Studies in Maine Geology

Volume 4: Igneous and Metamorphic Geology

Edited by Robert D. Tucker and Robert G. Marvinney

Walter A. Anderson, State Geologist
Maine Geological Survey
DEPARTMENT OF CONSERVATION

Studies in Maine Geology

Volume 4: Igneous and Metamorphic Geology

Edited by

Robert D. Tucker
Director, Cartography and Information Services
Maine Geological Survey

Robert G. Marvinney
Physical Geologist
Maine Geological Survey

Walter A. Anderson, State Geologist

Maine Geological Survey
DEPARTMENT OF CONSERVATION

1989

Copyright © 1989 by the Maine Geological Survey, Department of Conservation. All rights reserved. Printed in the United States of America. No part of this publication may be reproduced, stored in a retrieval system, or transmitted, in any form or by any means, electronic, mechanical, photocopying, recording, or otherwise, without the prior written permission of the publisher.

Cover photograph:

Pillowed and brecciated diabase in granite matrix as exposed near Mahar Flowage in the Moosehorn National Wildlife Refuge near Baring, Maine. This is part of an extensive unit thought to be the product of commingled granitic and gabbroic magmas in the Bays-of-Maine igneous complex. See "Commingled gabbroic and granitic magmas in the northern Bays-of-Maine igneous complex, Calais area" by M. D. Hill and R. N. Abbott, Jr., this volume. Photograph by W. B. Thompson.

The laws and policies of Maine and the United States prohibit discrimination in Department of Conservation programs and/or employment because of race, religion, national origin, sex, age, or handicap. Any person who believes discrimination has occurred should contact the Commissioner, Maine Department of Conservation, Station #22, Augusta, ME 04333; Telephone (207) 289-2211.

Published under Appropriation 4501-2300

Studies in Maine Geology

Papers to commemorate the 150th anniversary of
C. T. Jackson's reports on the geology of Maine

Studies in Maine Geology

Papers to commemorate the 150th anniversary of
C. T. Jackson's reports on the geology of Maine

Charles Thomas Jackson (1805-1880)

Foreword

During the period 1836-1839, Charles Thomas Jackson conducted the first comprehensive, government-funded survey of the geology of the state of Maine. As part of our commemoration of the 150th anniversary of that monumental undertaking, the Maine Geological Survey is publishing *Studies in Maine Geology*, a series of 6 volumes which cover a broad spectrum of geological investigations. The response to our initial call for papers was overwhelming not only in number, but also in the quality of contributions, which would have been well received by professional journals. I appreciate the efforts of each contributor in ensuring the success of these volumes.

Many issues have challenged the geologic community since the time of that first survey. Jackson was charged with the seemingly insurmountable task of surveying the geology of the entire state over a period of 3 field seasons without the aid of accurate maps or modern equipment. One of the main objectives of his work was to assess the potential for mineral deposits, coal, and building materials in this unexplored territory. In the latter part of the 19th century the geological issues of the state concerned sources of dimension stone and pegmatite gemstones. During this period, the gold and silver rushes accelerated the pace of geologic exploration in Maine, causing a short-lived metal-mining boom. In the first half of the 20th century and with the advent of two world wars, the need for "strategic minerals" once again stimulated geologic investigation. The economic downturn in the domestic minerals industry of the past few decades has reversed and interest in exploration and extractive commodities is once again rapidly gaining ground in the state.

Today, a growing environmental awareness has led to a concern for protecting our resources, both now and in the future. Geologic information provides the basis for a multitude of decisions aimed at confronting the complex problems of modern society. Primary issues are those of ground water resources and contamination, coastal development and shoreline protection, and the disposal of nuclear wastes in geological repositories.

To meet the changing and expanding needs of the state over the past century and a half, the Maine Geological Survey has been under the auspices of many different government departments, culminating in its current position within the Department of Conservation. Since Jackson's time, the survey has expanded from essentially a one-man agency to include full bedrock and surficial geology, marine geology, hydrogeology, and cartographic divisions. In spite of the changes in issues and manpower, one of the primary objectives of the Maine Geological Survey has remained unchanged since Jackson's time: to provide the public with the highest quality information about the geology of the state of Maine. These volumes meet the challenge of that objective.

Walter A. Anderson
Director and State Geologist
Maine Geological Survey
DEPARTMENT OF CONSERVATION
Augusta, Maine

Acknowledgments

Studies in Maine Geology began as a project to commemorate 150 years of geologic investigation in Maine. The original intent was to assemble a volume of papers which summarized our current understanding of all aspects of the geology of Maine. As word of the project spread, however, the volume grew into a six-volume set centered around three broad subject categories: structure and stratigraphy, igneous and metamorphic geology, and Quaternary geology.

The publication of a project of this size involves the time and goodwill of a great many people. The editors thank Marc Loiselle who initiated the project and contacted the authors. The illustrations and manuscript assembly were done by the Cartography and Information Services Division of the Maine Geological Survey. Additional editorial assistance was provided by Steve Dickson, Woody Thompson, Tom Weddle, and John Williams. Particular thanks are given to Ben Wilson, John Poisson, and Bob Johnston who drafted many of the illustrations and to Cathy Stultz and Cheryl Fiore who typed and corrected the manuscripts. We also wish to thank the geologists who willingly undertook the task of reviewing the manuscripts.

Scientific Reviewers

Richard N. Abbott
Michele L. Aldrich
John N. Aleinikoff
William I. Ausich
Fred Barker
Daniel S. Barker
Patrick J. Barosh
M. Jacques Béland
Daniel F. Belknap
Henry N. Berry IV
Francis S. Birch
Gary M. Boone
Harold W. Borns, Jr.
Wallace A. Bothner
Arthur J. Boucot
Dwight C. Bradley
Julie Brigham-Grette
F. William Cambray
C. Page Chamberlain
Lindgren L. Chyi
J. Michael Clinch
Steven M. Colman
Pierre A. Cousineau
John W. Creasy
James L. Cullen
Michael F. Diggles
William E. Doll
G. Nelson Eby
Gordon B. Fader
Roy L. Farnsworth
Duncan M. FitzGerald
Leslie R. Fyffe
Olcott Gates
Henri E. Gaudette
Robert F. Gerath
Richard A. Gilman
Richard P. Goldthwait
Charles V. Guidotti
Lindley S. Hanson
Matthew Heizler
J. Christopher Hepburn
O. Don Hermes
David A. Hewitt
Malcolm D. Hill
John P. Hogan
Michael J. Holdaway
William R. Holland
Arthur M. Hussey II
Andrew J. Hynes
J. Steven Kite
Edward Laine
E. Melanie Lanctot
Helen Lang
Pierre J. Lesperance
Marc C. Loiselle
Thomas V. Lowell
Allan Ludman
Jim Luetgert
Daniel R. Lux
John B. Lyons
Thomas J. Malterer
Lawrence C. Matten
Y. T. Maurice
Gregory J. McHone
Garry D. McKenzie
Robert L. McMaster
Calvin F. Miller
Robert H. Moench
R. Damian Nance
Thomas Nichols
Jackson Odum
Robert N. Oldale
William J. Olszewski
Philip H. Osberg
James K. Otton
Tom L. Phillips
Steven R. Pinette
Stephen G. Pollock
Thomas L. Potter
Ross D. Powell
A. G. Pronk
Douglas W. Rankin
Robert Raymond, Jr.
John B. Reid, Jr.
Michael J. Retelle
John C. Ridge
Peter S. Rosen
Martin E. Ross
David C. Roy
Arthur A. Ruitenberg
Donald F. Sangster
Matthew Scott
Allen A. Seamen
Carol Simpson
James W. Skehan
John F. Slack
Geoffrey W. Smith
Dale A. Springer
Ralph Stea
George C. Stephens
David B. Stewart
Peter Stringer
John R. Suter
Mark T. Swanson
Spencer R. Titley
Walter E. Trzcienski, Jr.
Allan B. Tanner
David L. Westerman

Contents

Foreword i

Acknowledgments ii

Compositional variation of plutonism in the coastal Maine magmatic province: mode of origin and tectonic setting 1
John P. Hogan and A. Krishna Sinha

Commingled gabbroic and granitic magmas in the northern Bays-of-Maine igneous complex, Calais area 35
Malcolm D. Hill and Richard N. Abbott, Jr.

Geochemistry of the granite-gabbro complex on Vinalhaven Island, Maine 45
Christopher B. Mitchell and J. Michael Rhodes

Geology and geochemistry of the Rattlesnake Mountain igneous complex, Raymond and Casco, Maine 63
John W. Creasy

Preliminary studies of five Mesozoic stocks in the Newfield 15' quadrangle, Maine 79
Richard A. Gilman

Petrographic and geochemical variations within the Songo pluton, western Maine 87
David Gibson and Daniel R. Lux

Geochronology of the Songo pluton, western Maine 101
Daniel R. Lux, David Gibson, and P. J. Hamilton

$^{40}Ar/^{39}Ar$ isotopic dating of the Horserace quartz diorite and its bearing on age relationships in the Katahdin batholith - Traveler rhyolite system 115
A. Scott Denning and Daniel R. Lux

Interpretation of the regional significance of the Chain Lakes massif, Maine, based upon preliminary isotopic studies 125
Michael M. Cheatham, William J. Olszewski, and Henri E. Gaudette

Geochemistry of the Catheart Mountain porphyry copper deposit, Maine 139
Robert A. Ayuso

Multiple thermal metamorphism of the Digdeguash Formation in the contact aureole of the Pocomoonshine gabbro-diorite, southeastern Maine 163
Allan Ludman, Sandra L. Bromble, and James M. DeMartinis

Maine Geological Survey
Studies in Maine Geology: Volume 4
1989

Compositional Variation of Plutonism in the Coastal Maine Magmatic Province: Mode of Origin and Tectonic Setting

John P. Hogan
A. Krishna Sinha
Department of Geological Sciences
Virginia Polytechnic Institute and State University
Blacksburg, Virginia 24061

ABSTRACT

Proterozoic(?) to Devonian metasedimentary and metavolcanic rocks of the northeast-trending, fault-bounded lithotectonic terranes of eastern coastal Maine, between Penobscot and Passamaquoddy Bay, have been pervasively intruded by over one hundred individual Silurian to Early Carboniferous mafic and felsic plutons. Mafic magmatism generally preceded felsic magmatism, although field evidence suggests that commonly these magmas were spatially and temporally related. The large volume and close spatial and temporal relationship of mafic and felsic plutonism within this area suggest a possible genetic relationship. We propose that mafic and felsic plutonic rocks within this region be considered collectively as the coastal Maine magmatic province.

On the basis of the presence of syn-plutonic mafic dikes, gradational contacts between mafic and felsic plutons, and the presence of mafic enclaves, plutons in the coastal Maine magmatic province can be divided into four types representing the relative degree of association of mafic and felsic magmas. End members are mafic plutons that have crystallized without interaction with a felsic magma (type I) and felsic plutons that have crystallized without interaction with a mafic magma (type II). Types III and IV are hybrid granitoid and gabbroic plutons that have had their original compositions modified by interaction with a magma(s) of markedly different composition during the course of crystallization. Using this classification scheme, contact relationships, subsurface distribution, modal mineralogy, and mineral and whole rock chemistry are examined for the plutons to determine possible compatible tectonic settings and thermal history for eastern coastal Maine during the Early to Middle Paleozoic.

Plutonism within the magmatic province is compatible with an extensional tectonic regime. Underplating (Wones, 1976a) and intraplating of mantle-derived mafic magmas, represented by type I plutons, provided the heat source to induce partial melting of a variably dehydrated crustal source region(s) for generation of the type II felsic plutons. The diversity of granitic plutons present in the coastal Maine magmatic province reflects the potential diversity in mineral assemblages present in the source region during partial melting as well as the possibility of later modification of the original magma composition through mixing/mingling with mafic magmas to produce hybrid pluton types III and IV. In general, the bimodal plutonism with alkalic tendencies that characterizes the coastal Maine magmatic province postdates assembly of the proposed lithotectonic terranes. Pluton emplacement may have been structurally controlled by preexisting faults. The presence of prominent dextral transcurrent faults suggests that rift-related magmatism could have occurred within a region of transtension in a transcurrent fault system. However, the orientation of relatively younger, Devonian, felsic batholiths coincides with a system of step-over faults that would require a change from a transtensional to transpressional regime prior to their intrusion, suggesting that plutonism within this region is sensitive to changes in the geometry of the transcurrent fault system.

INTRODUCTION

Large geographic areas intruded by voluminous plutonic rocks, such as the Mesozoic-Cenozoic coastal batholith of Peru (Pitcher, 1978) or the Lachlan fold belt of southeastern Australia (White and Chappell, 1983) are classified as magmatic provinces. Eastern coastal Maine, from west of Penobscot Bay north to Passamaquoddy Bay, has been pervasively intruded by over one hundred mafic and felsic plutons, spanning ages from Late Silurian to Early Carboniferous (Fig. 1, Tables 1 and 2). These plutons range in size from less than 1 km^2 to the 1670 km^2 Deblois granitoid batholith. Mafic plutonic rocks, such as gabbro, diorite, quartz-gabbro, and anorthosite, account for approximately 8% and felsic granitoids, predominantly granite with some quartz monzonite, and minor granodiorite represent 37% of the total 14,694 km^2 of the study area. Extended and repeated intrusion of plutons has resulted in younger intrusions transecting large portions of older plutons, suggesting that this represents a minimum estimate of mafic and felsic magmatic activity within the area. Previous reviews of plutonism in eastern coastal Maine have generally considered mafic and felsic plutonism separately (Chapman, 1962b, 1968; Page, 1968; Thompson, 1984). However, the large volume of magmatism and the close spatial and potential temporal relationship of mafic

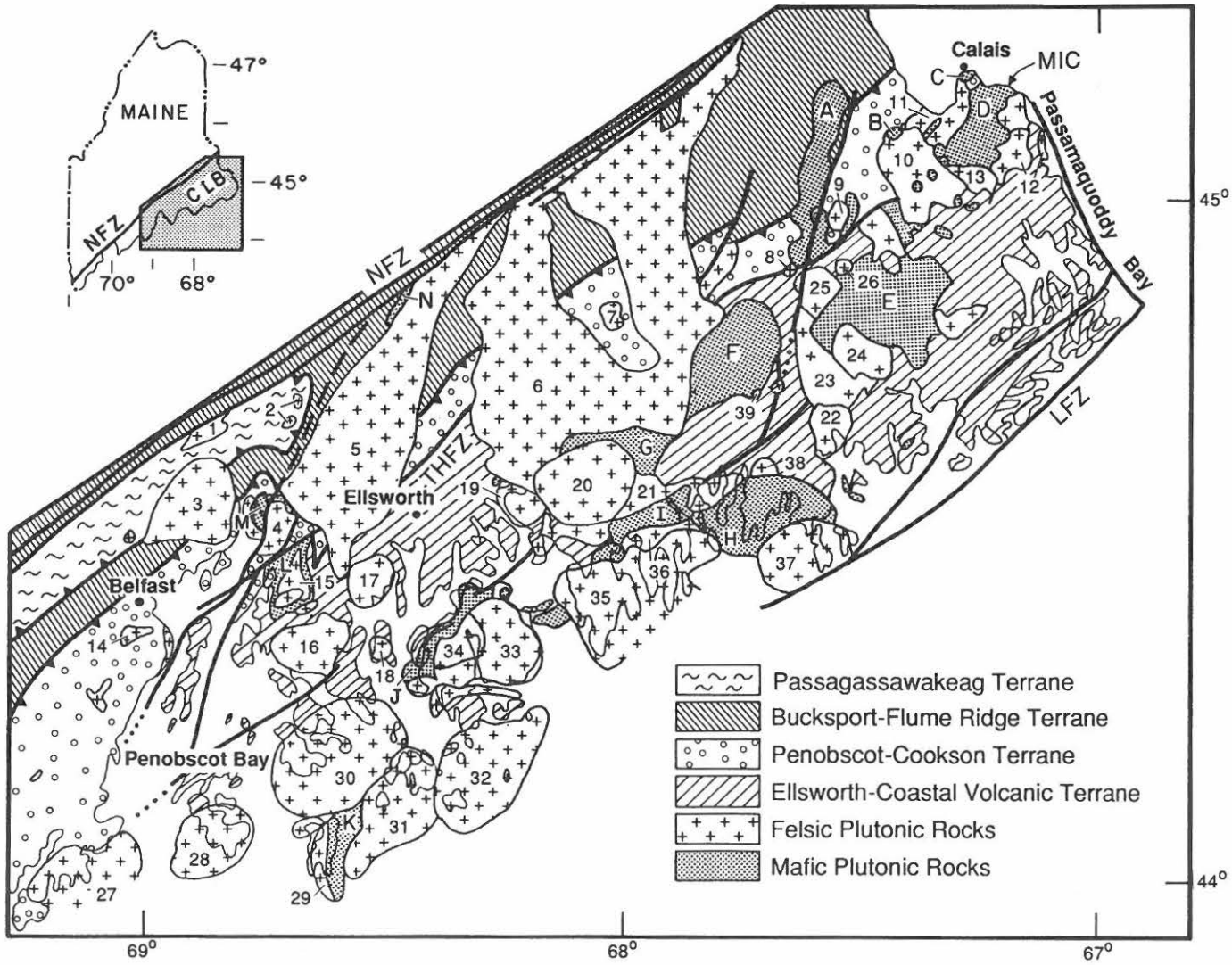

Figure 1. Generalized geologic map of a portion of the Fredrickton Trough and the coastal lithotectonic block, southeastern Maine, as modified from Osberg et al. (1985). Major tectonic elements include northeast-southwest trending lithotectonic terranes as well as prominent dextral transcurrent fault zones, such as the Norumbega fault zone (NFZ), the Turtle Head fault zone (THFZ), and the Lubec fault zone (LFZ), as well as associated N20-30°E step-over faults. Numbers correspond to felsic plutons and letters to mafic plutons identified in Table 1. The location of the Moosehorn Igneous Complex (MIC) referred to in the text is shown by the arrow.

TABLE 1. APPROXIMATE AREA OF PLUTONIC ROCKS IN THE COASTAL MAINE MAGMATIC PROVINCE.
(Pluton number and letter correspond to those in Figure 1).

FELSIC PLUTONS			MAFIC PLUTONS		
	Pluton Name	Area (km^2)		Pluton Name	Area (km^2)
1	Winterport	n.i.	A	Pocomoonshine	137
2	Stricklen Ridge	n.i.	B	Staples Mt.	3
3	Mt. Waldo	157	C	St. Stephen	2
4	Wallamatogus	34	D	Calais gabbro/diorite	105
5	Lucerne	625	E	Gardner Lake	244
6	Deblois	1670	F	Peaked Mt./Tibbettstown	190
7	Spruce Mt.	36	G	Cherryfield/Tibbettstown	44
8	Indian Lake	6	H	Pleasant Bay/Jonesport	169
9	Rocky Brook	14	I	Milbridge	44
10	Meddybemps	126	J	Mt. Desert	41
11	Baring	44	K	Isle Au Haut	51
12	Red Beach	36	L	South Penobscot	37
13	Charlotte	23	M	Leaches Point	16
14	Northport	14	N	Parks Pond	6
15	South Penobscot	31	O	Miscellaneous	79
16	Sedgwick	88			
17	Blue Hill	41			
18	Long Island	12			
19	Sullivan	36		Total area considered	14694
20	Tunk Lake	175			
21	Cherryfield	60		Area of felsic plutonic rocks	5422
22	Jonesboro	46			
23	Whitneyville	95		Area of mafic plutonic rocks	1134
24	Marshfield	58			
25	Bog Lake	36		Total area of plutonic rocks	6556
26	Round Lake Hills	5			
27	Spruce Head/Clark Island	147			
28	Vinalhaven	128			
29	Isle Au Haut	28			
30	Deer Isle	308			
31	Swans Lake	174		Percentage of total area considered	
32	Frenchboro	245			
33	Cadillac Mt.	158		Felsic plutonic rocks	37
34	Somesville	59			
35	Gouldsboro	360		Mafic plutonic rocks	8
36	Steuben	119			
37	Great Wass Island	124		Total for plutonic rocks	45
38	Highlands	8			
39	Pyroxene Granite	2			
	Miscellaneous	95		n.i. = not included	

and felsic plutons in eastern coastal Maine suggest a genetic relationship. Because of this we prefer to view plutonism in this area collectively as the coastal Maine magmatic province.

A correspondence between the composition of plutonic rock suites that comprise magmatic provinces and their associated tectonic environment has long been recognized by geologists (Harker, 1909; Benson, 1926; Martin and Piniwinskii, 1972; Petro et al., 1979; Pitcher, 1982, 1983). In well studied tectonic settings where magmatism is related to subduction, systematic variations in geochemical and isotopic characteristics exist for plutons with respect to their location from the trench (Kistler and Peterman, 1973; Taylor and Silver, 1978; DePaolo, 1981). The constant replenishment of source material through the subduction process to the site of melting is reflected in the repetition of intrusive sequences of magma types, ± gabbro, quartz-diorite, tonalite, granodiorite, and granite, within the overlying arc (Bateman et al., 1963; Bateman, 1983). In contrast, incremental melting of the same source region material can result first in the generation of low temperature, hydrous, peraluminous magmas followed by progressively higher temperature, drier, metaluminous melts and finally by anhydrous, peralkaline plutons (Brown and Fyfe, 1970). This sequence of magma types is compatible with rift-related tectonic settings where underplating of mantle derived magmas can provide the heat to melt the overlying source region (Wones and Sinha, 1988). In magmatic provinces where the tectonic setting is poorly constrained, analysis of the physical, petrographic, chemical, and isotopic characteristics of the plutonic rocks as well as establishment of sequences of magma types can be used to develop tectonic models that will be compatible with the characteristics of the

TABLE 2: RADIOMETRIC AGES OF PLUTONIC ROCKS IN THE COASTAL MAINE MAGMATIC PROVINCE.
(Pluton name and number correspond to those in Table 1 and Figure 1)

No.	Pluton Name	U/Pb (Zircon)	Rb/Sr (Whole Rock†)	Rb/Sr (Mineral†)	K/Ar (Mineral)
1	Winterport	412±14[14]*			
2	Stricklen Ridge	412±16[14]			
3	Mt. Waldo		382±10[4]		325±10(B)[15]
4	Wallamatogus		367±20[4]	323(B)[5]	330(B)[5]
				382(M)[5]	384(M)[5]
5	Lucerne	380±4[14]	371±21[6]	325(B)[5]	356(B)[5]
			393±13[4]		
6	Deblois		393±17[6]		367(B)[5]
10	Meddybemps			354(B)[5]	404(B)[5]
					354(B)[5]
12	Red Beach		385±6[9]	372(B)[5]	407(B)[5]
					401(B)[5]
13	Charlotte			382(B)[5]	406(B)[5]
15	South Penobscot	424±6[10]	394±15[4]		360+15[4]
		436±9[10]			
16	Sedgwick		387±15[4]		413±15[4]
17	Blue Hill		374±10[4]	362(B)[5]	387(B)[5]
19	Sullivan				369(B)[5]
20	Tunk Lake				357±10(B)[1]
22	Jonesboro				363(B)[5]
25	Bog Lake				363(B)[5]
27	Spruce Head/ Clark Island				367±11(B)[15]
28	Vinalhaven		353±7[2]		399(B)[4]
30	Deer Isle				
	Oak Point Phase		349±1[3]	336±12(B)[15]	354(B)[5]
				258±15(F)[15]	
	Stonington Phase		334±21[3]		350(B)[5]
					360(B)[5]
33	Cadillac Mt.		361±35[7]		397(Hfls)[5]
34	Somesville		410±16[7]		389(B)[5]
35	Gouldsboro		377±19[8]		
A	Pocomoonshine				423±24(H)[12]
					408±14(B)[12]
C	St. Stephen				407±20(H)[11]
					357±16(B)[11]
N	Parks Pond	410±4[13]	388±6[13]		365(B)[5]

* References indicated by superscripts, and the mineral used for dating in ( )
† All Rb/Sr ages reported are for $\lambda Rb^{87} = 1.42 \times 10^{-11}$ /yr.

1) Brookins, 1976
2) Brookins et al., 1973
3) Brookins and Spooner, 1970
4) Brookins, in Wones, 1976a
5) Faul et al., 1963
6) Loiselle et al., 1983
7) Metzger and Bickford, 1972
8) Metzger et al., 1982
9) Spooner and Fairbairn, 1970
10) Stewart et al., 1988
11) Wanless et al., 1973
12) Westerman, 1972
13) Eriksson and Williams, in press
14) Zartman and Gallego, 1979
15) Zartman et al., 1970

(B) Biotite
(M) Muscovite
(H) Hornblende
(F) Feldspar
(Hfls) Hornfels

associated plutonism. The purpose of this paper is to examine plutonism within the coastal Maine magmatic province in terms of the physical, petrographic, major element, and selected trace element characteristics of the associated plutons and interpret their role in the tectono-thermal evolution of the crust of eastern coastal Maine during Early to Mid-Paleozoic times.

The composition of plutonic rock suites has also been interpreted to be inherited from their source region (Chappell and White, 1974; White and Chappell, 1977). However, besides restite unmixing, compositional variation in plutons can also be produced by processes such as fractional crystallization, assimilation, or magma mixing. Modification of the original composition of the magma by these processes, except for restite unmixing, can act to obscure information about source region characteristics. In the coastal Maine magmatic province, the spatially intimate association of mafic and felsic plutons suggests that magmas of distinct composition may have been temporally and genetically related. Compositional variation of plutonism within this region has the possibility of reflecting various degrees of hybridization of felsic and mafic magmas through magma mixing and/or mingling during the course of crystallization. This process is important to identify because the chemistry of a magma that has interacted with melts of markedly different composition can be significantly modified (Eichelberger, 1978; Gamble, 1979; Reid et al., 1983). The resultant magma may even retain isotopic characteristics formed during magma mixing and therefore may not yield a meaningful whole rock Rb-Sr isotopic age (Faure, 1977). Therefore, the chemical characteristics of plutons derived from interaction of several magmas should be viewed with some caution, as their chemical signature may no longer reflect those of a single source region and could lead to erroneous tectonic interpretations.

With this caveat in mind, we have chosen to group plutons in the coastal Maine magmatic province into four broad types based on the possibility that mixing/mingling of felsic and mafic magmas may have been a viable process during the crystallization of a particular pluton. In this paper we use field observations such as gradational contacts between mafic and felsic plutons, the presence of syn-plutonic dikes, bimodal mafic/felsic dikes, and the presence of mafic enclaves to initially classify plutonic rocks of this province. The end member compositions of the four intrusive types are represented by mafic plutons (type I) and felsic plutons (type II) which, at the present level of exposure, appear to have crystallized without any interaction with a magma(s) of markedly different composition.

The two hybrid types are plutons where field evidence suggests that mixing and/or mingling of mafic and felsic magmas may have been an important process in their petrogenesis. Type III plutons are dominantly granitic, but have interacted to some degree with mafic magma(s). Type IV plutons are dominantly gabbroic, but have interacted with felsic magma(s) during the course of crystallization. Assignment of a pluton to type III or type IV in this paper is not intended as a final conclusion that magma mixing is the process responsible for the compositional

variation observed in these plutons; it is a preliminary classification based on field observations and needs to be considered in future investigations of plutons belonging to these two types. Detailed petrologic studies are required to determine the extent to which processes, such as assimilation, restite unmixing, fractional crystallization, or magma mixing may have operated in a pluton to produce the observed compositional variation. Several such detailed studies on plutonic rocks in the coastal Maine magmatic province, classified in this paper as either type III or type IV plutons, have recently been completed that stress the importance of magma mixing in the petrogenesis of these plutons (Mitchell, 1986; Stewart et al., 1988; Hill and Abbott, this volume; Mitchell and Rhodes, this volume).

Type II plutons, because they are the least likely to have interacted with a mafic magma(s), have the greatest potential for retrieval of information concerning the nature of the crustal source region(s) beneath the coastal Maine magmatic province. Although comparisons of modal, whole rock, and selected trace element chemistry support distinctions made by this classification scheme, these data also indicate that type II plutons can be further subdivided into units/superunits in the sense of Pitcher (1979) and potentially into suites in the sense of White and Chappell (1983). Identification of potential plutonic suites will provide a framework for geochemical and isotopic analysis to determine the geometry and spatial distribution of source regions beneath the coastal Maine magmatic province. This information will further constrain tectonic models proposed for eastern coastal Maine.

Modal and whole rock chemical data for selected plutons in the coastal Maine magmatic province have been compiled from a wide range of sources. The data presented have not been normalized in terms of areal extent of the pluton vs. the number of analyses. Several plutons that have been well studied and adequately sampled are used as type examples (Table 3) to illustrate major characteristics of the coastal Maine magmatic province. However, many of the plutons have either limited or no data available on the distribution, relationship, or chemistry of rock types present. This necessitates that some plutons be left

TABLE 3. CHARACTERISTICS OF INTRUSIVE TYPES IN THE COASTAL MAINE MAGMATIC PROVINCE.

	Type I	Type IIa	Type IIb	Type III	Type IV
Principal rock types	Gabbro, norite, diorite ± anorthosite	Granite	Granite ± alkali-feldspar granite	Granite, granodiorite quartz monzonite ± alkali-feldspar granite	Quartz monzodiorite-monzogabbro, gabbro, diorite, monzonite
Primary phases	Ol, Opx, Cpx Hbl ± Bio	Bio-Mu ± Gar Bio	Bio ± Hbl Bio	Bio-Mu ± Gar Bio ± Hbl, Bio	Bio ± Hbl ± Opx ± Cpx ± Ol(?)
Accessory mineralogy	Apatite, ilmenite pyrrhotite, pentlandite chalcopyrite	Ilmenite, monazite zircon, tourmaline apatite	Ilmenite, zircon apatite, +allanite +tourmaline	Magnetite, ilmenite, sphene, fayalite, aegerine-augite reibeckite, apatite, allanite	Magnetite, zircon apatite, sphene
Textures	Magmatic layering, cryptic layering,	Variable, medium to coarse grained, seriate to subporphrytic	Homogeneous coarse grained seriate to porphyritic	Variable, medium to coarse grained, seriate to porphyritic	Variable, medium to fine grained
Intrusive style	Stratiform sills, dikes, laccoliths	Subcircular stocks	Large elongated batholiths	Subcircular stocks, or multiple intrusions forming igneous complexes e.g. Moosehorn Igneous Complex	
Enclave types	Metasedimentary xenoliths, autoliths	Metasedimentary xenoliths, autoliths		Mafic enclaves common in zones and evenly distributed Autoliths, metasedimentary xenoliths	
Dikes	Tonalitic pegmatites	Aplites and pegmatites Common	Uncommon	Aplites and pegmatites, Mafic dikes	
Alumina saturation index	0.73 ± .1	1.13 ± .1 (1.34-0.99)	1.05 ± .02 (1.09-1.00)	1.00 ± .1 (1.26-0.89)	0.72 ± .2 (Gabbros) 0.68 ± .05 (Parks Pond)
Mean SiO_2 content	47.5 ± 3.7	74.6 ± 1.1	71.9 ± 2.0	72.5 ± 1.8	47.3 ± 7.4 (Gabbros) 57.9 ± 1.2 (Parks Pond)
Rb/Sr ratio	<1 : 2	>2 : 1	>2 : 1	<2 : 1	<2 : 1
Type examples	Pocomoonshine Pleasant Bay	Blue Hill Wallamatogus	Lucerne Deblois	Deer Isle Spruce Head Cadillac Mt.	Parks Pond gabbro, diorite in igneous complexes

unassigned, while other plutons may be prematurely classified and may require a more in-depth study before a final assignment of type is made. Therefore, inferences drawn from this limited data base represent guidelines for future work designed to test and evaluate preliminary conclusions presented in this paper.

REGIONAL GEOLOGY

Recent analyses of the Appalachian-Caledonide orogen have proposed that it can be viewed as a mosaic of suspect terranes (Williams and Hatcher, 1982, 1983; Zen, 1983). Terrane analysis has been in progress in Maine where geochemical and isotopic studies of granitic plutons within a transect across central to coastal Maine defined three distinct crustal source regions (Loiselle and Ayuso, 1980; Andrews et al., 1983; Ayuso, 1986) that are consistent with terranes defined on the basis of gravity gradients (Phillips et al., 1985), deep seismic reflection traverses (Stewart et al., 1985), and contrasting stratigraphic and structural features (Zen, 1983). In southeastern Maine, the steeply dipping, northeast-trending, dextral, Norumbega fault zone (Wones and Thompson, 1979; Johnson and Wones, 1984) is suggested to represent the boundary which separates the crustal block of central Maine from the coastal lithotectonic block (Fig. 1) (Stewart and Wones, 1974; Wones and Stewart, 1976; Zen, 1983). The regional geology of the coastal lithotectonic block, from Penobscot to Passamaquoddy Bay, consists of a series of northeast-trending, fault-bounded lithotectonic belts (Osberg et al., 1985). Each belt consists of a unique package of lithologies, regional metamorphic mineral assemblages, and deformational history suggesting that the coastal lithotectonic block can also be considered as a collage of several distinct crustal blocks or terranes (Stewart and Wones, 1974; Wones and Stewart, 1976; Osberg, 1974, 1978; Zen, 1983).

In the Penobscot Bay area, the Passagassawakeag terrane (Wones and Stewart, 1976; Bickel, 1976) consists of complexly deformed, migmatitic, quartzo-feldspathic augen gneiss, metavolcanics, and calc-silicates all of suggested Precambrian or Proterozoic age (Stewart and Wones, 1974) as well as Cambro-Ordovician pelitic schists, siltstones, and quartzites. This lithologic package is pervasively intruded by numerous pre- to syn-tectonic granitoid dikes, sills, pegmatites, and small stocks (Trefethen, 1944; Stewart and Wones, 1974; Wones, 1976a; Kaszuba, 1986). The Passagassawakeag terrane is interpreted to be in fault contact with rocks of the Bucksport-Flume Ridge terrane (Stewart and Wones, 1974; Kaszuba and Wones, 1985; Osberg et al., 1985; Hussey, 1985). However, detailed mapping along this contact did not reveal any structural or metamorphic discontinuity (Kaszuba, 1986). The finely laminated and calcareous siltstones and minor sulfidic pelite of the Bucksport-Flume Ridge terrane are separated from the graphitic, sulfidic, aluminous pelites, siltstones, quartzites, graywacke, metabasalt, slates, and schists of the Penobscot-Cookson terrane by a high-angle reverse fault (Stewart and Wones, 1974; Ludman, 1981a). The Turtle Head fault zone separates the Ellsworth-coastal volcanic terrane from the Penobscot-Cookson terrane (Stewart and Wones, 1974). The Ellsworth-coastal volcanic terrane consists of polydeformed low-grade greenstones and quartzo-feldspathic chlorite schists which are unconformably overlain by a series of bimodal suites of basalts and rhyolites, agglomerates, pyroclastics, breccias, and flow-banded auto-brecciated domes, interbedded with minor calcareous siltstones, limestones, shales, and conglomerates (Gilman, 1961; McGregor, 1964; Wingard, 1961; Stewart and Wones, 1974; Gates and Moench, 1981; Pinette, 1983). Previous interpretations of the Norumbega fault zone and Turtle Head fault zone as terrane boundaries are supported by seismic reflection and refraction studies which suggest that these fault zones are steeply dipping to near-vertical tectonic boundaries. They separate distinct crustal packages that consist of approximately 12 km of Lower Paleozoic cover rocks that overlie Precambrian gneissic basement (Stewart et al., 1986; Unger et al., 1986).

Timing of Terrane Accretion in Coastal Maine

The exact timing of terrane accretion in eastern Maine remains unresolved. In the Penobscot Bay area, faults juxtaposing the Bucksport-Flume Ridge terrane, Penobscot-Cookson terrane and the Ellsworth-coastal volcanic terrane are intruded by the Lucerne pluton (Wones, 1980a) which has a $^{207/206}$Pb age of 380±4 Ma (Zartman and Gallego, 1979) and a Rb-Sr whole rock age of 371±21 Ma (Loiselle et al., 1983), establishing a minimum age for docking of terranes in the coastal region. In extreme southeastern Maine these terranes have been shown to share sedimentological as well as deformational histories since the Early Devonian, and radiometric ages on plutons intruding terrane boundaries suggest that these terranes acted as a structural entity since this time (Ludman, 1981a, 1986). Isolated occurrences of conglomeratic units basal to the Siluro-Devonian volcanic sequence along the southeastern Maine coast may be correlative based on stratigraphic position and lithologic similarities (Gates, 1969). These basal conglomerates unconformably overlie units of both the Penobscot-Cookson terrane and the Ellsworth-coastal volcanic terrane. If they prove to be correlative, it would require juxtaposition of these terranes in coastal Maine by the latest Silurian.

Juxtaposition of these terranes with the proposed crustal block of central Maine has been suggested to occur by movement along the Norumbega fault zone during the early Carboniferous after emplacement of the plutons (Zen, 1983; Ayuso, 1986). However, overlapping Silurian and Devonian cover sequences suggest that collectively these terranes, from the Ellsworth-coastal volcanic belt through central Maine, interacted and accreted to form a complex composite block during Cambro-Ordovician time that was sutured to cratonic North America prior to the Silurian (Ludman, 1986). Limited post-Acadian offset of plutons and cover rocks along major southwest-northeast-trending fault zones, such as the Norumbega fault zone, resulted from

reactivation of the earlier sutures which join distinct basement terranes and would not necessitate large-scale lateral transport along these faults during the Siluro-Devonian or later (Ludman, 1981a, 1986).

TYPE I PLUTONS

Type I plutons of the coastal Maine magmatic province consist of stratiform mafic plutons that crystallized, uninterrupted by the intrusion of felsic magmas, to produce layered intrusions comparable to the Skaergaard pluton (Wager and Brown, 1968). The Pocomoonshine (Westerman, 1972) and Pleasant Bay (Bickford, 1963) plutons (Fig. 1) have been chosen to represent the type examples for this category of plutons (Table 3).

Contact Relationships

The Pocomoonshine pluton intrudes both the Bucksport-Flume Ridge and the Penobscot-Cookson terranes. Contacts with the country rock are sharp and discordant, crosscutting the regional fabric and truncating tight, upright, isoclinal folds (Westerman, 1972; Ludman, 1981b). The intrusion is elongated in a N30°E direction and is discordant to the regional trend. A 2.4 to 3.2 km wide metamorphic aureole overprints chlorite-grade, lower greenschist regional metamorphism with a low pressure-high temperature contact facies assemblage (Westerman, 1972; Ludman, 1981b; Ludman et al., this volume). Local zones of partially melted country rock are present adjacent to the intrusion, and similar observations have been reported for other mafic intrusions within the coastal Maine magmatic province (Gilman, 1961; Westerman, 1972; Ludman, 1981b). Igneous layering is disrupted by high-angle dip-slip and strike-slip faulting with locally developed weak to strong foliation, brittle fracturing, and mylonites (Westerman, 1972; Ludman, 1981b). The Pocomoonshine pluton has been intruded by small felsic stocks which crosscut igneous layering and enclose xenoliths of the Pocomoonshine pluton. The pluton may have intruded by forceful injection with minor assimilation (Westerman, 1972). The presence of abundant xenoliths associated with roof pendants (Westerman, 1972) suggests that stoping may have been important. Emplacement of the pluton is suggested to have been strongly controlled by a preexisting N30°E fault system (Ludman, 1974; Biggi and Hodge, 1982).

The Pleasant Bay gabbro-diorite pluton is emplaced entirely within the Ellsworth-coastal volcanic terrane. Igneous laminations and layering in the Pleasant Bay gabbro-diorite pluton demonstrate that the pluton is a trough-shaped intrusion (Ward, 1972) which is discordant to the regional folding, rather than a folded sill as suggested by Bickford (1963). Magmatic layering and lithologic units within the Pleasant Bay pluton have also been truncated and disrupted by post-emplacement faulting (Terzaghi, 1946; Bickford, 1963).

Subsurface Distribution

The subsurface distribution of rock types related to the Pocomoonshine gabbro-diorite pluton is inferred from gravity data (Biggi and Hodge, 1982) and changes in the width of the contact aureole (Westerman, 1972). The pluton is believed to be a 1.5 km thick, sheet-like sill, that dips approximately 45° to the west, although the eastern contact has been modified by post-emplacement faulting and is now nearly vertical (Westerman, 1972; Ludman, 1981b). A pronounced positive Bouger anomaly over the northern portion of the complex supports Westerman's (1972) suggestion for accumulation of denser mafic minerals along the floor of the intrusion. Gravity data indicate a maximum thickness of 4.0 km for the Pleasant Bay pluton (Biggi and Hodge, 1982).

Textural Variation

Characteristic features of stratiform mafic intrusions such as igneous lamination, rhythmic layering, cryptic layering, and phase layering are displayed by one or both of these plutons. In the Pleasant Bay gabbro-diorite pluton, high concentrations of olivine, hypersthene, and augite form dark bands that alternate with layers modally abundant in plagioclase, giving an appearance similar to graded bedding (Bickford, 1963). These rhythmic layers may truncate other rhythmic layers in a manner suggestive of cross-bedding.

The Pocomoonshine pluton is compositionally zoned (Westerman, 1972). Troctolites at the roof of the intrusion are replaced by progressively more felsic rock types, quartz-biotite-hornblende diorite, towards the interior of the sill, forming a reverse phase layered sequence. A sequence, symmetrical to the reverse phase layered upper portion of the chamber, is believed to have accumulated on the unexposed floor, indicating crystallization proceeded from the walls inward to the center of the pluton (Westerman, 1972). The stratiform nature of phase layering in the Pleasant Bay pluton has been disrupted by post-emplacement faulting, making correlation with stratigraphic position difficult (Bickford, 1963). A proposed section based on field and petrographic observations places cumulate mafic rocks at the base, grading progressively upwards into extremely differentiated quartz-bearing, fayalitic, leuco-gabbronorites (Bickford, 1963).

Modal Analysis and Mineralogy

Modal data for the Pocomoonshine (Westerman, 1972) and Pleasant Bay plutons (Bickford, 1963) indicate that rocks in both plutons can contain both pyroxene and hornblende, in excess of 5%, as well as biotite in amounts that vary from 0 to 11% for rocks of the Pleasant Bay pluton and 0 to 20% in the Pocomoonshine pluton. Rocks have been divided into two groups on the basis of the presence or absence of olivine before being plotted in the ternary systems olivine-plagioclase-pyroxene and

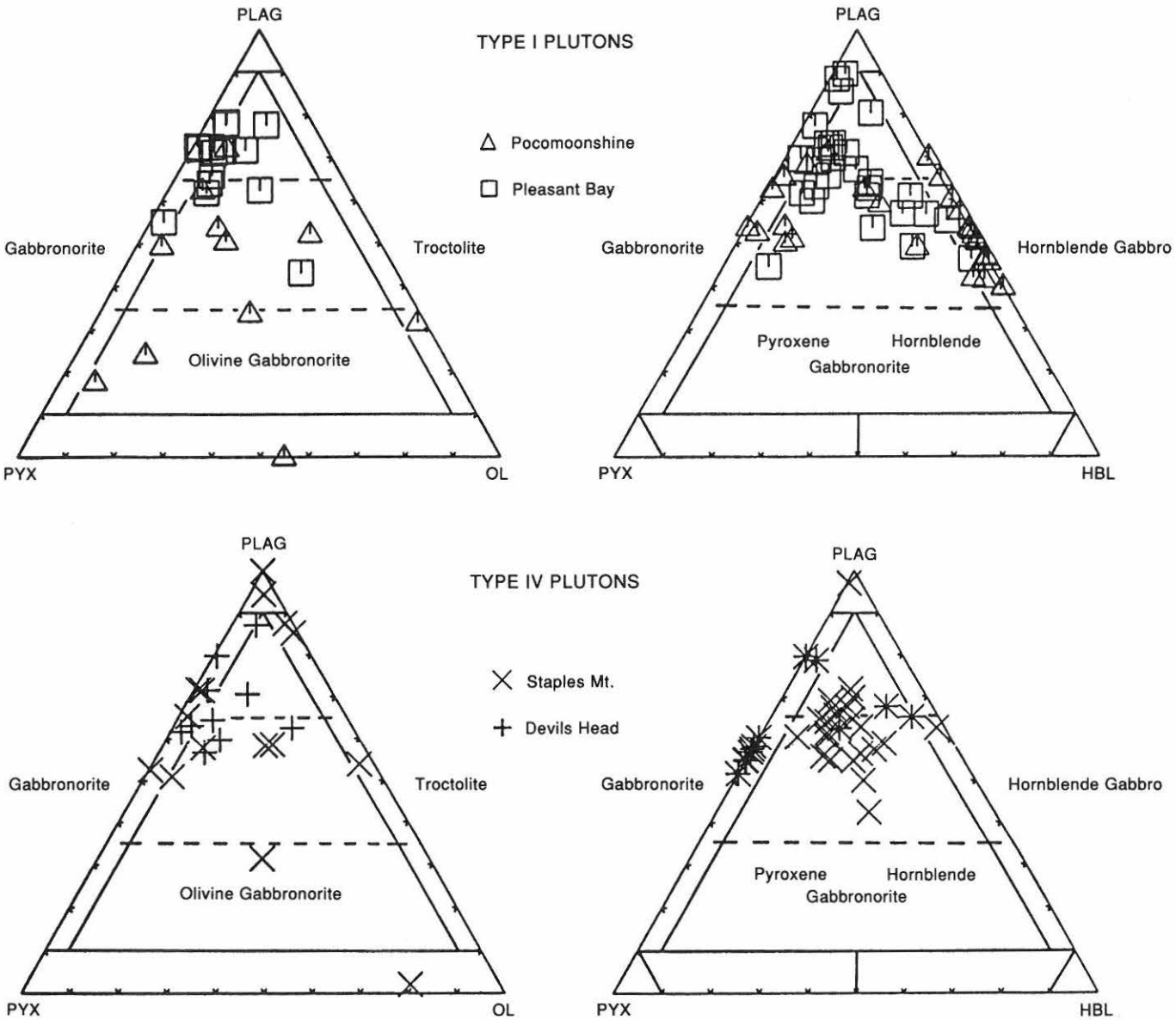

Figure 2. Modal analysis of selected mafic plutonic rocks from the coastal Maine magmatic province. Data for the type I Pocomoonshine and Pleasant Bay plutons are compiled from Westerman (1972) and Bickford (1963). Data for the type IV Staples Mountain and Devils Head mafic plutonic rocks associated with the Moosehorn Igneous Complex (Jurinski, 1987) are compiled from Coughlin (1986), Amos (1963), and Jurinski (1987). Field boundaries are those of Streckeisen (1976).

hornblende-plagioclase-pyroxene (Fig. 2) for classification purposes using the nomenclature suggested by Streckeisen (1976).

Olivine-bearing lithologies of the Pleasant Bay pluton are in general more leucocratic than rocks from the Pocomoonshine pluton. The majority of olivine-bearing lithologies from the Pocomoonshine pluton are dispersed throughout the olivine-plagioclase-pyroxene ternary diagram (Fig. 2). Rock types present in the Pocomoonshine pluton (ultramafic to leuco-olivine-gabbronorite, mela-troctolites and mela-gabbronorites) reflect accumulation of mafic minerals in contrast to the plagioclase cumulates present in the Pleasant Bay pluton.

Olivine-absent samples from the Pleasant Bay pluton display an antipathetic modal variation of plagioclase and pyroxene with hornblende (Fig. 2). Rocks range from leuco-gabbronorites and leuco-pyroxene-hornblende-gabbronorites, through the pyroxene-hornblende-gabbronorite field towards the hornblende-gabbro field and along the plagioclase-hornblende join. In contrast, olivine-absent samples from the Pocomoonshine pluton plot along or close to either the plagioclase-pyroxene join, as gabbronorite, or the plagioclase-hornblende join as hornblende-gabbro. Relatively few samples from the Pocomoonshine pluton plot within the pyroxene-hornblende-

gabbronorite field; those that do are biased toward either the gabbronorite field or the hornblende-gabbro field. The presence of a continuous modal variation within the Pleasant Bay pluton and its absence in the Pocomoonshine pluton is a marked difference between these otherwise similar intrusions.

Rocks of the Pocomoonshine pluton become increasingly more felsic from the roof towards the core of the body (Westerman, 1972). Cumulate troctolites, which occur within 50 meters of the roof, are underlain by olivine-gabbronorite and gabbronorite with minor amounts of olivine. Underlying this zone is a layer of olivine-absent gabbronorite and pyroxene-hornblende-gabbronorite, below which is found pyroxene-hornblende-gabbronorite with minor amounts of pyroxene. The core of the pluton consists of hornblende-gabbro and hornblende-diorite. Some of the hornblende-diorites contain significant amounts of biotite (2-12%) and quartz (tr-14%). Rare, sporadic occurrences of olivine-norite and feldspathic-hornblende-biotite-peridotite are believed to represent autoliths of ultramafic layers (Westerman, 1972). The peridotites all contain numerous xenoliths. A similar stratiform sequence has been proposed for the Pleasant Bay pluton (Bickford, 1963). Mafic cumulates (olivine-gabbronorite) are believed to have formed along the floor of the intrusion and grade progressively upward to more felsic, quartz-bearing leuco-gabbronorite.

Mineral Compositional Variation

Cryptic layering is present in both plutons. Mineral compositional changes, as determined by optical methods (Bickford, 1963; Westerman, 1972), indicate overall trends of Fe and Na enrichment as crystallization proceeds in both magmas. Plagioclase in the Pocomoonshine varies from An_{95} in cumulate troctolite to An_{38} in biotite-quartz-hornblende-diorite. Plagioclase compositions vary from An_{95} to An_{85} as olivine varies from Fo_{86} to Fo_{64} with orthopyroxene exhibiting little compositional variability (En_{83}-En_{80}). A larger compositional range exists for plagioclase (An_{65}-An_{38}) and orthopyroxene (En_{73}-En_{47}) in olivine-absent rocks. Plagioclase in hornblende-gabbros that contain minor amounts of pyroxene are discontinuously zoned with cores of $An_{85\text{-}75}$ mantled by rims of $An_{55\text{-}50}$. The transition from core to rim is sharp. This compositional gap in An content is mimicked in the pluton by a bimodal distribution of plagioclase compositions in olivine-bearing samples (An_{95}-An_{85}) vs. olivine-absent samples (An_{65}-An_{38}).

Mineral compositions for rocks of the Pleasant Bay pluton are more evolved than the Pocomoonshine pluton. Olivine and pyroxene compositions (Fo_{62}; En_{52}; $Wo_{44}En_{42}Fs_{14}$) in the more mafic rocks are iron-rich and coexist with normally zoned plagioclase (An_{87core}-An_{22rim}). Pyroxene compositions become progressively more iron-rich (En_{49}; $Wo_{43}En_{37}Fs_{17}$) and plagioclase more sodic (An_{60core}-An_{25rim}) in the quartz-bearing gabbronorite. Final crystallization in the Pleasant Bay pluton is represented by extreme iron enrichment. Quartz-bearing leuco-olivine-gabbronorite contains iron-rich pyroxenes (En_{37}; $Wo_{42}En_{21}Fs_{36}$), plagioclase (An_{65core}-An_{15rim}), and the appearance of fayalitic olivine ($Fo_{8.6}$) in contrast to the crystallization sequence observed in the Pocomoonshine pluton. Early crystallization of anhydrous phases progressively enriches the H_2O content in the magmas of the Pocomoonshine and Pleasant Bay plutons as expressed by the appearance of magmatic hornblende and finally magmatic biotite during the later stages of crystallization (Westerman, 1972).

Chemistry

The Pocomoonshine pluton has a mean SiO_2 content of 46±3.2 wt% with a range from 38.3 to 54.1 wt% (Fig. 3). The mean value of Fm, (FeO*/FeO*+MgO wt%, where FeO* = FeO + .89 Fe_2O_3) is 48 and TiO_2 ranges from 0.1 to 2.6 wt%. Available analyses from the Pleasant Bay pluton are characterized by a mean SiO_2 content of 52.8±3.4 wt%, Fm of 64, and TiO_2 of 1.2-2.1 wt%, suggesting that these rocks formed from a slightly more fractionated magma than the Pocomoonshine pluton. Three analyses from the Pocomoonshine pluton exhibit a range in Ba of 52-200 ppm, in Sr of 176-402 ppm, and Rb of 23-44 ppm (Fig. 4).

TYPE II PLUTONS

Type II granitic plutons are those in which mafic enclaves, bimodal dikes, syn-plutonic mafic dikes, or other field observations suggestive of mixing or commingling of mafic and felsic magmas have not been recognized. They are considered on the basis of field observations to have crystallized without interaction with mafic magma(s). Significant differences in textures, modal mineralogy, major element chemistry, trace element chemistry, abundance of aplites and pegmatites, as well as the volume of intrusion allow the broad category of type II plutons to be provisionally subdivided into two suites. The first suite, type IIa, is high silica (74.6±1.1 wt%), peraluminous, medium to coarse grained, seriate to subporphyritic, subcircular granitic stocks (Table 3). In contrast, type IIb plutons have a lower average silica content (71.9±2.0 wt%), are metaluminous, coarse grained with megacrystic alkali-feldspar phenocrysts, seriate to porphyritic, elongated granitoid batholiths. Recognition of granitic suites, such as type IIa and IIb, in the coastal Maine magmatic province may yield important information on the nature and distribution of the source regions for these magmas and therefore aid in constraining the tectono-thermal evolution of the crust beneath the coastal Maine magmatic province during the Paleozoic.

Type IIa

This group is well represented throughout the coastal Maine magmatic province and includes plutons such as the Spruce Mt.,

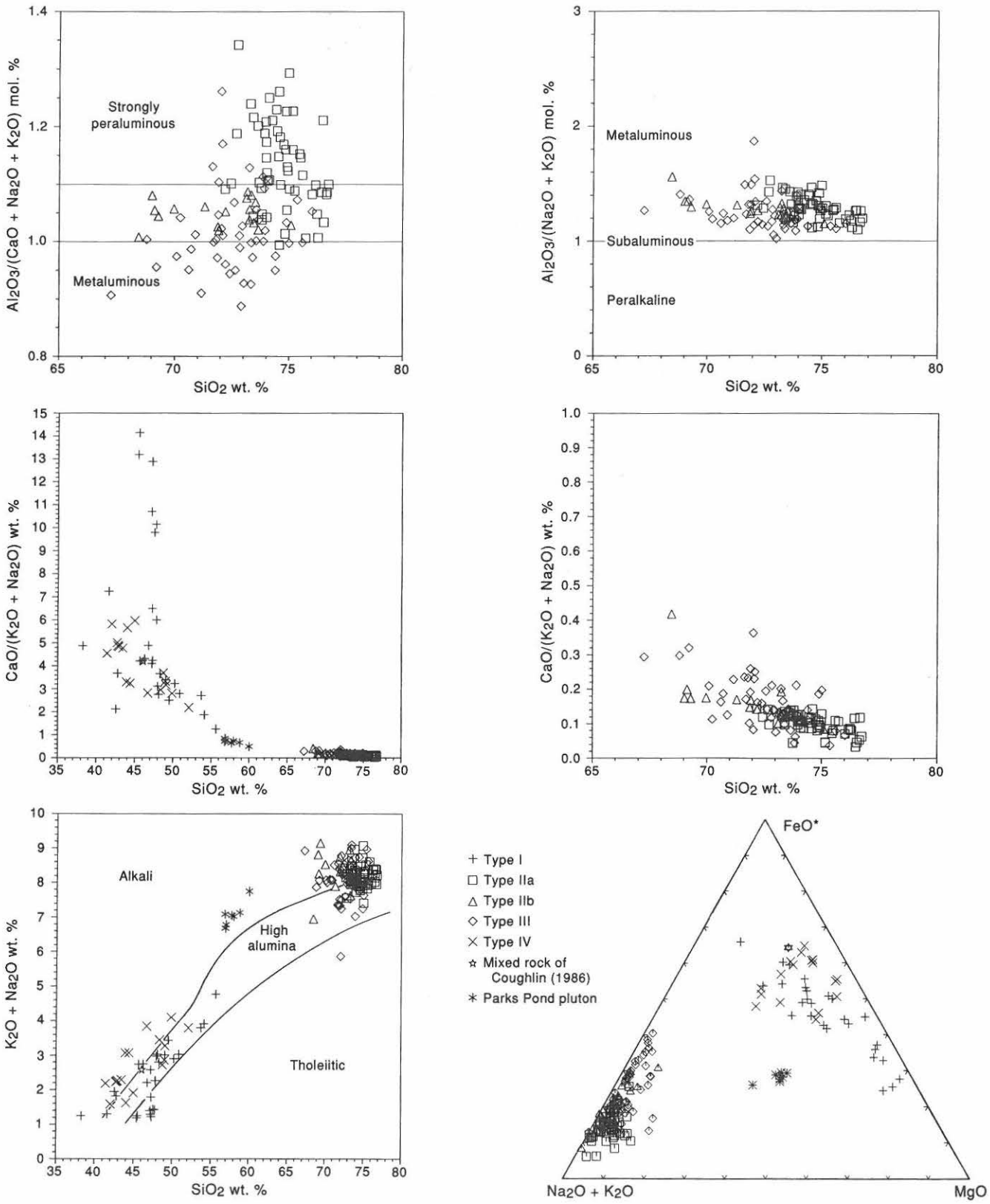

Figure 3. Comparative major element chemistry of pluton types of the coastal Maine magmatic province. Data compiled from Carl et al. (1984), Carl (pers. commun., 1985), Coughlin (1986), Eriksson (pers. commun., 1986), Stewart (1956), Westerman (pers. commun., 1985), Wones (unpubl. data), and Hogan and Sinha (unpubl. data).

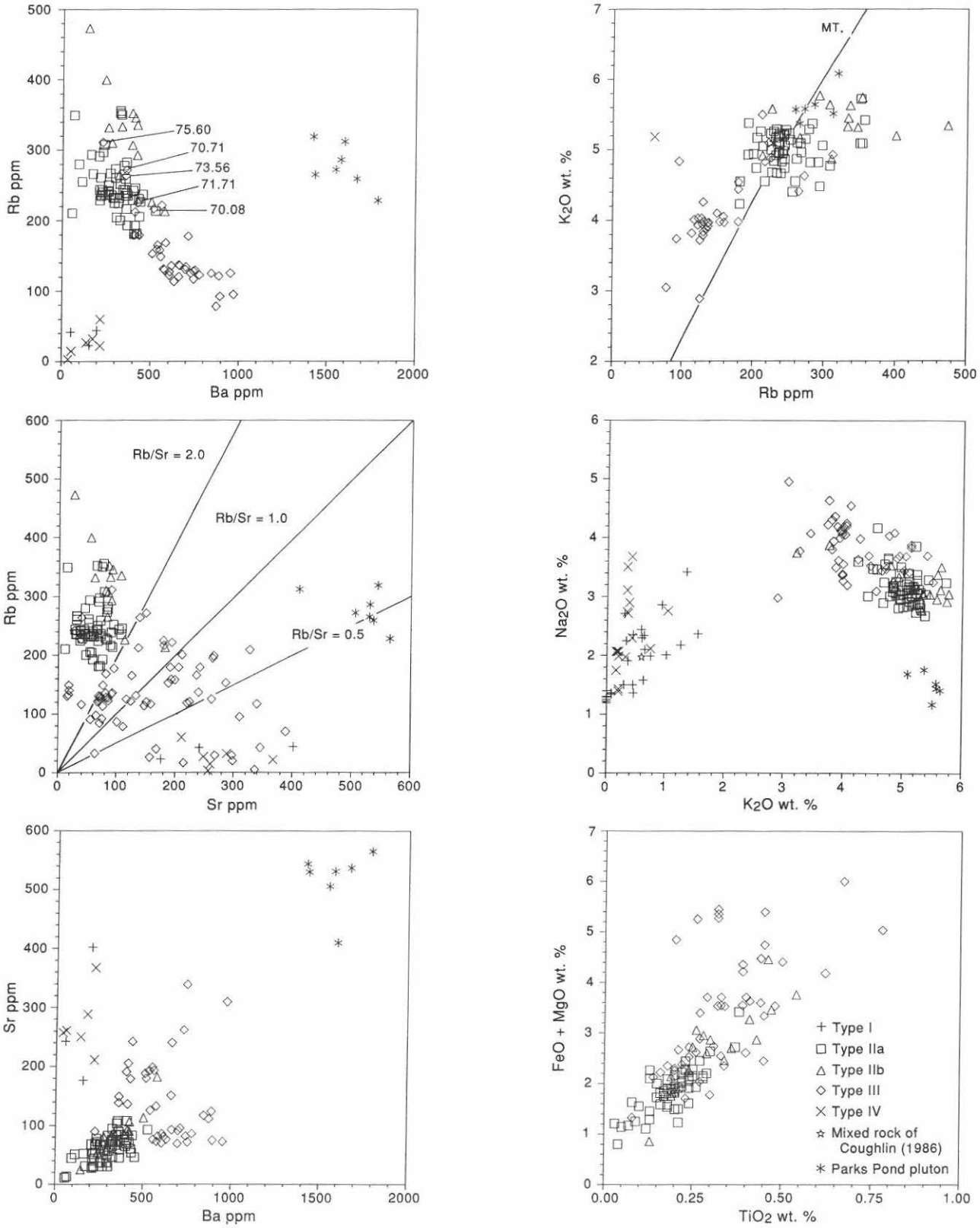

Figure 4. Comparative chemistry of selected trace elements and major elements for pluton types of the coastal Maine magmatic province. MT is the Main Trend of Shaw (1968). Values of SiO_2 for the Mount Waldo pluton are given in the Rb vs. Ba plot. Sources of data are the same as in Figure 3 except for additional Rb/Sr data from Spooner and Fairbairn (1970), Brookins and Spooner (1970), and Metzger et al. (1982).

Indian Lake, and Marshfield granites (Fig. 1). Typically, these plutons are small intrusions and range in size from less than a square kilometer to several tens of square kilometers. They may occur as isolated plutons (e.g. Long Island granite) or can form part of an igneous complex (e.g. Somesville pluton). The Wallamatogus and Blue Hill plutons are the representative examples of type IIa plutons (Table 3).

Contact Relationships. Contacts with country rocks are generally discordant, irregular, sharp, and truncate earlier folds and associated fabrics. Dikes emanating from the granites intrude the hornfelsed country rock, and commonly exploit joints and fractures associated with emplacement. The majority of plutons exhibit some form of alignment of platy minerals in a flow foliation. Fabrics related to deformation are localized to areas disrupted by post-emplacement faulting. Prominent faults cut and/or truncate contacts of the Wallamatogus pluton and many type IIa plutons experience some degree of post-emplacement deformation related to faulting.

Enclaves within these plutons can usually be related to the country rocks which they intrude. These xenoliths are generally larger, angular, and more abundant near the contacts and become progressively smaller and rounded towards the center of the intrusion. They occur within several meters of the contact, as in the Wallamatogus pluton, or more or less evenly distributed throughout, as in the Blue Hill pluton. Large, rotated, angular blocks of country rock near the margins of the Blue Hill, Wallamatogus, Sedgwick, and other plutons suggest that stoping was an important emplacement mechanism for intrusion of these plutons.

Contact aureoles 1-2 km wide , characterized by andalusite-cordierite + sillimanite assemblages, overprint the regional lower greenschist metamorphic assemblage (Wingard, 1961; Wones, 1976a). However, portions of contact aureoles may be complex, as in the case of the Wallamatogus pluton where part of the contact aureole is characterized by a wide zone of metasomatized hornfels, that in places is net-veined and plastically deformed. The aureole has been intruded by several generations of aplite, pegmatite and fine grained granitic dikes that often persist for several hundreds of meters from the contact of the main body of the pluton.

Subsurface Distribution. Gravity modeling over the Wallamatogus and Blue Hill pluton characterizes these intrusions as thin (~2 km) tabular sheets with gentle outward-dipping contacts (Sweeney, 1976). The Waldoboro pluton, a possible type II intrusion southwest of Penobscot Bay, is also modeled as a thin, 1.6 km or less, gently dipping sill (Hodge et al., 1982). This style of emplacement may be characteristic of some type IIa intrusions, but gravity and seismic data indicate steep to nearly vertical contacts and ~ 6.0 to 7.0 km thickness for the Sedgwick pluton (Stewart et al., 1986), demonstrating that more than one style of emplacement has been adopted by type IIa plutons.

Textural Variation. It is likely that the majority of type IIa plutons are texturally inhomogeneous as detailed mapping generally reveals that they can be subdivided into distinct facies based on textural and mineralogical changes. Several plutons exhibit narrow, discontinuous, and texturally variable border phases that are generally finer grained and may have formed as the result of quenching during intrusion (Chapman, 1968; Karner, 1968). However, the reverse is also true as in the Wallamatogus pluton where the marginal facies is generally coarse grained and in places characterized by megacrystic alkali-feldspar phenocrysts which decrease in abundance towards the center of the pluton (Hogan, in prep.). The granite progressively grades through a seriate and then porphyritic zone to a fine grained approximately equigranular interior. Intrusive contacts between these facies have not been observed. The Somesville pluton shows similar textural variation from a coarse grained facies through a subporphyritic facies to a generally finer grained equigranular core (Chapman, 1974).

In contrast, textural facies in the Blue Hill pluton have sharp intrusive internal contacts as well as gradational boundaries. At least seven textural varieties exist, which range in size from several square kilometers to discontinuous zones and pods at the outcrop scale. Unlike the approximate concentric zonation of the Wallamatogus pluton, they are asymmetrically distributed. Grain size and color variations are also present in the neighboring Sedgwick pluton and have been reported for the Long Island pluton (Wingard, 1961) as well as the Indian Lake pluton (Westerman, 1972), although the areal extent and distribution of these facies is unknown.

The abundance of aplite and pegmatite dikes varies in type IIa plutons. Dikes as well as irregular pegmatitic pods are common in the Blue Hill pluton. In this and the Sedgwick pluton, aplite and pegmatite dikes appear to be asymmetrically distributed and are more common along the southeastern margins. In contrast with its contact zone, aplite or pegmatite dikes are uncommon within the interior of the Wallamatogus pluton. Miarolitic cavities have also been observed in several of these plutons, and together with the abundance of aplites and pegmatites, they indicate that these plutons crystallized from magmas that were near vapor saturation for a portion of their crystallization history.

Modal Analysis and Mineralogy. The peraluminous nature of type IIa plutons is reflected in their minor and accessory mineralogy by the presence of aluminous biotite, ± muscovite, ± garnet, and ± tourmaline. Type IIa plutons which contain biotite as the dominant accessory phase, such as the Somesville, Sedgwick, and Blue Hill plutons, are compositionally restricted and plot in the center of the granite field (Fig. 5). The color index of these plutons is generally less than 10%, and the absence of a systematic variation with quartz, alkali-feldspar, or plagioclase emphasizes the mineralogically homogeneous nature of the plutons. Muscovite and biotite alternate as the dominant accessory mineral in various portions of the Wallamatogus pluton. Modally, the Wallamatogus pluton plots within the granite field, overlapping the biotite dominated type IIa intrusions, but with a considerably larger scatter. The noticeable decrease in color index with increasing plagioclase content in the Wallamatogus

pluton is in direct contrast to typical trends for granites and suggests the presence of feldspar cumulates. Primary muscovite and garnet have been observed in the Sedgwick and Blue Hill plutons as minor accessory phases, whereas they can be relatively common in portions of the Wallamatogus pluton. Tourmaline occurs in variable amounts as both a primary magmatic phase and with quartz as a late stage fracture filling.

Chemistry. Following the classification of Shand (1955), type IIa plutons are, in general, peraluminous to strongly peraluminous with a mean value of 1.1±0.1 for ANCK = (Al_2O_3/(CaO+Na_2O+K_2O) mol%) with a range from 1.0 to 1.3 (Fig. 3). Type IIa plutons form a well defined field in terms of their alkali content with a Na_2O/K_2O ratio slightly less than one. The low $CaO/(K_2O+Na_2O)$ ratios of type IIa plutons reflect the relatively low CaO contents of these plutons (CaO ~ 0.8±0.2 wt%). Type IIa plutons are characterized by a mean SiO_2 value of 74.7±1.1 wt% and range from 72.2 to 76.7 wt%. A positive correlation between FeO*+MgO against TiO_2 is displayed by type IIa plutons. Type IIa plutons, in general, form a well defined field at lower values of FeO*+MgO (1.9±0.4 wt%) with a narrow range in TiO_2 (0.2±0.1 wt%).

Type IIa plutons have Rb/Sr ratios > 2.0 with a range in Rb of 181 ppm to 356 ppm and a mean Sr content of 61±23 ppm (Fig. 4). K/Rb ratios of type IIa plot along the main fractionation trend for granitic magmas as discussed by Shaw (1968). They have a mean Rb content of 248±40 ppm and a mean K_2O content of 5.0±0.3 wt%. Type IIa plutons show a limited range in Rb/Ba and Sr/Ba ratios forming well defined fields.

Type IIb

The large volume of magma represented by the Lucerne (~625 km^2) and Deblois (~1670 km^2) plutons (Table 1) as well as their extremely coarse grained appearance, distinctive megacrystic alkali-feldspar phenocrysts, paucity of aplites and pegmatites, and metaluminous composition distinguishes these plutons from type IIa. A complete description of the petrology of the Lucerne pluton is given by Wones (1980a). It represents the type example for type IIb plutons.

Contact Relationships. In contrast to the common subcircular stocks of type IIa plutons, the Lucerne and Deblois granites form large elongated batholiths that intrude several lithotectonic terranes. Several of the faults associated with the terrane boundaries do not offset the contacts of these plutons, nor can any deformation be associated with the trace of these fault zones through the plutons. However, movement associated with the Norumbega fault zone truncates and/or offsets the northern contacts of both these plutons (Loiselle and Wones, 1979a; Wones, 1980a). Although the majority of the Lucerne pluton has been reported as being massive, ductile deformation zones within the granite produce mylonitic fabrics that parallel the intrusive western contact (Wones, 1980a).

Contacts of the Lucerne pluton with the country rock are sharp and, in general, the granite retains its megacrystic texture up to the contact, although in some instances a slight reduction in phenocryst size within 2-3 cm of the contact has been observed. A similar chill zone, less than a meter wide, has been

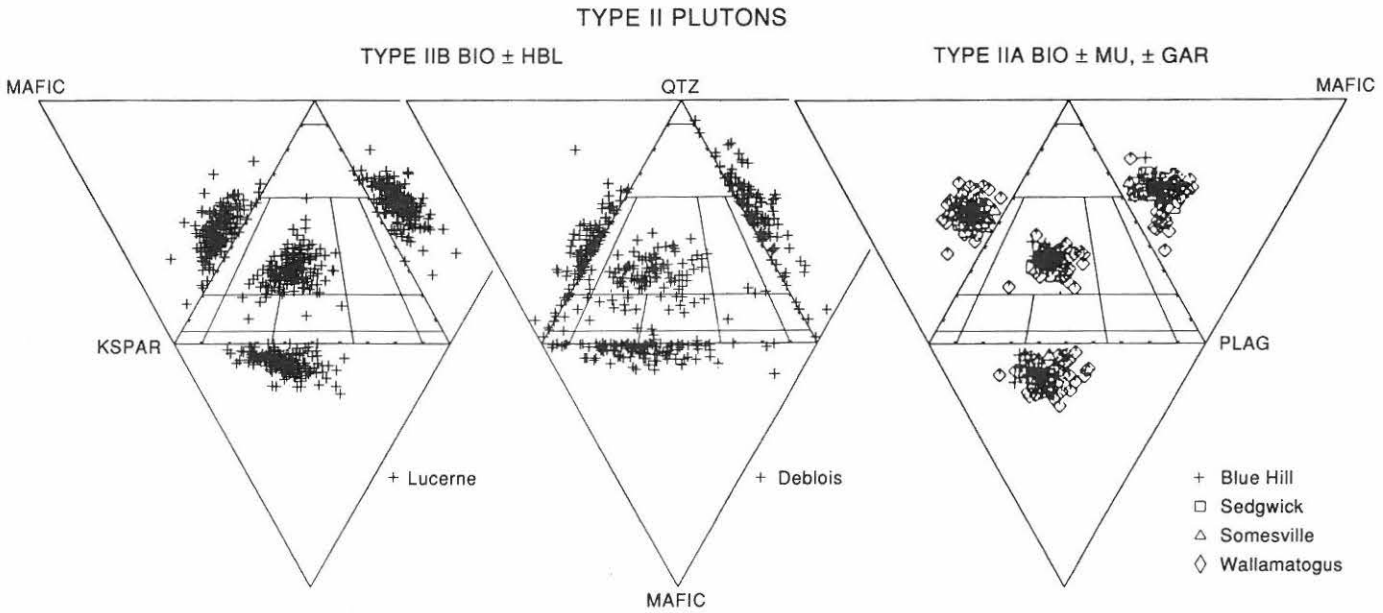

Figure 5. Modal analysis of selected type II plutons from the coastal Maine magmatic province. Data compiled from Wones (1980a), Wones (unpubl. data), Carl et al. (1984), Carl (pers. commun., 1986), and Hogan and Sinha (unpubl. data). Field boundaries are from Streckeisen (1976).

reported for the Deblois pluton (Gilman, 1961). Xenoliths of country rock occur within a few meters of the contact of the Lucerne pluton (Wones, 1980a), but enclaves commonly occur in swarms in the interior of the pluton. Roof pendants are present in both the Lucerne and Deblois plutons (Wones, 1980a; Loiselle and Wones, 1979a). Dikes of the Lucerne granite emanating from the pluton are rare and, when present, generally occur within several tens of meters of the contact.

Metamorphic effects of the Lucerne pluton persist for up to 1.0 km from the contact and overprint the lower greenschist facies assemblages (Novak, 1979). Calcareous country rocks near the contact contain tremolite-diopside-zoisite±wollastonite assemblages, and pelitic rocks are characterised by andalusite and corundum (Novak, 1979).

Subsurface Distribution. Gravity modeling of the subsurface distribution of these plutons indicates inwardly dipping contacts for the Deblois pluton, and straight, steep contacts for the Lucerne granite (Hodge et al., 1982). Apparently, upon reaching higher levels in the crust, the Deblois pluton spread out laterally, while the presence of a system of steeply dipping N30°E faults strongly influenced the shape of the Lucerne magma chamber. The Lead Mountain facies of the Deblois pluton is estimated to be a maximum of 12.5 km thick while the average thickness of the Lucerne granite is ~6.5 km, with zones thicker than 7.0 km showing a strong linear trend parallel to N30°E (Hodge et al., 1982). These two plutons together represent the most substantial contribution of felsic magma to the upper crust in the coastal Maine magmatic province.

Textural Variation. The bulk of the Lucerne pluton is a texturally homogeneous, coarse grained, seriate granite (Wones, 1980a). A central medium grained porphyritic core facies with 1-3 cm wide miarolitic cavities represents approximately 10% of the intrusion (Loiselle and Ayuso, 1980). This porphyritic variety has been observed in one place adjacent to the margin and exhibits gradational contacts with the seriate facies (Wones, 1980a).

Textural variations are present in the Deblois pluton, but little information is available about their extent and distribution. The Deblois pluton, previously considered as two separate intrusions -- the Lead Mountain granite to the west and Cranberry Lakes granite to the east -- may be a single coherent intrusion (Wones, 1984; Loiselle and Wones, 1979a). The Lead Mountain facies is generally coarser grained and shows less textural variability than the Cranberry Lakes facies which can vary from medium to coarse grained and porphyritic to equigranular (Gilman, 1961). Feldspars in a rapakivi relationship are more abundant in the Lead Mountain facies than in the Cranberry Lakes facies (Karner, 1962) and are similar to those in the Lucerne granite (Wones, 1980a). Aplite dikes and pegmatites are rare in both the Lucerne (Wones, 1980a) and Deblois (Gilman, 1961) plutons, indicative of the low volatile contents of these melts (Andrews et al., 1983).

Modal Analysis and Mineralogy. In general, type IIb plutons show greater variability in the relative percentages of quartz, alkali-feldspar, plagioclase, and mafic minerals than type IIa intrusions (Fig. 5). The majority of rock types in the Lucerne pluton and both facies of the Deblois pluton are granite. The dominant mafic phase in type IIb plutons is biotite with variable amounts of hornblende. This accessory mineralogy reflects the weakly peraluminous to dominantly metaluminous nature of these magmas.

In comparison to the well-studied Lucerne pluton, limited information is available for the Deblois pluton. The color index for the Deblois pluton is considerably lower than that of the Lucerne pluton and type IIa plutons. The Lead Mountain facies is characterized by the presence of hornblende, whereas the Cranberry Lakes facies is dominantly a biotite-granite (Loiselle and Wones, 1979a). Considerable scatter in the modal data for the pluton indicates the presence of alkali-feldspar-granite, alkali-feldspar-quartz-syenite, and quartz-syenite as well as the presence of quartz-monzonite, granodiorite, and quartz-monzodiorite (Fig. 5). It is not clear if this scatter is the result of cumulate processes, multiple intrusions, contamination, or reflects inherent properties of the magma.

Chemistry. Type IIb plutons have a mean ANCK of 1.05±0.02, with a range from 1.0 to 1.1 indicating they are metaluminous to weakly peraluminous (Fig. 3). They are slightly higher in K_2O for approximately the same Na_2O content (Loiselle and Ayuso, 1980) and have a higher mean CaO content (1.33±0.47 wt%) than type IIa plutons, whereas their mean SiO_2 content of 71.9±2.0 wt% and a range of 68.4 to 75.1 wt% is lower. Although the mean FeO*+MgO (2.7±0.8 wt%) and TiO_2 content (0.3±0.1 wt%) is higher than type IIa plutons, they also exhibit a positive correlation between FeO*+MgO and TiO_2 contents.

Type IIb plutons possess a larger range in Rb content (213 to 473 ppm) and slightly greater mean Sr content (87.85±36.25 ppm) than type IIa (Fig. 4). Type IIb plutons, as characterized by the Lucerne pluton, also have a higher mean Rb (322.00±68.52 ppm) and mean K_2O (5.55±0.30 wt%) content and have lower K/Rb ratios than the main K/Rb fractionation trend for granites as discussed by Shaw (1968). Rb/Ba plots distinguish between type IIa and IIb due to the Rb-enriched nature of the Lucerne pluton. However, type IIa and IIb plutons are indistinguishable from each other in a plot of Sr vs. Ba where they define a tight cluster with relatively low values of Sr and Ba in comparison with other granitoids in the coastal Maine magmatic province.

TYPE III PLUTONS

Type III granitic plutons are identified through field evidence which indicates possible involvement with a mafic magma at some time during the course of crystallization. The presence of mafic enclaves, mafic enclave swarms, crosscutting mafic dikes, the occurrence of composite dikes (dikes consisting of a mixture of mafic enclaves within a felsic matrix), or the existence of a gradational contact defined by a large compositional gradient within a short distance towards an adjacent gab-

broic pluton are the characteristics used to recognize type III plutons.

Type III plutons are represented by granite, granodiorite, alkali-feldspar granite, and quartz monzonite of diverse accessory mineralogy. Examples of hornblende-biotite, biotite, biotite-muscovite, biotite-muscovite-garnet, and alkali-feldspar dominated aegirine-augite-hornblende granitoid plutons exist. This wide variety is not really surprising as a somewhat similar diversity in accessory mineralogy is present in type IIa and IIb plutons. Type III plutons are potentially examples of type II partial melts that have been modified by interaction with a mafic magma.

Contact Relationships

In the coastal Maine magmatic province, type III plutons can occur as individual plutons, although they are more commonly represented by an assemblage of spatially and possibly temporally associated mafic and felsic magmas that have coalesced as a result of multiple intrusion. This collection of plutons will be referred to as an igneous complex, and it can consist of a variety of pluton types as defined in this paper. Igneous complexes represent an intrusive style that is a common characteristic of the coastal Maine magmatic province. Examples of these complexes include the Mount Desert Igneous Complex (Chapman, 1970, 1974), the South Penobscot Igneous Suite (Stewart et al., 1988), the Isle Au Haut Igneous Complex (Luce, 1962), as well as the Moosehorn Igneous Complex (Jurinski, 1987; Hill and Abbott, this volume).

Contacts with Gabbroic Plutons

The Baring granite, a seriate biotite-granite of the Moosehorn Igneous Complex, is in intrusive contact with the layered gabbro of the Staples Mountain pluton as well as the Calais gabbro-diorite (Jurinski, 1987). Contacts between gabbro and granite have been described as intrusive breccias with angular xenoliths of gabbro in a granitic matrix, as well as gradational, from gabbro to granite, with intervening zones of diorite and granodiorite (Amos, 1963; Coughlin, 1986; Jurinski, 1987). Within the contact zone, the modal mineralogy of the Baring granite exhibits progressive and variable changes towards granodiorite compositions while the gabbro changes progressively towards hornblende-quartz-gabbro and diorite (Coughlin, 1986).

Mafic Enclaves

Within the Baring pluton, removed from the gabbro-granite contacts, local zones with a high density of mafic enclaves are common and are similar to other type III plutons in close spatial association with gabbroic intrusions. Mafic enclaves are irregularly distributed throughout the Spruce Head pluton and in places comprise several percent of the rock mass (Chayes, 1952). An intervening contact zone of coarse grained, hornblende-diorite to granodiorite exists between the biotite-muscovite Spruce Head pluton (Fig. 1) and an adjacent hornblende-gabbro (Guidotti, 1979).

Mafic enclaves are also common in individual granitoid plutons isolated from known and mappable contacts with mafic intrusions. Mafic enclaves are a common occurrence in the Oak Point phase of the Deer Isle pluton (Stewart, 1956; Wones, 1976a). Enclaves range in size from tens of centimeters to a meter and generally have irregular cuspate margins. The mineralogy of these mafic enclaves consist of hornblende, plagioclase (An_{22-27}), biotite, quartz, sphene, apatite ± epidote, and ore and are modally very similar to mafic enclaves of the composite dikes which intrude the Oak Point granite (Stewart, 1956). Feldspars in rapakivi relationship are a common occurrence in the Oak Point granite and can also be found within the mafic enclaves, which in some cases host pods of finer-grained granite mineralogically similar to the enclosing Oak Point granite.

Mafic enclaves in the Tunk Lake pluton are usually gabbro-diorite with medium to coarse grained interiors and fine grained margins, although enclaves with no distinguishable interior are also present (Karner, 1974). Mafic enclaves tend to be concentrated towards the marginal zones of the Tunk Lake pluton (Karner, 1974), whereas in the Mount Waldo granite they occur throughout the pluton as finer grained suboval clots which are mineralogically similar to the granite, but with a higher color index (Trefethen, 1944). Alkali-feldspar has also been observed within these enclaves.

Mafic and Bimodal Dikes

Several episodes of basaltic dike emplacement (from pre-regional metamorphic to Late Triassic) have been established for part of the coastal Maine magmatic province (Wingard and Brookins, 1964). A detailed study of the relative ages of basaltic dikes on Mount Desert Island documented at least one set concurrent with intrusion of the Cadillac Mountain granite (Chapman and Wingard, 1958). Type III plutons such as the Deer Isle, Mount Waldo, Tunk Lake, Gouldsboro, Sullivan, and Cadillac Mountain plutons are commonly cut by quartz-diorite dikes and basaltic dikes as well as Mesozoic alkalic mafic dikes (Stewart, 1956; Trefethen, 1944; Karner, 1968; Chapman and Wingard, 1958).

Composite dikes, consisting of mafic enclaves in a felsic granitoid matrix, intrude layered gabbro of the Mount Desert Igneous Complex (Chapman, 1962a). Mafic enclaves within the dikes have cuspate margins and often exhibit pillow lava type structures. Typically, the mafic enclaves consist of a coarse grained interior encased in a fine grained shell. These textures may represent chill zones formed during quenching of the mafic magma (Wager and Bailey, 1953). Within the enclaves, plagioclase exhibits swallowtail or H-shaped skeletal morphologies, and alkali-feldspar xenocrysts are rimmed by

plagioclase overgrowths (Chapman, 1962a). These textures can be attributed to a magma mixing origin (Hibbard, 1981). A major element and REE study of these composite dikes suggested that commingling of mafic and felsic magmas best explained their origin (Taylor et al., 1980). Although these dikes occur within the gabbro of the Mount Desert Igneous Complex, similar composite dikes intrude the Oak Point phase of the Deer Isle pluton (Stewart, 1956).

Subsurface Distribution

Information concerning shapes and sizes of plutons and the possible presence of large bodies of mafic rocks at depth, beneath type III plutons, can be inferred from geophysical data. Seismic profiles across the Deer Isle pluton reveal steeply dipping sides and a possible floor at ~6.0 km depth (Stewart et al., 1986). Modeling of gravity data also indicated a maximum thickness of ~6.0 km, but suggested that the pluton's sides dip gently, forming a bowl-shaped intrusion (Hodge et al., 1982). Gravity measurements over the Deer Isle pluton preclude the presence of substantial mafic rocks at depth; however, both the Cadillac Mountain granite (2.5 km thick) and the Gouldsboro pluton (0.8 km thick) may be represented as thin sheets which lie structurally above a gently dipping, flat-bottomed, ~3.0 to 5.5 km thick mafic sill (Hodge et al., 1982).

Textural Variations

Type III plutons exhibit a similar range in textural variability as type II plutons. Texturally homogeneous type III plutons, such as the medium grained, hypidiomorphic-granular Sullivan pluton (Karner, 1962, 1968), are less common than the general case in which several textural varieties are recognized within a single pluton. For example, the majority of the Mount Waldo pluton is coarse grained, equigranular to seriate, but subporphyritic. Medium to fine grained varieties do occur, although their spatial distribution is not well mapped (Trefethen, 1944; Sweeney, 1972; King, 1977). Detailed mapping of the Tunk Lake pluton documented a systematic increase in the textural variability towards the core of the pluton (Karner, 1968). Coarse grained granites of the Tunk Lake pluton are hypidiomorphic-granular, seriate-porphyritic, subporphyritic, or porphyritic with gradational contacts. Fine grained and aplitic varieties, ranging in form from irregular sheet-like masses to dikes, as well as miarolitic cavities and granophyric textures are more common in the center of the intrusion (Karner, 1962, 1968).

Modal Analysis and Mineralogy

Type III plutons are characterized by a wide variety of granitoids with a diverse accessory mineralogy. Alkali-feldspar-granite and quartz-alkali-feldspar-syenite crop out in the type III Tunk Lake and Cadillac Mountain plutons (Fig. 6). Although limited modal data is available for the Cadillac Mountain granite, the distribution of various rock types in the Tunk Lake pluton is well documented (Karner, 1962, 1968). Like the type IIb Deblois pluton, the Tunk Lake granite varies in rock type from granite to alkali-feldspar-granite and quartz-alkali-feldspar-syenite. The color index for all three plutons is uniformly low.

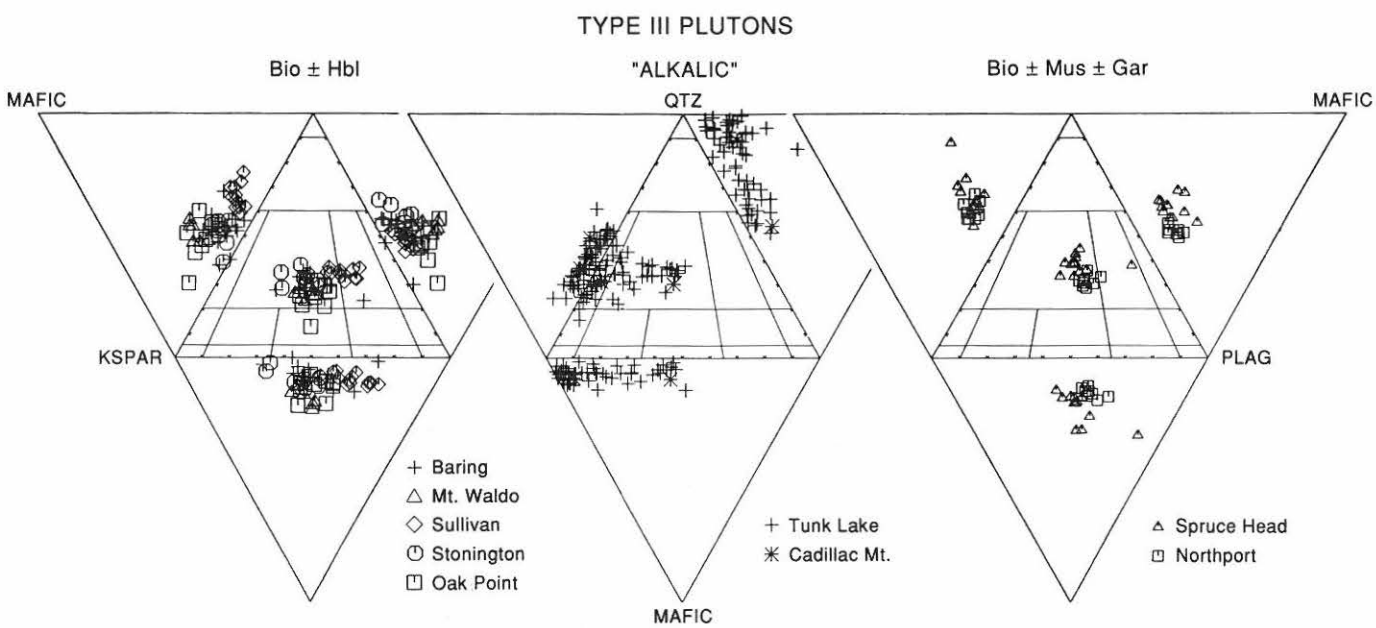

Figure 6. Modal analysis of selected type III plutons from the coastal Maine magmatic province. Data compiled from Carl et al. (1984), Carl (pers. commun., 1986), Chayes (1952), Jurinski (pers. commun., 1986), Karner (1968), Stewart (1956), and Hogan and Sinha (unpubl. data). Field boundaries from Streckeisen (1976).

The dominant mafic phase in the Cadillac Mountain pluton is hornblende; biotite is rare (Chapman, 1974).

Mineralogically distinct facies, as characterized by their mafic mineral assemblage, are concentrically arranged within the Tunk Lake pluton (Karner, 1968). The marginal assemblage consists of aegirine-augite, fayalite, and magnetite. These phases are progressively replaced inward by hornblende with minor amounts of riebeckite, then hornblende and biotite, and finally biotite alone as the dominant mafic phase. Alkali-feldspar-granite and its distinctive accessory mineralogy is restricted to within a few kilometers of the margin, whereas the bulk of the pluton is biotite-granite.

In contrast to the similarities that exist between the type III (Cadillac Mountain and Tunk Lake) and IIb (Deblois) plutons that have alkaline affinities, systematic differences do exist in the modal and accessory mineralogy between other type III plutons (Fig. 6) and their type II counterparts (Fig. 5). In general, type III plutons appear to have a higher color index than type II plutons. Type III biotite-muscovite + garnet plutons, such as the Northport and Spruce Head plutons, are more granodioritic in contrast to the biotite-muscovite + garnet type IIa plutons which plot in the granite field. Similarly, the dominantly biotite-bearing Sullivan pluton straddles the granite-granodiorite boundary in contrast with the type IIa biotite-granite of the Sedgwick pluton. Type III plutons where hornblende is present as an accessory phase in addition to biotite (e.g. the Oak Point phase of the Deer Isle pluton or the Mount Waldo granite) are modally lower in quartz and higher in plagioclase than the type IIb Lucerne pluton. Although the bulk of the Sullivan and Baring plutons is biotite-granite and the Spruce Head pluton a biotite-muscovite-granite, hornblende has been reported to occur in all three plutons (Karner, 1968; Jurinski, 1987; Chayes, 1952). The presence of hornblende in the Spruce Head pluton is spatially associated with the gradational gabbro-granite contact (Chayes, 1952) and is likely to be xenocrystic. The presence of hornblende in type IIb intrusions may reflect an intrinsic characteristic of the source region, whereas the hornblende in type III magmas may have a more complex origin and could be directly related to a mixing event or reflect an intrinsic characteristic of the source region, or both.

Chemistry

Type III plutons exhibit a greater diversity in chemistry than both suites of type II plutons (Figs. 3 and 4). Type III plutons range from approximately subaluminous, ANK=1.02, where ANK = ($Al_2O_3/(Na_2O+K_2O)$), to strongly peraluminous, ANCK=1.26. The mean SiO_2 content for type III plutons is 72.56±1.78 wt% with a large range from 67.24 to 76.02 wt%. Type III plutons have a higher mean CaO content, 1.31±0.54 wt%, and a range of 0.34-2.62 wt% with slightly lower K_2O contents for approximately the same Na_2O contents as type II plutons. The majority of high Na_2O values (>4.00 at $K_2O \sim 4.0$) for type III plutons are from the hypersolvus Cadillac Mountain granite. The Cadillac Mountain granite is an exception in that Na_2O/K_2O is greater than one (Carl et al., 1984), as is also true for one sample from the type IIb Deblois pluton. Type III plutons exhibit a large range in TiO_2 (0.08-0.78 wt%) and FeO*+MgO (1.33-6.01 wt%), with a positive correlation between FeO*+MgO and TiO_2 contents.

Type III plutons define a broad field in Rb vs. Sr plots with Rb/Sr ratios that are generally <2.0 (Fig. 4). The K/Rb ratios of type III plutons plot close to the main fractionation trend for granitic magmas (Shaw, 1968). However, they form two groups, one overlapping with type IIa plutons while the second group is characterized by higher K/Rb ratios than the main trend and lower mean Rb (139.33±64.27 ppm) and K_2O (4.23±0.60 wt%) contents. Type III plutons also form a broad field in the Sr vs Ba plots. The low Sr, high Ba analyses are from the hornblende-alkali-feldspar Cadillac Mountain granite. The other type III granites have significantly higher Sr concentrations and a large range in Ba and Sr content. Rb and Ba contents of most type III plutons form a well defined field with lower Rb and higher Ba content than type II plutons.

TYPE IV PLUTONS

Type IV plutons are mafic magma(s) that have interacted to varying degrees with felsic magma(s). They are characterized by quartz-monzodiorite, monzogabbro, monzonite, quartz-diorite, quartz-gabbro, and the mafic granitoids of the Parks Pond pluton. Type IV plutons can occur as isolated plutons as in the case of the Parks Pond pluton (Cavalero, 1965; Wones, 1976a, 1980a; Eriksson and Williams, in press), or more commonly they are associated with igneous complexes, such as the Moosehorn Igneous Complex (Jurinski, 1987; Hill and Abbott, this volume) or the South Penobscot Intrusive Suite (Stewart et al., 1988), as intervening zones of texturally variable hybrid rocks at the contact of gabbroic and granitoid rocks.

Contact Relationships

The Moosehorn Igneous Complex is comprised of an intimate association of plutons ranging from gabbro to granite near Calais, Maine (Amos, 1963; Jurinski, 1987) and may extend southwest to include granite plutons and gabbroic rocks associated with the Gardner Lake gabbro-diorite of Gilman (1961) and Westerman (1980). Isolated, discrete, irregularly shaped areas of layered and massive gabbronorite which crop out throughout the central portion of the Moosehorn Igneous Complex are similar to rock types cropping out at Staples Mountain (Amos, 1963). Complex contact relationships have been observed between isolated layered mafic gabbro and felsic rocks in the central portion of the Moosehorn Igneous Complex (Jurinski, 1987; Hill and Abbott, this volume). Mafic rocks in this zone are surrounded by progressively more felsic rock types. Contact relationships exhibit a regular gradation from gabbronorite through microcline-hornblende-gabbro to hornblende-

diorite and granodiorite (Amos, 1963). Hybrid rocks range from brecciated gabbro to gabbroic enclaves and diabase pillows in a dioritic-granodioritic matrix to granodiorite with sporadic enclaves of gabbro and can occur either as a border phase on the granodiorite or as isolated patches in the gabbro (Hill and Abbott, this volume). Bimodal composite dikes of diabase pillows in a granodioritic matrix crosscut the gabbroic rocks (Hill and Abbott, this volume). A similar relationship occurs in the South Penobscot Intrusive Suite where granitic magma of the central core comes in contact with the mafic rocks of the border zone, resulting in the development of hybrid intermediate rocks with numerous mafic enclaves (Stewart et al., 1988). In general, for the South Penobscot Intrusive Suite the transition from mafic gabbroic rocks at the margin to granitic rocks in the core is gradational (Stewart et al., 1988). The occurrence of several intermediate rock types associated with contact breccias in the igneous complexes has been attributed to both reaction of gabbroic rocks with the infiltrating Baring granite (Coughlin, 1986; Jurinski, 1987) or to magma mixing (Stewart et al., 1988; Hill and Abbott, this volume).

The Parks Pond pluton, an example of an isolated type IV pluton, is intruded by the Lucerne granite and itself intrudes the Bucksport Formation (Cavalero, 1965; Wones, 1976a, 1980a; Eriksson and Willaims, in press). Along the contact of the Parks Pond pluton, the Bucksport Formation has been partially melted (Russell and Wones, 1984; Russell, 1984). The northern contact of the pluton is truncated by the Norumbega fault zone (Wones, 1976a), and mylonite and fracture zones related to the Norumbega fault zone occur throughout the pluton (Eriksson and Wones, 1983). The pluton is fine to medium grained equigranular and is characterized by abundant mafic enclaves with features typical of magma mingling (Eriksson, 1985).

Subsurface Distribution

At least two different styles of intrusion for igneous complexes are suggested by geophysical modeling. Modeling of gravity data for the Gardner Lake gabbro-diorite suggests a limited thickness of gabbro (0.5 - 1.0 km) underlain by an extensive thickness (5.0 - 6.5 km) of coalescing granitic stocks (Biggi and Hodge, 1982). Modeling of gravity, magnetic, and seismic data over the South Penobscot Intrusive Suite as summarized in Stewart et al. (1988) suggests that this pluton has a steep-walled hopper shape, with mafic rocks of the border zone extending deeply below the northern and southwestern portions of the central granitic core.

Textural Variation

The mafic rocks at Staples Mountain reveal a well layered, differentiated sequence that crystallized from olivine-gabbronorite at the margins inward to a pyroxene-hornblende-gabbronorite in a manner similar to the type I Pocomoonshine pluton (Coughlin, 1986). Igneous layering consists of both phase layering and rhythmically alternating noritic and anorthositic layers (Amos, 1963; Coughlin, 1986). Other features commonly associated with stratiform mafic bodies, such as igneous lamination, cross-bedding and graded bedding have been reported, as well as a high density of cumulate olivine lenses (Coughlin, 1986). Similar layered gabbroic rocks crop out on the margin of the South Penobscot Intrusive Suite (Stewart et al., 1988). Remnants of layered gabbro associated with these igneous complexes are remarkably similar to the type I plutons.

Textures such as chill margins in mafic rocks along the contact with granite, irregular cuspate margins of felsic dikes intruding mafic rocks, and the incorporation of phenocrysts from felsic rocks into subrounded amorphous mafic enclaves suggest that two magmas of distinct composition were present at the same time. Mineral textures in the hornblende-diorite, such as embayed calcic plagioclase phenocrysts rimmed by alkali-feldspar and hornblende overgrowths on ragged remnants of clinopyroxene, (Amos, 1963) suggest that extensive interaction between granitic and gabbroic rocks may have occurred to produce this hybrid rock.

Modal Analysis and Mineralogy

Available modal data for the northern extent of the Moosehorn Igneous Complex (Amos, 1963; Abbott, 1977, 1978; Coughlin, 1986; Jurinski, 1987) reveals the compositionally expanded nature of these complexes (Fig. 7). High concentrations of samples occur within the gabbro/diorite/anorthosite field at the plagioclase apex, as well as within the granite field. Samples are scattered throughout the intermediate rock types, the quartz-bearing gabbro-diorite and monzo-gabbro-diorite, with some occurrences in the granite-granodiorite, tonalite, and quartz-monzonite fields. A similar modal distribution of rock types has been documented for the South Penobscot Intrusive Suite (Stewart et al., 1988). Type IV plutonic rocks occurring within igneous complexes are represented by these intermediate hybrid rock types.

Modal analysis of the Parks Pond pluton reveals the complex, heterogeneous nature of the body. It consists of granite, quartz-syenite, and quartz-monzonite, but has a color index that ranges from 35-66% with a large variability in the modes of mafic phenocrysts such as biotite (7-41%) and clinopyroxene (9-24%) (Eriksson and Wones, 1983).

Mineral Compositional Variation

Mineral analyses from the Staples Mountain pluton (Coughlin, 1981, 1986) exhibit a limited range of chemical variation. Olivine is iron-enriched (Fo_{55-53}) and plagioclase is normally zoned with the most calcic phenocrysts occurring in the cumulate layers (An_{70}-An_{53}) and the more sodic compositions (An_{56-53}) found in the rythmically layered norite and anorthosite in the core of the intrusion. Orthopyroxene ($En_{63.9}Fs_{34.0}Wo_{2.1}$-$En_{59.5}Fs_{38.4}Wo_{2.1}$) and clinopyroxene ($En_{42.1}Fs_{16.1}Wo_{41.8}$-

$En_{40.5}Fs_{15.4}Wo_{43.9}$) show a limited compositional range from the more mafic margin to the felsic core. Modally and mineralogically, the Staples Mountain pluton is similar to type I plutons.

In the Parks Pond pluton, orthopyroxene, clinopyroxene, and biotite crystallized early followed by plagioclase, alkali-feldspar, and quartz (Eriksson and Wones, 1983). Magnetite contains up to 7.5 wt.% Cr_2O_3 and a high temperature of intrusion (~900°C) has been calculated from the TiO_2 content of biotite (3.4-5.0 wt.%) and compositions of coexisting ortho- and clinopyroxene (Eriksson, 1985).

Chemistry

Limited chemical data is available for mafic and intermediate rock types from the Moosehorn Igneous Complex. Analyses from gabbroic rocks have a SiO_2 range of 41.04 to 52.08 wt% and a TiO_2 range of 1.02 to 4.81 wt% with a mean Fm ratio of 63.5 (Fig. 3). Analyses from the gradational contacts between the layered gabbro and granite, where hybridization of type I and II magmas is evident, are lacking. One analysis is available from the contact between the Baring granite and Staples Mountain pluton (Coughlin, 1986), and it has been plotted for comparison (Figs. 3 and 4). Limited analyses of type I and IV gabbroic plutons define a field that overlaps with the low Rb, high Sr side of type III intrusions (Fig. 4).

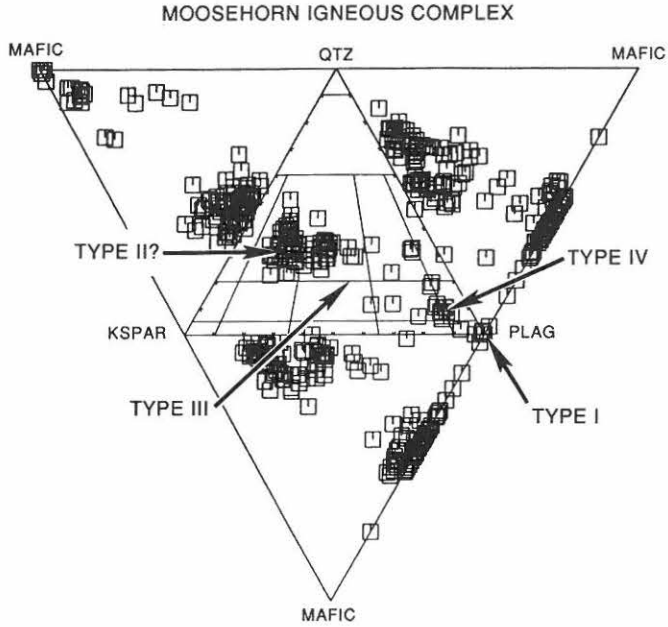

Figure 7. Modal analysis of mafic and felsic plutonic rocks associated with the Moosehorn Igneous Complex. Data compiled from Amos (1963), Abbott (1978), Coughlin (1986), and Jurinski (pers. commun., 1986). Field boundaries are those of Streckeisen (1976). Fields of rock types within the complex are similar to pluton types present in the coastal Maine magmatic province as a whole, suggesting that the processes operating in the igneous complexes may be equivalent to those which produced similar compositional variability within the coastal Maine magmatic province.

Data on mineral compositional variation within intermediate hybrid type IV plutonic rocks are scarce. Plagioclase phenocrysts exhibit a large compositional range (An_{50-28}) with calcic cores and oscillatory zoned rims (Amos, 1963). The marginal portions of plagioclase phenocrysts are commonly embayed and rimmed by alkali-feldspar, quartz, and hornblende (Amos, 1963). Alkali-feldspar occurs with quartz as coarse grained, interstitial aggregates, and the abundance of irregularly shaped alkali-feldspar phenocrysts within the microcline-hornblende-gabbro increases as contacts with granitic rocks are approached (Amos, 1963).

The anomalous nature of the Parks Pond pluton with respect to other plutons in the coastal Maine magmatic province is immediately apparent in comparitive diagrams of whole rock chemical analyses. The pluton is alkalic (Fig. 3), and with the available analyses from the coastal Maine magmatic province, is the only intermediate pluton with a SiO_2 range of 55.5-57.8 wt% (Eriksson and Wones, 1983; Eriksson, 1985). The pluton has Rb (228-319 ppm) and K_2O (5.09-6.08 wt%) contents similar to that of the felsic magmas, but is enriched in Sr (410-565 ppm) and Ba (1420-1790 ppm) and lower in mean Na_2O (1.52±0.20 wt%) than the granitic rocks (Fig. 4). Rb/Sr ratios are similar to type III intrusions and the K/Rb ratio straddles the main trend for plutonic rocks (Fig. 4). A mantle origin has been suggested for the Parks Pond magma based on the Cr-rich nature of the whole rocks (400-500 ppm) and of the magnetite compositions, up to 7.5 wt% Cr_2O_3, but an initial Sr^{87}/Sr^{86} ratio of 0.7099±.0.0012 (2 s.d.) suggests a complex magmatic history for the pluton (Eriksson, 1985).

DISCUSSION

Plutons in the coastal Maine magmatic province appear to have been intruded by a combination of dilation, doming, fracturing, and stoping of the country rocks. The mode of emplacement for many of the plutons may have been by ring dike intrusion and cauldron subsidence (Chapman, 1968). This style of intrusion, as well as the presence of contact breccias, low pressure contact aureoles superimposed on lower greenschist facies regional metamorphic assemblages, chill margins, roof pendants, and miarolitic cavities, attests to the high level, epizonal nature of these plutons. Several granites, such as the Sedgwick pluton, possibly intrude their own volcanics (Brookins et al., 1973), and the presence of granophyric textures, as described for the Red Beach pluton (Abbott, 1978), are consistent with a subvolcanic environment. Mineral composition and phase equilibria studies suggested that the majority of the Lucerne pluton crystallized at temperatures between 650°C and 700°C at 1.0 to 2.0 kb (Wones, 1980a). Such data are consistent with field observations that suggest a shallow level of emplacement for plutons of the coastal Maine magmatic province.

Several observations suggest that fractional crystallization of magmas in the coastal Maine magmatic province occurred at this shallow emplacement level. The well developed magmatic layering and orderly progression of rock types from cumulate troctolite inwards toward quartz-biotite-horndblende-diorite in type I plutons is compatible with fractional crystallization. Whole rock chemistry from the Pocomoonshine pluton supports a model in which melanocratic-gabbronorite (±olivine) and gabbronorite (±olivine) represent mafic cumulates of a water-rich, high-alumina, tholeiitic, basaltic magma that fractionated to produce hornblende-gabbro (Westerman, 1972, 1981). Type II granitic plutons are rarely texturally homogeneous. They generally consist of several rock types which become more differentiated with increasingly younger relative age. Modal variation towards the alkali-feldspar apex (Fig. 5) within the Lucerne pluton has been interpreted to reflect cumulate processes operative during crystallization of the granite, and segregations of alkali-feldspar phenocrysts on the scale of meters to tens of meters across, observed in road cuts, support this idea (Wones, 1980a). The preservation of magmatic layering, textural variability, chill margins, and cumulates in conjunction with high temperature-low pressure contact aureoles superimposed on low-grade regional metamorphic assemblages implies that these magmas were intruded, with relatively low initial phenocryst content, into shallow levels of the crust before significant fractional crystallization took place. The rapid ascent necessary for crystallization at these shallow emplacement levels may have been facilitated by fractures.

Compositional variation produced by the accumulation of varying proportions of minerals as the result of fractional crystallization can be observed in major and trace element plots (Figs. 3 and 4). In general, for the type III Mount Waldo pluton, Rb increases and Ba decreases with increasing SiO_2, defining a trend that parallels the distribution of Rb vs. Ba analyses of type II plutons. This suggests that the negative correlation between Rb and Ba observed for pluton types may reflect compositional variation within individual plutons produced by selective crystal accumulation. Similarly, the positive correlation between FeO*+MgO against TiO_2 that exists for pluton types may, in part, reflect varying modal abundances of mafic minerals such as biotite in early vs. later crystallizing textural varieties within a pluton. A negative correlation of Rb and Sr for the Lucerne pluton has previously been suggested as the result of fractional crystallization (Loiselle and Ayuso, 1980).

Comparative Chemistry of Pluton Types

Compositional variation within plutons and within pluton types may, in part, be explained by fractional crystallization. However, distinctions made between pluton types on the basis of field observations are supported by differences in several plots of major and selected trace element chemistry. For example, significant differences in the Rb/Sr ratios for plutons in the Penobscot Bay area have been previously recognized (Carl et al., 1984), and it appears that the Rb/Sr ratio of plutons is an effective discriminator between granitoid intrusive types as defined by this paper (Fig. 4). Type II plutons generally have an Rb/Sr ratio ≥2.0, whereas type III plutons are characterized by Rb/Sr ratios ≤2.0. Pluton types also define separate fields with limited overlap in plots of Rb vs. Ba and Sr vs. Ba. However, type IIa and IIb plutons commonly do not define separate fields that adequately distinguish between pluton types in several plots. Differences between types III, IIa, and IIb are more subtle in plots of Na_2O vs. K_2O, FeO*+MgO vs. TiO_2, and K_2O vs. Rb where significant overlap between pluton types can occur.

Several possibilities exist that may explain the overlap of some analyses in plots that appear for the most part to discriminate between pluton types. Type III granitoids have the largest range of Rb/Sr ratios and several type III analyses plot within the field of type II plutons (Fig. 4). One of the analyses is from the Mount Waldo granite. This sample is significantly lower in MgO, FeO*, CaO, Ba and significantly higher in SiO_2, K_2O, and MnO than the rest of the analyses of that granite, suggesting that it represents a late stage fractionate. The rest of the type III analyses which overlap the type II field are from the Red Beach pluton near Calais, Maine. The data on whole rock samples are from Spooner and Fairbairn (1970), and information on rock type or sample location within the Red Beach pluton was not reported. The Red Beach pluton is a mineralogically and texturally composite hornblende, biotite-hornblende, biotite-granite (Amos, 1963; Abbott, 1977) associated with the Moosehorn Igneous Complex. Chemical and modal variation expressed by several phases of the pluton, including spatially associated gabbro and diorite, have been interpreted to represent an igneous series formed as the result of crystal fractionation (Abbott, 1977, 1978). Whole rock strontium isotopic analyses from the Red Beach pluton (Spooner and Fairbairn, 1970) do not define an isochron. The presence of internal intrusive contacts between different phases of the Red Beach pluton (Amos, 1963; Abbott, 1977, 1978) in conjunction with the scatter in the isotopic data suggests that this may be a composite intrusion comprised of multiple magmas rather than a consanguineous fractionation suite. A second possible explanation is that the original magma has been inhomogeneously modified to varying degrees by mixing with a mafic magma. The presence of more than one magma or modification through magma mixing is suggested by the plot of Rb/Sr ratios which places samples from the Red Beach pluton in both the type II and III fields.

Several similarities between type II and type III plutons in conjunction with subtle differences in modal mineralogy and major and trace element chemistry suggest that type III plutons have been derived from similar source regions as type II plutons, but have had their original chemical characteristics modified by interaction with a mafic magma. Type III plutons with similar accessory mineralogies as type IIa or type IIb plutons have higher plagioclase to alkali-feldspar ratios and are shifted out of the granite field towards granodiorite or quartz-monzonite compositions (Figs. 5 and 6). These differences are also reflected in

major and selected trace element chemistries. Type III plutons have higher $CaO/(Na_2O+K_2O)$ ratios, lower Rb/Sr ratios, and higher concentrations of FeO^*+MgO, and TiO_2 (Figs. 3 and 4). Biotite-muscovite±garnet-bearing type III plutons also have consistently lower mean SiO_2 contents than their type IIa counterparts. These differences are compatible with the addition of small amounts of mafic magma to the crystallizing felsic pluton through processes such as magma mixing to produce the type III plutons. Modification of the original chemical composition of the felsic magma in a similar manner by magma mixing combined with fractional crystallization has been documented for the granitoid rocks of the South Penobscot Intrusive Suite (Stewart et al., 1988).

An antipathetic modal relationship between alkali-feldspar and color index is displayed, to varying degrees, by type III plutons which are also characterized by a larger range in their plagioclase/alkali-feldspar ratio than type II plutons. The Oak Point phase of the Deer Isle pluton, a hornblende-biotite-granite, has a modally higher plagioclase content and color index than the spatially associated Stonington biotite-granite. Brookins and Spooner (1970), on the basis of strontium isotopic analyses, suggested that these two phases of the Deer Isle pluton were consanguineous. The lower color index and presence of alkali-feldspar segregations, which contain minor amounts of plagioclase and quartz, suggest that a similar mechanism of fractional crystallization as proposed by Wones (1980a) for the Lucerne granite operated in the Deer Isle pluton to produce the observed compositional variability. The Oak Point phase is, however, characterized by the presence of abundant mafic enclaves which are uncommon to rare in the Stonington granite. The effects of possible mixing with a basaltic magma may be reflected by the higher plagioclase content and the presence of hornblende in the Oak Point pluton. It is likely that the observed compositional variability in this type III pluton is the result of several processes which may include fractional crystallization as well as magma mixing.

Magmatism within the Moosehorn Igneous Complex is representative of the entire coastal Maine magmatic province. Modal variation within this igneous complex can be represented as four groups which roughly correspond to the four pluton types defined for the coastal Maine magmatic province (Fig. 7). The stratiform, layered mafic sill at Staples Mountain may represent a portion of the original mafic magma which crystallized earlier near the margin of the pluton, but isolated from interaction with felsic magma. The modal mineralogy of these rocks plots at the plagioclase apex, along the plagioclase-mafic join, and at the mafic apex in the quartz-mafic-alkali-feldspar ternary system. The suggestion that the isolated occurrences of gabbroic rocks in the Moosehorn Igneous Complex, such as the Staples Mountain pluton, are remnants of a larger stratiform mafic body (similar to type I plutons) that has been disrupted by later intrusion of felsic magmas (Amos, 1963) is supported by the strong similarities in modal mineralogy and mineral and whole rock chemistry of type I plutons and gabbroic rocks from this complex. Hornblende- and biotite-hornblende granite occur as volumetrically minor facies associated with the dominantly biotite-granite plutons of the Moosehorn Igneous Complex (Amos, 1963). Within the interior of this complex, large areas of biotite-granite devoid of mafic enclaves exist (Jurinski, pers. commun., 1987). These plutons are modally very similar to type II plutons in that they are compositionally restricted and plot within the granite field. These data suggest the presence of domains of felsic magmas which crystallized in isolation from interaction with mafic magma(s). These domains may be similar to type II plutons.

The formation of hybrid rock types within these igneous complexes can then be considered as a model for the formation of type III and IV plutons within the coastal Maine magmatic province. Modal analyses of rocks from contact zones between granitic and gabbroic rocks reveal two distinct groups of modified magmas representing type III and IV plutons. Modified mafic magma or type IV plutons were formerly gabbro and now contain alkali-feldspar, quartz, and possibly biotite as the result of interaction with felsic magma to form hybrid quartz-monzodiorite, quartz-monzogabbro, quartz-gabbro, quartz-diorite, and tonalite. Type III plutons are represented by quartz-monzonite and granodiorite, which are modally higher in plagioclase and mafic minerals than the associated granite as the result of hybridization with mafic melts. This shift in quartz content and alkali-feldspar/plagioclase ratio for hybrid rock types in the Moosehorn Igneous Complex is similar to the variation observed between type II plutons and their type III counterparts.

Aspects of mafic and felsic magma interaction as a function of composition, initial crystallinity, water content, initial temperatures, and mass fraction of the end members has been examined by Frost and Mahood (1987). Their findings suggest that under most circumstances the basaltic end member quenches in the felsic magma to form enclaves and that hybridization to form magmas of intermediate composition, tonalite or mafic granodiorite, can occur only when the compositional difference is less than 10.0 wt% SiO_2 or the mass fraction of the mafic magma is greater than 0.5. Their observations potentially explain (1) the restriction of hybrid intermediate magmas to narrow, intervening zones between the contacts of gabbro and granite within igneous complexes (where the mass fraction of the mafic magma remains high), (2) the paucity of intermediate rock types at a regional scale within the coastal Maine magmatic province, and (3) the presence of mafic enclaves as the dominant field evidence that type III plutons may have interacted with a limited amount of mafic magma.

Intrusive Style in the Coastal Maine Magmatic Province

Contacts of plutons are generally sharp and discordant, and crosscut the regional fabric and folds (Fig. 1). Several large plutons intrude major fault zones that juxtapose distinct lithologies without significant offset along their contacts (Fig.

1). However, prominent faults also crosscut and/or truncate contacts of some plutons (Wallamatogus, Great Wass Island, Lucerne, Deblois, South Penobscot Intrusive Suite), and many plutons show evidence of localized post-emplacement deformation related to faulting (Wones, 1980a; Ludman, 1981b; Loiselle and Wones, 1979a; Stewart et al., 1988). The majority of plutons in the coastal Maine magmatic province, with the exception of a few small intrusions in the Passagassawakeag terrane, are considered to be post-tectonic, post-regional metamorphic, and to have intruded after assembly of the various lithotectonic terranes.

In general, smaller plutons such as Vinalhaven, Long Island, and Great Wass Island tend to be roughly circular or elliptical in shape. Larger intrusions such as the Lucerne and Deblois plutons are angular, elongated batholiths that often transect several lithotectonic terranes (Fig. 1). The bases of plutons in the Penobscot Bay area, as determined by geophysical methods, occur at depths of six to ten kilometers, entirely within the Paleozoic cover sequence (Hodge et al., 1982; Stewart et al., 1985, 1986). It is suggested, based on this observation, that granitic magmas have spread out laterally into their present shape only after the magma reached the upper crustal lithologies above the underlying Precambrian(?) basement rocks (Stewart et al., 1986).

Fault-controlled emplacement has been suggested for both felsic and mafic plutons (Chapman, 1968; Sweeney, 1976; Biggi and Hodge, 1982; Hodge et al., 1982). Gravity modeling over several plutons indicates a strong spatial correlation between the projected location of prominent faults and the subsurface distribution of the majority of the mass of these plutons (Hodge et al., 1982). These data strongly suggest that preexisting faults may have controlled the location and shape of many of the intrusions in the coastal Maine magmatic province (Biggi and Hodge, 1982; Hodge et al., 1982; Sweeney, 1976). The intrusion of elliptical stocks in eastern coastal Maine may have occurred at the intersection of two sets of steep crustal fracture zones (Chapman, 1968). While plutons appear to be related to the regional structure in that they are intruded along fault zones, observed faults do not necessarily correspond with Chapman's (1968) proposed grids (Wones, 1976a).

Pluton Emplacement within a Transcurrent Fault Zone

It is likely that the orientation and shape of some intrusions within the coastal Maine magmatic province are controlled by the presence of a preexisting fault system. Juxtaposition of lithotectonic terranes along prominent N60°E fault boundaries (e.g. Turtle Head fault zone) as well as apparent dextral offset of these linear belts along N20-30°E faults can be seen in several places along the strike of the Penobscot-Cookson terrane (Fig. 1) and must have occurred prior to emplacement of plutons such as the Mount Waldo, Lucerne, Deblois, and Pocomoonshine. The long axes of the Lucerne pluton, the Lead Mountain and Cranberry Lakes facies of the Deblois pluton, and the Pocomoonshine pluton are at high angles to the regional strike of the major fault systems and the lithotectonic terranes. The axes of these batholiths coincide with the N20-30°E fault system that links several of the major N60°E-trending dextral fault zones of eastern coastal Maine.

Depending on the relative geometry and movement of associated transcurrent fault zones, intervening regions can be areas of extension or compression and are referred to as either transtensional or transpressional fault zones (Aydin and Page, 1984). Relative motions along major N60°E fault zones within the coastal Maine magmatic province (Norumbega fault zone, Turtle Head fault zone, Lubec fault zone, Fig. 1) indicate that this area was a region of dextral shear (Stewart, 1974; Wones and Stewart, 1976; Johnson and Wones, 1984; Ludman, 1986). An en-echelon system of dextral shear zones with sinistral step-over geometry, which appears to be the case for eastern coastal Maine, can be characterized by high-angle reverse faults within the shear zone (Aydin and Page, 1984). Such high-angle reverse faults are present within the N20-30°E fault system that coincides with Penobscot Bay (Osberg et al., 1985), suggesting that these faults may have formed as a part of the dextral shear zone which is so prominent in this area. The geometry of step-over faults within this dextral shear zone is compatible with a transpressional regime. The orientation of the larger batholiths coincides with the N20-N30°E step-over fault system, suggesting that these large plutons exploited the existence of this fault system and intruded after initiation of this transpressional tectonic regime.

Tectonic Setting of the Coastal Maine Magmatic Province

Unique assemblages of Mesozoic and Cenozoic plutonic rocks have been correlated with specific tectonic settings; this correlation has been found to extend to Paleozoic rocks as well (Pitcher, 1982). Plutonic rocks from different tectonic settings have been characterized by their mineralogy, mode, aluminum saturation index, enclave types, duration of plutonism, and intrusive style. Similarly, a series of mineralogical and chemical criteria have been used to successfully distinguish between Mesozoic and Cenozoic plutonic rocks generated at compressional vs. extensional plate boundaries (Martin and Piniwinskii, 1972; Petro et al., 1979). Compositional intrusive sequences are also characteristic of tectonic setting. Repetitive intrusion of the compositional series ±gabbro, quartz diorite, tonalite, granodiorite, and granite that is characteristic of plutonic arcs, has been attributed to constant replenishment of similar source material to the site of melting by subduction processes (Bateman et al., 1963; Bateman, 1983). Incremental melting of a static source region to first produce low-temperature, hydrous, peraluminous magmas followed by higher temperature, drier, metaluminous magmas and finally by high-temperature, anhydrous peralkaline plutons (Brown and Fyfe, 1970) is more compatible with a rift related tectonic setting where underplating of mantle-derived magmas can provide the heat to melt the overlying source region (Wones and Sinha, 1988). In magmatic

provinces where the tectonic setting is poorly known, characterization of plutonic rocks in terms of physical, petrographic, and chemical characteristics, as well as intrusive sequences, can be used to develop tectonic models compatible with the associated plutonism (Wones, 1980b). Using this approach, we will attempt to identify tectonic settings and develop a model for magma genesis consistent with mineralogical and chemical characteristics and intrusive style of plutonism in the coastal Maine magmatic province.

Type I plutons have mineral and chemical characteristics suggestive of crystallization from magmas with affinities transitional between alkalic and tholeiitic basalts. Chemical analyses of mafic rocks, including samples associated with the igneous complexes (Fig. 3), straddle the alkalic/tholeiitic boundary as proposed by Macdonald and Katsura (1964). They are suggestive of having been in equilibrium with magmas that had dominantly high alumina to alkalic affinities as proposed by Kuno (1966). Nepheline and quartz normative samples are present in the Pocomoonshine pluton (Westerman, pers. commun., 1985) although primary minerals, indicative of a strongly alkalic nature such as nepheline or alkali-feldspar, have not been reported from type I plutons (Bickford, 1963; Westerman, 1972). In the AFM ternary diagram (Fig. 3), type IV plutons appear to be iron- and alkali-enriched with respect to type I plutons. However, the two groups do overlap and together they display an overall minor alkali- and iron-enrichment trend. The type IV Parks Pond pluton plots alone in the alkalic field of the AFM ternary diagram, reinforcing its unique character with respect to plutonism in the coastal Maine magmatic province.

Peraluminous and metaluminous granitoid plutons can occur in both compressional and extensional tectonic environments, however, peralkaline compositions appear to be restricted to regions of extension (Petro et al., 1979). The high alumina to alkali, type II granitoid plutons of the coastal Maine magmatic province can be subdivided into at least two suites, each characterized by its own chemical and mineralogical signature. The high silica, weak to strongly peraluminous, type IIa plutons are characterized by aluminous biotite, ±muscovite, ±garnet. The lower silica, higher CaO contents and metaluminous to weakly peraluminous nature of type IIb plutons is reflected by the presence of aluminous biotite ±hornblende. Both suites of type II plutons are modally dominated by monzogranite. However, the type IIb Deblois pluton also contains alkali-feldspar granite (Fig. 5). The Deblois pluton has been inferred to have crystallized from a relatively anhydrous magma with an intrinsically low oxygen fugacity, suggestive of potential affinity with granite generated in anorogenic settings (Andrews et al., 1983; Loiselle and Wones, 1979a, 1979b; Loiselle et al., 1983; Collins et al., 1982). Hypersolvus, aegirine-augite, riebeckite, alkali-feldspar granite of alkaline affinity is represented in the coastal Maine magmatic province by the type III Tunk Lake and Cadillac Mountain plutons (Fig. 6).

The calc-alkaline index (the value of SiO_2 where $CaO/(Na_2O+K_2O)=1$), a variation of the Peacock Index (Peacock, 1931), has been successful in discriminating between extensional and compressional tectonic settings for igneous provinces (Petro et al., 1979). The calc-alkaline index for the coastal Maine magmatic province falls in the alkali-calcic range (51-56% SiO_2), and although displaying considerable scatter at low silica values (Fig. 3), it is comparable to plutonic rock suites generated in extensional tectonic settings.

Plutonism in the coastal Maine magmatic province is best described as being bimodal. The paucity of intermediate plutonic rocks in these analyses from the coastal Maine magmatic province is clearly demonstrated in the plots of K_2O+Na_2O vs. SiO_2 and CaO/K_2O+Na_2O vs. SiO_2 (Fig. 3). The dominant plutonic rock types in the coastal Maine magmatic province consist of high-alumina to alkali gabbro and granite with the intermediate SiO_2 compositions restricted to the type IV Parks Pond pluton and some hybrid plutonic rocks cropping out within the igneous complexes. The bimodal nature of the province is again emphasized in the AFM ternary diagram (Fig. 3) where gabbroic rocks define an iron enrichment trend in contrast to the granitoids which plot along the iron-alkali join. Available intermediate rock analyses are again restricted to the alkalic Parks Pond pluton. The bimodal nature of plutonism in the coastal Maine magmatic province is reflected by the intimate spatial association of mafic and felsic magmatism within the igneous complexes, an intrusive style that is characteristic of the coastal Maine magmatic province.

Plutons in the coastal Maine magmatic province have a variety of geometries and an intrusive style which contrasts sharply with that of plutonic arcs. Plutons occur as individual diapiric or thin sheet-like bodies, dispersed isolated complexes comprised of multiple plutons, and multiple batholiths. Emplacement appears to be influenced by the presence of preexisting crustal fractures. Several plutons expand laterally upon intruding the upper crustal Paleozoic section (Hodge et al., 1982; Stewart et al., 1986), others form ring dikes and appear to have been emplaced by cauldron subsidence (Chapman, 1968). In contrast, magmatism over Cordilleran subduction zones is characterized by great, multiple linear batholiths consisting of arrays of composite cauldrons (Pitcher, 1982) with steeply dipping intrusive contacts and large tabular batholiths oriented parallel to the regional trend (Wones, 1980b). The thin (<2 km) sheet-like plutons that are present in the coastal Maine magmatic province appear to be absent in the Sierra Nevada batholith (Wones, 1980b) and although linear, tabular, plutons do exist in the coastal Maine magmatic province, their orientation is at a high angle to the regional trend, in contrast to those of the Sierra Nevada batholith.

The bimodal nature of plutonism, the iron-enrichment trend in the AFM ternary diagram, the alkali-calcic calc-alkaline index, the overall high-alumina to alkaline nature of the magmas, the presence of granite with alkaline tendencies, as well as the style of intrusion are all characteristics of plutonism generated in an extensional tectonic setting and contrasts sharply with plutonism associated with subduction zone processes. The as-

sociation of a transcurrent fault zone with magmatism that is characteristic of an extensional rifting environment suggests that this fault zone was transtensional during part of its history. Siluro-Devonian bimodal volcanism in the coastal volcanic belt may have been localized by normal block faulting along the margins of an extensional rift graben (Gates and Moench, 1981), a feature that would be compatible with a transtensional fault geometry. Thinning of the lithosphere and upwelling of the underlying mantle may have produced the early mafic magmatism in the coastal Maine magmatic province. However, emplacement of the large, felsic, type IIb, granitoid plutons may have been controlled by a preexisting transcurrent fault system with a transpressional geometry. The significant volume of felsic plutonism in the province during the middle Paleozoic represents a large-scale thermal instability of the underlying crust. Ponding of basaltic magmas at the base of the crust was proposed by Wones (1976b) as a heat source to promote partial melting. A change from an early transtensional fault geometry, which allowed for rapid ascent of basaltic magmas to high levels in the crust, to one of transpression may have restricted the bulk of the mafic magmatism to the base of the crust, triggering the large degree of partial melting represented by these granitic batholiths. This complex history suggests that a long term relationship existed between Middle to Late Paleozoic magmatism of an extensional tectonic affinity with movements along portions of a major transcurrent fault zone.

Tectono-Thermal Evolution of Compositionally Distinct Granitoid Magmas in the Coastal Maine Magmatic Province

The successively higher temperature of intersection of the H_2O-saturated granite solidus with the dehydration reactions for muscovite and quartz, and biotite and quartz in rocks of peraluminous as well as metaluminous bulk compositions, is responsible for the generation of granitic magmas with initially distinct compositions, mineralogies, water contents, and temperatures (Brown and Fyfe, 1970; Clemens and Wall, 1981; Clemens, 1984). Lower temperature granitic magmas formed from incongruent melting of muscovite will have the highest $xH_2O^{(MELT)}$ contents; those formed from Fe-rich biotite will have a moderate $xH_2O^{(MELT)}$ content, and higher temperature melts formed from melting reactions involving Mg-rich biotite will have the lowest $xH_2O^{(MELT)}$ content (Wones, 1981). Melting reactions in source rocks that involve either biotite and feldspar or amphibole and feldspar assemblages should have similar water contents because of the overlap of the stability fields of biotite and amphibole (Wones, 1981). Characteristics of granitic melts would be determined by vapor-absent melting of the appropriate hydrous phases present in the source rocks at various metamorphic grades and levels in the crust.

Thermal decomposition of muscovite in muscovite-quartz-alkali-feldspar assemblages to produce a strongly peraluminous, low temperature hydrous melt at mid-crustal levels occurs at temperatures below 700°C (Thompson and Tracy, 1977). Upon crystallization, these melts, which contain small concentrations of non-minimum melt components such as CaO, TiO_2, MgO, and FeO*, would crystallize some combination of peraluminous phases, such as muscovite, aluminous biotite, garnet, and/or Al_2SiO_5 (Clemens and Wall, 1981). These characteristics are typical of the strongly peraluminous type IIa plutons such as the Wallamatogus, Spruce Mountain, and Indian Lake plutons. The strongly peraluminous type III plutons such as the Spruce Head or Northport plutons may have formed in a similar manner, but were modified at some point in their history by interaction with a mafic magma.

Melts produced from the decomposition of biotite at temperatures above the thermal stability of muscovite and quartz have been recognized as being important in the generation of granitic magmas (Brown and Fyfe, 1970; Clemens and Wall, 1981; Clemens, 1984). The thermal stability of biotite is expanded by compositional substitutions such as $Ti^{VI}O_2 = (FeMg)^{VI}(OH)_2$ and F = OH; melting may occur over a range in temperatures from 750°C to 850°C depending on the composition of biotite and the coexisting mineral assemblage (Clemens and Wall, 1981). Granitic magmas generated by partial melting due to the thermal instability of biotite alone will have significantly lower $xH_2O^{(MELT)}$ than melts derived from source rocks also containing muscovite. Melts generated from aluminous compositions may evolve along reactions such as

$$\text{Bio} + Al_2SiO_5 + \text{Feldspars} \rightarrow \text{Gar} + \text{K-Fld} + \text{Melt} \qquad (1)$$

and produce water-undersaturated, higher temperature melts, with relatively low contents of refractory components such as CaO, TiO_2, and MgO (Clemens and Wall, 1981; Clemens, 1984). The degree of aluminum saturation of granites crystallizing from these melts will depend on the modal percentage of aluminous phases involved in partial melting. Melting by reactions such as this may produce moderately peraluminous, biotite-dominated type IIa plutons such as the Sedgwick or Blue Hill granites and contaminated counterparts such as the type III Sullivan biotite-granite.

In weakly peraluminous or metaluminous source rocks, biotite may persist to higher temperatures during high-grade thermal metamorphism. Generation of melt by decomposition of biotite will be of the form

$$\text{Bio} + \text{Qtz} + \text{Fld} \rightarrow \text{Opx} + \text{K-Fld} + \text{Melt} \pm \text{Gar, Cord} \qquad (2)$$

(Clemens 1984). Because partial melting of biotite in the presence of other aluminous phases begins at higher H_2O fugacities and lower temperatures than pure biotite, partial melts derived from peraluminous metasedimentary source rocks will have relatively higher water contents than those derived from metaluminous source rocks (Hoffer and Grant, 1980; Wones, 1981). Depending on the composition of biotite, melts generated by reactions of this type will be strongly water-undersaturated, metaluminous to weakly peraluminous, and will have relatively

low SiO_2 content and be slightly enriched in refractory components such as Ca, Ti, Fe, and Mg (Clemens and Wall, 1981). Granitic magmas in the coastal Maine magmatic province that appear to have formed as a result of incongruent melting of biotite are the type IIb plutons such as the Lucerne and Deblois granites. The lower activity of H_2O, lower K/Rb ratios and higher absolute K_2O and Rb contents in comparison to type IIa plutons reflect the decomposition of biotite during partial melting of the source. A potassium-rich quartz-plagioclase-biotite gneiss, depleted in muscovite and H_2O by an earlier metamorphic event, has been suggested as a likely source for the Lucerne magma (Wones, 1980a). The type III Mount Waldo pluton is possibly a modified counterpart of the type IIb Lucerne pluton.

Several plutons in the coastal Maine magmatic province are characterized by the presence of hypersolvus, alkali-feldspar granite, high Na_2O+K_2O content, and late-crystallizing sodic amphiboles and closely resemble the high temperature, relatively anhydrous, fluorine-rich, A-type granites of Loiselle and Wones (1979b), Collins et al. (1982), and Whalen et al. (1987). These characteristics are suggested to have been inherited from the partial melting of source region material that has been metamorphosed to granulite facies conditions (Collins et al., 1982; Clemens et al., 1986). The production of granitic magmas from granulites in quantities sufficent enough to allow migration of the melt from the source region at geologically reasonable temperatures is limited by the availabilty of a volatile component (Collins et al., 1982). The increased thermal stability of fluorobiotite and fluoro-amphibole to granulite facies conditions suggests that thermal decomposition of these phases may provide the necessary volatile component to induce vapor-absent partial melting of a granulite source (Collins et al., 1982; Clemens et al., 1986). At elevated temperatures (>830°C), reactions of the type

$$\text{F-rich (Bio,Hbl)} + \text{Qtz} + \text{Fld} \rightarrow \text{(Opx,Cpx)} + \text{K-Fld} + \text{Melt} \quad (3)$$

have been suggested for the formation of granitic melts from rocks at granulite facies conditions (Clemens et al., 1986; Collins et al., 1982). High temperature, vapor-absent partial melting of granulite source regions by reactions of this type could form the small volume of relatively anhydrous, high temperature, fluorine-rich, granitic magmas due to the dehydrated, low H_2O nature of the source region as well as the presence of additional volatile species such as fluorine during partial melting (Clemens et al., 1986). High Na_2O+K_2O content of these magmas may be attributed to the thermal decomposition of biotite, amphibole, and the albite component, and reflect the relatively refractory nature of calcic plagioclase (Clemens et al., 1986).

Melting of lower crustal granulite facies source regions by vapor-absent partial melting along reactions similar to reaction 3 may have produced magmas which crystallized to form the type III Cadillac Mountain and Tunk Lake plutons. Intrusion of basaltic magma has been suggested as an extracrustal heat source that could produce the high crustal temperatures necessary for melting to take place along reactions of this type (Clemens et al., 1986) and may explain the close spatial association of mafic magmas with type III plutons of alkaline affinity in the coastal Maine magmatic province.

A general chronological pattern of intrusion has been proposed for the province, where the earliest magmas intruded are gabbroic (type I) followed by peraluminous plutons (type IIa) then by biotite, biotite-hornblende metaluminous granite (type IIb) with the youngest intrusions being of an alkaline affinity (Wones and Sinha, 1988). This chronological sequence for emplacement of granitic magmas from early intrusion of low-temperature, hydrous, peraluminous magmas, to sequentially higher temperature, metaluminous magmas to progressively more anhydrous magmas is predicted by Brown and Fyfe (1970) for incremental melting of an initially hydrous source rock on the basis of the progressive increase in temperature required to obtain thermal instability of first muscovite, then biotite, and finally hornblende for vapor-absent melting. Peraluminous magmas such as the type IIa Wallamatogus pluton would be produced first. Successive melting of the same source region would produce the metaluminous, H_2O-undersaturated Lucerne granite (type IIb) leaving behind a relatively anhydrous residuum, which upon additional melting might produce the drier magmas such as represented by the Tunk Lake pluton.

However, deviations from this idealized compositional intrusive sequence can be found within the coastal Maine magmatic province and neighboring regions. Recent geochronological investigations have established a Silurian age for the Cadillac Mountain pluton (D. Lux, pers. commun., 1986). Peralkaline granitic plutonism of similar age has been identified south of the magmatic province within the Gulf of Maine and in the Avalonian terranes of southeastern New England where both Middle to Late Ordovician and Middle to Late Devonian peralkaline plutonism is present (Hermes et al., 1978; Hermes and Zartman, 1985). In southern New Brunswick, Canada, granites with A-type affinities span a range of ages from the Siluro-Devonian to the Carboniferous (Payette and Martin, 1987; Whalen, 1986) and may also precede intrusion of peraluminous to metaluminous granitic magmas.

Extraction of a peraluminous to metaluminous partial melt from the source region has been proposed as a dehydration mechanism to produce anhydrous granulite facies assemblages prior to generation of granitic magmas with A-type affinities (Collins et al., 1982; Clemens et al., 1986). However, granulite facies assemblages can also be formed by mineral dehydration reactions alone, liberating H_2O without the removal of a melt fraction (Nesbitt, 1980), resulting in a potential source region for granitic magmas with A-type affinities. The presence of rift-related, bimodal Siluro-Devonian volcanic rocks extending from approximately Passamaquoddy Bay to Penobscot Bay (Gates and Moench, 1981; Pinette, 1983) indicates that this area was a region of high heat-flow prior to intrusion of the majority of plutons in the coastal Maine magmatic province. Efficient convection of heat away from the base of the crust during incipient

rifting by the liberation of volatiles during mineral dehydration reactions may have supressed the role of partial melting in the formation of anhydrous granulite facies assemblages in the lower crust beneath the magmatic province. After dehydration of the lower crust occurs, continued underplating of mantle-derived magmas results in additional heat that can no longer be rapidly transferred from the base of the crust by migration of a volatile component. Initial melting of the anhydrous lower crust during the early stages of rifting could form the early granitic magmas of A-type affinity.

During the early stages of rifting, the high heat-flow from the mantle may have produced a vertical metamorphic gradient in the crust. The anhydrous granulites of the lower crust would give way to progressively more hydrous lower amphibolite to greenschist facies assemblages at successively shallower levels. The initial extensional environment created by the transtensional fault geometry may have facilitated access of mantle-derived magmas to higher levels in the crust. This rapid transfer of heat to low-grade, biotite-muscovite-bearing hydrous source regions could trigger partial melting of these source regions to form the type IIa plutons. In some instances crustal partial melts and their heat source, the mantle-derived high-temperature mafic magmas, interacted to varying degrees to form the type III and IV plutons as well as the igneous complexes that are characteristic of the magmatic province.

Intrusion of the large metaluminous type IIb batholiths and younger plutons with alkaline affinities occurred after this transcurrent fault zone became transpressional. Restriction of mafic magmas to the lower crust in a transpressional environment would result in partial melting of the more dehydrated source regions, such as a quartzo-feldspathic biotite-hornblende gneiss to produce the type IIb plutons and the anhydrous granulites of the lower crust for the source region of the younger granites of alkaline affinity.

The relationship between tectonic setting, pluton type, and thermal history of the crust in eastern coastal Maine is summarized in Figure 8, an idealized schematic cross section of the coastal Maine magmatic province. Transfer of heat from the mantle to the overlying crust is accomplished by ascent of mantle-derived magmas. These magmas may become trapped at various levels in the overlying crust. Mantle-derived magmas trapped at the lithologic boundary between the lower crust and mantle may provide the heat necessary to melt relatively anhydrous source materials to generate crustal magmas with A-type affinities, whereas those that intrude higher levels in the crust may induce partial melting of progressively less dehydrated source regions to form either type IIa or IIb plutons. Mantle-derived magmas, facilitated by the presence of crustal fractures, may ascend to near surface levels in the crust where they crystallize to form the type I layered mafic plutons or are subsequently intruded by crustal-derived magmas to form the bimodal igneous complexes that are characteristic of the province. Interaction between the crustal magmas and their heat source, the mantle-derived magmas, results in formation of the compositional hybrid type III granitic plutons and/or the type IV intermediate to mafic plutons of the coastal Maine magmatic province.

CONCLUSIONS

Proposed Models for Terrane Accretion in Coastal Maine

Juxtaposition of disparate lithologies of varying structural complexity and metamorphic grade along fault boundaries in the Penobscot Bay region has led to the suggestion that these lithotectonic belts of eastern Maine are best represented as suspect terranes (Stewart and Wones, 1974; Wones and Stewart, 1976; Osberg, 1974, 1978; Bickel, 1976; Zen, 1983). Plate tectonic models proposed to explain the juxtaposition and amalgamation of these terranes in the Early- to Mid-Paleozoic differ considerably on the role of subduction. One model proposed telescoping of a complex continental margin, comprised of a series of small ocean basins separating microcontinental blocks, through subduction of the intervening oceanic crust along consuming plate margins (Osberg, 1978; McKerrow and Ziegler, 1971; Rast and Stringer, 1975; Dewey and Kidd, 1974; Ruitenberg and Ludman, 1978; Poole, 1976). Subduction terminated with successive accretion of each outboard terrane onto the North American margin along thrust faults. Volcanic and plutonic rocks of eastern coastal Maine are proposed to represent remnants of a former volcanic arc overlying a subduction zone (Osberg, 1978; McKerrow and Ziegler, 1971; Dewey and Kidd, 1974; Ruitenberg and Ludman, 1978; Poole, 1976; Gates et al., 1984).

Alternative models for terrane accretion suggest that subduction of oceanic crust played a minor role in the assembly of the different terranes (Wones and Stewart, 1976; Wones, 1976b, 1980b; Andrews et al., 1983; Ayuso, 1986). Amalgamation of these terranes is believed to have occurred through lateral transport of distinct structural/stratigraphic crustal blocks over large distances along major dextral transcurrent faults during the Acadian compressional event (Wones and Stewart, 1976). Geochemical and isotopic characteristics of the source regions of plutons intruding these terranes cannot be correlated across proposed terrane boundaries, suggesting that observed discontinuities between terranes at the surface persist at depth, maintaining the integrity of these terranes into the lower crust. These data are suggested to be consistent with the assembly of distinct crustal blocks along transcurrent faults (Andrews et al., 1983; Ayuso, 1986).

Characteristics of Siluro-Devonian to Carboniferous plutonism in the coastal Maine magmatic province appears to be more compatible with magmatism related to an extensional plate tectonic environment. Plutonism postdated terrane assembly in eastern coastal Maine and the strong structural control of dextral transcurrent faults on the emplacement of plutons suggests that intrusion of magmas into the overlying crust was facilitated by the presence of a preexisting transcurrent fault system. Changes

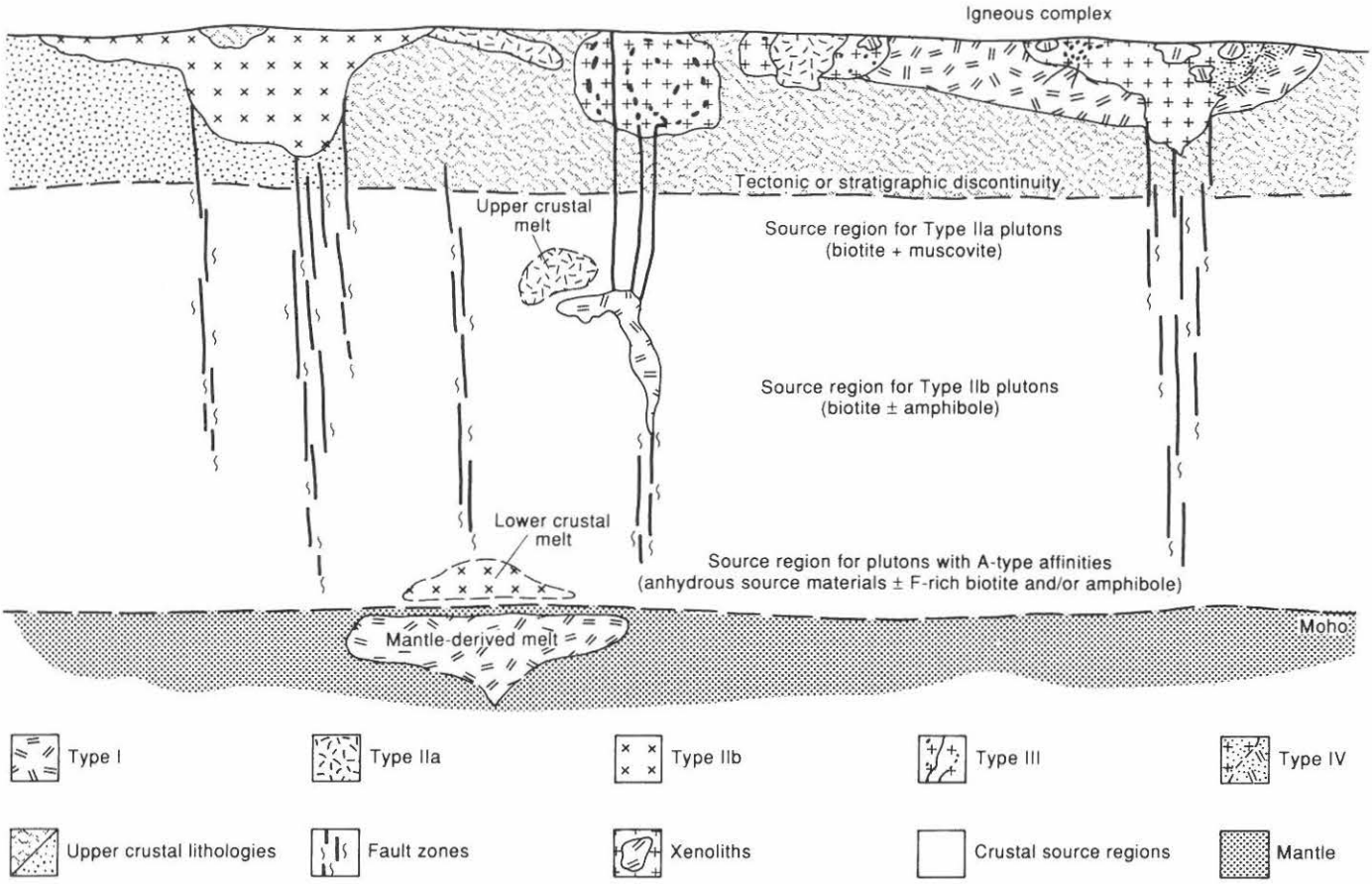

Figure 8. Schematic cross section (not to scale) of the coastal Maine magmatic province. Upper crustal lithologies are in fault contact with each other and may be either autochthonous or allochthonous over the underlying source region(s). Mantle-derived magmas act as the heat source to induce melting of source region(s) and crystallize to form type I intrusions. Melting of different crustal levels produces felsic magmas with unique mineralogical and compositional characteristics which reflect the metamorphic assemblage of the source. These magmas crystallize to form type IIa or IIb plutons. Interaction between crustal melts and their heat source (characterized by the presence of synplutonic mafic dikes, mafic enclaves, or gradational contacts between mafic and felsic rocks) results in the formation of hybrid type III or IV plutons. Close spatial association, but not necessarily a close temporal association, of different pluton types is expressed by the presence of igneous complexes.

in the geometry of this fault system resulted in different periods of intraplating and underplating of mantle-derived magmas resulting in partial melting of crustal source regions at various metamorphic grades which gave rise to compositionally distinct granitoid magmas. Interaction between crustal- and mantle-derived partial melts during crystallization may have resulted in variable degrees of hybridization of felsic and mafic magmas.

Comparison of the Coastal Maine Magmatic Province with Neighboring Regions

In New Brunswick, Canada, Fyffe et al. (1981) subdivided plutons into types A through H on the basis of field relationships, texture, mineralogy, and chemistry. Several features of Siluro-Devonian to Carboniferous plutonism in the southern plutonic belt of New Brunswick, summarized here from Fyffe et al. (1981), suggest that a similar petrogenetic and tectonic setting exists for this region and the coastal Maine magmatic province. Plutonism has been interpreted to be coeval and to also postdate faulting associated with the later stages of the Acadian orogeny. Early mantle-derived mafic magmas (type A ~ type I), intruded along faults, were subsequently intruded by a texturally and compositionally diverse group of felsic granitoids (type B ~ type III), often resulting in the formation of hybrid rocks (type A-B ~ type IV) of intermediate composition. This mafic-felsic association corresponds to the igneous complexes of the Maine province. These intrusions were subsequently followed by water-saturated, peraluminous, muscovite-bearing granites (type D ~ type IIa) and water-undersaturated, metaluminous, megacrystic, biotite±hornblende granites (type F ~ type IIb), and then by equigranular biotite±muscovite granites (type H ~ type IIa). The intrusive sequence of granitoids progressively changes

towards more felsic and potassic compositions (Fyffe et al., 1981). Recent work in this area has also described the occurrence of both Siluro-Devonian and Carboniferous peralkaline magmatism associated with hybrid and basic rocks (Whalen, 1986; Payette and Martin, 1987) that would correspond to the type III Cadillac Mountian and Tunk Lake plutons of the coastal Maine province.

Subduction-related magmatism as an origin for plutonism in southern New Brunswick was ruled out in favor of initially localized melting of the crust by intrusion of mafic magmas followed by widespread melting due to radioactive heating of a continental crust tectonically overthickened during the Taconic orogeny (Fyffe et al., 1981). Alternatively, the association of Siluro-Devonian peralkaline magmatism with graben formation has been interpreted to represent rift-related igneous activity related to extension during the Siluro-Devonian (Payette and Martin, 1987). The presence of Siluro-Devonian ductile, dextral, transcurrent fault zones in this region (Leger and Williams, 1986) as well as the similarity in plutonic styles suggests that Early to Middle Paleozoic plutonism in southern New Brunswick may have also been related to mantle upwelling beneath a transtensional transcurrent fault zone.

Siluro-Devonian plutonism in the Nashoba terrane and Avalonian terranes of southeastern Massachusetts and Rhode Island (Hepburn et al., 1987) is also similar in some respects to plutonism in the coastal Maine magmatic province. The salient characteristics of plutonism in these terranes as summarized by Hepburn et al. (1987) are presented here for comparison. The Avalonian terranes are characterized by a 650 to 600 Ma period of coarse grained, calc-alkaline, hornblende-biotite, tonalite-granodiorite-granite intrusions that has not yet been identified in the coastal Maine magmatic province. Late Ordovician to Devonian plutonism generally exhibits alkaline affinities and can also be associated with contemporaneous gabbroic plutons, suggesting strong similarities with the type III Cadillac Mountain and Tunk Lake plutons of the Maine province. Carboniferous plutonism in the Avalonian terranes is represented by the peraluminous Narragansett Pier granite. The Nashoba terrane experienced widespread bimodal plutonism commencing possibly as early as the Middle to Late Ordovician and waning in the Early Devonian. The oldest intrusion is represented by the 446±32 Ma peraluminous, foliated, and non-foliated Andover pluton. Mafic to intermediate magmas consisting of gabbroic cumulates (possible type I plutons?), tonalite, and hornblende-biotite-diorite were intruded during the Silurian and Early Devonian. Granitic crustal partial melts coexisted with mafic magmas associated with the 430±5 Ma Sharpners Pond diorite, suggesting that intermediate compositions may be the result of magma mixing and could possibly have an origin similar to that of type IV plutons. Some of the igneous complexes present in the Maine province have a similar age and association of magma compositions as the Sharpners Pond diorite.

Although the character of plutonism in the coastal Maine magmatic province can be readily extended into southern New Brunswick, correlation with similar age plutonism in southeastern New England remains tenuous at present. Plutonism in the Nashoba terrane may have resulted through subduction related processes during the Siluro-Devonian, whereas Late Ordovician to Devonian plutonism in the Avalonian terrane is more characteristic of anorogenic magmatism on a stable cratonic platform (Hepburn et al., 1987). Juxtaposition of these distinct plutonic regimes may reflect accretion along transcurrent faults during the Mid-Paleozoic (Hepburn et al., 1987). However, similarities with temporally equivalent plutonism in the coastal Maine magmatic province suggest that a similar thermal disturbance triggered partial melting of the crust beneath both regions. If this is the case, then compositional differences of granitoid plutons across terrane boundaries may reflect partial melting of distinct source regions juxtaposed by transcurrent faulting prior to plutonism, suggesting that southeastern New Brunswick, Canada, eastern coastal Maine, southeastern Massachusetts, and Rhode Island shared a common Middle Ordovician to Siluro-Devonian tectonic history. However, it is clear that several problems remain to be resolved before the relationship between plutonism in the coastal Maine magmatic province and southern New England is fully understood.

Tectonic Implications of Possible Crustal Source Region Geometries Beneath the Coastal Maine Magmatic Province

Petrologic and geochemical characteristics of plutonism in Maine have been correlated with unique fault-bounded lithologic crustal domains (Loiselle and Ayuso, 1980; Andrews et al., 1983; Ayuso, 1986). Distinct differences between source region characteristics for granitic plutons intruded into opposing sides of proposed terrane boundaries, such as the Norumbega fault zone, were used to suggest that these discontinuities persist into the lower crust as fundamental tectonic boundaries, reflecting juxtaposition of discrete source regions by transcurrent faulting (Loiselle and Ayuso, 1980; Andrews et al., 1983; Ayuso, 1986). In eastern coastal Maine, southeast of the Norumbega fault zone, the majority of magmatism appears to have postdated assembly of the proposed terranes by transcurrent dextral fault motions. Individual plutons, such as the type IIb Lucerne pluton, may intrude several of the lithotectonic blocks; several examples of a pluton type, such as the type IIa Wallamatogus and Blue Hill plutons, can intrude several different terranes within the coastal Maine magmatic province.

This suggests two possiblities for source region geometries beneath the magmatic province (Fig. 9). The first case (Fig. 9) is one in which vertical packages of unrelated, but compositionally similar, source region lithologies are juxtaposed along transcurrent faults. These distinct source regions become progressively more dehydrated with increasing depth in the crust. Partial melting of source rocks at similar metamorphic grades beneath each terrane is controlled by vapor-absent melting reactions in equivalent mineral assemblages resulting in

formation of compositionally similar types of granitic melts. The granite magmas (type II) intrude upper crustal lithologies that overlie the source region of their respective terrane. Mineralogically and compositionally, these magmas may appear very similar, but if the source region beneath each terrane is sufficently distinct, compositionally similar granites across terrane boundaries should be isotopically distinguishable. Transcurrent faults that juxtapose distinct upper crustal lithologies would maintain their integrity as terrane boundaries in the lower crust. This model is a variant of those proposed by Wones (1976b), Loiselle and Ayuso (1980), Andrews et al. (1983), and Ayuso (1986).

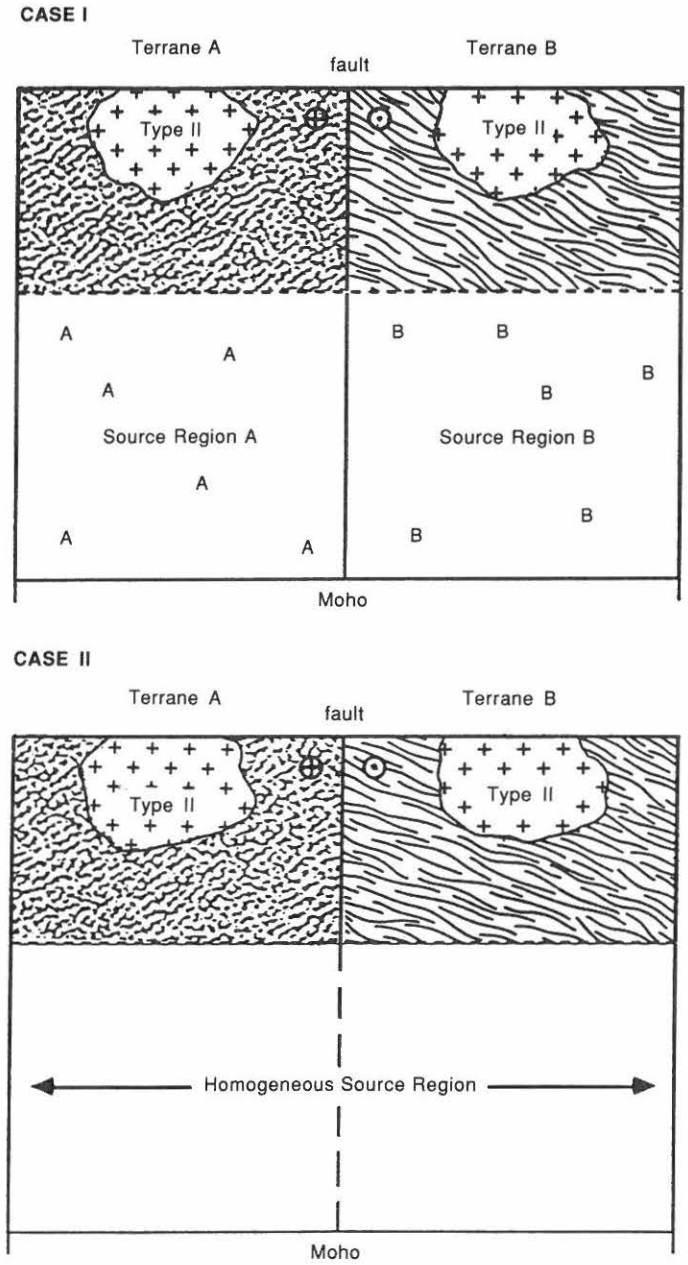

Figure 9. Possible source region geometries in the coastal Maine magmatic province. In case I distinct vertical packages of upper crustal lithologies and their source regions represent separate terranes A and B that have been juxtaposed by transcurrent faulting. In case II, a compositionally and isotopically homogeneous source region underlies both terranes A and B. In case I upper crustal lithologies may be either autochthonous or allochthonous above the underlying source regions, whereas case II is compatible with an allochthonous cover sequence overlying the source region.

A second possibility (case II, Fig. 9) arises if the presence of type II granites in several terranes reflects the presence of a common, laterally extensive, mineralogically and chemically homogeneous source rock that exists beneath several of the proposed terranes. Isotopic characteristics of compositionally similar type II granites cropping out in separate terranes would be similar if they originate by equilibrium partial melting from the same source rock layer that underlies both terranes. Superposition of different pluton types within the same terrane may be due to increasing metamorphic grade of this source rock with depth or the horizontal stacking of chemically and compositionally distinct source regions at different metamorphic grades beneath the terranes. Isotopic characteristics of distinct granite types (types IIa and IIb) within the same terrane should be dissimilar if they form by partial melting of different horizontally stacked source rock layers and similar if they formed by incremental partial melting of the same source rock. In this second case, proposed terrane boundaries between upper crustal lithologies would not represent fundamental tectonic boundaries in the source regions immediately beneath these terranes. In case I upper crustal lithologies may be either autochthonous or allochthonous above the underlying source regions, whereas case II is compatible with an allochthonous cover sequence overlying the source region.

Isotopic studies are presently underway to determine the internal consistency of granitoid types IIa and IIb, distinguished on the basis of mineralogical, major element, and limited trace element chemistry (Hogan and Sinha, in prep.). These data should provide a means to test between successively derived melts from a single source region vs. distinct melts derived from unique, vertically stacked source regions beneath the coastal Maine magmatic province as well as determine the lateral continuity of the source regions beneath proposed terrane boundaries and to evaluate the role of transcurrent faulting in the assembly of terranes in eastern coastal Maine. Determination of the isotopic characteristics of type I gabbros is also in progress to determine the possible role of mantle-derived melts in the formation of hybrid type III and IV plutons in the coastal Maine magmatic province.

ACKNOWLEDGMENTS

We thank Marc Loiselle, O. Don Hermes and the editors Robert D. Tucker and Robert G. Marvinney for their careful reviews which greatly improved the clarity and presentation of ideas in this manuscript. We also thank Dave Stewart, Joe Arth, Susan Eriksson, Joe Jurinski, Robert Ayuso, and the late Dave

Wones for discussions with us on plutonism in eastern coastal Maine. A special thanks to Dave Westerman for showing us several of the mafic plutons in southeastern Maine and for making available to us his data on the Pocomoonshine pluton. We also thank Jim Carl and Susan Eriksson for the use of unpublished data on selected plutons and the help of David Anderson and Allan Ludman in obtaining unpublished theses. The technical support of Karen Hogan is greatly appreciated. This study was partially supported through grants from the Geological Society of America, Sigma Xi, the Maine Geological Survey, and the National Science Foundation, Grant #EAR8416575.

REFERENCES CITED

Abbott, R. N., 1977, Petrology of the Red Beach granite near Calais, Maine: Ph.D. dissert., Harvard Univ., Cambridge, Mass., 223 p.

Abbott, R. N., 1978, Geology of the Red Beach granite, *in* Ludman, A. (ed.), New England Intercollegiate Geological Conference guidebook for field trips in southeastern Maine and southwestern New Brunswick, p. 17-37.

Amos, D. H., 1963, Petrology and age of plutonic rocks, extreme southeastern Maine: Geol. Soc. Amer., Bull., v. 74, p. 169-193.

Andrews, A. S., Loiselle, M. C., and Wones, D. R., 1983, Granite plutonism as an indicator of microplates in the Paleozoic of central and eastern Maine: Earth Planet. Sci. Lett., v. 66, p. 151-165.

Aydin, A., and Page, B. M., 1984, Diverse Pliocene-Quaternary tectonics in a transform environment, San Francisco Bay region, California: Geol. Soc. Amer., Bull., v. 95, p. 1303-1317.

Ayuso, R. A., 1986, Lead isotopic evidence for distinct sources of granite and for distinct basements in the northern Appalachians, Maine: Geology, v. 14, p. 322-325.

Bateman, P. C., 1983, A summary of critical relations in the central part of the Sierra Nevada batholith, California, U.S.A.: Geol. Soc. Amer., Mem. 159, p. 241-259.

Bateman, P. C., Clark, L. D., Huber, N. K., Moore, J. G., and Rhinehart, C. D., 1963, The Sierra Nevada batholith - a synthesis of recent work across the central part: U.S. Geol. Surv., Prof. Paper 414D, 46 p.

Benson, W. N., 1926, The tectonic conditions accompanying the intrusion of basic and ultrabasic igneous rocks: National Academy of Sciences, Washington, D.C., Mem. 1, v. 19, 90 p.

Bickel, C. E., 1976, Stratigraphy of the Belfast quadrangle, Maine: Geol. Soc. Amer., Mem. 148, p. 97-128.

Bickford, M. E., 1963, Petrology and structure of layered gabbros at Pleasant Bay, Maine: Jour. Geol., v. 71, p. 215-237.

Biggi, R. J., and Hodge, D. S., 1982, Gravity studies over the Bays of Maine Igneous Complex: Geol. Soc. Maine, Bull., v. 2, p. 1-15.

Brookins, D. G., 1976, Geochronologic contributions to stratigraphic interpretation and correlation in the Penobscot Bay area, eastern Maine, *in* Page, L. R. (ed.), Contributions to the stratigraphy of New England: Geol. Soc. Amer., Mem. 148, p. 129-146.

Brookins, D. G., Berdan, J. M., and Stewart, D. B., 1973, Isotopic and paleontologic evidence for correlating three volcanic sequences in the Maine coastal volcanic belt: Geol. Soc. Amer., Bull., v. 84, p. 1619-1628.

Brookins, D. G., and Spooner, C. M., 1970, Isotopic ages of the Oak Point and Stonington granites, eastern Penobscot Bay, Maine: Jour. Geol., v. 78, p. 570-576.

Brown, G. C., and Fyfe, W. S., 1970, The production of granitic melts during ultrametamorphism: Contrib. Mineral. Petrol., v. 28, p. 310-318.

Carl, J. D., Liptak, A. R., Savitz, S. L., Schmidt, D. T., Shay, S. G., Tom, V. J., and Wink, J. T., 1984, Geochemical characteristics of granitoid plutons in the Penobscot Bay area Maine: Northeastern Geology, v. 6, p. 12-24.

Cavalero, R. A., 1965, Geology of the Clifton Township area in the Orono and Great Pond quadrangles, Maine: M.S. thesis, Univ. Maine, Orono, 116 p.

Chapman, C. A., 1962a, Diabase-granite composite dikes, with pillow like structure, Mount Desert Island, Maine: Jour. Geol., v. 70, p. 539-564.

Chapman, C. A., 1962b, Bays-of-Maine igneous complex: Geol. Soc. Amer., Bull., v. 73, p. 883-888.

Chapman, C. A., 1968, A comparison of the Maine coastal plutons and the magmatic central complexes of New Hampshire, *in* Zen, E-an, White, W. S., Hadley, J. B., and Thompson, J. B., Jr. (eds.), Studies of Appalachian geology: northern and maritime: Interscience, New York, p. 385-396.

Chapman, C. A., 1970, The geology of Acadia National Park: The Chatham Press, Old Greenwich, Conn., 128 p.

Chapman, C. A., 1974, Bedrock geology of Mount Desert Island, in Osberg, P. H. (ed.), New England Intercollegiate Geological Conference guidebook for field trips in east-central and north-central Maine, p. 140-153.

Chapman, C. A., and Wingard, P. S., 1958, Physical control and age of dike formation in the Maine coastal region: Geol. Soc. Amer., Bull., v. 69, p. 1193-1195.

Chappell, B. W., and White, A. J. R., 1974, Two contrasting granite types: Pacif. Geol., v. 8, p. 173-174.

Chayes, F., 1952, The finer-grained calc-alkaline granites of New England: Jour. Geol., v. 60, p. 207.

Clemens, J. D., 1984, Water contents of silicic to intermediate magmas: Lithos, v. 17, p. 273-287.

Clemens, J. D., Holloway, J. R., and White, A. J. R., 1986, Origin of an A-type granite: experimental constraints: Am. Mineral., v. 71, p. 317-324.

Clemens, J. D., and Wall, V. J., 1981, Crystallization and origin of some peraluminous (S-type) granitic magmas: Can. Mineral., v. 19, p. 111-132.

Collins, W. J., Beams, S. D., White, A. J. R., and Chappell, B. W., 1982, Nature and origin of A-type granites with particular reference to southeastern Australia: Contrib. Mineral. Petrol., v. 80, p. 189-200.

Coughlin, S. P., 1981, The petrology of the Staples Mountain intrusive, southeastern Maine: Geol. Soc. Amer., Abs. with Prog., v. 13, p. 126.

Coughlin, S. P., 1986, Petrology of the Staples Mountain Igneous Complex, Calais quadrangle, southeastern Maine: M.S. thesis, Queens College, New York, 138 p.

DePaolo, D. J., 1981, A neodymium and strontium isotopic study of the Mesozoic calc-alkaline granitic batholith of the Sierra Nevada and Peninsular Ranges, California: Geophys. Res., v. 86, p. 10470-10488.

Dewey, J. F., and Kidd, W. S. F., 1974, Continental collisions in the Appalachian-Caledonian orogenic belt: variations related to complete and incomplete suturing: Geology, v. 2, p. 543-546.

Eichelberger, J. C., 1978, Andesite volcanism and crustal evolution: Nature, v. 275, p. 21-27.

Eriksson, S. C., 1985, The Parks Pond pluton: a mantle-derived mafic granite: Geol. Assoc. Canada, Mineral. Assoc. Canada, Joint Annual Meeting, Abs. with Prog., v. 10, p. A17.

Eriksson, S. C., and Williams, I. S., in press, Inherited zircons from the Paleozoic Parks Pond pluton, Maine: direct evidence for Archean components in the Avalon basement: Geol. Soc. Amer., Bull.

Eriksson, S. C., and Wones, D. R., 1983, The Parks Pond pluton, eastern Maine: evidence for cratonization or orogenic activity: Geol. Soc. Amer., Abs. with Prog., v. 15, p. 118.

Faul, H., Stern, T. W., Thomas, H. H., and Elmore, P. L. D., 1963, Ages of intrusion and metamorphism in the northern Appalachians: Am. Jour. Sci., v. 261, p. 1-19.

Faure, G., 1977, Principles of isotope geology: John Wiley and Sons, Inc., New York, 464 p.

Frost, T. P., and Mahood, G. A., 1987, Field, chemical, and physical constraints on mafic-felsic magma interaction in the Lamarck granodiorite, Sierra Nevada, California: Geol. Soc. Amer., Bull., v. 99, p. 272-291.

Fyffe, L. R., Pajari, G. E., Jr., and Cherry, M. E., 1981, The Acadian plutonic rocks of New Brunswick: Maritime Sed. and Atlantic Geol., v. 17, p. 23-36.

Gamble, J. A., 1979, Some relationships between co-existing granite and basaltic magmas and the genesis of hybrid rocks in the tertiary central complex of Slieve Gullion, Northeast Ireland: Volcan. Geotherm. Res., v. 5, p. 297-316.

Gates, O., 1969, Lower Silurian-Lower Devonian volcanic rocks of New England coast and southern New Brunswick, *in* Kay, M. (ed.), North Atlantic-Geology and Continental Drift, International Conference, 1967, Gander, Symposium: Am. Assoc. Petrol. Geol., Mem. 12, p. 484-503.

Gates, O., Hussey, A. M., II, and Osberg, P. H., 1984, Acadian thrust plates in coastal Maine: Geol. Soc. Amer., Abs. with Prog., v. 16, p. 17.

Gates, O., and Moench, R. H., 1981, Bimodal Silurian and Lower Devonian volcanic rock assemblages in the Machias-Eastport area Maine: U.S. Geol. Surv., Prof. Paper 1184, 32 p.

Gilman, R. A., 1961, Petrology and structure of the Milbridge-Whitneyville area Maine: Ph.D. dissert., Univ. Illinois, Urbana, 130 p..

Guidotti, C. V., 1979, Preliminary bedrock geology of the Tenants Harbor and a portion of the Friendship 7.5' quadrangles Maine: Maine Geol. Surv., Open-File Rept. 79-16, 12 p.

Harker, A., 1909, Natural history of igneous rocks: Macmillan, New York, 384 p.

Hepburn, J. C., Hill, M., and Hon, R., 1987, The Avalonian and Nashoba Terranes, eastern Massachusetts, U.S.A.: an overview: Maritime Sed. Atlantic Geol., v. 23, p. 1-12.

Hermes, O. D., Ballard, R. D., and Banks, P. O., 1978, Upper Ordovician peralkaline granites from the Gulf of Maine: Geol. Soc. Amer., Bull., v. 89, p. 1761-1764.

Hermes, O. D., and Zartman, R. E., 1985, Late Proterozoic and Devonian plutonic terrane within the Avalon zone of Rhode Island: Geol. Soc. Amer., Bull., v. 96, p. 272-282.

Hibbard, M. J., 1981, The magma mixing origin of mantled feldspars: Contrib. Mineral. Petrol., v. 76, p. 158-170.

Hodge, D. S., Abbey, D. A., Harbin, M. A., Patterson, J. L., Ring, M. J., and Sweeney, J. F., 1982, Gravity studies of subsurface mass distributions of granitic rocks in Maine and New Hampshire: Am. Jour. Sci., v. 282, p. 1289-1324.

Hoffer, E., and Grant, J. A., 1980, Experimental investigation of the formation of cordierite-orthopyroxene paragenesis in pelitic rocks: Contrib. Mineral. Petrol., v. 73, p. 15-22.

Hussey, A. M., II, 1985, The bedrock geology of Bath and Portland 2o sheets, Maine: Maine Geol. Surv., Open-File Rept. 85-87, 80 p.

Johnson, T. D., and Wones, D. R., 1984, Sense and mode of shearing along the Norumbega fault zone, eastern Maine: Geol. Soc. Amer., Abs. with Prog., v. 16, p. 27.

Jurinski, J. B., 1987, The Baring pluton: contaminated granite of the Moosehorn Igneous Complex: Honors Thesis, Virginia Polytechnic Institute and State Univ., Blacksburg, Virginia, 48 p.

Karner, F. R., 1962, Petrology of the Tunk Lake granite pluton, southeastern Maine: Ph.D. dissert., Univ. Illinois, Urbana, 94 p.

Karner, F. R., 1968, Compositional variation in the Tunk Lake granite pluton, southeastern Maine: Geol. Soc. Amer., Bull., v. 79, p. 193-221.

Karner, F. R., 1974, The concentrically zoned Tunk Lake pluton: Devonian melting-anomaly activity?, *in* Osberg, P. H. (ed.), New England Intercollegiate Geological Conference guidebook for field trips in east-central and north-central Maine, p. 190-209.

Kaszuba, J. P., 1986, Polyphase deformation and metamorphism in the Penobscot Bay area, coastal Maine: M.S. thesis, Virginia Polytechnic Institute and State Univ., Blacksburg, Virginia, 100 p.

Kaszuba, J. P., and Wones, D. R., 1985, Early Devonian thrusting in the Penobscot Bay area, Maine: Geol. Soc. Amer., Abs. with Prog., v. 17, p. 27.

King, A. W., 1977, The petrology and geochemistry of the Mount Waldo granite, southeastern Maine: M.S. thesis, Univ. Maine, Orono, 79 p.

Kistler, R. W., and Peterman, Z. E., 1973, Variations in Sr, Rb, K, Na and initial $^{87}Sr/^{86}Sr$ in Mesozoic granitic rocks and intruded wall rocks in central California: Geol. Soc. Amer., Bull., v. 84, p. 3489-3511.

Kuno, H., 1966, Lateral variation of basalt magma type across continental margins and island arcs: Bull. of Volcanology, v. 29, p. 195-222.

Leger, A., and Williams, D. R., 1986, Transcurrent faulting history of southern New Brunswick, *in* Current Research, Part B: Geol. Surv. Canada, Paper 86-1B, p. 111-120.

Loiselle, M. C., and Ayuso, R. A., 1980, Geochemical characteristics of granitoids across the Merrimack synclinorium, eastern and central Maine, *in* Wones, D. R. (ed.), Proceedings, The Caledonides in the U.S.A.: Dept. Geology, Virginia Polytechnic Institute and State Univ., Blacksburg, Virginia, Mem. 2, p. 117-121.

Loiselle, M. C., Eriksson, S., Wones, D. R., and Sinha, A. K., 1983, Timing and emplacement of post-Acadian plutons in central and eastern Maine: Geol. Soc. Amer., Abs. with Prog., v. 15, p. 187.

Loiselle, M. C., and Wones, D. R., 1979a, Plutonism and Post-Acadian faulting in east-central Maine, *in* Hussey, A. M., II, and Westerman, D. (eds.), Field trips of the Geological Society of Maine, 1978-1983: Geol. Soc. Maine, Bull. 3, p. 72-84.

Loiselle, M. C., and Wones, D. R., 1979b, Characteristics and origin of anorogenic granties: Geol. Soc. Amer., Abs. with Prog., v. 11, p. 468.

Luce, R. W., 1962, Petrography of the igneous rocks, Isle au Haut, Maine: M.S. thesis, Univ. Illinois, Urbana, 27 p.

Ludman, A., 1974, Preliminary report on the geology of the Calais-Big Lake, Maine area: Maine Geol. Surv., Progress Rept., 30 p.

Ludman, A., 1981a, Significance of transcurrent faulting in eastern Maine and location of the suture between Avalonia and North America: Am. Jour. Sci., v. 281, p. 463-483.

Ludman, A., 1981b, Bedrock geology of the Big Lake 15' quadrangle, Maine: Maine Geol. Surv., Open-File Rept. 81-35, 37 p., 1 map.

Ludman, A., 1986, Timing of terrane accretion in eastern and east-central Maine: Geology, v. 14, no. 5, p. 411-414.

Macdonald, G. A., and Katsura, T., 1964, Chemical composition of Hawaiian lavas: Jour. Petrol., v. 5, p. 82-133.

Martin, R. F., and Piniwinskii, A. J., 1972, Magmatism and tectonic settings: Jour. Geophys. Res., v. 77, p. 4966-4975.

McGregor, J. D., 1964, Geology of the Ellsworth quadrangle and vicinity, Maine: Ph.D. dissert., Univ. Illinois, Urbana, 116 p.

McKerrow, W. S., and Ziegler, A. M., 1971, The Lower Silurian paleogeography of New Brunswick and adjacent areas: Jour. Geol., v. 79, p. 635-696.

Metzger, W. J., and Bickford, M. E., 1972, Rb-Sr chronology and stratigraphic relations of Silurian rocks, Mount Desert Island, Maine: Geol. Soc. Amer., Bull., v. 83, p. 497-504.

Metzger, W. J., Mose, D. G., and Nagel, M. S., 1982, Rb-Sr whole-rock ages of igneous rocks in the vicinity of Mount Desert Island, coastal Maine: Northeastern Geology, v. 4, p. 33-38.

Mitchell, C. B., 1986, Field and textural evidence for commingling of felsic and mafic magmas on Vinalhaven Island, Maine: Geol. Soc. Amer., Abs. with Prog., v. 18, p. 56.

Nesbitt, H. W., 1980, Genesis of the New Quebec and Adirondack granulites: evidence for their production by partial melting: Contrib. Mineral. Petrol., v. 72, p. 303-310.

Novak, S. W., 1979, Contact metamorphism of the Lucerne pluton, Hancock County, Maine: M.S. thesis, Virginia Polytechnic Institute and State Univ., Blacksburg, Virginia, 108 p.

Osberg, P. H., 1974, Foreword, *in* Osberg, P. H. (ed.), New England Intercollegiate Geological Conference guidebook for field trips in east-central and north-central Maine, p. iii-xv.

Osberg, P. H., 1978, Synthesis of the geology of the northeastern Appalachians, U.S.A., *in* Caledonian-Appalachian orogen of the north Atlantic region: Project 27 Intl. Geol. Correlation Project: Geol. Surv. Canada, Pap. 78-13, p. 137-148.

Osberg, P. H., Hussey, A. M., II, and Boone, G. M., 1985, Bedrock geologic map of Maine: Maine Geol. Surv., scale 1:500,000.

Page, L. R., 1968, Devonian plutonic rocks in New England, *in* Zen, E-an, White, W. S., Hadley, J. B., and Thompson, J. B., Jr. (eds.), Studies of Appalachian geology: northern and maritime: Interscience, New York, p. 371-383.

Payette, C., and Martin, R. F., 1987, The Welsford igneous complex, southern New Brunswick: rift related Acadian magmatism, in Current Research, Part A: Geol. Surv. Canada, Paper 87-1A, p. 239-248.

Peacock, M. A., 1931, Classification of igneous rock series: Jour. Geol., v. 39, p. 54-67.

Petro, W. L., Vogel, T. A., and Wilband, J. T., 1979, Major element chemistry of plutonic rock suites from compressional and extensional plate boundaries: Chemical Geol., v. 26, p. 217-235.

Phillips, J. D., Goldsmith, R., and Stewart, D. B., 1985, The regional setting of the Quebec-Western Maine seismic reflection profile: Geol. Soc. Amer., Abs. with Prog., v. 17, no. 1, p. 58.

Pinette, S. R., 1983, Stratigraphy, structure, metamorphism and volcanic petrology of islands in east Penobscot Bay, Maine: M.S. thesis, Univ. Maine, Orono, 140 p.

Pitcher, W. S., 1978, The anatomy of a batholith: Jour. Geol. Soc., London, v. 135, part 2, p. 157-182.

Pitcher, W. S., 1979, The nature, ascent and emplacement of granitic magmas: Jour. Geol. Soc., London, v. 136, p. 627-662.

Pitcher, W. S., 1982, Granite type and tectonic environment, *in* Hsu, K. J. (ed.), Mountain building processes: Academic Press Inc., London, p. 19-40.

Pitcher, W. S., 1983, Granite: typology, geological environment, and melting relationships, *in* Atherton, M. P., and Gribble, C. D. (eds.), Migmatites, melting and metamorphism: Proceedings of the Geochemical group of the Mineralogical Society, Shiva Publishing Ltd., p. 277-285.

Poole, W. H., 1976, Plate tectonic evolution of the Canadian Appalachian region: Report of activities, part B, Geol. Surv. Canada, p. 113-126.

Rast, N., and Stringer, P., 1975, Recent advances and interpretation of geological structures of New Brunswick: Geoscience Canada, v. 2, p. 15-25.

Reid, J. B., Jr., Evans, O. C., and Fates, D. G., 1983, Magma mixing in granitic rocks of the central Sierra Nevada, California: Earth Planet. Sci. Lett., v. 66, p. 243-261.

Ruitenberg, A. A., and Ludman, A., 1978, Stratigraphy and tectonic setting of early Paleozoic sedimentary rocks of the Wirral-Big Lake area, southwestern New Brunswick and southeastern Maine: Can. Jour. Earth Sci., v. 15, p. 22-32.

Russell, L. M., 1984, Petrogenesis of a migmatite, Penobscot County, Maine: ultrametamorphism or intrusion?: M.S. thesis, Virginia Polytechnic Institute and State Univ., Blacksburg, Virginia, 290 p.

Russell, L. M., and Wones, D. R., 1984, Petrogenesis of a migmatite, Penobscot County, Maine: ultrametamorphism or intrusion?: Geol. Soc. Amer., Abs. with Prog., v. 16, p. 61.

Shand, S. J., 1955, The eruptive rocks: J. Wiley and Sons, New York, 488 p.

Shaw, D. M., 1968, A review of K-Rb fractionation trends by covariance analysis: Geochim. Cosmochim. Acta, v. 32, p. 573-601.

Spooner, C. M., and Fairbairn, H. W., 1970, Relation of radiometric age of granitic rocks near Calais, Maine, to the time of Acadian orogeny: Geol. Soc. Amer., Bull., v. 81, p. 3663-3670.

Stewart, D. B., 1956, Rapakivi granite of the Deer Isle region, Maine: Ph.D. dissert., Harvard Univ., Cambridge, Mass., 150 p.

Stewart, D. B., 1974, Precambrian rocks of Seven Hundred Acre Island and development of cleavage in the Isleboro Formation, *in* Osberg, P. H. (ed.), New England Intercollegiate Geological Conference guidebook for field trips in east-central and north-central Maine, p. 86-90.

Stewart, D. B., Arth, J. G., and Flohr, M. J. K., 1988, Petrogenesis of the South Penobscot intrusive suite, Maine, *in* Sinha, A. K., Hewitt, D. A., and Tracy, R. J. (eds.), Frontiers in petrology: Am. Jour. Sci., v. 288-A, p. 75-114.

Stewart, D. B., Unger, J. D., and Phillips, J. D., 1985, Quebec-Western Maine seismic reflection profile 3B across the coastal volcanic belt Maine: Geol. Soc. Amer., Abs. with Prog., v. 17, p. 64.

Stewart, D. B., Unger, J. D., Phillips, J. D., Goldsmith, R., Poole, W. H., Spencer, C. P., Green, A. G., Loiselle, M. C., and St-Julien, P., 1986, The Quebec western Maine seismic reflection profile: setting and first years results, *in* Reflection seismology: the continental crust: Am. Geophys. Union, Geodynamics Series, v. 14, p. 189-199.

Stewart, D. B., and Wones, D. R., 1974, Bedrock geology of northern Penobscot Bay area, *in* Osberg, P. H. (ed.), New England Intercollegiate Geological Conference guidebook for field trips in east-central and north-central Maine, p. 223-239.

Streckeisen, A. L., 1976, To each plutonic rock its proper name: Earth Sci. Rev., v. 12, p. 1-33.

Sweeney, J. F., 1972, Detailed gravity investigation of the shapes of granitic intrusives, south-central Maine, and implications regarding their mode of emplacement: Ph.D. dissert., Univ. New York, Buffalo, 122 p.

Sweeney, J. F., 1976, Subsurface distribution of granitic rocks, south-central Maine: Geol. Soc. Amer., Bull., v. 87, p. 241-249.

Taylor, H. P., and Silver, L. T., 1978, Oxygen isotope relationships in plutonic igneous rocks of the Peninsular Range batholith, southern and Baja California: U.S. Geol. Surv., Open-File Rept. 78-701, p. 423-426.

Taylor, T. R., Vogel, T. A., and Wilband, J. T., 1980, The composite dikes at Mount Desert Island Maine: an example of co-existing acidic and basic magmas: Jour. Geol., v. 88, p. 433-444.

Terzaghi, R. D., 1946, Petrology of the Columbia Falls quadrangle, Maine: Maine Geol. Surv., Bull. 3, 18 p.

Thompson, A. B., and Tracy, R. J., 1977, Anatectic melting reactions in pelitic rocks: Am. Geophys. Union Trans. v. 58, p. 520.

Thompson, J. F. H., 1984, Acadian synorogenic mafic intrusions in the Maine Appalachians: Am. Jour. Sci., v. 284, p. 462-483.

Trefethen, J. M., 1944, Mount Waldo batholith and associated igneous rocks, Waldo County, Maine: Geol. Soc. Amer., Bull., v. 55, p. 895-904.

Unger, J. D., Stewart, D. B., and Phillips, J. D., 1986, A deep seismic reflection profile across the Merrimack synclinorium and coastal antiform of central Maine: Geol. Soc. Amer., Abs. with Prog., v. 18, p. 73.

Wager, L. R., and Bailey, E. B., 1953, Basic magma chilled against acid magma: Nature, v. 172, p. 68-69.

Wager, L. R., and Brown, G. M., 1968, Layered igneous rocks: Oliver and Boyd, Edinburgh and London, 588 p.

Wanless, R. K., Stevens, R. D., La Chance, G. R., and Delabio, R. N., 1973, Age determinations and geological studies (K-Ar isotopic ages report 11): Geol. Surv. Canada, Paper 73-2, p. 84-87.

Ward, J. G., 1972, Petrology of the rapakivi granite of the Great Wass Island pluton, Washington County, Maine: Ph.D. dissert., Univ. Illinois, Urbana, 236 p.

Westerman, D. S., 1972, Petrology of the Pocomoonshine gabbro-diorite, Big Lake quadrangle, Maine: Ph.D. dissert., Lehigh Univ., Bethlehem, Penn., 175 p.

Westerman, D. S., 1980, Geologic map of the Wesley 15' quadrangle Maine: Maine Geol. Surv., Open-File Map 81-90.

Westerman, D. S., 1981, Whole-rock chemistry and tectonic history of the Pocomoonshine gabbro-diorite, central Washington County, Maine: Geol. Soc. Amer., Abs. with Prog., v. 13, p. 183.

Whalen, J. B., 1986, A-type granites in New Brunswick, *in* Current Research, Part A: Geol. Surv. Canada, Paper 86-1A, p. 297-300.

Whalen, J. B., Currie, K. L., and Chappell, B. W., 1987, A-type granites: geochemical characteristics, discrimination and petrogenesis: Contrib. Mineral. Petrol., v. 95, p. 407-419.

White, A. J. R., and Chappell, B. W., 1977, Ultrametamorphism and granitoid genesis: Tectonophysics, v. 43, p. 7-22.

White, A. J. R., and Chappell, B. W., 1983, Granitoid types and their distribution in the Lachlan Fold Belt, southeastern Australia, *in* Roddick, J. A. (ed.), Circum-Pacific plutonic terranes: Geol. Soc. Amer., Mem. 159, p. 21-34.

Williams, H., and Hatcher, R. D., Jr., 1982, Suspect terranes and accretionary history of the Appalachian orogen: Geology, v. 10, p. 530-536.

Williams, H., and Hatcher, R. D., Jr., 1983, Suspect terranes: a new look at the Appalachian orogen, *in* Hatcher, R. D., Jr., Williams, H., and Zietz, I. (eds.), Contributions to the tectonics and geophysics of mountain chains: Geol. Soc. Amer., Mem. 158, p. 33-53.

Wingard, P. S., 1961, Geology of the Castine-Blue Hill area, Maine: Ph.D. dissert., Univ. Illinois, Urbana, 138 p.

Wingard, P. S., and Brookins, D. G., 1964, Age of basic dikes on the Castine-Blue Hill peninsula Maine: Geol. Soc. Amer., Spec. Pap. 82, p. 226.

Wones, D. R., 1976a, The Penobscot Bay area of Maine, *in* Pajari, G. E., Jr. (ed.), Field guide to the geology and plutonic rocks of southwest New Brunswick and the Penobscot Bay area of Maine: I.G.C.P. Project 27, Dept. Geology, Univ. of New Brunswick, New Brunswick, Canada, p. 69.

Wones, D. R., 1976b, Phanerozoic plutons of New England: Geol. Soc. Amer., Abs. with Prog., v. 8, p. 303-304.

Wones, D. R., 1980a, Contributions of crystallography, mineralogy, and petrology to the geology of the Lucerne pluton, Hancock County, Maine: Am. Mineral., v. 65, p. 411-437.

Wones, D. R., 1980b, A comparison between granitic plutons of New England, U.S.A. and the Sierra Nevada batholith, California, *in* Wones, D. R. (ed.), The Caledonides in the U.S.A., I.G.C.P. Project 27, p. 123-130.

Wones, D. R., 1981, Mafic silicates as indicators of intensive variables in granitic magmas: Mining Geol., v. 31(4), p. 191-212.

Wones, D. R., 1984, Gravity studies of subsurface mass distributions of granitic rocks in Maine and New Hampshire, a discussion: Am. Jour. Sci., v. 284, p. 792-794.

Wones, D. R., and Sinha, A. K., 1988, A brief review of early Ordovician to Devonian plutonism in the North American Caledonides, *in* Harris, A. L., and Fettes, D. J. (eds.), The Caledonian-Appalachian orogen: Geol. Soc. London, Spec. Pub. 38, p. 381-388.

Wones, D. R., and Stewart, D. B., 1976, Middle Paleozoic right-lateral strike-slip faults in central coastal Maine: Geol. Soc. Amer., Abs. with Prog., v. 8, p. 304.

Wones, D. R., and Thompson, W. B., 1979, The Norumbega fault zone: a major regional structure in central eastern Maine: Geol. Soc. Amer., Abs. with Prog., v. 11, p. 60.

Zartman, R. E., and Gallego, M. D., 1979, Radiometric ages: Compilation B, U.S. Geol. Surv., *in* Marvin, R. F., and Dobson, S. W. (eds.), Isochron West, The Bulletin of Isotopic Geochronology, no. 26, p. 18-19.

Zartman, R. E., Hurley, P. M., Krueger, H. W., and Giletti, B. J., 1970, A Permian disturbance of K-Ar radiometric ages in New England: its occurrence and cause: Geol. Soc. Amer., Bull., v. 81, p. 3359-3374.

Zen, E-an, 1983, Exotic terranes in the New England Appalachians - limits, candidates, and ages: a speculative essay, *in* Hatcher, R. D., Jr., Williams, H., and Zietz, I. (eds.), Contributions to the tectonics and geophysics of mountain chains: Geol. Soc. Amer., Mem. 158, p. 55-81.

Maine Geological Survey
Studies in Maine Geology: Volume 4
1989

Commingled Gabbroic and Granitic Magmas in the Northern Bays-of-Maine Igneous Complex, Calais Area

Malcolm D. Hill
Department of Geology
Northeastern University
Boston, Massachusetts 02115

Richard N. Abbott, Jr.
Department of Geology
Appalachian State University
Boone, North Carolina 28608

ABSTRACT

Field evidence from the northeastern end of the Bays-of-Maine Igneous Complex shows that coeval mafic and felsic magmas intruded the region during the Devonian. An intrusive complex of diabase pillows in a matrix of granite underlies an extensive region south of Calais, Maine, including much of the area occupied by the Baring portion of the Moosehorn National Wildlife Refuge. The mafic component displays a variety of contact features including: (1) fine-grained, quenched margins, pillowed form, with sharp boundaries against the granite matrix; (2) medium-grained, non-quenched margins, pillowed form, with diffuse contacts against the granite matrix; and (3) angular, brecciated fragments set in granite matrix, with either sharp or diffuse contacts with granite matrix. In some areas, the pillowed complex forms dikes within gabbro bodies.

The abundance of well-preserved pillows suggests that relatively little blending or homogenization of the basalt and rhyolite occurred at the level of outcrop exposure. Hence, we prefer the term "magma commingling" as used by Mitchell (1986) and Mitchell and Rhodes (this volume), rather than "magma mixing" for the event recorded in this area. When the basalt and rhyolite were juxtaposed, the viscosity of the basalt rose to a value higher than that of the rhyolite matrix, and a variety of pillow-matrix boundary types developed. Many pillows exhibit granite-healed, planar fractures, demonstrating a final, brittle stage in the evolution of the pillow-matrix system, before final crystallization of the matrix.

This bimodal basalt-rhyolite magmatism in the Bays-of-Maine Igneous Complex mimics the compositional features found in the Siluro-Devonian coastal volcanic belt and provides additional support for the hypothesis that these two major igneous complexes in coastal Maine are related.

INTRODUCTION

In this report we describe field relationships which indicate extensive commingling of felsic and mafic magmas near Calais, Maine, at the northeastern end of Chapman's (1962) Bays-of-Maine Igneous Complex. These observations derive from ongoing field studies in the Calais 15' quadrangle (Ludman and Hill, 1986, in prep.) and in the adjoining Devils Head, Red Beach, and Robbinston 7.5' quadrangles (Abbott, 1977, 1986).

The Bays-of-Maine Igneous Complex (Chapman, 1962) is an assemblage of granite and gabbro plutons extending from Penobscot Bay northeastward into New Brunswick. According

TABLE 1. SUMMARY OF PUBLISHED AGES (Ma) FROM THE CALAIS, MAINE, REGION.

	Rb-Sr	K-Ar	Reference
Red Beach granite	385 ± 6[a]		3
Red Beach granite	393[b]	415, 409 (bio.)	1
Charlotte granite	404[b]	414 (bio.)	1
Meddybemps granite	375[b]	412, 361 (bio.)	1
St. George pluton (New Brunswick)	386 ± 20[c]	399 (hbl.) 393 (bio.)	5
St. Stephen gabbro		418 (hbl.) 360 (bio.)	6
Eastport Fm. volcanics (intruded by Red Beach granite)	399 ± 3[c]		2
Pocomoonshine Lake gabbro		431 ± 24 (hbl.)	4

[a]Rb-Sr mineral isochron.
[b]Rb-Sr mica age.
[c]Rb-Sr whole rock age.
All ages recalculated from the original sources using the new decay constants for ^{87}Rb and ^{40}K from Steiger and Jaeger (1977).
References: (1) Faul et al., 1963; (2) Fullagar and Bottino, 1970; (3) Spooner and Fairbairn, 1970; (4) Westerman, 1972, 1973; (5) Pajari et al., 1974; (6) Wanless et al., 1973.

to Chapman (1962), the mafic magmatism preceded the felsic magmatism. In contrast, Mitchell (1986) and Mitchell and Rhodes (this volume) cited evidence for coexisting rhyolitic and basaltic magma at the southwestern end of the complex (Vinalhaven Island). We report similar observations from the northeastern end.

The Bays-of-Maine Igneous Complex is predominantly Devonian in age, although some of the gabbro may be Silurian. Table 1 summarizes the geochronological data published for rocks in the Calais area.* Westerman (1972, 1973) reported an age of 431±24 Ma for hornblende from the Pocomoonshine Lake gabbro in the Big Lake 15' quadrangle immediately west of our study area. In the Calais area (Fig. 1), the Red Beach granite (Amos, 1963; Abbott, 1986) intrudes the Eastport Formation of early Devonian or younger age (Berdan, 1971) and is in turn unconformably overlain by the Upper Devonian Perry Formation (Amos, 1963; Schluger, 1973; Abbott, 1986). Fullagar and Bottino (1970) obtained an age of 399±3 Ma for the Eastport Formation, dominated by data for the rhyolites. Spooner and Fairbairn (1970) reported a Rb-Sr whole rock "age" of approximately 392 Ma, obtained by combining data for the Charlotte granite, Meddybemps granite, and the Red Beach granite (Fig. 1), onto a single diagram. Faul et al. (1963) reported K-Ar ages of 414 Ma for the Charlotte granite, 412 and 361 Ma for the Meddybemps granite, and 415 and 409 Ma for the Red Beach granite. Spooner and Fairbairn (1970) determined a Rb-Sr mineral isochron age of 385±6 Ma for the Red Beach granite.

*All ages cited have been recalculated from the original references using the new decay constants suggested by Steiger and Jaeger, 1977. The conversion factors published in Dalrymple (1979) were used to correct all K-Ar ages.

It is clear from inspecting Table 1 that additional work is needed to clarify the ages of plutons in the Calais area - a conclusion that is not new to workers in this region. The Eastport Formation (399 Ma) is intruded by both the Charlotte granite and the Red Beach granite, hence the recalculated K-Ar ages for those plutons (409-415 Ma) are too old, if the Rb-Sr age for the Eastport Formation is correct. Although the field evidence we describe below suggests that mafic and felsic magmas coexisted during at least part of the Devonian, the uncertainty in ages precludes addressing questions such as the length of time during which gabbroic magmas were injected into the crust, and whether there are genetic links between the gabbroic plutonism and the granitic magmatism in toto.

PETROLOGY OF COMMINGLED PLUTONIC UNITS

Amos (1963) subdivided the plutons in the Calais area into seven units: (1) norite and gabbro; (2) diorite; (3) the Baring granite; (4) the Meddybemps granite; (5) the Charlotte granite; (6) the granite of Magurrewock Lakes; and (7) the Red Beach granite. Our field studies indicate that extensive commingling

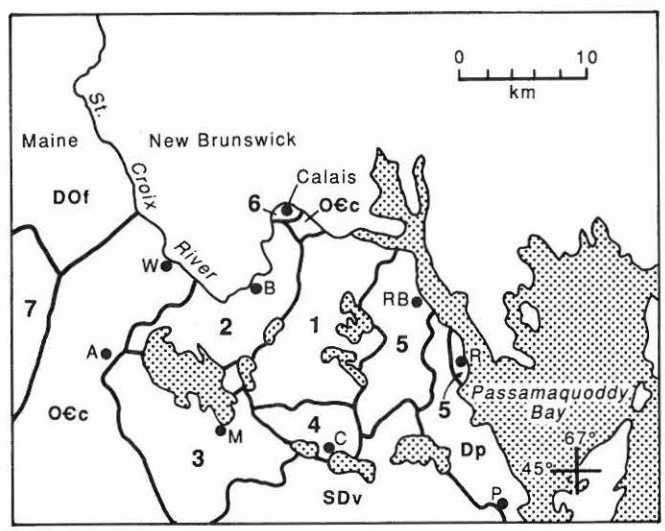

Figure 1. Generalized geologic map of the Calais area, Maine after Osberg et al. (1985). Plutonic units: (1) Zone of extensive magma commingling, approximately coincident with the "diorite" unit of Amos (1963). This unit contains gabbro, diorite, granodiorite, dikes, and irregular zones of diabase pillows in a granite matrix, and mixed rocks of hybrid compositon which are not easily separable, even at map scales greater than 1:24,000. (2) Baring granite. (3) Meddybemps granite. (4) Charlotte granite. (5) Red Beach granite. (6) St. Stephen gabbro. (7) Pocomoonshine gabbro. Not shown: small bodies of the granite of Magurrewock Lakes. Sedimentary and volcanic rock units: (OCc) Cookson Fm. (SDv) Maine coastal volcanics: Eastport, Edmunds, Leighton and Quoddy Formations. (DOf) Flume Ridge Fm. (Dp) Perry Fm. Geographic locations: (A) Alexander; (B) Baring; (C) Charlotte; (M) Meddybemps; (P) Perry; (R) Robbinston; (RB) Red Beach; (W) Woodland. Areas with dot pattern = lakes.

has occurred between mafic and felsic magma. The evidence comes mostly from Amos' (1963) diorite unit, which we have incorporated into our map unit 1 (Fig. 1). This unit is extremely heterogeneous, consisting of (1) gabbro (plagioclase with An > 50); (2) diorite (plagioclase with An < 50); (3) granodiorite; (4) dikes and irregular zones of diabase pillows in a granitic matrix; and (5) mixed rocks of hybrid composition. The granitic rocks in this unit are most likely related to the Baring granite. We emphasize that all of these compositions are contained within the composite unit labeled "1" on Figure 1; a description of each of the units follows. For more detailed field relations, see the maps in Abbott (1986) and Ludman and Hill (in prep.).

Gabbro

A wide range of gabbroic compositions occurs in the Calais region, including olivine gabbro, norite, anorthositic norite, hypersthene gabbro, hornblende gabbro, and leucogabbro (Amos, 1963; Westerman, 1972, 1973; Coughlin, 1983). The gabbros generally contain plagioclase (An_{70-40}), hornblende, augite, orthopyroxene, biotite, magnetite, sphene, and apatite. Some samples contain either olivine or quartz ± orthoclase. Secondary chlorite, sericite, and epidote also occur. Generally, the gabbro is homogeneous in outcrop scale although locally, rhythmic bedding is well-developed, as at Staples Mountain in the Calais quadrangle (Coughlin, 1983; Ludman and Hill, 1986, in prep.) and at Pocomoonshine Mountain in the Big Lake quadrangle (Westerman, 1972, 1973). We have found that areas shown on Amos' (1963) map as "norite-gabbro" generally contain a distinctive, porphyritic gabbro with buff to tan plagioclase phenocrysts up to 4 cm in diameter.

Diorite

Diorite (sensu stricto - plagioclase < An_{50}) is the predominant mafic plutonic component within the Calais quadrangle. The diorite lacks olivine, and clinopyroxene occurs as relict cores in hornblende grains, rather than as the discrete grains which occur in the gabbro bodies. Except for a few olivine-rich gabbros, the color index of many of the diorites is as high as that in some gabbro. The diorites are predominantly plagioclase-hornblende-biotite-bearing rocks; the hornblende:biotite ratio varies from >1 to <1. Interstitial quartz occurs in some diorites. In some areas, a distinctive foliated diorite with igneous laminations of hornblende-rich and feldspar-rich bands occurs. These occur in discontinuous, isolated outcrops in the Calais quadrangle (Ludman and Hill, in prep.).

Granodiorite

Granodiorite, within unit 1 of Figure 1, occurs primarily in northeast-southwest elongate bodies that intruded gabbro. The granodiorite is intruded by the Red Beach granite, Charlotte granite, and smaller bodies of biotite granite. The last of these belong to Amos' (1963) granite of Magurrewock Lakes. Typically, the granodiorite contains plagioclase (An_{50-29}), hornblende, biotite, quartz, perthite, magnetite, and apatite. Chlorite, epidote and sericite are secondary minerals. This unit displays gradational compositional variations over a wide range, from diorite and quartz diorite to granite.

At the southwest end of the Bays-of-Maine Igneous Complex, Mitchell (1986) noted that local patches of granodiorite were formed by mixing between basaltic pillows and the surrounding rhyolite matrix. He suggested that large, homogeneous granodiorite plutons, which intrude the felsic-mafic pillowed complex, might have formed by more efficient blending of the two compositions at depth.

Mixed Rocks

The mixed rocks unit of Abbott (1986), within unit 1 of Figure 1, consists of rounded to angular inclusions of gabbro, with smaller proportions of diabase pillows (see following description and Figs. 3, 6). The inclusions and diabase pillows are set in a dioritic to granitic matrix of variable composition. Where the volume percent of inclusions or the degree of disaggregation of the inclusions is great, the color index of the rock is high. Fragments of gabbro range in size from centimeters up to hundreds of meters, while the diabase pillows are usually less than 30 cm in size, but can reach 2 m or more. The rocks form a continuum from essentially inclusion-free granodiorite to essentially homogeneous gabbro. At one extreme, the unit might best be described as brecciated gabbro; at the other, as granodiorite with sporadic inclusions of gabbro. Consequently, the placement of the contact between the mixed rocks and the gabbro, and that between the mixed rocks and the granodiorite is somewhat subjective.

There are two modes of occurrence of this mixed rock unit: (1) as a border facies of the granodiorite intrusions, and (2) as isolated patches in the gabbro. The second mode of occurrence may represent apophyses of the first in the fractured roofs of subjacent bodies of granodiorite. The different areas of granodiorite exposed at the surface may all be parts of a single body.

Pillow Diabase

Diabase is found sporadically throughout the northern part of the area, where it is integrally related to gabbro, granite, and granodiorite. Within our study area, diabase occurs only as pillows or fragmented inclusions in an intermediate or felsic host. Dikes or other intrusive forms of diabase have not been observed to crosscut any of the gabbroic or granitic bodies in the area.

The diabase pillows have a variety of forms and a wide range of sizes up to several meters. The shapes include (1) simple well-rounded pillows (Fig. 2a); (2) crenated pillows, outward-pointing lobes alternating with inward-pointing cusps (Figs. 2b,

Figure 2. Nature of the boundary between diabase pillows and surrounding granite matrix. (a) Simple, well-rounded diabase pillows. (b) Crenate pillow. (c) Margin of an amoeboid pillow. Scale bar is 25 cm.

3, 4); (3) amoeboid pillows, outward-pointing lobes alternating with inward-pointing lobes (Fig. 2c); and (4) angular inclusions (Fig. 5). For each type of inclusion the margins may be sharp or diffuse. The composition of the surrounding material becomes more mafic as the margins of the pillows become more diffuse. The simple, well-rounded pillows commonly occur in aggregates in which the pillows have been deformed against one another (Fig. 2a). This deformation suggests that the diabase was plastic when it was in contact with the felsic host.

The proportion of the matrix varies substantially, regardless of the pillow type, from isolated pillows in an otherwise homogeneous felsic matrix to more than 90% pillows. In the latter case, the pillows tend to have coalesced, perhaps by gravity settling, such that most of the interstitial felsic magma has been expelled. Commonly, all that remains of the matrix is a thin film between pillows and anti-crenated volumes of felsic rock (inward-pointing lobes alternating with outward-pointing cusps).

Fine grained, thin (2 to 5 mm) rinds on the simple and crenate pillows have been interpreted to result from quenching. These rinds are predominantly composed of fine grained, brown-pleochroic biotite. Although similar biotite is present in the interiors of the pillows, it is much less abundant than hornblende. These relationships suggest some degree of chemical exchange across the mafic/felsic interface.

We have no evidence to indicate which component (felsic or mafic) was emplaced into the crust first. The basalt was quenched to form diabase pillows, whose initial shapes would be controlled by the surface tension of the congealing mafic magma against the surrounding felsic magma. This would produce the simple, rounded pillows. The crenated shapes may represent deformed pillows, or pillows that were frozen in the process of subdividing. The amoeboid pillows would indicate a more fluid interdigitation of the two magmas. The absence of quenched margins on the amoeboid pillows suggests that the felsic host for these pillows was unusually hot compared with the felsic magma which encased the simple and crenated pillows.

Many diabase pillows have been intruded along narrow fractures by the felsic matrix, presumably at a time when the pillows were essentially crystallized, but the matrix was still fluid (Fig. 3a). The angular diabase inclusions probably represent the fragments of more thoroughly fractured pillows (Fig. 5).

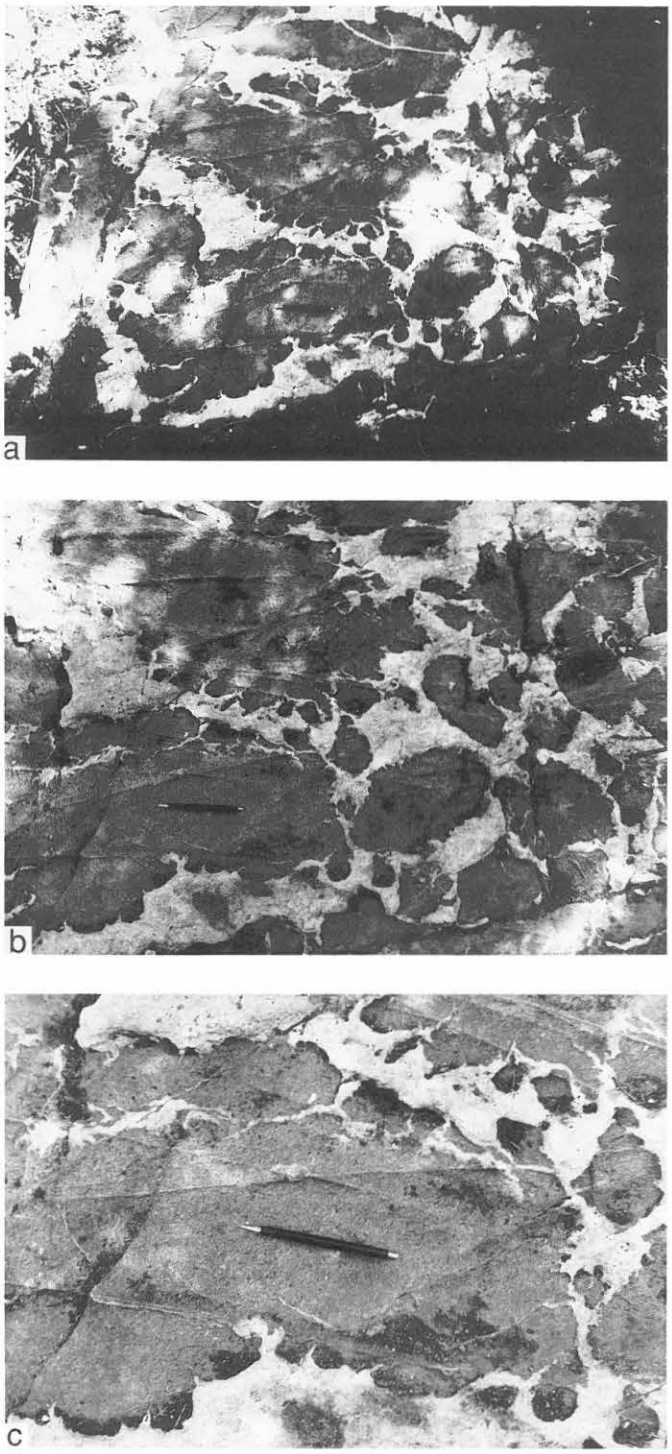

Figure 3. Pavement exposure of pillowed diabase in granite matrix, east of junction of South Ridge Trail and Beaver Trail, Moosehorn National Wildlife Refuge. Pencil is in the same position in each photo. (a) Note fractured pillow at top, healed by matrix granite. (b) Note presence of both cuspate (pillowed) and angular (brecciated) diabase blocks. (c) Close-up of pillowed diabase. The diabase at this locality exhibits quenched margins at granite contacts. However, the dark shading in the photo is caused by pine needles accumulated in the depressions left by weathering of the less resistant diabase. Silicified joints which crosscut the diabase were more resistant to weathering.

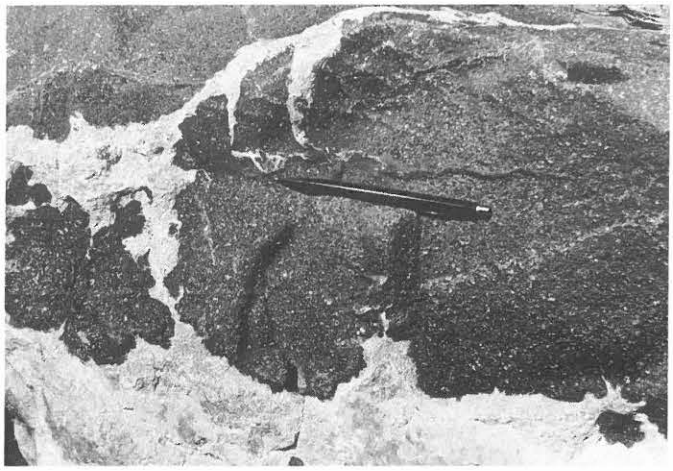

Figure 4. Plagioclase-phyric diabase pillow in granite matrix, Snare Meadow, Moosehorn National Wildlife Refuge. Pencil for scale. Dark rind in diabase at granite contact marks the quenched margin of the pillow. Note evidence near the pencil tip for fracture and rotation of the diabase pillow while the granite could still flow.

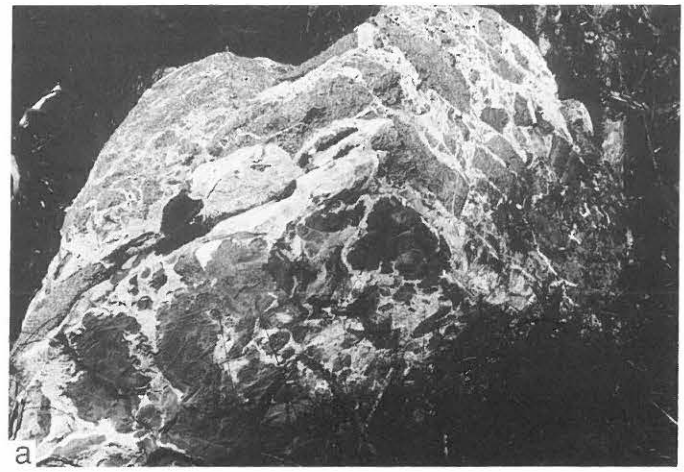

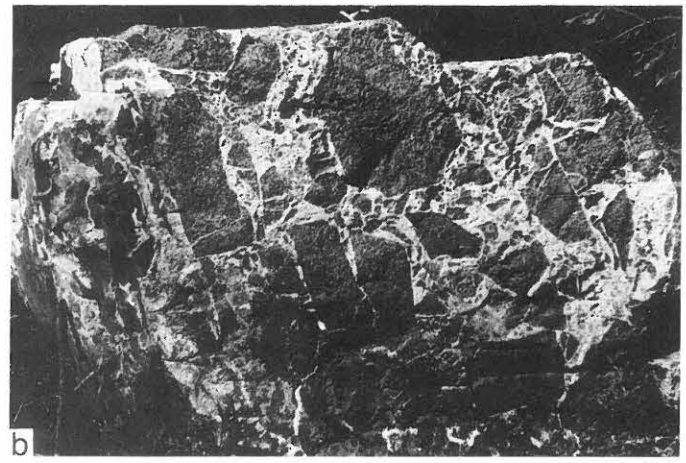

Figure 5. Two sides of a single, 1.5 m float block along the Beaver Trail, near Mahar Flowage, Moosehorn National Wildlife Refuge. (a) Pillowed and brecciated diabase in granite matrix. (b) Primarily brecciated diabase fragments in granite matrix. The large octagonal fragment at top-center, as well as the two rectangular fragments below it, can easily be located in the upper-right face of the block in Fig. 5a.

Angular gabbro fragments are commonly medium-grained equigranular immediately adjacent to the granite contacts; they show no evidence of quenching.

Diabase pillow complexes, i.e., diabase plus felsic matrix, locally constitute dikes, rarely exceeding 4 meters in width, in the gabbro. Angular fragments of gabbro are also present in the granodiorite matrix of these dikes and the walls are rarely exposed. Figure 6 is a sketch map of one side of a diabase pillow dike. The dike trends north-south and is zoned with respect to the proportion of diabase pillows. There is a swarm of north-south-trending diabase pillow dikes cutting the gabbro immediately south of Vose Pond.

Diabase pillows as well as angular fragments of gabbro also characterize the mixed rocks associated with the granodiorite unit. It may be that the diabase pillow dikes are simply apophyses of these mixed rocks. If so, then, in accordance with Mitchell's (1986) model, the whole of the granodiorite may be a well-homogenized hybrid of the diabasic magma and a granitic magma, with the diabase pillows being preserved only where quenched along the margins of the granodiorite (mixed rocks) and in dikes.

Baring Granite

The Baring granite (unit 2 on Fig. 1) is a medium to coarse grained biotite ± hornblende granite. Most samples have a seriate texture and contain quartz, plagioclase with minor zoning (An_{26-23} cores, An_{21} rims), perthitic microcline, biotite, hornblende, apatite, zircon, and opaque minerals. Allanite occurs in some samples, and myrmekitic intergrowths occur in some, but not all specimens. Generally, outcrops of Baring granite are massive and medium to coarse grained. Locally, there are coarse grained, porphyritic variants with alkali feldspars to 2-3 cm. A quenched, porphyritic facies, which we interpret as part of the Baring granite, with rapakivi mantling and inclusions of basalt blebs occurs locally adjacent to the diabase pillow zones.

Where the granite occurs as thin lenses or septa in the pillowed diabase or mixed rocks zones, the percentage of hornblende is noticeably higher than in outcrops of homogeneous granite. This effect is most strongly developed in outcrops which contain pillows or breccia fragments with diffuse boundaries. In other locations, particularly adjacent to diabase pillows which display very sharp, quenched margins against the granite, the granite is finer grained than normal Baring granite and contains an unusually low proportion of mafic minerals. The fine grain size of the matrix granite indicates a greater nucleation rate compared with normal Baring granite.

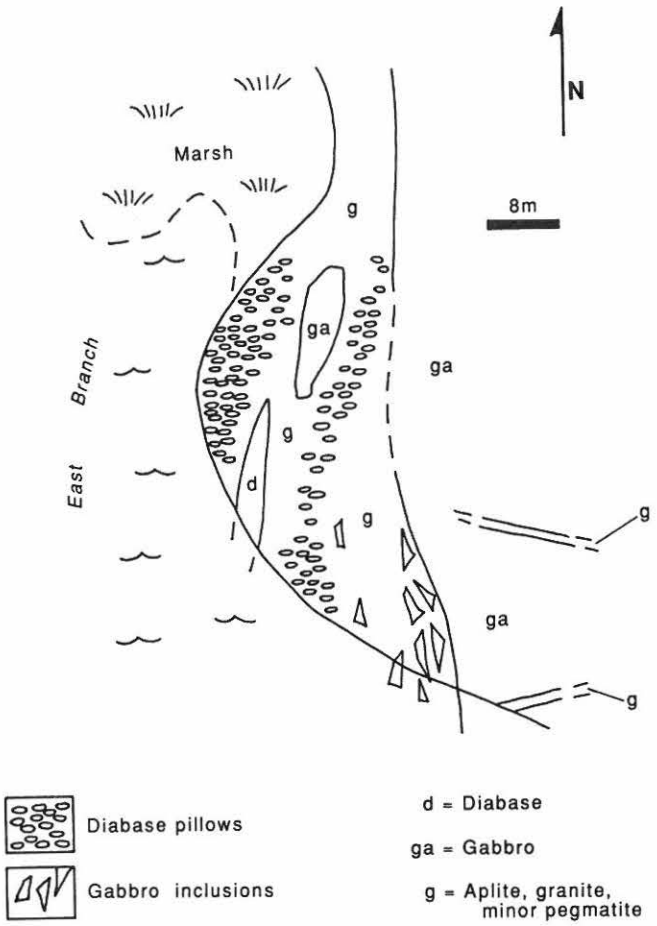

Figure 6. Map of east wall of a dike containing diabase pillows. The pillow complex is exposed on the east bank of East Branch, approximately 1 km. northeast of Vose Pond. Scale bar is 8 m.

The relative dearth of mafic minerals in the granite suggests either (1) that nucleation of quartz and feldspars was enhanced while nucleation of biotite and hornblende was suppressed at the (higher temperature? dryer?) contacts with the molten diabase; or (2) that some or all components needed to stabilize hydrous silicates (OH?) were effectively removed from the granite magma at the contact, presumably by diffusion into the "chilled" (800 - 1000°C ?) diabase pillow. We note (1) that scattered amygdules filled with quartz, biotite, and hornblende occur in some, but not all, of the quenched diabase pillows; and (2) the quenched margins of the diabase pillows are predominantly composed of fine-grained biotite - in contrast to the pillow interiors, where the predominant mafic silicate is hornblende.

DISCUSSION

In recent years, volcanologists have shown that eruptions from chemically zoned or stratified magma chambers are not uncommon in the geologic record (Hildreth, 1981; Bacon, 1986). There can be no doubt that juxtaposition of two magmas occurs and could be preserved in the plutonic regime as well (Reid et al., 1980; Reid and Eichelberger, 1981; Whalen, 1985; Mitchell, 1986; Mitchell and Rhodes, this volume; Whalen and Gariépy, 1986). The ellipsoidal to amoeboid forms and the presence of quenched margins in diabase pillows set in granite matrix demonstrate that magma commingling has been preserved over a wide outcrop area in the Calais region. The common observation of sharply-defined margins on the diabase pillows in the Calais area (Fig. 4) demonstrates that no substantial degree of mixing (or blending) of the two compositions has occurred at the present level of erosion. It is quite likely, however, that some degree of elemental and isotopic exchange has occurred across the pillow:matrix interface. The biotite-rich pillow rims and the increased hornblende content of some pillow-matrix granite compared with normal Baring granite in areas free of inclusions attests to local hybridization between the two magmas.

The textural preservation of the pillowed complex may derive from relatively rapid cooling at shallow depth. We discuss below the possibility that some of the magmatism recorded in the adjacent Silurian-Devonian coastal volcanic belt may be related to that which formed the Bays-of-Maine plutonic complex. If so, the lack of andesite compositions in the bimodal basalt-dacite/rhyolite volcanic suite of the Eastport Formation (Gates and Moench, 1981) also attests to limited mixing.

The presence of angular or brecciated inclusions of one igneous rock type in another is often taken to indicate a greater age for the type which forms the inclusions. We have observed a number of outcrops which contain both amoeboid pillows and brecciated fragments; indeed, in many cases, thin granite veins continuous with and indistinguishable from the granite interpillow matrix cut undoubted pillows into angular fragments (Fig. 3). Hence, these results suggest that not all angular inclusions within a plutonic matrix need predate the host. For those outcrops of Baring granite with abundant angular gabbroic inclusions, but lacking convincing evidence for pillows (such as those exposed along Rte. 1 approximately 1 km south of Rte. 9), extensive geochemical and mineralogical studies will be needed to relate the brecciated fragments to either known pillowed complexes or to gabbros which may predate the Baring granite - gabbro intrusive complex (J. Jerinski, Ph.D. dissert. in progress, Virginia Tech. Univ.).

Physical Conditions during Magma Commingling

Abbott (1977, 1987) estimated that the Red Beach granite, the youngest of the Acadian granites in the area, was emplaced at a depth of 0.8 - 1.5 km. Hill (Ludman and Hill, in prep.) summarized geochemical evidence which suggests that the Baring granite, Charlotte granite, Meddybemps granite, and granite of Magurrewock Lakes are of similar origin, and have some mineralogical and geochemical features akin to A-type granites (Loiselle and Wones, 1979). Abbott (1987) related

some of these, specifically the Charlotte granite and the granite of Magurrewock Lakes, to the Red Beach granite. Whalen (1986) described A-type granites related to the St. George batholith in New Brunswick, of similar age to the granites in the Calais area and immediately northeast of our study area. At the southern end of the Bays-of-Maine complex, on Vinalhaven Island, Mitchell and Rhodes (this volume) report granite with some A-type affinities commingled with basaltic pillows in virtually the same field associations as those we describe from the northern end of the complex.

Clemens et al. (1986) reported 1 kb melting experiments on an A-type granite; for 1% dissolved water, the solidus temperature is about 875°C, and the liquidus temperature is over 1000°C. The granite that Clemens et al. (1986) studied became water-saturated at about 4% H_2O for the 1 kb pressure of the experiments. Assuming that these results are relevant to the Baring granite, they indicate that the granite would have been at relatively high temperatures at the time of mixing with the basalt to form the pillowed complexes.

Thompson (1974) summarized the results of melting experiments on a variety of basalts from Skye, whose compositions may be analagous to those of the parent magmas which formed the gabbros in the Calais area. Liquidus temperatures vary between approximately 1160 - 1260°C, depending on the basalt composition; solidus temperatures are not as well constrained, but are at or below 1050°C. The common occurrence of plagioclase-porphyritic gabbro in the Calais area, and the occasional presence of distinct plagioclase phenocrysts (Fig. 4), coupled with the absence of olivine or pyroxene phenocyrsts in the quenched diabase pillows, is compatible with shallow crystallization of a relatively Fe-rich magma under hydrous conditions (see data summarized for Skye and Snake River Plain lavas in Thompson, 1972). The abundance of amphibole and late crystallization of biotite in many gabbro samples supports crystallization under hydrous conditions. Temperatures in the range of 1200 - 1150°C are indicated by these relationships (Thompson, 1972).

In his summary of structural studies in the plutonic Querigut Complex, Marre (1986) discussed contact relationships between mafic inclusions and felsic host rock which are similar to the crenate and amoeboid pillows and brecciated fragments we observe in the Calais area. He noted that, for inclusions (Marre's "enclaves") such as our crenated pillows with an oak-leaf-shaped outline (Fig. 2b), the material of greater viscosity forms rounded lobes while the material of lower viscosity fills the sharp embayments. Our simple and crenate pillows (Fig. 2a, 2b) would develop when the viscosity of chilling basalt was somewhat greater than that of the felsic matrix. If the viscosities of the mafic and felsic magmas were more closely matched, the amoeboid boundaries of Figure 2c featuring smoothly interdigitating lobes without any sharp embayments, would develop. The amoeboid texture in Figure 2c may develop preferentially along the boundaries of larger basaltic masses, which would have a greater thermal mass than small basalt pillows, allowing the basalt to retain higher temperatures and a lower viscosity for a longer period of time.

The inferences we have drawn from our field observations about the relative viscosities in the mafic and felsic components are in apparent conflict with experimental viscosity data. Crystal-free basalt at 1200°C has a significantly lower viscosity, approximately 2 to 3 log(poise) units (Murase and McBirney, 1973), than rhyolite at 1000°C. The viscosity of rhyolite with 10% dissolved water at 1000°C is approximately 4 log(poise) units, vs. approximately 8 for rhyolite with 1% dissolved H_2O at the same temperature (Shaw, 1965).

Two effects may provide the means to reverse the normal difference in viscosity between mafic and felsic magmas, and to explain our field observations. First, the viscosity of crystallizing basalt increases rapidly with increasing phenocryst content, especially when crystallization exceeds 20% (Shaw et al., 1968). Upon mixing, the hotter basalt and cooler rhyolite will approach thermal equilibrium; crystallization of the basalt will accelerate while the rhyolite may locally become superheated. Second, because the viscosity of a magma is inversely related to its temperature, the viscosity of the basalt will increase and the viscosity of the rhyolite will decrease at the interface between the two magmas. Together, these effects must be sufficiently large to reverse the normal viscosity contrast between magmas of basaltic vs. rhyolitic composition, in order to explain our observations as well as those of Mitchell (1986), Mitchell and Rhodes (this volume), Whalen (1985), and Whalen and Gariépy (1986).

Although some of the angular breccia fragments in the pillowed outcrops may represent preexisting mafic wall rocks intruded by the Baring granite, the presence of fractured pillows in many of the same outcrops can only be reconciled with brecciation of the congealing mafic component soon after the mixing event. The textures indicate that, upon mixing, the basalt coalesced into pillows with chilled margins. The pillows deformed plastically to form the range of shapes shown in Figure 2. Due to their greater solidus temperature, crystallization in the pillows proceeded more rapidly than in the granite matrix. Eventually, some pillows fractured while the granite was still molten. Marre (1986) noted that it is difficult to generate fractures within more viscous inclusions by transmitting stress through surrounding, less viscous matrix, and appealed to earthquake shocks traversing the pluton. Perhaps thermal stresses in radially cooling pillows could overcome the tensile strength of the crystallizing diabase body. The implied volume increase of the brecciated fragments could easily be accommodated if the surrounding, less viscous felsic magma was still largely or partly molten.

In some areas, the interpillow granite is relatively fine-grained and nearly devoid of mafic silicates. Although we have no data for the water contents of the granite or of the diabase pillows, it is likely that the basalt had a lower (OH) content than the rhyolite at the time they were juxtaposed. It is possible that the rhyolite may have lost (OH) to the pillows by diffusion across

the interface. This effect could explain the dearth of hydrous silicates in these fine-grained granite zones and may explain the biotite-rich selvages of quenched pillows.

Regional Implications

Gabbro, diabase, and basalt occur throughout the Silurian-Devonian coastal volcanic belt, indicating a long-standing source of basaltic magma from Early Silurian to Early Devonian time (Gates, 1975). Felsic volcanic rocks also occur throughout the sequence (Bastin and Williams, 1914; Gates, 1975). Gates and Moench (1981) noted that the coastal volcanic belt is essentially a bimodal basalt-dacite/rhyolite suite, and tentatively suggested that the adjacent Bays-of-Maine Igneous Complex might be genetically related, more likely to the Eastport Formation bimodal volcanism than to the Silurian bimodal suite (O. Gates, pers. commun., 1987). Our work at the northeastern end of this complex, and that of Mitchell (1986) and Mitchell and Rhodes (this volume) at the southwestern end, provides compelling evidence that mafic and felsic magmas were coeval in the Bays-of-Maine Igneous Complex. Geochemical studies are in progress by us, by Mitchell, and by Jerinski (Ph.D. dissert., Virginia Tech. Univ.) on various aspects of the Bays-of-Maine Igneous Complex which will permit further comparison with the eruptive suite in the coastal volcanic belt.

ACKNOWLEDGMENTS

We appreciate the support of the Maine Geological Survey for our studies in the Calais area. The work was supported in part by the U.S. Geological Survey Cooperative Geological Mapping (COGEOMAP) Program, Cooperative Agreement No. 14-08-0001-A0249. David R. Wones had begun the re-study of the plutonic rocks in the Calais quadrangle. Following Wones' untimely death, Hill was assigned to complete the Calais mapping, and wishes to acknowledge his debt to the results of Dave's first field season. Discussions with Allan Ludman, Marc Loiselle, Dick Naylor, and Krishna Sinha have been useful in developing our ideas. We thank Fran Robinson and Darryl and Wanda McClure of the University of Maine at Machias camp in Princeton for logistical support. Doug Mullen and the staff of the Moosehorn Wildlife Refuge in Calais kindly provided maps, air photos, and access to exposures in the Refuge. Carroll Stewart and Lesley Abbott provided able field assistance through a variety of field conditions, pleasant and otherwise. We very much appreciate the comments and suggestions made by the reviewers, Ollie Gates and Richard Gilman.

REFERENCES CITED

Abbott, R. N., Jr., 1977, Petrology of the Red Beach granite near Calais, Maine: Ph.D. dissert., Harvard Univ., Cambridge, Mass., 223 p.

Abbott, R. N., Jr., 1986, Preliminary report on the bedrock geology of the Devils Head, Robbinston, and Red Beach 7-1/2' quadrangles, Maine: Maine Geol. Surv., Open-File Rept. No. 86-73, 36 p.

Amos, D. H., 1963, Petrography and age of plutonic rocks, extreme southeastern Maine: Geol. Soc. Amer., Bull., v. 74, p. 169-194.

Bacon, C. R., 1986, Magmatic inclusions in silicic and intermediate volcanic rocks: Jour. Geophys. Res., v. 91, p. 6091-6112.

Bastin, E. S., and Williams, H. S., 1914, Eastport Folio, Maine: U.S. Geol. Surv., Folio 192.

Berdan, J. M., 1971, Silurian to Early Devonian ostracodes of European aspect from the Eastport quadrangle, Maine: Geol. Soc. Amer., Abs. with Prog., v. 3., p. 18.

Chapman, C. A., 1962, Bays-of-Maine Igneous Complex: Geol. Soc. Amer., Bull., v. 73, p. 883-887.

Clemens, J. D., Holloway, J. R., and White, A. J. R., 1986, Origin of an A-type granite: experimental constraints: Am. Mineral., v. 71, p. 317-324.

Coughlin, S., 1983, Geology of the Staples Mountain Complex, Calais quadrangle, eastern Maine: M.S. thesis, Queens College, Flushing, N.Y., 113 p.

Dalrymple, G. B., 1979, Critical tables for conversion of K-Ar ages from old to new constants: Geology, v. 7, p. 558-560.

Faul, H., Stern, T. W., Thomas, H. H., and Elmore, P. L. D., 1963, Age of intrusion and metamorphism in the northern Appalachians: Am. Jour. Sci., v. 261, p. 1-19.

Fullagar, P. D., and Bottino, M. L., 1970, Rb-Sr whole rock ages of Silurian-Devonian volcanics from eastern Maine, *in* Shorter contributions to Maine geology: Maine Geol. Surv., Bull. 23, p. 49-52.

Gates, O., 1975, Geologic map and cross-section of the Eastport quadrangle, Washington County, Maine: Maine Geol. Surv., Map GM-3, 19 p.

Gates, O., and Moench, R. H., 1981, Bimodal Silurian and Lower Devonian volcanic rock assemblages in the Machias-Eastport area, Maine: U.S. Geol. Surv., Prof. Paper 1184, 32 p.

Hildreth, W., 1981, Gradients in silicic magma chambers: implications for lithospheric magmatism: Jour. Geophys. Res., v. 86, p. 10153-10192.

Loiselle, M. C., and Wones, D. R., 1979, Characteristics and origin of anorogenic granites: Geol. Soc. Amer., Abs. with Prog., v. 11, p. 468.

Ludman, A., and Hill, M., 1986, Bedrock geology of the Calais 15' quadrangle, Maine: Maine Geol. Surv., Open-File Map 86-72, 46 p.

Ludman, A., and Hill, M., in prep., Bedrock geology of the Calais 15' quadrangle, Maine: Maine Geol. Surv., Open-File.

Marre, J., 1986, The structural analysis of granitic rocks: North Oxford Academic Publishers, Ltd. (Elsevier), Amsterdam, 123 p.

Mitchell, C. B., 1986, Field and textural evidence for commingling of felsic and mafic magmas on Vinalhaven Island, Maine: Geol. Soc. Amer., Abs. with Prog., v. 18, p. 56.

Murase, T., and McBirney, A. R., 1973, Properties of some common igneous rocks and their melts at high temperatures: Geol. Soc. Amer., Bull., v. 84, p. 3563-3592.

Osberg, P. H., Hussey, A. M., II, and Boone, G. M., 1985, Bedrock geologic map of Maine: Maine Geol. Surv., scale 1:500,000.

Pajari, G. E., Jr., Trembath, L. T., Cormier, R. F., and Fyffe, L. R., 1974, The age of the Acadian deformation in southwestern New Brunswick: Can. Jour. Earth Sci., v. 11, p. 1309-1313.

Reid, J. B., Jr., and Eichelberger, J. C., 1981, Basaltic droplets in silicic host magmas: a comparison of mixed magmas in volcanic and plutonic settings: Trans. Amer. Geophys. Union, v. 62, p. 433.

Reid, J. B., Jr., Evans, O. C., and Fates, D. G., 1980, Quenched droplets of basaltic magma in granites of the Pliny Range, NH: Geol. Soc. Amer., Abs. with Prog., v. 12, p. 507.

Schluger, P. R., 1973, Stratigraphy and sedimentary environments of the Devonian Perry Formation, New Brunswick, Canada and Maine, U.S.A.: Geol. Soc. Amer., Bull., v. 84, p. 2533-2548.

Shaw, H. R., 1965, Comments on viscosity, crystal settling, and convection in granitic magmas: Am. Jour. Sci., v. 263, p. 120-152.

Shaw, H. R., Peck, D. L., Wright, T. L., and Okamura, R., 1968, The viscosity of basaltic magma: an analysis of field measurements in Makaopuhi lava lake, Hawaii: Am. Jour. Sci., v. 266, p. 225-264.

Spooner, C. M., and Fairbairn, H. W., 1970, Relation of radiometric age of granitic rocks, near Calais, Maine, to the timing of the Acadian orogeny: Geol. Soc. Amer., Bull., v. 81, p. 3663-3670.

Steiger, R. H., and Jaeger, E., 1977, Subcomission on geochronology: convention on the use of decay constants in geo- and cosmo-chemistry: Earth Planet. Sci. Lett., v. 36, p. 359-362.

Thompson, R. N., 1972, The 1-atmosphere melting patterns of some basaltic volcanic series: Am. Jour. Sci., v. 272, p. 901-932.

Thompson, R. N., 1974, Primary basalts and magma genesis: I. Skye, Northwest Scotland: Contrib. Mineral. Petrol., v. 45, p. 317-341.

Wanless, R. K., Stevens, R. D., LaChance, D. R., and Delabio, R. N., 1973, Age determinations and geological studies, K-Ar isotopic ages: Report 11, Geol. Surv. Canada, Paper 73-2.

Westerman, D. S., 1972, Petrology of the Pocomoonshine gabbro-diorite, Big Lake quadrangle, Maine: Ph.D. dissert., Lehigh Univ., 175 p.

Westerman, D. S., 1973, Geologic history and age relations of some igneous and metamorphic rocks in southeastern Maine: Geol. Soc. Amer., Abs. with Prog., v. 5, p. 236.

Whalen, J. B., 1985, The McGerrigle plutonic complex, Gaspé, Quebec: evidence of magma mixing and hybridization, in Current Research, Part A: Geol. Surv. Canada, Paper 85-1A, p. 795-800.

Whalen, J. B., 1986, A-type granites in New Brunswick, *in* Current Research, Part A: Geol. Surv. Canada, Paper 86-1A, p. 297-300.

Whalen, J. B., and Gariépy, C., 1986, Petrogenesis of the McGerrigle plutonic complex, Gaspé, Quebec: a preliminary report, *in* Current Research, Part A: Geol. Surv. Canada, Paper 86-1A, p. 265-274.

Maine Geological Survey
Studies in Maine Geology: Volume 4
1989

Geochemistry of the Granite-Gabbro Complex on Vinalhaven Island, Maine

Christopher B. Mitchell
IEP, Inc.
P.O. Box 1136
Portsmouth, New Hampshire 03801

J. Michael Rhodes
Department of Geology and Geography
University of Massachusetts
Amherst, Massachusetts 01003

ABSTRACT

The bimodal granite-gabbro association on Vinalhaven Island, Maine has spectacular textural and structural relationships that are interpreted to have resulted from commingling of contemporaneous mafic and felsic liquids. During this process, the felsic and mafic magmas retained their identities and produced composite zones of chilled basaltic pillows in a granite matrix. Approximately 100 samples have been analyzed for whole-rock major and trace element abundances. These data have been used to classify the rocks and evaluate their relationships.

The granites are homogeneous, high SiO_2 (72.55-77.35 wt %), two-feldspar, biotite ± hornblende, I-type, crustal, minimum-melt granites, with similar compositions to other granites from the Maine coastal lithotectonic belt. The mafic rocks, medium-grained gabbros to diorites and fine-grained chilled basalt pillows, have a range in composition (MgO 4.09-11.11 wt %) that can be explained by varying amounts of crystal fractionation of the proposed parental magma composition accompanied by crystal accumulation and contamination by the surrounding granite melt. The parental composition calculated for the mafic rocks is similar to type I MORB that has been enriched in K, Sr, Rb, Ba, and Al. The mafic magma is probably the product of partial melting and was enriched in these elements during emplacement. A second group of mafic samples is enriched relative to the other mafic samples, in high field-strength elements TiO_2, Zr, Nb, along with Sr.

The physical differences in composition, temperature, and viscosity between the mafic and felsic magmas allowed the mafic magmas to chill as pillows, which helped prevent mixing between the basalt and the granite melt in the composite zones. The mechanical breakdown of some of the pillow-granite contacts has aided selective mixing, which has produced limited hybridization. These contaminated samples are not the result of simple two-component mixing of the observed granite and proposed parental basalt composition.

INTRODUCTION

The Island of Vinalhaven lies 15 miles east of Rockland, Maine at the southern end of Penobscot Bay. It is made up of a 361 ± 7 Ma Devonian granite-gabbro association, intruding the 393 ± 6 Ma Silurian-Early Devonian(?) Vinalhaven rhyolite and Thorofare andesite (Brookins, 1976). The intrusive rocks are the southwesternmost exposure of the Bays-of-Maine Igneous Complex (Chapman, 1962a).

The Bays-of-Maine Igneous Complex is a large, essentially bimodal Devonian granite-gabbro association that trends 280 km east-northeast, parallel to tectonic strike, from southern

Penobscot Bay along the coast of Maine into New Brunswick, Canada. According to Chapman (1962a) it consists of earlier gabbroic phases, closely followed by at least two later granitic phases. Chapman (1962a, 1968) has placed the granites of Vinalhaven into the younger group termed the Maine coastal plutons, cutting the earlier phases of the complex. He suggested that the Maine coastal plutons are post-orogenic and were emplaced in association with cauldron subsidence. These plutons straddle the proposed Acadian suture, and therefore must have been emplaced in the late stages of, or after, the Acadian orogeny (Berry, 1986). Both these conclusions are in accord with that of Loiselle and Wones (1979) who state that the coastal plutons are anorogenic or A-type granites. This study shows that the granites on Vinalhaven were closely associated with the emplacement of the "earlier" mafic phase and that intimate commingling of the two magmas took place during their emplacement (Mitchell, 1986).

The Association of Mafic and Felsic Magmas

The relationship between coexisting felsic and mafic magmas has been a long-standing controversy in geology (e.g. Holmes, 1931; Walker and Skelhorn, 1966; Yoder, 1973). Such associations have been explained through fractional crystallization of a parental basaltic magma, various degrees of partial melting of single or multiple sources, restite contamination, and magma-mixing. Each theory has prevailed at some time in the past, with magma-mixing receiving considerable attention in the current literature.

The intimate association of mafic and felsic magmas is well documented throughout the geologic record. These associations manifest themselves as mixed magma ejecta, net-veined complexes, composite dikes and sills, and dikes of incompletely mixed, commingled mafic "pillows" in granite hosts. Examples include commingling in the Precambrian Tigalak intrusion, Labrador, Canada (Wiebe and Wild, 1983), the Tertiary Marsco suite on the Isle of Skye, Scotland (Harker, 1904; Wager et al., 1965; Vogel et al., 1984), and mixed magma ejecta in the 1875 eruption of Askja, Iceland (Sigurdsson and Sparks, 1981).

Bunsen (1851) first recognized the association of basalt and rhyolite in the lavas of Iceland. He suggested that the mixing of these magmas could be responsible for the genesis of the range of igneous rocks of Iceland and other similar associations. In his classic work on the Tertiary igneous rocks of Skye, Harker (1904) interpreted the composite dikes, sills, and ring dikes as a consequence of the simultaneous intrusion of mafic and felsic magmas. Wager and Bailey (1953) examined the details of net-veined complexes and attributed the textures to the chilling of mafic magma against a cooler felsic magma, which produced chilled margins on the mafic unit. They called this incomplete mixing of compositionally distinct magmas "commingling."

Many subsequent studies support the commingling hypothesis (Gibson and Walker 1963; Blake et al., 1965; Wager et al., 1965; Walker and Skelhorn 1966; Wiebe 1973, 1974, 1979, 1980, 1984; Yoder, 1973; Gamble, 1979; Taylor et al., 1980; Reid et al., 1983; Marshall and Sparks, 1984; Cantagrel et al., 1984; Vogel et al., 1984; Whalen and Currie, 1984; Brown and Becker, 1986), suggesting that the textures formed are the result of interaction when both magmas were liquid or largely liquid at the same time. Despite the overwhelming field and petrographic evidence for the commingling of mafic and silicic magmas, attempts to document the degree of liquid-liquid interaction with geochemical data have failed to support simple two-component mixing processes (Gamble, 1979; Taylor et al., 1980; Vogel et al., 1984; Whalen and Currie, 1984).

Other alternatives such as fluidization have been suggested for net-veining of mafic and felsic magmas (Reynolds, 1954). Chapman (1962b) suggested that the composite dikes of Mt. Desert Island, Maine were formed by net-veining, with a granite liquid intruding a solid gabbro host. Taylor et al. (1980) examined the Mt. Desert dikes and interpreted those dikes as having formed through commingling.

The well developed textural relationships and spectacular shoreline exposures on Vinalhaven Island make this an excellent location to study the commingling of mafic and felsic magmas. The purpose of this study is twofold: first to describe the chemistry of the intrusive rocks on Vinalhaven Island in order to place them in the regional and tectonic setting, and second to relate the chemical variation in the zones of commingling to the massive granite-gabbro association that makes up the majority of the island.

Throughout this paper the term commingling will be used to describe magmas which have mechanically mixed, but have retained their compositional identity. The terms hybridized and contaminated will be used interchangeably to describe situations where the magmas have interacted in such a manner that their compositions have been changed.

Methods

During the summers of 1984 and 1985, over 100 samples were collected from the granite-gabbro complex on Vinalhaven. Sample size for chemical analysis was based on the guidelines of Clanton and Fletcher (1976) and ranged from approximately 100 grams for fine-grained mafic material to 2,000 grams for medium-grained granite. Samples were analyzed for bulk rock chemistry major (Si, Ti, Al, Fe, Mn, Mg, Ca, Na, K, P) and trace (V, Cr, Ni, Zn, Ga, Sr, Y, Zr, Nb, Ba, La, Ce, Pb, Th, U) elements using X-ray fluorescence spectrometry (XRF) at the Department of Geology and Geography, University of Massachusetts, Amherst. Standard petrographic thin sections were examined for textural relations and mineralogical data.

Major elements analyses were done following modifications of the methods of Norrish and Hutton (1969). Trace-element abundances were determined using the methods of Norrish and Chappell (1967). Mass absorption coefficients for the

TABLE 1. REPRESENTATIVE ANALYSES FROM THE VINALHAVEN GRANITE-GABBRO ASSOCIATION.
MGAVG, average of 11 medium grained granites; FGAVG, average of 6 fine grained granites; M, representative granite matrix material (VH-62); E, representative evolved sample (VH-51); P, five-pillow average representing the starting liquid composition; C, representative cumulate sample (VH-49). Analytical precision estimates (1 σ) expressed as weight percentage or ppm. Complete Vinalhaven analyses are given in Appendix A, Table A1.

Sample	MCAVG	1-std	FGAVG	1-std	M	E	P	C	Analytical Precision
SiO_2	74.37	0.62	73.83	0.59	61.71	53.34	48.94	47.58	0.16
TiO_2	0.32	0.03	0.30	0.02	1.62	2.25	1.26	0.89	0.005
Al_2O_3	13.00	0.18	13.58	0.12	14.26	13.89	17.11	17.69	0.06
Fe_2O_3*	2.06	0.14	1.91	0.17	8.59	12.03	9.95	9.18	0.03
MnO	0.04	0.01	0.04	0.01	0.16	0.20	0.17	0.15	0.005
MgO	0.28	0.05	0.39	0.05	1.91	5.55	8.26	11.11	0.04
CaO	1.10	0.09	1.23	0.11	4.41	7.89	10.82	10.84	0.03
Na_2O	3.45	0.16	3.56	0.17	3.62	3.21	2.70	2.48	0.09
K_2O	5.07	0.07	5.08	0.15	3.10	1.48	0.54	0.18	0.003
P_2O_5	0.07	0.01	0.08	0.01	0.53	0.35	0.11	0.10	0.006
Total	99.86	0.33	99.84	0.32	99.90	100.20	99.90	100.18	---
Mg' val	0.26	---	0.29	---	0.31	0.48	0.62	0.71	---
A/CNK	0.99	---	1.00	---	0.82	0.65	0.69	0.74	---
Ba	227	28	357	18	219	140	41	2	6
Rb	230	15	251	13	116	58	27	5	0.26
Sr	47	5	59	2	168	298	202	228	1.7
Pb	23	2	25	5	16	1	4	3	0.1
Th	20	3	21	3	12	4	1	1	0.2
U	8	2	8	1	3	1	1	0	0.7
Zr	195	15	219	20	289	208	93	62	0.6
Nb	13.1	0.7	14.9	0.8	12.5	8.0	2.2	2.3	0.3
Y	48	6	39	3	59	44	26	15	0.3
V	17	2	17	2	101	254	190	125	2.5
Cr	4	1	6	1	5	198	243	252	2.0
Ni	2	2	5	1	3	40	127	251	1.0
Zn	32	4	27	5	96	113	74	62	0.6
Ga	17	0	16	1	21	22	17	15	0.5
Rb/Sr	5.0	---	4.2	---	0.7	0.2	0.1	0.0	---
K/Rb	183.9	---	168.1	---	221.8	212.0	178.0	334.0	---
Zr/Nb	15.0	---	14.7	---	23.1	26.0	42.8	27.0	---

*Total Fe expressed as Fe_2O_3
Mg'- value = mol. prop. Mg/(Mg+Fe) after adjusting Fe^{+3}/Total Fe as FeO = 0.1
A/CNK = mol. $Al_2O_3/(CaO + Na_2O + K_2O)$

samples were determined using a Compton scattering method modified after Reynolds (1967) and were used to correct for matrix differences between samples and standards. Calibrations were based on both natural rock and synthetic standards. Analytical precision for both major and trace element analyses are given in Table 1.

Fifteen samples, selected on the basis of the XRF data, were analyzed for rare earth elements REE (La, Ce, Nd, Sm, Eu, Tb, Yb, Lu) and additional trace elements (Hf, Ta, Th, U) by Instrumental Neutron Activation Analysis (INAA) at the Department of Geology and Geophysics, Boston College.

Chondrite normalizing values are from F. A. Frey (pers. commun. to J. M. Rhodes, 1982). In all REE diagrams, samples are normalized to chondrites and Gd has been linearly estimated from Sm to Yb chondrite-normalized abundances to better define the Eu anomaly.

Geology of Vinalhaven Island

The most complete geologic study of Vinalhaven Island was made by Smith et al. (1907) in their description of the geology of the Penobscot Bay quadrangle. The geologic relationships from their map of the Vinalhaven area were transferred to the Vinalhaven 15' quadrangle and used as a base for this study. Figure 1 is a reproduction of their work with the addition of the contact for the fine-grained granite and the location of the zones of commingling of granitic and mafic magmas. Smith et al. (1907) did not map the fine-grained granite on Vinalhaven Island as a separate unit. The fine-grained granite was, however, well known during the early 1900's for its use as a building stone. Dow (1965) studied the Vinalhaven rhyolite, Thorofare andesite and Calderwood Formation on the northern portion of the island in conjunction with his work on North Haven Island. These units

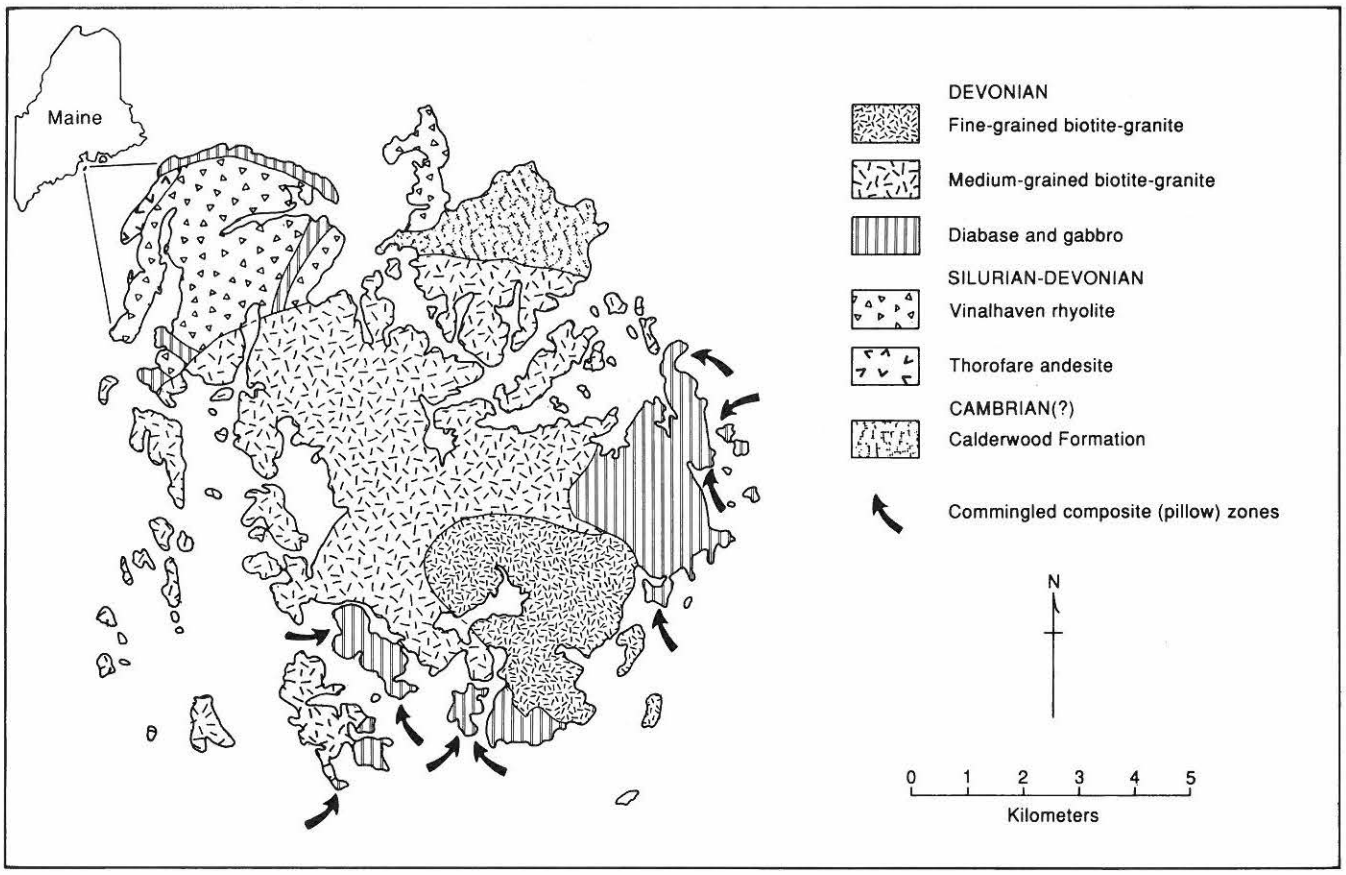

Figure 1. Generalized geologic map of Vinalhaven Island, Maine, after Smith et al. (1907), showing Cambrian(?) Calderwood Formation, Silurian-Early Devonian(?) Vinalhaven rhyolite and Thorofare andesite, Devonian granite-gabbro complex with early mafic phase, and later medium-grained hornblende-biotite granite cut by fine-grained biotite granite. Arrows indicate zones of commingled composite zones.

are intruded by the granite-gabbro association which makes up the southern three-quarters of Vinalhaven Island. Brookins (1976) dated a number of Devonian granites in Maine using Rb/Sr whole rock methods and obtained an age of 361 ± 7 for the medium-grained granite on Vinalhaven, with an initial $^{87}Sr/^{86}Sr$ value of 0.705 ± 0.001.

The intrusive rocks on Vinalhaven consist of early mafic phases ranging from olivine gabbro to diorite which are cut by a later medium-grained hornblende-biotite granite that is in turn intruded by a fine-grained biotite-granite. The association is bimodal in nature and does not show a continuous compositional gradation from basalt to granite (Fig. 2). During the emplacement of the medium-grained granite, commingling with the mafic phase occurred, producing many composite zones of basalt "pillows" and gabbro xenoliths in a granitic to granodioritic matrix. The locations of these zones are shown in Figure 1. Throughout this paper the term "pillow" will refer to the 10x10 cm to 1x5 m globules of basalt enclosed in granite; the term "matrix material" will refer to the granitic material interstitial to the basalt pillows. In addition to the granites and matrix material there are late-stage aplite dikes that cut all other intrusive units.

THE COMPOSITE ZONES

The intimate association of commingled felsic and mafic magmas on Vinalhaven Island has resulted in well developed basalt pillows which chilled within a granite matrix similar to those described by Wager and Bailey (1953). These composite zones range from large, 100 m x 20 m, sill-like sheets (Fig. 3a), to small, 5 m x 15 cm dikes that cut the gabbros. The pillows have a planar orientation that is parallel to the contact of the composite zones with the gabbro host. The extreme differences in composition, temperature, and viscosity between the mafic and felsic magmas have prevented them from thoroughly mixing together, allowing the pillows to retain their identity within the granite matrix (Fig. 3b-c).

Within these composite zones, the basalt pillows and granitic matrix material behaved in a very plastic manner. Pillows range from simple spheres to complex shapes with varying

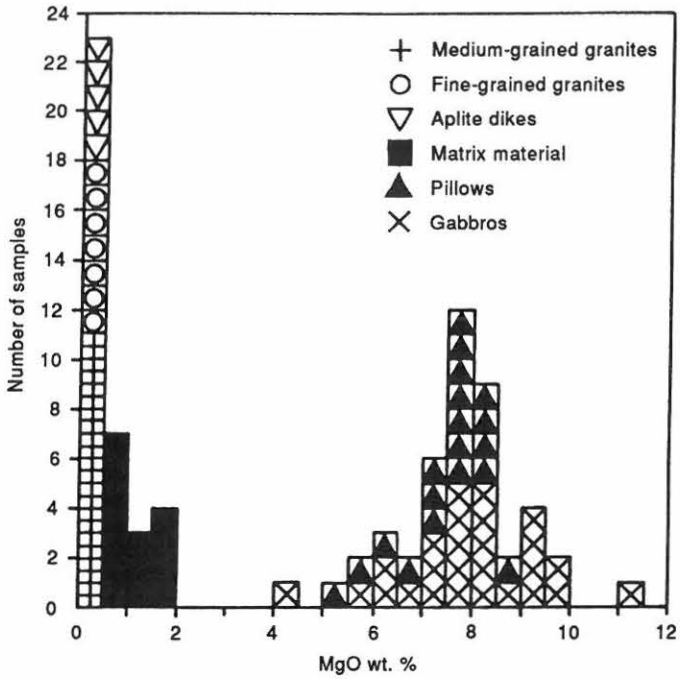

Figure 2 (at left). MgO histogram for all analyzed Vinalhaven samples, showing granites <0.5; matrix material 0.5-2.0; gabbro 4.0-11.8; pillows 5.5-8.9 (all wt. %). The gap in composition reflects the bimodal nature of the association. Data given in Appendix A.

Figure 3 (below). Photographs of basalt pillows in granite matrix from zones of commingling. (a) Sheet-like nature of the composite sill in contact with the gabbro. (b) Close-up of a composite zone illustrating fluidity of interaction. (c) Compaction of pillows and matrix in a dike. (d) Rotated close-up of the spoon-like structure in lower center of (c); note the sharpness of the contact.

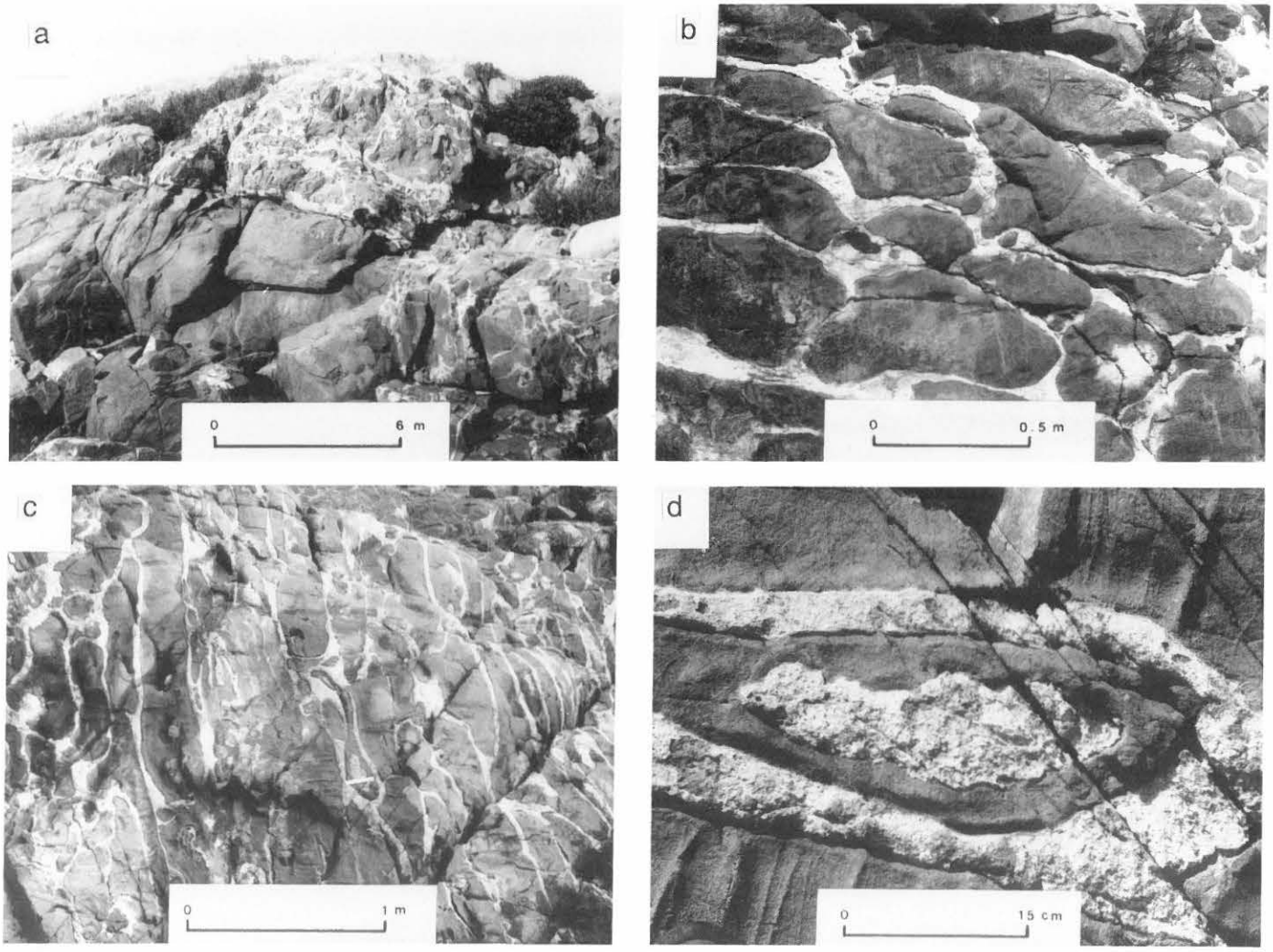

amounts of thinning, bending, and necking. This very fluid behavior has produced some spectacular structures (Fig. 3) with relationships suggesting that both the pillows and matrix were liquid, or largely liquid, at the same time (Mitchell, 1986).

The pillows have sharp, fine-grained margins containing biotite and hornblende that has partially replaced pyroxene within a plagioclase-rich matrix. The concentration of hornblende and biotite has produced a 2-3 centimeter green rind on the outer edges of the pillows. Grain size increases towards the center of pillows and is accompanied by an increase in the concentration of pyroxene and a concurrent decrease in the abundance of hornblende and biotite. This concentration of hydrous phases at the margins of the pillows is probably the result of contamination by the surrounding granite melt and is limited to the outer rind. The pillow centers show little to no evidence of contamination by the granite.

Some pillows have engulfed granite and contain quartz and microcline phenocrysts. These phenocrysts are very similar to those present in the granite except they are rimmed by biotite, hornblende, and some pyroxene, and are clearly out of equilibrium. Their presence suggests that the granite matrix contained phenocrysts prior to the commingling process. The pillows must have incorporated these phenocrysts while the basalt and granite were liquid and liquid plus crystals.

The granitic matrix material is fairly homogeneous. Chemically and petrographically, it is broadly similar to and probably is the equivalent of the medium-grained granite that crops out over most of the island. The contacts of the matrix with the pillows are fine-grained and the matrix appears to have remelted at the pillow interface, perhaps as the result of superheating by the basalt pillows. Most of the matrix material has seen very little contamination by the pillow material. The exception is in areas where there has been some deformation. Here the edges of the pillows have been mechanically broken and the mafic material comminuted into the granite matrix. This largely mechanical interaction results in matrix material with a slightly intermediate composition (see Fig. 2 and sample M, Table 1), accompanied by an increase in hornblende and biotite.

The clear-cut field relations on Vinalhaven suggest that the chemical variation in the composite zones should be the result of mixing of felsic and mafic magmas. In the following sections, detailed chemical analyses will be used to describe the intrusive rocks on Vinalhaven, and demonstrate that simple two component mixing of the observed mafic and felsic end members present in the composite zones is not solely responsible for the observed compositional variation.

THE GRANITES

The medium-grained granite on Vinalhaven, named "Vinalhaven Coarse" by the quarrymen of the late 1800's, is pink and medium-grained with about equal proportions of quartz, plagioclase (An_{12-22}), and microcline, and less than 10% mafic phases consisting of chiefly hornblende and biotite. Accessory

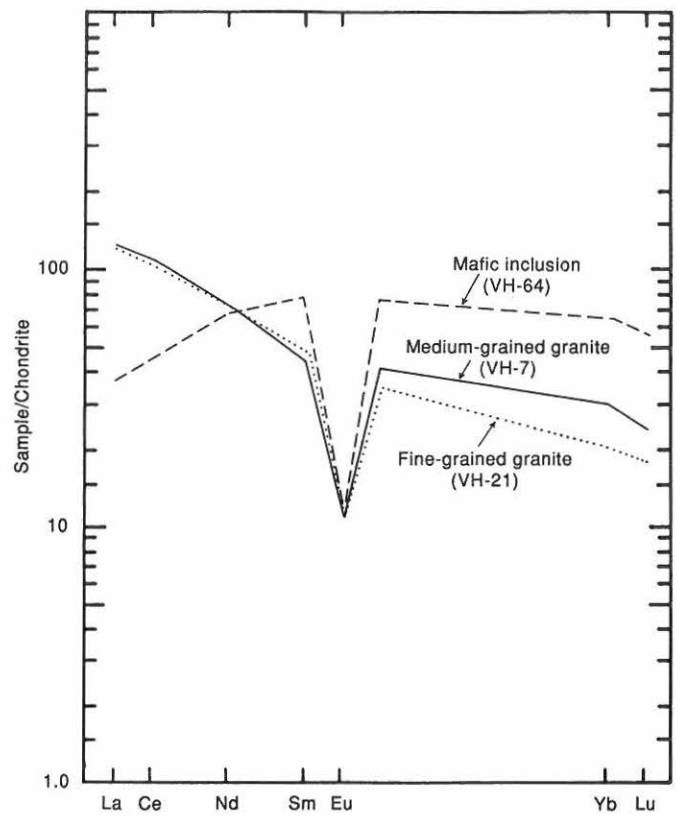

Figure 4. Chondrite-normalized REE plot for representative felsic samples. It is important to notice the difference between the pattern for the mafic inclusion (VH-64) and the mafic samples as in Figure 9.

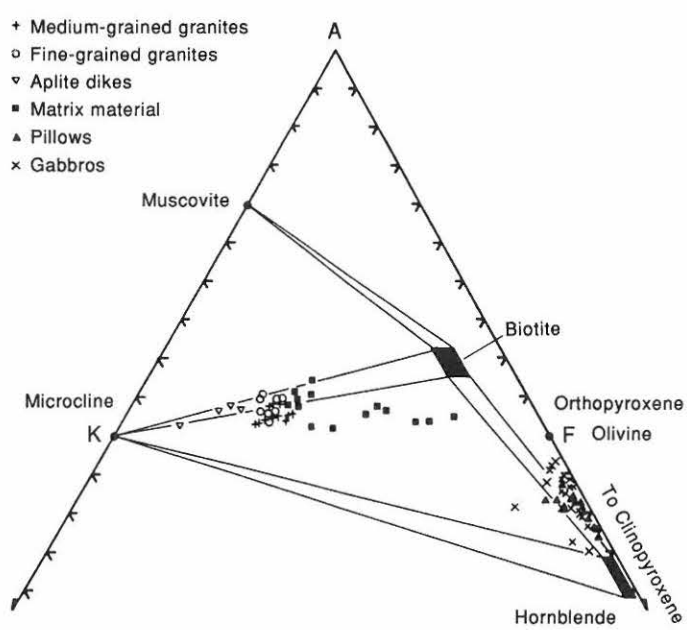

Figure 5. AKF projection from plagioclase and quartz with molar whole rock and mineral compositions. $A = Al_2O_3 + Fe_2O_3 + TiO_2 - Na_2O - K_2O - (CaO - 10/3\ P_2O_5)$, $K = K_2O$, $F = FeO + MnO + MgO - TiO_2$. Biotite and hornblende compositions from granites of similar composition (Deer et al., 1962; Rhodes, 1969).

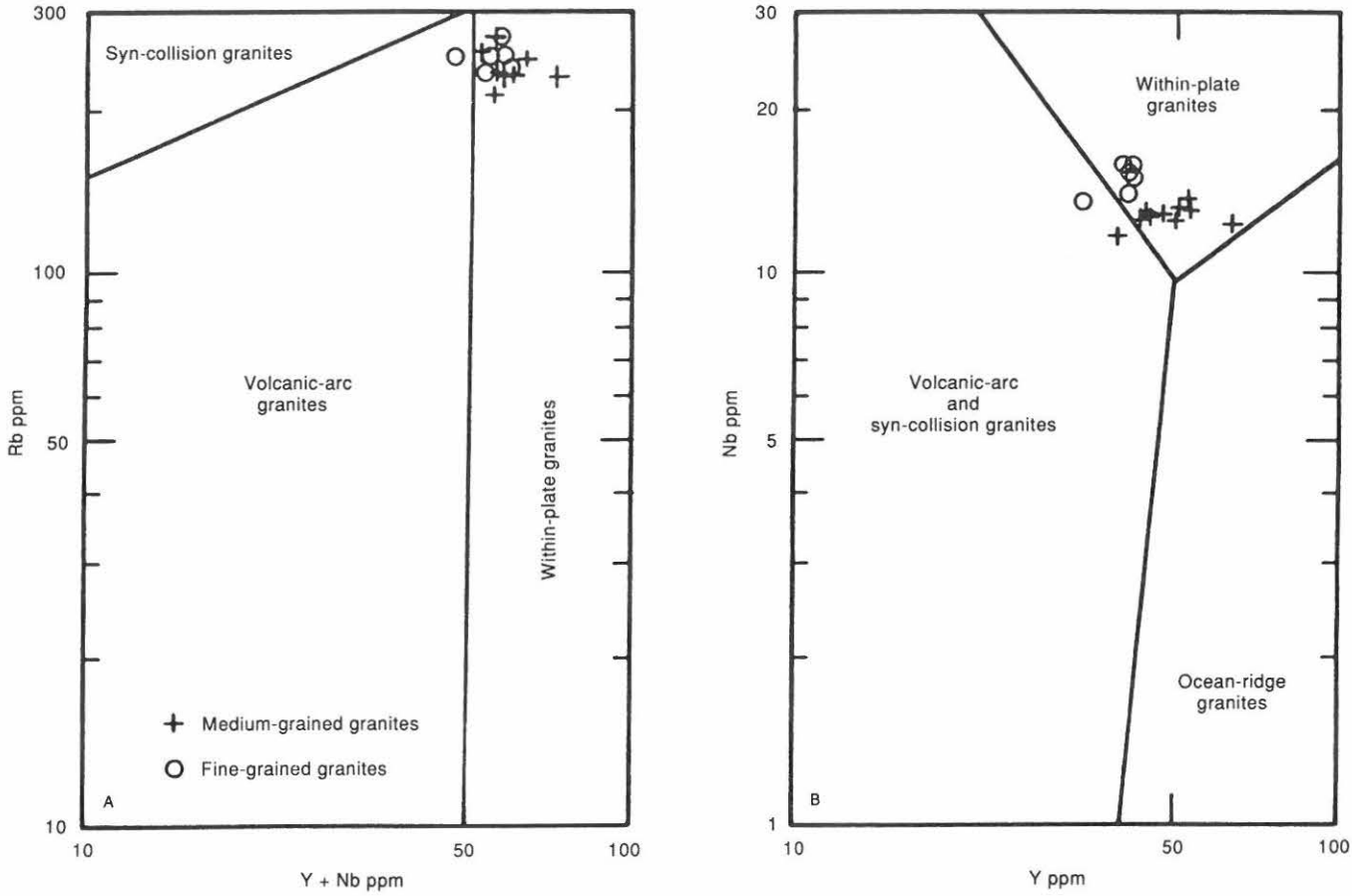

Figure 6. (a) Rb vs Y+Nb and (b) Nb vs Y tectonic discriminant diagrams after Pearce et al. (1984).

phases include magnetite, ilmenite, apatite, sphene, zircon, and allanite. Large alkali feldspar phenocrysts have exsolved to a fine-grained intergrowth of microcline and plagioclase. These are responsible for the rock's pink color. In rare samples these phenocrysts have plagioclase rims forming the so-called viborgite-type Rapakivi texture. There is some sericitization of the plagioclase and alteration of biotite to chlorite.

The fine-grained granite is gray, with equal proportions of quartz, plagioclase (An_{15-22}), and microcline, and less than 5% biotite. Accessory minerals include magnetite, ilmenite, apatite, zircon, sphene, and allanite. The principal petrographic difference between the two granites is one of grain size and the presence of hornblende in the medium-grained variety. On the basis of field and petrographic evidence, Stewart (1956) correlated the Vinalhaven medium- and fine-grained granites with the Sherwood granite on Deer Island and Crotch Island granite on Crotch Island respectively.

The medium- and fine-grained granites are both very homogeneous, have similar compositions, and appear to be the product of similar magmas with slightly different cooling histories. This would account for the presence of hornblende and increased grain size in the medium-grained granite. Table 1 gives the average chemical compositions for the two granites. They are metaluminous ($Al_2O_3/CaO + K_2O + Na_2O < 1$ molar) to mildly peraluminous, subalkaline, and correspond with the I-type classification of Chappell and White (1974) with <1% normative corundum, no modal aluminous minerals, and initial $^{87}Sr/^{86}Sr$ between 0.704-0.706 (Brookins, 1976).

Chondrite (CH) normalized rare earth elements (REE) patterns for the two granites are very similar (Fig. 4). They are enriched in light REE, 100-50 times CH, have large negative Eu anomalies, and an overall negative slope to their patterns. The medium-grained granite contains more Yb and Lu than the fine-grained granite. This relative enrichment of heavy REE is probably a function of hornblende content. Hornblende is enriched in the heavy REE relative to the granites (Hanson, 1978); thus, its presence in the medium-grained granite could be responsible for the observed differences in Yb and Lu in the two granites.

In order to examine the relationship between the whole rock chemistry and observed mineralogy, all Vinalhaven samples (felsic and mafic rocks) have been plotted on an AKF projection (Fig. 5). Average analyses of hornblende and biotite taken from the literature for rocks of similar compositions (Deer et al. 1962; Rhodes, 1969) have been plotted to show their general location on such a projection. Biotite is the key mineral composition

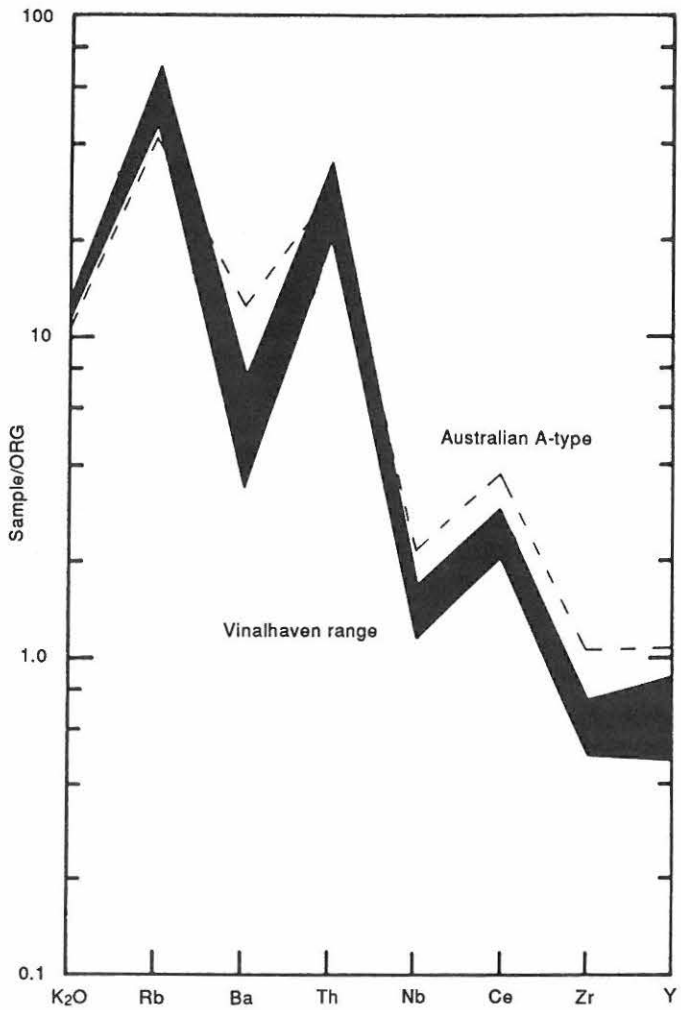

Figure 7. Modified "spider diagram" with samples normalized to Ocean Ridge Granites (ORG) after Pearce et al. (1984). Shaded field, range for medium- and fine-grained Vinalhaven granites; dashed line, average Australian A-type granites from White and Chappell (1983).

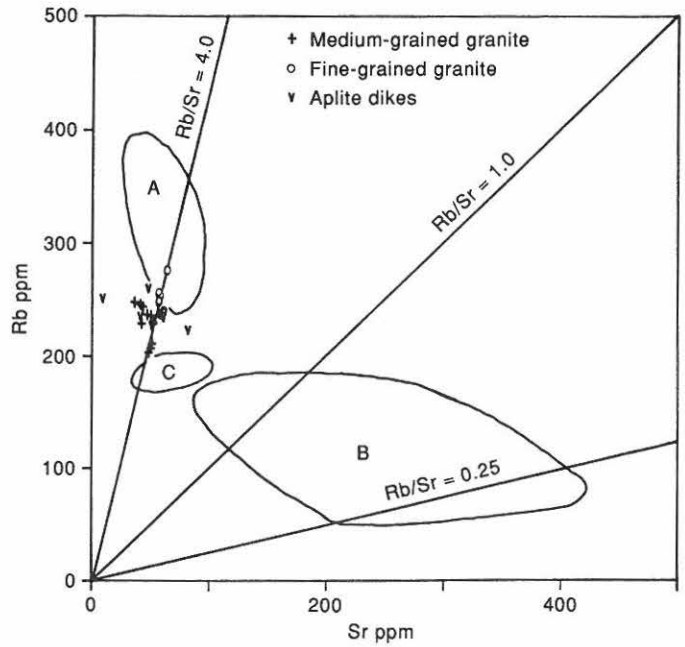

Figure 8. Plot of Rb vs Sr for granites from Vinalhaven. Fields A, B, and C for other Maine granites are taken from Loiselle and Ayuso (1980). Outlined fields include: A-Lucerne and Lead Mountain plutons; B-Bottle Lake complex, Center Pond pluton, and Seboeis foliated granitoid; C-Seboeis non-foliated granite and Katahdin pluton.

because its location controls the biotite-microcline tie line separating the muscovite-biotite-microcline-plagioclase field from the hornblende-biotite-microcline-plagioclase field. All Vinalhaven samples lack a primary aluminous phase and plot within the hornblende-biotite-microcline-plagioclase field, with some samples falling on or close to the inferred biotite-microcline tie line. S-type granites (Chappell and White, 1974) contain muscovite and other aluminous phases and would plot above the biotite-microcline tie line, whereas I-type granites lacking aluminous phases would plot along or below the biotite-microcline tie line.

The mineralogy, both essential and accessory (e.g. sphene), and the presence of mafic inclusions also support an I-type classification. In addition to their I-type characteristics, however, these granites show many of the compositional attributes of A-type, anorogenic granites (Barker et al., 1975; Loiselle and Wones, 1979; Collins et al., 1982; Anderson, 1983; White and Chappell, 1983; Whalen et al., 1987). Although there is some confusion over the definition of A-type granitoids, they tend to be subalkaline and metaluminous, with enrichment of incompatible elements (K, Zr, Nb) and depletion of compatible elements (Cr, Ni, Ba, Sr) relative to other granite types with comparable silica contents. The chemical characteristics of the granites from Vinalhaven are similar to those of proposed anorogenic suites.

In order to evaluate the tectonic environment in which these rocks were emplaced, they are compared to granites of known tectonic environment using trace element discriminant diagrams (Pearce et al., 1984). The granites on Vinalhaven plot in the field of within-plate granites on Nb vs Y and Rb vs Y+Nb diagrams (Fig. 6). This point is illustrated further using a modified "spider diagram" (Fig. 7), in which samples are normalized to an ocean ridge granite (Pearce et al., 1984). This multi-element pattern also compares closely with granites from within-plate environments. All are high in normalized Rb and Th, and are depleted in Ba, producing a substantial Ba anomaly. This anomaly is a common characteristic of granites of the within-plate suite. This pattern is also similar to granites from the post-orogenic suite (Pearce et al., 1984). The averages of 31 Devonian A-type granites from eastern Australia (White and Chappell, 1983) show a very similar pattern to those from Vinalhaven (Fig. 7). Thus, on the basis of their trace elements, both fine- and medium-grained granites on Vinalhaven show similar characteristics to

granites from known within-plate and post-orogenic environments.

In order to compare the granites of Vinalhaven to other Maine plutons, their Rb and Sr abundances have been plotted on Figure 8. Although the absolute abundances are transitional between groups A and C of Loiselle and Ayuso (1980), Rb/Sr ≥ 4.0 is consistent with group A, representing other plutons of the Maine coastal lithotectonic belt (Loiselle and Ayuso, 1980; Ayuso, 1986).

THE MAFIC SUITE

Characterization

The mafic rocks on Vinalhaven have been divided on the basis of their field occurrence. The intrusive rocks are grouped together as "gabbros" and the fine-grained rocks from the composite zones are referred to as "pillows." Each group shows a range in composition. The gabbros are medium-grained and range from true olivine two-pyroxene gabbros to hornblende-biotite diorites. The pillows are fine-grained basalts and contain varying amounts of olivine, clinopyroxene, plagioclase, biotite, and hornblende. Major and trace element abundances for the mafic suite show a wide range in composition (Appendix A). Compatible elements (CaO, Al_2O_3, Ni, Cr) decrease with decreasing MgO. Incompatible elements (TiO_2, K_2O, Na_2O, Zr, Nb, Y, Th) increase with decreasing MgO. The gabbros and pillows are very similar in composition, with the pillows showing a more restricted range within that of the gabbros (Fig. 2).

Samples with 8.9-11.8 wt% MgO are thought to have accumulated olivine and plagioclase crystals, are depleted in highly incompatible elements (60-79 ppm Zr, <2.5 ppm Nb, <3 ppm Th), and are low in moderately incompatible elements (0.85-1.56 wt% TiO_2, 15-25 ppm Y). They have flat chondrite normalized REE patterns approximately 10 times chondrite, which are depleted relative to other Vinalhaven samples (Fig. 9). These samples have Mg'-values of 0.64-0.71 and are enriched in compatible elements (169-355 ppm Cr, 177-251 ppm Ni). Most samples show little textural evidence of contamination or alteration.

Samples with MgO 4.1-7.5 wt%, have Mg'-values of 0.48-0.64 and show strong evidence for both crystal fractionation and contamination by the surrounding granite. Modal hornblende and biotite increase with decreasing MgO, as do the incompatible elements (122-294 ppm Zr, 4.4-8.0 ppm Nb, 1-7 ppm Th, 23-44 ppm Y, 0.97-2.51 wt% TiO_2). Their chondrite normalized REE patterns are enriched relative to the other mafic samples (Fig. 9). These patterns show varying amounts of fractionation and contamination relative to samples with lower MgO contents. The presence of large Eu anomalies in some samples suggest that they may have incorporated varying amounts of granitic material. The compatible elements decrease (40-114 ppm Ni, 136-248 ppm Cr) as MgO decreases. Although there is overlap, these samples show more evolved compositions for all elements compared to the other mafic samples.

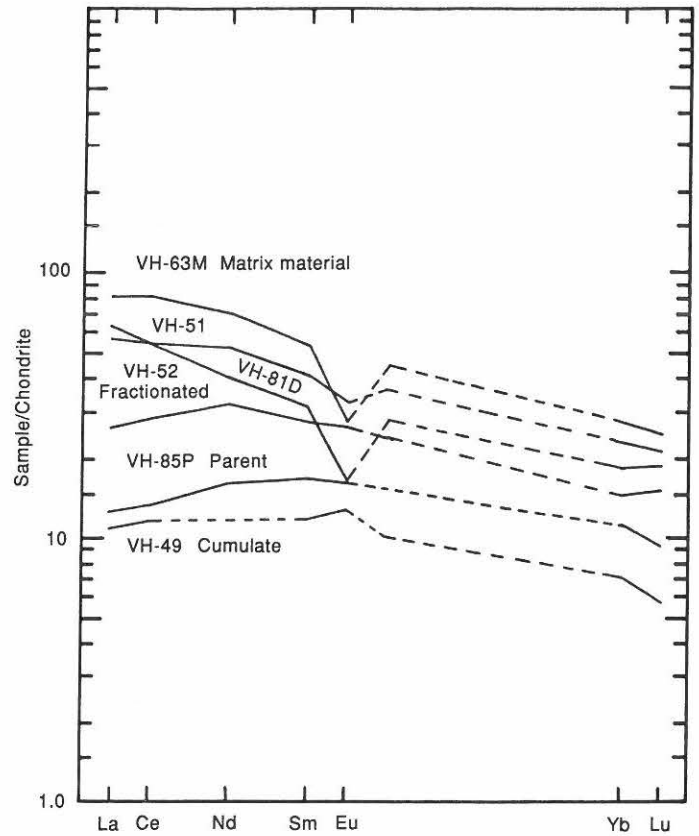

Figure 9. Chondrite-normalized REE diagram for selected mafic samples. VH-85P represents approximate parental composition. VH-49 is a cumulate sample. The other samples represent varying amounts of crystal fractionation and contamination. Samples with negative Eu anomalies have been contaminated by a granitic component.

Interpretation

Much of the compositional diversity of the mafic suite is thought to result from the combined effect of crystal accumulation and fractionation, and contamination by the surrounding granite magma. Samples with MgO between 7.5-8.5 are most abundant and are taken to represent compositions closest to the parental mafic magmas. Within this range, fine-grained pillow interiors are probably closest in composition to that of the mafic melt, since rapid cooling will have minimized the effects of crystal fractionation and accumulation. In addition, petrographic inspection shows that biotite and hornblende, possible evidence for granitic contamination, are restricted to the pillow rims. Thus pillow cores show little evidence of contamination by the granite matrix and should reflect a composition close to the original magma. The average of 5 such pillow cores with MgO between 7.5-8.5 has been taken to represent the

composition of the parental mafic magma. This five pillow average will be referred to as "P" and is given in Table 1. Pillow VH-85P has the composition closest to the calculated average. It has a flat chondrite-normalized REE pattern approximately 15 times chondrite. This pattern will be used to represent the parental REE pattern. The composition is similar to those reported for Type I mid-ocean ridge basalts (MORB) (Basaltic Volcanism Study Project, 1981), with the exception of enrichment in K, Sr, Ba, Rb, and Al relative to MORB. This enrichment could in part be the result of interaction with the granite.

In order to compare the Vinalhaven mafic suite to basalts from known tectonic environment, data have been plotted on a Zr/Y vs Zr diagram (Fig. 10). These samples fall into two distinct groups. Samples with Zr/Y <4 lie in the MORB field and samples with Zr/Y >4 plot in the within-plate field (Pearce and Norry, 1979). On the basis of their major element chemistry (except TiO_2) the group of samples with Zr/Y >4 could be produced by fractional crystallization of the proposed parental magma P. It is not possible, however, to explain some of their trace element abundances by either fractionation of low Zr/Y parental melts, or by contamination of such a melt by the associated granites. The high Zr/Y group is enriched in other high field strength elements Nb and TiO_2, and also in Sr. These samples are limited to a single area in the composite zone on the south-central portion of the island. On the basis of their field relations and trace element chemistry, these samples could represent a later phase of mafic activity that was enriched in incompatible elements and are correspondingly depleted in compatible elements relative to the proposed parental composition P. This enrichment would explain why these samples plot in the within-plate field on the Zr/Y vs Zr diagram. These compositions are evidence for a second mafic magma.

Figure 11 plots Zr vs Nb for all analyzed Vinalhaven samples. These two elements are highly incompatible with respect to basaltic and mantle mineralogy. Their concentrations and, particularly, their ratios are thought to be immobile and only slightly modified by alteration and secondary processes (Humphris and Thompson, 1978). Varying amounts of partial melting, crystal fractionation and crystal accumulation may change the abundances of Zr and Nb, but should not change their ratio. Thus a suite of rocks from the same source would have constant Zr/Nb ratios. The majority of the mafic suite, and in particular samples with high MgO content, have Zr/Nb ≥30. This ratio is comparable to many island arc tholeiites and Type I mid-ocean ridge basalts (Basaltic Volcanism Study Project, 1981). Although the enriched samples have higher Zr and Nb abundances than the other mafic samples, their Zr/Nb ratios are not significantly different. The consistent Zr/Nb ratio for the gabbros and pillows suggests that they were derived from the same source. The granites, on the other hand, have markedly different Zr/Nb ratios (<15) and large negative Eu anomalies which suggests that they were not differentiated from the mafic suite and were probably the result of crustal melting (Ayuso, 1986).

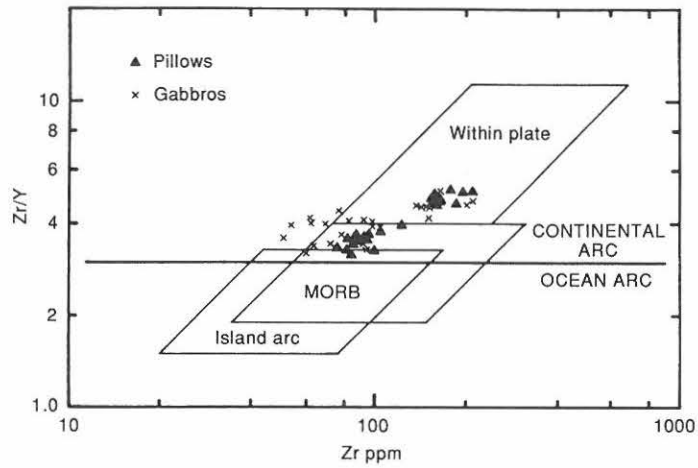

Figure 10. Zr/Y vs Zr tectonic setting discriminant diagram for basaltic rocks. Modified after Pearce and Norry (1979) and Pearce (1983).

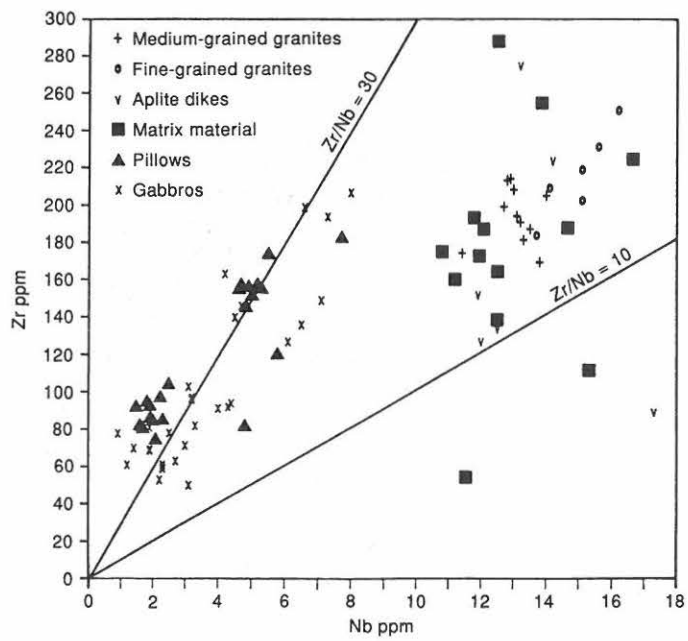

Figure 11. Zr vs Nb chemical variation diagram showing all analyzed Vinalhaven samples.

The Mafic Suite: Discussion

The wide range in composition for the mafic suite can be explained to a first approximation by a combination of crystal fractionation and accumulation from a parental basaltic magma modified by contamination. Figure 12 illustrates the interplay of crystal fractionation, accumulation, and contamination. The Vinalhaven samples have been projected from plagioclase onto the olivine-clinopyroxene-silica ternary diagram (Grove et al., 1982). The 1-atmosphere and inferred 1,000 bars P_{H2O} cotectics and reaction curves have been included for reference. The samples inferred to have accumulated olivine trend away from

P toward the olivine corner, whereas evolved samples trend toward more silica-rich compositions. Many of the evolved samples do not plot on or near the olivine-plagioclase-clinopyroxene saturation curve as they should if their composition is controlled solely by low pressure crystal fractionation. Instead, they trend directly towards the silica corner, or are intermediate between this trend and the three phase saturation curve. These samples are inferred to result from a combination of low pressure crystal fractionation and contamination by the granite along a proposed mixing line shown on Figure 12. These trends produce qualitative support for the idea that the range in composition in the mafic suite can be produced by varying amounts of crystal fractionation, crystal accumulation, and contamination by the granite. For a detailed discussion of the petrogenetic model of these samples see Mitchell (1988) and Mitchell and Rhodes (in prep).

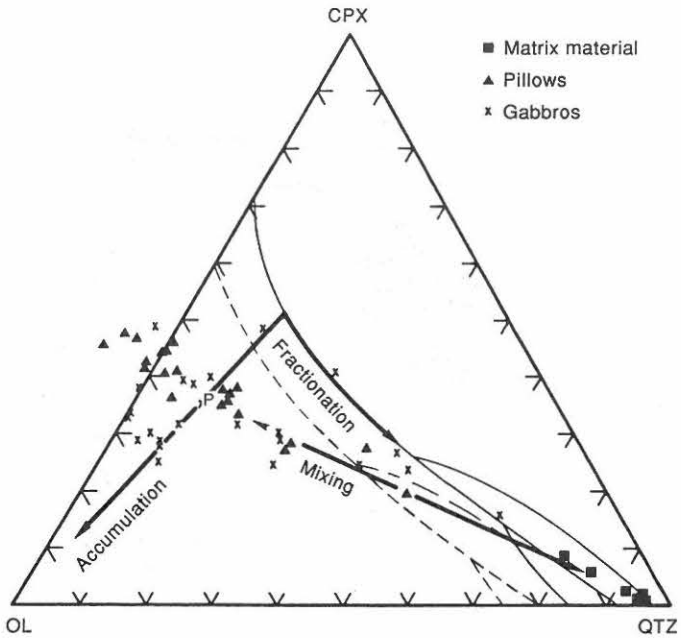

Figure 12. Projection from plagioclase onto the plane olivine (OL)-clinopyroxene (CPX)-silica (QTZ) after Grove et al. (1982). Solid phase boundaries modified from Grove et al. (1982), with the inclusion of data from Grove and Bryan (1983). Dashed curves are inferred phase boundaries for 1,000 bar P_{H2O} (Grove et al., 1982). P = parent composition; vectors indicate inferred fractionation, accumulation, and contamination trends.

CONCLUSIONS

(1) The intrusive rocks on Vinalhaven are bimodal and consist of minimum-melt granites formed by crustal melting and a suite of mafic rocks probably derived by partial melting in the mantle.

(2) The medium- and fine-grained granites are closely similar in composition and represent magma from the same source, with slightly different cooling histories. Both are I-type granites that show compositional similarities to anorogenic granites. Their Rb/Sr ratio >4 is consistent with other granites of the Maine coastal lithotectonic belt.

(3) On the basis of their trace element compositions, both granites on Vinalhaven are similar to granites from within-plate and post-orogenic tectonic environments, suggesting they could have been emplaced during the late stages of, or after the Acadian orogeny.

(4) The mafic suite consists of medium-grained gabbros to diorites and fine-grained basaltic pillows with a wide range in composition that can be explained by varying amounts of crystal fractionation, crystal accumulation, and contamination by the associated granites. The proposed parental composition is similar to Type I MORB that have been enriched in K, Sr, Rb, Ba, and Al.

(5) Commingling of the mafic and felsic magmas has produced composite zones of basalt pillows in a granite matrix. The pillows retained their own identity because of differences in composition, temperature, viscosity, and lack of convective mechanical mixing. Shapes and structures formed during mingling of the mafic and felsic magmas, along with chilled margins on the pillows, suggest that they and the granites were liquid or largely liquid at the same time.

(6) These commingled magmas show limited chemical interaction. Samples with intermediate (hybrid) compositions are not the product of simple two-component mixing of the proposed mafic parent (P) and granite end members.

DEDICATION

This work is dedicated to the memory of Michael A. B. Stratton who through his work with dyslexic children at the Carroll School Bounders Program has given me and many other students the opportunity to believe in ourselves and our own abilities. He first took me to Vinalhaven when I was 12 years old, and let me climb on, throw, and carry rocks. He introduced me to the wonders of the Maine coastal islands, and his stories about the old quarry men and the lives they lived is what got me interested in rocks in general and granites in particular. Without his help, I would never have realized that it is possible to do anything you want as long as you try hard enough. This work would never have been possible without the self confidence and "can do" attitude that I gained by working with Mike over the years.

ACKNOWLEDGMENTS

This work was supported in part by grants from the Geological Society of America and Sigma Xi. We are grateful to J. W. Sparks and L. K. Autio for assistance with XRF analyses and discussion of the data, and to R. Hon and A. Sheardin for the INAA analyses. CBM would also like to thank S. A. Morse and Peter Robinson for their direction during this project.

REFERENCES CITED

Anderson, J. L., 1983, Proterozoic anorogenic granite plutonism of North America: Geol. Soc. Amer., Mem. 161, p. 133-154.

Ayuso, R. A., 1986, Lead-isotopic evidence for distinct sources of granite and for distinct basement in the Northern Appalachians, Maine: Geology, v. 14, p. 322-325.

Barker, F., Wones, D. R., Sharp, W. N., and Desborough, G. A., 1975, The Pikes Peak batholith, Colorado Front Range, and a model for the origin of the gabbro-anorthosite-syenite-potassic granite suite: Precambrian Res., v. 2, p. 97-160.

Basaltic Volcanism Study Project, 1981, Basaltic volcanism on the terrestrial planets: Pergamon Press Inc., New York, 1286 p.

Berry, H. N., IV, 1986, Bedrock geology of the Camden Hills, Maine: M.S. thesis, Univ. Maine, Orono, 138 p.

Blake, D. H., Elwell, R. W. D., Gibson, I. L., Skelhorn, R. R., and Walker, G. P. L., 1965, Some relationships resulting from the intimate association of acid and basic magmas: Quart. Jour. Geol. Soc. Lond., v. 121, p. 31-49.

Brookins, D. G., 1976, Geochronologic contributions to stratigraphic interpretation and correlation in the Penobscot Bay area, eastern Maine: Geol. Soc. Amer., Mem. 148, p. 129-145.

Brown, P. E., and Becker, S. M., 1986, Fractionation, hybridisation and magma-mixing in the Kialineg Centre, East Greenland: Contrib. Mineral. Petrol., v. 92, p. 57-70.

Bunsen, R. W., 1851, Uber die Processe Vulkanischen Gesteinsbildungen Island: Annalen der Physik und Chemie, v. 83, p. 197-272.

Cantagrel, J. M., Didier, J., and Gourgaud, A., 1984, Magma mixing: origin of intermediate rocks and "enclaves" from volcanism to plutonism: Phys. Earth and Planet. Inter., v. 35, p. 63-76.

Chapman, C. A., 1962a, Bays-of-Maine Igneous Complex: Geol. Soc. Amer., Bull., v. 73, p. 883-888.

Chapman, C. A., 1962b, Diabase-granite composite dikes, with pillow-like structure, Mount Desert Island, Maine: Jour. Geol., v. 70, p. 539-564.

Chapman, C. A., 1968, A comparison of the Maine coastal plutons and the magmatic central complexes of New Hampshire, *in* Zen, E-an, White, W. S., Hadley, J. B., and Thompson, J. B., Jr. (eds.), Studies of Appalachian geology: northern and maritime: Wiley-Interscience, New York, p. 385-396.

Chappell, B. W., and White, A. J. R., 1974, Two contrasting granite types: Pacific Geology, v. 8, p. 173-174.

Clanton, U. S., and Fletcher, C. R., 1976, Sample size and sampling errors as the source of dispersion in chemical analyses: Proc. 7th Lunar Sci. Conf., p. 1413-1428.

Collins, W. J., Beams, S. D., White, A. J. R., and Chappell, B. W., 1982, Nature and origin of A-type granites with particular reference to southeastern Australia: Contrib. Mineral. Petrol., v. 80, p. 189-200.

Deer, W. A., Howie, R. A., and Zussman, J., 1962, Rock forming minerals: William Clowes and Sons, London, v. 2, 379 p., and v. 3, 270 p.

Dow, G. M., 1965, Petrology and structure of North Haven Island and vicinity, Maine: Ph.D. dissert., Univ. Illinois, Urbana, 146 p.

Gamble, J. A., 1979, Some relationships between co-existing granitic and basaltic magmas and the genesis of hybrid rocks in the Tertiary central complex of Slieve Gullion, northeast Ireland: Jour. Vol. Geotherm. Res., v. 5, p. 297-316.

Gibson, I. L., and Walker, G. P. L., 1963, Some composite lavas and related composite dikes in Eastern Iceland: Proc. Geol. Assoc., v. 74, p. 301-318.

Grove, T. L., and Bryan, W. B., 1983, Fractionation of pyroxene-phyric MORB at low pressure: an experimental study: Contrib. Mineral. Petrol., v. 84, p. 293-309.

Grove, T. L., Gerlach, D. C., and Sando, T. W., 1982, Origin of calc-alkaline series lavas at Medicine Lake Volcano by fractionation, assimilation and mixing: Contrib. Mineral. Petrol., v. 80, p. 160-182.

Hanson, G. N., 1978, The application of trace elements to the petrogenesis of igneous rocks of granitic composition: Earth and Planet. Sci. Lett., v. 38, p. 26-43.

Harker, A., 1904, The Tertiary igneous rocks of Skye: Mem. Geol. Surv. U.K., James Hedderick and Sons, Glasgow, 481 p.

Holmes, A., 1931, The problem of the association of acid and basic rocks in central complexes: Geol. Mag., v. 68, p. 241-255.

Humphris, S. E., and Thompson, G., 1978, Trace element mobility during hydrothermal alteration of oceanic basalts: Geochim. Cosmochim. Acta, v. 42, p. 127-136.

Loiselle, M. C., and Ayuso, R. A., 1980, Geochemical characteristics of granitoids across the Merrimack synclinorium, eastern and central Maine: I.G.C.P. Project 27, Caledonide Orogen, p. 117-121.

Loiselle, M. C., and Wones, D. R., 1979, Characteristics and origin of anorogenic granites: Geol. Soc. Amer., Abs. with Prog., v. 11, p. 468. Marshall, L. A., and Sparks, R. S. J., 1984, Origin of some mixed-magma and net-veined ring intrusions: Jour. Geol. Soc. Lond., v. 141, p. 171-182.

Mitchell, C. B., 1986, Field and textural evidence for commingling of felsic and mafic magmas on Vinalhaven Island, Maine: Geol. Soc. Amer., Abs. with Prog., v. 18, p. 56.

Mitchell, C. B., 1988, Geochemistry of the granite-gabbro complex on Vinalhaven Island, Maine: an investigation of the commingling of mafic and felsic magmas: M.S. thesis, Univ. Massachusetts, Amherst, 111 p.

Mitchell, C. B., and Rhodes, J. M., in prep., Geochemical evidence for the mechanical constraint on the mixing between mafic and felsic magmas: the Vinalhaven granite-gabbro complex.

Norrish, K., and Chappell, B. W., 1967, X-ray fluorescence spectrography, in Zussman, J. (ed.), Physical methods in determinative mineralogy: Acad. Press, New York, p. 161-211.

Norrish, K., and Hutton, J. T., 1969, An accurate X-ray spectrographic method for the analysis of a wide range of geological samples: Geochim. Cosmochim. Acta, v. 33, p. 431-453.

Pearce, J. A., 1983, Role of the sub-continental lithosphere in magma genesis at continental margins, *in* Hawkesworth, C. J., and Norry, M. J. (eds.), Continental basalts and mantle xenoliths: Shiva Publishing Co., Cheshire, U.K., p. 230-250.

Pearce, J. A., Harris, N. B. W., and Tindle, A. G., 1984, Trace element discrimination diagrams for the tectonic interpretation of granitic rocks: Jour. Petrol., v. 25, p. 956-983.

Pearce, J. A., and Norry, M. J., 1979, Petrogenetic implications of Ti, Zr, Y, and Nb variations in volcanic rocks: Contrib. Mineral. Petrol., v. 69, p. 33-47.

Reid, J. B., Jr., Evans, O. C., and Fates, D. G., 1983, Magma mixing in the granitic rocks of the central Sierra Nevada, California: Earth and Planet. Sci. Lett., v. 66, p. 243-261.

Reynolds, D. L., 1954, Fluidization as a geological process and its bearing on the problem of intrusive granites: Am. Jour. Sci., v. 252, p. 577-614.

Reynolds, R. C., Jr., 1967, Matrix corrections in trace element analysis by X-ray fluorescence: estimation of mass absorption coefficents by Compton scattering: Amer. Mineral., v. 48, p. 1133-1143.

Rhodes, J. M., 1969, The geochemistry of a granite-gabbro association at Hartly, New South Wales: Ph.D. dissert., Australian National Univ., Canberra, 315 p.

Sigurdsson, H., and Sparks, R. S. J., 1981, Petrology of rhyolitic and mixed magma ejecta from the 1875 eruption of Askja, Iceland: Jour. Petrol., v. 22, p. 41-81.

Smith, G. O., Bastin, E. S., and Brown, G. W., 1907, Geologic Atlas of the United States-Penobscot Bay Folio: U.S. Geol. Surv., Folio 149, 14 p.

Stewart, D. B., 1956, Rapakivi granite of the Deer Isle region, Maine: Ph.D. dissert., Harvard Univ., Cambridge, 150 p.

Taylor, T. R., Vogel, T. A., and Wilband, J. T., 1980, The composite dikes at Mount Desert Island, Maine: an example of coexisting acidic and basic magmas: Jour. Geol., v. 88, p. 433-444.

Vogel, T. A., Younker, L. W., Wilband, J. T., and Kampmueller, E., 1984, Magma mixing: the Marsco suite, Isle of Skye, Scotland: Contrib. Mineral. Petrol., v. 87, p. 231-241.

Wager, L. R., and Bailey, E. B., 1953, Basic magma chilled against acid magma: Nature, v. 172, p. 68-69.

Wager, L. R., Vincent, E. A., Brown, G. M., and Bell, J. D., 1965, Marscoite and related rocks of the western Red Hills complex, Isle of Skye: Philos. Trans. Roy. Soc. London, v. A257, p. 273-307.

Walker, G. P. L., and Skelhorn, R. R., 1966, Some associations of acid and basic igneous rocks: Earth Sci. Rev., v. 2, p. 93-109.

Whalen, J. B., and Currie, K. L., 1984, The Topsail igneous terrane, western Newfoundland: evidence for magma mixing: Contrib. Mineral. Petrol., v. 87, p. 319-327.

Whalen, J. B., Currie, K. L., and Chappell, B. W., 1987, A-type granites: geochemical characteristics, discrimination and petrogenesis: Contrib. Mineral. Petrol, v. 95, p. 407-419.

White, A. J. R., and Chappell, B. W., 1983, Granitoid types and their distribution in the Lachland fold belt southeastern Australia: Geol. Soc. Amer., Mem. 159, p. 21-34.

Wiebe, R. A., 1973, Relations between coexisting basaltic and granitic magmas in a composite dike: Am. Jour. Sci., v. 273, p. 130-151.

Wiebe, R. A., 1974, Coexisting intermediate and basic magmas, Ingonish, Cape Breton Island: Jour. Geol. v. 82, p. 74-87.

Wiebe, R. A., 1979, Fractionation and liquid immisciblity in an anorthositic pluton of the Nain Complex, Labrador: Jour. Petrol., v. 20, p. 239-269.

Wiebe, R. A.. 1980, Commingling of contrasted magmas in the plutonic environment: example from the Nain Anorthosite complex: Jour. Geol., v. 88, p. 197-209.

Wiebe, R. A., 1984, Commingling of magmas in the Bjerkrem-Sogndal Lopolith (southwest Norway): evidence for the composition of residual liquids: Lithos, v. 17, p. 171-188.

Wiebe, R. A., and Wild, T., 1983, Fractional crystallization and magma mixing in the Tigalak layered intrusion, the Nain Anorthosite complex, Labrador: Contrib. Mineral. Petrol., v. 84, v. 307-344.

Yoder, H. S., Jr., 1973, Contemporaneous basaltic and rhyolitic magmas: Am. Mineral., v. 58, p. 151-171.

APPENDIX A. WHOLE ROCK MAJOR AND TRACE ELEMENT ANALYSES FOR THE VINALHAVEN GRANITE-GABBRO ASSOCIATION.

TABLE A1. VINALHAVEN WHOLE ROCK ANALYSES

	MEDIUM GRANITES										
Sample No.	VH-1	VH-2	VH-3	VH-4	VH-5	VH-6	VH-7	VH-8	VH-9	VH-10	VH-11
SiO_2	73.60	73.56	73.84	74.78	75.06	74.37	74.38	75.31	75.23	74.08	73.81
TiO_2	0.36	0.36	0.37	0.03	0.30	0.33	0.31	0.27	0.29	0.36	0.33
Al_2O_3	13.07	13.23	13.14	12.85	12.73	13.18	12.96	12.73	12.90	12.92	13.24
Fe_2O_3*	2.23	2.19	2.27	2.01	1.99	2.12	2.01	1.82	1.86	2.14	2.06
MnO	0.05	0.04	0.04	0.04	0.04	0.04	0.04	0.03	0.03	0.04	0.04
MgO	0.42	0.42	0.43	0.34	0.33	0.38	0.35	0.29	0.34	0.45	0.40
CaO	1.24	1.19	1.20	0.99	0.99	1.14	1.06	0.95	1.08	1.20	1.11
Na_2O	3.49	3.20	3.35	3.55	3.51	3.70	3.32	3.65	3.54	3.21	3.38
K_2O	5.05	5.23	4.98	5.09	5.04	5.01	5.11	5.00	5.10	5.05	5.16
P_2O_5	0.09	0.08	0.08	0.07	0.07	0.08	0.07	0.06	0.07	0.08	0.07
Total	99.60	99.49	99.70	100.01	100.04	100.34	99.60	100.14	100.43	99.53	99.59
Mg'-value	0.27	0.27	0.27	0.25	0.25	0.26	0.26	0.24	0.27	0.29	0.28
A/CNK	0.97	1.01	1.00	0.98	0.98	0.97	1.00	0.97	0.97	1.00	1.01
Ba	247	264	259	212	195	225	197	174	226	252	242
Rb	231	212	230	230	245	238	247	249	204	208	237
Sr	52	51	52	42	43	47	41	36	48	50	50
Pb	22	22	23	23	26	22	26	24	21	21	22
Th	19	17	19	22	28	19	23	25	17	19	18
U	8	6	12	5	7	8	10	9	7	7	7
Zr	215	209	214	192	182	206	188	170	175	200	195
Nb	12.9	13.0	12.8	13.2	13.3	14.0	13.5	13.8	11.4	12.7	13.1
Y	49	44	61	45	44	52	51	52	39	43	46
V	19	19	20	14	17	19	17	13	17	19	17
Cr	4	6	5	3	3	5	5	3	3	6	4
Ni	2	1	0	0	4	6	2	3	3	4	1
Zn	31	31	38	30	29	32	39	27	26	32	34
Ga	17	18	17	17	17	17	17	17	16	17	17
Rb/Sr	4.4	4.2	4.4	5.5	5.7	5.1	6.0	6.9	4.3	4.2	4.7
K/Rb	181.4	204.7	179.7	183.7	170.7	174.7	171.7	166.6	207.5	201.5	180.7
Zr/Nb	16.7	16.1	16.7	14.5	13.7	14.7	13.9	12.3	15.4	15.7	14.9
Zr/Y	4.4	4.8	3.5	4.2	4.2	4.0	3.7	3.3	4.5	4.7	4.2

*Total Fe expressed as Fe_2O_3

Mg'-value = mol. prop. Mg/(Mg+Fe) after adjusting Fe^{3+}/total Fe as FeO = 0.1

A/CNK = mol. $Al_2O_3/(CaO+Na_2O+K_2O)$

TABLE A1. CONTINUED.

Sample No.	FINE GRANITES VH-20	VH-21	VH-22	VH-23	VH-24	VHL-26	APLITE DIKES VH-27	VH-28	VH-29	VH-30	VH-97	VH-102
SiO_2	74.72	72.79	73.53	73.79	73.46	74.28	74.23	76.55	72.55	77.35	75.48	75.28
TiO_2	0.31	0.35	0.27	0.28	0.32	0.28	0.30	0.17	0.37	0.07	0.18	0.23
Al_2O_3	13.38	13.78	13.64	13.63	13.58	13.46	13.57	12.74	14.13	12.58	13.26	13.18
Fe_2O_3*	1.99	2.18	1.77	1.74	2.10	1.77	1.82	1.27	2.00	0.81	1.23	1.55
MnO	0.04	0.05	0.03	0.03	0.04	0.03	0.03	0.02	0.03	0.02	0.01	0.02
MgO	0.38	0.48	0.35	0.33	0.44	0.36	0.39	0.22	0.48	0.04	0.18	0.27
CaO	1.27	1.38	1.12	1.08	1.33	1.10	1.30	0.72	1.47	0.50	0.75	0.98
Na_2O	3.58	3.35	3.36	3.48	3.61	3.68	3.88	3.45	3.70	3.46	3.54	3.44
K_2O	4.98	5.14	5.25	5.21	5.10	5.09	4.78	5.14	5.39	5.46	5.47	5.29
P_2O_5	0.08	0.08	0.08	0.07	0.08	0.09	0.07	0.05	0.10	0.01	0.04	0.06
Total	99.72	99.56	99.40	99.64	100.04	100.14	100.37	100.31	100.22	100.30	100.15	100.30
Mg'-value	0.27	0.30	0.28	0.27	0.29	0.29	0.30	0.25	0.32	0.08	0.22	0.26
A/CNK	0.98	1.02	1.03	1.02	0.98	0.99	0.97	1.02	0.97	1.01	1.01	1.00
Ba	341	370	350	376	326	361	377	221	611	17	298	280
Rb	242	278	258	255	239	250	236	237	225	253	262	229
Sr	61	64	57	58	58	57	61	41	82	9	48	51
Pb	22	22	32	25	19	32	21	23	23	27	27	23
Th	22	26	18	22	22	17	20	20	20	28	20	22
U	10	6	9	7	8	6	9	10	6	11	8	5
Zr	204	252	211	233	220	185	225	128	276	90	135	153
Nb	15.1	16.2	14.1	15.6	15.1	13.7	14.2	12.0	13.2	17.3	12.5	11.9
Y	42	41	40	41	40	34	37	32	35	43	34	36
V	19	18	18	13	21	17	16	9	24	3	7	11
Cr	6	7	5	6	5	5	4	4	7	2	1	3
Ni	3	5	5	4	6	5	3	5	7	1	1	5
Zn	31	29	20	30	31	18	27	18	28	16	11	15
Ga	17	17	17	16	17	16	15	14	17	16	17	17
Rb/Sr	4.0	4.3	4.5	4.4	4.1	4.4	3.9	5.8	2.7	28.1	5.5	4.5
K/Rb	170.8	153.4	168.9	169.6	177.1	169.0	168.1	180.0	198.8	179.1	173.3	191.7
Zr/Nb	13.5	15.6	14.9	14.9	14.6	13.5	15.8	10.7	20.9	5.2	10.8	12.9
Zr/Y	4.9	6.1	5.2	5.6	5.5	5.5	6.1	4.0	7.9	2.1	4.0	4.2

Sample No.	GABBROS VH-40	VH-41	VH-42	VH-43	VH-44	VH-45	VH-46	VH-47	VH-48	VH-49	VH-50	VH-51	VH-52
SiO_2	48.58	48.43	49.39	48.18	51.58	52.85	52.22	47.75	47.77	47.58	54.82	53.34	47.94
TiO_2	1.53	1.18	0.96	1.86	0.81	1.24	1.07	1.03	0.98	0.89	0.78	2.25	1.90
Al_2O_3	17.11	18.31	18.44	16.35	18.20	16.15	16.58	19.61	19.07	17.69	15.23	13.89	16.77
Fe_2O_3*	10.39	9.19	8.16	11.53	7.66	8.85	7.95	7.64	7.92	9.18	7.21	12.03	11.52
MnO	0.16	0.15	0.14	0.19	0.12	0.14	0.14	0.12	0.12	0.15	0.13	0.20	0.19
MgO	8.31	9.47	9.01	7.74	7.96	7.43	7.01	9.56	9.79	11.11	8.03	5.55	8.25
CaO	9.92	10.76	10.08	10.83	9.96	9.62	11.59	11.80	11.24	10.84	10.07	7.89	9.24
Na_2O	2.91	2.47	3.03	2.73	2.90	2.77	2.82	2.66	2.54	2.48	2.44	3.21	3.16
K_2O	0.64	0.26	0.46	0.44	0.85	0.96	0.64	0.12	0.15	0.18	1.05	1.48	0.48
P_2O_5	0.23	0.13	0.11	0.23	0.07	0.06	0.12	0.09	0.07	0.10	0.07	0.35	0.24
Total	99.77	100.33	99.77	100.06	100.10	100.06	100.12	100.36	99.64	100.18	99.84	100.20	99.68
Mg'-value	0.61	0.67	0.69	0.57	0.67	0.62	0.64	0.71	0.71	0.71	0.69	0.48	0.59
A/CNK	0.73	0.77	0.77	0.66	0.76	0.70	0.63	0.76	0.77	0.74	0.65	0.65	0.74

Total Fe expressed as Fe_2O_3
Mg'-value = mol. prop. Mg/(Mg+Fe) after adjusting Fe^{3+}/total Fe as FeO = 0.1
A/CNK = mol. $Al_2O_3/(CaO+Na_2O+K_2O)$

TABLE A1. CONTINUED.

Sample No.	GABBROS (Cont.) VH-40	VH-41	VH-42	VH-43	VH-44	VH-45	VH-46	VH-47	VH-48	VH-49	VH-50	VH-51	VH-52
Ba	66	33	46	67	53	67	48	3	24	24	67	140	60
Rb	29	8	18	26	40	34	30	5	6	5	43	58	12
Sr	234	235	225	228	206	194	197	287	253	228	159	298	274
Pb	6	2	4	6	7	7	4	3	2	3	6	10	3
Th	2	2	2	1	3	2	2	0	0	1	4	4	1
U	1	1	1	1	2	1	1	0	0	0	2	1	1
Zr	93	79	71	141	83	72	97	79	62	62	92	208	164
Nb	4.3	2.5	1.4	4.5	3.3	3.0	3.2	0.9	1.2	2.3	4.0	8.0	4.2
Y	27	22	18	31	20	21	24	18	15	15	23	44	32
V	189	151	136	228	110	189	177	139	138	125	141	254	149
Cr	167	169	355	215	139	291	336	159	328	252	369	198	138
Ni	139	177	187	96	116	93	64	244	216	251	72	40	119
Zn	86	61	63	92	51	62	58	51	60	62	55	113	85
Ga	17	17	17	19	18	18	17	16	16	15	16	22	19
Rb/Sr	0.1	0.0	0.1	0.1	0.2	0.2	0.2	0.0	0.0	0.0	0.3	0.2	0.0
K/Rb	183.2	237.1	212.1	140.4	176.8	233.1	176.8	215.8	232.4	333.8	202.7	211.8	319.2
Zr/Nb	21.6	31.6	50.7	31.3	25.2	24.1	30.3	87.6	51.7	27.0	23.1	26.0	39.1
Zr/Y	3.4	3.6	3.9	4.5	4.1	3.4	4.1	4.4	4.0	4.1	4.0	4.7	5.2

Sample No.	GABBROS (Cont.) VH-53	VH-54	VH-56	VH-57	VH-58	VH-80D	VH-81D	VH-87D	VH-88DU	VH-92D	VH-93D	VH-94D	VH-200D
SiO_2	55.56	48.83	56.93	53.74	53.75	49.59	61.10	49.10	49.03	49.80	55.88	51.23	50.82
TiO_2	1.17	2.51	1.04	0.32	0.33	2.44	0.97	1.81	1.21	1.16	0.88	1.15	1.00
Al_2O_3	15.73	15.82	15.56	17.76	18.09	14.34	14.91	16.05	17.35	16.78	15.72	16.12	17.00
Fe_2O_3*	8.22	12.83	7.87	6.78	7.35	12.66	6.75	11.39	9.58	9.48	7.69	9.36	9.06
MnO	0.15	0.21	0.16	0.12	0.11	0.22	0.12	0.19	0.17	0.16	0.16	0.17	0.15
MgO	5.35	6.48	5.37	7.82	7.75	6.20	4.09	7.37	8.87	8.44	6.94	7.83	8.18
CaO	8.80	8.84	7.98	9.47	8.79	9.87	5.71	10.26	10.25	10.40	8.45	9.65	10.21
Na_2O	3.49	3.48	2.53	3.02	2.51	3.27	4.06	3.31	2.45	3.11	3.03	3.14	2.90
K_2O	1.41	0.89	2.15	1.11	1.15	0.84	2.60	0.63	1.14	0.51	1.36	0.83	0.76
P_2O_5	0.20	0.36	0.19	0.03	0.03	0.32	0.10	0.21	0.09	0.10	0.09	0.11	0.06
Total	100.07	100.24	99.78	100.17	99.86	99.75	100.40	100.30	100.04	99.93	100.21	100.17	100.12
Mg'-value	0.56	0.50	0.58	0.70	0.68	0.49	0.55	0.56	0.65	0.64	0.64	0.62	0.64
A/CNK	0.68	0.69	0.74	0.76	0.85	0.59	0.75	0.65	0.73	0.68	0.72	0.68	0.70
Ba	116	96	225	71	72	104	134	84	47	62	112	96	60
Rb	52	29	108	51	51	42	131	28	94	20	58	35	35
Sr	222	282	448	214	226	231	152	222	225	197	160	188	194
Pb	7	7	7	8	8	6	14	5	0	5	9	6	3
Th	5	2	5	3	3	2	11	2	1	1	5	3	3
U	1	1	3	2	2	1	8	0	1	1	3	2	1
Zr	128	195	137	51	54	200	150	147	82	98	95	104	64
Nb	6.1	7.3	6.5	3.1	2.2	6.6	7.1	4.7	1.9	3.2	4.4	3.1	2.7
Y	33	39	30	14	14	44	37	33	23	25	29	26	19
V	154	246	157	57	47	305	135	222	163	173	145	166	158
Cr	62	151	130	178	98	153	112	194	243	276	248	219	227
Ni	19	70	40	119	124	46	51	84	166	133	100	159	123
Zn	70	107	72	63	50	107	58	89	72	70	80	74	76
Ga	19	22	18	15	15	22	17	19	16	19	16	17	16
Rb/Sr	0.2	0.1	0.2	0.2	0.2	0.2	0.9	0.1	0.4	0.1	0.4	0.2	0.2
K/Rb	225	225.6	165.2	180.6	187.1	166.0	164.7	186.7	100.6	211.6	194.6	196.8	180.2
Zr/Nb	21.0	26.7	21.1	16.5	24.5	30.3	21.1	31.3	43.2	30.6	21.6	33.5	23.7
Zr/Y	3.9	5.0	4.5	3.5	4.0	4.6	4.1	4.5	3.6	4.0	3.3	4.0	3.4

*Total Fe expressed as Fe_2O_3
Mg'-value = mol. prop. Mg/(Mg+Fe) after adjusting Fe^{3+}/total Fe as FeO = 0.1
A/CNK = mol. $Al_2O_3/(CaO+Na_2O+K_2O)$

TABLE A1. CONTINUED.

Sample No.	GABBROS (Cont.) VH-201D	VH-203D	GRANITE MATRIX MATERIAL VH-62M	VH-63M	VH-74M	VH-75M	VH-68M	VH-69M	VH-86M	VH-91M	VH-95M	VH-98M	VH-99M
SiO_2	49.57	49.61	61.71	63.95	71.62	68.77	72.78	73.41	73.25	73.10	74.65	69.63	67.69
TiO_2	0.99	0.85	1.62	1.28	0.55	0.68	0.39	0.38	0.38	0.89	0.38	0.80	1.03
Al_2O_3	17.60	17.85	14.26	14.47	13.49	14.19	13.29	13.35	13.68	13.39	12.55	13.12	14.32
Fe_2O_3*	8.87	8.36	8.59	6.81	3.13	4.17	2.55	2.37	2.21	2.44	2.30	4.82	4.98
MnO	0.14	0.13	0.16	0.11	0.07	0.07	0.04	0.04	0.02	0.04	0.03	0.08	0.08
MgO	9.89	9.40	1.91	1.63	0.84	1.36	0.73	0.66	0.68	0.69	0.58	1.69	1.11
CaO	9.54	9.99	4.41	3.81	1.87	2.60	1.67	1.52	1.60	1.50	0.93	3.14	2.88
Na_2O	3.01	2.83	3.62	3.65	3.66	3.17	3.51	3.30	3.21	3.55	2.76	2.99	3.79
K_2O	0.56	0.81	3.10	3.51	4.61	4.31	4.76	4.55	4.44	4.76	5.82	3.53	3.91
P_2O_5	0.08	0.07	0.53	0.29	0.10	0.12	0.08	0.07	0.07	0.07	0.08	0.19	0.24
Total	100.25	99.90	99.90	99.50	99.95	99.46	99.80	99.64	99.54	99.94	100.09	99.98	100.02
Mg'-value	0.69	0.69	0.31	0.32	0.35	0.39	0.36	0.36	0.38	0.36	0.33	0.41	0.31
A/CNK	0.77	0.75	0.82	0.86	0.94	0.97	0.95	1.02	1.05	0.98	1.00	0.91	0.91
Ba	59	48	219	267	209	338	218	222	243	227	299	240	247
Rb	21	39	116	118	212	141	194	180	155	193	214	99	135
Sr	213	215	168	130	64	98	58	61	73	60	56	109	139
Pb	5	5	16	17	22	20	24	22	18	22	23	14	16
Th	2	2	12	11	21	12	18	20	13	20	21	15	13
U	1	1	3	3	4	3	4	5	5	4	10	6	5
Zr	60	70	289	256	187	226	172	165	176	173	189	491	139
Nb	2.3	1.9	12.5	13.8	12.1	16.6	11.9	12.5	10.8	11.9	14.6	10.9	12.5
Y	18	18	59	53	48	48	40	43	34	41	46	58	45
V	138	127	101	96	48	62	28	28	31	28	27	74	90
Cr	298	342	5	13	11	22	15	13	15	12	6	17	4
Ni	195	180	3	7	4	11	6	7	8	5	3	5	3
Zn	61	60	96	76	45	52	39	30	23	34	24	54	45
Ga	17	17	21	19	18	19	17	16	17	17	16	16	19
Rb/Sr	0.1	0.2	0.7	0.9	3.3	1.4	3.4	3.0	2.1	3.2	3.8	0.9	1.0
K/Rb	220.1	171.3	221.8	246.9	180.5	253.7	203.6	209.8	237.7	204.7	225.7	295.9	240.4
Zr/Nb	26.1	36.8	23.1	18.5	15.5	13.6	14.5	13.2	16.3	14.5	13.0	45.0	11.1
Zr/Y	3.3	4.0	4.9	4.9	3.9	4.7	4.3	3.9	5.1	4.2	4.1	8.4	3.1

Sample No.	GRANITE MATRIX MATERIAL (Cont.) VH-200M	VH-201M	VH-202M	VH-203M	BASALT PILLOWS VH-60P	VH-68P	VH-69P	VH-80P	VH-81P	VH-84P	VH-85P	VH-86P	VH-91P
SiO_2	70.22	72.37	68.25	72.93	48.54	48.43	48.65	48.14	48.80	49.28	48.92	50.15	48.67
TiO_2	0.66	0.33	0.76	0.35	1.31	1.35	1.29	1.92	1.29	1.36	1.13	1.24	1.30
Al_2O_3	13.99	14.40	14.34	13.79	16.99	17.00	16.99	16.35	17.00	17.78	17.81	16.75	16.91
Fe_2O_3*	3.79	1.98	4.44	2.19	10.14	10.33	10.09	11.54	10.11	9.45	9.42	9.77	10.09
MnO	0.07	0.03	0.08	0.03	0.17	0.17	0.17	0.18	0.16	0.16	0.15	0.17	0.16
MgO	1.26	0.70	1.88	0.76	8.14	8.32	8.37	7.48	8.11	7.62	8.46	7.99	8.37
CaO	2.29	1.74	3.49	1.73	10.81	10.96	11.05	10.55	11.14	10.36	10.99	10.28	11.10
Na_2O	3.50	3.85	3.95	3.84	2.90	2.74	2.46	2.64	3.01	2.91	2.90	2.49	2.51
K_2O	4.46	4.66	2.94	4.24	0.44	0.68	0.55	0.57	0.28	1.32	0.27	0.78	0.31
P_2O_5	0.13	0.10	0.15	0.10	0.14	0.11	0.09	0.25	0.10	0.11	0.09	0.10	0.09
Total	100.36	100.16	100.28	99.94	99.84	100.08	99.70	99.61	100.0	100.35	100.14	99.72	99.50
Mg'-value	0.40	0.41	0.46	0.41	0.61	0.61	0.62	0.56	0.61	0.61	0.64	0.62	0.62
A/CNK	0.95	0.99	0.89	0.98	0.68	0.68	0.69	0.68	0.67	0.71	0.71	0.71	0.69

*Total Fe expressed as Fe_2O_3
Mg'-value = mol. prop. Mg/(Mg+Fe) after adjusting Fe^{3+}/total Fe as FeO = 0.1
A/CNK = mol. $Al_2O_3/(CaO+Na_2O+K_2O)$

TABLE A1. CONTINUED.

Sample No.	GRANITE MATRIX MATERIAL (Cont.) VH-200M	VH-201M	VH-202M	VH-203M	BASALT PILLOWS (Cont.) VH-60P	VH-68P	VH-69P	VH-80P	VH-81P	VH-84P	VH-85P	VH-86P	VH-91P
SBa	230	429	190	331	39	29	26	71	32	63	37	73	32
Rb	175	168	111	163	22	38	27	31	12	120	10	36	12
Sr	80	99	99	85	206	197	203	233	203	190	214	193	211
Pb	19	17	14	20	2	6	6	3	5	3	4	1	3
Th	17	18	12	20	1	0	1	1	1	0	2	1	1
U	7	4	3	3	0	1	1	1	1	1	0	1	0
Zr	193	55	112	161	87	99	86	158	93	96	87	106	76
Nb	11.8	11.5	15.3	11.2	2.3	2.2	2.0	4.9	1.5	1.8	1.9	2.5	2.1
Y	43	31	42	29	25	30	25	33	26	26	24	28	22
V	57	30	84	30	189	204	200	230	189	201	166	194	188
Cr	20	11	41	12	228	259	261	212	239	274	211	257	254
Ni	14	10	17	9	129	126	127	89	127	148	129	126	106
Zn	40	24	54	25	72	84	76	81	73	67	66	77	84
Ga	17	17	17	16	16	18	16	20	17	18	18	16	17
Rb/Sr	2.2	1.7	1.1	1.9	0.1	0.2	0.1	0.1	0.1	0.6	0.0	0.2	0.1
K/Rb	211.5	230.2	219.8	215.9	171.4	148.5	169.7	151.4	193.6	91.3	220.8	179.8	212.3
Zr/Rb	16.4	4.8	7.3	14.4	37.8	45.0	43.2	32.3	62.1	53.3	45.8	42.3	36.1
Zr/Y	4.5	1.8	2.7	5.6	3.5	3.3	3.4	4.8	3.6	3.7	3.7	3.8	3.4

Sample No.	BASALT PILLOWS (Cont.) VH-95P	VH-96P	VH-98PI	VH-98PO	VH-99PI	VH-99PM	VH-99PO	VH-100PI	VH-100PO	VH-101P	VH-200P	VH-201P	VH-202P	VH203P
SiO_2	55.59	47.85	52.32	52.33	52.58	49.11	48.46	47.62	47.97	48.02	48.51	51.93	48.23	48.61
TiO_2	1.04	1.92	2.07	2.01	1.26	1.84	1.84	1.92	1.91	1.91	1.33	1.42	1.24	1.28
Al_2O_3	15.89	16.47	15.43	15.22	16.64	16.26	16.43	16.34	16.49	16.59	16.72	16.43	17.29	17.36
Fe_2O_3*	7.88	11.76	11.10	11.05	8.73	11.19	11.31	11.68	11.63	11.57	10.56	9.65	9.97	9.17
MnO	0.15	0.19	0.22	0.18	0.15	0.19	0.18	0.19	0.19	0.19	0.18	0.20	0.17	0.16
MgO	6.05	7.87	5.70	5.46	7.34	7.49	7.63	7.90	7.76	7.81	8.24	6.63	8.94	8.39
CaO	7.91	10.74	8.67	9.07	9.02	10.19	10.39	10.70	10.71	10.71	11.24	9.08	11.48	11.81
Na_2O	3.19	2.72	3.50	3.68	3.14	3.01	2.65	3.02	2.96	2.80	2.93	3.53	2.57	2.66
K_2O	1.76	0.43	0.71	0.64	1.40	0.57	0.68	0.41	0.56	0.52	0.22	1.29	0.45	0.44
P_2O_5	0.10	0.26	0.27	0.29	0.11	0.24	0.24	0.24	0.26	0.25	0.10	0.18	0.09	0.10
Total	99.55	100.19	99.98	99.93	100.36	100.28	99.81	100.02	100.43	100.38	100.01	100.32	100.44	99.97
Mg'-value	0.60	0.57	0.50	0.49	0.62	0.57	0.57	0.57	0.57	0.57	0.61	0.58	0.64	0.64
A/CNK	0.74	0.67	0.69	0.65	0.72	0.67	0.68	0.66	0.66	0.67	0.66	0.69	0.68	0.66
Ba	126	67	59	67	85	88	80	60	65	63	22	153	18	24
Rb	121	14	48	34	65	38	40	9	21	19	8	57	17	25
Sr	164	245	205	203	210	233	236	240	238	239	204	187	188	185
Pb	11	3	12	5	8	5	3	4	6	9	3	8	4	3
Th	7	1	4	3	4	2	2	1	1	1	0	4	1	1
U	7	0	2	2	1	1	1	0	0	0	0	1	0	1
Zr	122	157	185	208	83	147	158	154	159	159	94	176	82	84
Nb	5.8	4.6	7.7	7.4	4.8	4.8	5.3	5.0	4.7	5.2	1.9	5.5	1.7	1.6
Y	31	34	40	41	23	32	33	32	33	34	26	34	25	26
V	154	231	263	237	168	217	224	230	228	232	203	185	204	204
Cr	186	209	136	126	200	195	205	210	211	215	263	161	292	286
Ni	91	97	44	45	114	95	103	98	102	105	111	97	154	158
Zn	70	86	91	91	68	88	82	85	89	92	73	89	85	69
Ga	18	19	22	20	17	20	18	19	18	19	18	18	17	16
Rb/Sr	0.7	0.1	0.2	0.2	0.3	0.2	0.2	0.0	0.1	0.1	0.0	0.3	0.1	0.1
K/Rb	120.7	255.5	123.4	156.7	178.7	124.5	141.5	373.5	219.3	228.4	225.1	187.8	219.7	146.1
Zr/Nb	21.1	34.1	24.0	28.1	17.3	30.6	29.8	30.8	33.8	30.6	49.5	32.0	48.2	52.5
Zr/Y	3.9	4.7	4.7	5.1	3.6	4.6	4.9	4.8	4.8	4.7	3.6	5.1	3.2	3.2

*Total Fe expressed as Fe_2O_3
Mg'-value = mol. prop. Mg/(Mg+Fe) after adjusting Fe^{3+}/total Fe as FeO = 0.1
A/CNK = mol. $Al_2O_3/(CaO+Na_2O+K_2O)$

TABLE A2. VINALHAVEN WHOLE ROCK ANALYSES (INAA).

Sample No.	VH-7	VH-21	VH-41	VH-49	VH-51	VH-52	VH-81D	VH-62M	VH-63M	VH-95M	VH-68P	VH-85P	VH-95P	VH-64
La	40.8	41.0	4.4	3.6	17.9	8.4	19.8	34.0	26.2	30.0	26.0	4.0	14.0	12.2
Ce	94.6	93.4	13.3	10.0	46.4	24.5	46.2	82.9	70.3	67.5	27.9	11.4	33.8	40.4
Nd	43.4	43.5	9.5	5.7	30.7	18.8	23.4	47.4	40.9	31.0	22.5	9.6	18.7	36.5
Sm	8.47	8.16	3.01	2.15	7.28	4.88	5.60	10.34	9.10	7.42	4.57	3.00	4.64	14.16
Eu	0.64	0.80	1.19	0.89	2.20	1.79	1.08	2.44	1.82	0.70	1.31	1.14	1.15	0.75
Tb	1.79	1.70	0.45	0.30	1.12	0.68	1.10	1.60	1.46	1.64	0.54	0.55	0.83	2.87
Yb	5.82	4.15	2.06	1.44	4.48	2.90	3.67	5.85	5.45	5.03	2.28	2.23	3.00	12.87
Lu	0.80	0.63	0.34	0.20	0.71	0.51	0.55	0.93	0.82	0.73	0.40	0.33	0.46	1.92
Hf	6.3	7.3	2.3	1.6	6.5	4.2	4.5	8.0	7.7	6.6	2.6	2.2	3.6	6.1
Ta	3.6	3.6	0.5	0.3	1.0	0.6	1.2	2.3	2.4	4.4	0.6	0.5	1.0	2.9
Th	24.8	25.7	0.5	0.2	4.9	0.7	11.3	11.8	11.1	24.9	0.5	0.6	6.5	19.8
U	7.2	5.1	-	-	-	-	6.6	2.2	1.8	8.4	-	-	6.3	5.9
Zr/Hf	29.7	34.5	34.7	38.1	31.8	39.4	33.1	36.2	33.2	28.9	38.4	38.9	34.0	33.6
Ta/Nb	0.3	0.2	0.2	0.1	0.1	0.1	0.2	0.2	0.3	0.3	0.3	0.3	0.2	0.1
Sample/CH														
La	123.7	124.4	13.4	10.8	54.3	25.5	59.8	103.2	79.3	90.9	78.6	12.2	42.3	37.0
Ce	107.5	106.1	15.1	11.4	52.7	27.8	52.5	94.2	79.8	76.7	31.7	13.0	38.4	46.0
Nd	72.3	72.5	15.8	9.5	51.2	31.3	38.9	79.1	68.2	51.7	37.4	16.0	31.1	60.9
Sm	46.8	45.1	16.6	11.9	40.2	27.0	30.9	57.1	50.3	41.0	25.2	16.6	25.6	78.2
Eu	9.3	11.6	17.2	12.9	31.9	25.9	15.7	35.4	26.3	10.1	19.0	16.5	16.7	10.8
Tb	38.1	36.2	9.6	6.4	23.8	14.5	23.4	34.0	31.1	34.9	11.4	11.7	17.7	61.1
Yb	29.1	20.8	10.3	7.2	22.4	14.5	2.8	29.3	27.3	25.2	11.4	11.2	15.0	64.6
Lu	23.6	18.5	10.0	5.9	20.9	15.0	133.2	27.4	24.1	21.5	11.7	9.7	13.5	56.5
(La/Sm)CH	2.6	2.8	0.8	0.9	1.4	0.9	1.9	1.8	1.6	2.2	3.1	0.7	1.7	0.5
(Yb/Sm)CH	0.6	0.5	0.6	0.6	0.6	0.5	0.1	0.5	0.5	0.6	0.5	0.7	0.6	0.8

Maine Geological Survey
Studies in Maine Geology: Volume 4
1989

Geology and Geochemistry of the Rattlesnake Mountain Igneous Complex, Raymond and Casco, Maine

John W. Creasy
Department of Geology
Bates College
Lewiston, Maine 04240

ABSTRACT

Early Jurassic igneous rocks exposed in Casco and Raymond, Maine, intrude quartz monzonite and migmatite of the Carboniferous Sebago pluton. Northeast-trending dikes of trachyte, nepheline trachyte, and minor lamprophyre emanate from, but in part predate, the spatially associated silica saturated and undersaturated alkali syenites of the Rattlesnake Mountain pluton. These rocks, termed the Rattlesnake Mountain igneous complex, are assigned to the White Mountain magma series on the basis of age, mineralogy, and texture and constitute the most easterly known occurrence of this distinct petrotectonic suite.

Several bodies of syenite are distinguished by texture, abundance, and proportion of ferrohastingsite and biotite, and abundance of nepheline. In order of decreasing relative age these are: melanocratic syenite, medium-grained biotite-ferrohastingsite syenite, coarse-grained ferrohastingsite syenite, fine-grained chilled syenite, nepheline-bearing syenite, and nepheline syenite.

Compositions of trachyte and nepheline trachyte closely parallel those of ferrohastingsite syenite and nepheline-bearing syenite, respectively. However, correlated variations in Sr and Rb abundances and in Ba/Sr values define one group of rocks that contain cumulus alkali feldspar, e.g. ferrohastingsite syenite. Compositions of a second group are representative of residual liquids and require removal of alkali feldspar, e.g. nepheline syenite and dike rocks. The variations of Sc and LREE abundances in the plutonic rocks require fractionation or accumulation of minerals, e.g. amphibole ± sphene and apatite, that have partition coefficients >1 and that preferentially incorporate the HREEs. These chemical data are consistent with the accumulation or fractionation of alkali feldspar, amphibole, and accessory minerals such as sphene and apatite. The presence of alkali feldspar and hornblende as phenocrysts in dike rocks supports this conclusion.

Outcrops of melanocratic syenite are observed to be mechanical mixtures produced by the intrusion of syenitic magma into rocks of lamprophyric composition. Major and trace element abundances generally fall on a simple mixing line between these two end member compositions.

Sr isotopic data from the pluton (Creasy, 1988) indicate an Sr initial ratio of 0.7027. This requires derivation of the syenites from melts of strongly depleted mantle or by partial melting of Rb depleted lower crust (mafic granulite ?).

PETROTECTONIC SETTING

Syenite and nepheline syenite occur at Rattlesnake Mountain in Raymond and Casco, Maine (DeMartinis, 1976; Carter et al., 1979; Whitaker, 1984) and constitute the Rattlesnake Mountain pluton. Porphyritic trachyte and nepheline-bearing trachyte form nearly linear swarms of dikes spatially associated with the pluton (Griffith, 1983). The pluton and dikes together are termed

the Rattlesnake Mountain igneous complex and are assigned by Creasy et al. (1986) and Creasy (1988) to the White Mountain magma series (Billings, 1956).

The Rattlesnake Mountain pluton has field and petrographic characteristics typical of the White Mountain magma series (Fig. 1). It is clearly discordant with the surrounding granitoids (and migmatites) of the Sebago batholith of Carboniferous age (Aleinikoff et al., 1985; Hayward and Gaudette, 1984) and has a well developed chilled margin. The syenites exhibit massive hypidiomorphic-granular textures and lack metamorphic foliation although a primary flow texture is developed in some rocks. The essential mineral constituents are microperthite, subordinate nepheline and ferrohastingsite, and locally biotite and ferrohedenbergite or aegerine-augite; muscovite and other peraluminous minerals are absent.

In contrast to most intrusive centers of the White Mountain magma series, swarms of dikes are associated with the Rattlesnake Mountain pluton (Fig. 2). Dikes of trachyte and nepheline-bearing trachyte are thin (cm-scale) and generally sparse within the pluton. However, only 1 km to the northeast, 52 dikes with an aggregate width of 113 m intrude a zone 1.2 km wide. Southwest of the pluton, 42 dikes totalling 47 m in width occur in a zone 0.9 km wide. The average orientation of these dikes is N54^{o}E $\pm$ 14° with vertical dip (Griffith, 1983) and is controlled by a regional joint orientation (Creasy, 1979). These data indicate a NW-SE crustal dilation of 10% and 5%, respectively. The dikes decrease in width and number with increasing distance from the pluton. Arcuate or ring dikes typically associated with major intrusive centers of the White Mountain magma series are lacking here.

All known occurrences of feldspathoidal syenite in northern New England (Fig. 1), including the Rattlesnake Mountain pluton, define a nearly linear array that trends N55^{o}E. Most occurrences are assigned to the White Mountain magma series: for example, Pleasant Mountain (Jenks, 1934; Sanders, 1971) and Randall Mountain (Gilman, 1978), Maine; Red Hill, New Hampshire (Pirsson and Washington, 1907; Wellman, 1971; Size, 1972); and Cuttingsville, Vermont (Eggleston, 1918).

An Rb-Sr whole-rock isochron age of 205 $\pm$ 2 Ma for the Rattlesnake Mountain pluton (Creasy, 1988) is consistent ($\pm 2\sigma$)with K-Ar ages (H. Krueger, pers. comm., 1985) of 192 $\pm$ 7 Ma for syenite and of 196 $\pm$ 8 Ma for trachyte. These ages fall within the older (200-165 Ma) of the two major periods of White Mountain magmatism (Foland and Faul, 1977; Eby and Creasy, 1983; McHone and Butler, 1984). The syenites at Red Hill, New Hampshire, yield a similar age of 198 $\pm$ 3 Ma (Rb-Sr isochrons, Foland and Friedman, 1977). However, K-Ar ages for feldspathoidal rocks at Pleasant Mountain (Foland and Faul, 1977), Randall Mountain (Weston Geophysical Research, 1977), and Cuttingsville (Armstrong and Stump, 1971) fall within the younger White Mountain magma series (100-130 Ma) of Eby (1985a,b,c). Nepheline syenite in Litchfield, Maine (Barker, 1965) is assigned to the Mesozoic coastal New England igneous province (McHone and Butler, 1984) primarily on the basis of significantly older K-Ar dates of 234 $\pm$ 5 Ma and 244 $\pm$ 5 Ma (Burke et al., 1969).

The ages and regional distribution of these feldspathoidal syenites hint at some long-lived lithospheric control for the occurrence of undersaturated felsic magmas. The regional trend of plutons parallels both the regional orientation of abundant mafic dikes of Permo-Triassic age (McHone, 1978) and of dikes of the Rattlesnake Mountain igneous complex. This trend, N55^{o}E, intersects at high angle the NNW trend of the voluminous, oversaturated intrusives of the White Mountain magma series (Fig. 1). Hence, while early Mesozoic magmatism is considered an expression of rifting (Creasy and Eby, 1983; McHone and Butler, 1984), the the spatial distribution and temporal association of mafic magmas, undersaturated felsic magmas, and oversaturated felsic magmas likely signal differing structural domains within the crust and differing source regions within the continental lithosphere.

The rocks of the Rattlesnake Mountain igneous complex exhibit systematic variations in mineralogy, chemistry, and relative age that are the subject of this paper. These data document the petrologic evolution of an undersaturated magma system and thus provide a rare opportunity to evaluate the formation of undersaturated felsic rocks within the continental crust.

GEOLOGY

The elliptical pluton is exposed over an area of 8 km^2 on Rattlesnake Mountain in the northwest corner of the Raymond, Maine, 7 1/2' quadrangle (Fig. 3). This mountain is a series of several hills joined by low saddles to the main summit (elevation 1035') which provide 600 feet of vertical relief on the pluton. The main summit is elongate to the northeast with a steep southeast-facing slope providing nearly continuous exposure. The dikes are best exposed on Pismire Mountain and Tenny Hill to the northeast (Fig. 2) and on a ridge paralleling Maine Route 121 to the southwest of the pluton. These dikes extend to Black Cat Mountain, a distance of 7 km to the northeast, and to Sebago Lake, a distance of 10 km to the southwest (Griffith, 1983).

The Rattlesnake Mountain pluton intrudes granitoids and migmatites of the Carboniferous Sebago batholith (Osberg et al., 1985). DeMartinis (1976) described these rocks from the vicinity of Rattlesnake Mountain as consisting of a medium- to coarse-grained two-mica quartz monzonite (CQM of Table 1) containing inclusions and regionally-oriented septa of oligoclase-biotite schist and gneiss. Pegmatite and aplite dikes are present in most outcrops of country rock. A narrow arcuate body of biotite granite crops out along the northwest margin of the pluton. This granite is demonstrably older than the syenite, but is inferred to be younger than the quartz monzonite. It is distinguished from the quartz monzonite (DeMartinis, 1976) by the abundance (~6%) of small schist inclusions, the lack of muscovite, the greater ratio of alkali feldspar:plagioclase, and

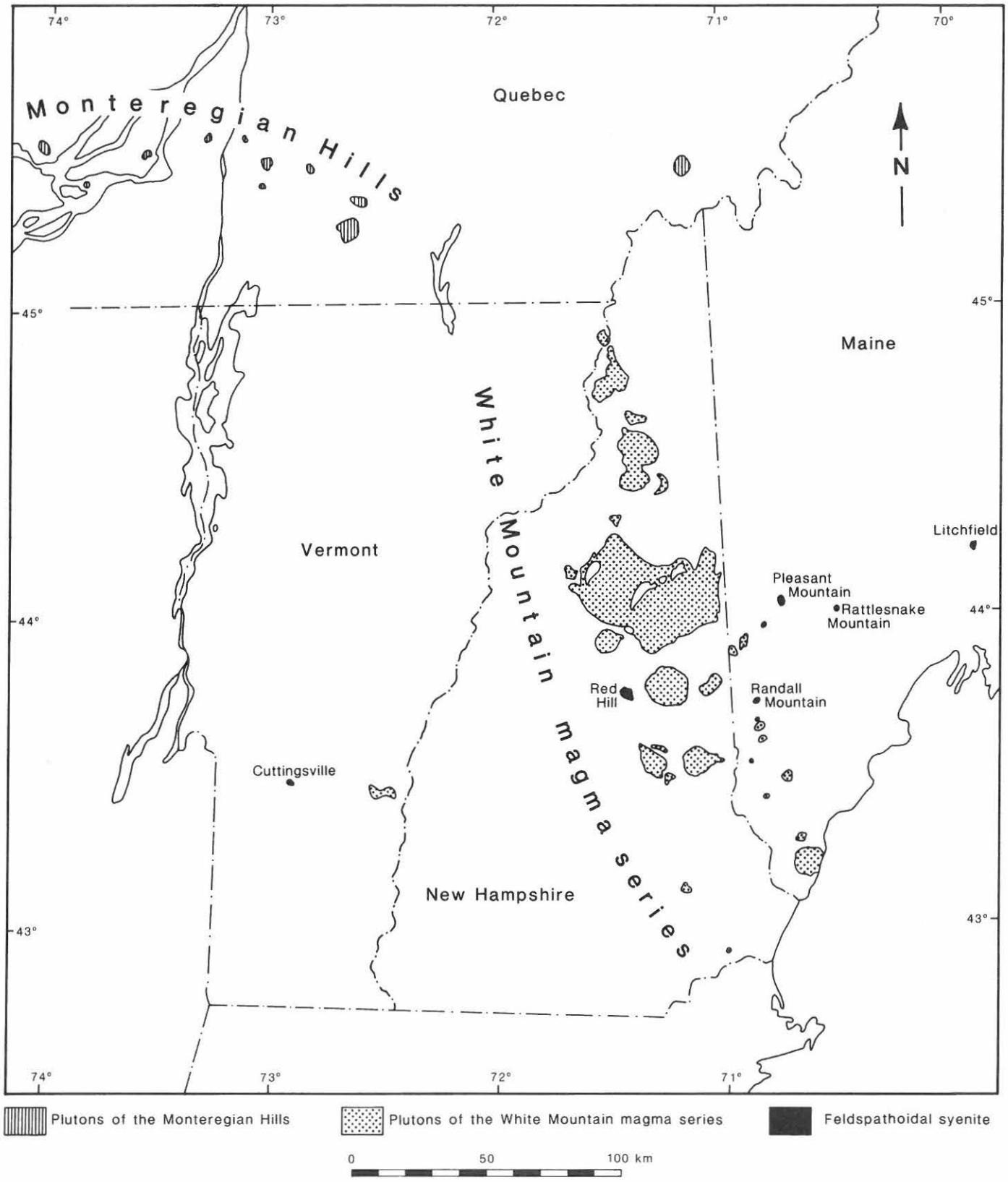

Figure 1. Map showing the distribution of the White Mountain magma series and the location of specific localities referred to in text.

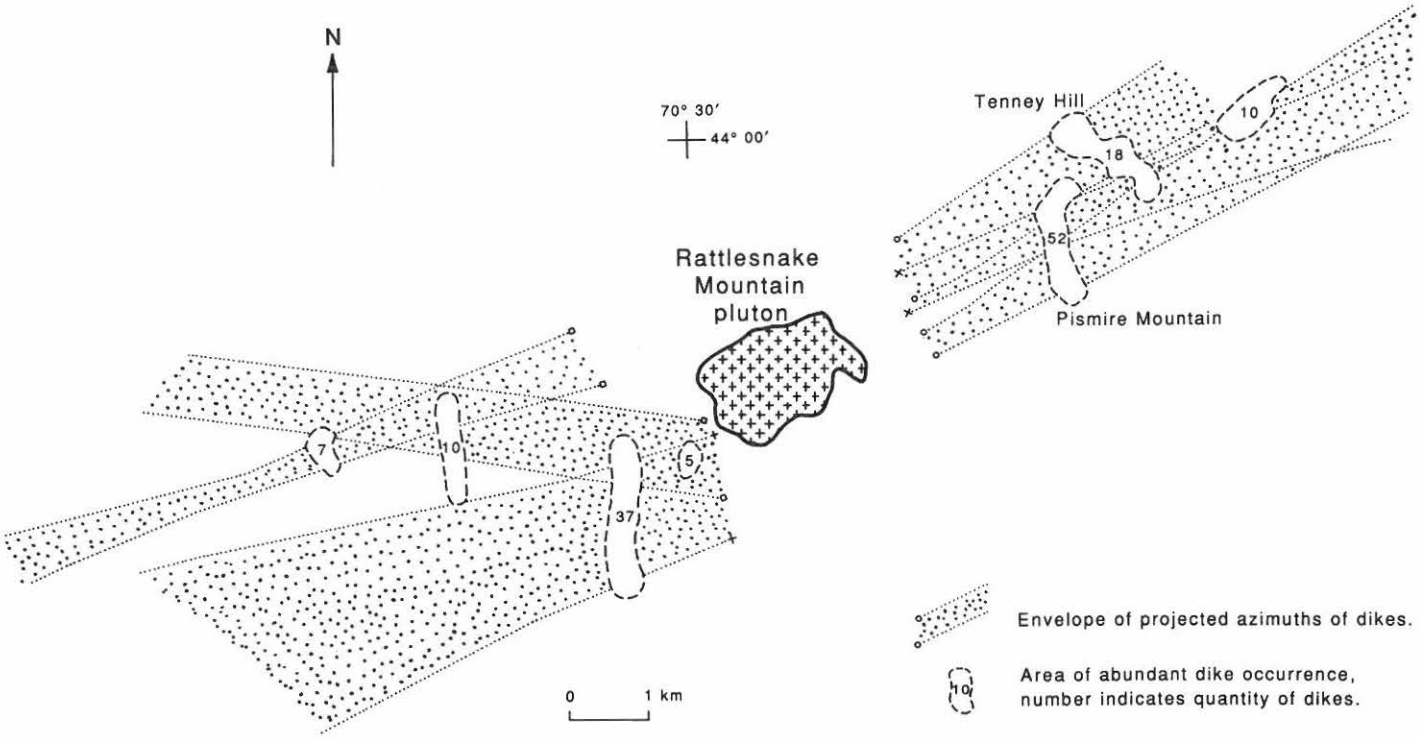

Figure 2. Map illustrating the spatial relations of the Rattlesnake Mountain pluton and associated dike swarm (modified after Griffith, 1983).

TABLE 1. AVERAGE MODES OF ROCKS FROM RATTLESNAKE MOUNTAIN IGNEOUS COMPLEX.

	ROCK UNIT[1]					
	CQM	HBT	NET	FHS	NBS	NS
MINERAL						
Orthoclase	24	42 ± 4	39 ± 6	7 ± 4	19 ± 5	4 ± 1
Oligoclase	34	39 ± 5	40 ± 7	4 ± 1	1	2
Microperthite	0	4 ± 1	0	75 ± 7	62 ± 12	63 ± 2
Quartz	36	0	0	0	0	0
Nepheline	0	0	4 ± 2	0	3 ± 2	16 ± 2
Biotite	5	2 ± 1	5 ± 3	1 ± 1	1	1
Muscovite	3	0	0	0	0	0
Ferrohastingsite	0	7	8 ± 3	11 ± 6	12 ± 3	8 ± 2
Aegirine-augite	0	0	1	3 ± 3	1	2
Fayalite	0	0	0	tr	0	0
Zircon	tr	tr	tr	tr	tr	tr
Apatite	0	tr	tr	tr	tr	tr
Allanite	0	0	0	tr	tr	0
Sphene	0	tr	tr	tr	tr	tr
Opaques	tr	3	2	tr	1	1
Chlorite	0	tr	tr	0	tr	0
Calcite	0	1	1	0	0	0
Sericite	0	tr	tr	tr	1	3
Number of samples	2	5	8	16	7	2

[1]CQM = quartz monzonite of Sebago pluton, HBT = hornblende trachyte, NET = nepheline trachyte, FHS = ferrohastingsite syenite, NBS = nepheline-bearing syenite, NS = nepheline syenite.

locally, the presence of sodic amphibole. The latter was attributed to alkali metasomatism adjacent to the intruding syenite (DeMartinis, 1976). This granite is similar to other non-foliated subaluminous granites, e.g. the Black Cat granite (Creasy, 1979), occurring within peraluminous rocks of the Sebago batholith.

The pluton (Fig. 3) is composed chiefly of coarse-grained ferrohastingsite syenite; nepheline-bearing syenites comprise about 20% of exposures. Other minor but distinctive lithologies include fine-grained syenite forming a chilled margin to the pluton and mafic syenite of hybrid origin. The chilled margin of the pluton is well exposed at several locations and dips outward at 35° except along the northwest where dips of 76-80° are recorded. A lamprophyre dike or plug (?) within the pluton is intruded by the ferrohastingsite syenite. The presence of hybridized syenites (Fig. 3) suggests that more extensive occurrences of lamprophyric rocks may have been present prior to emplacement of the pluton. As noted above, dikes of trachyte, nepheline trachyte, and lamprophyre are thin and generally sparse within the pluton.

Several distinct lithologic units are recognized within the Rattlesnake Mountain pluton (DeMartinis, 1976; Carter et al., 1979; Whitaker, 1984; Creasy et al., 1986). In order of decreasing relative age these are (Fig. 1): mafic hybridized syenite (HYS), medium-grained biotite-ferrohastingsite syenite (FBS), coarse-grained ferrohastingsite syenite (FHS), fine-grained syenite (CHS), nepheline-bearing syenite (NBS), and nepheline syenite (NS).

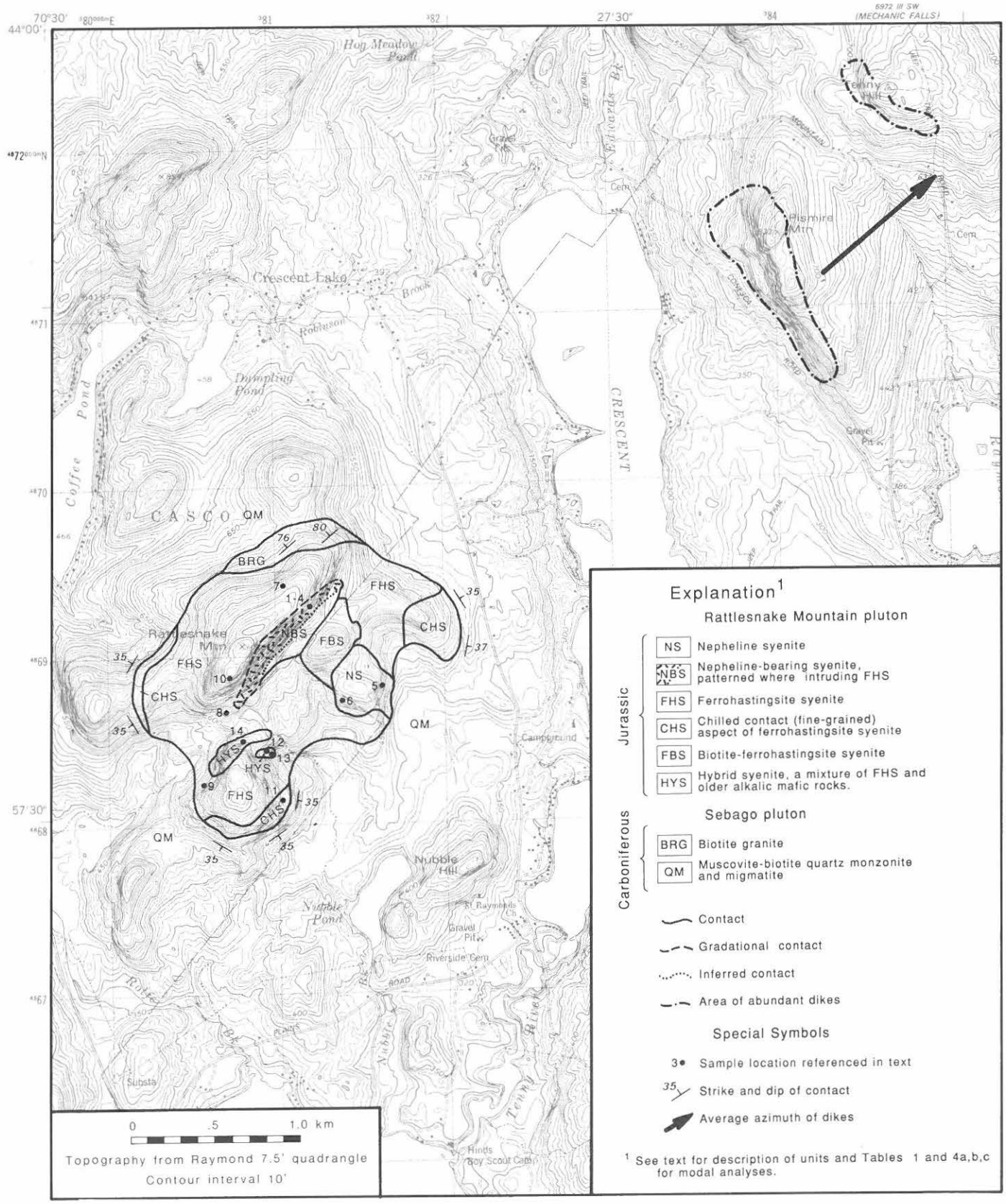

Figure 3. Geologic map of the Rattlesnake Mountain pluton (modified after Whitaker, 1984).

Coarse-grained ferrohastingsite syenite (FHS of Table 1) is the most abundant rock type. Microperthite and ferrohastingsite dominate the mineral assemblage; orthoclase and oligoclase are the only other minerals commonly present in greater than trace amounts. The feldspar:amphibole ratio ranges from 3:1 to 25:1 (average 10:1) and although variations are at the outcrop scale, no systematic variations in this ratio are seen across the pluton. Occasional grains of aegirine-augite are present in thin section and usually are rimmed by ferrohastingsite (Fig. 4). Other typical accessory minerals include sphene, apatite, zircon, allanite, and magnetite. The subhedral crystal shapes of feldspar and ferrohastingsite indicate simultaneous crystallization (or accumulation) of these two minerals. In nearly all other syenites of the White Mountain magma series, amphibole is an interstitial, late crystallizing mineral (Creasy, 1974). Cumulate textures are not recognized within the ferrohastingsite syenite, but this does not preclude the presence of significant cumulus alkali feldspars (Creasy et al., 1979). The sparsely distributed nepheline (~1 grain/m^2) is present in the ferrohastingsite syenite as interstitial grains; no quartz has been observed in hand samples or thin section.

Medium-grained biotite-ferrohastingsite syenite is found as ellipsoidal inclusions (~5-15 cm) within the coarse-grained syenite and as a separate body in the center of the pluton. It is distinguished from the coarser syenite by a greater abundance of biotite (up to 15%), a greater proportion of orthoclase and oligoclase relative to microperthite (particularly noted within inclusions), and a finer grain size (DeMartinis, 1976). The amphibole:biotite ratio ranges from 5:1 to 1:1 within this unit, although no systematic variation is recognized.

The term hybrid syenite is here used to designate rocks resulting from the injection and disaggregation of lamprophyre by syenitic magma. Hybrid syenites occur in the southwestern part of the pluton and in outcrop range from largely mafic material injected by syenitic dikes to largely syenitic material with a high color index. In thin section, the latter exhibit a disequilibrium mineral assemblage, e.g. strongly zoned titanaugite xenocrysts are rimmed by augite and ferrohastingsite (Fig. 5).

Significant amounts of nepheline are present in two units of the Rattlesnake Mountain pluton. Nepheline-bearing syenite (NBS of Table 1) forms an elongate body in the northern part of the pluton. It is medium- to fine-grained and distinguished by the presence of 2-10% nepheline. Nepheline syenite (NS of Table 1) crops out in the northeast part of the pluton. It is readily distinguished by its medium-grained bostonitic texture (Fig. 6) and up to 15-25% pink angular nepheline ($Ne_{68}Ks_{32}$, Carter et al., 1979). Microperthite is the dominant feldspar in both units. Some samples of the nepheline-bearing syenite have a sub-parallel feldspar lamination (Fig. 7); similar textures present in nepheline-sodalite syenite at Red Hill, New Hampshire, are considered by Size (1972) to be of cumulate origin. The late magmatic crystallization of nepheline is illustrated by thin sections of nepheline syenite (Fig. 6): nepheline fills triangular interstices formed by randomly arrayed laths of microperthite. The nepheline syenite thus appears to represent a quenched liquid rather than a cumulus mineral assemblage. Both units contain about 8-12% ferrohastingsite and minor aegirine-augite and biotite. Weak sericitic alteration of microperthite is noted in most specimens of the nepheline syenite.

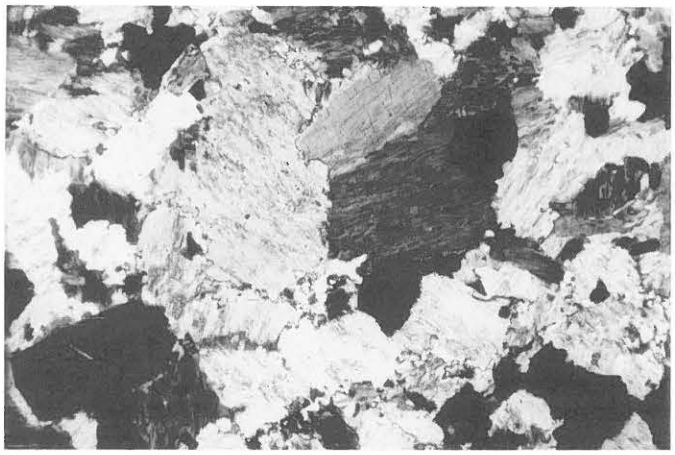

Figure 4. Ferrohastingsite syenite (FHS) shows aegerine-augite partially resorbed and enclosed by subhedral ferrohastingsite. Field of view is 5.8 mm (long dimension).

Figure 5. Hybrid syenite (HYS) shows disequilibrium mineral assemblage of titanaugite resorbed and rimmed by augite and minor barkevikite; a reaction rim of ferrohastingsite encases the augite. Field of view is 5.8 mm (long dimension).

The dikes of the Rattlesnake Mountain igneous complex are broadly divided into three lithologic types (Griffith, 1983; see Table 1). These are in order of decreasing abundance (as percentage of dike population): porphyritic hornblende trachyte (75%), porphyritic nepheline trachyte (20%), and lamprophyre and basalt (5%).

Porphyritic hornblende trachyte (HBT of Table 1) forms dikes up to 13 m wide, although more than 2/3 of the dikes are

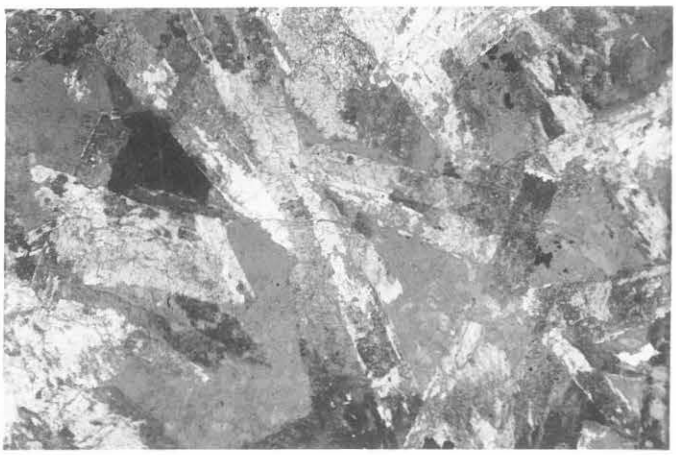

Figure 6. Bostonitic texture of nepheline syenite (NS) has randomly arrayed laths of alkali feldspar forming angular interstices occupied by nepheline, aegerine-augite, ferrohastingsite, and accessory minerals. Field of view is 5.8 mm (long dimension).

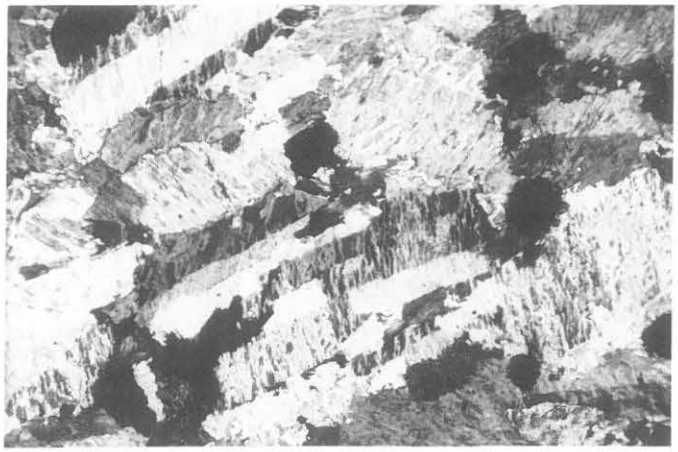

Figure 7. Lamination of alkali feldspar is present in some samples of the nepheline-bearing syenite (NBS). Field of view is 5.8 mm (long dimension).

less than 2 m wide. Phenocrysts of orthoclase (typically 30% of sample) and hornblende (5%) are set in a fine-grained trachytic groundmass consisting of orthoclase, albite, hornblende, magnetite, and biotite. Some samples are mildly peralkaline with minor amounts of aegirine-augite and riebeckite present in the groundmass. Weak to moderate sericitic alteration of feldspars is typical; hornblende phenocrysts are altered to assemblages containing calcite, chlorite, and magnetite. A variant of the trachyte described as hornblende microsyenite by Griffith (1983) contains abundant small partially digested inclusions of calcareous metasediments.

Dikes of porphyritic nepheline trachyte (NET of Table 1) are widely distributed, but most abundant near the pluton (Griffith, 1983). Phenocrysts (30% of rock) of zoned albite-oligoclase, orthoclase, hornblende, biotite, and rarely, nepheline, are set in a groundmass that includes the same minerals. Nepheline (1-10%) has two distinct occurrences: as rims on plagioclase phenocrysts and as grains interstitial to feldspar laths in the groundmass. Although nepheline is difficult to discern in hand sample and is most easily identified by staining, samples with abundant nepheline are gray and contrast with the light brown typical of the hornblende trachyte. The minor minerals of the groundmass and the alteration assemblages are similar to those of the hornblende trachyte.

Mafic dikes are rare and their immediate relation to the Rattlesnake Mountain complex may be solely spatial rather than genetic, since no comparable mafic plutonic rocks are present and mafic dikes are ubiquitous throughout much of southwestern Maine. Lamprophyre has a typical Ti-rich mineralogy: phenocrysts of unresorbed olivine, titanaugite, and magnetite in a groundmass of oligoclase, barkevikite, magnetite, and minor titanaugite. Basalt samples contain phenocrysts of partially resorbed olivine, augite, and plagioclase in a groundmass which consists of plagioclase, hornblende, magnetite, and biotite.

GEOCHRONOLOGY AND ISOTOPE GEOLOGY

The silica undersaturated rocks of the Rattlesnake Mountain pluton preclude a magma source containing modal or normative quartz and any significant contamination with metamorphosed sediments and granitic rocks of the upper crust. The source of the critically saturated syenites is not similarly constrained. A single parental magma for both saturated and undersaturated syenites is suggested, but not required, by the field evidence.

The Sr isotope systematics of 10 samples from the Rattlesnake Mountain pluton provide a basis for evaluating the source(s) and possible contamination of the parental magma(s). Samples of syenite (n = 3), nepheline-bearing syenite (n = 4), nepheline syenite (n = 2), and chilled marginal syenite (n = 1) correspond to those analyzed for major and minor elements (see Geochemistry). Concentrations of Rb and Sr and their isotopic ratios vary widely in these rocks (Table 2), e.g. $^{87}Rb/^{86}Sr$ ranges from 0.5 to 176. Nine samples define an isochron age of 205.5 Ma (MSWD = 2.2) and an initial $^{87}Sr/^{86}Sr$ of 0.7027 ± 0.004 (Figs. 8a and 8b). This extremely low initial Sr ratio is consistant with depleted mantle values (Eby, 1985c) and precludes significant amounts of contamination with Rb-rich crustal materials. The presence of excess radiogenic Sr and of normative quartz in the chilled marginal syenite (Fig. 8b) suggest only local contamination during emplacement.

Contamination may also be evaluated with a plot of initial $^{87}Sr/^{86}Sr$ (@ 205.5 Ma) versus 1/Sr for the ten samples (Fig. 9, also Table 2). In such a plot, a linear array of data points with a non-zero slope would suggest mixing of two components having different initial $^{87}Sr/^{86}Sr$ ratios (Faure, 1977). Nepheline syenite and nepheline-bearing syenite have low initial Sr ratios (generally 0.7027 ± 0.001) and show no clear evidence of incorporating Rb-rich materials. A sample of nepheline syenite has an intial

TABLE 2. ANALYTICAL DATA FOR RB-SR WHOLE-ROCK ISOCHRON, RATTLESNAKE MOUNTAIN PLUTON.

Sample[1]	Rb (ppm)	Sr (ppm)	Measured $^{87}Rb/^{86}Sr$	Measured $^{87}Sr/^{86}Sr$	Initial[2] $^{87}Sr/^{86}Sr$
FERROHASTINGSITE SYENITE:					
FHS 8	81.5	435.0	0.5408±.0067	0.70449±.00056	0.702916
FHS 9[3]	77.0	358.4	0.6211±.0077	0.70461±.00056	0.702796
FHS 10	87.0	200.0	1.2577±.0157	0.70523±.00056	0.701551
CHS 11	138.0	83.0	4.8277±.0323	0.7267 ±.00056	0.712602
NEPHELINE-BEARING SYENITE:					
NBS 1	87.4	207.1	1.2202±.0152	0.70507±.00056	0.701506
NBS 2	87.8	84.6	3.0022±.0201	0.71138±.00035	0.702607
NBS 3	146.7	74.0	5.7462±.0385	0.72013±.00036	0.703341
NBS 4[3]	135.5	44.7	8.6822±.0581	0.73009±.00036	0.704717
NEPHELINE SYENITE:					
NS 5[3,4]	169.2	6.2	80.2411±2.888	0.93762±.00853	0.703122
NS 6[3,4]	187.2	3.2	175.7231±1.616	1.20855±.003202	0.695023

[1] sample descriptors are the same as those used in Tables 2 and 3, and Fig. 3.
[2] calculated for 205.5 Ma, decay constant = 1.42 x 10-11.
[3] five powder replicate analyses made of this sample.
[4] high correlation of variations in measured isotopic ratios due to slight inhomogeneities in powder.

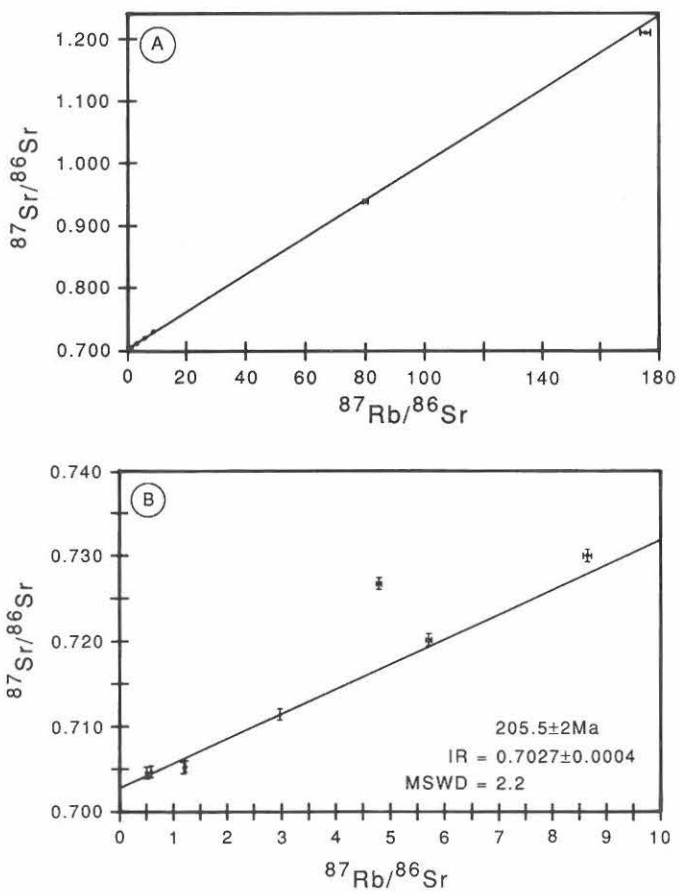

Figure 8. (a) Rb-Sr whole-rock isochron for Rattlesnake Mountain pluton (see also Table 2). (b) Detail of Rb-Sr whole-rock isochron for samples with values of $^{87}Rb/^{86}Sr < 10$.

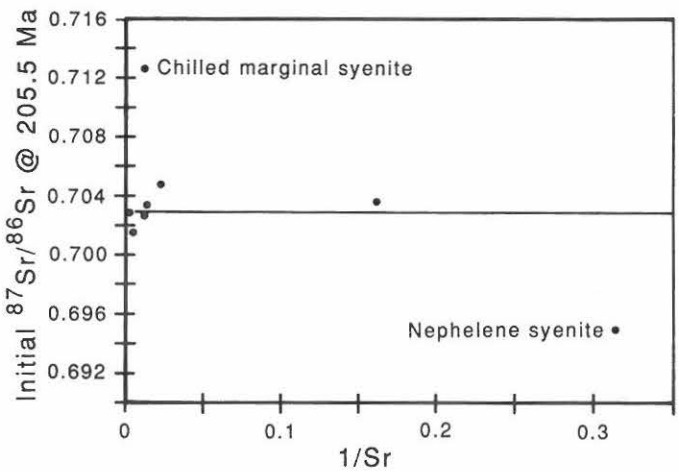

Figure 9. Variation of initial $^{87}Sr/^{86}Sr$ of individual samples calculated for the isochron age (205.5 Ma).

$^{87}Sr/^{86}Sr$ of 0.695; assuming that 0.7027 is the correct initial value yields a calculated age of 202.4 Ma for this sample. This slightly younger age is consistent with the relative age of the nepheline syenite and its central location within the pluton. Syenite, the most abundant rock type and that for which a crustal origin *might* be postulated, also has low initial Sr ratios. The sample of marginal syenite is clearly anomalous in this plot; an initial $^{87}Sr/^{86}Sr$ of >0.712 is indicative of crustal contamination.

These data contrast with isotopic data from other silica undersaturated intrusive complexes where higher initial Sr ratios and evidence of crustal contamination are observed (see Fig. 1 for locations). Foland and Friedman (1977) report a whole-rock Sr initial ratio of 0.7033 for syenites at Red Hill, New Hampshire; mineral isochrons for nepheline syenite have initial Sr ratios of 0.70463 and 0.70418. The authors (Foland and Friedman, 1977) suggest that syenites and nepheline syenites at Red Hill may have had (isotopically) different source regions or the same (mantle) source, but with assimilation of crustal material indicated for the nepheline syenite. Chen et al. (1984) suggest a depleted mantle source for several White Mountain intrusives (initial $^{87}Sr/^{86}Sr$ = 0.7033-0.7040), including Red Hill and Pleasant Mountain, although all showed isotopic evidence for some form of crustal contamination.

Crustal contamination of mantle-derived melts generally is invoked for several silica saturated to oversaturated intrusive complexes (initial $^{87}Sr/^{86}Sr$ = 0.7033-0.7038) of the White Mountain magma series (Chen et al., 1984; Foland et al., 1985; Loiselle, 1978; Randall et al., 1983) although Eby (1985c) notes little crustal contamination at Mt. Pawtuckaway, New Hampshire. Saturated to oversaturated rocks of the voluminous White Mountain batholith have higher initial Sr ratios (0.7039-0.7060) and originate in the lower crust (Eby and Creasy, 1983).

The Sr isotopic data for the Rattlesnake Mountain pluton (a) indicate that there was no significant contamination of the magma by Rb-rich crustal materials and (b) are consistent with

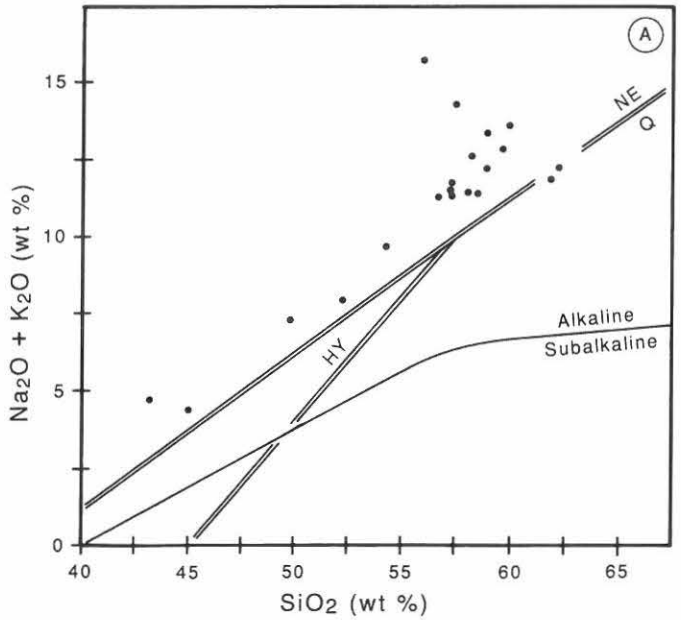

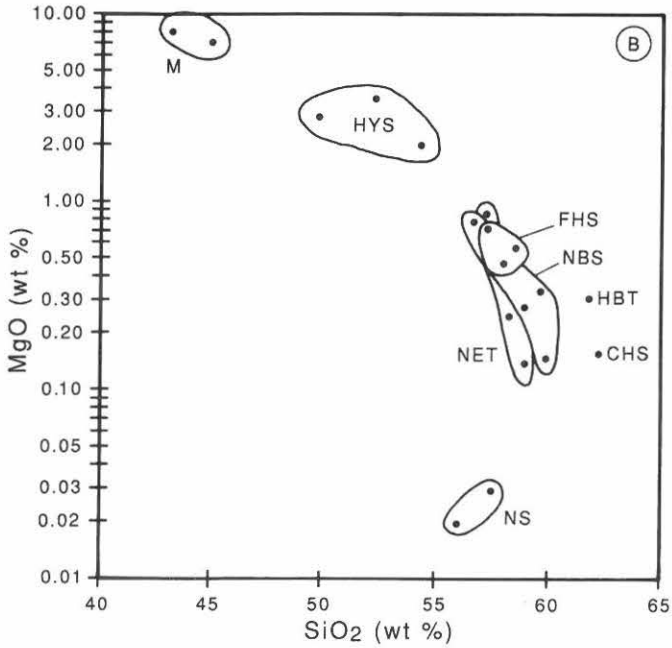

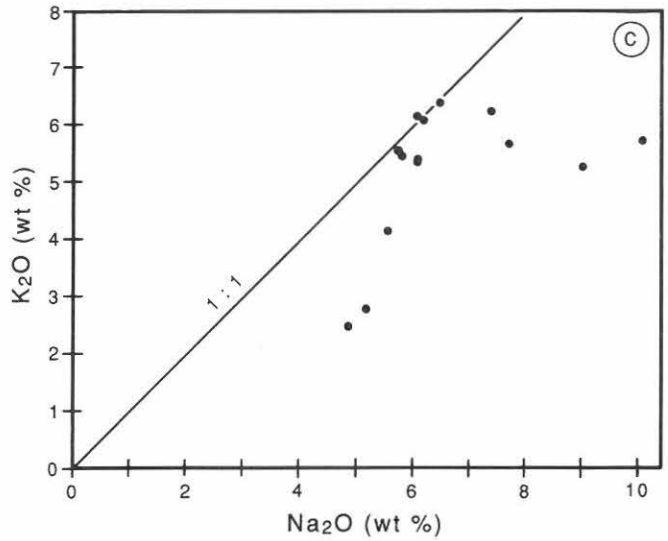

Figure 10. (a) Total alkalis-silica variation diagram for Rattlesnake Mountain igneous complex. Boundary between alkaline and subalkaline fields from Miyashiro (1978); boundaries separating undersaturated (NE normative), saturated (HY normative) and oversaturated (Q normative) compositions from Broustet (1986). (b) Magnesia-silica variation diagram for Rattlesnake Mountain igneous complex (see Tables 3a,b,c). Note logarithmic scale for MgO values. (c) Potash-soda variation diagram for Rattlesnake Mountain igneous complex (see Tables 3a,b,c).

the premise that fractionation of a single mantle-derived magma generated the observed rocks of the Rattlesnake Mountain pluton.

GEOCHEMISTRY

Twenty whole rock analyses are presented for the Rattlesnake Mountain igneous complex in Tables 3a,b,c; modes for these analyzed rocks are given in Tables 4a,b,c. These geochemical data document the differences between and within the plutonic units and the similar compositional range for dikes and pluton. Systematic variations in the concentration of major and trace elements generally have been interpreted to reflect increasing degrees of crystal fractionation and correlate with decreasing relative age. Trace element data suggest that some samples of ferrohastingsite syenite and nepheline-bearing syenite are cumulate rocks. Other samples of these units, as well as the nepheline syenite and the dikes represent original or fractionated liquid compositions (hereafter termed fractionates). The hybrid syenites have major and trace element abundances that generally fall on simple mixing lines between ferrohastingsite syenite and lamprophyre.

Despite the restricted range of silica values (56-62%), striking variations are present among the major element oxides. A plot of total alkalis versus silica (Fig. 10a) illustrates the alkaline composition of these rocks. Here, as in the magnesia versus silica diagram (Fig. 10b), the plutonic rocks and felsic dikes form a coherent and coincident group. An increase in alkalis and a decrease in magnesia correspond with increasing modal nepheline (Tables 4a,b,c) and with increasing silica content. However, values for the nepheline syenite reverse the trend of increasing silica content--silica decreases with increasing alkalis and decreasing magnesia. Compositions of the hybrid syenite are separate and displaced towards those of the mafic dikes. Similar trends are shown by other major element oxides, e.g. CaO and TiO_2, when plotted against silica.

TABLE 3a. MAJOR AND TRACE ELEMENT ANALYSES FOR RATTLESNAKE MOUNTAIN PLUTON: NEPHELINE-BEARING SYENITE (NBS), NEPHELINE SYENITE (NS), AND NEPHELINE TRACHYTE (NET).[1]

Descriptor[2] Bates #	NBS 1 1508	NBS 2 1507	NBS 3 1506	NBS 4 1505	NS 5 1504	NS 6 1511	NET 7 1513
SiO_2 [wt %]	56.70	58.90	59.60	59.90	57.50	56.00	58.90
Al_2O_3	17.10	17.70	18.10	19.10	19.90	21.40	18.20
FeOtotal	7.91	5.74	5.15	3.81	4.53	2.85	5.44
MnO	0.27	0.18	0.21	0.16	0.17	0.11	0.18
MgO	0.79	0.28	0.34	0.15	0.03	0.02	0.14
CaO	2.93	2.01	1.39	0.97	0.90	0.35	0.79
Na_2O	5.82	6.06	6.49	7.39	9.04	10.10	7.71
K_2O	5.49	6.19	6.38	6.26	5.29	5.76	5.70
P_2O_5	0.21	0.08	0.09	0.04	0.04	0.02	0.50
TiO_2	0.65	0.33	0.27	0.14	0.03	0.01	0.15
LOI	0.54	0.00	0.23	0.16	0.70	1.16	0.47
TOTAL	98.41	97.47	98.25	98.08	98.13	97.78	98.18
(Na+K)/Al	0.91	0.94	0.97	0.99	1.04	1.07	1.04
Q	0	0	0	0	0	0	0
NE	5.2	5.1	6.7	10.8	19.7	27.5	10.8
Sc [ppm]	6.0	2.7	3.4	0.6	0.5	0.5	0.5
V	17.4	2.6	1.3	1.0	2.0	0.0	0.9
Cr	13.9	13.1	16.7	16.7	16.0	11.8	26.7
Co	5.0	5.0	5.0	5.0	5.0	5.0	5.0
Ni	9.7	6.6	7.3	11.0	9.0	6.1	10.5
Zn	147.4	92.0	101.4	70.6	80.0	69.9	100.6
Rb	87.0	88.0	146.0	136.0	169.0	187.0	180.0
Sr	207.0	85.0	74.0	42.0	6.2	3.3	46.0
Zr	670.8	507.7	638.1	830.7	682.0	705.1	1135.6
Nb	203.9	169.1	159.7	91.2	60.4	33.6	129.5
Hf	19.0	13.0	15.0	15.0	16.0	15.0	25.0
Ba	794.6	383.5	319.4	90.6	6.2	1.2	113.9
La	105.0	72.0	83.0	58.0	77.0	32.0	83.0
Ce	170.0	122.7	128.3	89.9	101.9	50.9	97.6
Sm	16.1	12.6	9.7	6.0	4.0	2.0	5.2
Ta	7.0	5.0	6.0	5.0	4.0	4.0	8.0
Th	11.0	8.0	10.0	7.0	17.0	15.0	27.0

TABLE 3b. MAJOR AND TRACE ELEMENT ANALYSES OF RATTLESNAKE MOUNTAIN PLUTON: FERROHASTINGSITE SYENITE (FHS), CHILL SYENITE (CHS) AND HYBRID SYENITE (HYS).[1]

Descriptor[2] Bates #	FHS 8 1515	FHS 9 1517	FHS 10 1514	CHS 11 1510	HYS 12 1516	HYS 13 1512	HYS 14 1509
SiO_2 [wt. %]	58.50	58.00	57.30	62.20	49.80	54.30	52.30
Al_2O_3	17.90	18.40	17.40	17.90	18.40	18.40	16.70
FeOtotal	5.55	5.26	7.18	4.56	8.35	6.94	8.06
MnO	0.19	0.15	0.22	0.12	0.22	0.17	0.21
MgO	0.58	0.48	0.72	0.16	2.86	2.03	3.59
CaO	2.35	2.36	2.54	0.94	6.98	4.27	5.92
Na_2O	6.08	6.09	5.75	6.20	4.85	5.55	5.17
K_2O	5.36	5.39	5.59	6.09	2.48	4.16	2.80
P_2O_5	0.17	0.19	0.18	0.03	0.54	0.39	0.38
TiO_2	0.50	0.53	0.65	0.12	1.64	1.26	1.46
LOI	0.23	0.47	0.85	0.07	1.00	0.62	0.31
TOTAL	97.41	97.32	98.38	98.39	97.12	98.09	96.90

[1] Major element analyses determined by X-ray fluorescence (X-ray Assay Laboratories, Inc.); Sc, Co, Hf, La, Sm, Ta, and Th by instrumental neutron activation (X-ray Assay Laboratories, Inc.); Rb and Sr by isotope dilution (University of New Hampshire); all other trace elements by X-ray fluorescence (University of Massachusetts).

[2] Refer to Fig. 3 for sample location.

TABLE 3b. CONTINUED.[1]

Descriptor[2] Bates #	FHS 8 1515	FHS 9 1517	FHS 10 1514	CHS 11 1510	HYS 12 1516	HYS 13 1512	HYS 14 1509
(Na+K)/Al	0.88	0.86	0.89	0.94	0.58	0.74	0.69
Q	0	0	0	0	0	0	0
NE	2.9	3.6	3.7	0	3.6	4	2.4
Sc [ppm]	3.7	4.7	3.6	0.8	12.0	7.1	16.0
V	4.5	3.9	8.9	2.5	101.3	48.7	101.8
Cr	11.3	17.3	11.4	28.0	44.8	34.1	85.5
Co	5.0	5.0	5.0	5.0	15.0	12.0	20.0
Ni	7.2	9.2	8.1	9.3	26.7	20.7	42.3
Zn	92.3	78.1	110.7	41.4	145.7	101.1	117.9
Rb	100.0	81.0	87.0	138.0	80.0	110.0	90.0
Sr	425.0	435.0	200.0	83.0	881.0	595.0	541.0
Zr	301.8	244.0	400.4	1015.2	489.0	386.6	323.8
Nb	128.5	122.5	184.8	159.3	109.5	108.8	106.3
Hf	8.0	6.0	11.0	26.0	13.0	9.0	8.0
Ba	1957.3	1841.6	726.8	183.2	848.0	1174.3	873.4
La	66.0	63.0	73.0	77.0	68.0	64.0	65.0
Ce	95.7	82.3	118.9	77.8	87.8	83.2	88.5
Sm	8.9	9.0	11.3	7.3	10.2	8.3	8.6
Ta	3.0	5.0	5.0	8.0	5.0	4.0	5.0
Th	4.0	4.0	5.0	18.0	7.0	8.0	7.0

[1] Major element analyses determined by X-ray fluorescence (X-ray Assay Laboratories, Inc.); Sc, Co, Hf, La, Sm, Ta, and Th by instrumental neutron activation (X-ray Assay Laboratories, Inc.); Rb and Sr by isotope dilution (University of New Hampshire); all other trace elements by X-ray fluorescence (University of Massachusetts).

[2] Refer to Fig. 3 for sample location.

TABLE 3c. MAJOR AND TRACE ELEMENT ANALYSES FOR DIKES FROM RATTLESNAKE MOUNTAIN IGNEOUS COMPLEX: MAFIC (M), NEPHELINE TRACHYTE (NET) AND HORNBLENDE TRACHYTE (HBT).[3]

Descriptor Bates #	M 15 860	M 16 868	NET 17 862	NET 18 863	NET 19 867	NET 7 1513	HBT20 874
SiO_2 [wt. %]	43.20	45.00	57.30	57.20	58.20	58.90	61.80
Al_2O_3	13.90	14.70	18.40	18.80	18.00	18.20	17.20
FeOtotal	15.10	14.00	6.94	7.60	6.59	5.44	6.87
MnO	0.18	0.16	0.18	0.15	0.19	0.18	0.09
MgO	8.13	7.10	0.74	0.88	0.25	0.14	0.31
CaO	8.48	7.52	1.87	1.15	1.55	0.79	0.64
Na_2O	2.67	2.60	6.36	6.51	6.62	7.71	5.72
K_2O	2.09	1.80	5.43	5.02	6.02	5.70	6.20
P_2O_5	0.41	0.51	0.18	0.24	0.06	0.50	0.08
TiO_2	2.86	2.70	0.60	0.72	0.24	0.15	0.36
TOTAL	97.02	96.09	98.00	98.27	97.72	97.71	99.27
(Na+K)/Al	0.48	0.42	0.89	0.86	0.97	1.04	0.94
Q	0	0	0	0	0	0	2.4
NE	3.4	0	3.1	7.7	0	10.8	0
Sc [ppm]	28	21	2.8	3	0.9	0.5	4.3
Cr	240	210	40	50	40	40	50
Co	43	34	5	8	2		2
Rb	40	110	120	140	140	180	160
Sr	540	510	330	320	120	46	120
Zr	220	170	550	530	770	1136	840

[3] Major and minor element analyses determined by X-ray fluorescence except Sc and Co by instrumental neutron activation; all by X-ray Assay Laboratories, Inc.

TABLE 4a. MODES FOR CHEMICALLY ANALYZED SAMPLES OF RATTLESNAKE MOUNTAIN PLUTON: NEPHELINE-BEARING SYENITE (NBS) AND NEPHELINE SYENITE (NS).

Descriptor Bates No.	NBS 1 1508	NBS 2 1507	NBS 3 1506	NBS 4 1505	NS 5 1504	NS 6 1511
MINERAL						
Microperthite	71	77	47	75	61	64
Orthoclase	5	5	37	5	3	5
Oligoclase	1	2	1	tr	3	2
Quartz	0	0	0	0	0	0
Nepheline	3	2	tr	10	14	18
Biotite	0	0	1	0	1	0
Ferrohastingsite	16	9	13	9	10	6
Aegirine-augite	2	1	1	1	3	2
Fayalite	0	0	0	0	0	0
Zircon	tr	0	0	0	0	0
Apatite	tr	0	tr	tr	tr	tr
Allanite	tr	0	0	0	0	0
Sphene	tr	0	tr	tr	0	0
Opaques	tr	3	tr	tr	2	tr
Sericite	2	1	tr	0	3	3

TABLE 4b. MODES FOR CHEMICALLY ANALYZED SAMPLES OF RATTLESNAKE MOUNTAIN PLUTON: FERROHASTINGSITE SYENITE (FHS), CHILL SYENITE (CHS) AND HYBRID SYENITE (HYS).

Descriptor Bates No.	FHS 8 1515	FHS 9 1517	FHS 10 1514	CHS 11 1510	HYS 12 1516	HYS 13 1512
MINERAL						
Microperthite	74	70	73	76	6	26
Orthoclase	5	9	3	12	42	36
Oligoclase	3	2	4	3	2	5
Quartz	0	0	0	0	0	0
Nepheline	0	0	0	0	0	0
Biotite	tr	4	2	0	16	11
Ferrohastingsite	14	12	14	1	21	12
Aegirine-augite	3	1	3	tr	12	4
Fayalite	0	0	0	8	0	0
Zircon	tr	tr	tr	tr	tr	0
Apatite	tr	tr	tr	0	tr	tr
Allanite	0	0	tr	0	0	tr
Sphene	0	tr	tr	0	0	0
Opaques	0	tr	tr	tr	tr	tr
Sericite	3	2	1	0	1	2

Soda equals or exceeds potash (Fig. 10c) and is substantially greater in nepheline syenite. This same relationship is generally true at Red Hill (Size, 1972; Quinn, 1937), but potash exceeds soda in a greater proportion of samples from that locality. With respect to alumina saturation, atomic (Na+K)/Al increases from metaluminous values in ferrohastingsite syenite (0.86-0.94) and nepheline-bearing syenite (0.91-0.99) to peralkaline values in nepheline syenite (1.04-1.07). Dikes show similar values (Table 3a,b,c). Normative nepheline (NE, Tables 3a,b) ranges from about 3% in ferrohastingsite syenite to more than 20% in nepheline syenite. The chilled syenite is just saturated, and the

TABLE 4c. MODES FOR CHEMICALLY ANALYZED SAMPLES FOR DIKES FROM RATTLESNAKE MOUNTAIN IGNEOUS COMPLEX: MAFIC (M), NEPHELINE TRACHYTE (NET), AND HORNBLENDE TRACHYTE (HBT).

Descriptor Bates No.	M 15 860	M 16 868	NET 17 862	NET 18 863	NET 19 867	NET 7 1513	HBT 20 874
MINERAL							
Orthoclase	20	17	41	35	36	42	36
Oligoclase	29	38	33	44	41	38	44
Quartz	0	0	0	0	0	0	1
Nepheline	0	0	5	3	7	5	0
Biotite	0	0	3	8	1	8	3
Ferrohastingsite	18	12	13	6	10	4	7
Riebeckite	0	0	0	0	2	0	0
Aegirine-augite	0	0	2	tr	0	tr	0
Olivine	10	8	0	0	0	0	0
Zircon	tr	tr	tr	tr	tr	tr	tr
Apatite	1	2	tr	tr	tr	tr	tr
Sphene	0	0	tr	tr	tr		tr
Opaques	10	20	2	2	2	1	3
Chlorite	tr	tr	tr	tr	tr	tr	tr
Calcite	2	tr	1	1	1	1	1
Sericite	tr	tr	tr	tr	tr	tr	tr

hornblende trachyte dike contains a small amount of normative quartz (Q). To calculate the norms, total iron as analytically determined was recast into FeO and Fe_2O_3 in the ratio of 1.1:1, an average value for syenite and nepheline syenite (Le Maitre, 1976). This value is consistent with those determined for rocks at Red Hill (Quinn, 1937), but typically is greater than 2:1 in syenites from the White Mountain magma series and Monteregian Hills (Eby, 1985a, and unpublished data). Norms calculated using a larger ratio would show increased amounts of nepheline.

The same general trends noted above for the major elements are apparent in the trace element data with some qualification. Concentrations of some trace elements, for example Sr and Rb, in hybrid syenites do not fall neatly on a simple mixing line between end-member compositions. Although these rocks are shown on subsequent variation diagrams, they are not pertinent to the present discussion and are not discussed further. The compositions of dikes and of plutonic rocks show generally coherent grouping of trace element compositions, but do not exhibit the coincidence shown by the major element oxides, such as MgO. This is significant when assessing the composition of the parental magma(s) and the extent of feldspar fractionation and/or accumulation in the generation of the felsic plutonic rocks. To facilitate description of the trace element diagrams, analyses in Tables 3a,b,c (and Tables 4a,b,c) are serially numbered (1-20) and have a unit descriptor, for example NET 18. Sample locations are indicated in Figure 3.

Concentrations of Rb and Sr versus silica are plotted on Figures 11a and 11b. These elements show wide ranges in abundance with extreme Sr depletion and Rb enrichment shown by nepheline syenite. Mineral/matrix partition coefficients for

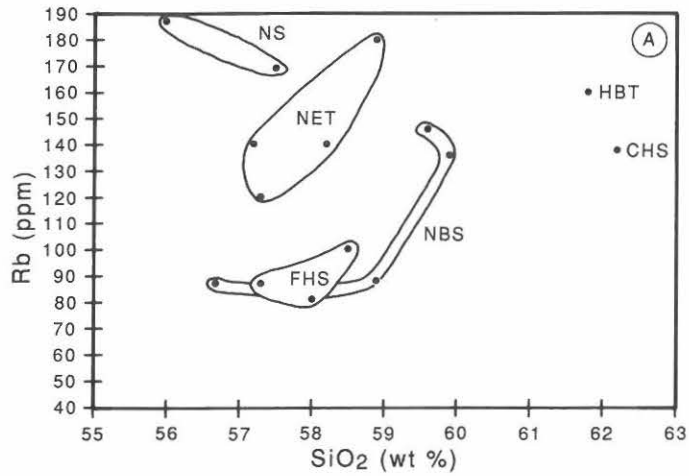

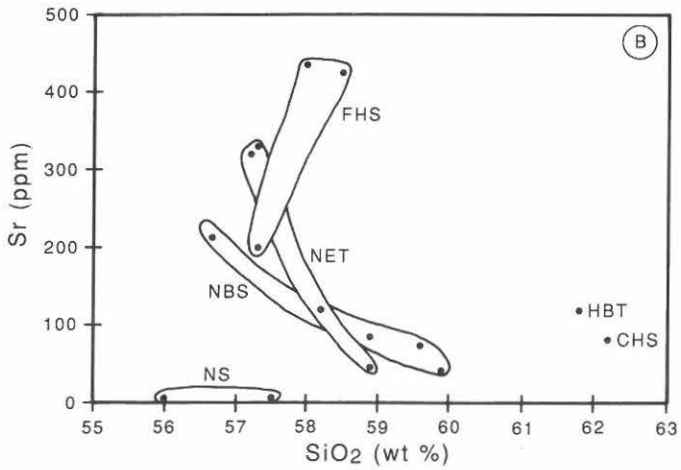

Figure 11. (a) Variation in Rb abundance as a function of silica content for the Rattlesnake Mountain igneous complex (see Tables 3a,b,c). (b) Variation in Sr abundance as a function of silica content for the Rattlesnake Mountain igneous complex (see Tables 3a,b,c).

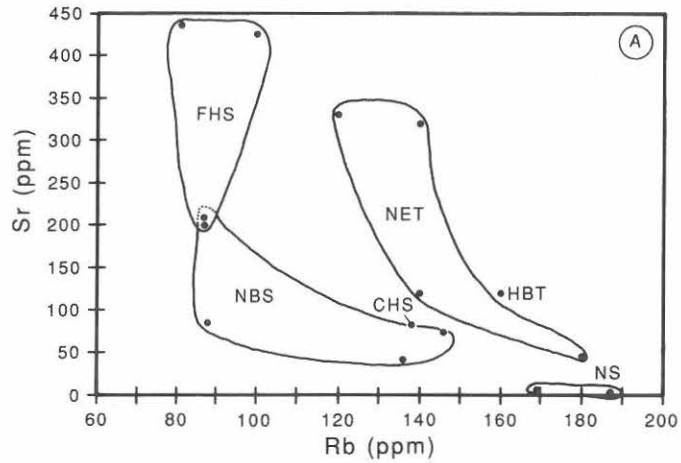

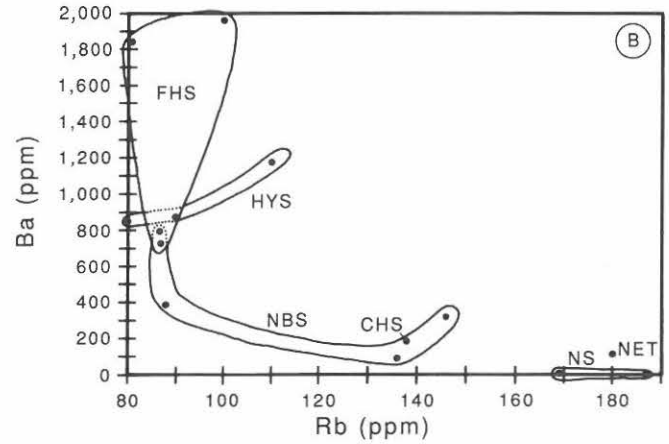

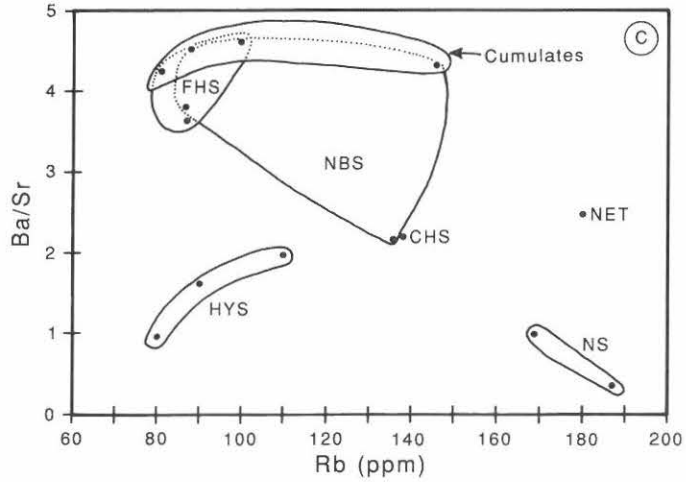

Figure 12. (a) Variation in Sr abundance as a function of Rb concentration for the Rattlesnake Mountain igneous complex (see Tables 3a,b,c). (b) Variation in Ba abundance as a function of Rb concentration for the Rattlesnake Mountain pluton. Ba abundances not available for dikes except NET 7 (see Tables 3a,b,c). (c) Variation of Ba/Sr as a function of Rb concentration for the Rattlesnake Mountain pluton (see Tables 3a,b,c). Field of probable cumulate samples is outlined.

Rb are much less than 1 for all rock-forming minerals except biotite (Henderson, 1982). Although present in rocks of the Rattlesnake Mountain complex (Tables 1; 4a,b,c), biotite appears late in the crystallization sequence and was not a fractionating phase. Hence, Rb concentration can be used as an indicator of magmatic evolution (Eby, 1985a, p. 429) in these rocks. On a plot of Sr versus Rb (Fig. 12a), the usual negative correlation of Sr with Rb is documented. Of greater significance are the distinctions apparent between the dikes and pluton. Nepheline trachyte has Rb and Sr concentrations that equal or exceed concentrations in nepheline-bearing syenite. The hornblende trachyte has greater Rb and Sr than does ferrohastingsite syenite or chilled marginal syenite.

Ba concentrations in the plutonic rocks do not describe a simple variation trend (Fig. 12b). Although overall a negative

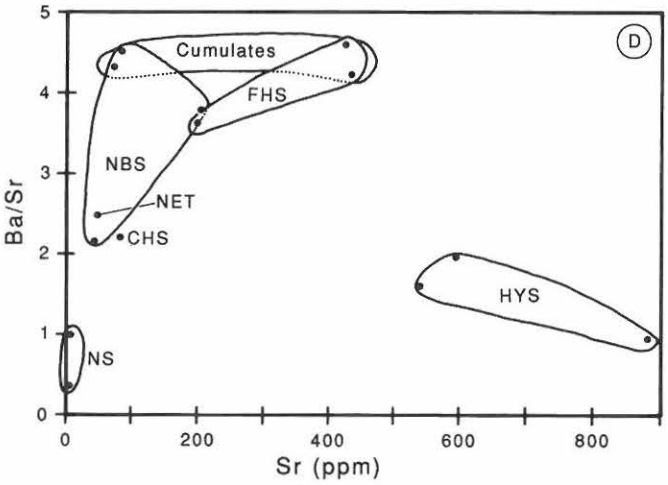

Figure 12 (Continued). (d) Variation of Ba/Sr as a function of Sr concentration for the Rattlesnake Mountain pluton (see Tables 3a,b,c). Field of probable cumulate samples is outlined.

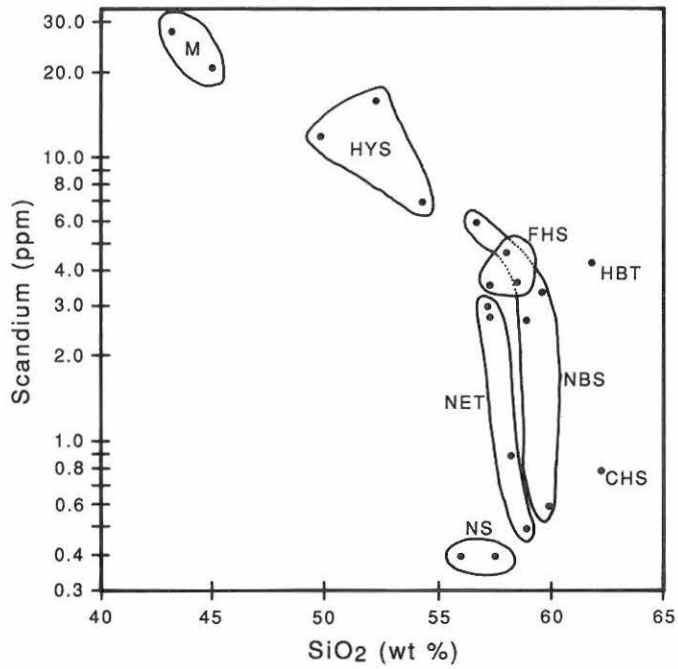

Figure 13. Variation in Sc abundance as a function of silica content for the Rattlesnake Mountain igneous complex (see Tables 3a,b,c). Note logarithmic scale for Sc values.

correlation of Ba with Rb is generally indicated, all samples of ferrohastingsite syenite and two of nepheline-bearing syenite (NBS 1 and 2, Table 3a) have strikingly different Ba concentrations (383-1841 ppm) for the same low Rb value (~90 ppm). Ba/Sr values generally decrease with increasing Rb concentration (Fig. 12c) and with decreasing Sr concentration (Fig. 12d), but low Rb samples (excluding hybrid syenites) have Ba/Sr values that are approximately constant.

The compositions of dike rocks most closely represent liquid compositions, and the variations in trace element abundances as shown by nepheline trachyte may approximate a liquid line of descent (Fig. 12a). Both plagioclase and alkali feldspar generally have partition coefficients »1 for Sr (and «1 for Rb), but partition coefficients for Ba are «1 in plagioclase and »1 in alkali feldspar (Henderson, 1982). Thus the variations observed in Sr and Rb concentrations (Fig. 12a) and in Ba/Sr values (Fig. 12b) are consistent with fractionation of alkali feldspar.

Similar variations in trace element abundances are shown by nepheline-bearing syenite. However, the presence of cumulus textures in some samples suggest that less fractionated (Rb-poor) samples may be cumulates (NBS 1 and NBS 2, Table 3a). Furthermore, if hornblende trachyte (HBT 20, Table 3c) or chilled syenite (CHS 11, Table 3b) is representative of parental compositions for the ferrohastingsite syenite, then the abundance of Rb and Sr requires the presence of cumulus alkali feldspar in all samples of ferrohastingsite syenite. Additional support for a cumulate origin may be indicated by the Ba data. For example, Ba concentrations in the plutonic rocks do not describe a simple variation trend (Fig. 12b). Although overall a negative correlation of Ba with Rb is generally indicated, all samples of ferrohastingsite syenite and two of nepheline-bearing syenite (NBS 1 and 2, Table 3a) have strikingly different Ba concentrations (383-1841 ppm) for the same low Rb value (~90 ppm). Ba/Sr values decrease with increasing Rb concentration (Fig. 12c), but the group of low Rb samples have Ba/Sr values that are approximately constant.

The trends in Rb and Sr concentration defined by nepheline trachyte and nepheline-bearing syenite are distinct, but converge at high Rb values. Protracted fractionation of alkali feldspar from liquids on either trend could produce the Rb-enriched and Sr-depleted nepheline syenite.

An alternate explanation (Creasy et al., 1986) suggests that Rb-poor samples of ferrohastingsite syenite are representative of the parental magma. Fractionation of alkali feldspar could produce the observed trends of Ba and Sr depletion and Rb enrichment in the plutonic rocks. However, this could not explain the Rb and Sr concentrations observed in the felsic dike rocks.

Scandium abundances decrease with increasing silica content (Fig. 13) and Rb values and are positively correlated with TiO_2 abundance (Tables 3a,b,c). The scandium content of liquids is decreased by the removal of clinopyroxene and amphibole (partition coefficients ≥20), biotite (~10), and magnetite (~4) (Henderson, 1982). The occurrence of amphibole and lesser amounts of clinopyroxene in all rocks and especially as phenocrysts in dikes suggests that crystallization of these minerals controlled the Sc distribution. Ferrohastingsite syenite and nepheline-bearing syenite (NBS 1 and 2, Table 3a) have greater Sc values than do felsic dikes. This is consistent with the accumulation of amphibole in the plutonic rocks.

The light rare earth elements (LREE) La, Ce, and Sm (Tables 3a,b,c) are approximately constant in total abundance. La/Sm values increase exponentially with increasing Rb and decreasing Sc, a result of decreasing Sm concentrations. That total LREE concentrations remain constant despite the fractionation and/or accumulation of alkali feldspar (partition coefficients «1) requires that some other phase control their behavior. Fractionation of a major mineral, such as amphibole, with Sc and LREE partition coefficients »1 (Hyndman, 1985, p. 116) and preferentially incorporating the heavier rare earths, could account for the observed variation. Other minor minerals, such as apatite, have the appropriate partition coefficients (Henderson, 1982) for the rare earth elements. Given the strong negative correlation P_2O_5 with Rb (Tables 3a,b,c), continuous crystallization and removal of apatite could also account for the variation in rare earth values.

CONCLUSIONS

Rocks of the Rattlesnake Mountain igneous complex exhibit systematic variations in the concentrations of major and trace elements. These variations are the result of accumulation or fractionation of alkali feldspar, amphibole, and accessory minerals such as sphene and apatite. The presence of alkali feldspar and hornblende as phenocrysts in dike rocks supports this conclusion.

The samples of nepheline trachyte (and possibly nepheline-bearing syenite, NBS 3 and NBS 4) document changes in liquid composition resulting from the fractionation of alkali feldspar and amphibole from an assumed parental liquid represented by sample NET 17. Samples of nepheline-bearing syenite and nepheline syenite define a similar fractionation trend, although samples NBS 1 and NBS 2 are in part cumulate assemblages. Hornblende trachyte and chilled marginal syenite are similar in composition to, but more fractionated than, ferrohastingsite syenite although the chemistry of the latter suggests they are also cumulate rocks. Nepheline syenite represents the final highly fractionated residual liquid marked by extreme depletion of Ba, Sr and MgO and enrichment in Rb and Th.

Field relations clearly show that nepheline-bearing syenite and nepheline trachyte are younger than ferrohastingsite syenite; it is therefore assumed that nepheline trachyte is also younger than hornblende trachyte. The restriction of the nepheline-bearing syenite to an elongate body on strike with the dike swarm (and parallel to a prominent topographic lineament) suggests that emplacement of nepheline-bearing syenite and nepheline trachyte were synchronous and related events. Likewise, the compositional similarity of chilled syenite and hornblende trachyte, as well as the lack of trachytic dikes cutting the pluton, suggest a similar link between hornblende trachyte and ferrohastingsite syenite. The hornblende trachyte and ferrohastingsite syenite account for the great bulk of exposed rocks, but the range of compositions shown by these units is restricted in comparison with nepheline trachyte and nepheline-bearing syenite. Hence, silica undersaturated compositions apparently evolved late, but rapidly, in the crystallization history if the proportions presently observed are representative of the entire pluton.

The relative position within the magma chamber represented by present erosional levels can be estimated by upward projection of dips (~35°) measured along the contact of the pluton and country rocks. Calculations by Whitaker (1984) assuming a spherical pluton would place the roof of the chamber about 100 m above the summit of Rattlesnake Mountain. Thus present exposures are within the uppermost part (upper margin ?) of the pluton.

A petrogenetic model for the Rattlesnake Mountain igneous complex assumes the emplacement of a critically saturated syenitic magma within highest crustal levels, a process facilitated by regional NW-SE extension during Jurassic time. The abundant trachytic dikes injected as a NE-SW trending swarm were precursors of the ascending magma chamber. Cooling at the margins of the magma chamber promoted the inward crystallization and accumulation or stagnation (?) of abundant alkali feldspar, and lesser ferrohastingsite and clinopyroxene, to produce ferrohastingsite syenite. Residual liquids evolved to increasingly undersaturated and peralkaline compositions. Fracturing of the partially solidified magma chamber, perhaps as a result of continued regional extension, tapped the residual liquids of this or a subjacent chamber to produce nepheline trachyte in the country rock and, within the upper margin of the chamber, nepheline-bearing syenite. Flow differentiation or syn-crystallization tectonic processes may have separated liquid from crystals, producing cumulus fractions within the nepheline-bearing syenite. Solidification of the final residuum yielded peralkaline nepheline syenite; the lack of dikes of comparable composition and texture preclude forceful injection of this highly evolved composition.

The spatial and temporal association of these plutonic rocks and of lamprophyre suggests a possible genetic link: fractionation of a mafic melt within the lower crust or upper mantle produces a critically saturated syenitic magma that migrates into the upper crust where further fractionation accompanies solidification.

ACKNOWLEDGMENTS

I acknowledge several Bates College students: J. DeMartinis, W. Griffith, and S. Whitaker, whose senior research forms a significant part of this manuscript, and the field assistance of A. Carter, C. Curtis, and J. Karb. H. E. Gaudette kindly provided access to the isotope laboratory, GSL/EOS, of the University of New Hampshire. I gratefully acknowledge W. J. Olszewski and H. E. Gaudette of the University of New Hampshire who gave freely of their time to train the author in the finer points of Rb-Sr isotope analysis. Joel Sparks kindly performed the X-ray fluorescence analyses at the University of

Massachusetts. D. S. Barker and W. J. Olszewski provided helpful and insightful reviews of the manuscript. Any errors of fact or interpretation remain the sole responsibility of the author. Partial support for this research was provided by NSF grant EAR-86 00058 to G. Nelson Eby.

REFERENCES CITED

Aleinikoff, J. N., Moench, R. H., and Lyons, J. B., 1985, Carboniferous U-Pb age of the Sebago batholith, southwestern Maine: metamorphic and tectonic implications: Geol. Soc. Amer., Bull., v. 96, p. 990-996.

Armstrong, R. L., and Stump, E., 1971, Additional K-Ar dates, White Mountain magma series, New England: Am. Jour. Sci., v. 270, p. 331-333.

Barker, D. S., 1965, Alkalic rocks at Litchfield, Maine: Jour. Petrol., v. 6, p. 263-280.

Billings, M. P., 1956, The geology of New Hampshire, Part II, Bedrock geology: New Hampshire State Planning and Development Commission, Concord, 203 p.

Broustet, J-M., 1986, Étude du magmatisme mésozoïque anorogénique de la province des White Mountains (Nouvelle Angleterre, États-Unis); ses relations avec l'overature de l'Ocean Atlantique: Ph.D. dissert., Univ. Bordeaux III, Bordeaux, 691 p.

Burke, W. H., Otto, J. B., and Denison, R. E., 1969, Potassium-argon dating of basaltic rocks: Jour. Geophys. Res., v. 74, p. 1082-1086.

Carter, A., Curtis, C., and Karb, J., 1979, The Rattlesnake Mountain pluton, Raymond and Casco, Maine: unpub. student research project, Bates College, Lewiston, Maine, 10 p.

Chen, J., Foland, K. A., Gilbert, L. A., and Randall, K. A., 1984, Depleted mantle sources for Mesozoic plutons of New England and southern Quebec: Geol. Soc. Amer., Abs. with Prog., v. 16, p. 469.

Creasy, J. W., 1974, Mineralogy and petrology of the White Mountain batholith, Franconia and Crawford Notch quadrangles, New Hampshire: PhD. dissert., Harvard Univ., Cambridge, Massachusetts, 430 p.

Creasy, J. W., 1979, Preliminary bedrock geology of the Poland 15' quadrangle, Maine: Maine Geol. Surv., Open-File Report 79-15, 18 p.

Creasy, J. W., 1988, Strontium isotope geology of the Rattlesnake Mountain pluton, southwestern Maine: depleted mantle signature: Geol. Soc. Amer., Abs. with Prog., v. 20, p. 14.

Creasy, J. W., and Eby, G. N., 1983, The White Mountain batholith as a model of Mesozoic felsic magmatism in New England: Geol. Soc. Amer., Abs. with Prog., v. 15, p. 549.

Creasy, J. W., Eby, G. N., and Wood, S. A., 1979, Geochemistry of the Hart Ledge complex, White Mountain batholith, New Hampshire: Geol. Soc. Amer., Abs. with Prog., v. 11, p. 38.

Creasy, J. W., Whitaker, S. B., and Griffith, W. C., 1986, Rattlesnake Mountain, Maine--new occurrence of undersaturated felsic rocks, White Mountain magma series: Geol. Soc. Amer., Abs. with Prog., v. 18, p. 10.

DeMartinis, J. M., 1976, Petrology of the Rattlesnake Mountain pluton, Maine: B.S. thesis, Bates College, Lewiston, Maine, 40 p.

Eby, G. N., 1985a, Monteregian Hills II. Petrography, major and trace element geochemistry, and strontium isotopic geochemistry of the eastern intrusions: Mounts Shefford, Brome, and Megantic: Jour. Petrol., v. 26, p. 418-448.

Eby, G. N., 1985b, Age relations, chemistry, and petrogenesis of mafic alkaline dikes from the Monteregian Hills and younger White Mountain igneous provinces: Can. Jour. Earth Sci., v. 22, p. 1103-1111.

Eby, G. N., 1985c, Sr and Pb isotopes, U and Th chemistry of the alkaline Monteregian and White Mountain igneous provinces, eastern North America: Geochim. et Cosmochim. Acta, v. 49, p. 1143-1154.

Eby, G. N., and Creasy, J. W., 1983, Strontium and lead isotope geology of the Jurassic White Mountain batholith, New Hampshire: Geol. Soc. Amer., Abs. with Prog., v. 15, p. 188.

Eggleston, J. W., 1918, Eruptive rocks at Cuttingsville, Vermont: Am. Jour. Sci., v. 45, p. 377-410.

Faure, G., 1977, Principles of isotope geology: John Wiley and Sons, New York, 464 p.

Foland, K. A., and Faul, F., 1977, Ages of the White Mountain intrusives--New Hampshire, Vermont, and Maine: Am. Jour. Sci., v. 277, p. 888-904.

Foland, K. A., and Friedman, I., 1977, Application of Sr an O isotope relations to the petrogenesis of the alkaline rocks of the Red Hill complex, New Hampshire, USA: Contrib. Mineral. Petrol., v. 65, p. 213-225.

Foland, K. A., Henderson, C. M. B., and Gleason, J., 1985, Petrogenesis of the magmatic complex at Mount Ascutney, Vermont, USA: I. Assimilation of crust by mafic magmas based on Sr and O isotopic and major element relationships: Contrib. Mineral. Petrol., v. 90, p. 331-345.

Gilman, R. A., 1978, Bedrock geology of the Newfield 15' quadrangle, Maine: Maine Geol. Surv., Open-File Rept. 78-10, 20 p.

Griffith, W. C., 1983, Trachyte and nepheline trachyte dike swarm, Raymond and Casco, Maine: B.S. thesis, Bates College, Lewiston, Maine, 74 p.

Hayward, J. A., and Gaudette, H. E., 1984, Carboniferous ages for the Sebago and Effingham plutons, Maine and New Hampshire: Geol. Soc. Amer., Abs. with Prog., v. 16, p. 22.

Henderson, P., 1982, Inorganic geochemistry: Pergamon Press, Oxford, 353 p.

Hyndman, D. W., 1985, Petrology of igneous and metamorphic rocks, second edition: McGraw-Hill, New York, 786 p.

Jenks, W. F., 1934, Petrology of the alkaline stock at Pleasant Mountain, Maine: Am. Jour. Sci., Series 5, v. 28, p. 321-340.

Le Maitre, R. W., 1976, The chemical variability of some common igneous rocks: Jour. Petrol., v. 17, p. 589-637.

Loiselle, M. C., 1978, Geochemistry and petrogenesis of the Belknap Mountains complex and Pliney Range, White Mountain series, New Hampshire: Ph.D. dissert., Mass. Inst. Tech., Cambridge, 302 p.

McHone, J. G., 1978, Distributions, orientations, and ages of mafic dikes in central New England: Geol. Soc. Am., Bull., v. 89, p. 1645-1655.

McHone, J. G., and Butler, J. R., 1984, Mesozoic igneous provinces of New England and the opening of the North Atlantic ocean: Geol. Soc. Amer., Bull., v. 95, p. 757-765.

Miyashiro, A., 1978, Nature of alkalic volcanic rock series: Contrib. Mineral. Petrol., v. 66, p. 91-104.

Osberg, P. H., Hussey, A. M., II, and Boone, G. M., 1985, Bedrock geologic map of Maine: Maine Geol. Surv., scale 1:500,000.

Pirsson, L. V., and Washington, H. S., 1907, Contributions to the geology of New Hampshire; No. III, On Red Hill, Moultonboro: Am. Jour. Sci., 4th series, v. 23, p. 257-276, 433-447.

Randall, K. A., Foland, K. A., Raczek, I., and Henderson, C. M. B., 1983, Evolution of the Pliney complex, northern New Hampshire: isotopic and chemical relationships: Geol. Soc. Amer., Abs. with Prog., v. 15, p. 666.

Quinn, A., 1937, Petrology of the alkaline rocks at Red Hill, New Hampshire: Geol. Soc. Amer., Bull., v. 48, p. 373-402.

Sanders, R. P., 1971, Petrology of the syenitic intrusive complex, Pleasant Mountain, Maine: Ph.D. dissert., Univ. Illinois, Urbana, 130 p.

Size, W. B., 1972 , Petrology of the Red Hill syenitic complex, New Hampshire: Geol. Soc. Amer., Bull., v. 83, p. 3747-3760.

Wellman, T. R., 1971, Feldspathoidal rocks of the Red Hill igneous complex, New Hampshire: Jour. Geol., v. 79, p. 621-627.

Weston Geophysical Research, 1977, Geological investigation for the Pilgrim Unit II of Boston Edison: U.S. Nuclear Regulatory Commission Document BE-5G 7603, Appendix G-6, 19 p.

Whitaker, S. B., 1984, Geology of the Rattlesnake Mountain igneous complex, Raymond and Casco, Maine: B.S. honors thesis, Bates College, Lewiston, Maine, 109 p.

Maine Geological Survey
Studies in Maine Geology: Volume 4
1989

Preliminary Studies of Five Mesozoic Stocks in the Newfield 15' Quadrangle, Maine

Richard A. Gilman
State University of New York
College at Fredonia
Fredonia, New York 14063

ABSTRACT

Five discordant plutons ranging in composition from quartz diorite to granite and alkaline syenite are exposed in the Newfield, Maine 15' quadrangle. Two of the five plutons contain xenoliths of volcanic or hypabyssal rocks. Only the Abbott Mountain stock shows an internal complexity that is suggestive of magmatic differentiation; each of the other four stocks consist of a single phaneritic rock type. Where exposed, contacts are moderate-to-steep, abrupt, and marked by brecciation of the country rock and by quartz enrichment of the pluton. Emplacement of the plutons did not affect the orientation of the schistosity in the adjacent country rocks, thus suggesting emplacement by fracturing and stoping. Three of the plutons contain syenites that carry small amounts of Na-rich pyroxene and fayalite as well as occasional feldspathoids.

The five plutons are part of a band of Mesozoic stocks (the White Mountain Magma Series of Billings, 1956) that extends from the Maine coast through central and northern New Hampshire. This has recently been subdivided by McHone and Butler (1984), who include the Abbott Mountain stock within their coastal New England province.

Chemical analyses of the Abbott Mountain stock show minor chemical differences between the three recognized varieties of syenite, and suggest that the leucocratic syenite may be a differentiate of the enclosing fayalite syenite. The stock has been dated at 221±8 Ma (Foland and Faul, 1977).

INTRODUCTION

In recent years several studies have provided new data on the ages of a group of Mesozoic alkalic plutons exposed in a belt extending from southern Maine to the Monteregian Hills of Quebec, and have led to models for incorporating these bodies into the plate tectonic scheme (McHone and Butler, 1984; Crough, 1981; McHone, 1981; Foland and Faul, 1977). While all of the plutons are considered to be post-tectonic in the sense that none show the effects of Paleozoic tectonism and metamorphism, the range in published ages, from 240 Ma to 85 Ma, remains wide. Some authors have attempted to fit this age range to the drifting of the North American plate over one or more hot spots (Crough, 1981; Morgan, 1981), while others relate the magmatism to leaky transform faults (Uchupi et al., 1970) or extensional fracturing (McHone and Butler, 1984). The problem of origin remains unresolved.

The plutons have been generally referred to as members of the White Mountain Magma Series (Billings, 1956). More recently, however, McHone and Butler (1984) have suggested a further subdivision of these plutons based on age, distribution, and petrologic character. Of particular interest here is their proposed separation of plutons in southern Maine -- their coastal New England province -- from the main group of plutons belonging to the White Mountain Magma Series province in New Hampshire. The two proposed provinces abut approximately along the Maine/New Hampshire border (McHone and Butler, 1984, Fig. 1) in the vicinity of the Abbott Mountain stock, one of the five small plutons exposed in the Newfield quadrangle (Gilman, 1978, 1983). The purpose of this paper is to document the field and petrographic character of these plutons and to present preliminary chemical studies of one of them (Abbott

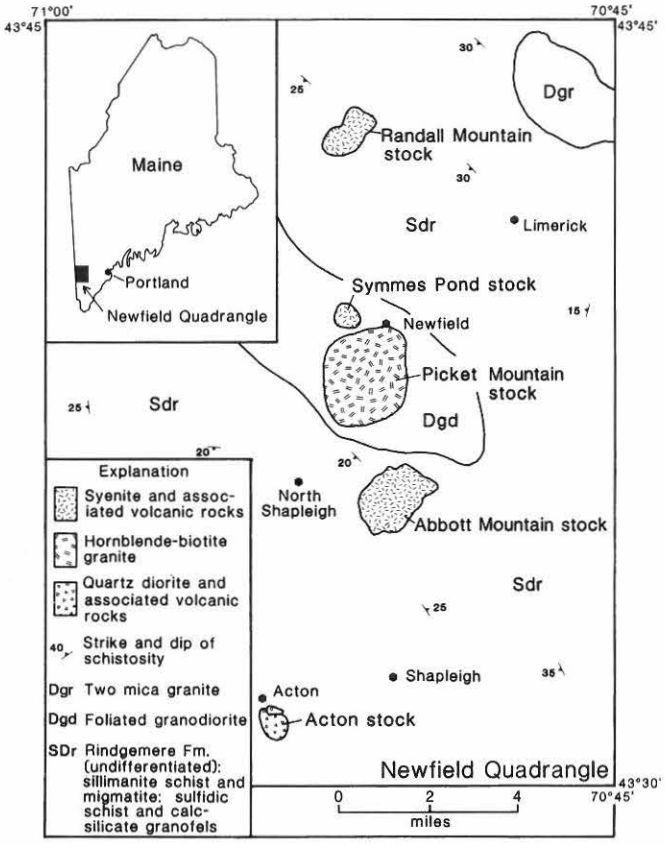

Figure 1. Regional setting of the five plutons studied in the Newfield 15' quadrangle, Maine.

Mtn.) in the hope that it will generate interest in additional investigations of a more detailed geochemical/petrologic nature.

REGIONAL SETTING

The five plutons are distributed along a more-or-less north-south line in the center of the Newfield quadrangle (Fig. 1). The stocks intrude a host rock consisting of granodiorite and sillimanite-grade schist and migmatite of the Rindgemere Formation (Silurian-Devonian). They vary in composition from quartz diorite to alkali syenite and granite, and some have associated aphanitic (volcanic?) members. The stocks are postkinematic, showing no effects of metamorphic overprinting, and are sharply discordant with respect to the structural trends of the host rock near their contacts. The stocks have been given appropriate geographic names; from north to south they are the Randall Mountain, Symmes Pond, Picket Mountain, Abbott Mountain, and Acton stocks.

RANDALL MOUNTAIN STOCK

Randall Mountain is located in the north-central part of the Newfield quadrangle between the villages of South Parsonsfield and East Parsonsfield (Fig. 2). The pluton is easily accessible on all sides by means of blacktop and gravel roads. The area is completely forested except for bald ledges at the summit of Randall Mountain. Nevertheless, there are good exposures on the steep south and southeast slopes and on the ridge crests, but north-facing slopes are more gentle and outcrops there are scarce.

The stock consists of (1) fine- to medium-grained, gray to brown syenites, and (2) gray, fragmental, trachyte porphyry.

Syenite is the most abundant rock type. Hornblende and/or biotite are visible in hand specimen while pyroxene was recognized only in thin section. The rocks vary from a porphyritic phase carrying up to 30% phenocrysts (dominantly feldspar of 2.0 to 4.0 mm length) set in a fine-grained groundmass, to an equigranular, medium-grained phase with feldspar grains averaging 3.0 to 5.0 mm with a maximum length of 10.0 mm. This textural variation does not appear to be mappable and the change from one type to another is gradual. Mafic minerals are conspicuous, but never amount to more than 5% of the rock.

Neither igneous lamination nor other primary structures were found in outcrop, although loose blocks on the ridge northeast of the summit of Randall Mountain show a well developed parallel arrangement of feldspar crystals. Variations of the syenite may be seen in a traverse up the south side of the mountain; the syenite at the summit is an equigranular, medium-grained type.

The syenites have been subdivided into porphyritic and equigranular types for thin section descriptions. The equigranular type is characterized by 2.0 to 5.0 mm, subhedral, interlocking orthoclase laths with minor fine-grained interstitial feldspar. Orthoclase usually constitutes more than 95% of the rock. It is always dusted by alteration products, commonly shows Carlsbad twinning, and consists of either homogeneous orthoclase or patchy microperthite. Interstitial nepheline and albite were found in one specimen each. Mafic minerals consist of biotite, clusters of fine-grained green hornblende, and pyroxene. The pyroxene occurs as euhedral to subhedral, 0.5 to 1.0 mm grains which in some cases show deep green colors indicative of aegirine-augite, and is commonly altered in part to hornblende. Of the accessory minerals, sphene is particularly evident, occurring in large, subhedral grains.

In thin section the porphyritic syenite shows 3.0 to 5.0 mm phenocrysts primarily of K-feldspar with lesser amounts of plagioclase, pyroxene, hornblende and biotite, set in a groundmass of feldspar, mafics, and accessory minerals ranging from 0.2 to 0.8 mm in diameter. Phenocrysts constitute from 5 to 30% of the rock. K-feldspar phenocrysts are usually subhedral and display an irregular, microperthitic intergrowth over the entire grain. Clinopyroxene phenocrysts are pale green and show faint pleochroism. The groundmass consists primarily of feldspar laths, frequently displaying a weak trachytic texture. Hornblende, augite, biotite, and accessories complete the groundmass. Sphene is again the most abundant accessory. Two of the specimens studied contain nepheline as either phenocrysts

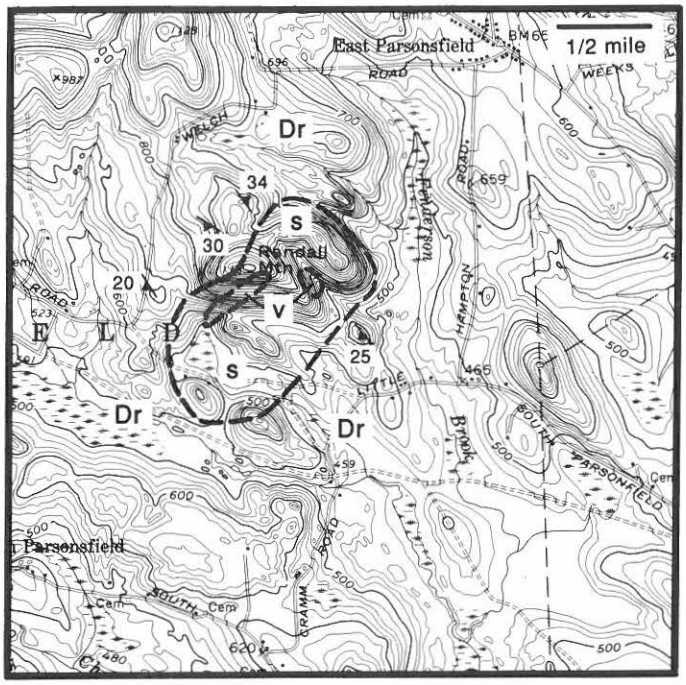

Randall Mountain stock

s	Syenite
v	Fragmental porphyry
Dr	Rindgemere Formation
20	Strike and dip of foliation
———	Exposed contact
— —	Covered contact

Figure 2. Location and composition of the Randall Mountain stock.

or interstitial fillings, and three specimens have small amounts of sodalite as subhedral, dodecahedral phenocrysts or as interstitial grains.

Light-gray porphyries, some of which carry xenoliths, occur both as dikes cutting the syenite and as inclusions within the syenite. The two varieties show only minor differences in thin section and are indistinguishable in hand specimen. Figure 2 shows two areas of fragmental trachyte porphyry that are interpreted as large xenoliths. In hand specimen these rocks consist of feldspar phenocrysts (2.0 to 4.0 mm long) and rock fragments enclosed in a gray, aphanitic groundmass. Primary flow structures were not observed. When present, rock fragments are subangular and range in size from 1 to 15 cm, the smaller ones being the most common. Fragments and/or phenocrysts constitute from 20 to 40% of the rock.

In thin section the phenocrysts are predominantly anhedral to subhedral orthoclase with minor perthitic intergrowths. Plagioclase phenocrysts were observed in a few samples, but always subordinate to orthoclase. Other phenocrysts include clinopyroxene and biotite. Clusters of subhedral, interlocking orthoclase grains represent either compound phenocrysts or fragments of an early phase of the syenite. Rock fragments consist of trachyte commonly showing well developed flow structure. The groundmass consists of subparallel laths of feldspar that sometimes wrap around rock fragments and phenocrysts. Augite, hornblende, biotite, and accessories are also present.

Dikes of fragmental trachyte porphyry are similar to the rocks just described, the major microscopic difference being the tendency for the groundmass to be allotriomorphic-granular rather than trachytic. Rock fragments include trachyte and syenite. A small dike cutting the syenite on the summit of Randall Mountain consists of 0.2 mm to 0.4 mm laths of subhedral orthoclase with a homogeneous pilotaxitic texture. A pink felsite dike in the valley east of the summit is distinctly different from others in the area. It consists of 0.2 mm laths of plagioclase with minor interstitial quartz in a groundmass showing a well developed trachytic texture.

The contact of the syenite with the country rock is exposed on the west side of Randall Mountain in a zone approximately 30 meters wide consisting of angular blocks of schist enclosed in pinkish, quartz-bearing syenite. The contact dips steeply to the northwest. Elsewhere the contact is not exposed, but the limits of the body are fairly well delineated by exposures of the surrounding country rocks. The contact is discordant, there being no deflection of the regional schistosity.

ABBOTT MOUNTAIN STOCK

Abbott Mountain lies just east of the village of North Shapleigh (Fig. 3). Exposures are excellent along the tops of ridges and are good on the steeper slopes, but lower slopes and the surrounding areas are generally covered by thick glacial deposits. Fresh samples are frequently difficult to obtain due to the rounded, weathered nature of the exposures; bald outcrops are often covered with thin sheets of crumbled rock. The area is accessible by dirt road on the north side, and by discontinued roads on the south and west sides and through the center.

The stock consists predominantly of a brown to gray, coarse-grained syenite with fine-grained diorite dikes at the margin. The coarse-grained syenite has been subdivided into three varieties on the basis of microscopic study. The most widespread type contains fayalite and aegirine-augite as minor constituents. A second variety is similar to this, but in addition contains minor amounts of quartz. The third variety is nearly devoid of mafic minerals.

The fayalite syenite (ops on Fig. 3) contains from 90 to 95% euhedral-to-subhedral, randomly arranged feldspar laths averaging 5.0 mm in length with maximum lengths of 10.0 mm. The

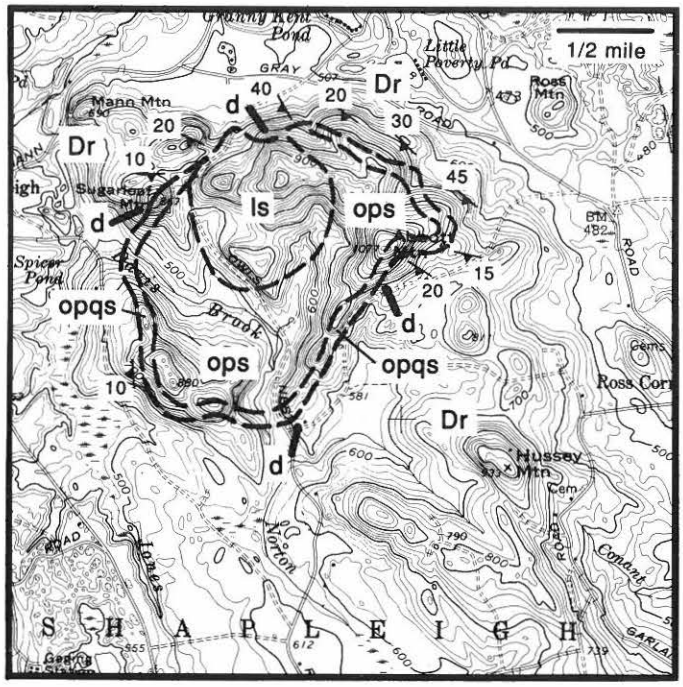

Abbott Mountain stock

ls	Leucocratic syenite
ops	Olivine-pyroxene syenite
opqs	Olivine-pyroxene-quartz syenite
d	Diorite dike
Dr	Rindgemere Formation
20	Strike and dip of foliation
——	Exposed contact
— —	Covered contact

Figure 3. Location and composition of the Abbott Mountain stock.

feldspar is dominantly orthoclase or microcline microperthite with patches and veins of albite distributed either uniformly throughout the grain or restricted to grain margins. Pyroxene constitutes from 2 to 7% of the rock and usually occurs in 0.5 to 2.0 mm euhedral-to-subhedral grains, commonly with hornblende alteration. The pyroxene is a darker green than common augite, suggesting aegirine-augite, but pleochroism is faint or nonexistent. Fayalite (sign (-), 2V approximately 40°) constitutes up to 3% of the rock and is found as 0.5 to 2.0 mm equant, anhedral grains that are partially altered along fractures to red iddingsite and a yellowish serpentine. In some grains the original olivine has been completely replaced. Biotite, apatite, zircon, and opaques complete the assemblage. This variety occurs in the east, south, and west parts of the area, including Abbott Mountain where there are abundant exposures.

The quartz syenite (opqs on Fig. 3) contains minor interstitial quartz; otherwise it is similar to the fayalite syenite. Orthoclase and microcline microperthite constitute 85 to 95% of the rock occurring as subhedral grains ranging from 4.0 to 8.0 mm in length. Grains of medium green, non-pleochroic aegirine-augite are usually subhedral and average 1.0 mm in diameter; some have been totally altered to secondary minerals. Quartz varies in amounts from a trace to 8% and occurs as anhedral grains (less than 0.5 mm) in the interstices between feldspar laths. Relatively large (up to 0.5 mm) grains of euhedral zircon are also found in this variety. Biotite, apatite, and opaques complete the assemblage. This variety has been found only in the contact zones of the stock and appears to form a nearly continuous shell between the country rock and the syenite of the interior.

The leucocratic syenite contains feldspar as the only essential mineral, with mafic and accessory minerals never constituting more than one or two percent of the rock. The feldspar consists of euhedral to subhedral grains ranging from 4.0 to 8.0 mm long. Both microperthite and antiperthite are present in various ratios, but antiperthite is frequently the more abundant. The K-feldspar is commonly clear in the center of the grains and perthitic at the margins; microcline twinning is sometimes present. The antiperthite consists of albite showing extremely thin twin lamellae and patches of K-feldspar. Accessory minerals are hornblende, zircon, and opaques. This variety is found in the north-central part of the stock, but its boundaries and contact relations are not well known. One sample from the margin carries small amounts of aegirine-augite and fayalite suggesting that it is gradational into the fayalite syenite.

Fine-grained (0.1 to 1.0 mm) diorite consists of approximately equal amounts of weakly zoned, intermediate plagioclase (An_{35-50}) and mafic grains arranged in an intergranular texture. Augite constitutes about 35 percent of the rock and usually occurs as subhedral interstitial grains, but occasionally is found in larger, poikilitic grains. Biotite occurs in small, red-brown irregular plates and constitutes 5 to 10% of the rock. Brown hornblende is occasionally associated with augite. Accessories are apatite and opaques. This lithology has been found in several localities at the margin of the stock where it occurs as brown-weathering dikes that cut the country rock. Inclusions of the diorite have been found enclosed in the border phase of the syenite.

Aplite dikes cut the syenite and consist of stubby, euhedral to subhedral phenocrysts of orthoclase (1.0 to 2.0 mm) embedded in a fine-grained (0.2 mm) groundmass of quartz and feldspar. Riebeckite and biotite are present in small amounts.

Field observations and petrographic study demonstrate a consistent pattern in the distribution of the major rock types of the stock. The diorite is only found at the margin of the stock as dikes cutting the country rock. These are isolated intrusions rather than a continuous body such as a ring dike. Fracturing and

dike emplacement may have been extensive in the area now occupied by the syenite. The dikes may also extend farther out into the country rock, but exposures are limited and they have not been found more than a few tens of meters from the stock margin.

The quartz-bearing phase of the syenite has been found only at the margin of the stock at several locations. Because the rock was not recognized as a separate type during field mapping, no attempt was made to establish the continuity of this type around the entire stock. The massive, coarse-grained rock, however, probably forms a marginal phase about a hundred meters wide around most of the body except along the northern edge.

The fayalite syenite constitutes the main body of the stock on the west, south, and east sides.

The leucocratic syenite is found in the north-central part of the stock. Sampling was not specifically planned to determine its extent because distinctive microfeatures of this unit were not recognized in the field. One sample, apparently representing the margin of this unit from the ridge northwest of Abbott Mountain, has a mineral assemblage intermediate between the leucocratic syenite and the fayalite syenite. The contact, therefore, has been drawn through this location; elsewhere it has been drawn separating known exposures of the two rock types based on microscopic study.

The relative ages of the rock units are defined on the basis of cross-cutting relations, inclusions, and inferred petrogenetic trends. The diorite dikes are clearly the oldest phase of intrusive activity. These cut the schist and pegmatite country rock and are in turn cut, brecciated, and included in the syenite. No indications of the relative ages of the quartz syenite and the fayalite syenite were observed. Both rocks are medium-to coarse-grained and it is possible that their contact is gradational. Likewise, there is evidence of a transitional contact between the fayalite syenite and the leucocratic syenite. The decrease in mafic constituents of the leucocratic syenite may reflect a later stage of differentiation, thus suggesting a younger age relative to the fayalite syenite. Riebeckite-bearing aplite dikes are younger than the fayalite syenite, but are of unknown age relative to the leucocratic syenite.

The attitude of the contact with the country rock is well displayed on several of the ridges. On Abbott Mountain the contact can be followed along the southeast side nearly to the summit. The outcrop pattern indicates that the contact dips southeastward. Similar outcrop patterns are found at several localities around the margin of the stock; on the north side the contact dips northward at as little as 30°, but on Sugarloaf Mountain the contact is nearly vertical. The overall shape of the contact is that of a dome with dips ranging from moderate (30°) to nearly vertical, the former predominating.

The stock is discordant with respect to the foliation in the surrounding schist. This is best shown along the northeastern margin where the schistosity strikes uniformly northwestward with a westerly dip. There has been no reorientation of the schistosity as a result of the intrusion of the stock.

Foland and Faul (1977) obtained a K/Ar date of 221±8 Ma for the fayalite syenite. Earlier work by Christopher (1969) using apatite fission-track geochronology gave an age of 119 Ma. That date is now interpreted as an unroofing date rather than a crystallization age (Foland and Faul, 1977).

Chemical analyses of eight samples from the Abbott Mountain stock are given in Table 1. It is evident that the three varieties of syenite are similar chemically. However, of the three, the leucocratic syenite is considerably lower in CaO and MgO, and is slightly higher in Na_2O. The increased abundance of free quartz at the margin of the stock is not clearly reflected in the variations in chemistry. Thus no major SiO_2 contamination by the country rock is apparent. However, norm calculations (Table 2) show a greater than threefold increase in quartz in the border phase. Normative feldspar compositions are nearly constant throughout the body with only a slight increase in albite toward the leucocratic syenite, and an accompanying decrease in orthoclase and anorthite. Considering the trace elements, only the leucocratic syenite shows any appreciable difference from the other syenites in that Rb, Zr, and Nb are higher, and Sr and Ba are lower.

SYMMES POND STOCK

The Symmes Pond stock lies just east of Symmes Pond (Fig. 4). Its margins are poorly defined, but neighboring outcrops of schist and granite limit the size to approximately that shown on the map. A breccia zone can be observed on the south side of Hall Road where it crosses the southwest side of the stock. The stock consists of green-brown, coarse-grained syenite containing fragments of foliated granodiorite country rock. The syenite contains small amounts of sulfides including molybdenite and has been the site of minor prospecting in past years. In thin section the rock consists of 95% microperthite and about 2 to 3% each of fayalite and clinopyroxene. The fayalite is partially altered to serpentine and occurs as 1.0 mm equant grains. The clinopyroxene is medium green and non-pleochroic, possibly an aegirine-augite. The petrographic and mineralogical character of this syenite is similar to the fayalite syenite of the Abbott Mountain stock. Dikes of tan trachyte are found cutting the country rock on the hill northeast of the stock.

PICKET MOUNTAIN STOCK

The Picket Mountain stock lies just south and west of the village of Newfield (Fig. 4). Outcrops are limited to ridges on Picket, Knox, and Zekes Mountains and in the Little Ossipee River at Newfield. The contact can be established within a few meters on the west slope of the small hill east of Picket Mountain where the granite is in contact with pegmatite and foliated granodiorite.

The stock consists of a homogeneous gray-brown, medium-grained, equigranular to subporphyritic granite. The mafic minerals are biotite and hornblende. The feldspar is dominantly

TABLE 1. WHOLE ROCK CHEMICAL ANALYSES: ABBOTT MOUNTAIN

	Diorite		Quartz syenite		Fayalite syenite		Leucocratic syenite	
Sample	23	56	16	40	15	31	24	26
MAJOR ELEMENTS (wt.%)								
SiO_2	51.6	48.7	63.2	61.7	60.0	61.6	63.7	61.7
TiO_2	2.44	4.54	0.43	0.52	0.55	0.48	0.28	0.53
Al_2O_3	13.4	13.5	16.9	16.8	17.0	17.1	17.8	17.9
Fe total	13.1	14.2	4.59	5.92	4.62	6.11	4.45	5.64
MnO	0.22	0.26	0.16	0.19	0.16	0.21	0.13	0.07
MgO	7.37	7.13	0.36	0.45	0.52	0.37	0.08	0.09
CaO	7.86	7.76	1.11	2.01	2.08	1.78	0.09	0.08
Na_2O	2.96	2.17	5.71	5.77	6.32	6.02	7.11	7.48
K_2O	0.43	0.29	6.40	5.13	5.13	6.04	5.40	5.00
P_2O_5	0.42	1.13	0.08	0.21	0.23	0.28	0.05	0.03
LOI	0.23	0.38	0.85	0.70	1.47	0.23	1.08	1.08
Total	100.00	99.98	100.0	99.6	99.1	100.3	100.3	99.7
TRACE ELEMENTS (ppm)								
Cr	250	240	20	20	20	10	20	10
Rb	40	20	220	170	130	120	230	230
Sr	430	980	80	270	440	40	10	10
Y	10	30	40	40	30	40	20	20
Zr	130	470	1010	330	230	140	420	540
Nb	40	140	90	80	60	60	100	250
Ba	240	360	290	980	2170	390	60	90

XRF analyses by X-RAY ASSAY LAB. LTD., Don Mills, Ontario.
* Total iron as Fe_2O_3.

TABLE 2. CIPW NORMS: ABBOTT MOUNTAIN

	Diorite		Quartz syenite		Fayalite syenite		Leucocratic syenite	
Sample	23	56	16	40	15	31	24	26
quartz	2.71	6.36	3.54	4.90	1.28	1.01	1.48	-
orthoclase	2.54	1.71	37.82	30.30	30.32	35.7	31.9	29.5
albite	25.05	18.36	48.32	48.8	53.31	50.9	60.1	60.9
anorthite	22.01	26.24	1.58	4.8	3.9	1.18	0.12	0.2
corundum	-	-	-	-	0.37	-	0.22	0.11
hypersthene	26.8	28.09	-	-	1.29	-	0.24	-
magnetite	2.26	2.45	4.05	5.25	3.73	5.64	4.15	4.53
ilmenite	4.63	8.62	0.82	0.99	1.04	0.91	0.53	1.0
hematite	-	-	0.16	0.19	0.40	0.04	-	0.5
apatite	0.97	2.62	0.19	0.49	0.53	0.65	0.12	0.07
diopside	11.68	3.99	1.9	2.42	-	1.99	-	-
wolastonite	-	-	0.38	0.29	-	1.11	-	-
nepheline	-	-	-	-	-	-	-	0.2
olivine	-	-	-	-	-	-	-	0.1

Note: Calculations used $Fe_2O_3/FeO = 2$

K-feldspar, sometimes present as phenocrysts, and chalky-weathering plagioclase. Quartz is visible in all samples.

Thin section study shows that the rock is comprised of about 25% quartz, 50% microperthite, 20% plagioclase, and 5% mafics. Quartz ranges in size from tiny interstitial grains up to grains 3.0 mm in diameter. Microperthite phenocrysts are up to 5.0 mm long, show Carlsbad twinning, and a vein-type perthitic intergrowth. Plagioclase is restricted to small (0.5 mm) subhedral grains in the groundmass. Biotite and hornblende are ragged. Hornblende is less abundant than biotite and is often altered to matted biotite.

ACTON STOCK

The Acton stock is a small body of quartz diorite located on the east side of Grant Road approximately midway between Acton and South Acton (Fig. 5). Part of the area is an apple orchard and therefore is easily accessible. A few exposures are

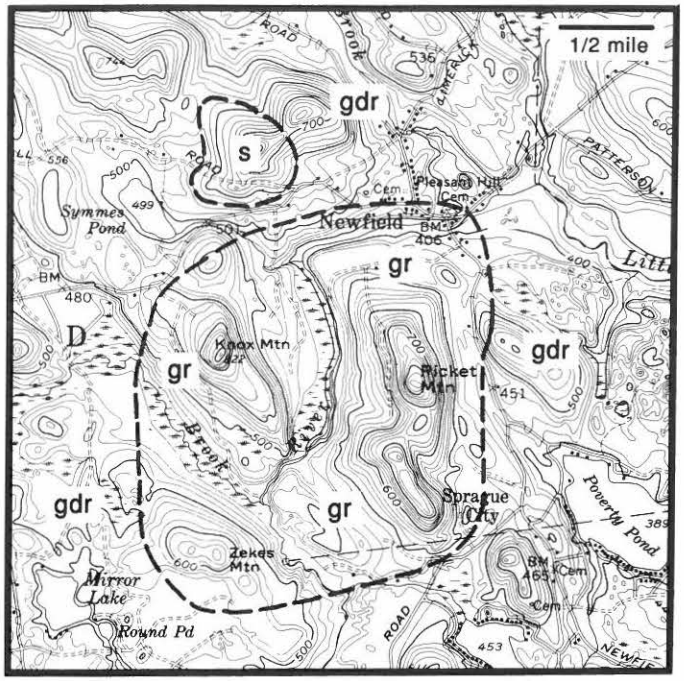

Picket Mountain and Symmes Pond stocks

s	Syenite
gr	Biotite-hornblende granite
gdr	Foliated grandiorite
——	Exposed contact
— —	Covered contact

Figure 4. Location and composition of the Symmes Pond and Picket Mountain stocks.

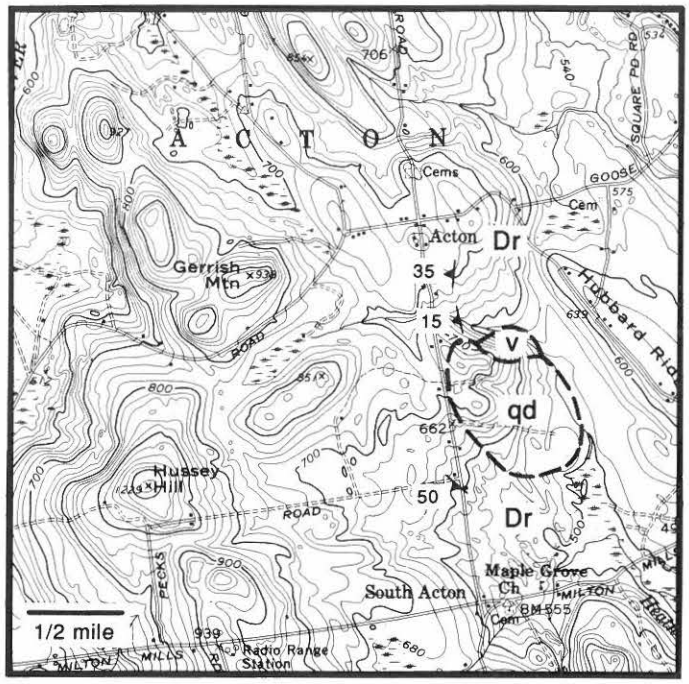

Acton stock

v	Fragmental volcanics
qd	Quartz diorite
Dr	Rindgemere Formation
15 ⟨	Strike and dip of foliation

Figure 5. Location and composition of the Acton stock.

found in the orchard itself, but most large exposures are in the surrounding woods. The shape of the stock is not well known because of the lack of outcrops on the south and east sides.

Two rock units are present: medium-grained, gray-weathering quartz diorite, and dark gray porphyritic and fragmental andesite. The contact between the two units is not exposed but, based on the absence of quartz diorite fragments in the fragmental andesite, it is tentatively concluded that the quartz diorite is the younger.

The medium- to coarse-grained, gray quartz diorite constitutes most of the body. Igneous lamination is evident in a few exposures. In thin section the rock consists of approximately 80% plagioclase, 15% pyroxene, and 5% opaque minerals, apatite, and quartz. The plagioclase is occasionally strongly zoned, but unzoned grains (An_{50}) are abundant. The grains are subhedral with interpenetrating grain margins and may be surrounded by finer-grained, anhedral plagioclase. Grains average about 4.0 mm, but are as large as 8.0 mm long. Orthopyroxene and clinopyroxene are subhedral, average 1.0 mm in diameter, and are partially altered to fibrous amphibole and biotite. Interstitial quartz is present in minor amounts. A fine-grained border phase is exposed along the west margin and is sometimes the host of a breccia containing fragments of hornfelsed schist. Small dikes of tan aplite cut the medium-grained quartz diorite.

Dark gray, porphyritic and fragmental andesite constitutes the northern part of the body, but the contact with the country rock has not been found. The rock is massive and has abundant phenocrysts of light gray-weathering plagioclase and small, angular fragments of dark, aphanitic rock types that are seen most clearly on weathered surfaces. In thin section the rock consists of 20% plagioclase phenocrysts set in a microcrystalline groundmass of plagioclase, biotite, and opaques. In some cases the plagioclase phenocrysts appear to be fragments of phenocrysts having sharp but irregular edges. At one location a

10 cm dike of lighter colored fragmental rock cuts the andesite. The fragments are usually less than 3 cm in diameter, subangular, and consist of various aphanitic rocks and schist. The fragments are set in a matrix of microcrystalline biotite, feldspar, and quartz. The andesite is also cut by a dike of tan felsite.

SUMMARY AND PETROLOGIC IMPLICATIONS

The characteristics of the five plutons along with petrologic implications can be summarized as follows:

(1) All the stocks are post-tectonic in that none show overprinting of tectonism or metamorphism. In the past they have been considered members of the White Mountain Magma Series, but recently McHone and Butler (1984) have separated the Abbott Mountain stock from the series on the basis of radiometric age (221±8 Ma; Foland and Faul, 1977) to include it with an older igneous province they call the coastal New England province. While none of the other four plutons of this study have been dated, neighboring plutons of known ages are either Early Jurassic or Early Cretaceous (Foland et al., 1971; Foland and Faul, 1977).

(2) The most abundant rock type is alkali syenite that in many cases carries Na-rich pyroxene and fayalite, and in a few instances includes nepheline and sodalite. Quartz diorite and granite are present in one stock each.

(3) With the possible exception of the Abbott Mountain stock there is no evidence of magmatic differentiation. Each of the other stocks consists of a single phaneritic rock type that may show localized textural variations, but is mineralogically homogeneous. The Abbott Mountain stock, on the other hand, shows a distribution of fayalite syenite and leucocratic syenite that suggests differentiation may have taken place. Chemical analyses of the Abbott Mountain stock indicate that differences exist between the three varieties of syenite, but that detailed geochemical studies are needed to further explore the effects, if any, of magmatic differentiation.

(4) Two of the stocks (Acton and Randall Mountain) include aphanitic rocks that predate the coarse-grained members. In both cases these volcanic, or hypabyssal, rocks contain abundant lithic fragments of other aphanitic igneous lithologies. This is similar to the pattern found in the Burnt Meadow Mountain complex a few miles to the north, (Gilman, 1977, 1979) as well as in other White Mountain Magma Series plutons (Billings, 1956).

(5) The discordant nature of the plutons suggest fracturing and stoping as the emplacement mechanism. Where the margins of the plutons are exposed on Randall and Abbott mountains, the contacts dip steeply-to-moderately outward from the center of the pluton. This suggests that in these two cases the present erosion surface may be close to the top of domal-shaped intrusions.

ACKNOWLEDGMENTS

I want to express my thanks to the Maine Geological Survey for their continued support for mapping in the Newfield quadrangle. Also to my wife, Carmen, for typing the manuscript as well as helping with revisions, and to J. Berkley and two anonymous reviewers for reading and improving the final draft.

REFERENCES CITED

Billings, M. P., 1956, The geology of New Hampshire, part II, Bedrock geology with colored map (1955): New Hampshire State Planning and Development Commission, Concord, 203 p.

Christopher, P. C., 1969, Fission track ages of younger intrusives in southern Maine: Geol. Soc. Amer., Bull., v. 80, p. 1809-1814.

Crough, S. T., 1981, Mesozoic hotspot epeirogeny in eastern North America: Geology, v. 9, p. 2-6.

Foland, K. A., and Faul, H., 1977, Ages of the White Mountain intrusives-New Hampshire, Vermont and Maine, U.S.A.: Am. Jour. Sci., v. 277, p. 888-904.

Foland, K. A., Quinn, A. W., and Giletti, B. J., 1971, K-Ar and Rb-Sr Jurassic and Cretaceous ages for intrusions of the White Mountain Magma Series, northern New England: Am. Jour. Sci., v. 270, p. 321-330.

Gilman, R. A., 1977, Geology of the Kezar Falls quadrangle, Maine: Maine Geol. Surv., Map GM-4, 15 p.

Gilman, R. A., 1978, Bedrock geology of the Newfield 15' quadrangle, Maine: Maine Geol. Surv., Open-File Report 78-10, 20 p.

Gilman, R. A., 1979, Geology of the Burnt Meadow Mountains igneous complex, Oxford County, Maine: Geol. Soc. Maine, Bull. 1, p. 29-41.

Gilman, R. A., 1983, Mesozoic plutonic-volcanic rocks of the Newfield quadrangle, Maine: Geol. Soc. Amer., Abs. with Prog., v. 15, p. 188.

McHone, J. G., 1981, Comment on "Mesozoic hotspot epeirogeny in eastern North America": Geology, v. 9, p. 341-343.

McHone, J. G., and Butler, J. R., 1984, Mesozoic igneous provinces of New England and the opening of the North Atlantic Ocean: Geol. Soc. Amer., Bull., v. 95, p. 757-765.

Morgan, W. J., 1981, Hotspot tracks and the opening of the Atlantic and Indian Oceans, *in* Emiliani, C. (ed.), The oceanic lithosphere: The Sea, v. 7, Wiley, New York, p. 443-487.

Uchupi, E., Phillips, J. D., and Prada, K. E., 1970, Origin and structure of the New England seamount chain: Deep-Sea Research, v. 17, p. 483-494.

Maine Geological Survey
Studies in Maine Geology: Volume 4
1989

Petrographic and Geochemical Variations within the Songo Pluton, Western Maine

David Gibson
Daniel R. Lux
Department of Geological Sciences
University of Maine
Orono, Maine 04469

ABSTRACT

Field and petrographic investigations of the 382 Ma old Songo pluton, western Maine, have revealed that it can be subdivided into two petrographic varieties. A typical I-type granodiorite containing biotite, ± hornblende, and sphene crops out in the northwestern, northern, and northeastern parts of the pluton. Biotite-granodiorites containing Ti-rich biotite occur in the central and southern areas. The distribution of the latter facies appears to be spatially associated with the outcrop pattern of the 325 Ma Sebago two-mica granite and with numerous pegmatites. A gradational boundary is inferred between the two petrographic varieties of the Songo pluton.

Microprobe data confirm that biotites from the two petrographic varieties differ in TiO_2 and to a lesser degree MnO wt.%. These biotite analyses show a trend of decreasing Mn and increasing Ti within the pluton. Continuous variation in biotite compositions also corroborates the gradation between the two Songo types.

Major element geochemical data show that the petrographic varieties overlap in composition but that, on average, the biotite-hornblende-sphene granodiorites are less felsic (i.e. lower SiO_2 and higher TiO_2, Fe_2O_3(T), CaO and P_2O_5 wt.%) than their biotite-granodiorite counterparts. Whereas the major element data define linear, continuous trends with SiO_2, the trace elements do not. Some of the biotite-granodiorites are mildly peraluminous, with A/CNK ratios greater than 1:1.

The combined field, petrographic, and geochemical evidence suggest that parts of this I-type granodiorite may have been modified by the subsequent intrusion of the Sebago granite. The dual effects of reheating and fluid migration associated with the emplacement of the latter may have produced the mineralogical variation in those parts of the Songo pluton adjacent to the Sebago granite and the pegmatites. This thermal event may also have caused open-system behavior of trace elements in the Songo pluton. The major element geochemistry of the pluton appears to have remained largely unchanged.

INTRODUCTION

The Songo granodiorite pluton is one of a number of post-Acadian granitic intrusions presently exposed on the northwestern limb of the Kearsarge - central Maine synclinorium in western and northwestern Maine (Fig. 1). It covers an area of approximately 300 km^2 in the Bethel and Bryant Pond 15' quadrangles and intrudes metasedimentary rocks of Silurian and early Devonian age. It is truncated to the southeast by the Moll Ockett normal fault and is intruded by the Speckled Mountain quartz monzonite, which is the northern extension of the Sebago two-mica granite. The Songo pluton was originally mapped by Fisher (1962) and Guidotti (1965) and has been assigned to the New Hampshire plutonic series of Billings (1956).

U-Pb zircon (Lux and Aleinikoff, 1985) and Rb-Sr whole rock isochron results (Lux et al., this volume) indicate a crystal-

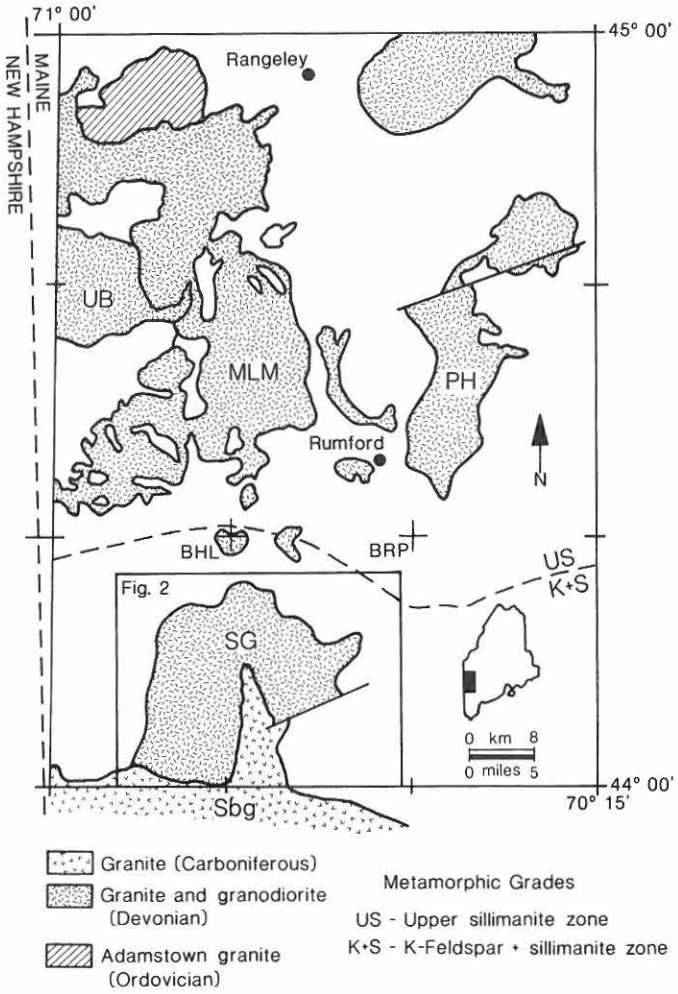

Figure 1. Map showing the distribution of granitic plutons in part of western Maine. (UB - Umbagog; MLM - Mooselookmeguntic; PH - Phillips; SG - Songo; Sbg - Sebago). The Bethel (BHL) and Bryant Pond (BRP) quadrangles are also labeled.

lization age of 382 Ma for the Songo pluton. This is comparable to ages of other plutons in this area, for example 371±6 Ma for the Mooselookmeguntic pluton (Moench and Zartman, 1976) and 382±3 Ma for the Umbagog pluton (Moench, 1984). However, $^{40}Ar/^{39}Ar$ dating of hornblende from the Songo pluton reveals that they have disturbed argon release spectra and plateau ages, averaging at 304 Ma, which are significantly younger than the crystallization age (see Lux et al., this volume).

These young, reset hornblende ages and petrographic data from the metamorphic rocks of the area led Lux and Guidotti (1985) to suggest that some of the high-grade metamorphism in western Maine was closely related in time and space to the emplacement of the Sebago granite. The latter has been dated at 325 Ma by both the Rb-Sr whole rock isochron (Hayward and Gaudette, 1984) and the U-Pb zircon methods (Aleinikoff, 1984). This suggests that this metamorphic event is Carboniferous in age rather than Devonian as previously believed (Holdaway et al., 1982, and Guidotti et al., 1983). Further evidence from calculated thermal models by De Yoreo et al. (1989) strongly suggests that the Sebago pluton was an adequate heat source for this metamorphism, given that it is a thin (ca. 1 km), north-dipping sheet-like intrusion (Hodge et al., 1982).

The initial reconnaissance sampling for the argon dating study (D. R. Lux) revealed certain petrographic variations within the Songo pluton. In some areas the granodiorite contains biotite, hornblende, and sphene, a mineral assemblage characteristic of I-type granites (Chappell and White, 1974). In other parts of the pluton the granodiorite lacks hornblende and sphene and contains biotite as the only mafic phase. In addition, preliminary petrographic observations revealed that this biotite has a distinctive red/brown pleochroism indicative of high TiO_2 contents. This is a mineralogical feature often associated with peraluminous S-type granites (see Table 1 of Pitcher, 1982). Thus the Songo pluton presents an opportunity to investigate a seemingly individual intrusion within which internal petrographic varieties are present.

This contribution presents field, petrographic, and geochemical data for the Songo granodiorite and associated rocks within the pluton. The aims of this study are, (1) to elucidate the field relations of the two petrographic varieties and hence ascertain whether the Songo pluton is zoned or composite, (2) to investigate the origin of this internal variation, and (3) to examine the effects on the Songo pluton of the later emplacement of the Sebago granite.

ANALYTICAL METHODS

Geochemical bulk rock analyses of 41 samples from the Songo pluton were performed at the Department of Geology, The Queen's University of Belfast, N. Ireland. The whole rock analyses were performed on a Phillip's PW 1410/20 X-ray fluorescence spectrometer with interchangeable W and Cr X-ray tubes. Most major elements were analyzed off fused glass discs except for MgO and CaO, which along with the trace elements, were determined on pressed powder pellets. A set of international silicate standards, along with some internal laboratory standards, were employed to construct calibration lines. SiO_2 and Al_2O_3 analyses were duplicated for each sample and these varied usually by <0.1% and <0.17% respectively from the averages. Precisions for SiO_2, Al_2O_3, TiO_2, Fe_2O_3 (as total), CaO, Na_2O and K_2O were less than 1% of the total concentrations and less than 3% for MgO, MnO, and P_2O_5. Trace element precisions were less than 1% for Rb, Sr, Ba, Zr, and Y and <5% for Th, Zn, Nb, and Ni.

Biotite microprobe analyses were performed at the University of Maine on a MAC 400S system with an accelerating potential of 15 Kv and a beam current of 0.03 micro-amps. Silicate mineral standards were utilized and the matrix correction factors employed are those of Bence and Albee (1968).

FIELD RELATIONS AND PETROGRAPHY

The Songo granodiorite is typically medium grained and equigranular although some variations in grain size and texture are observed. The granodiorite is commonly foliated and in some outcrops it is intensely banded (see below). The outer contacts of the pluton are fairly well exposed and are often associated with migmatites. No contact aureole is evident around the Songo pluton nor would one be expected because of the high grade of regional metamorphism (Ksp + Sill). Metasedimentary xenoliths, probably of local origin, are preserved in the Songo pluton, but nowhere are they abundant. Igneous type enclaves are also recognized at some localities as well as biotite-rich schlieren.

Field and petrographic investigations have confirmed that two varieties of granodiorite are present within the Songo pluton. One facies is characterized by the presence of red/brown, Ti-rich biotite and is referred to here as the biotite-granodiorite. In contrast, the other granodioritic variety contains black biotite, and usually hornblende and sphene (referred to as the BHS-granodiorites). However, more extensive sampling of the pluton has revealed that, in some parts of this facies, there is variation in this standard mineral assemblage (see below). Usually, the two petrographic varieties can be identified in the field either by the presence of hornblende and/or sphene, or by the color of the biotite. In particular, the red/brown sheen of biotite from the biotite-granodiorites is distinctive.

Recent field mapping has revealed that the two petrographic varieties crop out in discrete areas (Fig. 2). The BHS-granodiorites crop out in the northwestern, northern, and northeastern parts of the pluton with a small subsidiary area northeast of East Stoneham. The biotite-granodiorites are observed in the central and southern parts of the pluton and close to the northern extension of the Sebago granite. Indeed, there appears to be a strong spatial association between the biotite-granodiorite facies of the Songo pluton and the contact of the latter with the Sebago granite. In addition to the main area, biotite-granodiorite is also observed close to major pegmatite bodies and adjacent to large metasedimentary xenoliths.

A gradational boundary is inferred between the two Songo varieties and no intrusive contact has been observed. Evidence from petrographic observations, biotite mineral chemistry, and whole-rock geochemical data (as detailed below) appears to support this proposed gradation.

In the BHS-granodiorite, black biotite is the most abundant mafic phase and is ubiquitous throughout this facies. In thin section it is typically brown-green and inclusions of zircon and apatite are common. Hornblende is sub- to euhedral and up to 5 mm in length. Preliminary microprobe analyses suggest they are a calcic variety. Plagioclase is generally unzoned, sub- to euhedral and occasionally has sericitized cores. It greatly exceeds K-feldspar in abundance with the latter being sub- to anhedral and interstitial. Quartz often exhibits evidence of being strained with undulose and sectorial extinction. Of the accessory phases, sphene is the most abundant and is usually euhedral. Apatite is also present, occurring both as inclusions in biotite and as discrete grains (up to 0.2 mm). Zircon occurs generally as inclusions in biotite and appears to lack any petrographic characteristics of an inherited component (e.g. rounded cores or zonal growth lines). Magnetite, the primary Fe-Ti oxide phase, and allanite are also present in minor amounts. Myrmekitic intergrowths of plagioclase, K-feldspar, and quartz are common. Some muscovite is also observed, but its characteristics strongly suggest that it is secondary. Therefore, on petrographic grounds, the BHS-granodiorites have an I-type mineralogy.

However, there is some variation of the characteristic mineral assemblage of the BHS-granodiorites, with a decrease in the abundance of hornblende and sphene. In some parts of this facies hornblende is absent, but the presence of both black biotite and sphene confirm that these samples are part of this petrographic variety. Therefore there is a gradation from biotite-hornblende-sphene granodiorites to biotite-sphene granodiorites within this facies.

In the biotite-granodiorite, biotite is the only mafic silicate present. It has a distinctive red-brown pleochroism in thin section which is usually indicative of high TiO_2 contents (Deer et al., 1975). Plagioclase is sub- to euhedral and unzoned. Commonly its twin planes are warped and diffuse and, in highly deformed samples of the biotite-granodiorite, it is heavily sericitized. K-feldspar is generally subhedral and interstitial. The quartz in the biotite-granodiorite appears highly strained and is often cracked, embayed, and exhibits sectorial extinction. Apatite and zircon are the most abundant accessory phases and commonly occur as inclusions in biotite. Fe-Ti oxides (mag-

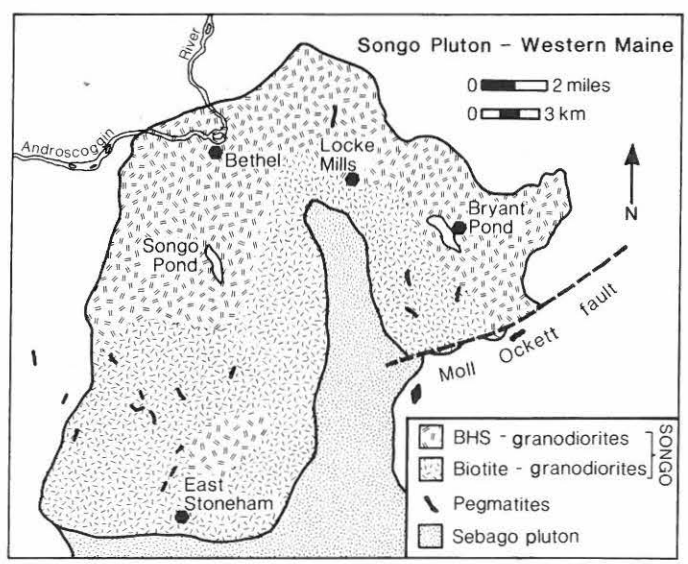

Figure 2. Generalized map of the Songo pluton showing the disposition of the two petrographic varieties. The Sebago granite and some of the larger pegmatites are also shown.

netite + ilmenite, some of which may be secondary) and allanite are present in minor amounts. Myrmekitic intergrowths are also observed in this facies. Subsidiary amounts of muscovite are present and although the majority of grains appear to be secondary, there is evidence to suggest that a small amount of primary muscovite is present in this part of the pluton. In contrast to the BHS-granodiorites, the biotite-granodiorites exhibit some S-type characteristics.

The petrographic characteristics described above are fairly constant for each Songo type. Variations are observed however, and in some biotite-granodiorite samples the biotites have less extreme red/brown pleochroism (cf. to normal examples of this facies) and some resorbed anhedral sphene, possibly of a secondary origin, is observed. In addition, biotites from some BHS-granodiorites occasionally show incipient development of red/brown pleochroism. These "intermediate" petrographic characteristics are observed in samples from outcrops geographically between the two main Songo varieties and may be evidence of a gradation between them.

Modal analyses reveal that most samples from the two petrographic varieties of the Songo pluton plot in the granodiorite field of the Streckeisen (1976) classification diagram (Fig. 3b), though some are more strictly termed tonalites. There is a large degree of overlap between the two varieties on the Q-A-P triangle with an overall trend of increasing quartz contents and decreasing plagioclase contents. Similarly, there is a large degree of overlap in total mafic content between the BHS-granodiorites (15-28%) and the biotite-granodiorites (13-25%), as illustrated by Figure 3a. The modal data also show that both plagioclase and total mafic content decrease with increasing quartz levels (see Figs. 3a and c).

The Songo pluton is cut by numerous pegmatitic bodies, most of which have a simple mineralogy (i.e. quartz, K-feldspar, muscovite ± biotite ± garnet), although some also contain beryl, tourmaline, and apatite. They commonly occur as dikes or larger irregular masses, and field relations suggest that there may have been more than one generation of pegmatite emplacement. The pegmatites appear to be more abundant in the central part of the pluton, coincidental with the area of biotite-granodiorite. Guidotti et al. (1986) suggest that their general preponderance in western Maine is due to the emplacement of the Sebago pluton from which they may have been derived. Small bodies of leucocratic two-mica ± garnet granite are commonly associated with some of the larger pegmatites. The field relations of the former are ambiguous. They may be contemporaneous with the pegmatites, or younger. These leucocratic granites may also be related to the Sebago granite. Geochemical data presented in Table 4 may shed further light on this idea.

Deformation features are not only observed at a microscopic scale as described above, but also on a macroscopic scale within the Songo pluton. In the field, the granodiorite is commonly foliated. This is usually defined by the mafic phases + plagioclase and generally trends between 30°W to 30°E of N. At some localities plagioclase phenocrysts up to 3 cm in length are aligned parallel to the foliation. Commonly, the foliation is crenulated and is especially well developed in the central area of biotite-granodiorite. Indeed, the latter is often highly deformed and in many outcrops distinct mafic and felsic banding is observed. In addition to this banding, large plagioclase grains are developed, giving the rock the general appearance of an augen gneiss (e.g. 3 miles southwest of Songo Pond).

In summary, two main petrographic varieties are observed within the Songo pluton, each of which crops out in distinct parts of the intrusion. The BHS-granodiorites have an I-type mineralogy, whereas the biotite-granodiorites have some S-type characteristics. Pegmatites are regionally abundant, but within the Songo pluton they are especially common in the areas underlain by the biotite-granodiorite. Similarly, deformation features are better developed in this area, although foliations are observed over much of the Songo pluton.

BIOTITE MINERAL CHEMISTRY

The variation in biotite petrography is one of the most important parameters on which the subdivision of the Songo granodiorite is based. To elucidate the origin of the observed petrographic variations, it was important to investigate the mineral chemistry of biotites from the Songo pluton. Seventy-four biotites, from nine samples, were analyzed by electron microprobe. The samples chosen for analysis are from both petrographic varieties including possible intermediate types, spanning the range of whole-rock compositions (see Table 3). The results are given in Table 1 as averages +/- one standard deviation for each sample and are displayed graphically in Figure 4.

Most geochemical parameters do not distinguish between biotite from either Songo type (Table 1). Significantly, TiO_2 and to a lesser extent MnO are the exceptions to this generalization. Biotites from the BHS-granodiorite have, on average, lower

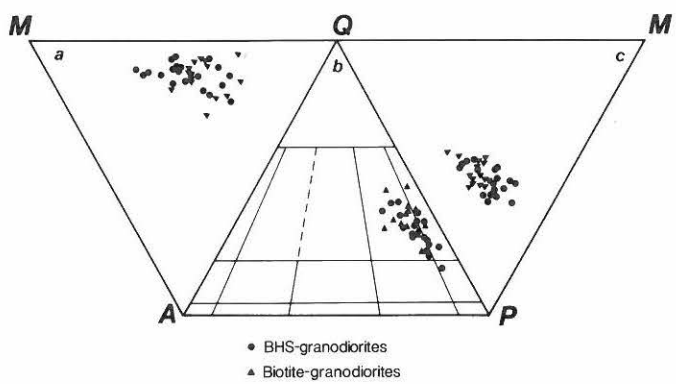

Figure 3. (a,b,c) Variations in modal mineral abundances within the Songo pluton plotted on quartz-alkali feldspar - plagioclase - total mafic content (Q-A-P-M) diagrams. 3b also shows the granitoid classification fields of Streckeisen (1974). (Some data points omitted due to overlap).

TABLE 1. AVERAGE MICROPROBE ANALYSES AND STRUCTURAL FORMULA UNITS (± ONE STANDARD DEVIATION) OF BIOTITES FROM SELECTED SAMPLES OF THE SONGO PLUTON.

Samples SG-7, 38, 10, 18, and 23 are BHS-granodiorites and are arranged, from left to right, in order of increasing SiO_2 values of their host whole-rocks (see Table 2). SG-34, 5, 16, and 40 are biotite-granodiorites. Number of biotites analysed per sample is given in brackets.

	SG-7 (8)	SG-38 (10)	SG-10 (8)	SG-18 (8)	SG-23 (6)	SG-34 (9)	SG-5 (9)	SG-16 (8)	SG-40 (8)
SiO_2	36.34 ± 0.29	36.93 ± 0.61	36.39 ± 0.78	36.29 ± 0.50	36.33 ± 0.12	36.35 ± 0.17	35.93 ± 0.60	35.66 ± 0.40	35.93 ± 0.39
Al_2O_3	16.75 ± 0.34	16.33 ± 0.67	16.06 ± 0.24	16.31 ± 0.45	17.02 ± 0.17	16.49 ± 0.31	16.48 ± 0.20	18.83 ± 0.36	17.63 ± 0.52
TiO_2	2.80 ± 0.17	2.78 ± 0.46	2.43 ± 0.19	2.50 ± 0.43	3.10 ± 0.19	3.23 ± 0.16	3.43 ± 0.19	3.60 ± 0.17	3.60 ± 0.16
MgO	10.55 ± 0.17	11.11 ± 0.26	11.42 ± 0.13	10.61 ± 0.39	11.23 ± 0.23	11.19 ± 0.17	11.30 ± 0.19	10.01 ± 0.24	10.52 ± 0.22
MnO	0.25 ± 0.06	0.26 ± 0.04	0.27 ± 0.03	0.37 ± 0.04	0.39 ± 0.05	0.16 ± 0.03	0.29 ± 0.02	0.08 ± 0.02	0.28 ± 0.07
FeO	18.33 ± 0.19	18.47 ± 0.18	18.85 ± 0.13	19.36 ± 0.28	17.83 ± 0.13	18.81 ± 0.15	18.10 ± 0.23	18.00 ± 0.24	17.62 ± 0.37
BaO	0.25 ± 0.27	0.07 ± 0.08	0.06 ± 0.11	0.11 ± 0.11	0.54 ± 0.15	0.26 ± 0.15	0.49 ± 0.13	0.03 ± 0.04	0.15 ± 0.10
K_2O	9.77 ± 0.15	9.45 ± 0.29	9.80 ± 0.14	9.68 ± 0.19	9.77 ± 0.18	9.43 ± 0.34	9.67 ± 0.19	9.80 ± 0.13	9.27 ± 0.28
Na_2O	0.19 ± 0.04	0.14 ± 0.03	0.14 ± 0.03	0.17 ± 0.04	0.12 ± 0.02	0.12 ± 0.03	0.14 ± 0.04	0.17 ± 0.02	0.14 ± 0.08
Fe/(Fe+Mg)	0.494±0.004	0.483±0.006	0.481±0.007	0.506±0.12	0.471±0.007	0.486±0.004	0.473±0.006	0.502±0.006	0.484±0.008
FORMULA UNITS ON THE BASIS OF 22 OXYGENS									
Si	5.541±0.039	5.590±0.087	5.550±0.066	5.549±0.028	5.477±0.013	5.497±0.018	5.456±0.047	5.355±0.038	5.543±0.058
Al^{IV}	2.459±0.039	2.410±0.087	2.450±0.066	2.451±0.028	2.523±0.013	2.503±0.018	2.544±0.047	2.645±0.038	2.568±0.058
Al^{VI}	0.551±0.035	0.504±0.051	0.437±0.039	0.488±0.084	0.500±0.024	0.435±0.051	0.405±0.048	0.689±0.047	0.574±0.036
Ti	0.321±0.018	0.317±0.051	0.278±0.023	0.288±0.048	0.352±0.021	0.367±0.018	0.391±0.024	0.406±0.020	0.409±0.017
Mg	2.398±0.037	2.508±0.070	2.596±0.041	2.418±0.100	2.523±0.053	2.522±0.041	2.557±0.049	2.241±0.046	2.370±0.050
Mn	0.032±0.007	0.033±0.005	0.035±0.003	0.048±0.006	0.049±0.006	0.021±0.004	0.037±0.003	0.010±0.001	0.035±0.009
Fe	2.338±0.029	2.339±0.033	2.404±0.037	2.476±0.044	2.248±0.016	2.379±0.020	2.299±0.043	2.261±0.030	2.227±0.049
Ba	0.015±0.016	0.005±0.005	0.004±0.007	0.006±0.006	0.032±0.009	0.015±0.009	0.029±0.008	0.002±0.001	0.009±0.006
K	1.901±0.022	1.824±0.057	1.907±0.029	1.889±0.044	1.878±0.033	1.819±0.066	1.874±0.035	1.879±0.028	1.885±0.047
Na	0.059±0.010	0.040±0.008	0.042±0.008	0.052±0.013	0.036±0.007	0.036±0.008	0.042±0.012	0.048±0.007	0.042±0.023

TiO_2 wt.% (2.4 - 3.1%) than those from the biotite-granodiorite (3.2 - 3.6%). The highest TiO_2 biotite values are observed in those samples (SG-16 and 40) which are geographically closest to the Sebago granite. In addition to the variation in TiO_2, there is also good discrimination between biotites from both petrographic types based on their MnO concentrations. Biotites from the BHS-granodiorite have, on average, higher MnO wt.% (0.25 - 0.39%) than their counterparts in the biotite-granodiorite (0.08 - 0.29%).

Further conclusions from the biotite data given in Table 1 are: (1) Samples SG-23 and 34, which may be intermediate varieties, have biotite TiO_2 values in between those of biotite from the two main Songo types. (2) Within the BHS-granodiorite there is a trend of decreasing biotite TiO_2 values with increasing SiO_2 contents of the host whole-rock (see also Fig. 5). (3) Fe/Fe+Mg ratios for all the biotites from the Songo pluton are fairly constant and have a restricted range of values (0.473-0.506).

Figures 4a-d are plots of individual biotite oxide pairs on a series of variation diagrams. It is apparent from these plots that there is overall continuous variation in the composition of biotites from the Songo pluton. This would tend to support the suggestion that there is a gradation between the two Songo types. It is significant, however, that the data plot in two distinct groups, each corresponding to the petrographic varieties. This distinction is primarily based on differences in TiO_2 concentrations. For example, Figure 4d shows that for a given Fe/Fe + Mg ratio, biotites from the biotite-granodiorite have significantly higher TiO_2 levels than those of the BHS-granodiorite. Only when Ti and Mn are considered jointly (Fig. 4c) is there almost complete separation of the two sets of biotite data. Furthermore, there is a general trend of decreasing Mn with increasing Ti through the entire biotite sequence.

The general relationship between biotite chemistry and whole-rock compositions is shown on a plot of biotite TiO_2 versus SiO_2 wt.% of the host rock (Fig. 5). As noted above, there is a general decrease of biotite TiO_2 with increasing SiO_2 of the host within the BHS-granodiorites, except for SG23 which is possibly an intermediate sample. In contrast, biotite TiO_2 levels remain fairly constant in the biotite-granodiorites and even SG-40, which has one of the most evolved whole-rock compositions of the entire Songo pluton (SiO_2 = 71%), has biotite TiO_2 wt.% similar to SG-5 which has a SiO_2 whole-rock value of 64 wt.%.

The electron microprobe data for the biotites confirm the petrographic subdivision described above. Biotites from the biotite-granodiorite have significantly higher TiO_2 concentrations and lower MnO values than those from the BHS-granodiorite. The data also support the suggestion that there is a gradation between the two varieties of the Songo pluton.

WHOLE-ROCK GEOCHEMISTRY

Whole-rock geochemical data for 39 Songo granodiorites are presented in Table 2 and also in summarized form in Table

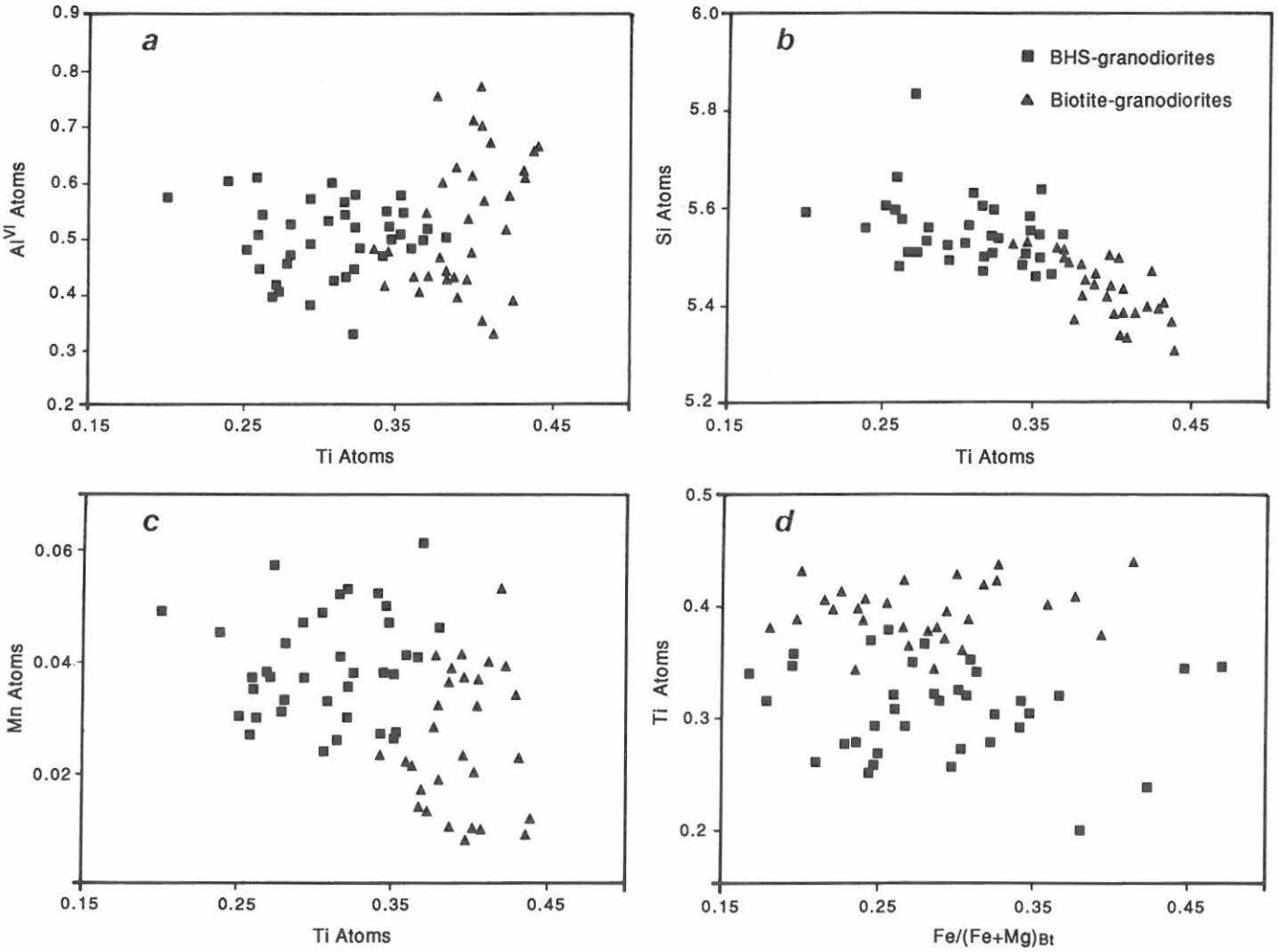

Figure 4. Bivariate plots of individual biotite oxide pairs. Figures 4a,b and c are of Al^{vi}, Si, and Mn atoms per formula unit versus Ti atoms per formula unit; 4d is of Ti atoms per formula unit against Fe/(Fe+Mg)Biot. Note the overall continuous trends in biotite composition on all the diagrams and the distinction between biotites from the BHS-granodiorites and the biotite-granodiorites.

3. Results for samples of the two-mica granite, which is associated with the pegmatites within the Songo pluton and data for the Sebago granite, are given in Table 4 and discussed below. The major and trace element data for the Songo granodiorites are plotted on a series of bivariate diagrams (Fig. 6 and 8) using SiO_2 as a fractionation index.

Table 3 shows that there is a significant amount of major element compositional variation within the Songo pluton. SiO_2 levels range from 57.5 to 71 wt.%, though the majority of samples fall within the range 61 to 68 wt.%. TiO_2, Fe_2O_3 (total), and CaO also vary significantly within the pluton. The data show that there is considerable compositional overlap between the two petrographic varieties. The BHS-granodiorites have generally less evolved chemistries. On average they contain lower SiO_2 and higher Al_2O_3, TiO_2, Fe_2O_3 (total), MnO, MgO, CaO, and P_2O_5 wt.% compared to the biotite-granodiorites. Furthermore, the BHS-granodiorites have generally lower Larsen Index and molecular A/CNK values than their biotite-granodiorite counterparts (see Table 3).

From examination of the whole-rock analyses and accompanying sample localities, it does not appear that the Songo pluton is zoned in any regular fashion. That is to say it does not display comparable systematic petrographic and geochemical variations observed in many symmetrically zoned plutons, e.g. the Loch Doon pluton, Scotland (Tindle and Pearce, 1981) or the Center Pond pluton, Maine (Scambos et al., 1986). Nevertheless, samples from the central and southwestern part of the pluton (e.g. SG-59, -2, -14 and -11), independent of their petrographic variety, do have more evolved chemistries (SiO_2 > 65%, TiO_2 <0.75%, L.I. > 15) compared to samples from the north and northeastern outcrops of the intrusion (e.g. SG-19, -6, -7 and -36). The latter, which are all BHS-granodiorites, have distinctly

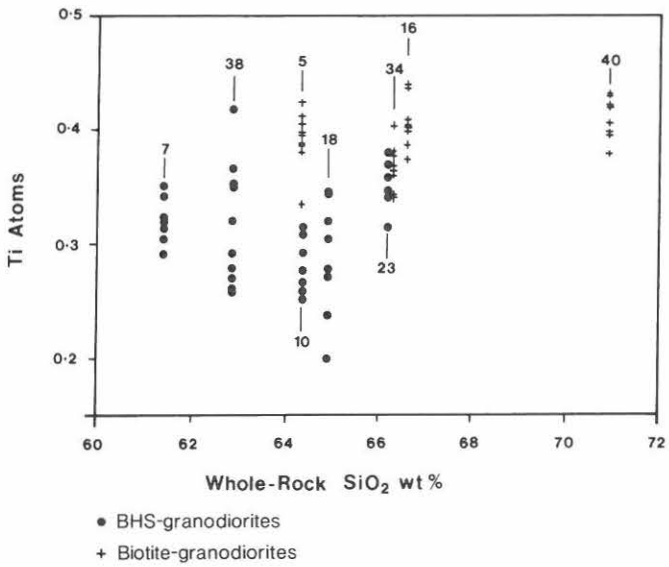

Figure 5. Plot of Ti atoms per formula units for biotites against SiO_2 wt. % of their host whole-rocks. Sample numbers are the same as those given in Table 2.

less evolved compositions. Therefore, it does appear that the central and southwestern parts of the Songo pluton are more felsic, at least on the basis of major element geochemistry.

The major element Harker diagrams (Fig. 6) reveal that the Songo granodiorites define single, essentially continuous compositional trends that have linear correlations with SiO_2. All the major elements (except for Na_2O and K_2O) decrease as SiO_2 levels increase through the series, with correlation coefficients ranging from -0.71 for MnO to -0.92 for CaO. Na_2O increases slightly through the series as SiO_2 rises, but K_2O does not appear to vary systematically through the pluton. Figure 6 also illustrates the extent to which the BHS-granodiorites and biotite-granodiorites overlap in composition, and the more evolved chemistry of some samples of the latter facies.

Figure 7, a plot of molecular A/CNK against SiO_2 wt.%, again shows that the two Songo varieties overlap in composition. The majority of samples have values between 1 and 1.1, but some biotite-granodiorites have ratios >1.1. There appears to be a slight, overall increase in A/CNK ratios with increasing SiO_2 wt.% through the Songo series.

In addition to the major element compositional variation described above, there are also differences in trace element concentrations within the Songo pluton. Table 3 reveals, however, that there is even less geochemical discrimination between the two petrographic varieties when the trace elements are considered, with many parameters almost totally overlapping. There is some trace element distinction between the two Songo types with the BHS-granodiorites having higher Sr and Ba ppm contents and slightly higher levels of Rb, Zr, Zn, and Ni ppm than the biotite-granodiorites. Nb, Th, and Y ppm are fairly constant throughout the pluton.

Trace element concentrations were also plotted on variation diagrams, but they generally lack systematic variation when plotted against SiO_2 wt.% or indeed any other fractionation index (e.g. Larsen Index or K/Rb ratios). Only plots of Rb, Sr, Zr, and Zn are presented here (Fig. 8), as the other trace elements are either fairly constant or lack any coherent trends. Figure 8 shows that Rb generally increases through the BHS-granodiorites, but that there is greater scatter in many of the more evolved biotite-granodiorite samples. In general, Sr ppm is constant in the BHS-granodiorites, but declines in some biotite-granodiorites. Only Zr and Zn vary systematically with SiO_2, both decreasing in abundance through the Songo sequence as SiO_2 increases. In general therefore, these trace element trends are in marked contrast to the linear trends observed on the major element bivariate diagrams.

DISCUSSION

The petrographic and geochemical variations of the Songo pluton may have been produced by a magmatic process(es) at the time of emplacement, as a result of post-crystallization modification, or by a combination of these mechanisms. The most likely cause of any post-crystallization modification would be the metamorphic event associated with the emplacement of the Sebago granite at around 325 Ma. The possibility that the petrographic and geochemical variations were produced independently (at different times) must also be explored. The main factors in assessing the origin of the internal variations of the Songo pluton are, (1) the disposition of and relationship between the petrographic varieties, (2) the nature of the geochemical variations within the pluton, and (3) the possible effects of the intrusion of the Sebago granite.

The distribution of the two Songo petrographic varieties has been described above. The major observation is that the biotite-granodiorites are spatially related to the outcrop pattern of the Sebago granite (Fig. 2). Away from the latter, biotite-granodiorites occur near the larger pegmatites.

The relationship between the Sebago granite and the pegmatites is unclear. The preponderance of the latter in western Maine has been linked to the proposal that the Sebago granite underlies much of the area (Guidotti et al., 1986). A model which depicts pegmatitic fluids streaming off the upper (top) surface of the Sebago magma is reasonable, but difficult to test. A possible solution might be to examine the leucocratic two-mica granites which are often associated with the pegmatites. These may be small pockets of "Sebago-type" magma, associated with the pegmatitic fluids or alternatively they may be batches of local anatectic melt. Table 4 presents analyses of two samples of leucocratic granite and for comparison the range of analyses for 21 samples of the Sebago granite. The data for the leucocratic granites usually fall within the range of the Sebago analyses and there is some geochemical affinity. However, this is not proof that they are comagmatic with the Sebago granite. Investigation

TABLE 2. MAJOR AND TRACE ELEMENT ANALYSES (XRF) OF THE SONGO GRANODIORITES.
$Fe_2O_3(T)$ = total iron measured as Fe_2O_3; L.I. - Larsen Index (= 1/3 SiO_2 + K_2O - Fe_2O_3 + MgO + CaO) (Larsen, 1938);
A/CNK = Molecular Al/Molecular Ca + Na + K; N + K wt % = total alkalis. BDL - below detection limits. Samples with an asterisk are biotite-granodiorites.

	SG-1	SG-2	SG-3	SG-6	SG-7	SG-10	SG-15	SG-17	SG-18	SG-19	SG-20	SG-23	SG-29
SiO_2	63.84	65.86	57.53	60.61	61.39	64.35	62.23	61.84	64.9	61.9	63.86	66.17	62.32
Al_2O_3	16.97	16.79	19.03	18.65	17.8	16.27	17.56	17.47	16.66	17.04	17.04	16.75	17.75
TiO_2	0.755	0.643	1.048	0.896	0.921	0.801	0.954	0.905	0.696	0.83	0.793	0.688	0.848
Fe_2O_3T	4.12	3.72	5.87	4.51	5.13	4.38	4.52	4.89	3.77	5.02	4.49	3.74	4.95
MnO	0.072	0.07	0.079	0.066	0.08	0.08	0.063	0.079	0.067	0.079	0.074	0.074	0.071
MgO	1.78	1.63	3.14	2.45	2.47	1.93	2.21	2.41	1.53	2.31	2.06	1.63	2.07
CaO	4.09	3.64	5.16	4.29	4.66	4.01	4.67	5.05	3.67	4.72	4.43	3.49	4.5
Na_2O	3.77	4.09	3.39	3.67	3.53	3.51	3.64	3.34	3.63	3.58	3.49	3.94	3.51
K_2O	2.99	2.24	2.9	3.19	2.4	3.36	2.38	2.37	3.8	2.85	2.14	2.39	2.44
P_2O_5	0.24	0.179	0.736	0.383	0.315	0.219	0.352	0.28	0.272	0.295	0.261	0.232	0.315
Total	98.63	98.86	98.88	98.72	98.69	98.91	98.58	98.63	98.99	98.62	98.64	99.1	98.77
L.I.	14.28	15.2	7.91	12.14	10.6	14.49	11.72	10.63	16.46	11.43	12.45	15.59	11.69
A/CNK	1.005	1.065	1.052	1.079	1.055	0.974	1.029	1.013	0.994	0.971	1.058	1.087	1.069
N+Kwt%	6.76	6.33	6.29	6.86	5.93	6.87	6.02	5.71	7.43	6.43	5.63	6.33	5.95
Rb ppm	112	103	146	164	130	109	75	83	112	100	100	129	111
Sr	610	496	609	609	631	598	1030	672	645	627	803	543	645
Ba	848	527	772	978	676	925	965	820	935	883	1056	545	1028
Zr	171	143	152	161	208	180	197	191	173	196	189	157	259
Th	11	7	4	BDL	10	12	7	8	14	7	8	15	16
Zn	64	61	118	79	86	65	70	68	58	70	67	67	84
Y	21	18	22	14	19	27	19	32	20	20	19	20	16
Nb	14	15	14	14	15	18	14	19	15	11	13	14	10
Ni	21	16	30	24	24	29	19	44	15	23	20	14	4

	SG-30	SG-35	SG-36	SG-38	SG-47	SG-48	SG-52	SG-53	SG-59	SG-4*	SG-5*	SG-8*	SG-9*
SiO_2	64.72	66.23	61.6	62.83	67.72	63.15	63.36	66.88	66.68	63.7	64.29	70.18	64.24
Al_2O_3	17.74	16.32	16.88	16.87	16.66	16.62	16.45	16.39	16.06	17.67	16.67	15.53	17.69
TiO_2	0.693	0.685	0.975	0.874	0.644	0.904	0.926	0.704	0.715	0.72	0.803	0.404	0.671
Fe_2O_3T	4.12	3.82	5.33	5.12	3.28	5.06	5.06	3.53	3.8	4.25	4.44	2.48	3.83
MnO	0.072	0.065	0.086	0.079	0.054	0.082	0.085	0.059	0.067	0.064	0.072	0.044	0.062
MgO	1.9	2.15	2.57	2.16	1.52	2.3	2.43	1.55	1.55	2.53	2.55	1.12	1.59
CaO	4.19	3.91	4.91	4.67	3.36	4.49	4.55	3.53	3.69	4.3	4.36	2.69	3.77
Na_2O	3.35	3.34	3.24	3.51	3.55	3.56	3.31	3.68	3.47	3.25	3.06	3.56	3.56
K_2O	2.21	2.65	2.77	2.6	3.25	2.65	2.32	2.94	3.27	2.17	2.15	3.25	3.23
P_2O_5	0.251	0.205	0.323	0.291	0.224	0.316	0.329	0.249	0.246	0.227	0.262	0.129	0.234
Total	99.25	99.38	98.68	99.0	100.26	99.13	98.82	99.51	99.55	98.88	98.66	99.39	98.88
L.I.	13.57	14.85	10.49	11.59	17.66	11.85	11.4	16.62	16.46	12.32	12.23	20.35	15.45
A/CNK	1.143	1.055	0.978	0.988	1.077	0.984	1.014	1.047	1.007	1.139	1.091	1.089	1.092
N+Kwt%	5.56	5.99	6.01	6.11	6.8	6.21	5.63	6.62	6.74	5.42	5.21	6.81	6.79
Rb ppm	115	96	92	88	108	95	105	115	111	90	94	124	110
Sr	617	548	669	672	802	627	671	617	649	544	602	381	604
Ba	1122	846	938	825	1042	653	1054	661	893	346	858	700	1416
Zr	245	154	214	217	152	210	217	156	189	146	176	121	192
Th	16	9	12	5	12	12	6	17	14	6	16	12	16
Zn	76	63	76	75	54	82	75	57	60	73	67	43	72
Y	18	17	21	22	10	16	19	24	20	30	21	16	14
Nb	12	8	12	15	11	11	12	16	15	11	17	11	10
Ni	5	22	31	20	13	26	25	12	14	29	33	15	3

TABLE 2. CONTINUED.

	SG-11*	SG-12*	SG-13*	SG-14*	SG-16*	SG-33*	SG-34*	SG-40*	SG-43*	SG-46*	SG-49*	SG-51*	SG-58*
SiO_2	69.65	64.19	65.51	65.16	66.58	66.35	66.29	70.9	64.73	67.05	64.34	64.88	66.83
Al_2O_3	15.78	17.04	17.07	17.54	16.19	17.05	16.74	14.77	16.56	15.66	17.21	17.63	16.39
TiO_2	0.581	0.817	0.678	0.601	0.658	0.598	0.767	0.505	0.871	0.764	0.805	0.706	0.694
Fe_2O_3T	3.07	4.42	3.8	3.68	3.88	3.35	4.04	2.89	4.57	4.14	4.66	3.89	4.12
MnO	0.053	0.073	0.062	0.056	0.052	0.048	0.056	0.058	0.069	0.066	.0.69	0.062	0.045
MgO	1.25	2.19	1.45	1.45	1.71	1.2	2.08	1.43	2.33	2.03	1.85	1.78	1.72
CaO	3.25	4.42	3.75	3.96	3.29	3.51	3.95	2.76	4.28	3.72	4.26	4.06	3.21
Na_2O	3.58	3.35	3.6	3.64	3.72	3.61	3.74	3.41	3.13	3.47	3.35	3.43	3.95
K_2O	2.29	2.25	2.69	2.59	2.36	3.39	1.83	2.78	2.34	1.99	2.3	2.57	1.99
P_2O_5	0.129	0.245	0.263	0.248	0.312	0.278	0.256	0.139	0.315	0.239	0.246	0.251	0.23
Total	99.63	98.99	98.87	98.93	98.75	99.38	99.75	99.64	99.2	99.13	99.09	99.26	99.18
L.I.	17.94	12.62	15.53	15.22	15.67	17.45	13.86	19.33	12.74	14.45	12.98	14.47	15.22
A/CNK	1.105	1.066	1.091	1.097	1.105	1.067	1.093	1.083	1.071	1.071	1.093	1.116	1.312
N+Kwt%	5.87	5.6	6.29	6.23	6.08	7.0	5.57	6.19	5.47	5.46	5.65	6.0	5.94
Rb ppm	93	111	112	108	121	140	85	97	110	108	109	109	123
Sr	512	644	629	606	544	530	689	475	683	480	489	618	398
Ba	501	947	1001	1240	466	1043	925	1054	911	264	372	989	249
Zr	139	161	174	193	149	130	182	141	200	225	211	201	167
Th	BDL	3	10	5	10	4	9	7	7	4	3	12	10
Zn	53	66	63	64	68	54	55	44	74	77	76	70	84
Y	13	23	22	12	18	20	15	16	19	10	12	12	15
Nb	11	16	14	10	14	15	13	10	15	11	12	11	16
Ni	7	24	9	4	19	5	18	25	23	18	6	8	15

of the isotopic systematics of these leucocratic granites might further constrain their origin, especially because the Sebago granite has distinctive Sr and O isotopic values. It is, however, reasonable to expect that at least some of the pegmatites were derived from the Sebago magma.

Much of the data presented above strongly suggest that the two petrographic varieties grade into each other - no intrusive contact is observed. Several lines of evidence support this view: (1) Petrographic observations detailed above reveal that certain samples from localities in between the main Songo types have "intermediate" petrographic characteristics. (2) There is continuous variation of biotite TiO_2 values (Fig. 4) from samples of both petrographic varieties, including data for the intermediate examples. (3) There is a lack of compositional hiatuses on any major or trace element bivariate plots (Figs. 6 and 8). The likelihood that the boundary between the two Songo types is gradational, rather than an intrusive contact, implies that the petrographic varieties do not represent the crystallized products of separate intrusive magma batches and thus the Songo pluton is not a composite body.

The geochemical data for the Songo pluton provide further insight into the origin of the internal variations of this intrusion. As noted above, the BHS-granodiorites and the biotite-granodiorites are generally not geochemically distinctive and there are continuous major element trends. Thus it appears that the Songo pluton probably crystallized from a single magma batch. The fact that there is no major distinction between the petrographic varieties and their geochemistry may also suggest that the process(es) which produced them were temporally distinct.

Compositional variation within granitoid plutons has been assigned to a variety of processes such as (1) fractional crystallization of a primary basic/intermediate magma, (2) assimilation of crustal material by a primary magma, (3) mixing of two independently derived magmas, or (4) a restite unmixing process as described by White and Chappell (1977). Distinction between these mechanisms often relies heavily on the levels and variations of the trace elements as they are more sensitive indicators of fractionation processes than the major elements. In the case of the Songo pluton any discussion of these magmatic processes is seriously restricted by the general lack of regular trace element trends within the pluton.

Nevertheless, the restite unmixing process can be largely ruled out. The Songo pluton lacks many of the recognized petrographic characteristics of this mechanism such as abundant dioritic inclusions, mottled plagioclase cores, and acicular apatites (see White and Chappell, 1977). Furthermore, it is difficult to explain both the distribution of petrographic variations within the pluton and the lack of coherent trace element trends by a magma mixing process.

Fractional crystallization may be the most favorable process responsible for the geochemical variations of the Songo pluton. The declining levels of CaO, TiO_2, and P_2O_5 with increasing SiO_2 contents may represent the fractionation of plagioclase, sphene + Fe-Ti oxides, and apatite respectively. The only systematic variation in trace element levels, Zr and Zn, might be

TABLE 3. SUMMARY OF MAJOR AND TRACE ELEMENT, L.I. AND MOLECULAR A/CNK RESULTS FOR THE SONGO PLUTON. Mean and standard deviation values on top line, min.-max. in brackets.

	SONGO GDs (N=39)	BHS-GDs (N=22)	Bt.-GDs (N=17)
SiO_2 wt%	64.74 ± 2.60	63.64 ± 2.38	66.17 ± 2.14
	(57.53 70.90)	(57.53 67.72)	(63.7 70.9)
Al_2O_3	16.89 ± 0.81	17.08 ± 0.74	16.66 ± 0.82
	(14.77 19.03)	(16.06 19.03)	(14.77 17.69)
TiO_2	0.76 ± 0.13	0.81 ± 0.12	0.69 ± 0.12
	(0.40 1.05)	(0.64 1.05)	(0.40 0.87)
Fe_2O_3T	4.19 ± 0.71	4.47 ± 0.67	3.85 ± 0.59
	(2.48 5.87)	(3.28 5.87)	(2.48 4.66)
MnO	0.067 ± 0.011	0.073 ± 0.008	0.059 ± 0.009
	(0.044 0.086)	(0.054 0.086)	(0.044 0.073)
MgO	1.95 ± 0.45	2.08 ± 0.41	1.78 ± 0.44
	(1.12 3.14)	(1.52 3.14)	(1.12 2.55)
CaO	4.03 ± 0.59	4.26 ± 0.52	3.74 ± 0.53
	(2.69 5.16)	(3.36 5.16)	(2.69 4.42)
Na_2O	3.53 ± 0.21	3.55 ± 0.19	3.49 ± 0.22
	(3.06 4.09)	(3.24 4.09)	(3.06 3.95)
K_2O	2.62 ± 0.46	2.73 ± 0.43	2.48 ± 0.45
	(1.83 3.80)	(2.14 3.80)	(1.83 3.39)
P_2O_5	0.269 ± 0.093	0.296 ± 0.108	0.235 ± 0.054
	(0.129 0.736)	(0.179 0.736)	(0.129 0.315)
L.I.	14.02 ± 2.62	13.14 ± 2.47	15.17 ± 2.35
	(7.91 20.35)	(7.91 17.66)	(12.23 20.35)
A/CNK	1.06 ± 0.05	1.03 ± 0.04	1.09 ± 0.02
	(0.97 1.14)	(0.97 1.14)	(1.07 1.14)
Tot. Alk.	6.15 ± 0.53	6.28 ± 0.48	5.98 ± 0.51
	(5.21 7.43)	(5.56 7.43)	(5.21 7.00)
Rb ppm	109 ± 17	109 ± 20	108 ± 14
	(75 164)	(75 164)	(85 140)
Sr	611 ± 111	654 ± 106	555 ± 88
	(381 1030)	(496 1030)	(381 689)
Ba	828 ± 261	863 ± 163	781 ± 344
	(249 1416)	(527 1122)	(249 1416)
Zr	180 ± 31	188 ± 31	171 ± 29
	(121 259)	(143 259)	(121 225)
Th	9 ± 4	10 ± 4	8 ± 4
	(BDL 17)	(BDL 17)	(BDL 16)
Zn	69 ± 13	72 ± 13	65 ± 11
	(43 118)	(54 118)	(43 84)
Y	19 ± 5	20 ± 4	17 ± 5
	(10 32)	(10 32)	(10 30)
Nb	13 ± 2	14 ± 2	13 ± 2
	(8 19)	(8 19)	(10 17)
Ni	18 ± 9	21 ± 9	15 ± 9
	(<5 44)	(<5 44)	(<5 33)

explained by the continuous removal of zircon and perhaps hornblende. The fact that the Songo pluton lacks any obvious combined petrographic and geochemical variations, which are commonly observed in zoned plutons and would probably result from this process, is a drawback to this model. However it may be that the later emplacement of the Sebago granite overprinted/destroyed any systematic petrographic and compositional variation. The more felsic central and southwestern parts of the pluton as described above might be the remnants of such combined variations.

It is difficult, however, to explain both the geochemical and petrographic variations of the Songo pluton by a fractional crystallization mechanism alone. The fact that the petrographic varieties overlap geochemically argues against the biotite-granodiorites being differentiates of the BHS-granodiorites. However, this does not rule out the possibility that the mineralogical variations may have been superimposed on a fractional crystallization series.

An alternative model is that the Songo pluton represents a fractionally crystallizing I-type magma which had been con-

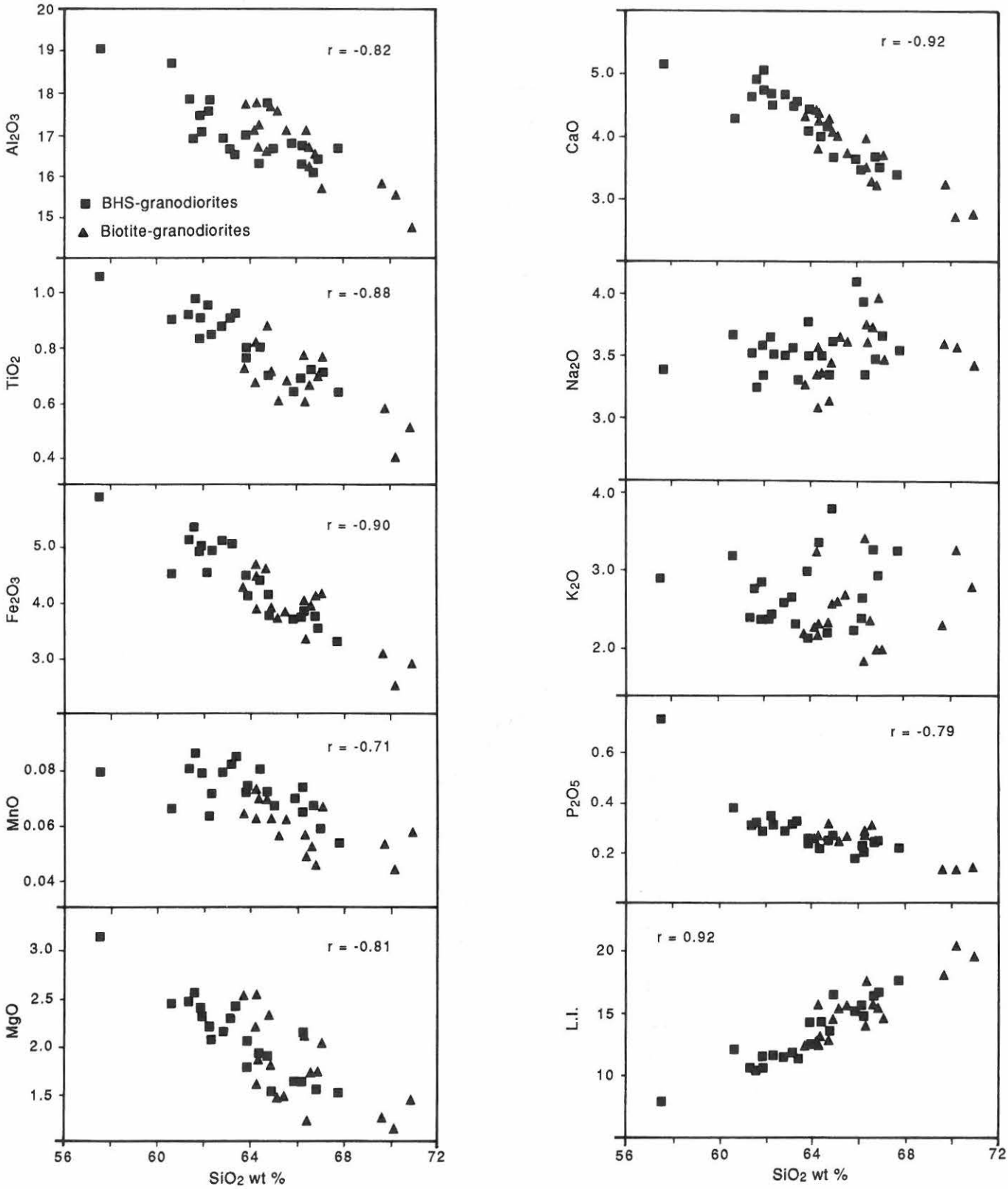

Figure 6. Major element Harker diagrams for the Songo granodiorites. The correlation coefficient (r) is given for each of the oxides (except Na_2O and K_2O). L.I. = Larsen Index (i.e. 1/3 SiO_2 + K_2O - Fe_2O_3(T) + MgO + CaO) (Larsen, 1938). (Some data points omitted due to overlap).

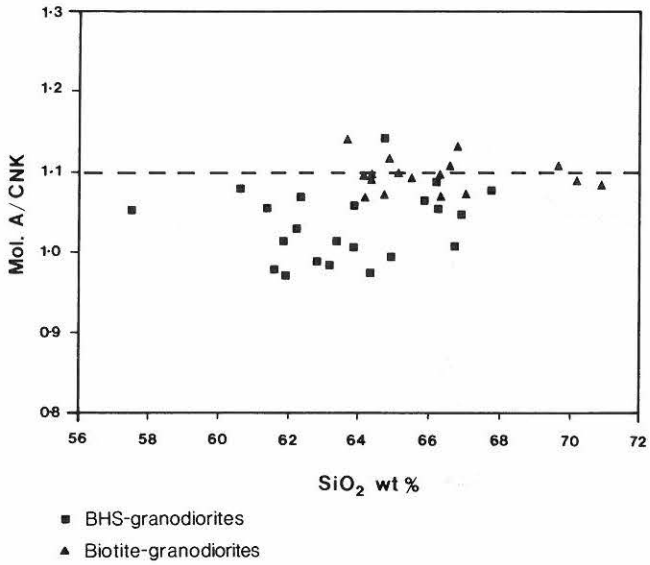

Figure 7. Molecular Al/molecular Ca + Na + K (A/CNK) plotted against SiO_2 wt. % for the Songo granodiorites. Note that some biotite-granodiorites have A/CNK > 1.1.

TABLE 4. GEOCHEMICAL DATA FOR TWO SAMPLES OF THE LEUCOCRATIC GRANITE OBSERVED WITHIN THE SONGO PLUTON AND, FOR COMPARISON, THE RANGE IN COMPOSITION OF 21 SAMPLES OF THE SEBAGO GRANITE (GIBSON, UNPUBLISHED DATA).

	85-45	85-50	SEBAGO DATA MIN.	MAX.
SiO_2	73.58	75.5	71.31	75.83
Al_2O_3	14.53	15.03	14.62	16.11
TiO_2	0.285	0.076	0.082	0.362
Fe_2O_3T	1.33	0.68	0.66	2.35
MnO	0.013	0.012	0.016	0.097
MgO	0.52	0.12	0.15	0.64
CaO	0.9	0.52	0.78	2.66
Na_2O	2.94	4.22	2.71	4.49
K_2O	6.24	4.49	2.84	6.41
P_2O_5	0.103	0.13	0.058	0.434
Total	100.44	100.78	--	--
L.I.	28.02	28.34	21.22	27.76
A/CNK	1.099	1.179	1.00	1.46
N+Kwt%	9.18	8.71	6.20	9.39
Rb ppm	211	332	91	434
Sr	207	19	48	455
Ba	526	BDL	13	879
Zr	225	28	53	250
Th	33	3	BDL	41
Zn	53	45	<5	80
Y	14	12	BDL	42
Nb	10	11	<5	36
Ni	BDL	BDL	BDL	BDL

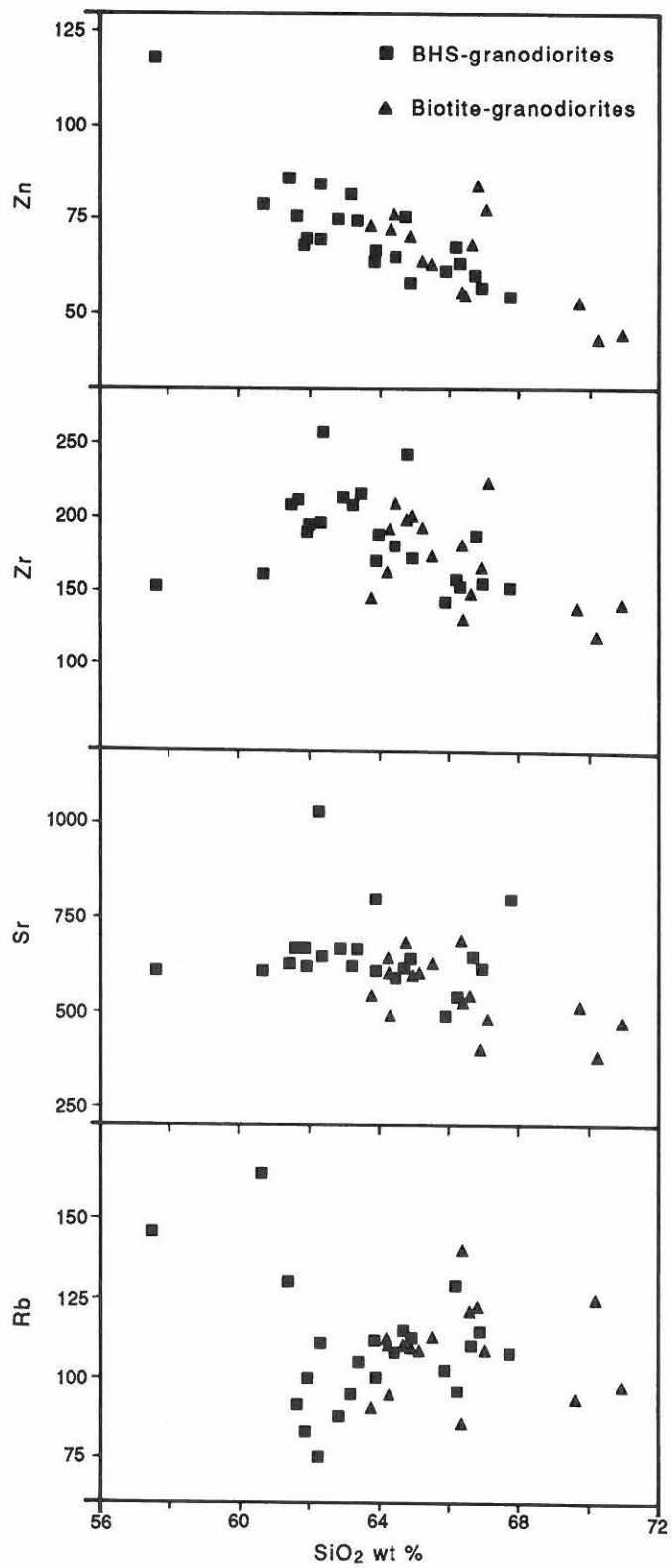

Figure 8. Plots of Rb, Sr, Zr, and Zn ppm versus SiO_2 wt. % for the Songo granodiorites.

taminated with crustal material. This might explain both the geochemical and petrographic variations, in that assimilation of aluminous metasedimentary xenoliths could increase the A/CNK ratio and also increase the stability field of biotite relative to hornblende. The increase in TiO_2 in biotite from the biotite-granodiorite may indicate that there was not another Ti-bearing phase crystallizing from the melt in certain parts of the pluton. This, however, does not explain the overall spatial distribution of the biotite-granodiorite or indeed the irregular trace element trends. It is hoped that ongoing research of the Sr and O isotopic systematics of the Songo pluton will help to further test this model.

One of the main problems in discussing the geochemical aspects of the pluton is the different behavior of the major and trace elements. Whereas the major elements vary regularly through the Songo pluton, the trace elements generally lack coherent trends. Any magmatic process such as fractional crystallization or restite unmixing which produced major element variations would invariably have resulted in systematic changes in trace element levels. Assuming this was the case, it appears therefore that the distribution of trace elements within the Songo pluton may have been subsequently altered.

Another model which should be considered is the effect of changes in the intensive variables (pH_2O, fO_2, T, and P) during crystallization on biotite composition. Speer (1987) has shown that petrographic variations in the Liberty Hill pluton, South Carolina can be explained by changes in the intensive variables as opposed to differentiation or multiple intrusion mechanisms. Significantly though, Speer states that biotites from the Liberty Hill pluton are generally similar in composition. This is in contrast to the compositional variation observed in the Songo biotites. Indeed, the variation of biotite composition within the BHS-granodiorites may point to a differentiation mechanism (see Fig. 5 and Table 1). However, more detailed electron microprobe data for the Fe-Ti oxides and hornblende would be necessary to examine any changes of the intensive parameters during the crystallization of the Songo pluton.

The effects of the emplacement of the thin (ca. 1 km), laterally extensive Sebago granite resulted in widespread metamorphism in western Maine (Lux and Guidotti, 1985). Temperatures within the Songo pluton were raised above the argon closure temperature for hornblende (500°C) as evidenced by their reset $^{40}Ar/^{39}Ar$ ages (Lux et al., this volume). In addition, abundant pegmatites, which were probably derived from the underlying Sebago magma, intruded the Songo pluton. Evidently there was considerable fluid migration through the pluton. It is suggested that this combination of reheating and widespread fluid migration may have resulted in the formation of the biotite-granodiorites in those parts of the Songo pluton closest to the Sebago granite or the pegmatites. In effect, the Sebago granite could have modified parts of this essentially I-type granodiorite by a process similar to that which produced K-feldspar + sillimanite-grade metamorphism in the country rocks.

Two further lines of evidence suggest that the thermal effects of the Sebago granite might have produced the petrographic variations evident in the Songo pluton. Firstly, Lux et al. (this volume) have shown that the Rb-Sr whole-rock isotopic systematics for the Songo pluton have been disturbed. They suggest that scatter in $^{87}Rb/^{86}Sr$ and $^{87}Sr/^{86}Sr$ data, especially among the biotite-granodiorites (see their Fig. 2), could be due to open-system trace element mobility coincidental with the thermal event associated with the emplacement of the Sebago granite.

Secondly, the variation in biotite chemistry within the Songo pluton may also point to the Sebago granite as the cause of the petrographic variations. Specifically, Figure 4c identifies a general trend of decreasing MnO and increasing TiO_2 contents in the biotites of the pluton. In fact these parameters almost discriminate between biotites from both petrographic varieties. Deer et al. (1975) state that the composition (and color) of biotite varies with metamorphic grade, and frequently a decrease in MnO (and Fe^{2+}, Fe^{3+}) and an increase in TiO_2 and MgO can be correlated with increasing metamorphic grade. This is the trend which is observed on a localized scale within the Songo pluton, as the highest Ti-lowest Mn biotite values are observed adjacent to the contacts with the Sebago granite. In fact, Guidotti (1984) recognized a general trend of increasing Ti in biotites with increasing grade of metamorphism from the rocks of western Maine. It would appear that this trend is also recognized from within the Songo pluton itself.

SUMMARY

The important conclusions of this study are as follows:

(1) The pluton can be subdivided into two petrographic varieties. The BHS-granodiorite has an I-type assemblage (biotite, + hornblende and sphene), whereas the biotite-granodiorite contains only Ti-rich biotite. Several lines of evidence suggest that there is a gradation between these two petrographic varieties.

(2) The two facies of the Songo pluton outcrop in distinct areas. The biotite-granodiorites are exposed in the central and southern parts of the pluton adjacent to the Sebago granite and also occur near large pegmatitic bodies. It is inferred that at least some of the latter were derived from the Sebago granite.

(3) Biotite mineral chemistry supports the petrographic subdivision of the Songo pluton and the gradation between the two Songo types. In addition, the trend of decreasing MnO with increasing TiO_2 values for the Songo biotites is similar to that observed for metamorphic rocks with increasing grade of metamorphism.

(4) Geochemical data reveal that neither petrographic variety is distinct, and therefore the Songo pluton is probably not a composite intrusion. The major elements vary systematically, having linear continuous trends with SiO_2. The trace elements, however, generally lack coherent trends and may have experienced open-system mobility.

The main conclusion of this study is that parts of the Songo pluton may have been subsequently modified by the later emplacement of the Sebago granite and pegmatites derived therefrom. A combination of reheating and fluid migration could have resulted in changes in biotite chemistry, thus producing the observed petrographic variation. In addition, this thermal event may have caused open-system mobility of trace elements and disturbance of the Rb-Sr isotopic system. The uncoupled nature of the petrographic and compositional variations suggests that they were produced at different times. In effect, the major element geochemistry of the pluton has been largely preserved but the mineralogy of parts of the Songo pluton has been altered.

The Songo pluton may therefore represent an I-type granodiorite which has been modified by a later thermal event. A similar situation may also have occurred in the southern parts of the Mooselookmeguntic pluton which also contains red/brown biotites and has suffered the metamorphic effects of the Sebago granite.

ACKNOWLEDGMENTS

We wish to thank Marty Yates (University of Maine) for extensive help with the electron microprobe analyses and Dr. I. G. Meighan and the technical staff at Queen's University, Belfast, N. Ireland for performing the whole-rock geochemical analyses. This manuscript benefited greatly from many helpful comments and suggestions from Dr. R. N. Abbott, John Hogan, and Diane Solie. Funding for the field work and analyses was provided by the National Science Foundation grant # ISP8011448.

REFERENCES CITED

Aleinikoff, J. N., 1984, Carboniferous uranium-lead age of the Sebago batholith, southwestern Maine: Geol. Soc. Amer., Abs. with Prog., v. 16, p. 1.

Bence, A. E., and Albee, A. L., 1968, Empirical correction factors of the electron microanalysis of silicates and oxides: Jour. Geol., v. 76, p. 382-403.

Billings, M. P., 1956, The geology of New Hampshire, Part II- bedrock geology: New Hampshire State Planning and Development Commission, Concord, New Hampshire, 203 p.

Chappell, B. W., and White, A. J. R., 1974, Two contrasting granite types: Pacific Geology, v. 8, p. 173-174.

Deer, W. A., Howie, R. A., and Zussman, J., 1975, An introduction to the rock-forming minerals: Longman, 528 p.

De Yoreo, J. J., Lux, D. R., and Guidotti, C. V., 1989, A thermal model for carboniferous metamorphism near the Sebago batholith, *in* Tucker, R. D., and Marvinney, R. G. (eds.), Studies in Maine Geology, Volume 3 - igneous and metamorphic geology.

Fisher, I. S., 1962, Petrology and structure of the Bethel area, Maine: Geol. Soc. Amer., Bull., v. 73, p. 1395-1420.

Guidotti, C. V., 1965, Geology of the Bryant Pond quadrangle: Maine Geol. Surv., Bull. 16, 116 p.

Guidotti, C. V., 1984, Micas in metamorphic rocks, *in* Bailey, S. W. (ed.), Micas: Reviews in Mineralogy, v. 13, p. 357-467.

Guidotti, C. V., Gibson, D., Lux, D. R., De Yoreo, J. J., and Cheney, J. T., 1986, Carboniferous metamorphism on the north upper side of the Sebago batholith, *in* Newberg, D. W. (ed.), New England Intercollegiate Geological Conference guidebook for field trips in southwestern Maine, p. 306-341.

Guidotti, C. V., Trzcienski, W. E., and Holdaway, M. J., 1983, A northern Appalachians metamorphic transect-Eastern Townships, Quebec to the central Maine coast: regional trends in the geology of the Appalachians - Caledonian Hercynian - Mauritanide orogen: D. Reidel, Boston, p. 235-247.

Hayward, J. A., and Gaudette, H. E., 1984, Carboniferous age of the Sebago and Effingham plutons, Maine and New Hampshire: Geol. Soc. Amer., Abs. with Prog., v. 16, p. 22.

Hodge, D. A., Abbey, D. A., Harkin, M. A., Patterson, J. A., Ring, M. J., and Sweeney, J. R., 1982, Gravity studies of subsurface mass distributions of granitic rocks in Maine and New Hampshire: Am. Jour. Sci., v. 282, p. 1289-1324.

Holdaway, M. J., Guidotti, C. V., Novak, J. M., and Henry, W. E., 1982, Polymetamorphism in medium to high-grade pelitic metamorphic rocks, west central Maine: Geol. Soc. Amer., Bull., v. 93, p. 572-584.

Larsen, E. S., 1938, Some new variation diagrams for groups of igneous rocks: Jour. Geol., v. 46, p. 505-520.

Lux, D. R., and Aleinikoff, J. N., 1985, ^{40}Ar-^{39}Ar and U-Pb geochronology of the Songo pluton, western Maine: Geol. Soc. Amer., Abs. with Prog., v. 17, p. 32.

Lux, D. R., and Guidotti, C. V., 1985, Evidence for extensive Hercynian metamorphism in western Maine: Geology, v. 13, p. 696-700.

Moench, R. H. (ed.), 1984, Geological map of the Sherbrooke - Lewiston area, Maine, New Hampshire and Vermont: U.S. Geol. Surv., Open-File Report 84-0650.

Moench, R. H., and Zartman, R. E., 1976, Chronology and styles of multiple deformation, plutonism and polymetamorphism in the Merrimack synclinorium of western Maine, *in* Lyons, P. C., and Brownlow, A. H. (eds.), Studies of New England geology: Geol. Soc. Amer., Mem. 146, p. 203-238.

Pitcher, W. S., 1982, Granite type and tectonic environment, *in* Hsu, K. J. (ed.), Mountain building processes: Academic Press, p. 19-40.

Scambos, T. A., Loiselle, M. C., and Wones, D. R., 1986, The Center Pond pluton: the restite of the story (phase separation and melt evolution in granitoid genesis): Am. Jour. Sci., v. 286, p. 241-280.

Speer, J. A., 1987, Evolution of magmatic AFM mineral assemblages in granitoid rocks: the hornblende + melt = biotite reaction in the Liberty Hill pluton, South Carolina: Am. Mineral., v. 72, p. 863-878.

Streckeisen, A., 1976, To each plutonic rock its proper name: Earth Sci. Reviews, v. 12, p. 1-33.

Tindle, A. G., and Pearce, J. A., 1981, Petrogenetic significance of in situ fractional crystallization in the zoned Loch Doon pluton, Scotland: Contrib. Mineral. Petrol., v. 78, p. 196-207.

White, A. J. R., and Chappell, B. W., 1977, Ultrametamorphism and granitoid genesis: Tectonophysics, v. 43, p. 7-22.

Maine Geological Survey
Studies in Maine Geology: Volume 4
1989

Geochronology of the Songo Pluton, Western Maine

Daniel R. Lux
David Gibson
Department of Geological Sciences
University of Maine
Orono, Maine 04469

P. J. Hamilton
Scottish Universities Research and Reactor Centre
East Kilbride, Scotland G75 0QU

ABSTRACT

Rb/Sr and $^{40}Ar/^{39}Ar$ isotopic age data for rocks and minerals of the Songo pluton are presented. The whole rock Rb/Sr isotopic data for the hornblende- and sphene-bearing phase of the Songo pluton is interpreted to date the crystallization of the pluton at 382±34 Ma. The scatter of Rb/Sr data on whole rock isochron diagrams and young $^{40}Ar/^{39}Ar$ ages (303-305 Ma) with disturbed release spectra for hornblendes are attributed to a heating event related to the intrusion of the two-mica granite of the Sebago batholith. $^{40}Ar/^{39}Ar$ release spectra for biotites all define plateau ages in the range of 247-256 Ma and are interpreted to indicate regional cooling through the biotite closure temperature in response to regional uplift and erosion at that time.

INTRODUCTION

It has recently become apparent that anatexis of the lower crust can be expected in regions with thickened continental crust because of the combined effect of added heat production and the insulating properties of crustal rocks (Thompson and England, 1984; De Yoreo et al., in press). This endothermic process can modify the steady state geotherm and also provide the opportunity for heat transfer via convective as well as conductive processes. Furthermore, conductive heat transfer may be of paramount importance in producing the metamorphism characteristic of low-P metamorphic terranes (Lux et al., 1986; Barton et al., in press; Lux, 1986). In such terranes, granitic magmas may serve as transient heat sources that drive low-P metamorphic reactions and are therefore the key to understanding the thermal evolution of such regions.

If magmatic heat transfer is indeed the primary process by which low-P metamorphic belts are produced, the following statements are true. (1) Crystallization ages for plutonic rocks effectively date distinct episodes of low-P metamorphism. (2) The thermal anomaly related to the emplacement of plutons is truly transient as plutons, unless of extraordinary volume, cool rapidly to the local ambient temperature. (3) Isotopic ages for minerals may date either the crystallization age of a pluton, regional cooling related to erosion and uplift, or cooling following a later heating event.

Mineral ages can provide several different types of valuable information. In the event that $^{40}Ar/^{39}Ar$ ages for minerals with markedly different closure temperatures agree, very rapid cooling rates are implied for the initial stages of cooling, and therefore mineral ages effectively date the formation of the pluton. In addition, they clearly demonstrate that the ambient temperature at the time of emplacement of the pluton was lower than the closure temperature for the mineral with the lowest concordant age. This information can be used to estimate the geothermal gradient at the time the pluton was emplaced, assuming the depth

of emplacement of the pluton can be determined independently. Alternatively, if all mineral ages are discordant, they must be interpreted with caution and without further information, can only be interpreted as the time of last cooling through their closure temperature. In this case two alternatives exist. They may represent the time of regional cooling, which is a function of uplift and erosion or they may represent cooling following a later thermal event.

Given the applications of such geochronological studies in elucidating thermal conditions, the Songo pluton was chosen for study. Isotopic dating was undertaken using the Rb-Sr whole rock isochron method in order to determine the age of crystallization of the pluton. Furthermore, $^{40}Ar/^{39}Ar$ isotopic ages were determined for both hornblende and biotite from the pluton in an attempt to determine the post-crystallization thermal history of the region.

The Songo pluton is located within the regional low-P terrane of western Maine on the NW limb of the Kearsarge-central Maine synclinorium (Fig. 1). It crops out over some 300 km^2, primarily in the Bethel and Bryant Pond 15' quadrangles. Since it was initially mapped (Fisher, 1962; Guidotti, 1965), it has been recognized as one of the New Hampshire Magma Series plutons which are characterized as a suite of generally non-foliated plutons that range in composition from intermediate to granitic (Billings, 1956).

Several lines of evidence exist which constrain the age of the Songo pluton. The Songo pluton is discordant and intrudes metasedimentary rocks that are Silurian to Devonian in age. The youngest stratigraphic unit cut by the Songo pluton is a metapelite that is locally metamorphosed to K-feldspar + sillimanite grade and is believed to be of Gedinnian age. This age designation is based on correlation with the Carrabassett Formation which is lithologically similar and is laterally continuous (Osberg et al., 1985). The Songo pluton is itself intruded by a younger granite, the Speckled Mountain quartz monzonite which is the northern extension of the Sebago batholith (Guidotti, 1965), and by numerous aplite and two mica granite dikes, and pegmatites. Previous geochronological investigations by both the Rb/Sr whole rock isochron and U/Pb zircon methods have established the crystallization age of the Sebago batholith as being between 325 and 336 Ma (Aleinikoff et al., 1985; Hayward, 1989). Thus, on the basis of these relationships, the

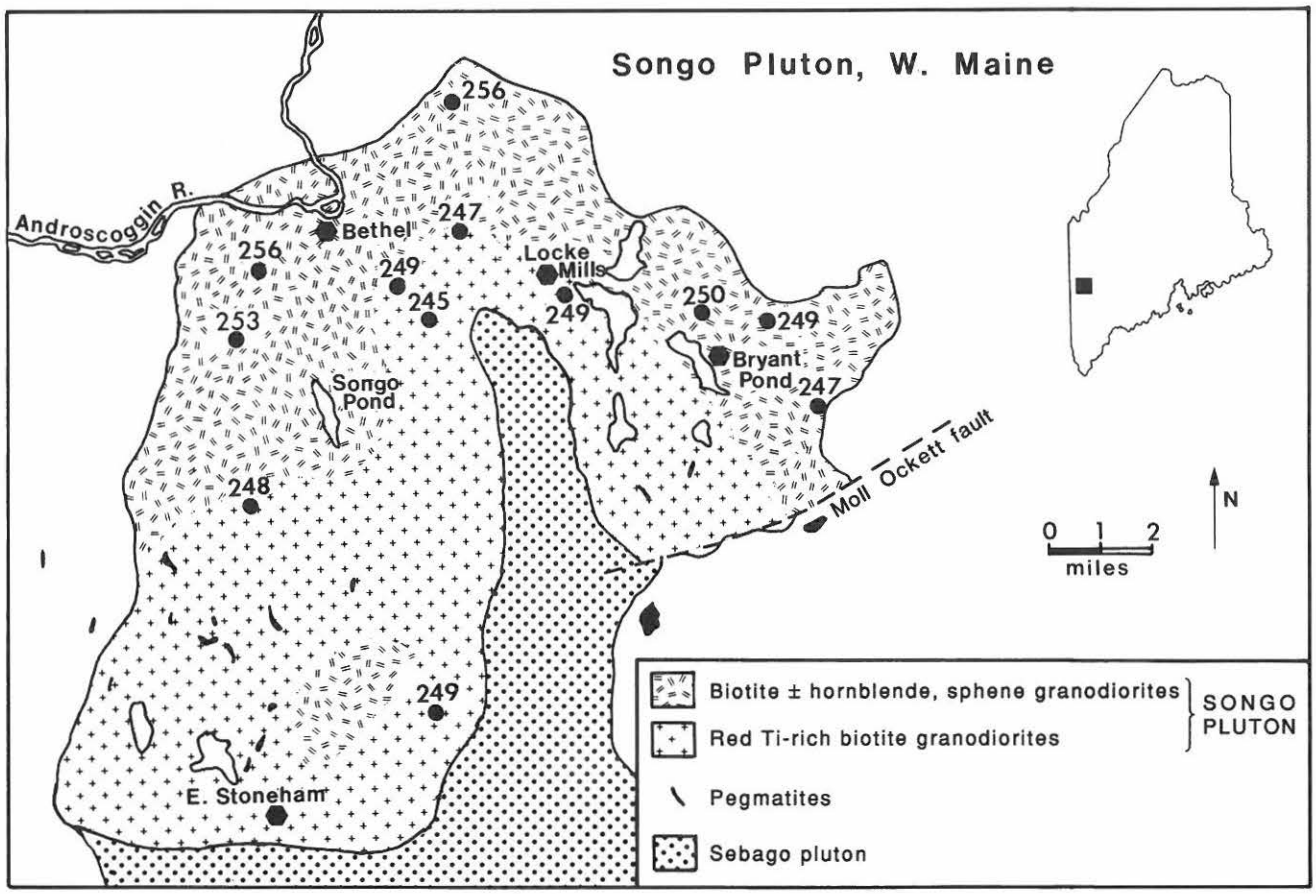

Figure 1. Map of the Songo pluton, western Maine showing the localities of biotites samples and their ages. The localities labeled 256, 256, and 253 are the hornblende localities.

formation of the Songo pluton is restricted to the time period Gedinnian to 325 Ma (approximately the end of the Mississippian period).

Some isotopic data exists which supports a middle Devonian age for the Songo pluton. Lux and Aleinikoff (1985) suggested that the Songo pluton had an age of about 382 Ma based on U/Pb isotopic age determinations for zircons. However, the data are discordant and are difficult to interpret. The discordance could be the result of either loss of radiogenic Pb or incorporation of an inherited Pb component. In either case there is sufficient doubt in the age to warrant further isotopic dating.

The Songo pluton is principally composed of medium grained equigranular granodiorite and quartz diorite (Guidotti et al., 1986; Gibson and Lux, this volume). It is generally nonfoliated, but has a distinct biotite foliation or intense compositional banding at some localities. Enclaves that appear to have both igneous and sedimentary textures are present, but are not common. Two distinct petrographic varieties of granodiorite are recognized (Fig. 1). One is characterized by the presence of biotite (with distinctly green pleochroism) and sphene, ± hornblende (hereafter referred to as BHS granodiorite). The second type lacks both hornblende and sphene. Biotites of this variety are characterized by a distinctive red-brown pleochroism (hereafter biotite granodiorite). More extensive petrographic descriptions of these varieties are given by Gibson and Lux (this volume).

The Songo pluton lacks a distinct metamorphic contact aureole as all of the nearby country rocks are at K-feldspar + sillimanite grade and pegmatites and migmatites are common (Guidotti, 1963). The age of this metamorphism has traditionally been linked with the Acadian orogeny (Holdaway et al., 1982; Guidotti et al., 1983). However, it has recently been suggested that this metamorphism is Carboniferous in age and is related in time and space to the emplacement of the Sebago batholith, the metamorphism being essentially "regional" contact metamorphism (Lux and Guidotti, 1985; Lux et al., 1986; Aleinikoff et al., 1985).

ANALYTICAL METHODS

Samples were passed through a jaw crusher and a disk grinder in order to disaggregate the sample. Each sample was then sieved in order to create favorable grain size fractions which contained a majority of the sample as individual rather than composite grains. The -60+80 standard sieve mesh fraction was used for biotite separations and the -100+120 fraction was used for hornblende separations. Standard techniques were employed to produce biotite and hornblende separates with an estimated purity of >99.9%. The mineral samples were encapsulated in aluminum foil, sealed in silica glass vials, and irradiated. Most were irradiated at the nuclear reactor of the Phoenix Memorial Laboratory at the University of Michigan. Others were irradiated at the U.S. Geological Survey TRIGA reactor in Denver, Colorado following previously established procedures (Dalrymple et al., 1981). An intralaboratory mineral standard, MMhb-1 (Alexander et al., 1978), was used as the irradiation monitor. Samples were heated in a molybdenum crucible within an ultra-high vacuum Ar extraction system using radio frequency induction heating. Extraction temperatures were estimated using an optical pyrometer and uncertainties are estimated to be $\pm 50^{o}C$. A molecular sieve desiccant, CuCuO getter, and Zr-Al getter cartridge were used to purify the inert gases extracted from the samples. The isotopic composition of Ar was determined using an automated Nuclide 6-60-SGA 1.25 mass spectrometer. All data are extrapolated to inlet time values and ^{37}Ar is corrected for decay during the time interval between irradiation and analysis. Corrections are made for all interfering isotopes produced during irradiations (Dalrymple et al., 1981) using a correction factor determined from irradiated K and Ca salts.

Individual ages and uncertainties (two sigma) were calculated using equations given by Dalrymple et al. (1981). The criteria that were used for determining plateaus were those of Fleck et al. (1977), and the critical value test of Dalrymple and Lanphere (1969) was used to test for concordance between increments. The total gas age (t_g) represents a weighted average based on the total amount of ^{39}Ar in each increment. A plateau age (t_p) is the mean of the ages deemed to be concordant. Associated uncertainties represent two standard deviations plus an uncertainty in the J-value (estimated at 0.5%).

The Rb-Sr analyses were carried out at the Isotope Geology Unit, Scottish Universities Research and Reactor Centre (SURRC), East Kilbride, Scotland. Approximately 30 mg of whole rock powder were used to determine the $^{87}Sr/^{86}Sr$ ratios and Sr and Rb concentrations by isotope dilution. Following $HF+HNO_3+HCl$ dissolution of spiked samples, Rb and Sr were separated by conventional cation-exchange chromatography. Isotopic compositions were analyzed on a Vacuum Generators Isomass 54E mass spectrometer with $^{87}Sr/^{86}Sr$ ratios normalized to $^{86}Sr/^{88}Sr = 0.1194$. The NBS 987 $^{87}Sr/^{86}Sr$ ratio in the SURRC laboratory is 0.71027 ± 0.00001.

All of the decay constants and isotopic composition of K are those of Steiger and Jager (1977).

ANALYTICAL RESULTS

$^{87}Sr/^{86}Sr$ and $^{87}Rb/^{86}Sr$ ratios for eight whole rock samples from the BHS granodiorite and five samples of the biotite granodiorite are given in Table 1. The results are presented on isochron diagrams in Figures 2a and 2b. The samples of the BHS granodiorite define a best fit line whose slope corresponds to an age of 382±34 Ma with an $^{87}Sr/^{86}Sr$ initial ratio of 0.70528±0.00015 (Fig. 2a). Samples of the biotite granodiorite are shown in Figure 2b along with a reference isochron and have not been used for the age determination. The excessive scatter (M.S.W.D. = 28.07) of these data will be discussed below.

Three hornblendes and twelve biotites were analysed by the $^{40}Ar/^{39}Ar$ incremental heating technique and the results are presented in Tables 2 and 3.

TABLE 1. ANALYTICAL DATA FOR 13 WHOLE ROCK SAMPLES. The concentration of Rb and Sr are given in parts per million and both $^{87}Rb/^{86}Sr$ and ^{87}Sr are atomic ratios. Samples with an asterisk are from the biotite granodiorite.

Sample#	Rb(ppm)	Sr(ppm)	$^{87}Rb/^{86}Sr$	$^{87}Sr/^{86}Sr$
SG-15	88.69	1048.9	.24463	.70671
SG-1	125.2	588.9	.61510	.70852
SG-2	117.5	493.2	.68960	.70916
SG-3	161.8	621.9	.75301	.70960
SG-10	111.1	608.6	.52838	.70817
SG-19	109.2	618.5	.51087	.70796
SG-20	110.5	769.9	.41510	.70742
SG-6	193.4	567.1	.98694	.71053
SG-5*	104.7	594.0	.50989	.70795
SG-40*	107.9	459.9	.67867	.70877
SG-11*	94.56	499.8	.54755	.70908
SG-9*	120.6	639.0	.54604	.70853
SG-16*	120.8	546.9	.63909	.71022

The biotites are all characterized by nearly undisturbed release spectra (Fig. 3). In each case the initial heating steps have young ages relative to the plateau ages (t_p) that are defined by each release spectra. The t_p of each sample is in agreement with the total gas age (t_g) within the limits of analytical uncertainty. We accept the t_p ages as the best estimate of the time of last cooling through the closure temperature (T_c), the temperature at which the kinetics of Ar diffusion become sufficiently slow such that Ar loss effectively ceases.

The t_p for biotites range from 247±2 to 256±3 Ma. It is of interest to note that not all of the biotite ages agree within the limits of analytical uncertainties. Instead, the data can be viewed as two distinct groups in which all of the ages are concordant. Samples 82-52, 82-55, and 82-56 form one group in which the ages vary between 253 and 256 Ma with a mean of 255±3 Ma. These are all from the BHS granodiorite. The remaining nine biotites have an age range of 247 to 250 Ma, mean 248±2 Ma, and come from the biotite granodiorite.

In contradistinction to the biotites, the three hornblende samples have somewhat disturbed release spectra that reflect the heterogeneous internal distribution of ^{40}Ar. The release spectra for each of the hornblendes (Fig. 4) are similar and are characterized by the following features: (1) the initial increments have anomalously high apparent ages which greatly exceed the known crystallization age of the pluton. (2) These anomalously old ages are followed by a small dip in the release spectra. This is particularly well defined in sample 82-52 which has several increments in the range of 282-289 Ma (Fig. 4). (3) A majority of the Ar released from each sample defines a plateau in which successive increments have concordant apparent ages. These tp ages are 303, 304, and 305 Ma and average 304±2 Ma. This is the best estimate of the time of cooling through the T_c for diffusive loss of Ar in hornblende. (4) Finally, each sample has an abrupt gradient followed by several increments with distinctly higher apparent ages in the range of 310-316 Ma.

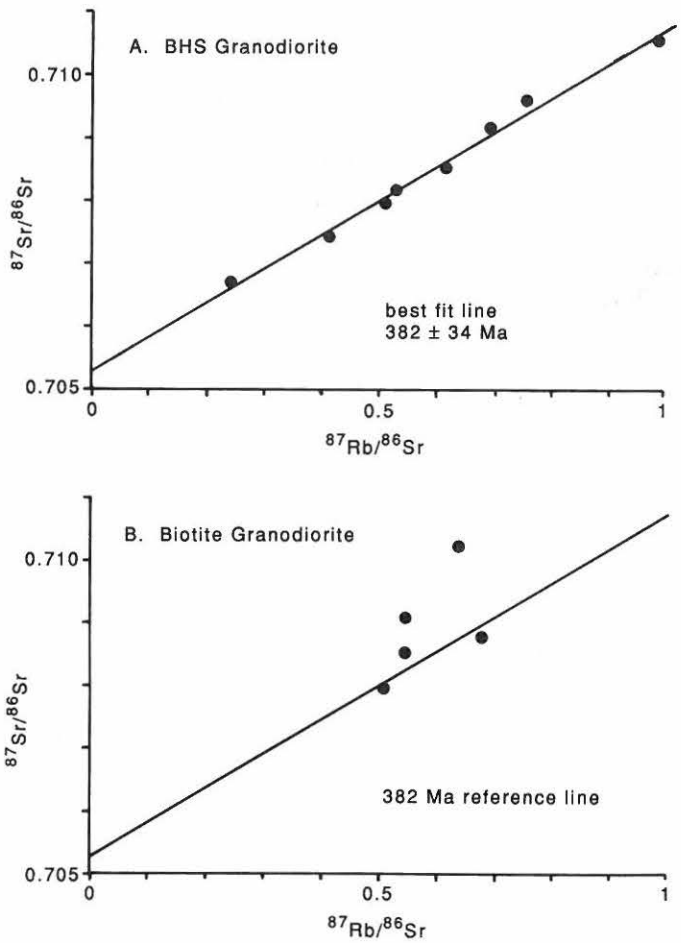

Figure 2. $^{87}Rb/^{86}Sr$ versus $^{87}Sr/^{86}Sr$ diagrams for whole rock samples of the Songo pluton. The upper diagram (a) gives the whole rock data for those samples of the BHS granodiorite phase only. The slope of the best fit line corresponds to an age of 382±34 Ma with an initial $^{87}Sr/^{86}Sr$ ratio of .70528±0.00002 (MSWD = 40.53). Note the considerable scatter of data points representing the biotite granodiorite (b) relative to the reference isochron from the BHS granodiorite data.

Another useful parameter in interpreting hornblende release spectra is the K/Ca ratio which can be determined as a by-product of the age determinations (Dalrymple et al., 1981). The K/Ca ratio is constant in each of these hornblendes after the first few increments (Table 2), indicating that the samples were homogeneous.

DISCUSSION

The geochronological data presented above raise important questions regarding the age and subsequent cooling history of the Songo pluton. The $^{87}Rb/^{86}Sr$ and $^{87}Sr/^{86}Sr$ whole rock data from the BHS granodiorite have some scatter about the best fit line (Fig. 2a). This random scatter could be the result of initial

TABLE 2. $^{40}Ar/^{39}Ar$ ANALYTICAL DATA FOR HORNBLENDES FROM THE SONGO PLUTON. MOLES OF ^{39}Ar ARE X 10^{-14}. APPARENT AGES ARE IN 10^4 YEARS.

TEMP °C	$^{40}Ar/^{39}Ar$	$^{37}Ar/^{39}Ar$	$^{36}Ar/^{39}Ar$	MOLES ^{39}Ar	%^{39}Ar	%^{40}Ar	K/Ca	APPARENT AGE
82-52	J = 0.009133							
500	199.60	1.951	0.2913	1.7	0.1	56.7	0.25	1286 ± 91
650	70.46	1.223	0.1745	3.5	0.2	26.8	0.40	289 ± 82
750	3	1.571	0.0494	4.9	0.3	56.2	0.31	287 ± 15
850	29.79	3.956	0.0394	11.8	0.7	61.0	0.12	282 ± 9
935	21.19	4.035	0.0059	115.8	6.8	91.8	0.12	300 ± 4
965	20.85	3.973	0.0037	173.4	10.1	94.8	0.12	305 ± 4
980	20.90	3.957	0.0036	155.5	9.1	94.9	0.12	305 ± 4
995	20.68	3.950	0.0030	215.2	12.6	95.7	0.12	305 ± 4
1010	21.01	3.948	0.0037	168.6	9.8	94.8	0.12	307 ± 4
1025	20.63	3.929	0.0025	314.1	18.3	96.4	0.12	306 ± 4
1040	21.12	3.920	0.0031	110.4	6.5	95.7	0.13	311 ± 4
1055	21.35	3.919	0.0031	82.8	4.8	95.7	0.13	314 ± 4
1080	21.39	3.931	0.0029	93.2	5.4	96.0	0.12	315 ± 4
1100	21.42	3.975	0.0028	99.4	5.8	96.2	0.12	316 ± 4
FUSE	21.41	3.963	0.0031	162.7	9.5	95.8	0.12	315 ± 4
TOTAL				1713.0				309
PLATEAU AGE								305 ± 2
82-55	J = 0.006153							
825	136.30	2.879	0.2604	4.1	0.3	43.5	0.17	564 ± 16
940	160.10	2.193	0.3822	3.5	0.3	29.4	0.22	461 ± 26
995	89.32	2.148	0.1952	4.5	0.3	35.4	0.16	324 ± 10
1025	36.67	3.820	0.0258	31.9	2.4	79.2	0.13	300 ± 5
1045	32.91	3.786	0.0146	98.0	7.3	86.9	0.13	296 ± 4
1055	31.48	3.735	0.0073	145.3	10.8	93.2	0.13	303 ± 4
1070	31.00	3.720	0.0057	187.4	13.9	94.6	0.13	303 ± 4
1080	60.75	3.709	0.0048	209.2	15.5	95.4	0.13	303 ± 4
1090	30.66	3.710	0.0047	220.0	16.3	95.5	0.13	302 ± 4
1100	30.98	3.703	0.0054	190.4	14.1	94.9	0.13	303 ± 4
1105	32.29	3.708	0.0088	66.4	4.9	91.1	0.13	306 ± 4
1110	31.96	3.724	0.0074	65.5	4.8	93.2	0.13	307 ± 4
1125	32.43	3.760	0.0077	52.4	3.9	93.0	0.13	310 ± 4
FUSE	32.29	3.835	0.0064	73.2	5.4	94.1	0.13	313 ± 4
TOTAL				1351.6				305
PLATEAU AGE								303 ± 4
82-56	J = 0.005804							
750	579.5	4.258	0.6103	0.2	0.1	48.6	0.02	2168 ± 76
825	149.8	2.342	0.0181	0.6	0.1	56.9	0.23	1101 ± 9
890	229.7	1.696	0.6255	1.3	0.1	16.3	0.32	419 ± 9
940	69.72	1.712	0.1194	1.5	0.2	31.7	0.32	330 ± 6
985	49.68	3.113	0.0637	2.2	0.3	40.3	0.17	300 ± 3
1000	42.96	3.826	0.0383	2.3	0.3	46.5	0.14	308 ± 5
1010	36.17	4.049	0.0170	5.7	0.7	67.4	0.13	303 ± 3
1040	33.27	3.909	0.0071	34.8	3.9	89.9	0.14	303 ± 3
1070	32.38	3.766	0.0038	209.6	23.7	95.7	0.14	304 ± 3
1085	31.67	3.727	0.0008	287.7	32.4	97.6	0.14	306 ± 3
1100	31.81	3.697	0.0005	189.6	21.5	97.5	0.14	310 ± 3
1110	32.79	3.733	0.0022	61.5	7.0	96.1	0.14	312 ± 3
1115	32.77	3.715	0.0023	21.5	2.4	91.0	0.14	311 ± 3
FUSE	34.44	3.891	0.0785	66.3	7.5	91.7	0.14	312 ± 3
TOTAL				873.7				311
PLATEAU AGE								304 ± 4

TABLE 3. $^{40}Ar/^{39}Ar$ ANALYTICAL DATA FOR BIOTITES FROM THE SONGO PLUTON. MOLES OF ^{39}Ar ARE X 10^{-14}. APPARENT AGES ARE IN 10^4 YEARS.

TEMP °C	$^{40}Ar/^{39}Ar$	$^{37}Ar/^{39}Ar$	$^{36}Ar/^{39}Ar$	MOLES ^{39}Ar	%^{39}Ar	%^{40}Ar	K/Ca	APPARENT AGE
BP-1	J = 0.005236							
350	29.56	0.0843	0.0368	4.7	0.3	63.2	6	168 ± 6
450	28.64	0.0080	0.0043	183.0	13.3	95.5	65	242 ± 2
650	28.39	0.0018	0.0011	529.0	38.6	98.9	289	247 ± 2
FUSE	28.72	0.0081	0.0012	656.0	47.8	98.7	64	250 ± 3
TOTAL				1372.7				247
PLATEAU AGE								249 ± 4
82-48	J = 0.009361							
465	19.61	0.3375	0.0352	14.9	0.5	47.0	1	150 ± 13
625	15.86	0.0049	0.0011	832.0	30.3	97.9	100	245 ± 3
730	16.40	0.0080	0.0010	275.1	10.0	98.1	61	248 ± 3
890	16.32	0.0319	0.0008	175.0	6.4	98.6	15	253 ± 5
980	15.90	0.0263	0.0008	716.0	26.0	98.5	19	247 ± 3
1100	15.98	0.0461	0.0006	406.0	14.8	98.8	11	247 ± 3
1175	15.88	0.1154	0.0008	309.0	11.2	98.5	4	247 ± 5
FUSE	20.49	0.4952	0.0162	21.5	0.8	76.7	1	248 ± 5
TOTAL				2749.4				246
PLATEAU AGE								247 ± 2
82-49	J = 0.009373							
465	76.19	0.1553	0.2481	2.1	0.1	3.8	3	48 ± 70
625	17.74	0.0584	0.0140	42.1	1.6	76.7	8	217 ± 6
730	16.71	0.0043	0.0032	273.7	10.6	94.3	115	248 ± 3
890	15.92	0.0020	0.0007	752.0	29.2	98.8	246	248 ± 3
995	16.41	0.0130	0.0017	206.7	8.0	96.9	38	251 ± 4
1100	16.10	0.0105	0.0008	471.7	18.3	98.5	47	250 ± 3
1175	15.96	0.0113	0.0007	683.8	26.5	98.7	43	248 ± 3
FUSE	16.98	0.0393	0.0034	145.8	5.7	94.0	12	252 ± 5
TOTAL				2577.9				248
PLATEAU AGE								250 ± 4
82-50	J = 0.009218							
465	20.41	0.0623	0.0425	12.2	0.4	38.5	8	126 ± 32
600	16.60	0.0029	0.0025	332.5	11.7	95.5	167	246 ± 3
730	16.08	0.0017	0.0005	767.7	27.0	99.2	281	247 ± 3
900	16.41	0.0031	0.0009	348.3	12.2	98.4	159	250 ± 3
980	16.22	0.0022	0.0006	537.5	18.9	98.9	221	249 ± 3
1065	16.09	0.0019	0.0005	635.3	22.3	99.1	255	247 ± 3
1175	16.35	0.0119	0.0010	194.2	6.8	98.2	41	249 ± 4
FUSE	21.49	0.0231	0.0204	17.3	0.6	72.0	21	240 ± 13
TOTAL				2845.0				247
PLATEAU AGE								249 ± 4

TABLE 3. CONTINUED.

TEMP °C	$^{40}Ar/^{39}Ar$	$^{37}Ar/^{39}Ar$	$^{36}Ar/^{39}Ar$	MOLES ^{39}Ar	%^{39}Ar	%^{40}Ar	K/Ca	APPARENT AGE
82-51	J = 0.009328							
465	42.81	0.6546	0.1329	3.7	0.1	8.3	1	60 ± 51
650	16.90	0.0024	0.0042	261.5	8.8	92.6	203	246 ± 4
730	16.01	0.0014	0.0008	552.3	18.7	98.5	342	247 ± 3
890	16.05	0.0016	0.0012	467.3	15.8	97.7	314	246 ± 3
995	16.38	0.0027	0.0019	254.6	8.6	96.7	181	248 ± 4
1090	15.83	0.0004	0.0005	1097.7	37.1	99.0	1287	246 ± 3
1175	16.14	0.0087	0.0009	298.7	10.1	98.3	56	249 ± 3
FUSE	19.66	0.0156	0.0130	26.2	0.9	80.4	31	248 ± 24
TOTAL				2962.0				247
PLATEAU	AGE							247 ± 4
82-53	J = 0.009331							
465	76.81	0.1769	0.2525	4.0	0.2	2.9	3	37 ± 42
650	17.04	0.0203	0.0073	171.6	6.7	87.3	24	234 ± 3
730	16.18	0.0031	0.0015	422.8	16.6	97.2	160	247 ± 3
890	16.04	0.0044	0.0010	469.6	18.4	98.2	112	247 ± 3
980	16.34	0.0102	0.0019	271.8	10.7	96.6	48	248 ± 3
1090	16.02	0.0086	0.0008	494.8	19.4	98.5	57	248 ± 3
FUSE	15.95	0.0132	0.0005	715.2	28.1	99.0	37	248 ± 3
TOTAL				2550.0				246
PLATEAU AGE								248 ± 2
82-54	J = 0.009268							
520	16.73	0.0052	0.0064	237.5	8.1	88.8	95	233 ± 4
625	16.08	0.0018	0.0014	628.2	21.5	97.4	267	245 ± 4
730	16.03	0.0024	0.0006	496.5	17.0	98.9	203	247 ± 3
890	16.31	0.0032	0.0015	163.3	5.6	97.3	153	247 ± 4
995	16.42	0.0059	0.0020	141.6	4.8	96.5	83	247 ± 3
1090	16.04	0.0022	0.0009	507.0	17.3	98.4	219	246 ± 3
1175	16.10	0.0038	0.0009	391.5	13.4	98.3	130	247 ± 3
FUSE	16.33	0.0241	0.0015	357.9	12.2	97.3	20	248 ± 4
TOTAL				2923.4				245
PLATEAU AGE								247 ± 3
82-52	J = 0.009381							
520	16.52	0.0251	0.0071	136.6	5.7	85.9	29	225 ± 4
600	16.80	0.0046	0.0017	317.5	13.3	97.0	106	257 ± 3
730	16.38	0.0030	0.0006	519.0	21.8	99.0	161	255 ± 3
890	16.84	0.0078	0.0019	160.9	6.7	96.7	63	257 ± 4
1010	16.51	0.0193	0.0007	724.6	30.4	98.7	25	257 ± 3
1100	16.36	0.0156	0.0008	447.6	18.8	98.7	31	254 ± 3
1175	17.23	0.0410	0.0026	70.3	3.0	95.6	12	259 ± 4
FUSE	43.10	0.0191	0.0924	9.3	0.4	36.7	26	249 ± 23
TOTAL				2385.7				254
PLATEAU AGE								256 ± 4

TABLE 3. CONTINUED.

TEMP °C	$^{40}Ar/^{39}Ar$	$^{37}Ar/^{39}Ar$	$^{36}Ar/^{39}Ar$	MOLES ^{39}Ar	%^{39}Ar	%^{40}Ar	K/Ca	APPARENT AGE
82-55	J = 0.010316							
400	17.06	0.0722	0.0498	13.1	0.5	13.7	7	43 ± 33
580	15.22	0.0093	0.0061	306.3	11.6	88.1	53	234 ± 4
700	14.98	0.0033	0.0010	654.3	24.8	98.1	147	255 ± 4
870	15.36	0.0105	0.0018	377.5	14.3	96.6	47	257 ± 4
970	15.10	0.0318	0.0011	661.1	25.0	97.9	15	256 ± 3
1050	15.05	0.0686	0.0008	512.1	19.4	98.4	7	257 ± 3
1100	15.65	0.0628	0.0029	92.9	3.5	94.6	8	256 ± 4
FUSE	20.68	0.1269	0.0204	23.5	0.9	70.9	4	254 ± 16
TOTAL				2640.8				252
PLATEAU AGE								256 ± 4
82-56	J = 0.010656							
450	20.29	0.1479	0.0641	15.4	0.7	6.7	3	26 ± 74
580	14.46	0.0113	0.0036	247.9	10.6	92.7	43	241 ± 4
700	14.45	0.0028	0.0011	220.1	9.4	97.7	178	253 ± 4
875	14.44	0.0047	0.0011	760.9	32.6	97.8	104	253 ± 3
975	14.42	0.0136	0.0008	501.6	21.5	98.3	36	254 ± 3
1050	14.42	0.0316	0.0009	388.9	16.7	98.1	15	253 ± 3
1100	14.64	0.0434	0.0017	175.9	7.5	96.6	11	253 ± 4
FUSE	20.12	0.1324	0.0206	21.5	0.9	69.8	4	252 ± 7
TOTAL				2332.2				250
PLATEAU AGE								253 ± 3
84-13	J = 0.004850							
815	32.08	0.0078	0.0094	152.1	19.6	91.3	63	240 ± 3
870	31.29	0.0019	0.0040	182.7	23.6	96.2	254	246 ± 3
960	32.24	0.0123	0.0052	101.1	13.0	95.2	40	250 ± 3
985	31.60	0.0134	0.0032	129.3	16.7	97.0	37	250 ± 3
1040	31.37	0.0150	0.0036	137.2	17.7	96.6	33	247 ± 3
FUSE	32.97	0.0178	0.0089	72.3	9.3	92.0	27	248 ± 3
TOTAL				774.6				246
PLATEAU AGE								248 ± 5
84-15	J = 0.004855							
800	35.32	0.0465	0.0229	5.9	0.8	80.8	11	234 ± 18
880	31.83	0.0035	0.0051	166.2	22.4	95.3	141	248 ± 3
960	31.79	0.0039	0.0043	131.0	17.6	96.0	127	249 ± 3
985	33.03	0.0032	0.0083	147.2	19.8	92.6	151	250 ± 3
1035	31.04	0.0050	0.0020	225.9	30.4	98.1	98	249 ± 3
FUSE	32.48	0.0049	0.0076	66.7	9.0	93.1	100	250 ± 5
TOTAL				742.9				249
PLATEAU AGE								249 ± 3

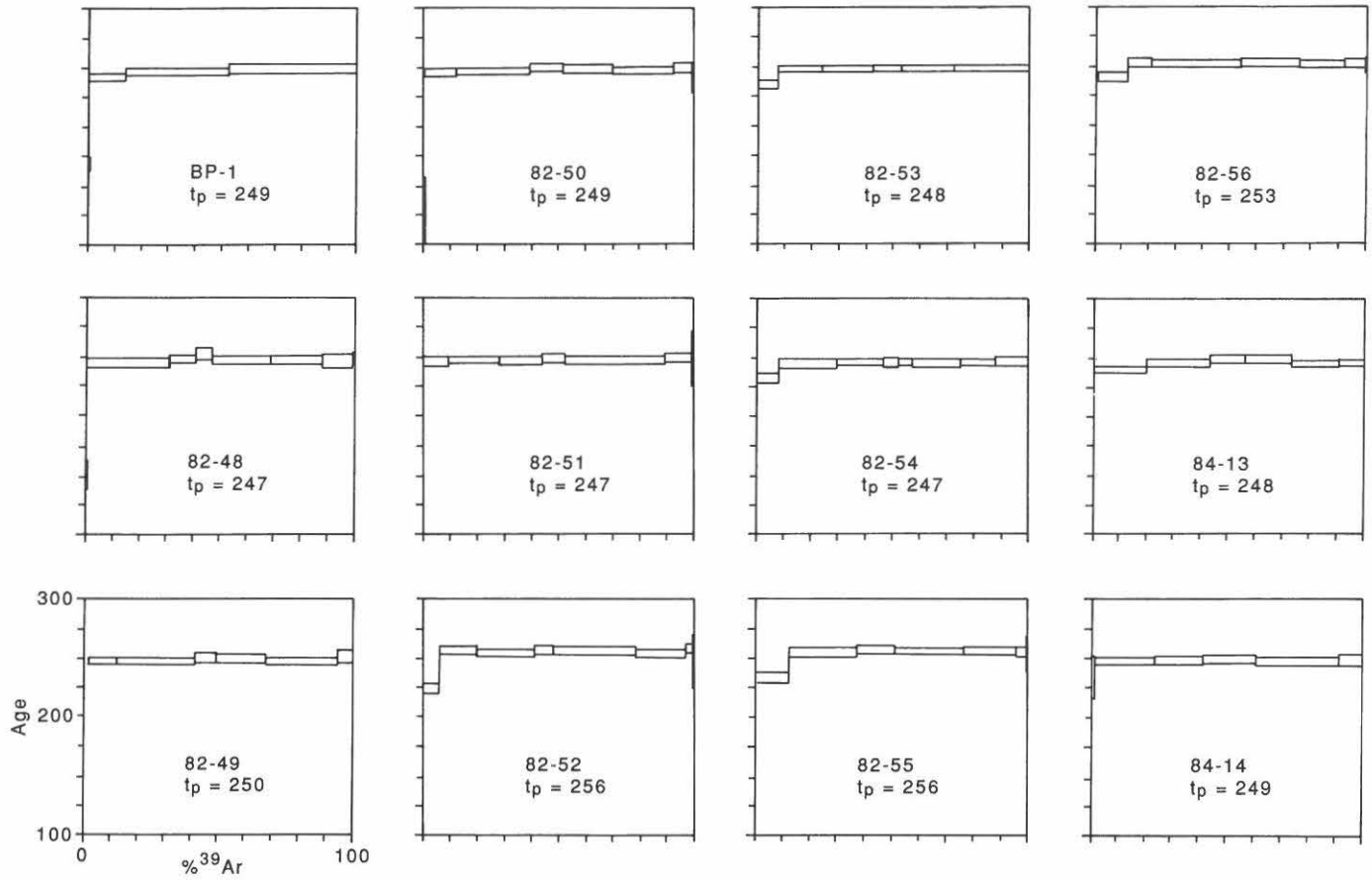

Figure 3. $^{40}Ar/^{39}Ar$ release spectra for twelve biotites samples are presented. The scales for each spectrum are as shown at the lower left hand corner. In each case the total gas age (t_g) agrees with the plateau age (t_p) and these can be found in Table 3. The spectra all define ages of about 250 Ma and suggest cooling through the biotite closure temperature at about that time.

variation in $^{87}Sr/^{86}Sr$ or alternatively could result from a period of open system behavior at some time following initial crystallization.

The Rb/Sr isotopic data used for the age determination comes only from samples of the BHS granodiorites. The five data points for the biotite granodiorites have additional scatter beyond that shown by the former type (Fig. 2b). We feel that this additional scatter is a function of Rb and Sr mobility during a period of open system behavior.

The two petrographic varieties of the Songo pluton have an interesting spatial relationship which may provide insight to the nature of the disturbed Rb/Sr systems. The BHS granodiorites are largely restricted to the northern part of the pluton and the biotite granodiorites are observed in the southern part (Fig. 1). In general, the latter separates the former from the two-mica granite of the Sebago batholith. This spatial relationship, in addition to several lines of evidence (Gibson and Lux, this volume), suggests that this may be a cause and effect relationship.

Geologic relationships only restrict the age to the interval Middle Devonian through Mississippian, and unfortunately the new Rb/Sr isotopic age determination, 382±34, does not significantly improve the situation. However, it does support the 382 Ma zircon age of Lux and Aleinikoff (1985). The data also support the idea that the Songo pluton is a member of the New Hampshire Magma Series as are other hornblende-bearing granodiorites of western Maine, including the Mooselookmeguntic, Hartland, Big Island Pond, Spider Lake, Chain of Ponds, and Umbagog plutons.

Isotopic age determinations for the two-mica granites of the Sebago batholith demonstrate that they are much younger, having crystallized about 325 to 336 Ma ago (Aleinikoff et al., 1985; Hayward, 1989). The recognition that the largest batholith in New England is Carboniferous rather than Devonian in age led to the suggestion that much of the metamorphism in the vicinity of the Sebago batholith was also Carboniferous in age with the former being the heat source for the metamorphism (Lux and Guidotti, 1985; Aleinikoff et al., 1985). However, it is still not clear how K-feldspar + sillimanite grade metamorphism, which occurs ten to twenty kilometers away from the exposed contacts of the batholith, could be caused by heat from the Sebago granites.

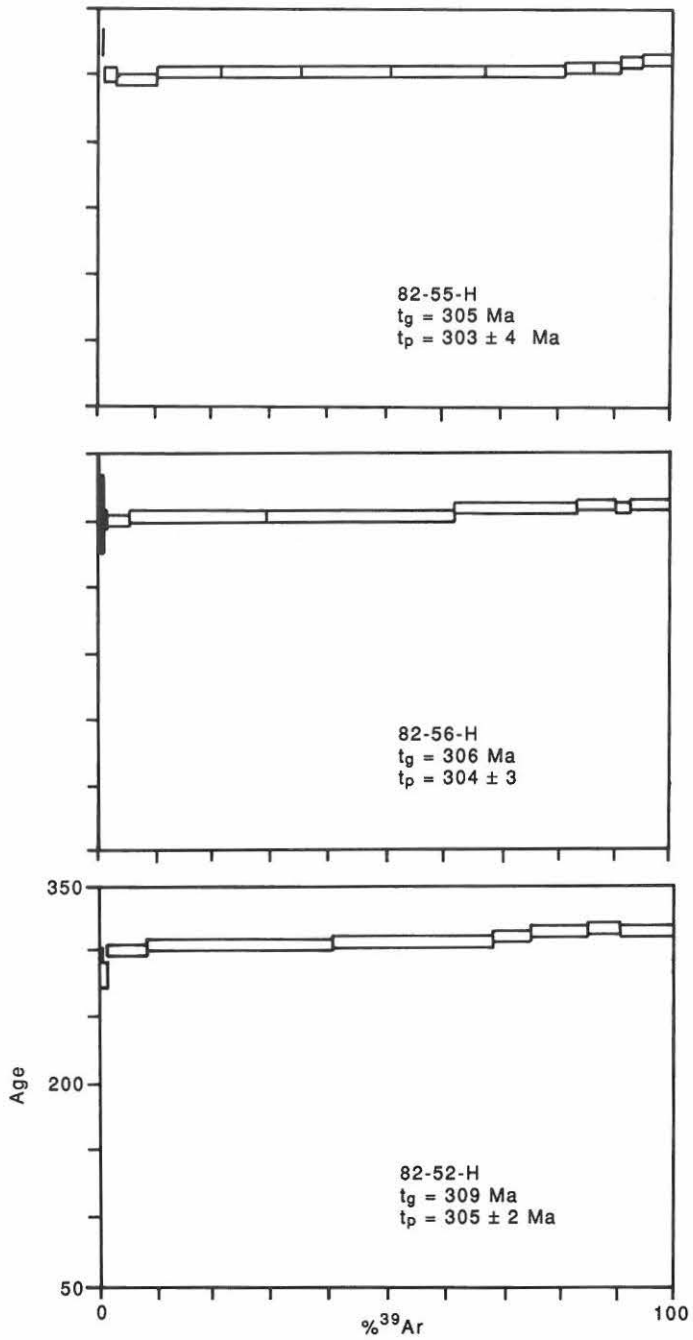

Figure 4. $^{40}Ar/^{39}Ar$ release spectra for three hornblende samples. The vertical and horizontal scales are the same on each age spectrum. Cooling through the closure temperature for Ar loss in hornblende occurred at about 304 Ma for all samples.

Modest topographic relief in the region precludes direct evidence bearing on the three-dimensional shape of the Sebago batholith. However, indirect observations of the shapes of plutons in western Maine and New Hampshire have been made through gravity surveys and modeling by Nielson et al. (1976), Kane and Bromery (1968), Carnese (1981), and Hodge et al. (1982). Their data show that plutons outside the New England high-grade metamorphic zone of western Maine often have marked negative gravity anomalies, suggesting that the plutons extend to significant depths and are rather equant in shape. Those plutons within the high-grade metamorphic zone lack significant gravity anomalies and appear to have the geometry of thin tabular sill-like bodies. Their gravity models suggest that many of the sill-like plutons dip northeasterly at a low angle (2-4 degrees) and extend far beyond their surface contacts (Nielson et al., 1976; Carnese, 1981; Hodge et al., 1982). This pluton geometry means that areas of high-grade metamorphism 10-20 km from the surface contact with a pluton may actually lie within 1 km of the contact with a pluton at depth. Therefore the sill-like plutons within the high-grade metamorphic zone are probable heat sources for much of the low-P metamorphism. See Lux et al. (1986) and De Yoreo et al. (in press) for a more complete discussion.

The extent and nature of the Carboniferous metamorphism surrounding the Sebago batholith have been outlined elsewhere (Guidotti et al., 1986; Guidotti, 1989; Lux and Guidotti, 1985). Some of the important features of this metamorphism found in the area north and northeast of the Sebago batholith include: (1) the zone of K-feldspar + sillimanite metamorphism; (2) extensive development of migmatites; and (3) intrusion of numerous rare mineral pegmatites. Numerous small granite dikes and other intrusive bodies are found throughout this same area (Guidotti, 1965; Fisher, 1962). The Songo pluton is also located within this zone of Carboniferous high-grade metamorphism and therefore must have experienced those same high-grade metamorphic conditions. Metamorphic transformations within the granodiorite are not particularly apparent because the mineral assemblages of the granodiorite were essentially stable at the P-T conditions of metamorphism. However, it is likely that much of the biotite foliation and intense mineral banding observed in the Songo pluton resulted from open system metamorphism related to the intrusion of the Sebago granites (Gibson and Lux, this volume).

We conclude that the scatter of the Rb/Sr data for the Songo pluton, especially that for the biotite granodiorite, is related to the intrusion of the Sebago two-mica granite as was the regional K-feldspar + sillimanite metamorphism, intrusion of rare mineral pegmatites, and possibly metamorphism of parts of the Songo pluton itself.

Further evidence that the Sebago batholith has caused a thermal disturbance of the region comes from the $^{40}Ar/^{39}Ar$ results of the hornblendes from the Songo pluton. $^{40}Ar/^{39}Ar$ ages for hornblende are considerably younger than the crystallization age for the Songo pluton and therefore require either that the ambient temperature at the time of emplacement of the Songo pluton was well above the T_c for hornblende and regional cooling in response to uplift and erosion was very slow, or that the K-Ar isotopic system of hornblendes was reset at a later time subsequent to the emplacement of the Songo pluton.

Arguments presented above demonstrate that the temperature of the Songo pluton was raised well above the closure temperature for Ar diffusion in hornblende at the time of intrusion of the Sebago batholith. Hence, whether the hornblendes had previously closed to Ar loss and subsequently opened or had never closed is impossible to say based on release spectra alone. Two lines of evidence suggest that the former is more likely.

Firstly, the closure temperature for hornblende, even at very slow cooling rates, is on the order of 500°C (Harrison, 1981). Mineral assemblages in the abundant pelitic schists around the Songo pluton provide no evidence to suggest that kyanite was ever a stable phase and thus the maximum burial of the region is restricted to pressures of the alumino-silicate triple point, about 14 km depth, or lower (Holdaway, 1971). Geobarometry of Holdaway et al. (1986) estimate a maximum pressure of 3.9 kbar for the region north of the Sebago batholith during Carboniferous time. For the hornblende ages to be the result of slow cooling, a minimum average geothermal gradient of about of 36°C/km, or about twice the present day New England geothermal gradient (Birch et al., 1968), would have been required during the time interval 382 to 304 Ma. Due to the convex nature of the geotherm, the near surface gradient would have been even greater. This is a tremendous energy requirement. Furthermore, if that gradient extended to greater depths, conditions for crustal melting (i.e. temperatures > saturated granite solidus) would be widespread at depths greater than 20 km. Almost all of the granites of the Kearsarge-central Maine synclinorium of western Maine, New Hampshire, and Massachusetts have been interpreted as being intrusive and are not the products of in situ melting, though many are peraluminous and most likely originated in the crust. Nonetheless, their intrusive nature argues against the high thermal gradients required above.

The second line of evidence comes from the release spectra. In the description of the release spectra given above it was shown that an age gradient was found in relatively high temperature increments following the plateau portion of the age spectrum. We suggest that this age gradient may represent a relict diffusion gradient that formed as ^{40}Ar was lost during a period of reheating related to the intrusion of the Sebago batholith.

These two lines of reasoning strongly suggest that the ambient temperature in the vicinity of the Songo pluton at the time of its intrusion was lower than the T_c for hornblende. The thermal disturbance associated with the emplacement of the Sebago batholith caused almost total Ar loss in hornblendes and they finally closed to Ar loss about 305 Ma ago. These results pose some problems with respect to the cooling history for the Sebago batholith presented by Aleinikoff et al. (1985). In particular, they presented U-Pb ages for monazites from the same samples they used for U-Pb age determinations on zircons in order to date the granites. One monazite was concordant at 272 Ma and the other had a slight reverse discordance with the following ages and isotopic ratios: $^{206}Pb/^{238}U$ = 294 Ma; $^{207}Pb/^{235}U$ = 293 Ma; and $^{207}Pb/^{206}Pb$ = 282 Ma. The best age for the latter was interpreted to be 282 Ma. These were interpreted as cooling ages following the intrusion of the Sebago batholith, and they assumed a closure temperature of 600°C, citing Gebauer and Grunenfelder (1979). However, Gebauer and Grunenfelder did not claim to know the closure temperature of monazite. They clearly stated that monazite "once formed can survive high-grade metamorphism(s) reaching temperatures of 600°C or more." This conclusion was based on the results of Koppel and Grunenfelder (1975) in which a single monazite separate from a sillimanite bearing quartzite xenolith gave an age that was older than monazites from the enclosing granite, but similar to the regionally metamorphosed country rocks. Based on this evidence they stated "we tentatively conclude that young monazites do not lose significant portions of their radiogenic lead even at temperatures above 600°C." This somewhat lengthy discussion has two purposes: (1) to point out that data bearing on the closure temperature of Pb loss in monazite are relatively sparse; and (2) to demonstrate that the available data provides no real information concerning the closure temperature of monazite.

Closure temperatures are not equivalent to resetting temperatures! Closure temperatures are based on the characteristics of Pb diffusion in monazite, grain size, and cooling rates. Resetting temperatures are a function of the characteristics of Pb diffusion in monazite, grain size, and the temperature and duration of a heating event. Because no data concerning the characteristics of Pb diffusion in monazite exist, and because the nature of the heating of the monazite studied by Koppel and Grunenfelder (1975) is not known, we know essentially nothing about the closure temperature for Pb loss in monazite. On the other hand, the database for hornblendes from granitic rocks is somewhat better. Harrison (1981) conducted a laboratory study of two hornblendes of differing composition and found them to have essentially the same characteristics for Ar diffusion. These correspond to a closure temperature of about 500°C when cooling rates are slow. Based on the isotopic results alone, we strongly favor the interpretation that regional cooling through 500°C occurred at about 305 Ma ago.

Geologic relations also favor our model of rapid cooling. De Yoreo et al., (1989) presented a thermal model which describes the cooling of the Sebago batholith. They demonstrate that cooling to the ambient temperature of the country rocks would occur very rapidly. The question then becomes, what is the ambient temperature of the country rocks? Arguments presented above suggest it was well below 600°C. The ambient temperature can be estimated if the thermal effects of the pluton are subtracted. This is difficult to do on the north or east side of the pluton because of the gentle northeasterly dip of the sill-like pluton, its consequent broad thermal aureole, and the presence of high-grade metamorphic zones related to earlier Acadian plutons. However, a detailed study of metamorphism in the vicinity of Gorham, Maine at the southern margin of the batholith (Thomson and Guidotti, 1989) sheds light on the pre-Sebago thermal structure on the underside of the pluton where temperatures would have been highest. In this area, closely spaced

isograds parallel the contact of the pluton and metamorphism drops off rapidly to garnet grade which represents the pre-Sebago thermal regime. This indicates that local ambient conditions at the time of intrusion of the Sebago batholith were well below 600°C. These data also make the interpretation of the monazite ages as the result of slow cooling untenable.

The significance of the monazite ages reported by Aleinikoff et al. (1985) becomes unclear, but very interesting. Several possibilities exist, but unfortunately definitive data do not. Perhaps the closure temperature for monazite is several hundred degrees lower than was assumed, though this seems unlikely. Another interpretation is that the concordant monazite actually dates the formation of the Sebago batholith. In general, inherited Pb gives rise to anomalously old U/Pb ages for zircons. Contamination of a magma with old, Rb-rich crustal components can also result in anomalously old whole-rock isochron ages. However, given the virtual concordance of the U/Pb and Rb/Sr ages, this interpretation also seems very unlikely. A third, and at this time favored, hypothesis is that the central and southern parts of the Sebago batholith were affected by a Permian thermal event that had little effect on the Songo pluton. This is supported by the data of West et al. (1988) who reported numerous ages in the range of 270-290 Ma for hornblendes from amphibolites in the Casco Bay Group lying just southeast of the Sebago batholith. Furthermore, one of the hornblendes dated in this study (82-52) has ages of 280-290 Ma in its first few increments which could be attributed to ^{40}Ar loss during a thermal event at that time.

We interpret the isotopic ages for biotites from the Songo pluton to date the time of closure to ^{40}Ar loss following a period of slow cooling following the intrusion of the Sebago batholith. The 12 biotites from the Songo pluton that were dated isotopically all have ages in the range 256-247 Ma. Harrison et al. (1985) have shown that in addition to cooling rate, the Fe/Mg ratio in biotite may influence the T_c, which, for igneous biotites, may be in the range of 280-300°C at slow cooling rates. Even with rather modest estimates of the paleogeothermal gradient, 20-25°C/km, it is likely that the biotites never closed to Ar loss prior to their final retention of ^{40}Ar at 250 Ma. The biotites therefore date the time of cooling through the T_c of biotite, approximately the 300°C isotherm, in response to uplift and erosion of the region. These data are consistent with other age data for micas from the region. De Yoreo et al. (1989) report $^{40}Ar/^{39}Ar$ ages for 9 coexisting biotite and muscovite pairs from the Sebago batholith. These have a range of 229-245 Ma for biotites and 240-246 Ma for muscovites. Hayward and Gaudette (1984) and Hayward (1989) reported Rb/Sr mineral isochrons of about 265 Ma for samples from the Sebago batholith. These data are mutually consistent and support the slow regional cooling hypothesis presented here as well as by De Yoreo et al. (in press) and by Dallmeyer and Van Breeman (1981).

The data presented above show that the biotites fall into two distinct populations, a group of green biotites (from the BHS granodiorite) with ages in the range 253-256 Ma and a group of red-brown biotites (from the biotite granodiorites) with ages in the range 247-250 Ma. We envisage two possible explanations for this distribution of ages. The green biotites having older isotopic ages are all found in the NW part of the pluton and may therefore represent regional differences in the time of cooling through the biotite T_c. If this is the cause of the age differences between the two biotite populations, the correlation of age grouping with color of the biotites is coincidental. However, the color of the biotites reflects (the red-brown biotites having higher TiO_2 contents; see Gibson and Lux, this volume) compositional differences and alternatively the two age populations could reflect a compositional dependence on biotite T_c as was demonstrated by Harrison et al. (1985). With the present database we are not prepared to choose between these two alternatives as either one appears viable. In either case, for the purposes of this paper, it is reasonable to conclude that all of the biotites cooled through the biotite T_c about 250 Ma ago.

CONCLUSIONS

The new isotopic data presented in this paper are summarized as follows: (1) New Rb/Sr whole rock isotopic data for samples from the BHS granodiorite phase of the Songo pluton yield an age of 382±34 Ma. However, the $^{87}Rb/^{86}Sr$ and $^{87}Sr/^{86}Sr$ data, especially for the biotite granodiorite phase, show some scatter. (2) $^{40}Ar/^{39}Ar$ dating of hornblende from the Songo pluton produces ages of about 304 Ma and suggests that hornblende ceased to lose radiogenic ^{40}Ar at that time. (3) $^{40}Ar/^{39}Ar$ isotopic ages for biotites fall in the range of 256-247 Ma and show that the biotites closed to radiogenic ^{40}Ar loss at about 250 Ma. The following are our conclusions based on the new isotopic data. Field relationships and previous isotopic age dating demonstrated that the Songo pluton was older than 325 Ma and younger than Early Devonian. The Rb/Sr whole rock data for samples from the BHS variety of the Songo pluton indicates an age of 382±34 Ma for crystallization, suggesting a Devonian age. Based on this evidence, it remains a member of the New Hampshire Magma Series like other hornblende-bearing granodiorites of western Maine such as the Hartland, Mooselookmeguntic, Chain of Ponds, Big Island Pond, Spider Lake, and Umbagog plutons. We attribute the scatter of $^{87}Rb/^{86}Sr$ and $^{87}Sr/^{86}Sr$ data, especially that of the biotite granodiorite phase, to open system behavior that occurred during the intrusion of the Sebago batholith.

Release spectra for the three hornblende samples are all disturbed. However, all have plateau ages of about 305 Ma which represents the time of cooling through the hornblende T_c following the Carboniferous metamorphic event. It is difficult to make an unambiguous interpretation of the disturbed release spectra preserved in these hornblendes, however we feel it is most likely that they are the result of both excess ^{40}Ar and a diffusion gradient related to ^{40}Ar loss during the Carboniferous regional metamorphic event. All biotites have nearly undisturbed release spectra with plateau ages of about 250 Ma. These record the time of last cooling through the T_c for Ar diffusion in biotite. The

large discordance between the hornblende and biotite ages are interpreted to indicate slow regional cooling in response to uplift and erosion during the time interval 305 to 250 Ma. Small differences in isotopic ages between those samples from the BHS granodiorites and the biotite granodiorites may be the result of either differences in regional cooling or more likely to compositional differences between the two groups of biotites.

ACKNOWLEDGMENTS

This work was supported by National Science Foundation grants EAR-82-06549 and ISP-8011448. The manuscript benefited greatly from comments by Dr. Henri Gaudette and an anonymous reviewer. In addition we would like to thank Matthew Heizler and Fritz Hubacher for their expert help.

REFERENCES CITED

Aleinikoff, J. N., Moench, R. H., and Lyons, J. B., 1985, Carboniferous U-Pb age of the Sebago batholith, southwestern Maine: Geol. Soc. Amer., Bull., v. 69, p. 990-996.

Alexander, E. C., Jr., Michelson, G. M., and Lanphere, M. A., 1978, MMhb-1: A new ^{40}Ar-^{39}Ar dating standard, *in* Zartman, R. E. (ed.), Short Papers of the Fourth International Conference, Geochronology, Cosmochronology. Isotope Geology: U.S. Geol. Surv., Open-File Rept. 78-701, p. 6-8.

Barton, M. D., Battles, D. A., Bebout, G. E., Capo, R. C., Christensen, J. N., Davis, S. R., Hanson, R. B., Michelsen, C. J., and Trim, H. E., in press, Mesozoic contact metamorphism in the western United States, *in* Ernst, W. G. (ed.), Metamorphism and crustal evolution, western co-terminous United States.

Billings, M. P., 1956, The geology of New Hampshire: Pt. II, Bedrock geology: New Hampshire State Planning and Devel. Comm., Concord, 203 p.

Birch, F., Roy, R. F., and Decker, E. R., 1968, Heat flow and thermal history in New England and New York, *in* Zen, E-an, White, W. S., Hadley, J. B., and Thompson, J. B. (eds.), Studies of Appalachian geology, northern and maritime: John Wiley & Sons, New York, p. 437-451.

Carnese, M. J., 1981, Gravity studies of intrusive rocks in west-central Maine: M.S. thesis, Univ. New Hampshire, Durham, N.H., 97 p.

Dallmeyer, R. D., and Van Breeman, O., 1981, Rb-Sr whole-rock and $^{40}Ar/^{39}Ar$ mineral ages of the Togus and Hallowell quartz monzonite and Three Mile Pond granodiorite plutons, south-central Maine: their bearing on post-Acadian cooling history: Contrib. Mineral. Petrol., v. 78, p. 61-73.

Dalrymple, G. B., Brent, E., Alexander, C., Jr., Lanphere, M. A., and Kraker, G. P., 1981, Irradiation of samples for $^{40}Ar/^{39}Ar$ dating using the Geological Survey TRIGA reactor: U.S. Geol. Surv., Prof. Pap. 1176, 55 p.

Dalrymple, G. B., and Lanphere, M. A., 1969, Potassium-argon dating: W. H. Freeman, San Francisco, 258 p.

De Yoreo, J. J., Lux, D. R., and Guidotti, C. V., 1989, A thermal model for Carboniferous metamorphism near the Sebago batholith, *in* Tucker, R. D., and Marvinney, R. G. (eds.), Studies in Maine geology, Volume 3 - igneous and metamorphic geology: Maine Geol. Surv.

De Yoreo, J. J., Lux, D. R., Guidotti, C. V., Decker, E. R., and Osberg, P. H., in press, The Acadian thermal history of western Maine: Jour. Metamorphic Geol.

Fisher, I. S., 1962, Petrology and structure of the Bethel Area, Maine: Geol. Soc. Amer., Bull., v. 73, p. 1365-1420.

Fleck, R. J., Sutter, J. F., and Elliot, D. H., 1977, Interpretation of discordant $^{40}Ar/^{39}Ar$ age-spectra of Mesozoic tholeiites from Antarctica: Geochim. Cosmochim. Acta, v. 41, p. 15-32.

Gebauer, D., and Grunenfelder, M., 1979, U-Th-Pb dating of minerals, *in* Jager, E., and Hunziker, J. C. (eds.), Lectures in isotope geology: Springer-Verlag, Berlin, p. 105-131.

Guidotti, C. V., 1963, Metamorphism of the pelitic schists in the Bryant Pond quadrangle, Maine: Amer. Mineral., v. 48, p. 722-791.

Guidotti, C. V., 1965, Geology of the Bryant Pond quadrangle, Maine: Maine Geol. Surv., Bull. 16, 116 p.

Guidotti, C. V., 1989, Metamorphism in Maine: an overview, *in* Tucker, R. D., and Marvinney, R. G. (eds.), Studies in Maine geology, Volume 3 - igneous and metamorphic geology: Maine Geol. Surv.

Guidotti, C. V., Gibson, D., Lux, D. R., De Yoreo, J. J., and Cheney, J. T., 1986, Carboniferous metamorphism on the north (Upper) side of the Sebago batholith, *in* Newberg, D. W. (ed.), New England Intercollegiate Geological Conference guidebook for field trips in southwestern Maine, p. 306-341.

Guidotti, C. V., Trzcienski, W. E., and Holdaway, M. J., 1983, A northern Appalachians metamorphic transect-Eastern Townships, Quebec to the central Maine coast, *in* Schenk, P. E. (ed.), Regional trends in the geology of the Appalachians - Caledonian-Hercynian-Mauritanide orogen: D. Reidel Pub. Co., p. 235-247.

Harrison, T. M., 1981, Diffusion of ^{40}Ar in hornblende: Contrib. Mineral. Petrol., v. 78, p. 324-331.

Harrison, T. M., Duncan, I., and McDougall, I., 1985, Diffusion of ^{40}Ar in biotite: temperature, pressure and compositional effects: Geochim. Cosmochim. Acta, v. 49, p. 2461-2468.

Hayward, J. A., 1989, Implications of the Rb-Sr and O isotopic systematics and geochemistry of some two-mica granites in northern New England, *in* Tucker, R. D., and Marvinney, R. G. (eds.), Studies in Maine geology, Volume 3 - igneous and metamorphic geology: Maine Geol. Surv.

Hayward, J. A., and Gaudette, H. E., 1984, Carboniferous age of the Sebago and Effingham plutons, Maine and New Hampshire: Geol. Soc. Amer., Abs. with Prog., v. 16, no. 1, p. 22.

Hodge, D. S., Abbey, D. A., Harkin, M. A., Patterson, J. A., Ring, M. J., and Sweeney, J. R., 1982, Gravity studies of subsurface mass distributions of granitic rocks in Maine and New Hampshire: Am. Jour. Sci., v. 282, p. 1289-1324.

Holdaway, M. J., 1971, Stability of andalusite and sillimanite and the aluminum silicate phase diagram: Am. Jour. Sci., v. 271, p. 97-131.

Holdaway, M. J., Dickerson, R. P., and Dutrow, B. L., 1986, Petrology and field relations of M_2 metamorphism in west-central Maine, *in* Newberg, D. W. (ed.), New England Intercollegiate Geological Conference guidebook for field trips in southwestern Maine, p. 240-253.

Holdaway, M. J., Guidotti, C. V., Novak, J. M., and Henry, W. E., 1982, Polymetamorphism in medium- to high-grade pelitic metamorphic rock, west-central Maine: Geol. Soc. Amer., Bull., v. 93, p. 572-584.

Kane, M. F., and Bromery, R. W., 1968, Gravity anomalies in Maine, *in* Zen, E-an, White, W. S., Hadley, J. B., and Thompson, J. B. (eds.), Studies in Appalachian geology, northern and maritime: John Wiley & Sons, New York, p. 415-423.

Koppel, V., and Grunenfelder, M., 1975, Concordant U-Pb ages of monazites from the Central Alps and the timing of the high temperature Alpine metamorphism, a preliminary report: Schweiz. Mineral. Petrogr. Mitt., v. 55, p. 129-132.

Lux, D. R., 1986, $^{40}Ar/^{39}Ar$ isotopic dating in low-pressure metamorphic terranes: an example from western Maine, U.S.A.: Terra Cognita, v. 6, p. 253.

Lux, D. R., and Aleinikoff, J. N., 1985, ^{40}Ar-^{39}Ar and U-Pb geochronology of the Songo pluton, western Maine: Geol. Soc. Amer., Abs. with Prog., v. 17, p. 32.

Lux, D. R., De Yoreo, J. J., Guidotti, C. V., and Decker, E. R., 1986, The role of plutonism in low-pressure metamorphic belt formation: Nature, v. 323, p. 794-797.

Lux, D. R., and Guidotti, C. V., 1985, Evidence for extensive Hercynian metamorphism in western Maine: Geology, v. 13, p. 696-700.

Nielson, D. L., Clark, R. G., Lyons, J. B., Englund, E. J., and Borns, D. J., 1976, Gravity models and modes of emplacement of the New Hampshire Plutonic Series: Geol. Soc. Amer., Mem. 146, p. 301-318.

Osberg, P. H., Hussey, A. M., II, and Boone, G. M., 1985, Bedrock geologic map of Maine: Maine Geol. Surv., scale 1:500,000.

Steiger, R. H., and Jager, E., 1977, Subcommission on geochronology: convention on the use of decay constants in geo- and cosmochronology: Earth Planet. Sci. Lett., v. 36, p. 359-362.

Thompson, A. B., and England, P. C., 1984, Pressure-temperature-time paths of regional metamorphism II: their inference and interpretation using mineral assemblages in metamorphic rocks: Jour. Petrol., v. 25, p. 929-955.

Thomson, J. A., and Guidotti, C. V., 1989, Carboniferous Barrovian metamorphism in Maine, *in* Tucker, R. D., and Marvinney, R. G. (eds.), Studies in Maine geology, Volume 3 - igneous and metamorphic geology: Maine Geol. Surv.

West, D. P., Jr., Lux, D. R., Guidotti, C. V., Hussey, A. M., II., and Newberg, D. W., 1988, $^{40}Ar/^{39}Ar$ mineral ages from the Casco Bay Group, southwestern Maine: Geol. Soc. Amer., Abs. with Prog., v. 20, p. 78.

Maine Geological Survey
Studies in Maine Geology: Volume 4
1989

$^{40}Ar/^{39}Ar$ Isotopic Dating of the Horserace Quartz Diorite and its Bearing on Age Relationships in the Katahdin Batholith-Traveler Rhyolite System

*A. Scott Denning**
Daniel R. Lux
Department of Geological Sciences
University of Maine
Orono, Maine 04469

**Present address:*
Department of Atmospheric Sciences
Colorado State University
Fort Collins, Colorado 80523

ABSTRACT

The Horserace quartz diorite is a small pluton that intrudes the Katahdin granite in north-central Maine. However, some field observations and geochemical data suggest that the Horserace quartz diorite may have been nearly contemporaneous with the Katahdin granite, which is believed to be the intrusive equivalent of the Traveler rhyolite. Stratigraphic control of the Traveler rhyolite is adequate such that reliable age data would provide an Early Devonian time scale correlation point. Thus, it was hoped that by dating the Horserace quartz diorite we could effectively date the Traveler rhyolite and provide an absolute time point for the stratigraphic time scale.

Four hornblende samples from the Horserace quartz diorite dated by the $^{40}Ar/^{39}Ar$ incremental heating technique yield plateau age spectra concordant at 2 sigma with a mean of 374.9± 3.2 Ma. Biotite samples from the Horserace quartz diorite do not yield plateau spectra, but total gas ages average 374 Ma, suggesting that the Horserace quartz diorite cooled quickly through the Ar closure temperatures for both hornblende and biotite (about 550°C and 350°C respectively). A single release spectrum for a biotite from the Katahdin granite yields a plateau age of 400.1 ± 1.0 Ma.

The new data demonstrate that the Horserace quartz diorite is 375 Ma old and data further suggest that the Katahdin granite is distinctly older, possibly 400 Ma old. These new results for the Horserace quartz diorite probably do not date the time of eruption of the Traveler rhyolite and therefore do not provide an absolute age calibration point for the stratigraphic time scale. The Traveler rhyolite does have great potential for providing such a calibration point and we recommend that future attempts to determine that point concentrate on direct age measurements of the Traveler rhyolite.

INTRODUCTION

The Katahdin batholith is a large body of felsic igneous rock in north central Maine. The batholith crops out over an area of approximately 2500 km^2 and is roughly elliptical in map pattern, with dimensions of about 65 by 40 km. A sketch map of the state of Maine shows the position and shape of the Katahdin batholith (Fig. 1). The batholith underlies much of Baxter State Park and

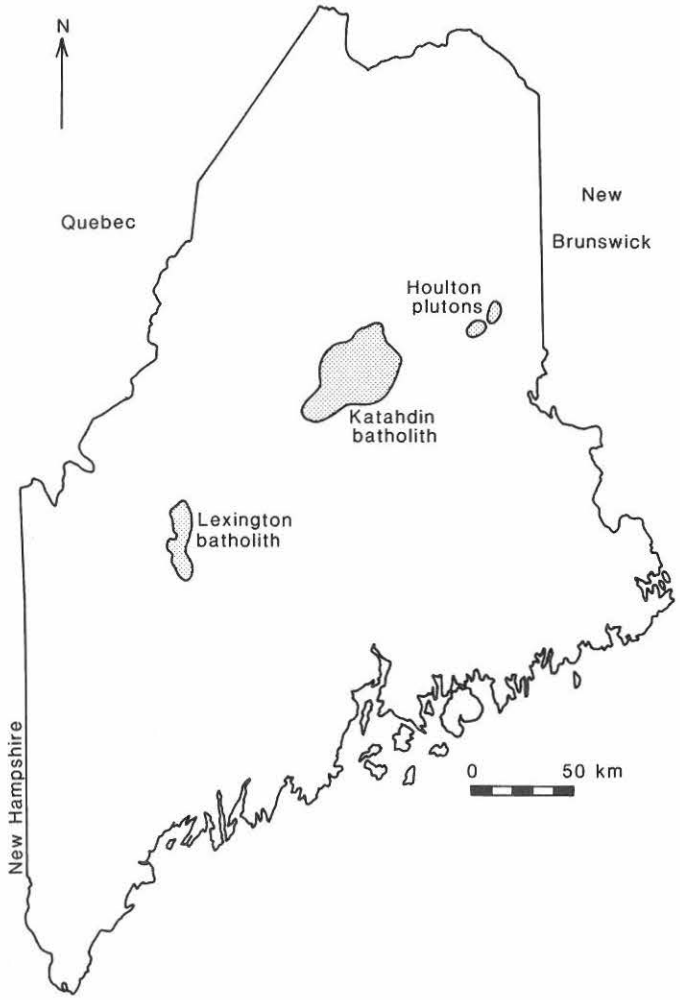

Figure 1. Map of Maine, showing the location of the Katahdin batholith and several other plutons in the dot pattern.

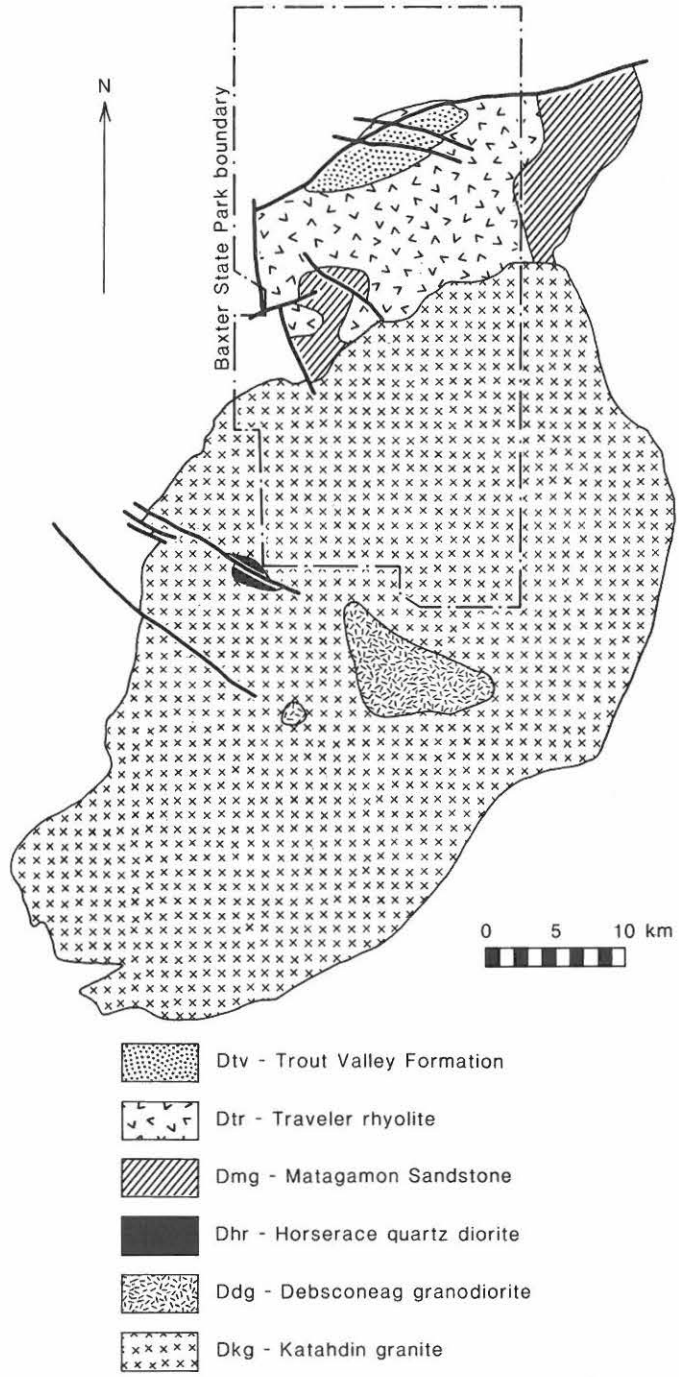

Figure 2. Geologic sketch map of the Katahdin batholith and vicinity showing various of the intrusive phases (after Hon, 1980).

also extends considerably to the south and west of the park. Mapping in the region has been completed by Rankin (1961), Griscom (1976), and Hon (1976).

A geologic sketch map showing the distribution of the major rock types of the Katahdin batholith is presented in Figure 2. The bulk of the batholith is comprised of biotite granite, i.e., the Katahdin granite. Two compositionally different units intrude the granite, namely the Horserace quartz diorite, a small stock about 6 by 2.5 km, and two bodies of the Debsconeag granodiorite. All three of these bodies crop out along the fault system associated with the West Branch of the Penobscot River, suggesting tectonic control for the site of the intrusions (Hon, 1980). There has been much interest in the age of the Katahdin batholith because of the good stratigraphic control on its stratigraphic equivalent, the Traveler rhyolite, and because the Katahdin granite intrudes folded Lower Devonian rocks, yet is itself undeformed.

A summary of the stratigraphic relationships of the Lower Devonian units of the area is presented in Figure 3. The base of the section considered here is the Seboomook Formation, of Siegenian age. It is overlain by the Matagamon Sandstone (Siegenian), which is in turn overlain by the Traveler rhyolite. The rhyolite is intruded by the Katahdin granite and is unconfor-

mably overlain by the Middle Devonian Trout Valley Formation (Rankin, 1980).

The Seboomook Formation in this area consists of a thick, sparsely fossiliferous sequence of graded beds consisting of fine grained sandstone, siltstone, and slate (turbidites). The Seboomook-Matagamon sequence has been interpreted as a westward-prograding delta (Hall et al., 1976; Pollock et al., 1988). These fossiliferous rocks are conformably overlain by the voluminous Traveler rhyolite volcanic sequence. Scattered pebbles of rhyolite are found in the upper few meters of the deltaic sequence suggesting that very little (if any) time elapsed between the deposition of the top of the sandstone and the ash flow eruptions producing the rhyolite (Rankin, 1961). In addition, Rankin (1961) also reported numerous clastic dikes of sandstone in the rhyolite, which he interpreted to mean that the sandstone was poorly consolidated during the deposition of the lower parts of the rhyolite. This further supports the suggestion of the similarity in age between the Siegenian Matagamon Sandstone and the Traveler rhyolite.

The Traveler rhyolite is unconformably overlain by a basal conglomerate of the Trout Valley Formation. Terrestrial plant fossils from the Trout Valley Formation are believed to be Middle Devonian in age (Rankin and Hon, 1987). The basal conglomerate contains felsite pebbles derived from the Traveler rhyolite. Rankin (1961) observed evidence of deformation in the Traveler rhyolite which is not seen in the Trout Valley Formation, suggesting an indefinite period of time elapsed between the end of the volcanism which produced the felsite and the deposition of the basal conglomerate of the Trout Valley Formation.

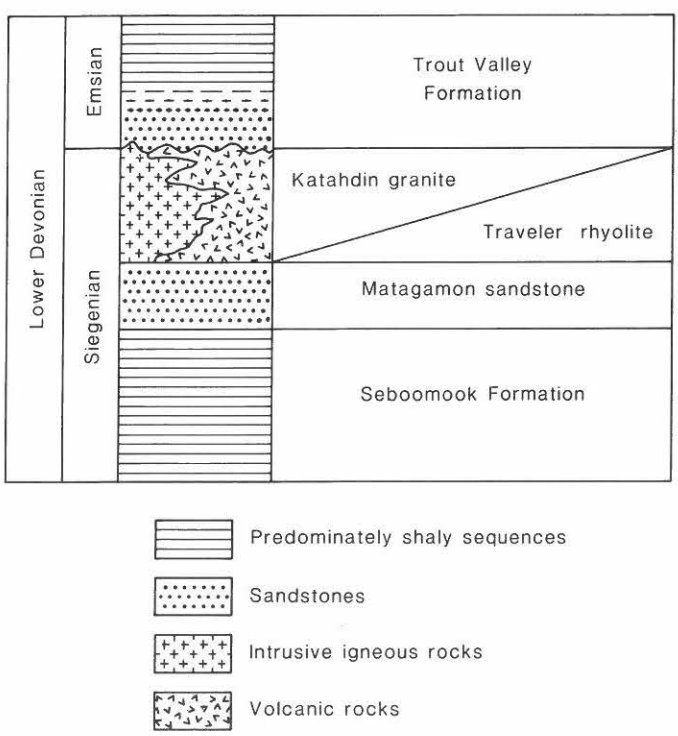

Figure 3. Stratigraphic relationships of Lower Devonian rocks in the study area.

The stratigraphic control on the age of the Traveler rhyolite is fairly good. Unfortunately, obtaining a reliable age of the Traveler rhyolite is complicated by the extensive recrystallization of these rocks in the time since they were extruded. Bottino et al. (1965) reported an Rb-Sr whole rock isochron age of 352 ± 10 Ma (calculated with the decay constants recommended by Steiger and Jager (1977) as are all other ages presented or discussed in this paper). The initial $^{87}Sr/^{86}Sr$ ratio is 0.7105.

The Traveler rhyolite is intruded by the Katahdin granite, but Rankin (1961) suggested that the two were comagmatic with the Traveler rhyolite being the volcanic equivalent of the Katahdin granite. Hon (1980, p. 75) showed by modeling of trace element abundances that "the Katahdin granite can be derived from the Traveler rhyolite magma if 15%-25% phenocrysts are removed by fractionation." Recent efforts to establish the chronology of these rocks have focused on dating the Katahdin granite as an equivalent of the Traveler rhyolite.

Loiselle et al. (1983) suggested that the Katahdin granite could be used as a geological time scale correlation point, making it possible to give an absolute age to rocks of this relative age anywhere in the world. If the granite and felsite are indeed contemporaneous, then it should at least be possible to determine a date for the late Siegenian, as the contact between the Matagamon Sandstone and the Traveler rhyolite is demonstrably conformable.

The age of the Katahdin granite has proved difficult to determine. Boucot (1954) reported an age of 363 Ma that was determined by the K/Ar method. Loiselle et al. (1983) reported two ages for the Katahdin batholith. One is a six point Rb/Sr whole rock isochron age of 388 ± 5 Ma, with an initial $^{87}Sr/^{86}Sr$ ratio of 0.7083. They also reported a $^{207}Pb/^{206}Pb$ age for zircons of 414 ± 4 Ma. These ages are not mutually consistent.

Because the Seboomook Formation contains Siegenian fossils, and the Seboomook-Matagamon sequence is overlain by the Traveler rhyolite, the age of formation of the Katahdin granite must be no older than Siegenian. Current estimates of the age of the Siluro-Devonian boundary include 405 Ma (Boucot, 1975), 408 Ma (Palmer, 1983), and 410 Ma (Spjeldnaes, 1978). Thus, if the zircon age reported by Loiselle et al. (1983) is accurate, estimates of this boundary must be somewhat young.

The present paper attempts to resolve the problem of the age of the Katahdin batholith by using the $^{40}Ar/^{39}Ar$ incremental heating technique. The $^{40}Ar/^{39}Ar$ method may be used for any mineral containing potassium, but is most useful for hornblende because of its relatively high closure temperature and because it is relatively stable during heating in the ultra-high vacuum furnace system during Ar extraction. Unfortunately, the Katahdin granite contains no hornblende. This paper, therefore, focuses on dating hornblende separates from the Horserace quartz diorite which intrudes the Katahdin granite.

The geochemical work of Brown and Hon (1984) has established that the Horserace quartz diorite is derived from a different magmatic source than the Katahdin granite and the Traveler rhyolite, and suggests the Debsconeag granodiorite may be a mixture of the Horserace and Traveler magmas. Nonetheless, they cited field evidence indicating the Katahdin granite was still at least partially molten at the time of intrusion of the Horserace quartz diorite. Contacts between the Katahdin granite and Horserace quartz diorite are observed to be wavy and irregular, and suggest that liquid phases of the two may have mixed. This phenomenon was also noted in the field by the authors. If the Katahdin granite was indeed still molten during intrusion of Horserace quartz diorite magma, then the two units should have been nearly contemporaneous.

If the Katahdin granite and Horserace quartz diorite formed contemporaneously and if both are also the same age as the Traveler rhyolite, then the age determined for the Horserace quartz diorite should be a good estimate of the age of the late Siegenian. Though intrusive into the Kathadin granite, Brown and Hon (1984) indicate that the granite was still partially molten when the quartz diorite was intruded, thereby strongly suggesting a temporal link. However, if the granite cannot be shown to be the same age as the quartz diorite, then the age of the latter still provides a lower limit to the age of the Katahdin granite and the Traveler rhyolite.

METHODS

Sampling localities are principally a series of well exposed outcrops along a 0.5 km transect on the south side of the West Branch of the Penobscot River between the Golden Road and Big Ambejackmockamus Falls. Samples 83-SD-1 and 83-SD-2 were collected from roadcut outcrops on the Golden Road near Big Eddy just west of the contact of the quartz diorite and the granite. Carrol Brown collected sample HQD-618-3A, but the exact locality was unspecified.

Mineral separates were obtained using standard methods including magnetic and heavy liquid separation techniques. Separates were at least 99% pure. The hornblende separates that were dated weighed 300-1000 mg, and biotite separates weighed about 100 mg.

All samples were irradiated in the U.S. Geological Survey TRIGA reactor in Denver, Colorado. One vial in each irradiation package contained flux monitor minerals of precisely known age. The monitor mineral used was an international standard, MMhb-1, whose age is known to be 519.4 Ma (Alexander et al., 1978).

Samples were heated incrementally in a molybdenum crucible within an ultra-high vacuum extraction furnace and purified using standard gettering techniques. The isotopic composition of the purified Ar was analyzed on a Nuclide 6-60-SGA 1.25 mass spectrometer.

Equations of Dalrymple et al. (1981) were used to calculate ages and estimate uncertainties. Release spectrum plateaus are defined as at least 50% of the gas in consecutive increments with the same age within a 2 sigma confidence interval. The plateau age reported is the unweighted mean of the ages of the increments falling within the limits of the plateau. Uncertainty reported for plateau ages is a 1 sigma confidence interval.

Closure temperatures were calculated by the method of Dodson (1979), using parameters from Harrison (1981) for hornblende and Harrison et al. (1985) for biotite.

RESULTS AND DISCUSSION

Analytical data from incremental heating and total fusion mass spectrometric analyses of samples from the Horserace quartz diorite and Katahdin granite are presented in Tables 1 and 2. Graphical illustrations of these data are presented in Figures 4 and 5. These age spectra are used to display the data qualitatively. Quantitative comparison of analytical data should be made using the numerical data presented in the Tables 1 and 2.

Five of the release spectra have plateaus as defined above. These are those for hornblendes from the Horserace quartz diorite (83-SD-3, 83-SD-4, 83-SD-6, and HQD-618-3A) and biotite from the Katahdin granite (83-SD-2). All of these plateau spectra show anomalously low ages for the first 5% or so of the gas released. This suggests minor episodic loss of $^{40}Ar_{Rad}$ at some indeterminate time since initial cooling. Because of this Ar loss the total gas age of each of these samples is lower than the plateau age. Plateau ages of the four hornblende samples from the Horserace quartz diorite are concordant within analyti-

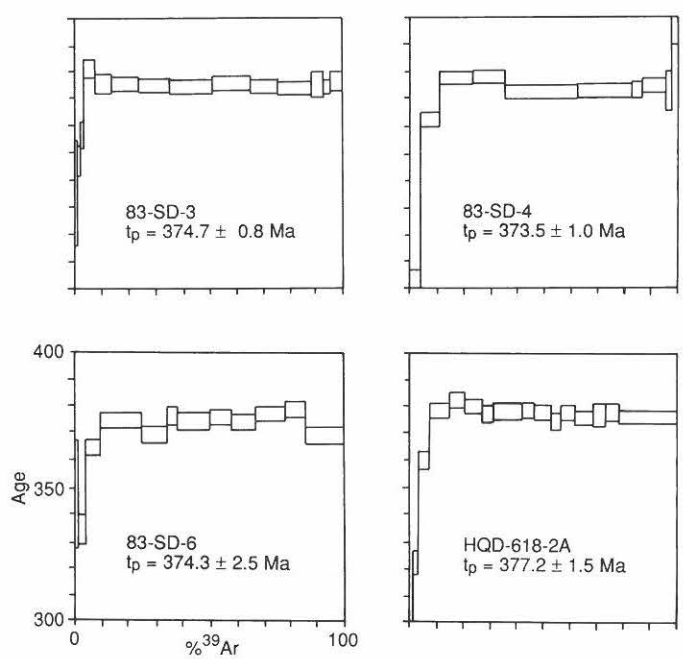

Figure 4. Age spectra of hornblende from samples of the Horserace quartz diorite (see Table 1). The vertical and horizontal scales are all as shown in the lower left. The box height for individual increments represents 2 sigma uncertainties. t_p - plateau age.

TABLE 1. INCREMENTAL RELEASE DATA FOR HORNBLENDE SAMPLES FROM THE HORSERACE QUARTZ DIORITE. MOLES ^{39}Ar HAS BEEN MULTIPLIED BY 10^{14} AND $\%^{40}Ar_{RAD}$ REPRESENTS THE PORTION OF ^{40}Ar DERIVED BY DECAY OF ^{40}K.

Temp °C	$^{40}Ar/^{39}Ar$	$^{37}Ar/^{39}Ar$	$^{36}Ar/^{39}Ar$	Moles ^{39}Ar	^{39}Ar %Total	$\%^{40}Ar$ RAD	K/Ca	Apparent Age Ma
83-SD-3 HORNBLENDE		J = 0.009263						
500	153.45	2.661	0.4602	1.50	0.3	11.4	0.18	274.0 ± 37.6
650	71.03	1.827	0.1663	3.45	0.6	30.8	0.26	335.2 ± 19.4
750	39.45	1.895	0.0566	5.43	0.9	57.6	0.26	347.0 ± 5.7
850	38.97	4.155	0.0534	6.94	1.2	59.5	0.12	356.4 ± 4.9
935	30.56	10.38	0.0209	25.60	4.4	79.8	0.05	380.9 ± 3.3
965	27.89	10.43	0.0132	43.46	7.5	86.0	0.05	375.3 ± 3.8
980	27.08	10.11	0.0104	57.47	10.0	88.6	0.05	375.1 ± 2.6
995	26.65	9.715	0.0090	66.16	11.5	90.1	0.05	374.6 ± 2.6
1010	26.12	9.222	0.0072	90.93	15.7	91.9	0.05	374.0 ± 2.5
1025	26.02	9.000	0.0063	83.09	14.4	92.8	0.05	375.5 ± 2.8
1040	26.14	8.933	0.0070	56.46	9.8	92.1	0.06	374.4 ± 2.5
1055	26.46	9.008	0.0083	39.89	6.9	90.7	0.05	373.7 ± 2.5
1080	26.59	9.463	0.0089	33.38	5.8	90.1	0.05	373.7 ± 2.5
1100	27.09	11.12	0.0108	26.95	4.7	88.2	0.04	375.0 ± 4.9
1120	28.72	12.53	0.0170	14.31	2.5	82.5	0.04	374.2 ± 2.8
Fuse	28.80	17.65	0.0184	22.67	3.9	81.2	0.02	376.3 ± 3.5
TOTAL				577.69	100.0			374.0
PLATEAU AGE								374.7 ± 0.8
83-SD-4 HORNBLENDE		J = 0.010917						
450	52.92	1.303	0.1231	15.06	3.3	31.3	0.38	301.6 ± 5.5
725	25.03	3.082	0.0167	33.48	7.4	80.3	0.16	362.4 ± 2.8
920	22.90	6.101	0.0071	57.33	12.6	90.8	0.08	378.0 ± 2.5
950	22.74	6.991	0.0069	54.08	11.9	91.1	0.07	378.0 ± 2.6
1010	22.04	9.028	0.0063	121.5	26.8	91.6	0.05	372.6 ± 2.5
1065	22.03	9.953	0.0064	89.97	19.8	91.4	0.05	373.3 ± 2.5
1090	23.34	9.977	0.0108	18.27	4.0	86.4	0.05	373.7 ± 2.9
1120	22.29	10.21	0.0070	41.54	9.2	90.8	0.05	375.1 ± 2.5
1130	26.46	10.17	0.0215	8.01	1.8	76.0	0.05	373.1 ± 7.2
1150	25.26	10.10	0.0125	13.62	3.0	85.4	0.05	396.3 ± 5.2
1175	124.0	9.789	0.3549	0.46	0.1	15.5	0.05	357.0 ± 65.2
Fuse	420.9	9.553	1.382	0.24	0.1	3.0	0.05	246.6 ± 198.1
TOTAL				453.60	100.0			371.9
PLATEAU AGE								373.5 ± 0.9
83-SD-6 HORNBLENDE		J = 0.010892						
450	79.11	3.842	0.2030	3.68	0.9	24.2	0.13	346.9 ± 20.0
725	41.29	2.903	0.0774	10.77	2.8	44.6	0.17	334.2 ± 5.6
920	25.89	9.350	0.0209	21.19	5.4	76.2	0.05	364.7 ± 3.0
980	23.11	10.27	0.0097	58.77	15.0	87.6	0.05	374.5 ± 2.7
1025	23.65	10.34	0.0127	37.02	9.5	84.1	0.05	369.2 ± 3.0
1040	24.89	10.20	0.0154	16.40	4.2	81.7	0.05	376.0 ± 3.3
1080	22.99	10.48	0.0094	45.85	11.7	88.0	0.05	374.6 ± 2.7
1090	23.49	10.83	0.0110	31.67	8.1	86.2	0.05	375.4 ± 2.8
1110	23.03	11.34	0.0099	35.98	9.2	87.3	0.04	373.8 ± 2.9
1130	22.66	11.39	0.0081	42.28	10.8	89.5	0.04	376.6 ± 2.6
1150	23.01	11.26	0.0089	28.79	7.3	88.6	0.04	378.4 ± 3.2
Fuse	22.62	9.508	0.0091	59.55	15.2	88.2	0.05	368.6 ± 2.8
TOTAL				391.96	100.0			371.8
PLATEAU AGE								374.3 ± 2.5

TABLE 1. CONTINUED.

Temp °C	$^{40}Ar/^{39}Ar$	$^{37}Ar/^{39}Ar$	$^{36}Ar/^{39}Ar$	Moles ^{39}Ar	^{39}Ar %Total	%^{40}Ar RAD	K/Ca	Apparent Age Ma
HQD-618-3A HORNBLENDE		J = 0.005865						
550	74.39	1.605	0.1785	2.79	0.9	29.1	0.31	216.9 ± 8.0
850	75.93	1.223	0.1447	5.93	2.0	43.7	0.40	321.9 ± 4.5
1020	58.78	4.168	0.0730	12.49	4.2	63.3	0.12	359.8 ± 3.4
1065	50.91	11.82	0.0419	22.21	7.4	75.7	0.04	378.2 ± 2.8
1090	49.39	12.58	0.0354	18.16	6.1	78.8	0.04	382.2 ± 2.9
1100	48.80	12.38	0.0343	19.04	6.4	79.3	0.04	379.9 ± 2.7
1110	51.64	12.04	0.0448	11.49	3.8	74.36	0.04	377.2 ± 3.1
1120	50.86	11.67	0.0418	32.76	11.0	75.75	0.04	378.0 ± 3.0
1130	49.87	11.34	0.0381	12.93	4.3	77.42	0.04	378.4 ± 2.9
1140	50.11	11.22	0.0391	17.94	6.0	76.94	0.04	377.8 ± 2.9
1150	50.44	11.00	0.0416	11.40	3.8	75.65	0.04	374.2 ± 3.1
1170	45.83	10.77	0.0245	15.59	5.2	84.20	0.05	377.7 ± 2.7
1180	46.40	10.72	0.0271	21.10	7.1	82.72	0.05	375.9 ± 2.7
1200	49.34	11.11	0.0369	12.81	4.3	77.92	0.04	376.8 ± 4.1
1220	54.38	11.37	0.0537	12.62	4.2	70.82	0.04	377.6 ± 3.2
Fuse	43.83	10.91	0.0184	69.53	23.3	87.60	0.05	376.2 ± 2.6
TOTAL				298.78	100.0			374.2
PLATEAU AGE								377.2 ± 1.5

TABLE 2. INCREMENTAL RELEASE AND TOTAL FUSION DATA FOR BIOTITES FROM THE HORSERACE QUARTZ DIORITE AND KATAHDIN GRANITE (83-SD-1 AND 83-SD-2). MOLES ^{39}Ar HAS BEEN MULTIPLIED BY 10^{14} AND %$^{40}Ar_{RAD}$ REPRESENTS THAT PORTION OF THE ^{40}Ar DERIVED BY DECAY OF ^{40}K.

Temp °C	$^{40}Ar/^{39}Ar$	$^{37}Ar/^{39}Ar$	$^{36}Ar/^{39}Ar$	Moles ^{39}Ar	^{39}Ar %Total	%^{40}Ar RAD	K/Ca	Apparent Age Ma
83-SD-1 BIOTITE		J = 0.009406						
650	16.10	0.0988	0.0118	252.2	16.1	78.3	4.96	202.2 ± 1.9
730	25.84	0.0230	0.0028	225.6	14.4	96.8	21.3	381.1 ± 2.5
890	26.14	0.0292	0.0013	241.9	15.5	98.5	16.8	391.2 ± 2.5
980	28.42	0.0312	0.0008	322.2	20.6	99.2	15.7	424.3 ± 2.7
1090	25.82	0.0471	0.0007	429.8	27.5	99.2	10.4	389.5 ± 2.5
1130	26.64	0.2334	0.0033	56.36	3.60	96.3	2.10	390.4 ± 3.3
1175	27.07	0.7211	0.0111	21.64	1.38	87.9	0.68	365.0 ± 7.3
Fuse	35.04	0.4531	0.0361	14.53	0.93	69.6	1.08	373.0 ± 6.8
TOTAL				1564.17	100.0			365.1
83-SD-1 TF BIOTITE		J = 0.006017						
Fuse	39.63	0.0509	0.0046	416.0	100.0	96.6	9.63	373.9 ± 2.4
83-SD-1 TF BIOTITE (duplicate)		J = 0.006017						
Fuse	39.57	0.0501	0.0046	323.4	100.0	96.6	9.78	373.2 ± 2.4
83-SD-2 BIOTITE		J = 0.009160						
500	20.55	0.0679	0.0109	115.0	4.59	84.3	7.22	265.7 ± 2.0
650	27.46	0.0097	0.0032	210.9	8.42	96.6	50.6	392.2 ± 2.8
830	27.34	0.0067	0.0012	692.0	27.6	98.8	73.6	398.6 ± 2.5
900	27.36	0.0131	0.0007	655.3	26.2	99.2	37.3	400.6 ± 2.6
980	27.49	0.0317	0.0017	801.5	32.0	98.8	15.5	400.7 ± 2.6
1050	28.12	0.5837	0.0034	23.9	0.96	96.4	0.84	400.7 ± 11.5
1100	41.03	0.6170	0.0544	4.89	0.20	60.8	0.80	372.0 ± 54.8
Fuse	186.15	0.7404	0.5511	1.25	0.05	12.5	0.66	350.0 ± 123.5
TOTAL				2504.83	100.0			393.1
PLATEAU AGE								400.1 ± 1.0

TABLE 2. CONTINUED.

Temp °C	$^{40}Ar/^{39}Ar$	$^{37}Ar/^{39}Ar$	$^{36}Ar/^{39}Ar$	Moles ^{39}Ar	^{39}Ar %Total	%^{40}Ar RAD	K/Ca	Apparent Age Ma
83-SD-2 TF BIOTITE		J = 0.006072						
Fuse	41.07	0.0438	0.0049	448.9	100.0	96.5	11.2	388.9 ± 2.5
83-SD-2 TF BIOTITE (duplicate)		J = 0.006072						
Fuse	41.28	0.0456	0.0052	298.1	100.0	96.3	10.7	389.9 ± 2.5
83-SD-3 BIOTITE		J = 0.009419						
600	10.03	0.2597	0.0478	0.01	0.8	41.5	1.89	162.9 ± 13.4
750	14.94	0.1082	0.0073	0.02	3.4	87.4	4.53	237.5 ± 1.7
840	24.16	0.0153	0.0024	0.15	23.3	97.1	32.0	369.8 ± 2.4
920	24.83	0.0182	0.0016	0.07	10.2	98.2	26.9	379.2 ± 2.5
1000	25.22	0.0357	0.0013	0.17	26.2	98.5	13.7	384.5 ± 2.5
1060	24.63	0.0358	0.0008	0.17	26.3	99.0	13.7	376.4 ± 2.5
1100	24.54	0.0730	0.0025	0.06	9.4	97.1	6.7	375.1 ± 2.6
Fuse	24.38	0.1433	0.1693	0.00	0.5	32.8	3.42	373.0 ± 12.4
TOTAL				0.66	100.00			370.8 ± 2.6
83-SD-8 BIOTITE		J = 0.010850						
375	83.51	0.3564	0.2508	1.66	0.2	11.3	1.38	175.8 ± 175.7
475	9.58	0.3379	0.0212	10.29	1.3	34.7	1.45	64.3 ± 11.6
625	21.70	0.0225	0.0023	170.3	20.8	96.9	21.8	370.7 ± 2.4
870	22.58	0.0343	0.0017	145.3	17.7	97.8	14.3	387.6 ± 2.6
970	22.59	0.0282	0.0011	125.4	15.3	98.6	17.4	390.7 ± 2.7
1100	22.53	0.0658	0.0021	117.1	14.3	97.2	7.45	384.6 ± 3.4
Fuse	22.25	0.0615	0.0022	249.7	30.5	97.1	7.96	379.7 ± 2.5
TOTAL				819.85	100.0			377.2
83-SD-8 TF BIOTITE		J = 0.006176						
Fuse	38.49	0.0553	0.0027	497.3	100.0	97.9	8.86	377.5 ± 2.5

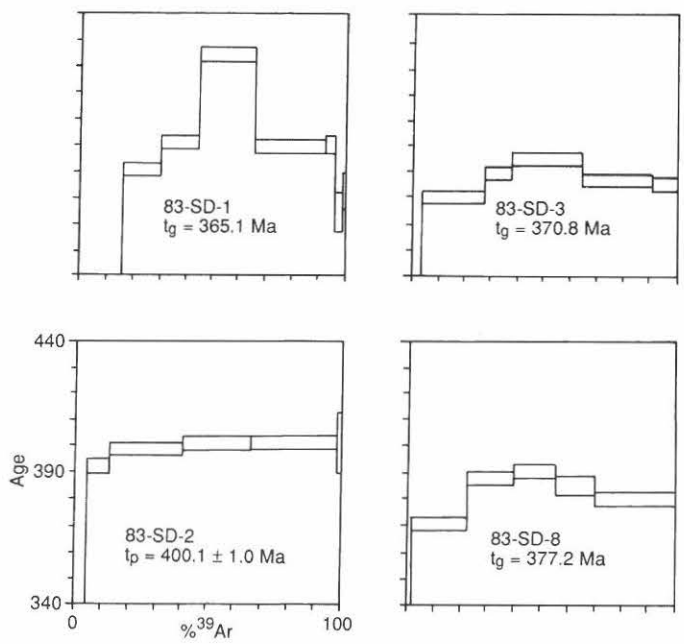

Figure 5. Age spectra of biotite from samples of the Horserace quartz diorite and Katahdin granite (83-SD-1 and 83-SD-2; see Table 2). The vertical and horizontal scales are all as shown in the lower left. The box height for individual increments represents 2 sigma uncertainties. t_p - plateau age, t_g - total gas age.

cal error, with a mean of 374.9 ± 1.6 Ma. This is interpreted as the time since the Horserace quartz diorite cooled through 550°C, the closure temperature calculated for these hornblende samples.

Biotite from the Katahdin granite, sample 83-SD-2 exhibits a well defined plateau, with 87% of the gas having the same calculated age 400.1 ± 1.0 Ma. Like the other plateau spectra, it steps up from very low ages in the first increment, suggesting minor episodic loss of $^{40}Ar_{Rad}$. The effect of this is seen in the fact that the total gas age is only 393.1 Ma. Ages obtained by the total fusion technique were also low, 388.9 Ma and 389.9 Ma. The plateau age of 400.1 ± 1.0 Ma is therefore probably a better estimate of the age of the Katahdin granite than the total fusion or total gas ages.

All other biotite samples analyzed exhibit unexpected "hump-shaped" release spectra. These spectra show anomalously low ages in early, low temperature release increments, as would spectra characteristic of $^{40}Ar_{Rad}$ loss. Ages for intermediate temperature increments are anomalously high, considerably older than the hornblende age of the rocks. Finally, at the higher temperatures and upon fusion of the sample, the ages of the gas released step back down.

Biotite sample 83-SD-1, also from the Katahdin granite, yields a total gas age of only 365.1 Ma, whereas biotite from the

same sample analyzed by the total fusion method yields ages of 373.2 and 373.9 Ma. These ages are difficult to reconcile with the total fusion and total gas ages of biotite from 83-SD-2 at 388.9, 389.9, and 393.1 Ma, respectively. One possible explanation could be Ar loss during a later heating event because the sample was collected within five dike widths of a basaltic dike. In light of these difficulties, the age of the Katahdin granite is not well determined by data presented in this paper, but the single plateau age of 400.1 ± 1.0 Ma for 83-SD-2 is the best estimate from the available $^{40}Ar/^{39}Ar$ data. This estimate falls halfway between the previously published Rb/Sr and U/Pb ages for the Katahdin granite.

CONCLUSIONS

The age of the Katahdin granite is not well determined by the data presented here. The hump-shaped biotite release spectra are problematic and the ages they yield should be used only with great caution. However, in this and other studies (Hubacher and Lux, 1987; Heizler, 1985; Tetley and McDougall, 1978), total gas ages for biotites with "hump-shaped" spectra have ages that are equal to hornblende plateau ages and in that respect appear to be meaningful. A single plateau spectrum (83-SD-2), however, is interpreted as the best estimate of the age of the Katahdin granite, 400.1 ± 1.0 Ma.

Recent age determinations by Hubacher and Lux (1987) for three small plutons southwest of Houlton, Maine, and by Gaudette and Boone (1985) for the Lexington pluton suggest that these may also be about 400 Ma in age. These occur along strike with the Katahdin batholith and the northeast-trending major axis of deformation of the Appalachians and probably represent an early belt of post-Acadian plutons.

The age of the Horserace quartz diorite is much more certain. The plateau ages of the four hornblende samples analyzed clearly indicate the quartz diorite had cooled to the hornblende closure temperature (about 550°C) 375 Ma ago. The two biotites from the Horserace quartz diorite have total gas ages that average 374 Ma and probably date the cooling through the biotite closure temperature, approximately 350°C. The rapid cooling rate implied for the temperature interval between biotite and hornblende closure temperatures can be confidently inferred back to solidus temperatures, and thus the concordant hornblende and biotite ages effectively date the time of intrusion of the Horserace quartz diorite at 375 Ma. This interpretation is also consistent with field relations which demonstrate that the Horserace quartz diorite is intrusive into the Katahdin granite.

The disparity between the ages of the Horserace quartz diorite and the Katahdin granite suggests that the assumption of contemporaneous cooling of the two units is invalid. Furthermore, the concordant biotite total gas ages and hornblende plateau ages for samples from the Horserace quartz diorite and the implied rapid cooling require that the host rocks, i.e. the Katahdin granite, were cool (less than the biotite closure temperature) when the Horserace quartz diorite was emplaced.

This is inconsistent with field observations described above which suggested that the Katahdin granite was still at least partially molten. Solidus temperatures for Katahdin granite magma are considerably lower than liquidus temperatures for Horserace quartz diorite, so it is conceivable that the latter Horserace quartz diorite magma may have locally melted some of the Katahdin granite upon intrusion along the fault it is observed to follow, thus producing the contact relationships.

The age of the Katahdin granite is constrained by the calculated age of the Horserace quartz diorite as at least 375 Ma old, because intrusive relationships clearly indicate the Katahdin granite is older than the Horserace quartz diorite. The assumption that the Katahdin granite and Traveler rhyolite are contemporaneous has not been rigorously tested in this paper. If this assumption is valid, then the age of the late Siegenian is at least as old as 375 Ma, and probably closer to 400 Ma. We recommend that further attempts to fix the absolute age as a geologic time scale calibration should concentrate on a direct determination of the age of the Traveler rhyolite.

ACKNOWLEDGMENTS

The authors would like to express their sincere appreciation to D. W. Rankin and L. L. Chyi for very helpful reviews of the manuscript. This work was supported by a grant (EAR-82-06549) from the National Science Foundation.

REFERENCES CITED

Alexander, E. C., Michelson, G. M., and Lanphere, M. A., 1978, MMhb-1: a new $^{40}Ar/^{39}Ar$ standard, *in* Zartman, R. E. (ed.), Short papers of the Fourth International Conference, Geochronology, Cosmochronology, Isotope Geology: U.S. Geol. Surv., Open-File Rept. 78-701, p. 6-8.

Bottino, M. L., Schnetzler, C. C., and Fullagar, P. D., 1965, Rb-Sr whole rock age of the Traveler and Kineo rhyolites, Maine, and its bearing on the duration of the Early Devonian: Geol. Soc. Amer., Spec. Paper 87, p. 15.

Boucot, A. J., 1954, Age of the Katahdin granite: Am. Jour. Sci., v. 252, p. 144-148.

Boucot, A. J., 1975, Evolution and extinction rate controls, *in* Developments in paleontology and stratigraphy: Elsevier, Amsterdam, v. 1, 427 p.

Brown, C., and Hon, R., 1984, Trace element geochemistry of a strongly fractionated quartz diorite body -- the Horserace quartz diorite of north-central Maine: Geol. Soc. Amer., Abs. with Prog., v. 16, no. 1, p. 6.

Dalrymple, G. B., Alexander, E. C., Jr., Lanphere, M. A., and Kraker, G. P., 1981, Irradiation of samples using the Geological Survey TRIGA reactor: U.S. Geol. Surv., Prof. Paper 1176, 55 p.

Dodson, M. H., 1979, Theory of cooling ages, *in* Jager, E., and Hunziker, J. C. (eds.), Lectures in isotope geology: Springer-Verlag, New York, p. 194-202.

Gaudette, H. E., and Boone, G. M., 1985, Isotopic age of the Lexington batholith: constraints on the timing of intrusion and Acadian metamorphism in western Maine: Geol. Soc. Amer., Abs. with Prog., v. 17, p. 19-20.

Griscom, A., 1976, Bedrock geology of the Harrington Lake area, Maine: Ph.D. dissert., Harvard Univ., Cambridge, 373 p.

Hall, B. A., Pollock, S. G., and Dolan, K. M., 1976, Lower Devonian Seboomook Formation and Matagamon Sandstone, northern Maine: a flysch basin-marginal delta complex, *in* Page, L. R. (ed.), Contributions to the stratigraphy of New England: Geol. Soc. Amer., Mem. 148, p. 57-63.

Harrison, T. M., 1981, Diffusion of ^{40}Ar in hornblende: Contrib. Miner. Petrol., v. 78, p. 324-331.

Harrison, T. M., Duncan, I. J., and McDougall, I., 1985, Diffusion of ^{40}Ar in biotite: temperature, pressure, and compositional effects: Geochemica et Cosmochemica Acta, v. 49, p. 2461-2468.

Heizler, M. T., 1985, Implications of ^{40}Ar/^{39}Ar incremental release geochronology of hornblende, biotite, and K-feldspar on the cooling history and proposed cooling model for the Chain of Ponds, Spider Lake, and Big Island Pond plutons, western Maine and Quebec: M.S. thesis, Univ. Maine, Orono, Maine, 212 p.

Hon, R., 1976, Geology, petrology and geochemistry of the Traveler rhyolite and Kathadin pluton (north-central Maine): Ph.D. dissert., Massachusetts Institute of Technology, Cambridge, 239 p.

Hon, R., 1980, Geology and petrology of igneous bodies within the Katahdin pluton, *in* Roy, D. (ed.), New England Intercollegiate Geological Conference guidebook for field trips in northeastern Maine and neighboring New Brunswick, p. 65-79.

Hubacher, P. A., and Lux, D. R., 1987, Timing of Acadian deformation in northeastern Maine: Geology, v. 15, p. 80-83.

Loiselle, M., Hon, R., and Naylor, R. S., 1983, Age of the Katahdin batholith, Maine: Geol. Soc. Amer., Abs. with Prog., v. 15, no. 3, p. 146.

Palmer, A. R., 1983, The decade of North American Geology Geologic Time Scale: Geol. Soc. Amer., Map and Chart Series MC-50.

Pollock, S. G., Boucot, A. J., and Hall, B. A., 1988, Lower Devonian deltaic sedimentary environments and ecology - examples from the Matagamon Sandstone, northern Maine, *in* Tucker, R. D., and Marvinney, R. G. (eds.), Studies in Maine Geology, Volume 1 - structure and stratigraphy, p. 81-99.

Rankin, D. W., 1961, Bedrock geology of the Katahdin-Traveler area, Maine: Ph.D. dissert., Harvard Univ., Cambridge, Mass., 317 p.

Rankin, D. W., 1980, The Traveler rhyolite and its Devonian setting, Traveler Mountain area, Maine, *in* Roy, D. (ed.), New England Intercollegiate Geological Conference guidebook to field trips in northeastern Maine and neighboring New Brunswick, p. 98-113.

Rankin, D. W., and Hon, R., 1987, Traveler rhyolite and overlying Trout Valley Formation and Kathadin pluton; a record of basin sedimentation and Acadian magmatism, north-central Maine: Geol. Soc. Amer., Centennial Field Guide - Northeastern Section, v. 5, p. 293-301.

Steiger, R. H., and Jager, E., 1977, Subcommission on geochronology: convention on the use of decay constants in geo- and cosmochronology: Earth and Planet. Sci. Lett., v. 36, no. 3, p. 359-362.

Spjeldnaes, N., 1978, The Silurian system, *in* Cohee, G. V., Glaessner, M. F., and Hedberg, H. D. (eds.), Contributions to the geologic time scale: Amer. Assoc. Petrol. Geol., Tulsa, Oklahoma, p. 341-345.

Tetley, N., and McDougall, I., 1978, Anomalous ^{40}Ar/^{39}Ar release spectra for biotites from the Berridale batholith, New South Wales, Australia, *in* Zartman, R. E. (ed.), Short Papers of the Fourth International Conference, Geochronology, Cosmochronology, Isotope Geology: U.S. Geol. Surv., Open-File Report 78-701, p. 427-430.

Maine Geological Survey
Studies in Maine Geology: Volume 4
1989

Interpretation of the Regional Significance of the Chain Lakes Massif, Maine based upon Preliminary Isotopic Studies

Michael M. Cheatham*
William J. Olszewski
Henri E. Gaudette
Institute for the Study of Earth, Oceans and Space
Science and Engineering Research Building
University of New Hampshire
Durham, New Hampshire 03824

**Present address:*
Department of Geological Sciences
Snee Hall
Cornell University
Ithaca, New York 14853

ABSTRACT

The Chain Lakes massif of northwestern Maine and adjacent Quebec contrasts sharply in lithology, metamorphism, deformation, and age with surrounding rocks, and has been considered a suspect terrane in the northern Appalachians. The massif is composed of aquagene metavolcanic and metasedimentary rocks, massive granofels and poorly stratified gneisses containing clasts of volcanic, plutonic, and sedimentary rocks which show evidence of previous deformation and metamorphism. Rocks of the Chain Lakes massif have been metamorphosed to upper amphibolite-granulite facies, although a later retrograde event (epidote-pumpellyite facies) is also recognized. Mild thermal effects and cataclasis resulted from overthrusting of the Boil Mountain ophiolite in the southern portion of the massif.

The massif has generally been assigned a Precambrian age. Although previous age work on the massif is ambiguous, stratigraphic constraints and isotopic results from surrounding rocks constrain the age of the massif only to the pre-Late Ordovician.

A total of 40 whole rock samples have been petrographically examined, 27 of which were analyzed by Rb-Sr and Sm-Nd isotopic techniques in order to determine the number, grades, and ages of the various metamorphic events affecting the massif, the age of the protolith material, and to constrain the age of deposition of the material in the massif. Petrographically, two distinct mineral assemblages characterize the rocks of the Chain Lakes massif. The first consists of quartz-plagioclase-sillimanite-biotite-muscovite, and relict K-feldspar (largely altered to white mica and epidote). The relict K-feldspar suggests second sillimanite grade associated with the upper amphibolite-granulite facies metamorphism. The second assemblage consists of extensive growth of chlorite, muscovite, epidote, and calcite, associated with retrograde metamorphism.

The Rb-Sr whole rock results are scattered, but yield an errorchron age of 684 ± 76 Ma. This is interpreted to represent the high-grade metamorphic event and resetting of the Rb-Sr whole rock systems at that time. Rb-Sr mineral analyses of three samples yield ages of 378, 394, and 419 Ma, interpreted as the result of resetting during a retrograde metamorphic event, possibly related to Acadian metamorphism and intrusion. Sm-Nd whole rock results are too limited to provide an isochron, but calculated crustal residence ages relative to depleted mantle range from

1050 to 1796 Ma. These crustal residence ages are in agreement with the Sr evolution of the massif (Sr crustal residence age of 1457 Ma) and zircon U-Pb results (1534 Ma).

The sedimentary rocks of the Chain Lakes massif were probably deposited between ~684 Ma and ~1500 Ma. The timing of the metamorphic events and the crustal residence ages for the massif are similar to other areas in New England, but no definitive correlations can be made at present. The isotopic signatures of the massif are similar to high-grade terrains of comparable age from other areas around the world.

The petrographic and isotopic results reinforce the unique nature of the Chain Lakes massif and point out the importance of the massif in understanding the tectonic evolution of the northern Appalachian orogen.

INTRODUCTION

The Chain Lakes massif of northwestern Maine and adjacent Quebec (Fig. 1) is composed dominantly of metamorphic rocks. Lying within the Gander Superterrane of Williams and Hatcher (1983), the Chain Lakes massif contrasts strikingly in lithology, metamorphic grade, and structural style with the surrounding Paleozoic rocks and is itself considered a "suspect terrane" (Williams and Hatcher, 1983; Zen, 1983a).

The age, origin, and relationships of the Chain Lakes massif to the surrounding rocks are uncertain, and except for small enclaves of Chain Lakes-like rocks in Quebec, no similar rocks are known in New England. In this regard, the massif is unusual, and an understanding of its geology, age, and evolution should reveal information pertaining to the early tectonic development of this part of the northern Appalachians. This paper reports the application of Rb-Sr and Sm-Nd whole rock isotopic methods and Rb-Sr mineral isotopic analyses to rocks of the massif. These analyses were carried out in order to obtain information about the age and origin of the Chain Lakes massif, the timing of thermal events affecting the rocks of the massif, and to provide information on the tectonic evolution of the massif in a regional context.

GEOLOGY OF THE CHAIN LAKES MASSIF

Lithology and Stratigraphy

The upper 1 km of the Chain Lakes massif is composed of aquagene metavolcanic and metasedimentary rocks. The

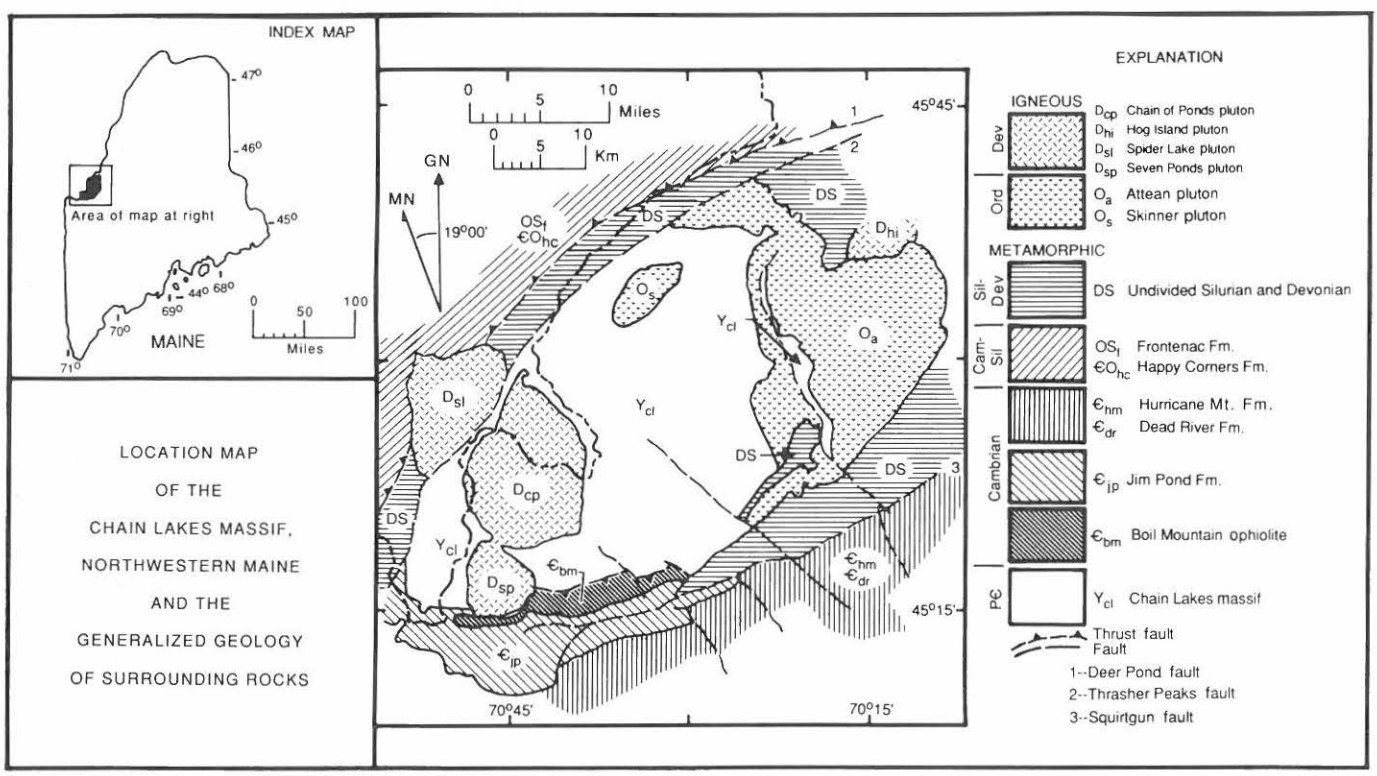

Figure 1. Location map of the Chain Lakes massif in northwestern Maine and the generalized geology of the surrounding rocks (from Moench, 1984).

remainder of the exposed massif consists dominantly of massive granofels to poorly stratified gneisses (Boudette et al., 1984). The term granofels, which has been applied to most of the rocks of the lower sequence of the Chain Lakes massif, is used to indicate high-grade metamorphic rocks where layering is cryptic or absent. Those units described as gneisses show a foliation interpreted to be parallel to compositional layering (Boudette, 1970; Biederman, 1984).

The granofels and gneisses consist of rocks with pebble- to boulder-sized clasts of vein quartz, mafic and felsic plutonic and volcanic rocks, and sedimentary rocks which show evidence of previous deformation and metamorphism (Boudette, 1970; Boudette and Boone, 1982). The clasts are supported by a matrix of quartz, plagioclase, biotite, chlorite, muscovite, and sillimanite (Boudette, 1970; Albee and Boudette, 1972; Boudette and Boone, 1982; Biederman, 1984; Boudette et al., 1984).

Boudette et al. (1984) divided the lower sequence of the Chain Lakes massif into eight geographic/lithologic units (Fig. 2). These are: (1) semipelitic gneiss at Twin Bridges; (2) layered granofels and gneiss at Bag Pond Mountain; (3) granofels and gneiss at Sarampus Falls; (4) massive granofels at Bugeye Pond; (5) polycyclic breccia at McKenney Pond; (6) spotted granofels at Kibby Mountain; (7) polymictic breccia at Kibby Mountain; and (8) diorite.

The stratigraphic relationships between these units are uncertain, although the diorite intrudes the spotted granofels at Kibby Mountain (6). Other than this relationship, no stratigraphic sequence is implied by the above list.

The metamorphic history of the massif is complex and still uncertain. The Chain Lakes massif has been metamorphosed to upper amphibolite-granulite facies (Boudette and Boone, 1982; Beiderman, 1984), but Boudette (1982) also recognized a retrograde metamorphic event of at least epidote-pumpellyite facies in both the Chain Lakes massif and the surrounding pre-Silurian rocks. He suggested an Ordovician age for this retrograde metamorphism. Additionally, local fault-related retrograde contact metamorphism due to the emplacement of the Boil Mountain ophiolite has affected the rocks of the massif. This zone is recognized by an increase in the size and amount of muscovite in the matrix of the rocks as the contact with the ophiolite complex is approached. The Devonian stratigraphic section around the Chain Lakes massif shows the effects of an Acadian prograde metamorphism to chlorite-biotite grade (Albee and Boudette, 1972; Biederman, 1984) prior to the intrusion of the undeformed and unmetamorphosed Lexington batholith at 399 Ma (Gaudette and Boone, 1985). Although the Acadian metamorphism appears to have had minimal effects on the mineralogy of the rocks of the massif, its effects on the Rb-Sr mineral ages are evident (see below).

Structure and Relationships to Surrounding Rocks

The Chain Lakes massif is bounded on the north, northwest, and west by the Thrasher Peaks fault (Fig. 1) which separates the massif from the cyclically bedded, well-graded, light gray to dark gray turbidites (Boucot, 1961; Albee and Boudette, 1972) of the Seboomook Group (Boudette et al., 1984; Boudette and Boone, 1984; Pollock, 1987). The Seboomook Group contains an early Devonian, Gedinnian-Siegenian age fossil assemblage (Boucot, 1961; Albee and Boudette, 1972).

The Attean pluton (Boudette, 1982; Lyons et al., 1983; Aleinikoff and Lyons, 1984), a hornblende-bearing quartz monzonite, intrudes the massif in the east. The eastern flank of the Attean pluton is unconformably overlain by the rocks of the Silurian and Devonian Moose River sequence (Boucot, 1961; Albee and Boudette, 1972; Boudette et al., 1984). This Siluro-Devonian sequence unconformably overlies the Chain Lakes massif (Boudette, 1970; Boudette et al., 1984) south of the Attean pluton (Fig. 1).

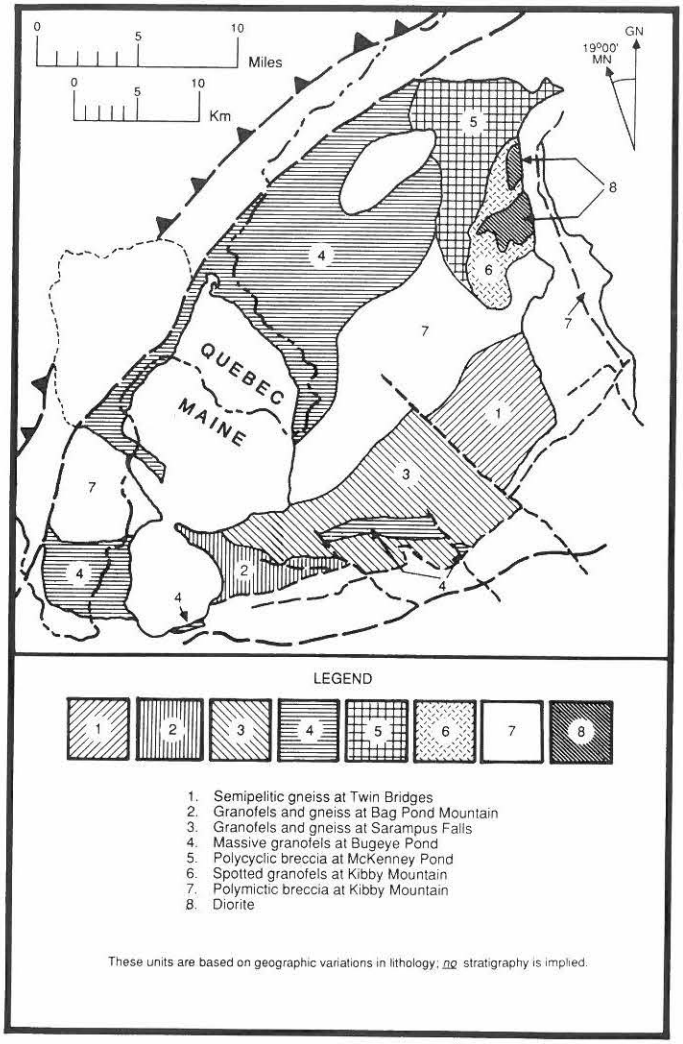

Figure 2. Geologic map (from Boudette et al., 1984) of the Chain Lakes massif showing the geographic variations in lithology. No stratigraphy is impled by these units.

To the southeast, south, and southwest the Chain Lakes massif is in contact with the Boil Mountain ophiolite and the Jim Pond Formation (Boudette, 1982). The Boil Mountain ophiolite is composed of layered harzburgite/lherzolite and pyroxenite, epidiorite/gabbro and clinopyroxenite, and calcic plagiogranite (Boudette, 1982). The Jim Pond Formation consists of pillow basalts at the base, overlain by vent facies felsic volcanic rocks, iron formation, and metaclastic rocks including mélange and quartzwacke olistostrome (Boudette, 1982). The contact of the Chain Lakes massif with the ophiolite complex is interpreted as a tectonic surface, probably a thrust fault along which the ophiolite complex has been ramped up on the massif (Boudette, 1982). Mild thermal metamorphism and cataclasis is associated with this contact (Boudette, 1982; and discussed above). The present contact between the Chain Lakes massif and the Boil Mountain ophiolite dips steeply to the south. The Jim Pond Formation overlies the Boil Mountain ophiolite and is also thrust over the massif along its southwesternmost margin.

In the west and southwest, the massif is intruded by the Chain of Ponds pluton, dominantly composed of granite with hornblende-bearing granodiorite, and the Seven Ponds pluton, a granite. On the northwest, the Chain Lakes massif is in fault contact with the Spider Lake pluton along the Thrasher Peaks fault (Fig. 1). A small body of granodiorite known as the Skinner pluton intrudes completely within the massif (Figs. 1, 2).

Preliminary interpretations of seismic reflection profiling (Stewart et al., 1985, 1986) from the Chain Lakes region showed that the massif is apparently floored by a southeasterly dipping décollement. They interpret this as a southeast over northwest thrust of either Acadian or Taconic age. The rocks of the Chain Lakes massif can be interpreted as allochthonous, and most probably derived from the southeast.

Besides the parts of the massif proper which occur across the international border in Quebec, small areas of Chain Lakes-like rocks occur to the northwest in Quebec (Williams and St-Julien, 1982; Cousineau and St-Julien, 1986).

Previous Work on the Age and Origin of the Chain Lakes Massif

Early geologic mapping in the Chain lakes massif was done by Marleau (1957) in Canada, and by Albee (1961) and Green and Guidotti (1968) who assigned rocks of the massif to the Ordovician, through correlation with the Ammonoosuc volcanics. Harwood (1970, 1973), working in the westernmost part of the massif, also considered the rocks of the Chain Lakes massif to be Ordovician in age, but assigned the rocks to the Magalloway Member of the Dixville Formation. West of the Seven Ponds pluton, Harwood (1973) described a coarse-grained biotite gneiss containing rounded masses of clear to milky white granular quartz in a matrix of quartz, plagioclase, biotite, muscovite, chlorite, sillimanite, and magnetite. This gneiss was also mapped as roof pendants within the Seven Ponds pluton (Harwood, 1973). Albee and Boudette (1972), while working in the eastern portion of the massif, recognized a similar lithology which they referred to as the "granofels unit", and assigned it to the pre-Silurian. Thin section study of this unit showed it to consist of quartz, feldspar (altered to white mica and clinozoisite), biotite, muscovite, chlorite, and more rarely sillimanite and garnet. Abundant polymictic lithic fragments were also noted.

Ages of the surrounding rocks constrain the age of the rocks of the Chain Lakes massif. Zircons from the Attean pluton yield an upper intercept age of 443 ± 4 Ma (Lyons et al., 1986). Zartman et al. (1970) report a K/Ar age of 370 Ma for the Chain of Ponds pluton. Lux (1983) obtained a $^{40}Ar/^{39}Ar$ hornblende age of 371 Ma for the Spider Lake pluton. Zircons from the calcic plagiogranite of the Boil Mountain ophiolite gave an age of 520 ± 12 Ma (Eisenberg, 1981). U-Pb analyses of zircons from the Jim Pond Formation give an age of 500 ± 10 Ma (Aleinikoff and Moench, 1985). The available isotopic results thus support a middle Ordovician or older age for the Chain Lakes massif.

The rocks of the Chain Lakes massif were originally assigned to the Precambrian by Ells (1887). Boudette (1970, 1982), Naylor et al. (1973), St-Julien and Hubert (1975), Lyons et al. (1982), Zen (1983a), Williams and Hatcher (1983), Biederman (1984), Moench (1984), and Osberg et al. (1985) have all upheld this age assignment based on the limited isotopic studies of the rocks of the Chain Lakes massif by Naylor et al. (1973) and Biederman (1984). The Naylor et al. study used U-Pb analyses of zircons from the matrix of the granofels. They obtained an upper intercept age of 1534 ± 59 Ma and a lower intercept of 153 ± 126 Ma (these ages and errors are recalculated by the present authors from the original data; Naylor, pers. comm., 1985). The upper intercept age was interpreted by Boudette and Boone (1982) to represent the age of prograde metamorphism. However, these ages are based on only two zircon fractions which are approximately 50% discordant and very close to one another. The true errors for these ages are unknown; the errors quoted above are for an assumed 1% experimental error, and thus no estimate of scatter can be made. In addition, as we discuss below there is evidence that these zircons contain a large fraction of grains of detrital origin which may represent different sources with a wide range of ages.

Biederman (1984) did not propose an age for the high-grade metamorphism in the Chain Lakes massif, but did suggest that the rocks of the massif passed through a temperature of 500°C in the very late Precambrian to early Cambrian. This age assignment is based on the $^{40}Ar/^{39}Ar$ release spectra obtained from two samples of hornblende from the Bugeye Pond member.

The origin of the Chain Lakes massif is even more uncertain than its age. Boudette and Boone (1982) have suggested that the Chain Lakes massif represents one of the following features: a tillite, a tectonic mélange, an olistostrome, an explosive volcanic assemblage, a plutonic roof complex, an infracrustal rift zone, or a metasuevite (impact origin) complex. The question of its origin remains open.

ANALYTICAL METHODS

A total of 40 samples, each approximately 15-20 kg in weight, were collected from various units within the massif. Every effort was made to collect the freshest possible material. However, megascopic examination of samples in the laboratory resulted in selection of 27 samples from the McKenney Pond, Bugeye Pond, and Sarampus Falls members for isotopic analysis. Rb/Sr and Sm/Nd whole rock and Rb/Sr mineral analyses were carried out in conjunction with petrographic examination of the rocks. Modal abundances of the minerals in each sample were determined by visual estimation in thin section.

Each whole rock sample was prepared for isotopic analysis by standard techniques. Minerals were separated from the whole rock samples by standard heavy liquid and magnetic separation procedures. Sample dissolution and chemical separation of Rb and Sr from the whole rock and mineral samples was done using HF-$HClO_4$ acid and cation exchange procedures. Sm and Nd were separated on anion exchange resin using nitric acid-methanol mixtures (Faris and Warton, 1962).

The isotopic compositions of Rb, Sr, Sm, and Nd were determined on a Nier-type, 9-inch radius, 60° sector, solid source mass spectrometer in the Isotope Geochemistry Laboratory at the University of New Hampshire. Rb, Sr, and Sm were analyzed as metals, Nd as an oxide. Sr analyses were corrected for fractionation to $^{86}Sr/^{88}Sr = 0.1194$ (Steiger and Jager, 1977). Nd ratios were normalized to a $^{146}Nd/^{144}Nd$ ratio of 0.72413 (Wasserburg et al., 1981). Analytical errors from powder replicates are $^{87}Rb/^{86}Sr = 1.0\%$; $^{87}Sr/^{86}Sr = 0.07\%$; coefficient of correlation = 0.011; $^{147}Sm/^{144}Nd = 0.2\%$; $^{143}Nd/^{144}Nd = 0.02\%$; coefficient of correlation = 0.01. All errors quoted are $\pm 1.0\ \sigma_m$. Isochrons are calculated using the equations of York (1969). Decay constants are those recommended by Steiger and Jager (1977) for Rb and U; the λ value used for ^{147}Sm was 6.54×10^{-12} yr^{-1} (DePaolo and Wasserburg, 1976). Replicate analyses of Eimer and Amend standard Sr carbonate during the course of the study gave a value of 0.70793 ± 0.00005 ($1.0\ \sigma_m$; N = 22) for $^{87}Sr/^{86}Sr$. Analyses of standard whole rock BCR-1 for Nd yielded a value of 0.511863 ± 0.000013 ($1.0\ \sigma_m$; N = 8) for $^{143}Nd/^{144}Nd$, which agrees well with the accepted value of 0.511847 (Wasserburg et al., 1981).

TABLE 1. MINERAL MODES

Sample	Q+	F(An)	B	M	C	A	S	E	O
MCKENNEY POND									
397	31	32(24)	3	10	9	tr	8	2	3
398z1	27	31(21)	11	13	10	tr	5	tr	2
399	29	36(25)	9	10	11	tr	3	tr	1
400	28	25(19)	8	10	7	tr	17	2	2
401	30	26(20)	8	15	9	tr	4	3	1
404	35	28(26)	5	15	10	tr	3	1	3
405	32	33(24)	3	12	13	1	2	2	1
SARAMPUS FALLS									
416z1*	30	30(17)	18	12	tr	tr	-	1	1
417	40	38(18)	5	15	tr	tr	-	tr	1
418	35	31(22)	11	15	3	1	-	1	2
419	30	28(24)	10	20	8	1	tr	1	2
420	32	28(23)	12	15	8	tr	-	1	2
421	34	24(19)	10	16	14	tr	-	tr	1
422	38	27(25)	8	8	12	1	-	tr	2
423	34	34(18)	6	10	12	1	-	1	2
424	40	15(25)	10	23	10	tr	-	tr	tr
425	40	15(24)	15	27	tr	tr	-	2	tr
426	38	27(18)	tr	10	23	tr	-	tr	1
427	46	33(20)	12	8	tr	tr	-	tr	1
436	46	30(24)	3	10	5	tr	2	tr	2
BUGEYE POND									
428	40	30(19)	tr	12	15	tr	-	1	1
429	35	20(22)	tr	25	18	tr	-	1	tr
430	30	20(23)	tr	10	37	tr	tr	tr	1
431	40	37(19)	4	10	6	tr	tr	tr	2
432	35	34(20)	6	14	10	tr	-	tr	1
433	39	30(18)	6	10	9	tr	-	3	2
434	43	30(19)	15	5	3	tr	2	tr	1
435	47	35(24)	7	4	3	tr	2	1	1

+Q - Quartz; F(An) - Feldspar, dominantly plagioclase but may include some potassium feldspar, value in parentheses is the anorthite content of the plagioclase; B - Biotite; M - Muscovite; C - Chlorite; A - Apatite; S - Sillimanite; E - Epidote; O - Opaque minerals, including ilmenite, magnetite, sulfides, etc. Short dashes indicate minerals not detected in thin section. All samples contain trace amounts of zircon.
*This sample includes 3% staurolite and 5% andalusite. This sample has not been analysed isotopically.

RESULTS

Petrography

Petrographic and isotopic analyses were carried out on the Sarampus Falls (13 samples, one sample 416z1 was not analyzed isotopically), Bugeye Pond (8 samples), and McKenney Pond (7 samples) members. Modal abundances of major minerals for each sample are provided in Table 1. Boudette et al. (1984) have indicated a mappable difference between the Sarampus Falls and Bugeye Pond members. Our examination of the 21 samples of these two members in both hand specimen and thin section could find no consistent difference between the two members, and for this reason our petrographic descriptions for these two members are treated together.

Megascopically, the Sarampus Falls and Bugeye Pond samples are medium to dark gray, medium grained, quartz-plagioclase-biotite-muscovite-chlorite gneisses and/or granofels, with minor clasts of quartz + feldspar and rare clasts of metapelite. Foliation, when present, is most apparent on the outcrop scale, but is also discernible in some hand specimens and thin sections.

Thin section examination shows the following ranges in mineral compositions: 30-47% quartz, 5-35% plagioclase, 0-18% biotite (showing some alteration), 4-27% muscovite, 0-35% iron-rich chlorite, 0-2% sillimanite, and varying trace amounts of apatite, ilmenite, magnetite, carbonate, epidote, tourmaline, and zircon. We have tentatively identified potassium feldspar (altered to white mica and epidote) in a few samples, but no analyses or staining have been done to corroborate this. Potassium feldspar has also been identified by Biedermann (1984) within a portion of the Sarampus Falls member.

The samples from the McKenney Pond member are all very similar in their textural relationships and mineral assemblages. Megascopically, the rocks are medium to dark gray, medium grained, quartz-plagioclase-biotite-chlorite-muscovite-sillimanite granofels. The samples analyzed are generally massive and lack foliation.

Thin section examination provides the following ranges in mineral composition: 25-35% quartz, 10-21% plagioclase, 3-11% partially altered biotite, 7-13% chlorite, 10-15% muscovite, 2-17% fibrous sillimanite, and variable trace amounts of carbonate, apatite, epidote, ilmenite, magnetite, zircon, and pyrite. Clasts are present and are typically composed of coarse-grained quartz and feldspar. Less common are clasts of metapelite consisting of fibrous sillimanite, biotite, chlorite, and muscovite. Albee and Boudette (1972) reported clasts with hornblende in this member, although none were found in the thin sections we examined.

Rb/Sr Whole Rock Results

The Rb-Sr isotopic results are listed in Table 2. A plot of all of the results for the three members is given in Figure 3. These data yield a regression line (errorchron) with an age of 684 ± 76 Ma and initial ratio of 0.7156 ± 0.0014 (MSWD = 12.39). If the three members are treated separately, the resulting three errorchrons (Fig. 4) vary in age, but overlap at 1.0 σ. The separate regression results are: McKenney Pond: 849 ± 202 Ma, initial

TABLE 2. Rb-Sr WHOLE ROCK ANALYSES

Sample	Rb(ppm)	Sr(ppm)	$^{87}Rb/^{86}Sr$	$^{87}Sr/^{86}Sr$
SARAMPUS FALLS				
417	100	245	1.185	0.7269
418	92	241	1.103	0.7269
419	101	245	1.192	0.7263
420	90	290	0.899	0.7248
421	94	224	1.212	0.7304
422	123	187	1.909	0.7334
423	91	183	1.438	0.7325
424	89	147	1.755	0.7327
425	114	180	1.825	0.7306
426	81	290	0.811	0.7236
427	90	286	0.910	0.7239
436	103	232	1.291	0.7266
BUGEYE POND				
428	86	176	1.410	0.7281
429	84	218	1.115	0.7275
430	60	276	0.622	0.7214
431	80	216	1.070	0.7260
432	91	215	1.212	0.7267
433	90	282	0.928	0.7245
434	93	199	1.351	0.7303
435	76	202	1.088	0.7297
MCKENNEY POND				
397	50	131	1.099	0.7248
398z1	67	139	1.418	0.7335
399	53	179	0.853	0.7227
400	89	158	1.636	0.7306
401	72	166	1.259	0.7297
404	81	145	1.615	0.7288
405	47	190	0.710	0.7199

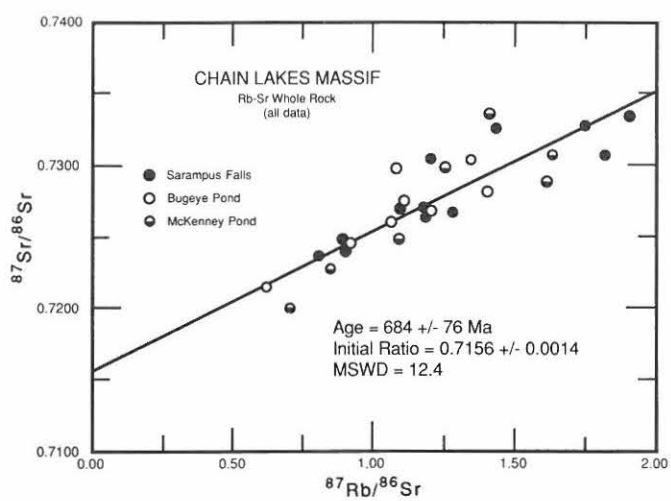

Figure 3. Rb-Sr whole rock diagram for all of the analyses of the Chain Lakes massif rocks carried out for this study. Errors are + 1.0 σ_m.

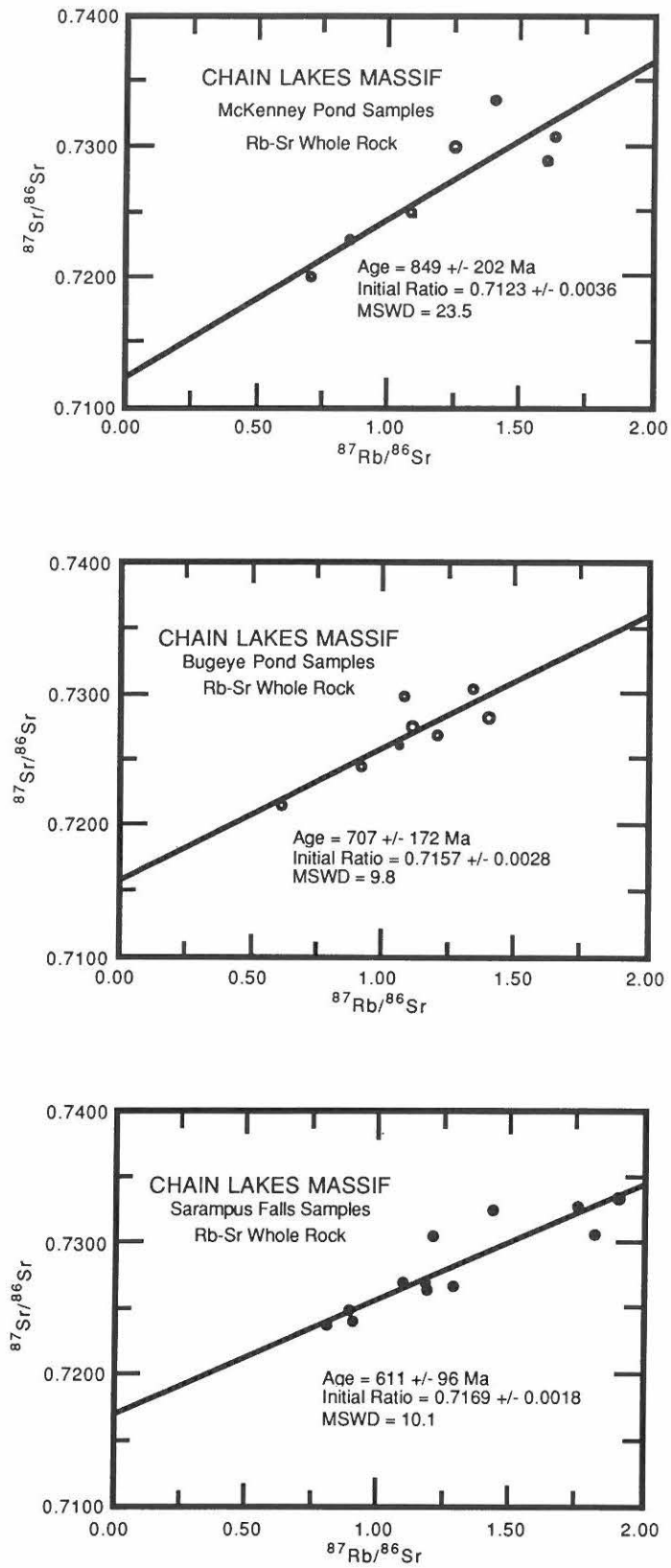

Figure 4. Rb-Sr whole rock diagrams for the individual lithologic units of the Chain Lakes massif. Errors are + 1.0 σ_m.

ratio = 0.7123 ± 0.0036, MSWD = 23.50; Bugeye Pond: 707 ± 172 Ma, initial ratio = 0.7157 ± 0.0028, MSWD = 9.83; Sarampus Falls: 611 ± 96 Ma, initial ratio = 0.7169 ± 0.0018, MSWD = 10.10.

There does not appear to be any significant difference in Rb and/or Sr contents of the three members (Table 2), or the relative positions of the three members on the isochron diagram (Fig. 3). This, combined with the generally similar mineralogies and textures of the the three members and similarity in rock type, led us to treat the isotopic results of all three members together. The results are obviously scattered, and the regression does not represent a true isochron. The scatter is probably the result of three major aspects of the Chain Lakes massif: (1) the granofels and gneiss represent a mixture of a number of rock types represented as clasts, each with a prior isotopic history; (2) the generally high grade of the early metamorphism of the massif which has most likely reset the Rb-Sr isotopic systematics on a whole rock scale; and (3) the variable effects of the Acadian metamorphism. In spite of these difficulties, we feel that the regression line "age" represents a significant event in the geologic evolution of the Chain Lakes massif. We interpret the regression line "age" as representing the approximate time of the first prograde metamorphic event that effected the massif. Our reasons for this interpretation are given in detail below.

Rb/Sr Mineral Analyses

Two samples of the Sarampus Falls member (UNH 420 and UNH 422) and one sample of the McKenney Pond member (UNH 401) were chosen for mineral separation and mineral Rb-Sr isotopic analyses. The individual mineral separates included a plagioclase fraction, muscovite fraction, and biotite fraction, and a heavy mineral fraction consisting mostly of opaque minerals (mainly magnetite, ilmenite, and pyrite), zircon, apatite, and biotite.

The results from these mineral analyses are listed in Table 3 and plotted in Figure 5. These mineral isochrons include the whole rock point for each sample. The isochron for UNH 401 does not include the heavy mineral or the biotite fraction, both of which were highly altered.

UNH 401 (McKenney Pond) gave an isochron (plagioclase-whole rock-muscovite) with an age of 378 ± 61 Ma, initial ratio = 0.7228 ± 0.0010, MSWD = 0.06. UNH 420 (Sarampus Falls) yields an isochron with an age of 419 ± 14 Ma, initial ratio = 0.7198 ± 0.0004, MSWD = 0.50; UNH 422 (Sarampus Falls) gives an isochron with an age of 394 ± 11 Ma, initial ratio = 0.7234 ± 0.0006, MSWD = 1.28. The ages for the three mineral isochrons agree within 1.0 σ of each other. We interpret these ages as representing a metamorphic event which reset the Rb-Sr isotopic systematics of the minerals. Ages ranging from 370 to 415 Ma are typical of ages for the Acadian orogeny in eastern New England. In northwestern Maine, near the Chain Lakes massif, the Acadian orogeny is constrained by the ages of the Attean quartz monzonite (443 Ma, Lyons et al., 1986), which has

TABLE 3. Rb-Sr MINERAL ANALYSES

Sample	Fraction	$^{87}Rb/^{86}Sr$	$^{87}Sr/^{86}Sr$
401	Feldspar	0.670	0.7264
	Muscovite	1.478	0.7307
420	Feldspar	0.549	0.7231
	Muscovite	3.702	0.7419
	Biotite	2.689	0.7356
	Heavy*	1.616	0.7299
422	Feldspar	1.218	0.7307
	Muscovite	6.475	0.7599
	Biotite	5.028	0.7512
	Heavy*	3.717	0.7447

*Heavy fraction is the suite of minerals that sinks in methylene iodide, no attempt was made to separate this fraction into separate pure mineral fractions.

been affected by Acadian metamorphism, and the Lexington batholith (399 Ma, Gaudette and Boone, 1985), which is unaffected by Acadian metamorphism. Plutons intruding the massif have dates as low as 370 Ma (see above). We interpret the mineral ages as representing resetting due to a combination of Acadian metamorphism and heating from the plutonic rocks that intrude the Chain Lakes massif. These events have undoubtedly contributed to the scatter seen in the combined whole rock regression line.

Sm/Nd Whole Rock Results

Sm-Nd isotopic analyses have been carried out on seven samples from the McKenney Pond member. The isotopic results are listed in Table 4. Although an isochron could not be drawn for these results because of the limited spread in $^{147}Sm/^{144}Nd$ ratios, crustal residence ages (T_{cr}) have been determined for each sample (Table 5). Crustal residence ages represent a hypothetical age at which the source of the material that makes up the massif was derived from a bulk earth source (CHUR, DePaolo and Wasserburg, 1976) or a depleted mantle (DM) source. The rocks of the Chain Lakes massif represent a mixture of sources and as a result, the crustal residence ages will represent a mixing age rather than the age at which a single and distinct source was derived from the mantle. Such mixture ages may have little to do with the geologic history or evolution of a rock unit (Arndt and Goldstein, 1987). However, other results (discussed below) suggest that the Chain Lakes crustal residence ages may provide information about the sources of material for the massif. The T_{cr} values are not affected by metamorphism, even high-grade metamorphism, as long as the Chain Lakes massif as a whole has remained a closed system. Our reasons for assuming closed system behavior for the Chain Lakes massif are discussed below.

The T_{cr} values for these seven samples range from 763 Ma to 1788 Ma with respect to CHUR, with an average of 1382 Ma. With respect to DM, the values range from 1050 Ma to 1796 Ma with an average of 1496 Ma. The implications of these T_{cr} values are discussed in more detail below.

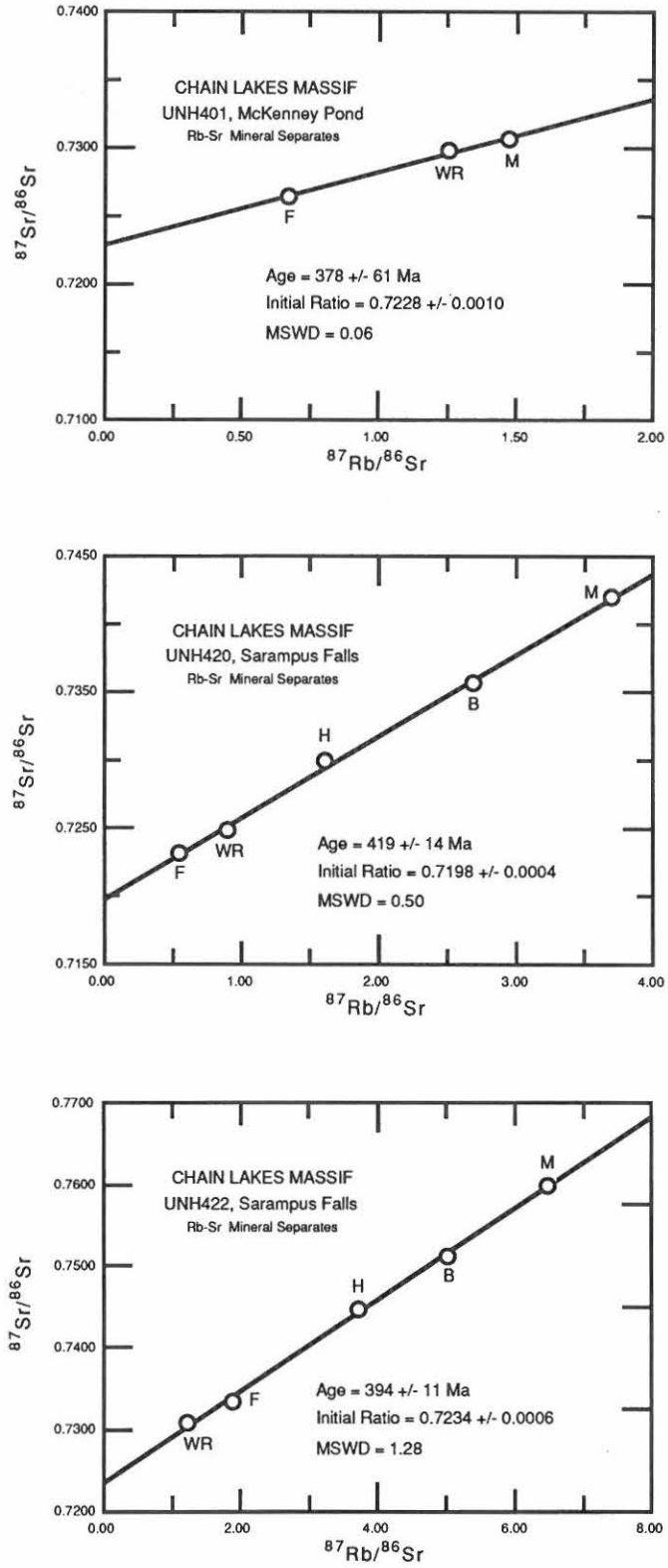

Figure 5. Rb-Sr mineral isochron diagrams for three samples of the Chain Lakes massif. F-feldspar fraction; WR-whole rock; H-heavy mineral fraction; B-biotite fraction; M-muscovite fraction. Errors are + 1.0 σ_m.

DISCUSSION

The mineral assemblages and textures of the Sarampus Falls, Bugeye Pond, and McKenney Pond members suggest that at least two, and possibly three, metamorphic events have affected the Chain Lakes massif. The first of these was a high-grade metamorphism that reached at least the first sillimanite isograd, and possibly the second sillimanite isograd (Biederman, 1984). Muscovite grew in all three members at the time of the high-grade metamorphism as shown by the inclusion of biotite in large muscovite grains. The rocks of the massif show high-grade textural equilibrium in the development of granoblastic and granoblastic-polygonal textures. The weak foliation seen in many of the rocks probably dates from this first high-grade event, since the foliation is generally defined by the high-grade minerals.

We interpret the 684 ± 76 Ma "age" as reflecting the resetting, either completely or partially, of the Rb-Sr systematics during this high-grade event. This "age" then gives at least an approximate age for the high-grade metamorphism.

There are a number of reasons for believing that the regression line age and the high-grade metamorphism are related:

TABLE 4. WHOLE ROCK Sm/Nd RESULTS

Sample	$^{147}Sm/^{144}Nd$	$^{143}Nd/^{144}Nd$
397	0.1040	0.51103
398z1	0.1016	0.51098
399	0.1092	0.51098
400	0.0911	0.51091
401	0.1030	0.51090
404	0.1076	0.51140
405	0.1058	0.51078

TABLE 5. Nd CRUSTAL RESIDENCE AGES AND ε_{Nd} AND ε_{Sr} VALUES FOR MCKENNEY POND SAMPLES

Sample	T_{cr}(CHUR)[1]	T_{cr}(DM)[1]	ε_{Nd}[2]	ε_{Sr}[2]
397	1347	1471	-15.96	288.1
398z1	1388	1499	-16.94	411.6
399	1508	1593	-16.94	258.3
400	1346	1459	-18.31	370.5
401	1532	1607	-18.50	357.7
404	763	1051	- 8.73	344.9
405	1788	1796	-20.85	218.6

[1]Crustal Residences Ages are in 10^6 years; CHUR parameters: $(^{147}Sm/^{144}Nd)_0 = 0.1967$, $(^{143}Nd/^{144}Nd)_0 = 0.511847$ (Wasserburg et al., 1981); Depleted Mantle (DM) parameters: $(^{147}Sm/^{144}Nd)_0 = 0.2300$, $(^{143}Nd/^{144}Nd)_0 = 0.512245$.
[2]ε values are relative to CHUR at the present time. CHUR parameters for Sr: $^{87}Rb/^{86}Sr = 0.0837$, $^{87}Sr/^{86}Sr = 0.7045$.

(1) The metamorphic grade was high enough to reset the Rb-Sr isotopic systems on the whole rock scale. The fine-grained matrix probably is more easily reset than the coarse-grained clasts, and this may contribute to the scatter in the isochron.

(2) This interpretation does not conflict with the other available geologic and geochronologic data presented above.

(3) This "age" is very similar to other ages (both metamorphic and intrusive) in eastern New England, as discussed below.

A period of high-grade metamorphism with a similar timing is seen in areas of New England and Maritime Canada. Gaudette et al. (1985) report a Rb-Sr whole rock age of 686 ± 30 Ma for the biotite gneiss of the Kelly's Mountain Complex of Cape Breton Island. Olszewski and Gaudette (in prep.) and Gaudette et al. (1983) report a Rb-Sr whole rock age of 692 ± 46 Ma for the amphibolite grade Folly River Schist (part of the Bass River Complex) of the Cobequid Highlands in Nova Scotia. Granitic gneisses that intrude the Bass River Complex yield Rb-Sr whole rock ages of 647 ± 22 Ma and 630 ± 18 Ma. A major period of intrusion and metamorphism occurs in the Green Head Group and associated rocks near Saint John, New Brunswick between 700 and 850 Ma (Olszewski and Gaudette, 1982) based on Rb-Sr whole rock and zircon U-Pb analyses. Cormier (1969) obtained a Rb-Sr whole rock age of 750 ± 80 Ma for the volcanic rocks of the Coldbrook Group which unconformably overlie the Green Head Group. In Maine, Stewart and Wones (1974) report an age of 750 ± 150 Ma by Rb-Sr whole rock analyses of foliated medium- to high-grade rocks on Seven Hundred Acre Island in Penobscot Bay. Stewart and Lux (1988) report a Rb-Sr whole rock age of 620 ± 20 Ma for a coarse muscovite pegmatite that intrudes these same rocks on Seven Hundred Acre Island. The same pegmatite yields a K-Ar age of 594 ± 18 Ma (Stewart and Lux, 1988). Argon release spectra from hornblendes separated from amphibolite and garnet-amphibolite on Seven Hundred Acre Island yield apparent ages of 670 and 650 Ma (Stewart and Lux, 1988). In south-central New Hampshire, Kelly et al. (1980) obtained a Rb-Sr whole rock age of 681 ± 16 Ma for a syntectonic intrusive in the Massabesic Gneiss Complex. A similar age was found by zircon U-Pb (681 ± 147 Ma). A zircon U-Pb age of 730 ± 26 Ma was obtained by Olszewski (1980) for the Fishbrook Gneiss of northeastern Massachusetts.

Most of these rocks have been included in the Avalonian terrane (Williams and Hatcher, 1983; Zen, 1983a; Zartman, 1988) of eastern New England. The similarity in timing of metamorphism between the Chain Lakes massif and these other units suggests three possibilities: that the timing of metamorphism is coincidental and that the Chain Lakes massif and Avalonia are two separate terranes that have never interacted; that they are two separate terranes which interacted in the late Precambrian to produce similar timing of metamorphism; or that the Chain Lakes massif represents Avalonian terrane.

This last possibility we feel can be dismissed because of numerous differences between the massif and typical Avalonian

terrane (e.g., southeastern Massachusetts). For example, there are no rocks like the Chain Lakes massif in the typical Avalonian terrane of southeastern New England (or anywhere else in New England for that matter), the grade of metamorphism of the rocks of the massif is significantly higher than that of most of the Avalonian terrane, and the Paleozoic geologic histories of the Chain Lakes massif and the Avalonian terrane are different (e.g., the Ordovician alkalic plutonism seen in southeastern Massachusetts is absent in the massif; the Cambrian is represented by shallow water marine facies sediments in Massachusetts, not ophiolite as in the Chain Lakes massif; Acadian metamoprhism is very weak in the Avalon terrane of southeastern Massachusetts).

In addition, the late Precambrian event in the Avalon terrane of southeastern Massachusetts is dominated by the intrusion of large calc-alkalic plutons, metamorphism is weak, and deformation is dominantly brittle shear and cataclasis (Zen, 1983b). In contrast, the rocks of the Chain Lakes massif underwent high-grade metamorphism in the late Precambrian as we suggest, it lacks major late Precambrian calc-alkalic plutonism, and deformation is dominantly ductile.

We feel that these are strong arguments against directly correlating the Chain Lakes massif with the Avalonian terrane. The similarity in timing may be fortuitous, but our tenative interpretation would be that it represents interaction between the Chain Lakes massif and the Avalonian terranes in the late Precambrian.

Our correlation of the high-grade metamorphism with the 684 Ma regression line "age" sets a minimum age for the formation of the Chain Lakes massif. A maximum age can be determined by the Sm-Nd provenance or crustal residence ages. The T_{cr} value relative to DM of 1496 Ma would represent the maximum age for the Chain Lakes massif. We realize that this T_{cr} value almost certainly represents a mixture of different sources with different crustal residence ages. However, the massif must be younger than the youngest source rock, and the youngest source rock can not be older than the average crustal residence age (or else the crustal residence age would be older). Thus, the Sm-Nd crustal residence age sets a maximum age for the massif. Additional support for the significance of this crustal residence age comes from Rb-Sr and U-Pb results as well.

Average crustal residence ages derived from Sm-Nd and Rb-Sr results assume that the Chain Lakes massif as a whole has remained closed to Sm, Nd, Rb, and Sr transport. Isotopic systems may be reset on both the mineral and whole rock scale, but if the massif as a unit remains closed, the isotopic systems will retain information about the average crustal residence ages for the sources. The closed system behavior of the Chain Lakes on the scale of the massif is suggested by the lack of evidence of partial melting or the removal by anatexis of a component of the massif. There is no evidence of long distance transport of Sr or Rb within the massif represented, for example, by extensive pegmatite or aplite dikes, epidote veins, etc., except near intrusions. Thus if the massif has remained a closed system, we can also calculate a crustal residence age from the average Rb-Sr isotopic results.

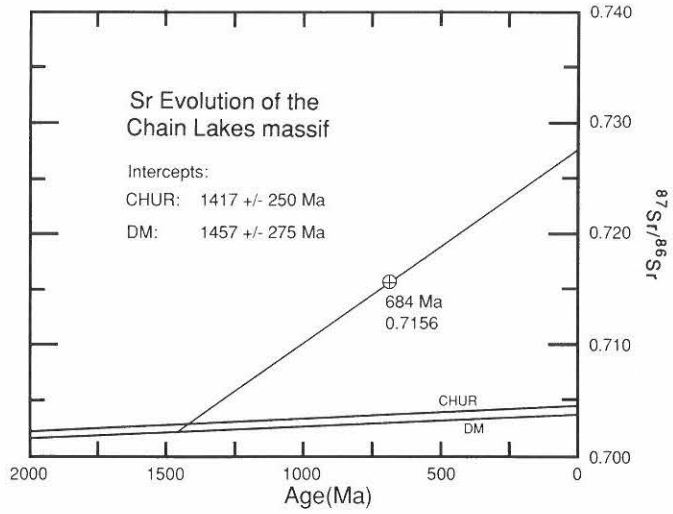

Figure 6. Sr evolution diagram for the Chain Lakes massif. The Sr evolution is based on extrapolation of the present average $^{87}Sr/^{86}Sr$ value for all of the samples analyzed (0.7275) back through the initial ratio at 684 Ma (circle with cross) to the intersections with a chondritic undifferentiated reservoir (CHUR) and typical depleted mantle (DM).

Figure 6 shows the Sr evolution for the Chain Lakes massif as a whole. Using the average $^{87}Sr/^{86}Sr$ value for the samples at present (0.7275), a chord has been constructed through that value and the value of the initial ratio at 684 Ma (0.7156). The intersection with a source with CHUR Sr parameters (McCulloch and Chappell, 1982) is 1417 Ma; the intersection with a depleted mantle source is 1457 Ma. The errors on these ages are 250 and 275 Ma respectively. The value for the depleted mantle intersection age (Sr T_{cr}) is very close to the value of 1496 Ma for the T_{cr} relative to depleted mantle obtained from the Nd data.

Both of these T_{cr} values are similar to the age of 1534 Ma from the zircon results of Naylor et al. (1973) discussed above. These zircons were taken from the matrix of the Sarampus Falls member. Examination of the zircon population from sample CLM-1 analyzed by Naylor et al. (1973), shows that the zircons are well rounded to subhedral, frosted and pitted grains. We interpret these characteristics as suggesting a detrital origin for the zircons from the matrix material.

The age of 1534 Ma for the zircon from the Sarampus Falls member of the Chain Lakes massif represents a mixture of zircons from different sources. However, its similarity to the T_{cr} values from the Sr and Nd results suggest that the massif may represent a well-mixed combination of sources. This crustal residence age of circa 1500 Ma may provide an upper limit for the age of the Chain Lakes massif. The isotopic results may constrain the age of the Chain Lakes massif between 684 Ma and 1500 Ma.

Certainly crustal residence ages must be approached cautiously (Arndt and Goldstein, 1987), but the similar crustal residence ages from three independent techniques suggest an average source age for the massif of ~1500 Ma.

Similar old, mixed source ages have been found for other rocks in New England and Maritime Canada. Olszewski and Gaudette (1982) found detrital zircons with ages of 1641 Ma in high-grade rocks of the Brookville Gneiss in New Brunswick. Olszewski (1980) found detrital zircons ranging in age from 1500 Ma to 2000 Ma in rocks of the Avalon terrane and the Nashoba block of southeastern Massachusetts. Old zircon components (>1000 Ma) are found in many of the binary granites in New England (Harrison et al., 1987). However, the significance of these similarities in age is at present unknown.

Although the age of the Chain Lakes massif can be tenatively constrained between 684 Ma and 1500 Ma, its exact age of formation (presumably deposition) cannot be determined based on the available data. The lowest Tcr age we obtained is 763 Ma by Sm/Nd for sample 404. Thus it is possible that portions of the Chain Lakes massif are as young as ~760 Ma. The material making up the Chain Lakes massif could have undergone a number of periods of erosion, transportation, deposition, lithification, and metamorphism between 1500 Ma and the high-grade metamorphism at ~684 Ma.

These age constraints on the Chain Lakes massif are consistent with its present day ε_{Nd} and ε_{Sr} values when compared to other Precambrian high-grade terrains. Figure 7 is an ε_{Nd} - ε_{Sr} diagram for the samples from the McKenney Pond member, based upon the data listed in Table 5. Data from key geologic provinces are also provided for comparison. The results for the Chain Lakes massif show high positive ε_{Sr} values and moderately negative ε_{Nd} values. Both are consistent with other high-grade gneissic terrains such as the Grenville (Area D in Fig. 7; McCulloch and Wasserburg, 1978), 1500 Ma granulites (Area E, Ben Othman et al., 1984), and Canadian Shield gneisses older than 2500 Ma (Area F, McCulloch and Wasserburg, 1978). Thus an old source age for the Chain Lakes massif is reasonable when compared to other areas.

CONCLUSIONS

Our major conclusions from this study are:

(1) The materials of the Chain Lakes massif were deposited sometime between ~1500 Ma and ~684 Ma based on Rb-Sr and Sm-Nd whole rock, and zircon U-Pb analyses.

(2) The sources for the sedimentary material of the Chain Lakes massif were derived from continental crust whose ultimate sources in the upper mantle average about 1500 Ma in age. The sedimentary material that made up the massif was probably a mixture of sources of different ages.

(3) The isotopic signatures of the rocks of the Chain Lakes massif are consistent with derivation from an older mixture of sources and are similar to high-grade areas of similar age from other parts of the world.

(4) The rocks of the Chain Lakes massif were metamorphosed to high grade at about 684 Ma, resetting the whole rock Rb-Sr systems.

(5) Subsequent low-grade metamorphic effects from the Acadian orogeny and the intrusion of plutons reset the Rb-Sr mineral ages at about 400 Ma.

(6) Although the Chain Lakes massif has many similarities in isotopic ages to other areas in New England and Maritime Canada, there are significant differences in rock types, geologic history, and metamorphism. The Chain Lakes massif cannot be reliably correlated with other rocks in the northern Appalachians, although it has probably interacted with other terranes since the late Precambrian. The massif appears to be a unique terrane in New England.

Our isotopic results cannot provide unequivocal information about the origin of the Chain Lakes massif. In fact, none of the possible modes of origin outlined by Boudette and Boone (1982) can be discounted based on this study. However, Archean or early Proterozoic ages of formation for the Chain Lakes massif as suggested by Boudette and Boone (1982) seem to be contrary to the available isotopic data.

Our results also support the idea that the Chain Lakes massif is not basement of Grenville affinity (Ayuso et al., 1987; Boudette and Boone, 1976; Naylor, 1975, 1976; Osberg, 1978; Stewart et al., 1985, 1986; Williams and Hatcher, 1983; Zen, 1983a), at least in the sense that it is directly related to Grenville rocks where high-grade metamorphism occurred at 900 to 1100

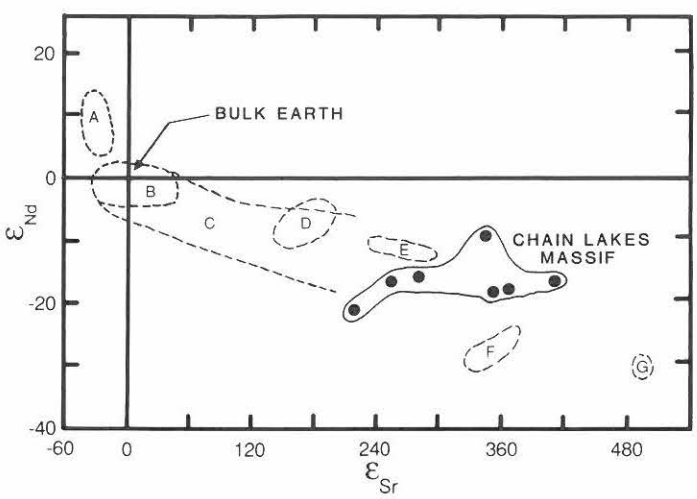

Figure 7. ε_{Nd}-ε_{Sr} diagram comparing results for the Chain Lakes massif with other rocks of varying age and location. The values for the Chain Lakes samples are listed in Table 5. The ε rock units from other areas that are plotted on the diagram are: A: MORB (O'Nions et al., 1979); B: Granitoid rocks older than 1000 Ma (Allegre and Ben-Othman, 1980); C: Granitoid rocks younger than 400 Ma (Allegre and Ben-Othman, 1980); D: Grenville gneisses (McCulloch and Wasserburg, 1978); E: 1500 Ma granulites (Ben-Othman et al., 1984); F: Canadian Shield gneisses older than 2500 Ma (McCulloch and Wasserburg, 1978); G: Liberian charnockites, 3300 Ma (Ben-Othman et al., 1984).

Ma. However, Grenville rocks may have been one of the sources for the sediments of the massif.

Recent work by Aleinikoff and Moench (1985, 1987), Barreiro and Aleinikoff (1985), and Ayuso et al. (1987) suggests that Precambrian rocks with isotopic signatures similar to the Chain Lakes massif may underlie the Kearsarge-central Maine synclinorium of New England (Lyons et al., 1982). Whether these basements have any relationship to the Chain Lakes massif is unknown. Other occurrences of rocks lithologically similar to the Chain Lakes massif are found only in Quebec within the mélange of the St. Daniel and Brompton Formations (Williams and St-Julien, 1982; Cousineau and St-Julien, 1986). These occurrences may be rafts of Chain Lakes rock rather than exposure of a Chain Lakes basement.

Rocks of the Chain Lakes massif are unique in the northern Appalachians. How widespread their occurrences are is presently unknown. The nature of the basement beneath the Kearsarge-central Maine synclinorium is also essentially unknown. Geophysical evidence (Stewart et al., 1985) is consistent with a greater extent of the Chain Lakes massif to the southeast than the surface expression in northwestern Maine suggests. It is important that tectonic models attempt to establish and evaluate what the existence and extent of this unique terrane means to the evolution of the northern Appalachian orogen.

ACKNOWLEDGMENTS

This study was part of the senior author's M.S. thesis submitted to the Department of Earth Sciences, University of New Hampshire. This project and investigation of the evolution of the Eastern Margin Precambrian Complexes have been supported by the National Science Foundation (Grants EAR-81-21423 and EAR-79-27093) to Henri E. Gaudette and William J. Olszewski. Dr. Richard S. Naylor graciously provided us with zircon sample CLM-1 from his earlier study. Thanks go to Gene Boudette for his continuing interest and insights, assistance in the field sampling program, and his willingness to read and comment upon many versions of the manuscript. We thank Dave Stewart for reading and commenting upon an early version of the paper, and John Aleinikoff, Chuck Guidotti, Marc Loiselle, and Bob Ayuso for careful and thoughtful reviews of the manuscript.

REFERENCES CITED

Albee, A. L., 1961, Boundary Mountain anticlinorium, west-central Maine and northern New Hampshire: U.S. Geol. Surv., Prof. Paper 424-C, p. C51-C54.

Albee, A. L., and Boudette, E. L., 1972, Geology of the Attean quadrangle, Somerset County, Maine: U.S. Geol. Surv., Bull. 1297, 110 p.

Aleinikoff, J. N., and Lyons, J. B., 1984, Feldspar-porphyritic granite of the Attean pluton, *in* Moench, R. H. (ed.), Geologic map of the Sherbrooke-Lewiston area: U.S. Geol. Surv., Open-File Rept. 84-0650, scale 1:250,000.

Aleinikoff, J. N., and Moench, R. H., 1985, Metavolcanic stratigraphy in northern New England--U/Pb zircon geochronology: Geol. Soc. Amer., Abs. with Prog., v. 17, p. 1.

Aleinikoff, J. N., and Moench, R. H., 1987, U/Pb geochronolgy and Pb isotopic systematics of plutonic rocks in northern New Hampshire: ensimatic vs. ensialic sources: Geol. Soc. Amer., Abs. with Prog., v. 19, p. 1.

Allegre, C. J., and Ben-Othman, D. B., 1980, Nd/Sr isotopic relationship in granitoid rocks and continental crust development: a chemical approach to orogenesis: Nature, v. 286, p. 335-342.

Arndt, N. T. and Goldstein, S. L., 1987, Use and abuse of crust-formation ages: Geology, v. 15, p. 893-895.

Ayuso, R. A., Horan, M. F., and Criss, R. E., 1987, Pb and oxygen isotopic geochemistry of the northern Maine plutonic belt: Geol. Soc. Amer., Abs. with Prog., v. 19, p. 3.

Barreiro, B. and Aleinikoff, J. N., 1985, Sm-Nd and U-Pb isotopic relationships in the Kinsman quartz monzonite, New Hampshire: Geol. Soc. Amer., Abs. with Prog., v. 17, p. 3.

Ben-Othman, D., Polve, M. and Allegre, C. J., 1984, Nd-Sr isotopic composition of granulites and constraints on the evolution of the lower continental crust: Nature, v. 307, p. 510-515.

Biederman, J. L., 1984, Petrology of the Chain Lakes massif along Route 27 in central-western Maine: a Precambrian high-grade terrane: M.S. thesis, Univ. Maine, Orono, Maine, 125 p.

Boucot, A. J., 1961, Stratigraphy of the Moose River synclinorium, Maine: U.S. Geol. Surv., Bull. 1111-E, p. 153-188.

Boudette, E. L., 1970, Pre-Silurian rocks in the Boundary Mountains anticlinorium, northwestern Maine, *in* Boone, G. M. (ed.), New England Intercollegiate Geological Conference guidebook for field trips in the Rangeley Lakes - Dead River Basin region, western Maine, p. C1-C21.

Boudette, E. L., 1982, Ophiolite assemblage of Early Paleozoic age in central western Maine, *in* St-Julien, P., and Beland, J. (eds.), Major structural zones and faults of the northern Appalachians: Geol. Assoc. Canada, Spec. Paper 24, p. 209-230.

Boudette, E. L., and Boone, G. M., 1976, Pre-Silurian stratigraphic succession in central western Maine: Geol. Soc. Amer., Mem. 148, p. 129-145.

Boudette, E. L., and Boone, G. M., 1982, Diamictite of the Chain Lakes massif of Maine: a possible metasuevite: Geol. Soc. Amer., Abs. with Prog., v. 14, p. 448.

Boudette, E. L., and Boone, G. M., 1984, Major boundaries in the geologic framework of western Maine: Geol. Soc. Amer., Abs. with Prog., v. 16, p. 5.

Boudette, E. L., Boone, G. M., Bothner, W. A., Marvinney, R. G., Moench, R. H., and Aleinikoff, J. L., 1984, Geologic map of the Sherbrooke $1^{\circ} \times 2^{\circ}$ quadrangle, Maine, New Hampshire and Vermont, *in* Moench, R. H. (ed.), Geologic map of the Sherbrooke-Lewiston area: U.S. Geol. Surv., Open-File Rept. 84-0650, scale 1:250,000.

Cousineau, P. A., and St-Julien, P., 1986, The Saint-Daniel Formation: a mélange along the Taconic Suture in southern Quebec, Canada: Geol. Soc. Amer., Abs. with Prog., v. 18, p 10.

Cormier, R. F., 1969, Radiometric dating of the Coldbrook Group of southern New Brunswick, Canada: Can. Jour. Earth Sci., v. 6, p. 393-398.

DePaolo, D. J., and Wasserburg, G. J., 1976, Nd isotopic variations and petrogenetic models: Geophys. Res. Letters, v. 3, p. 249-252.

Eisenberg, R. A., 1981, Chronostratigraphy of metavolcanic and associated intrusive rocks of the Boundary Mountain anticlinorium: Geol. Soc. Amer., Abs. with Prog., v. 13, p.131.

Ells, R. W., 1887, Report on the geology of a portion of the Eastern Townships (Quebec), relating more especially to the counties of Compton, Stanstead, Beauce, Richmond, and Wolfe: Canada Geol. Nat. Hist. Survey, 2nd Ann. Rept., Pt. J, 70p., with map.

Faris, J. P., and Warton, J. W., 1962, Anion exchange resin separation of the rare earths, yttrium, and scandium in nitric acid-methanol mixtures: Anal. Chem., v. 34, p. 1077-1080.

Gaudette, H. E., and Boone, G. M., 1985, Isotopic age of the Lexington batholith: constraints on timing of intrusion and Acadian metamorphism in western Maine: Geol. Soc. Amer., Abs. with Prog., v. 17, p. 19.

Gaudette, H. E., Olszewski, W. J., Jr., and Donohoe, H. V., 1983, Age and origin of the basement rocks, Cobequid Highlands, Nova Scotia: Geol. Soc. Amer., Abs. with Prog., v. 15, p. 136.

Gaudette, H. E., Olszewski, W. J., Jr., and Jamieson, R. A., 1985, Rb-Sr ages of some basement rocks, Cape Breton Highlands, Nova Scotia: 1985 Geol. Assoc. Can./Miner. Assoc. Can., Joint Ann. Mtg., Fredericton, NB., Canada, p. A20.

Green, J. C., and Guidotti, C. V., 1968, The Boundary Mountains anticlinorium in northern New Hampshire and northwestern Maine, *in* Zen, E-an, White, W. S., Hadley, J. B., and Thompson, J. B., Jr. (eds.), Studies of Appalachian geology: northern and maritime: Interscience Publishers, New York, p. 255-266.

Harrison, T. M., Aleinikoff, J. N., and Compston, W., 1987, Observations and controls on the occurrence of inherited zircon in Concord-type granitoids, New Hampshire: Geochim. et Cosmochim. Acta, v. 51, p. 2549-2558.

Harwood, D. S., 1970, Nature of the Taconic orogeny in the Cupsuptic quadrangle, west-central Maine, *in* Boone, G. M. (ed.), New England Intercollegiate Geological Conference guidebook for field trips in the Rangeley Lakes - Dead River Basin region, western Maine, p. H1-H19.

Harwood, D. S., 1973, Geology of the Cupsuptic and Arnold Pond quadrangles, Maine: U.S. Geol. Surv., Bull. 1346, 90 p.

Kelly, W. J., Olszewski, W. J., Jr., and Gaudette, H. E., 1980, The Massabesic Gneiss revisited: a Rb/Sr whole rock study of the Massabesic orthogneiss, southern New Hampshire: Geol. Soc. Amer., Abs. with Prog., v. 12, p. 45.

Lux, D. R., 1983, ^{40}Ar-^{39}Ar mineral ages for several plutons from western Maine: Geol. Soc. Amer., Abs. with Prog., v. 15, p. 147.

Lyons, J. B., Aleinikoff, J. N., and Zartman, R. E., 1986, Uranium-thorium-lead ages of the Highlandcroft Plutonic Suite, northern New England: Am. Jour. Sci., v. 286, p. 489-509.

Lyons, J. B., Boudette, E. L., and Aleinikoff, J. N., 1982, The Avalonian and Gander zones in central eastern New England, *in* St-Julien, P., and Beland, J. (eds.), Major structural zones and faults of the northern Appalachians: Geol. Assoc. Canada, Spec. Paper 24, p. 43-66.

Lyons, J. B., Zartman, R. E., and Aleinikoff, J. N., 1983, U-Pb ages of zircons from the Ordovician Highlandcroft Plutonic Suite and Silurian intrusives: Geol. Soc. Amer., Abs. with Prog., v. 15, p. 187.

Marleau, R. A., 1957, Preliminary report on East Megantic and Armstrong areas, electoral districts of Frontenac and Beauce, Quebec: Quebec Dept. Mines, Prelim. Rept. 362, p. 7.

McCulloch, M. T., and Chappell, B. W., 1982, Nd isotopic characteristics of S- and I-type granites: Earth Planet. Sci. Lett., v. 58, p. 51-64.

McCulloch, M. T., and Wasserburg, G. J., 1978, Sm-Nd and Rb-Sr chronology of continental crust formation: Science, v. 200, p. 1003-1011.

Moench, R. H. (ed.), 1984. Geologic map of the Sherbrooke-Lewiston area, Maine, New Hampshire, and Vermont: U.S. Geol. Surv., Open-File Rept. 84-0650, scale 1:250,000.

Naylor, R. S., 1975, Age provinces in the northern Appalachians: Ann. Rev. Earth Planet. Sci., v. 3, p. 485-494.

Naylor, R. S., 1976, Isotopic dating and New England stratigraphy: Geol. Soc. Amer., Mem. 148, p. 419-425.

Naylor, R. S., Boone, G. M., Boudette, E. L., Ashenden, D. D., and Robinson, P., 1973, Pre-Ordovician rocks in the Bronson Hill and Boundary Mountain anticlinoria, New England, USA: EOS, v. 54, p. 495.

Olszewski, W. J., Jr., 1980, The geochronology of some stratified metamorphic rocks in northeastern Massachusetts: Can. Jour. Earth Sci., v. 17, p. 1407-1416.

Olszewski, W. J., Jr., and Gaudette, H. E., 1982, Age of the Brookville Gneiss and associated rocks, southeastern New Brunswick: Can. Jour. Earth Sci., 19, p. 2158-2166.

Olszewski, W. J., Jr., and Gaudette, H. E., in prep., Rb-Sr ages and the evolution of the basement rocks, Cobequid Highlands, Nova Scotia.

O'Nions, R. K., Carter, S. R., Evensen, N. M., and Hamilton, P. J., 1979, Geochemical and cosmochemical applications of Nd-Sm isotope analysis: Ann. Rev. Earth and Planet. Sci., p. 11-38.

Osberg, P. H., 1978, Synthesis of the geology of the northern Appalachians, USA: Geol. Surv. Can., Paper 78-13, p. 137-147.

Osberg, P. H., Hussey, A. M., II, and Boone, G. M., 1985, Bedrock geologic map of Maine: Maine Geol. Surv., scale 1:500,000.

Pollock, S. G., 1987, The Lower Devonian slate problem of western and northern Maine revisited: Northeastern Geol., v. 9, p. 37-50.

Steiger, R. H. and Jager, E., 1977, Subcommission on geochronology: convention on the use of decay constants in geo- and cosmochronology: Earth Planet. Sci. Lett., v. 36, p. 359-362.

Stewart, D. B., Leutgert, J. H., Unger, J. D., and Phillips, J. D., 1985, Characterization of crust of Maine by seismic reflection and refraction: Geol. Soc. Amer., Abs. with Prog., v. 17, p. 727.

Stewart, D. B., and Lux, D. R., 1988, Lithologies and metamorphic age of the Precambrian rocks of Seven Hundred Acre Island and vicinity, Islesboro, Penobscot Bay, Maine: Geol. Soc. Amer., Abs. with Prog., v. 20, p. 73.

Stewart, D. B., Unger, J. D., Phillips, J. D., Goldsmith, R., Poole, W. H., Spencer, C. P., Green, A. G., Loiselle, M. C., and St-Julien, P., 1986, The Quebec-western Maine seismic reflection profile: setting and first year results, *in* Reflection seismology: the continental crust: Geodynamics Series, v. 14, Am. Geophys. Union, p. 189-199.

Stewart, D. B., and Wones, D. R., 1974, Bedrock geology of northern Penobscot Bay area, *in* Osberg, P. H. (ed.), New England Ingercollegiate Geological Conference guidebook for field trips in east-central and north-central Maine, p. 223-239.

St-Julien, P., and Hubert, C., 1975, Evolution of the Taconian orogen in the Quebec Appalachians: Am. Jour. Sci., v. 275A, p. 337-362.

Wasserburg, G. J., Jacobsen, S. B., DePaolo, D. J., McCulloch, M. T., and Wen, T., 1981, Precise determination of Sm/Nd ratios, Sm and Nd isotopic abundances in standard solutions: Geochim. et Cosmochim. Acta, v. 45, p. 2311-2323.

Williams, H., and Hatcher, R. D., Jr., 1983, Appalachian suspect terranes, *in* Hatcher, R. D., Jr., Williams, H., and Zietz, I. (eds.), Contributions to the tectonics and geophysics of mountain chains: Geol. Soc. Amer., Mem. 158, p. 33-53.

Williams, H., and St-Julien, P., 1982, The Baie Verte-Brompton line: Early Paleozoic continent-ocean interface in the Canadian Appalachians, *in* St-Julien, P., and Beland, J. (eds.), Major structural zones and faults of the northern Appalachians: Geol. Assoc. Can., Spec. Paper 24, p. 178-207.

York, D., 1969, Least squares fitting of a straight line with correlated errors: Earth Planet. Sci. Lett., v. 5, p. 320-324.

Zartman, R. E., 1988, Three decades of geochronologic studies in the New England Appalachians: Geol. Soc. Amer., Bull., v. 100, p. 1168-1180.

Zartman, R. E., Hurley, P. M., Krueger, H. W., and Giletti, B. J., 1970, A Permian disturbance of K-Ar radiometric ages in New England--its occurrence and cause: Geol. Soc. Amer., Bull., v. 81, p. 3359-3373.

Zen, E-an, 1983a, Exotic terranes in the New England Appalachians: limits, candidates, and ages: a speculative essay, *in* Hatcher, R. D., Jr., Williams, H., and Zietz, I. (eds.), Contributions to the tectonics and geophysics of mountain chains: Geol. Soc. Amer., Mem. 158, p. 55-81.

Zen, E-an, 1983b, Bedrock geologic map of Massachusetts: Mass. Dept. of Public Works, 3 sheets, scale 1:125,000.

Maine Geological Survey
Studies in Maine Geology: Volume 4
1989

Geochemistry of the Catheart Mountain Porphyry Copper Deposit, Maine

Robert A. Ayuso
U.S. Geological Survey
Reston, Virginia 22092

ABSTRACT

The Ordovician Catheart Mountain pluton is the best example of a porphyry copper system in the New England Appalachians. It intrudes the Ordovician Attean quartz monzonite in the Proterozoic Chain Lakes massif. The pluton consists of equigranular granodiorite intruded by porphyritic dikes of granite and granodiorite which contain up to 4% sulfides (pyrite, chalcopyrite, and molybdenite).

The equigranular host rocks and the porphyritic dikes are generally chemically similar, showing scattered compositional variations which reflect changes imposed on the pluton during crystallization and hydrothermal alteration. Most rocks are hydrated, containing high CO_2 and high S. The most intensely altered parts of the pluton are potassic (up to 6.9 wt % K_2O) and highly mineralized, especially with Cu (up to 3900 ppm), but also with Mo (up to 320 ppm). The host granodiorite and porphyritic dikes are depleted in Ca, Na, Fe^{2+} and Sr as a function of increasing Cu; the sulfide-rich rocks are enriched in Rb and they have high Fe^{3+}/Fe^{2+}, K/Na, and Rb/Sr values.

Abundances and ratios of the highly-charged cations (e.g. Zr, Hf, Ta, and Th) in the Catheart Mountain pluton resemble those in the Devonian granodiorites in the northern Maine plutonic belt. Abundances and ratios of the highly-charged cations in the Sally Mountain pluton, a nearby body also containing Cu and Mo mineralization, differ significantly from those in the Catheart Mountain pluton suggesting that the two plutons are not comagmatic. This is in agreement with lead isotopic compositions indicating that the Sally Mountain and Catheart Mountain plutons did not have the same source.

Magma for the Catheart Mountain pluton was probably generated in the subcontinental lithosphere from a source consisting of continental basement (Grenville or possibly Chain Lakes massif) and mantle-derived rocks. The host equigranular granodiorite represents a water-undersaturated magma emplaced into the upper crust. Volatile- and chloride-rich fluids in the porphyritic dikes leached the wall rocks and produced chemical reactions leading to the decomposition of magmatic minerals, remobilization of the major and many of the trace elements, oxidation of iron, and precipitation of chalcopyrite and molybdenite. Fluids may have been magmatic at the start of the hydrothermal activity, but included a component of high-^{18}O fluid originating from meteoric sources toward the waning stages of alteration.

INTRODUCTION

The Catheart Mountain pluton is in the northern Maine plutonic belt (Fig. 1), where it intrudes the Ordovician Attean quartz monzonite in the Proterozoic Chain Lakes massif, an allochthonous block that rests on Middle Proterozoic Grenvillian basement (Zen, 1983; St-Julien et al., 1983; Stewart et al., 1985). The Catheart Mountain pluton is probably one of the best examples of rocks associated with porphyry-style copper mineralization in the northern Appalachians of New England, and thus it is part of the so-called northern Appalachian porphyry province (Hollister et al., 1974).

The purpose of this paper is to summarize the field relations and major- and trace-element chemistry of the Catheart Moun-

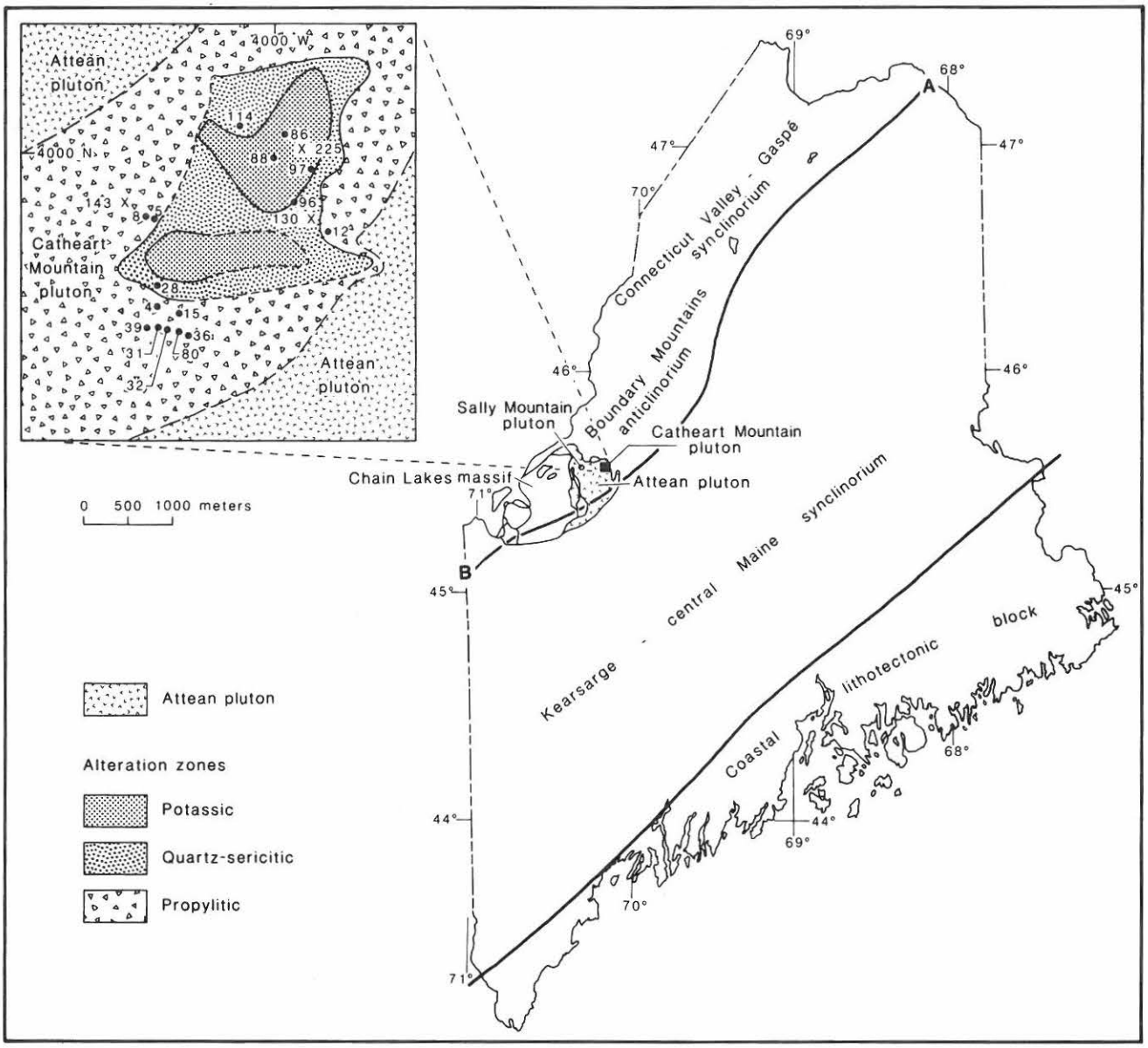

Figure 1. Map showing location of the Catheart Mountain and Sally Mountain plutons, the Chain Lakes massif, and structural features in Maine. Line A-B represents the southernmost extent of unexposed Grenville basement (Zen, 1983). The generalized map of the Catheart Mountain pluton shows the hydrothermal alteration zones, and location of the drill holes (solid circles) and surface samples (crosses) used in this study (modified from Schmidt, 1974).

tain pluton in order to better understand the genesis of the copper mineralization. Chemical information on the Catheart Mountain pluton is used to investigate changes in major- and trace element compositions as a function of increasing degree of mineralization and alteration. This is done in an effort to establish the relative elemental mobility produced by the hydrothermal events. Information on the immobile elements can then be used to compare the chemical affinities of the least altered parts of the Catheart Mountain pluton with granodioritic plutons from northern Maine, and to establish geochemical constraints on the sources of the felsic magmas.

Determining the magmatic affinities of the Catheart Mountain pluton is significant for exploration and economic assessment of granitic rocks because this pluton contains the best described porphyry copper deposit in New England, and also in light of current research aimed at synthesizing the regional metallogenesis of felsic intrusives in the northern Appalachians.

Geochemical studies emphasizing zoning of the chemical components in hydrothermally altered porphyry copper systems have been reported by Creasey (1965), Theodore and Nash (1973), Jambor (1974), Cox et al. (1975), Olade and Fletcher (1975), Chaffee (1976), Ford (1978), and Schwartz (1982).

These studies were generally done in the belief that more detailed knowledge of the compositional variations produced during the formation of porphyry copper deposits may help in locating poorly exposed porphyry copper deposits.

Previous work by Schmidt (1974) established a comprehensive framework for the study of rock alteration in the Catheart Mountain copper deposit. Schmidt (1974) described the hydrothermal alteration zones and provided a detailed description of the sulfide mineralogy. Subsequent investigations by Atkinson (1977) provided additional details of the alteration zones in the Catheart Mountain pluton.

Ayuso (1987) described the increasingly more aluminous compositions in white micas from the Catheart Mountain pluton as a function of increasing Cu and Mo content of the bulk rocks. Ayuso (1986a) and Ayuso et al. (1987, 1988) reported on the Pb and O isotopic geochemistry of the Catheart Mountain pluton in a study of granite rocks from northern Maine. The main conclusion of those studies was that the Catheart Mountain pluton and the Devonian granodiorite plutons from northern Maine were isotopically similar, suggesting that they had a similar source. In the Catheart Mountain pluton, lead-isotope values are relatively unradiogenic, and oxygen-isotope values indicate alteration by high-^{18}O fluids in the more intensely altered rocks.

FIELD AND PETROGRAPHIC RELATIONS

In addition to the Catheart Mountain pluton, two important igneous bodies are exposed in the area, the Attean quartz monzonite and the Sally Mountain pluton. Both the Catheart Mountain and Sally Mountain plutons intrude the Attean quartz monzonite, which in turn intrudes the southeast flank of the Boundary Mountains anticlinorium (Albee and Boudette, 1972) in the Proterozoic Chain Lakes massif (Naylor et al., 1973).

The Chain Lakes massif consists for the most part of diamictite, metasedimentary rocks (e.g. quartzite, feldspathic metasandstone), and some mafic metavolcanic rocks (Boone et al., 1970), which were regionally metamorphosed to sillimanite grade in the Proterozoic and subsequently retrograded to chlorite facies in the middle Paleozoic (Cheatham et al., 1985).

In the following sections, a brief description of the field relations and mineralogy of the igneous bodies is presented, followed by discussion of the geochemical data.

Catheart Mountain Pluton

The most abundant rock types in the Catheart Mountain pluton are fine- to medium-grained equigranular host rocks ranging from granite to granodiorite (referred to as quartz monzonites by Schmidt, 1974), and the numerous, irregularly-shaped porphyritic dikes also composed of granite and granodiorite (quartz porphyries of Schmidt, 1974). Both the host rocks and the dikes are mineralized, in contrast to the granitic rocks of the Attean quartz monzonite which are generally not mineralized.

Lyons et al. (1986) reported that muscovite from a quartz-molybdenite-white mica vein from the Catheart Mountain pluton had ages of 441 ± 8 Ma by the K-Ar method and 447 ± 10 Ma by the Rb-Sr method. This mineralization age is in good agreement with the zircon age of 443 ± 4 Ma obtained on the Attean quartz monzonite (Lyons et al., 1986), and thus is compatible with a comagmatic relation between the Catheart Mountain pluton and the Attean quartz monzonite.

Hydrothermal alteration is pervasive in the Catheart Mountain pluton. The freshest parts of the granitic rocks consist of alkali feldspar and plagioclase, quartz, biotite, accessory minerals (sphene, zircon, and apatite), and secondary minerals (epidote, sericite, chlorite, sphene, and hematite). In most samples, secondary minerals are abundant, and quartz and white mica are the predominant phases. Hydrothermal alkali feldspar and biotite are probably found only in the areas containing the most intensive alteration. In contrast, chlorite, calcite, and epidote are widely distributed throughout the hydrothermal zones.

Phenocrysts of quartz are probably the only textural features retained from the original igneous fabric in the Catheart Mountain pluton. Quartz grains are generally subhedral to euhedral and contain numerous embayments and indentations. Plagioclase phenocrysts are rare; most plagioclase grains are found in the groundmass where they are largely and progressively replaced by white mica and epidote. Biotite may have been the most abundant original mafic igneous mineral, but very little primary biotite remains, as it is replaced by chlorite and epidote. Hornblende may also have been a primary mineral in the Catheart Mountain pluton, but it did not survive the hydrothermal event.

Petrographic study of rock alteration of drill core samples allowed Schmidt (1974) to determine the regional hydrothermal alteration zones, and to suggest, on the basis of the general features of the alteration system, that it strongly resembled the zonation found in many other porphyry copper systems according to the model of Lowell and Guilbert (1970). Two main centers of alteration at Catheart Mountain were recognized (Fig. 1): a main alteration system and a smaller peripheral system. Alteration minerals include white mica, epidote, quartz, and secondary alkali feldspar, and these are generally arranged according to the regional pattern of zonation found in porphyry copper deposits.

Schmidt (1974) distinguished five major gradational regional alteration zones in the Catheart Mountain pluton, on the basis of the predominant alteration type found in the upper parts of the drill core. The regional alteration zones are, from least altered to most intensely altered, propylitic, outer phyllic, phyllic, quartzose potassic, and potassic. Figure 1 shows a generalized map of the propylitic, quartz-sericitic (outer phyllic and phyllic), and potassic (quartzose potassic and potassic) alteration zones in the Catheart Mountain pluton. Petrographic study of the core samples demonstrated the complex superposition of alteration events, reflecting the irregular distribution of the por-

phyritic dikes. No area of supergene enrichment was recognized.

Sulfides constitute as much as 4% of the porphyritic dikes and the equigranular host rocks of the Catheart Mountain pluton. In decreasing order of abundance the sulfides consist of pyrite, chalcopyrite, and molybdenite occurring within and controlled in their distribution by siliceous veinlets forming a stockwork oriented generally east-west. The sulfide minerals also occur as disseminated grains associated especially with the potassic alteration zone. The area near the interface between the potassic and the quartz sericitic (phyllic) alteration zone contains the highest abundance of ore minerals (Schmidt, 1974), in agreement with the general concepts of porphyry copper mineralization (Lowell and Guilbert, 1970). Stannite was reported to occur erratically in veins within the phyllic zone, and sphalerite in the propylitic zone (Hollister, 1978). Galena has also been reported in the vicinity. There is, however, no clear evidence of a regional zoning pattern of these minerals as a function of the intensity of the hydrothermal alteration.

A good correlation exists between the type of alteration, intensity of fracturing and veining, and intensity of mineralization, so that the highest amount of Cu and Mo, as well as the highest Cu/Mo ratio, is found in rocks of the potassic alteration zone that are closely associated with the porphyritic dikes. In the potassic zone the grade is about 0.2% Cu plus minor Mo (Hollister, 1978). Some of the veinlets in the propylitically altered parts of the system, according to Schmidt (1974), consist of a central zone containing the ore minerals and quartz sericitic (phyllic) alteration, surrounded by a K-feldspar-enriched alteration zone (potassic). This zonal arrangement at Catheart Mountain suggests that quartz sericitic alteration was superimposed on potassic alteration in the waning stages of the hydrothermal event (Ayuso, 1987), in agreement with the general superposition of alteration zones in many porphyry copper deposits (Titley, 1975, 1982; Gustafson and Hunt, 1975).

Sally Mountain Pluton

The Sally Mountain pluton is exposed in a small area consisting of small quartz porphyry plugs that intrude the Attean quartz monzonite (Albee and Boudette, 1972; Schmidt, 1974) (Fig. 1). Most of the Sally Mountain pluton is intensely altered, and the original mineral assemblage has been replaced by secondary minerals including K-feldspar, epidote, chlorite, and pyrite. Thus the original igneous mode is difficult to ascertain, but it was probably similar to that of the granites in the Catheart Mountain pluton which contain biotite as the most important mafic mineral. In most places the quartz porphyry plug appears intensely silicified, especially within the fractures containing potassic alteration, chalcopyrite, and molybdenite. In contrast to the Catheart Mountain pluton, quartz sericitic alteration is not well developed and the content of sulfide minerals is significantly lower in the Sally Mountain pluton.

Attean Quartz Monzonite

The Attean quartz monzonite in characteristically leucocratic, pink and green, and coarser grained than the Catheart Mountain pluton (Albee and Boudette, 1972). Other distinguishing features include prominent K-feldspar phenocrysts and lack of mineralization. The Attean quartz monzonite has a U-Pb zircon age of 443 ± 4 Ma (Lyons et al., 1986), and it intrudes the volcanic and volcaniclastic rocks that unconformably overlie the Proterozoic Chain Lakes massif.

Unconformably overlying the Attean quartz monzonite are greenschist-facies metasedimentary rocks of Silurian and Devonian age (Boone et al., 1970). Many samples of the Attean quartz monzonite are sheared and substantially altered; igneous textures in most samples of the pluton have been modified significantly. The least altered samples, however, are predominatly granitic and have a more restricted modal range than that of the Catheart Mountain pluton.

ANALYTICAL PROCEDURES

Drill cores from 116 holes of the Catheart Mountain pluton were made available by Scott Paper Co. for petrographic examination and sampling. A total of 45 samples was obtained from 18 of the drill cores. These samples were supplemented by 15 samples obtained on the surface in order to ensure that they were representative of the alteration zones and of the mineralized system (Fig. 1). Enough samples were obtained from each drill core to assure that the samples were representative of that section of the core. Polished microprobe sections were prepared for all samples, and 22 of them were used for detailed microprobe analyses (Ayuso, 1987). A special effort was made to obtain the least altered samples available from drill core to estimate the original composition of the Catheart Mountain pluton.

Most rocks were analyzed for 50 elements at the U.S. Geological Survey by the following techniques: major elements by rapid-rock methods (analysts F. Brown, D. Kobilis, and H. Kirschenbaum); Cl, F, and H2O by wet-chemical methods (analysts N. Rait and H. Smith); Rb, Sr, Ba, Y, and Zr by energy-dispersive X-ray fluorescence (analysts R. Johnson, L. Cox, and J. Jackson); rare-earth elements, U, Th, Ta, and ferromagnesian trace elements by instrumental neutron activation analysis (analysts C. Palmer and G. Wandless); Li, Mo, Sn, W, Zn, and Nb by wet-chemical methods (analysts A. Dorrzapf, P. Aruscavage, W. d'Angelo, and M. Doughten); Be by induction-coupled plasma and B by quantitative spectroscopy (analysts D. Golightly, J. Kane, and J. Fletcher).

GEOCHEMICAL RESULTS

A summary of the compositional changes in the Catheart Mountain pluton is presented in this section. The results are

useful in the study of wall-rock reactions, particularly in this attempt to unravel the magmatic affinities of the Catheart Mountain pluton on the basis of the most stable elements. Results are discussed starting with the major elements, volatiles, and sulfur -- elements whose contents are unlikely to have survived the hydrothermal event unchanged. The fugitive elements B, Be, and Li, and the large cations Rb, Sr, Cs, and Ba are discussed next; this is followed by a discussion of the rare-earth elements, Y, high-valence cations Zr, Hf, Nb, Ta, U, and Th, the ferromagnesian elements Co, Cr, Ni, Sc, and Zn, and the base metals Cu, Mo, Sn, and W.

Hydrothermal alteration variably affected host rocks and dikes in the Catheart Mountain pluton so that petrographic subgroups are readily distinguished on the basis of extent of fracturing and intensity of alteration. In addition to a group of rocks containing relatively few fractures and few sulfides, both the equigranular host rocks and porphyritic dikes each encompass a subgroup of rocks characterized by their highly fractured and altered nature. Such highly altered rocks are easily recognized because in addition to the thorough destruction of igneous fabric, they contain abundant sulfide ore minerals within the fractures and as disseminated grains. Thus, in the remainder of this report, the most intensely altered rocks of the equigranular host rocks and porphyritic dikes containing abundant sulfides will be referred to as the mineralized or sulfide-rich equigranular host rocks or as the mineralized or sulfide-rich porphyritic dikes, in contrast to the group of rocks characterized by fewer fractures and lower content of disseminated sulfides. This petrographic subdivision of the rocks in the Catheart Mountain pluton will be done in an effort to compare the relative patterns of enrichment and depletion in the major- and trace-elements between the sulfide-rich and sulfide-poor rock groups.

Composition-Volume Relations and Mobility of Components

The conversion of magmatic rocks into hydrothermally altered and mineralized porphyry copper systems is characterized by metasomatic reactions which drastically change the original magmatic compositions. It is possible, however, to estimate the extent to which components are affected by these exchange reactions by considering the change in rock volume and the change of individual chemical species (Gresens, 1967; Appleyard, 1980; Jamieson and Strong, 1981).

Establishing reasonable magmatic or original values for plutons associated with porphyry copper deposits is a problem that often arises in studies of this kind as a result of the chemical disturbance associated with hydrothermal processes. In assessing the primary compositions of such plutons, it is often assumed that the least altered, relatively sulfide-poor samples are suitable as base samples. Several samples of the Catheart Mountain pluton have relatively low H_2O, S, Cu, Mo, and CO_2 contents (e.g. CM-31-52, Table 1), and they could have been used to represent the original composition of the pluton and as a base for the calculations. Petrographic examination indicated, however, that such proposed samples also contained alteration products and were therefore rejected. In addition, the irregular shapes and distribution of the porphyritic dikes produced a complex superposition of alteration and chemical changes which also precluded reliable sampling of individual alteration zones.

Information on the composition-volume relations of the rock units in the Catheart Mountain pluton was obtained by comparing both the average composition of the sulfide-poor equigranular host rocks and porphyritic dikes, their sulfide-rich equivalents, and also by comparing the composition of individual samples from each of the four petrographic and chemical groups. Thus, the bulk chemical results represent the total chemical change in the transformation from relatively sulfide-poor to sulfide-rich rocks.

Tables 1 and 2 contain representative analyses of the equigranular host rocks, porphyritic dikes, and their mineralized or sulfide-rich equivalents in the Catheart Mountain pluton. Average compositions of these rocks were treated according to the relation:

$$x_n = a[f_v(g_B/g_A)c_n^B - c_n^A]$$

where x_n = the amount of material lost or gained of component n between A (represented by the relatively unaltered, unmineralized host rocks or porphyritic dikes) and B (represented by the sulfide-rich host rocks or porphyritic dikes); a = the amount in grams of each rock (this is conveniently assumed as 100 grams so that the results are found in wt %); f_v = the volume factor or the change between the final and the initial volume during the reaction from A to B; g = the specific gravity of A (average specific gravity of the host rocks or porpyritic dikes, 2.71 and 2.80, respectively) and B (average specific gravity of the sulfide-rich host rocks or dikes, 2.75 and 2.90, respectively); c_n = weight fraction of component n in A and B.

Transfer of a component from the generally sulfide-poor rocks to the sulfide-rich rocks can be estimated readily in this manner, and the results are best illustrated by calculating the change in the composition-volume relations, particularly for the intersection at $x_n = 0$ (gain-loss zero line) and $f_v = 1$ (isovolumetric transfer) (Gresens, 1967).

In the Catheart Mountain pluton, contents of the major oxides have been substantially disturbed (Fig. 2). For example, Fe^{2+}, Ca, Na, and possibly Mg have f_v values which intersect the gain-loss zero line higher than 1, indicating that these components were lost during the transformation of A to B (from the sulfide-poor rocks to sulfide-rich parts of the system); Sr and possibly Yb were also lost during this conversion. In contrast, Fe^{3+}, H_2O, and K have f_v values much lower than 1, suggesting that these components were gained during the transformation from the sulfide-poor to the sulfide-rich rocks in the Catheart Mountain pluton.

The relatively immobile major elements include Al, Ti, and Si. The apparent immobility of Si suggested by composition-volume relations in the Catheart Mountain pluton is unexpected, and contrasts with the general increase in silica found in many porphyry copper deposits elsewhere (e.g. Meyer and Hemley,

TABLE 1. REPRESENTATIVE ANALYSES OF THE EQUIGRANULAR HOST ROCKS OF THE CATHEART MOUNTAIN PLUTON, MAINE.

SAMPLE*	CM15-124 EHM**	CM36-1115 EHM	CM36-1092 EHM	CM32-424 EHM	CM36-1064 EHM	CM96-110 EHM	CM86-240 EHM	CM86-186 EHM	CMl4-384 EHM
SiO_2	67.70	68.70	69.00	69.00	69.20	69.30	69.40	71.10	71.90
Al_2O_3	14.70	13.70	14.10	14.60	14.80	14.70	14.70	14.60	13.80
Fe_2O_3	2.20	3.50	2.40	2.60	1.60	2.70	1.40	1.60	1.20
FeO	1.10	0.20	0.36	0.36	0.72	0.28	0.44	0.20	0.24
MgO	1.30	0.60	0.76	0.84	1.20	1.10	1.00	0.93	0.79
CaO	2.10	1.10	1.40	1.30	1.10	1.40	1.60	2.10	2.10
Na_2O	2.30	0.18	0.87	1.20	1.50	2.00	2.30	2.70	2.10
K_2O	4.50	6.40	6.50	5.30	6.10	4.70	5.50	4.70	4.20
TiO_2	0.39	0.31	0.35	0.43	0.37	0.37	0.18	0.31	0.18
P_2O_5	0.14	0.12	0.15	0.16	0.17	0.15	0.15	0.15	0.09
MnO	0.04	0.04	0.02	0.04	0.04	0.06	0.05	0.04	0.06
CO_2	1.10	0.86	1.10	1.10	0.96	0.48	1.30	0.18	1.80
S	1.10	2.40	1.70	1.50	0.89	1.60	0.73	0.56	0.55
Cl	.01	.01	.01	.01	.01	.01	.01	.01	.01
F	0.08	0.07	0.10	0.11	0.12	0.08	0.06	0.05	0.05
H_2O^+	1.80	1.50	1.40	1.60	1.70	1.60	1.30	1.20	1.60
H_2O^-	0.15	0.01	-	0.10	0.03	0.08	0.06	0.04	0.16
Subtotal	100.31	99.69	100.21	100.24	100.50	100.60	100.17	100.46	100.82
Less O	0.03	0.03	0.04	0.05	0.05	0.03	0.03	0.03	0.02
Total	100.28	99.66	100.17	100.19	100.45	100.57	100.14	100.43	100.80
Rb	169.	218.	213.	194.	224.	175.	194.	143.	108.
Cs	2.4	1.3	1.7	2.2	2.5	1.7	2.1	1.3	2.1
Sr	285.	93.	104.	153.	174.	232.	276.	392.	90.
Ba	774.	878.	855.	765.	877.	855.	789.	753.	815.
Y	9.	9.	9.	7.	9.	9.	7.	6.	7.
La	24.	28.	25.	23.	23.	25.	26.	23.	23.
Ce	44.	46.	41.	41.	43.	46.	43.	39.	38.
Nd	18.	17.	17.	16.	17.	18.	16.	16.	15.
Sm	2.7	2.7	2.4	2.6	2.5	2.7	2.5	2.4	2.3
Eu	0.64	0.59	0.59	0.57	0.65	0.64	0.56	0.55	0.49
Gd	-	-	-	-	-	-	-	-	2.1
Tb	0.19	0.16	0.18	0.19	0.2	0.18	0.19	0.17	0.16
Ho	-	-	-	-	-	-	-	-	-
Tm	0.21	0.15	0.12	0.15	0.15	0.16	0.14	0.11	0.16
Yb	0.2	0.1	0.4	0.6	0.3	0.6	0.1	0.3	0.1
Lu	0.07	0.07	0.07	0.07	0.07	0.07	0.06	0.05	0.06
Zr	118.	88.	99.	103.	106.	114.	112.	108.	107.
Hf	3.4	2.6	2.9	3.8	3.1	3.2	3.	2.9	2.8
Nb	6.6	7.8	8.	9.8	6.4	4.	7.2	5.6	4.4
Ta	0.54	0.47	0.49	0.66	0.50	0.47	0.52	0.65	0.4
Th	8.8	8.4	9.4	11.	10.	8.8	8.8	10.4	8.7
U	3.2	12.2	10.3	9.	5.	3.	3.6	4.3	2.2
Sc	5.2	3.8	4.5	4.6	4.9	4.8	4.0	4.1	3.0
Cr	14.1	10.5	11.4	13.8	12.3	9.3	9.9	10.4	6.3
Co	7.2	9.5	3.4	7.3	4.9	6.1	5.1	5.6	2.7
Ni	14.	8.1	6.9	11.	10.	9.4	8.8	9.4	5.
Cu	420.	3900.	1900.	1400.	1900.	2200.	620.	940.	160.
Zn	53.	53.	77.	107.	117.	30.	36.	34.	80.
Li	14.	15.	17.	14.	17.	11.	7.	9.8	7.
Be	1.7	1.0	1.3	1.5	1.8	1.5	1.7	1.6	1.
B	7.6	5.5	6.9	10.	8.8	4.8	7.5	7.7	14.
Sn	2.8	5.5	3.8	4.	2.5	5.	2.3	1.1	-
W	5.7	6.7	8.6	12.	6.2	6.9	3.9	2.4	5.6
Mo	11.	320.	40.	240.	16.	65.	120.	120.	54.
Sb	0.8	1.	0.6	0.7	0.6	0.6	0.9	1.	0.8

* Sample locations indicated by drill-core number and depth (in feet). Major oxides are in weight percent. Trace elements are in parts per million. R-225 (LP-I-4) and R-143 (LP-0-1) are surface samples.

** EHM refers to rocks from the mineralized equigranular host rocks; EH represents rocks from the unmineralized equigranular host rocks.

TABLE 1. CONTINUED.

SAMPLE*	CM80-673 EH**	R-225* EH	CM39-320 EH	CM114-442 EH	CM113-256 EH	CM31-210 EH	CM31-160 EH	CM31-52 EH	R-143* EH
SiO_2	64.20	67.10	67.80	67.90	68.30	68.50	68.70	70.70	70.90
Al_2O_3	16.80	16.30	15.50	16.00	14.90	15.40	14.80	15.00	15.00
Fe_2O_3	2.10	1.40	1.50	1.30	1.20	1.50	1.50	1.60	1.20
FeO	1.70	1.20	1.00	1.20	1.20	1.10	0.92	0.40	1.00
MgO	1.80	1.40	1.30	1.30	1.30	1.30	1.10	0.86	1.20
CaO	3.90	2.30	2.60	3.10	2.30	2.50	2.40	3.30	2.40
Na_2O	3.80	3.90	3.20	3.50	3.0	3.40	2.70	3.70	3.80
K_2O	2.50	3.10	3.70	3.10	4.30	3.90	4.50	2.50	3.40
TiO_2	0.44	0.33	0.32	0.33	0.32	0.31	0.31	0.26	0.30
P_2O_5	0.16	0.16	0.14	0.14	0.16	0.16	0.14	0.13	0.16
MnO	0.04	0.06	0.05	0.03	0.04	0.06	0.04	0.04	0.07
CO_2	0.48	0.04	0.46	0.16	0.92	0.15	0.91	0.10	0.03
S	0.19	0.33	0.58	0.16	0.68	0.37	0.84	0.05	0.24
Cl	.01	0.02	.01	.01	.01	.01	.01	.01	.01
F	0.07	0.07	0.07	0.06	0.05	0.06	0.07	0.04	0.04
H_2O^+	1.60	1.50	1.40	1.40	1.40	1.30	1.20	1.10	1.40
H_2O^-	0.11	0.07	0.08	0.08	0.09	0.08	0.08	0.06	0.07
Subtotal	99.89	99.28	99.70	99.76	100.16	100.09	100.21	99.84	101.21
Less O	0.03	0.03	0.03	0.03	0.02	0.03	0.03	0.02	0.02
Total	99.86	99.25	99.67	99.73	100.14	100.06	100.18	99.82	101.19
Rb	93.	103.	140.	97.	166.	126	168.	87.	96.
Cs	1.2	1.5	1.5	1.1	1.8	1.2	2.	0.9	1.3
Sr	609.	390.	459.	680.	370.	496.	329.	621.	512.
Ba	747.	741.	814.	754.	894.	777.	865.	456.	925.
Y	6.	9.	4.	5.	5.	4.	6.	5.	6.
La	-	24.	19.	20.	28.	-	-	-	21.
Ce	47.	42.	38.	41.	53.	34.	49.	41.	36.
Nd	19.	17.	15.	18.	21.	8.	18.	16.	12.
Sm	3.4	2.5	2.6	2.8	3.1	2.3	2.9	2.4	2.5
Eu	0.76	0.63	0.64	0.66	0.66	0.56	0.65	0.52	0.7
Gd	-	1.6	-	-	-	-	-	-	2.2
Tb	0.27	0.21	0.17	0.18	0.18	0.14	0.15	0.16	0.21
Ho		-	0.9		0.5		0.3		-
Tm	0.19	0.03		0.08	0.05	0.12	0.15		0.09
Yb	-	0.4	0.9	0.6	0.7	-	-	-	0.5
Lu	-	0.08	0.12	0.08	0.1	-	-	-	0.08
Zr	137.	113.	115.	121.	135.	106.	110.	113.	105.
Hf	3.6	3.2	3.	3.	3.3	3.	2.8	2.9	2.9
Nb	6.8	5.	5.4	6.	6.6	6.2	7.2	4.	7.
Ta	0.51	0.47	0.48	0.54	0.79	0.55	0.59	0.74	0.80
Th	8.4	7.	9.6	8.9	13.9	8.2	9.7	12.1	10.8
U	2.4	1.8	3.6	2.7	4.2	2.6	3.8	3.5	2.1
Sc	7.6	4.9	4.9	4.8	4.6	4.6	4.2	3.6	4.4
Cr	19.1	9.5	12.9	12.2	14.5	12.9	12.4	9.8	8.6
Co	8.3	4.4	6.1	5.8	6.	5.9	5.1	3.5	5.2
Ni	21.	12.	16.	15.	19.	18.	16.	13.	11.
Cu	58.	10.	600.	79.	320.	160.	450.	38.	74.
Zn	28.	35.	47.	37.	88.	51.	54.	33.	31.
Li	11.	14.	10.	8.1	10.	8.1	10.	7.9	11.
Be	1.9	1.6	1.6	1.9	1.9	1.8	1.5	1.6	1.6
B	8.6	17	6.2	6.2	5.7	6.6	7.1	8.6	5.7
Sn	1.9	3.1	1.1	0.5	1.7	0.9	1.8	0.8	2.3
W	0.88	1.6	3.8	1.	8.8	3.8	6.8	1.	2.
Mo	0.58	0.22	2.2	0.52	2.3	0.77	0.37	0.4	1.9
Sb	0.2	0.4	1.6	0.3	0.3	0.6	0.2	0.3	0.7

* Sample locations indicated by drill-core number and depth (in feet). Major oxides are in weight percent. Trace elements are in parts per million. R-225 (LP-I-4) and R-143 (LP-0-1) are surface samples.

** EHM refers to rocks from the mineralized equigranular host rocks; EH represents rocks from the unmineralized equigranular host rocks.

TABLE 2. REPRESENTATIVE ANALYSES OF THE PORPHYRITIC DIKES OF THE CATHEART MOUNTAIN PLUTON, MAINE

SAMPLE*	CM88-452 PDM**	CM28-159 PDM	CM32-642 PDM	CM28-260 PDM	CM4-350 PDM	CM39-463 PD**	CM31-282 PD	CM96-310 PD
SiO_2	64.50	66.90	67.40	67.40	70.70	65.40	65.60	66.10
Al_2O_3	15.30	13.80	14.80	14.50	12.50	15.10	15.60	15.90
Fe_2O_3	2.60	3.90	2.10	2.80	5.40	2.60	2.30	2.90
FeO	0.52	0.20	0.12	0.20	0.20	0.20	0.20	1.00
MgO	1.30	0.77	1.00	0.94	0.50	1.30	1.10	1.40
CaO	2.50	1.60	3.00	1.90	0.46	3.00	3.10	2.40
Na_2O	1.50	0.14	1.70	0.87	0.15	0.47	2.00	2.70
K_2O	4.60	6.00	4.30	5.20	4.10	5.70	4.50	3.50
TiO_2	0.38	0.29	0.31	0.32	0.27	0.33	0.37	0.38
MnO	0.04	0.04	0.06	0.02	0.01	0.07	0.06	0.06
CO_2	2.00	1.20	2.30	1.50	0.27	2.20	2.3	0.54
S	1.50	3.10	1.40	2.20	4.00	1.40	1.50	1.70
Cl	.01	.01	.01	.01	.01	.01	.01	.01
F	0.08	0.10	0.10	0.10	0.08	0.14	0.14	0.10
H_2O^+	2.10	1.70	1.80	1.80	1.70	2.00	1.7	1.80
H_2O^-	0.16	0.06	0.04	0.06	0.04	0.07	0.07	0.07
Subtotal	99.08	99.80	100.43	99.81	100.38	99.98	100.54	100.56
Less O	0.03	0.04	0.04	0.04	0.03	0.06	0.06	0.04
Total	99.05	99.76	100.39	99.77	100.35	99.92	100.48	100.5
Rb	148.	191.	154.	188.	155.	290.	210.	175.
Cs	2.2	2.1	3.6	3.	0.8	3.3	3.8	1.9
Sr	313.	97.	108.	76.	47.	104.	168.	372.
Ba	641.	855.	527.	662.	490.	590.	509.	647.
Y	6.	8.	11.	10.	9.	14.	7.	5.
La	32.	30.	27.	26.	28.	19.	19.	26.
Ce	54.	48.	46.	43.	52.	31.	39.	46.
Nd	21.	18.	17.	16.	20.	15.	7.	19.
Sm	3.1	2.6	2.8	2.6	3.	2.4	2.5	3.1
Eu	0.68	0.58	0.66	0.67	0.65	0.66	0.66	0.74
Gd	-	-	-	-	-	-	-	-
Tb	0.18	0.19	0.2	0.22	0.27	0.16	0.18	0.23
Ho	-	-	-	-	-	-	-	-
Tm	0.17	0.11	-	0.21	0.19	0.12	0.09	-
Yb	-	0.2	0.5	0.4	0.4	0.6	0.4	0.5
Lu	0.06	0.08	0.07	0.08	0.1	0.07	0.05	0.07
Zr	121.	137.	153.	148.	129.	97.	105.	129.
Hf	3.	3.6	4.1	4.	3.7	2.6	2.7	3.6
Nb	4.6	7.2	5.2	6.2	6.6	3.	3.6	4.4
Ta	0.38	0.58	0.46	0.58	0.5	0.31	0.29	0.43
Th	9.5	7.8	9.	8.2	8.7	5.4	6.2	7.7
U	3.7	4.7	2.5	2.4	3.3	2.6	2.1	2.6
Sc	5.1	3.52	3.9	3.78	3.7	5.1	4.6	6.2
Cr	10.5	5.6	8.3	9.9	6.6	6.9	9.1	11.3
Co	7.4	7.5	5.7	10.	15.6	5.	5.5	7.7
Ni	14.	8.8	6.9	7.5	11.	13.	10.	17.
Cu	2300.	2700.	1800.	3500.	3300.	780.	740.	520.
Zn	91.	86.	241.	125.	282.	197.	560.	48.
Li	10.	11.	8.	11.	12.	17.	13.	11.
Be	1.8	1.3	1.6	1.7	1.	2.2	1.7	1.8
B	8.7	7.5	21.	17.	40.	17.	16.	9.4
Sn	4.	7.3	3.4	5.9	13.	1.6	0.9	2.
W	7.	9.8	5.1	6.5	8.3	49.	27.	20.
Mo	20.	160.	31.	210.	84.	0.28	0.4	18.
Sb	1.4	17.7	60.5	5.	1.	2.	1.6	0.9

* Sample locations indicated by drill-core number and depth (in feet). Major oxides are in weight percent; trace elements are in parts per million.
** PDM represents samples from the mineralized porphyritic dikes; PD samples are from the unmineralized porphyrtic dikes.

TABLE 2. CONTINUED.

SAMPLE*	CM114-490 PD	CM12-370 PD	CM4-250 PD	CM5-680 PD	CM5-740 PD	CM4-300 PD	CM4-280 PD
SiO_2	66.70	66.80	67.40	67.80	68.00	69.30	69.70
Al_2O_3	16.10	15.90	15.30	15.00	15.10	14.10	14.30
Fe_2O_3	2.10	2.00	1.50	2.50	2.60	1.80	1.90
FeO	1.20	1.00	0.28	0.72	0.65	0.28	0.32
MgO	1.50	1.50	0.63	1.10	1.10	0.70	0.66
CaO	3.40	2.60	3.00	2.20	1.70	2.70	2.80
Na_2O	3.40	2.60	2.90	2.60	1.90	2.10	2.50
K_2O	2.70	3.30	3.40	3.90	4.20	3.90	3.50
TiO_2	0.38	0.39	0.24	0.29	0.28	0.25	0.24
MnO	0.05	0.05	0.02	0.05	0.04	0.05	0.05
CO_2	0.19	0.41	2.30	0.78	0.83	2.00	2.10
S	--	0.66	0.80	1.40	1.40	0.87	1.10
Cl	.01	.01	.01	.01	.01	.01	.01
F	0.08	0.07	0.10	0.07	0.09	0.07	0.07
H_2O^+	1.50	1.90	1.50	1.50	1.90	1.40	1.40
H_2O^-	0.15	0.12	0.08	0.09	0.10	0.08	0.08
Subtotal	99.45	99.30	99.46	100.01	99.90	99.60	100.72
Less O	0.03	0.03	0.04	0.03	0.04	0.03	0.03
Total	99.42	99.27	99.42	99.98	99.86	99.57	100.69
Rb	94.	136.	138.	127.	143.	137.	132.
Cs	1.5	2.1	1.9	1.9	1.9	2.1	2.2
Sr	861.	498.	156.	379.	249.	113.	135.
Ba	881.	869.	673.	756.	721.	814.	606.
Y	0.	6.	6.	4.	7.	7.	4.
La	22.	30.	23.	24.	21.	22.	21.
Ce	40.	57.	40.	43.	35.	37.	36.
Nd	17.	21.	14.	17.	14.	13.	17.
Sm	3.2	3.1	2.3	2.5	2.5	2.1	2.2
Eu	0.79	0.7	0.58	0.59	0.56	0.5	0.49
Gd	-	-	-	-	-	-	2.2
Tb	0.24	0.15	0.17	0.16	0.15	0.15	0.15
Ho	-	-	-	-	0.5	-	-
Tm	0.1	0.11	0.07	0.05	-	-	0.08
Yb	0.7	0.4	0.4	0.5	0.5	0.4	0.3
Lu	0.07	0.06	0.06	0.07	0.06	0.06	0.06
Zr	135.	133.	120.	105.	104.	99.	100.
Hf	3.5	3.	3.1	3.	2.7	2.8	2.6
Nb	5.	5.4	3.2	4.2	4.8	4.6	4.2
Ta	0.50	0.35	0.36	0.40	0.43	0.43	0.38
Th	7.1	9.8	9.1	9.4	8.9	8.3	9.
U	2.6	2.4	2.7	3.6	3.7	3.	2.7
Sc	6.1	5.5	3.5	4.3	4.2	3.5	3.5
Cr	13.7	12.	5.9	10.7	10.	6.3	5.6
Co	7.3	7.	3.2	8.1	7.4	4.	3.1
Ni	18.	12.	5.8	11.	11.	10.	6.8
Cu	240.	840.	180.	1500.	760.	280.	250.
Zn	52.	65.	46.	462.	92.	64.	53.
Li	10.	10.	8.7	10.	9.5	7.9	8.1
Be	2.	1.6	1.5	1.5	1.5	1.4	1.4
B	7.4	11.	16.	11.	6.7	23.	18.
Sn	1.5	1.4	1.5	2.6	2.4	1.4	1.8
W	2.5	12.	4.1	5.8	7.9	5.4	5.8
Mo	1.6	2.1	7.4	13.	4.3	30.	18.
Sb	0.2	1.6	0.4	0.3	0.5	0.8	0.3

* Sample locations indicated by drill-core number and depth (in feet). Major oxides are in weight percent; trace elements are in parts per million.
** PDM represents samples from the mineralized porphyritic dikes; PD samples are from the unmineralized porphyrtic dikes.

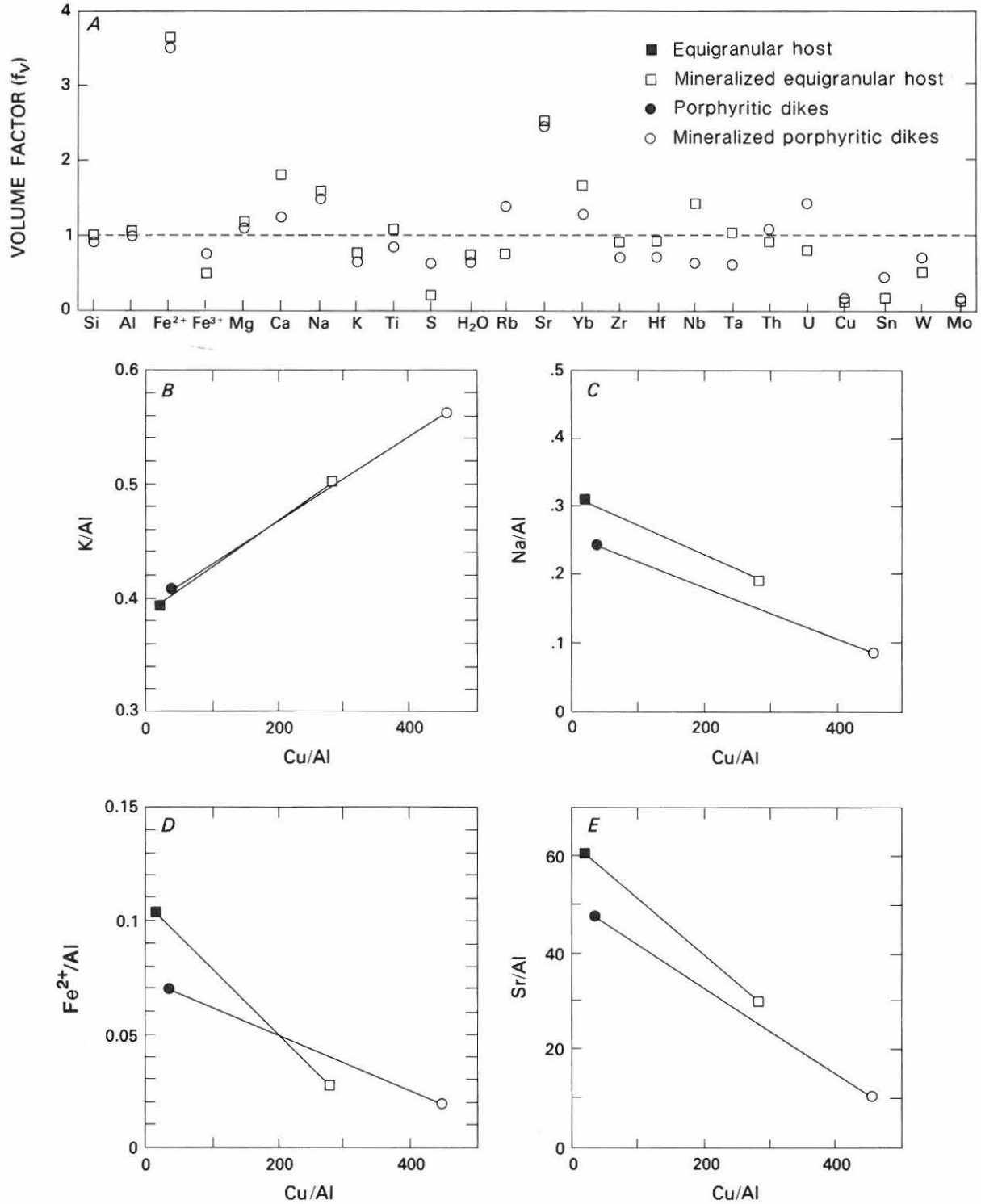

Figure 2. Summary diagram of composition-volume relations. (a) Variation of the volume factor (f_v) for the major and trace elements and base metals in the host rocks and porphyritic dikes of the Catheart Mountain pluton. Relatively immobile components have $f_v = 1$; components gained during alteration and mineralization have values of $f_v < 1$, and components lost from the system have values of $f_v > 1$ (see text for details). (b-d) Diagrams showing transfer of components in the average compositions of the equigranular host rocks (solid squares), sulfide-rich host rocks (open squares), porphyritic dikes (solid circles), and mineralized porphyritic dikes (open circles) as a function of Al, an immobile component in the Catheart Mountain pluton, and Cu, a component added to the system: (b) increasing K as a function of increasing Cu; (c) decreasing Na with increasing Cu; (d) decreasing Fe^{2+} with increasing Cu; and (e) decreasing Sr with increasing Cu.

1967; Ford, 1978; Schwartz, 1982). In the equigranular host rocks, Ti has f_v values of about 1 indicating the relative immobility of this component, but in the porphyritic dikes f_v values for Ti are slightly less than 1.

The high-valence cations Zr, Hf, Ta, and Th appear to have been relatively immobile; there is, however, a consistent difference in f_v values between the equigranular host rocks and the porphyritic dikes. In the equigranular rocks these incompatible elements have f_v values of about 1, in contrast to the porphyritic dikes which have values slightly lower than 1 for Zr, Hf, Nb, and Ta, indicating that these components might have been gained during hydrothermal alteration. Nb has f_v values greater than 1 in the equigranular rocks suggesting that it was lost during hydrothermal processes.

S, Cu, Sn, W, and Mo have f_v values much lower than 1, which is consistent with the addition of these components during mineralization.

Examples of the chemical changes converting sulfide-poor to sulfide-rich rocks in the Catheart Mountain pluton are summarized in Figures 2b-2f, where the elements are plotted as ratios to Al (an immobile element). These results illustrate the relative increase in K and decrease in Na, Fe^{2+}, and Sr during mineralization.

Major Elements

The range in SiO_2 is relatively narrow, from about 63 to 72%. One important chemical characteristic of the pluton as a whole is the general absence of chemical gradients within the equigranular host rocks and the porphyritic dikes as a function of increasing silica or of any other measure of chemical evolution. Similarly, there is no progressive compositional change from the equigranular host rocks to the porphyritic dikes. Figure 3 displays several of the more regular variations of the major elements with silica in the equigranular host rocks and in the porphyritic dikes.

The absence of progressive changes in the major oxides with silica strongly suggests that most of the major oxide compositions are not magmatic, in agreement with composition-volume relations indicating significant redistribution of the major oxides and with petrographic studies indicating abundant chlorite, hematite, white mica, and carbonate minerals especially in the more altered rocks of the Catheart Mountain pluton. Additional direct evidence of the chemical disturbance is demonstrated by the high CO_2, S, and H_2O contents which characterize even the rocks containing the lowest Cu and Mo (Tables 1, 2) compared to most calc-alkaline granites (e.g. Nockolds, 1954). Thus, on the basis of the major-element oxides, volatile content, and base-metal content of these rocks, no reliable chemical characterization can be made that gives a direct indication of the primary magmatic composition of the system or that satisfactorily classifies the Catheart Mountain pluton by means of ordinary schemes. This suggests that it is unlikely that the chemical variations of these elements are primary or that they can be used to unravel the magmatic evolution of the Catheart Mountain pluton.

On the alkali-silica (Fig. 4) and Alk-F-M plots (not shown), the equigranular host rocks fall generally within the field of calc-alkaline rocks, having alkali contents similar to those found in porphyry copper deposits at continental edges (summarized by Titley and Beane, 1981, and Beane and Titley, 1981). The equigranular host rocks generally have higher total alkali contents than do the porphyritic dikes. In contrast to the equigranular host rocks, the porphyritic dikes overlap significantly the tholeiitic field on the alkali-silica diagram (Fig. 4). Such comparisons, however, are unlikely to be meaningful as suggested by the composition-volume relations which indicate that the alkali elements have been substantially disturbed.

The most important compositional differences between the sulfide-poor and sulfide-rich equigranular host rocks and the porphyritic dikes are shown by the contents of K_2O, Na_2O, CaO, Fe_2O_3, and FeO (Fig. 3). The sulfide-rich equigranular host rocks differ from the sulfide-poor host rocks because they are depleted in CaO, Na_2O, and FeO, and because they are relatively enriched in K_2O and Fe_2O_3. The sulfide-rich porphyritic dikes show similar variations when compared to the unmineralized porphyritic dikes, except that the variations are not as pronounced, particularly for K_2O (Fig. 3).

In the Harker diagrams, values of SiO_2 have a tendency to remain unchanged (in agreement with composition-volume relations) within each of the petrographic groups, although silica increases slightly in the mineralized equigranular host rocks and decreases in the mineralized porphyritic dikes. Al_2O_3 decreases in the sulfide-rich rocks, but this again is in contrast to the composition-volume relations and the well-known tendency for Al_2O_3 to remain immobile during alteration (Meyer and Hemley, 1967).

In the equigranular mineralized host rocks MgO decreases in agreement with composition-volume relations and the overall depletion of this component in many porphyry copper systems (e.g., Ford, 1978). P_2O_5 and MnO contents show no meaningful changes between the different rock types.

Compared to the Catheart Mountain pluton, the Sally Mountain pluton is significantly enriched in SiO_2 and is relatively depleted in Al_2O_3, CaO, FeO, Fe_2O_3, MgO, TiO_2, P_2O_5, and MnO (Table 3).

F is higher in some of the samples of the mineralized equigranular host rocks relative to the unmineralized rocks, and this suggests the effects of hydrothermal alteration (Tables 1, 2). F contents as high as 0.14% in the porphyritic dikes, however, are only slightly higher than in high-Ca granites (Turekian and Wedepohl, 1961).

Cl contents as high as 0.02% are found in the sulfide-poor host rocks. These Cl values are equivalent to those in high-Ca granites, and they decrease as a function of increasing Cu. Samples from the Sally Mountain pluton are generally low in both F and Cl (Table 3).

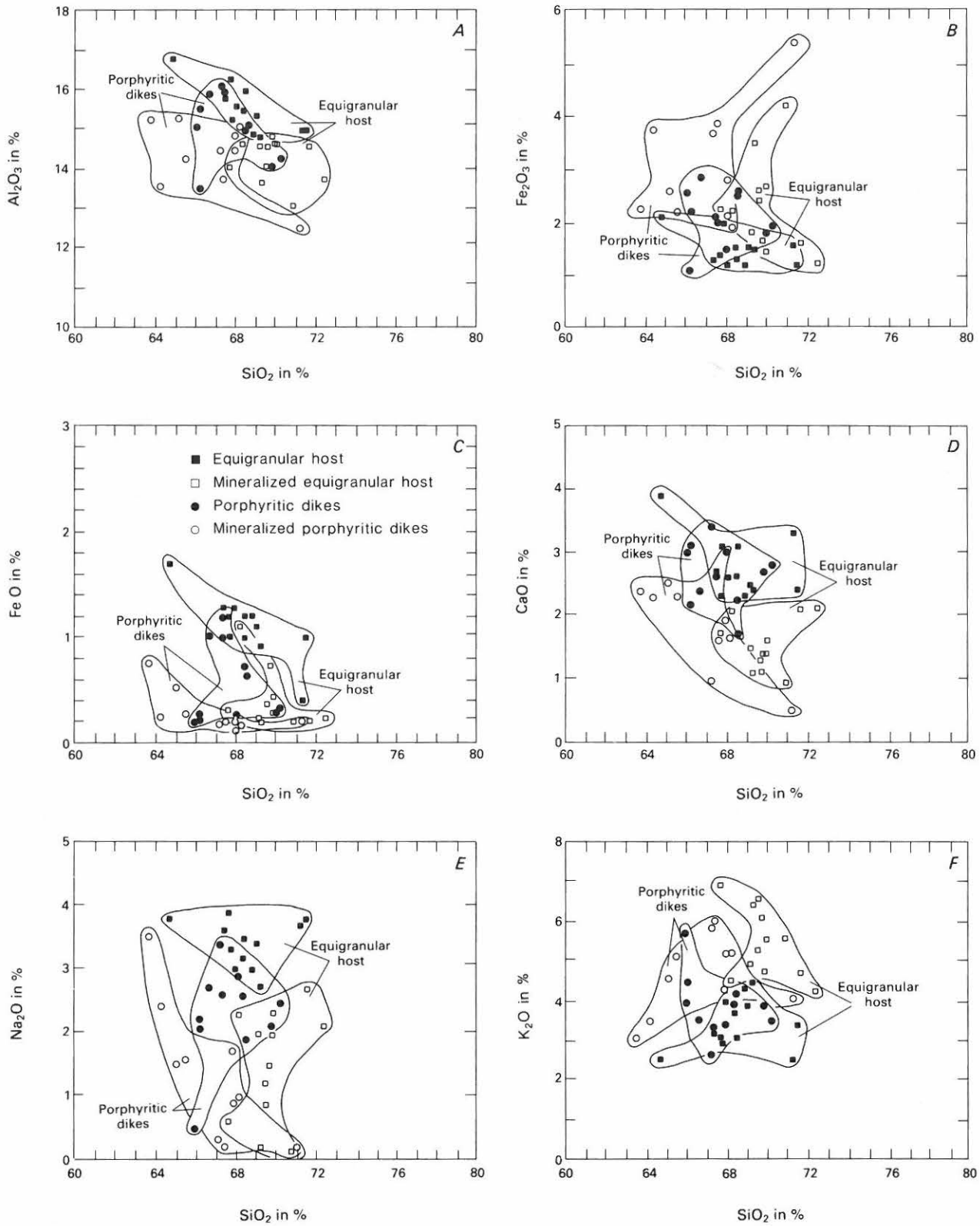

Figure 3. Variation diagrams for selected major oxides plotted against silica of the equigranular host (solid squares), mineralized equigranular host (open squares), porphyritic dikes (solid circles), and mineralized porphyritic dikes (open circles). Note that the equigranular host is higher in FeO, CaO, and Na_2O, and lower in K_2O relative to the mineralized equigranular host.

TABLE 3. REPRESENTATIVE ANALYSES OF THE SALLY MOUNTAIN PLUTON AND THE ATTEAN QUARTZ MONZONITE, MAINE

SAMPLE	SALLY ATO-2	SALLY ATO-6	SALLY ATO-7	SALLY ATO-1	ATTEAN SM90140	ATTEAN BA-766	ATTEAN SM90138	ATTEAN AQM-CL
Latitude	45°34'36"	45°34'39"	45°34'37"	45°34'37"	---	---	---	45°35'10"
Longitude	70°19'47"	70°19'47"	70°19'46"	70°19'48"	---	---	---	70°33'45"
SiO_2	75.50	76.50	76.50	78.40	69.50	70.20	70.30	79.30
Al_2O_3	13.30	12.50	13.20	10.50	14.80	14.50	14.40	12.10
Fe_2O_3	0.98	0.59	0.69	0.43	0.80	1.40	1.30	0.88
FeO	0.20	0.20	0.28	0.24	2.20	1.30	3.40	0.16
CaO	0.07	0.34	0.16	0.82	1.60	3.10	0.75	0.11
Na_2O	0.39	2.60	1.60	3.50	3.30	3.20	2.20	6.00
K_2O	7.50	5.50	5.90	4.90	4.40	3.80	4.90	0.31
TiO_2	0.20	0.18	0.33	0.12	0.28	0.47	0.27	0.13
P_2O_5	0.05	0.06	0.08	0.06	0.12	0.26	0.12	0.06
MnO	0.03	0.03	0.04	0.08	0.02	0.06	0.04	---
CO_2	0.03	0.12	0.05	0.25	0.04	0.05	0.08	0.07
S	---	0.093	0.013	---	---	---	---	---
Cl	.01	0.02	.01	.01	---	---	---	.01
F	0.04	0.02	0.05	---	---	---	---	0.01
H_2O^+	1.20	0.61	1.00	0.29	1.80	0.83	1.30	0.50
H_2O^-	0.11	0.10	0.11	0.04	0.03	---	0.04	0.15
Subtotal	100.21	99.70	100.45	99.82	100.39	100.04	100.30	99.85
Less O	0.02	0.01	0.02	---	0	0	0	0.01
Total	100.19	99.69	100.43	99.82	100.39	100.04	100.30	99.84
Rb	292.	179.	219.	182.	---	---	---	6.
Cs	1.7	1.6	1.8	1.	---	---	---	0.4
Sr	55.	76.	59.	69.	---	---	---	40.
Ba	555.	415.	452.	124.	---	---	---	75.
Y	12.	13.	10.	11.	---	---	---	65.
La	24.	38.	25.	49.	---	---	---	16.
Ce	30.	62.	50.	50.	---	---	---	36.
Nd	10.	19.	10.	14.	---	---	---	22.
Sm	2.	2.7	1.3	2.	---	---	---	6.4
Eu	0.31	0.41	0.24	0.27	---	---	---	0.69
Gd	---	---	---	---	---	---	---	---
Tb	0.11	0.16	0.08	---	---	---	---	1.34
Ho	---	---	---	---	---	---	---	1.5
Tm	0.08	---	---	0.09	---	---	---	0.95
Yb	0.6	0.8	0.7	1.	---	---	---	8.1
Lu	0.1	0.12	0.11	0.13	---	---	---	0.94
Zr	92.	92.	107.	83.	---	---	---	217.
Hf	2.7	3.	3.6	3.2	---	---	---	6.1
Nb	12.	9.	9.	18.	---	---	---	4.6
Ta	1.29	1.04	1.14	2.02	---	---	---	3.31
Th	30.8	26.7	24.8	35.4	---	---	---	3.8
U	3.2	3.4	2.9	5.9	---	---	---	1.3
Sc	1.95	1.43	1.63	1.8	---	---	---	6.88
Cr	3.4	1.1	1.9	0.68	---	---	---	---
Co	1.5	1.4	1.3	0.8	---	---	---	55.4
Ni	3.7	7.5	3.1	3.1	---	---	---	1.
Cu	---	86.	11.	15.	---	---	---	---
Zn	33.	9.	21.	11.	---	---	---	13.
Li	9.5	5.9	11.	3.8	---	---	---	2.
Be	3.3	2.	1.6	2.7	---	---	---	3.9
B	11.	3.4	10.	2.4	---	---	---	0.9
Sn	2.5	1.8	3.1	1.	---	---	---	0.9
W	5.	2.8	2.4	5.8	---	---	---	130.
Mo	0.13	0.27	1.3	---	---	---	---	0.9
Sb	0.1	0.1	0.1	0.1	---	---	---	0.3

* All samples from the Attean Quartz Monzonite with the exception of AQM-CL are from Schmidt (1974). Major oxides are in weight percent. Trace elements are in parts per million.

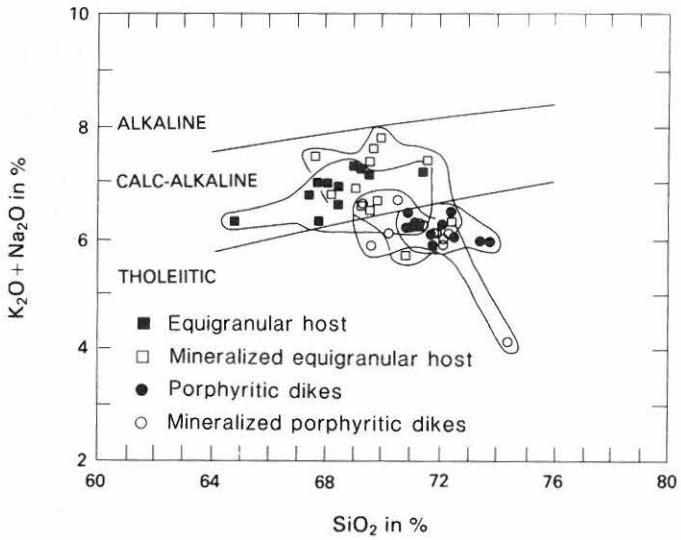

Figure 4. Kuno variation diagram. Equigranular host rocks and their mineralized parts shown as solid and open squares, respectively. Porphyritic dikes and their mineralized parts shown as solid and open circles. Most samples from the equigranular host rocks fall within the field of calc-alkaline rocks. Most samples of the porphyritic dikes are in the tholeiitic field. The alkali elements have been disturbed from their magmatic compositions as suggested by the composition-volume relations, and thus they cannot be used to classify the Catheart Mountain pluton.

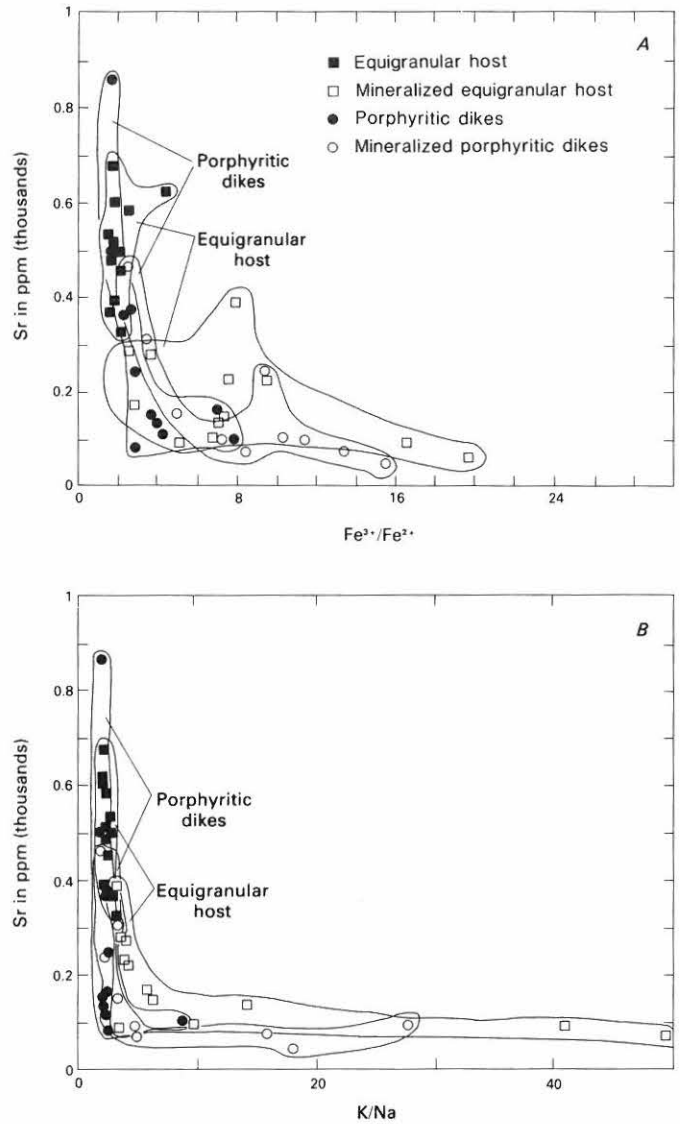

Figure 5. (a) Diagram showing the change in Sr vs. Fe^{3+}/Fe^{2+} in the Catheart Mountain pluton; and (b) Sr vs. K/Na. Sr decreases as a function of increasing oxidation of iron and with increasing K/Na, in a trend from the sulfide-poor to the sulfide-rich equigranular host rocks and porphyritic dikes.

Fugitive Elements

The elements B, Be, and Li show no affinity for either the mineralized or the more barren parts of the Catheart Mountain pluton, except for the moderate enrichment of B in a few samples of the porphyritic dikes compared to the equigranular host rocks. The Sally Mountain pluton is generally lower in B and Li than the rocks of the Catheart Mountain pluton.

Trace Elements

Large Cations. The contents of Rb, Sr, Cs, and Ba range widely (Tables 1, 2), and they are generally uncorrelated with silica. The patterns of enrichment in Rb and depletion in Sr in the sulfide-rich parts of the Catheart Mountain pluton, however, are significant. Sr contents also decrease as a function of decreasing Ca and increasing K/Na and Fe^{3+}/Fe^{2+} values (Fig. 5). Sr compositional variations are thus a reliable way to monitor chemical changes in the bulk rocks during hydrothermal alteration and mineralization.

Rb/Sr ratios are generally low in the Catheart Mountain pluton, from about 0.3 to 3, and they broadly increase with increasing Cu content of the equigranular host rocks as a result of increasing Rb and decreasing Sr (Tables 1, 2). Rb/Sr ratios of less than about 0.5 characterize the sulfide-poor parts of the equigranular host rocks of the Catheart Mountain pluton. This is in agreement with results from other porphyry copper systems showing a general increase in Rb/Sr in the most intensely altered parts of the hydrothermal system (e.g. Ford, 1978). In the porphyritic dikes, this general increase in Rb/Sr ratios between the sulfide-poor and the sulfide-rich porphyritic dikes is not evident.

K/Rb ratios range from about 15 to 33, and no general distinction can be made between the mineralized group of rocks and the more barren parts of the pluton.

Compared to the equigranular host rocks and the porphyritic dikes, the Sally Mountain pluton is generally low in Sr, Ba, and Cs (Table 3). These values are also significantly different from those in the ore-rich portions of the Catheart Mountain pluton.

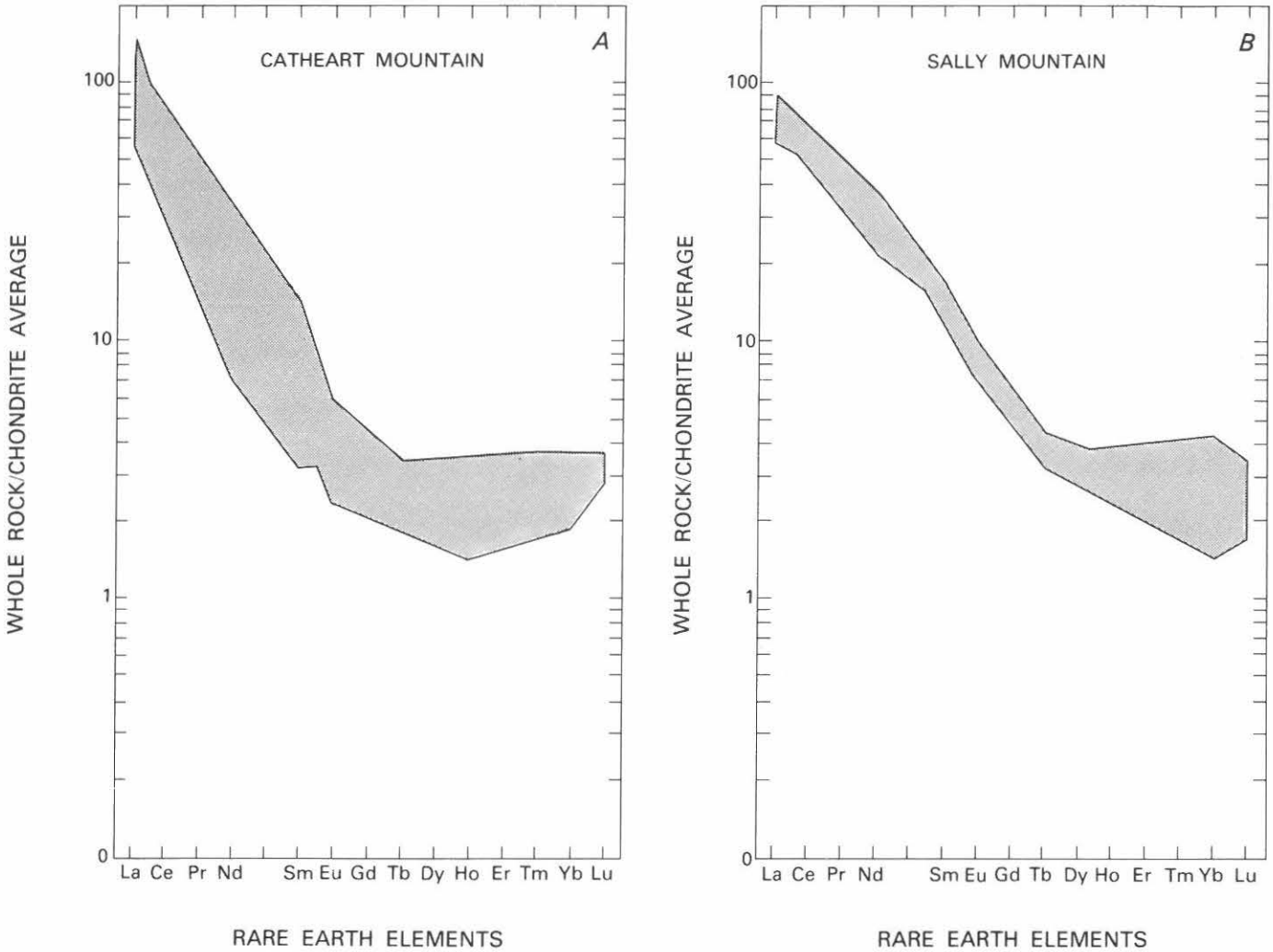

Figure 6. (a) Chondrite-normalized patterns of the rare earth elements in the Catheart Mountain pluton. The total variation in the REE patterns is relatively small within the pluton, and no significant difference exists between the rocks from the equigranular host rocks and porphyritic dikes. (b) Chondrite-normalized REE patterns of the Sally Mountain pluton.

Rare-Earth Elements. Values of the rare-earth elements (REE) in the equigranular host rocks and the porphyritic dikes indicate that the Catheart Mountain pluton is generally homogeneous (Tables 1, 2). REE contents in the sulfide-rich parts of the pluton are generally indistinguishable from the fresher, sulfide-poor, and less hydrothermally altered parts. In contrast, the content of Y in the host rocks is generally higher in the sulfide-rich samples relative to the sulfide-poor samples.

Chondrite-normalized REE patterns have steep negative slopes, characteristic of fractionated compositions (Fig. 6). They also show a wide range of chondrite-normalized Ce/Yb ratios (from 13.5 to 57.6), and they lack Eu anomalies. La ranges from about 60 to 100 times the average chondrite value, and Yb from 1.4 to 4.4 times.

Two important exceptions to the overall homogeneity in the Catheart Mountain pluton are the trend toward higher Th/Yb ratios (a measure of the slope of the heavy REE pattern) and Ce/Yb ratios (a measure of the difference between the light REE and the heavy REE) in the sulfide-rich equigranular host rocks compared to the sulfide-poor host rocks. This general tendency for slight depletion of the heavy REE in the Catheart Mountain pluton agrees with studies showing such changes as a function of increasing alteration in porphyry copper systems (Taylor and Fryer, 1982) as a result of REE fractionation between chloride-rich vapor and silicate melts (Flynn and Burnham, 1978). In contrast to the behavior of the heavy REE in porphyry copper systems, Hudson and Arth (1983) documented depletions in the light REE in evolved, tin-mineralized granites by removal of volatiles from the magma.

The Sally Mountain pluton has REE patterns that overlap the range in the light REE in the Catheart Mountain pluton, but that become progressively gentler in slope toward the middle

REE (Fig. 6). Ce/Yb (chondrite-normalized) ratios range from 12.5 to 26.8. The heavy REE form a trend similar to that of the Catheart Mountain pluton, flattening between Dy and Lu.

High-Valence Cations. Contents of the high-valence cations Zr, Hf, Nb, Ta, Th, and U show generally small changes as a function of silica content, degree of alteration or content of sulfide minerals (Tables 1, 2). This overall homogeneity is in agreement with composition-volume relations indicating that these elements were relatively immobile during alteration, especially in the equigranular host rocks. Significant exceptions to the general compositional pattern in this group of elements are shown by U in the equigranular host rocks and by Nb in the porphyritic dikes. Increasing U in the sulfide-rich host rocks with increasing Cu content results in decreasing Th/U ratio. In the porphyritic dikes, Nb increases as Cu increases.

The Sally Mountain pluton has a distinct compositional range compared to that of the Catheart Mountain pluton, and this may reflect the hydrothermal events or the more advanced stage of evolution of the granitic magma. Alternatively, such differences in these relatively immobile cations may also reflect a different source of the magmas.

Ferromagnesian Elements. The ferromagnesian elements Sc, Co, Cr, Ni, and Zn show no distinctive compositional patterns as a function of silica or Cu content in the Catheart Mountain pluton (Tables 1, 2). Two important exceptions are, however, that most samples from the sulfide-rich equigranular host rocks are slightly lower in Ni than the sulfide-poor host granodiorites, and that in the sulfide-rich porphyritic dikes the content of Zn is higher relative to the sulfide-poor dikes.

The Sally Mountain pluton is characterized by lower values of these elements than are found in the Catheart Mountain pluton (Table 3). This range in compositions is compatible with that of an aplitic part of an evolving magmatic system.

ECONOMIC GEOLOGY

The most important economic base metal in the Catheart Mountain pluton is Cu, but the pluton also contains anomalously high values of Mo, W, and Sn (Tables 1, 2). The range in Cu content is wide, from a few parts per million in the equigranular host rocks and the porphyritic dikes to about 3900 ppm in the sulfide-rich equivalents of these rocks. The maximum observed values for base metals accompanying Cu in the sulfide-rich rocks are 320 ppm Mo, 13 ppm Sn, 49 ppm W, and 560 ppm Zn (Fig. 7).

The Cu/Mo ratio has a wide range, but Schmidt (1974) determined a ratio of about 5 in the most intensely altered parts of the pluton. The Cu/Mo ratio tends to be lower as the rocks become more intensely altered and where the proportion of sulfide minerals increases. No consistent gradient or zoning of the base-metals exists in the Catheart Mountain pluton, although there is a general increase in the content of Zn as a function of increasing Cu in the porphyritic dikes.

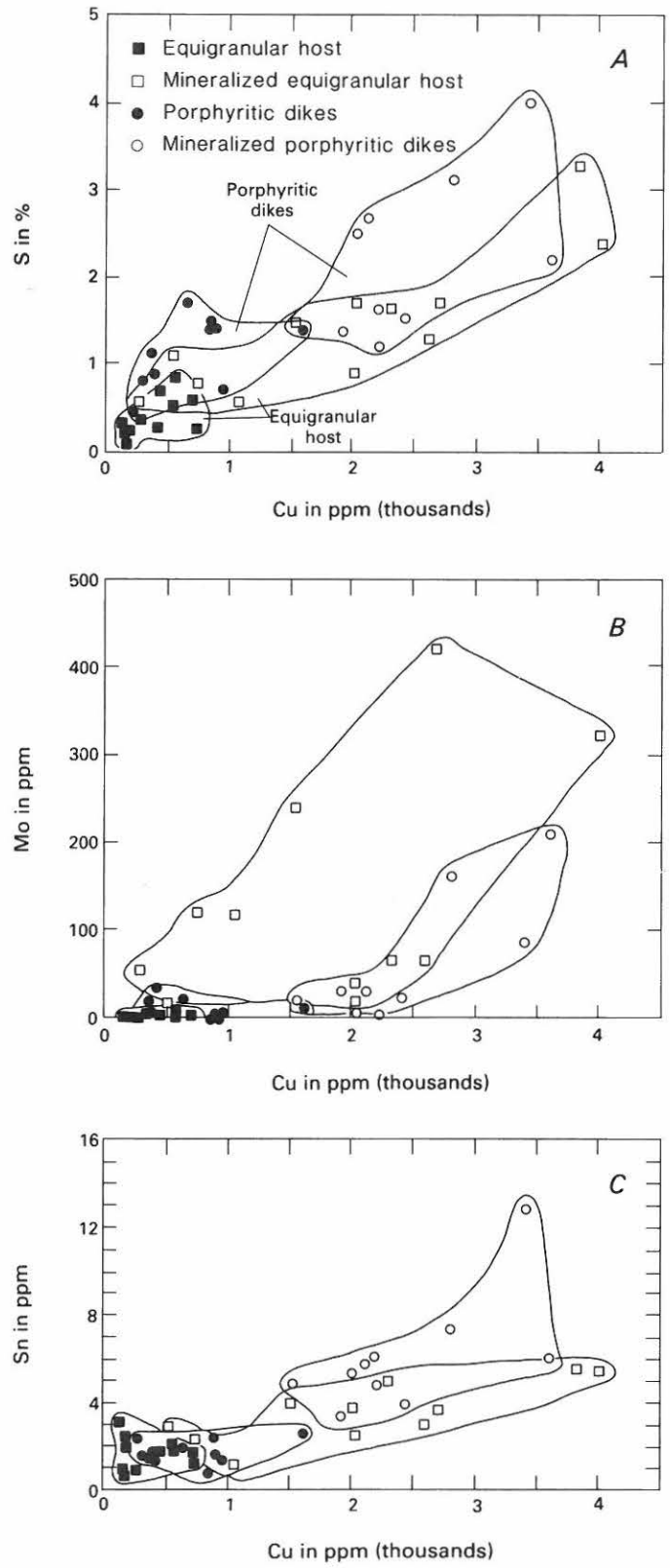

Figure 7. Variation diagrams for S, Mo, and Sn as a function of Cu content.

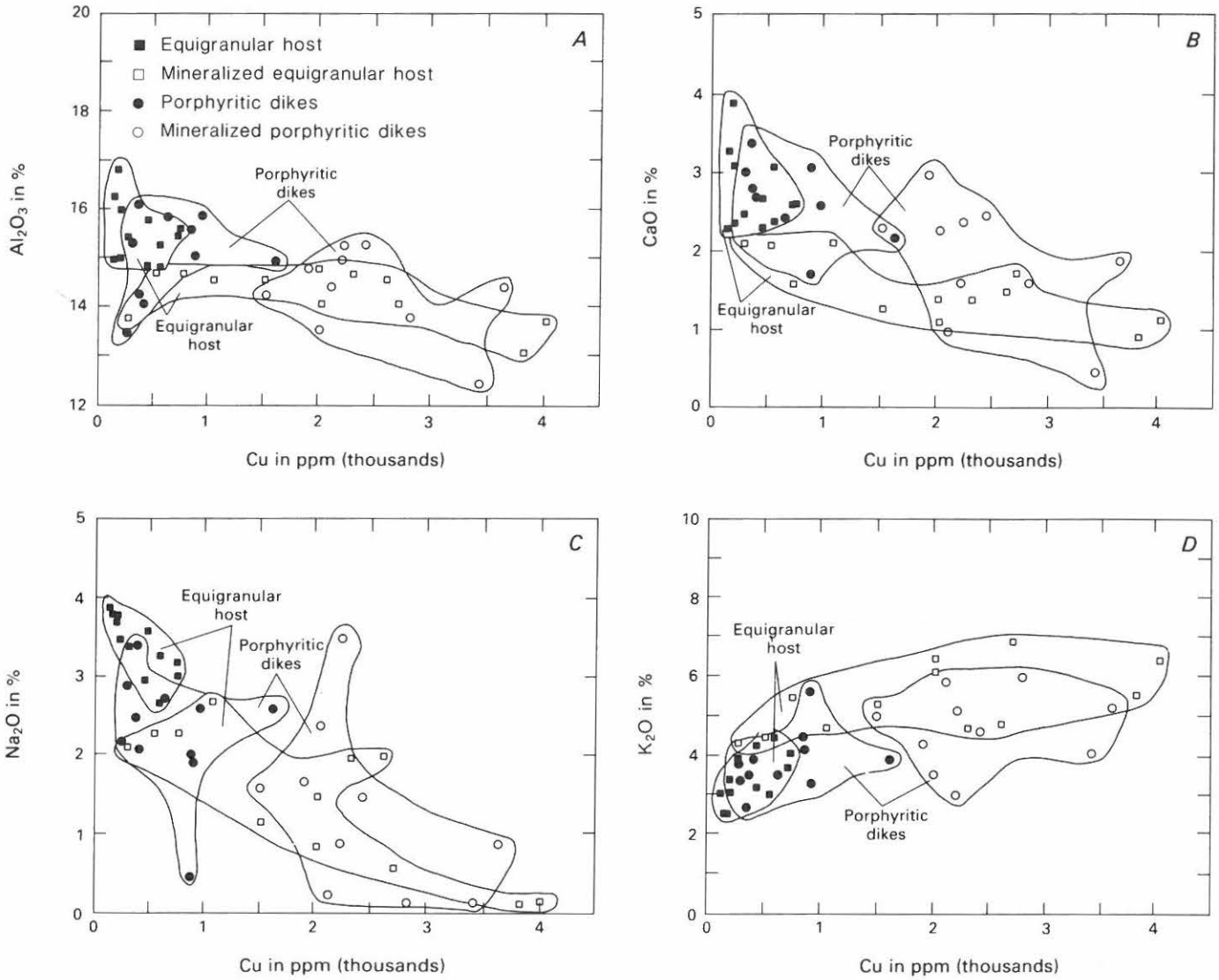

Figure 8. Variation diagrams for selected oxides including Al_2O_3, CaO, Na_2O, and K_2O as a function of the content of Cu. (a) Al_2O_3 decreases slightly as the content of Cu increases in the sulfide-rich equigranular host rocks. Composition-volume relations, however, indicate that Al_2O_3 was relatively immobile during the conversion of sulfide-poor to sulfide-rich equigranular host rocks. (b) CaO and (c) Na_2O generally decrease as the content of Cu increases in the equigranular host rocks and porphyritic dikes. (d) K_2O increases as a result of hydrothermal alteration and mineralization of the Catheart Mountain pluton.

Significant chemical changes in bulk composition accompanied the introduction of the base metals in the mineralized rocks of the Catheart Mountain pluton (Figs. 7-9). These results provide an account of the overall chemical change during alteration and mineralization, and are consistent with detailed geochemical studies of representative samples from individual stages of alteration in porphyry copper deposits elsewhere (e.g. Ford, 1978).

Samples from the equigranular host rock containing high Cu values are characterized by a relative depletion of CaO (less than 1.8%) and Na_2O (generally less than 2.7%), relative to samples containing less Cu in the sulfide-poor parts of the system. These sulfide-rich samples are also relatively enriched in K_2O (more than 4%), and they tend to have higher K/Na, and Fe^{3+}/Fe^{2+} ratios (Fig. 9).

There is no significant difference in total alkali content or in total iron content between the equigranular host rocks and the porphyritic dikes, or between the sulfide-rich and the more barren parts of the Catheart Mountain pluton. During alteration and mineralization, addition of K_2O, subtraction of Na_2O, and conversion of ferrous to ferric iron were maintained at nearly constant rates. This resulted in the total content of alkalies (K_2O + Na_2O) and iron remaining nearly unchanged.

Compositional variations in the large cations Rb and Sr also distinguish between the different parts of the Catheart Mountain pluton, especially in the equigranular host rocks. Sulfide-rich

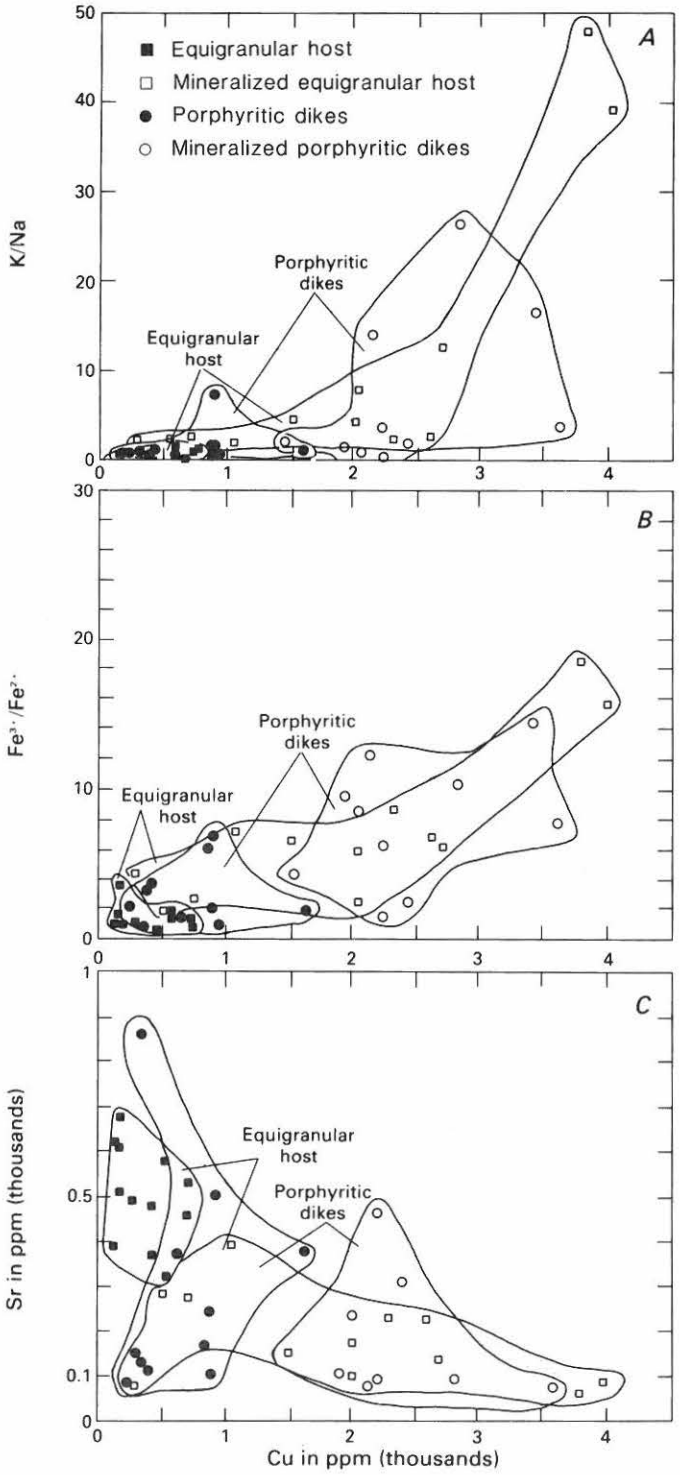

Figure 9. (a) Diagram showing the change in K/Na as a function of Cu content in the equigranular host and porphyritic dikes. Wall-rock reactions and potassium metasomatism produced an increase in the K/Na ratio during mineralization in the equigranular host rocks. (b) Diagram showing the general increase in the Fe^{3+}/Fe^{2+} ratio as Cu increases in the equigranular host rocks and porphyritic dikes. (c) Diagram showing the decrease in Sr with increasing Cu in the Catheart Mountain pluton.

samples containing >1000 ppm Cu tend to be relatively enriched in Rb (>150 ppm) and depleted in Sr (<300 ppm) (Fig. 9) and indicate a pattern of generally decreasing Rb/Sr values as a function of Cu content.

The Sally Mountain pluton is characterized by low abundances of the base metals (Table 3). For example, the highest Cu in the analyzed samples is 86 ppm, a value that is significantly lower than those in the equigranular host rocks, the porphyritic dikes, or in their mineralized equivalents in the Catheart Mountain pluton.

GEOCHEMISTRY OF THE CATHEART MOUNTAIN PLUTON

Geochemical Affinities and Possible Sources

Compositional variations in the granitic plutons are in many cases useful as chemical probes of the source region of felsic magma intruding different crustal segments. Processes affecting the magma during emplacement, however, may irrevocably modify its magmatic features so that the chemical information inherited from the source is drastically disturbed (e.g., Barker, 1981). For example, although ratios of incompatible elements are useful in establishing chemical constraints on the source region of felsic magmas (e.g., Pearce and Cann, 1973; Harris et al., 1986), these chemical variations may be disturbed by the effects of fractionation, by mixing of magmas from different sources, by the evolution and loss of a vapor phase, by coupled melting-fractionation events producing extensive reaction of melts and wall rocks, by contamination, and by assimilation of crustal rocks during plutonic emplacement (e.g., Taylor, 1980; DePaolo, 1981).

Fractionation of primary phases from granitic magma generally produces progressively more evolved rocks in a consistent way, and even though no abrupt changes are produced in the evolving geochemical signatures, the observed variations may be quite different from those inherited from the source region.

In the case of mineralized magmatic systems, the effects of hydrothermal alteration during the waning stages of crystallization are superimposed on the effects of fractionation and further modify the original magmatic signature. Flushing of vast amounts of reactive metasomatic solutions through cooling and largely solidified magmatic systems disturbs primary isotopic values (Taylor, 1974) and produces large-scale elemental redistribution through leaching of magmatic minerals, solution and complexing of metals (Helgeson, 1964), and precipitation of new minerals. Thus, in a hydrothermal system the pattern of enrichment and depletion of the chemical components depends on whether these are liberated through mineral decomposition and consequently lost or whether they are added from outside of the system. Alternatively, chemical components may be retained in resistant or in newly precipitating phases without substantial redistribution. The most resistant minerals, those that are slow

to dissolve or stable under the prevailing conditions, may thus retain chemical variations relatively unchanged from the magmatic regime; such compositional variations may be useful in constraining the type of source and chemical affinities of igneous systems affected by hydrothermal alteration.

In the case of the Catheart Mountain pluton, it seems reasonable to expect that fractional crystallization of rock-forming and accessory minerals systematically changed the composition that the magma inherited from its source. More importantly, however, it is also evident that hydrothermal alteration during the waning stages of crystallization resulted in drastic modifications of the original magmatic signature. Chemical variations in the Catheart Mountain pluton thus reflect changes imposed on the magma during crystallization and during hydrothermal alteration. As a result of these changes, variations of the major elements and many of the trace elements cannot be used to constrain the nature of the source rocks very precisely. For example, as shown above, most samples from the equigranular host rocks and the porphyritic dikes are hydrated and contain anomalously high Cu, Mo, CO_2, and S. In addition, the absence of progressive and consistent variations for most major oxides such as the alkali elements and iron as a function of silica indicates that these elements are not useful for classifying the pluton or for obtaining the original magmatic contents in the pluton. Similar disturbances are also evident for many of the trace elements, as exemplified by Rb and Sr.

The relatively moderate compositional ranges in Li, B, and Be, in the ferromagnesian elements (e.g. Cr, Co, Sc, and Ni), in the REE, and in the highly charged, high-field strength cations (especially Zr, Hf, Ta, and Th) suggest that their contents were not changed drastically even though the rocks were undergoing addition of substantial amounts of Cu and K transported in a highly reactive fluid. The moderate range in Li and B content is unexpected because these elements are lost readily during weathering and mild alteration (e.g., Ericksen and Salas, in press). In fact, this mobility of Li and B probably accounts for their relative enrichment near the ore zones in some porphyry copper deposits (Chaffee, 1976). Although this feature remains unrecognized in the Catheart Mountain pluton, the most straightforward interpretation of the distributions of Li and B in the Catheart Mountain pluton is that their general homogeneity is not a magmatic feature.

Be is enriched in plagioclase, particularly in the more evolved rocks within a sequence, and especially in those containing F-rich volatiles (Petrov, 1973). As the Catheart Mountain pluton exhibits obvious evidence of a strong hydrothermal event which includes decomposition of the primary feldspars and mafic minerals, it is also unlikely that the content of Be reflects the original composition of the granitic magma.

The ferromagnesian elements Co, Cr, Sc, Ni, and Zn show no distinct patterns of enrichment with respect to the content of Cu in the Catheart Mountain pluton, or to any measure of evolution. Although the ferromagnesian elements do not appear to have been significantly remobilized, the original carriers of these elements (e.g., biotite) were destroyed during the hydrothermal alteration. Thus the initial contents of the ferromagnesian elements in the magma are not easily discerned.

Previous studies have shown that the REE are useful for monitoring fluid evolution during hydrothermal alteration of porphyry copper deposits (Taylor and Fryer, 1980). In addition, it has also been established that REE mobility in hydrothermally altered granites is enhanced in F-rich fluids compared to Cl-rich fluids (Alderton et al., 1980). Thus, although it is likely that the abundances of the REE found in the Catheart Mountain pluton are not primary, there is no systematic change in the REE content of the Catheart Mountain pluton during its transformation from relatively sulfide-poor to sulfide-rich rocks. One possible explanation of this feature is that during potassic alteration, when the fluids were magmatic, hot, and saline, alteration of the granitic rocks produced enrichment of the light REE and a slight depletion in the heavy REE (Taylor and Fryer, 1982). Propylitic and phyllic alteration might have mobilized the REE as a group, perhaps resulting in a general depletion of REE relative to the initial magmatic values, but the REE were not mobilized and lost in great amounts.

An important exception to the overall homogeneity of the REE as a group is the possible loss of the heavy REE. This loss may reflect the change from a Cl- to a F-dominated fluid during hydrothermal alteration (Alderton et al., 1980), or perhaps result from the overprinting of the potassic by the phyllic or propylitic alterations (Taylor and Fryer, 1982).

Contents and ratios of the high-field-strength elements are also among the least variable in the Catheart Mountain pluton. Most of the highly charged cations are relatively immobile and insensitive to secondary processes (e.g., Pearce and Cann, 1973; Floyd and Winchester, 1975). In addition, these elements reside in accessory phases (e.g., apatite, zircon, and sphene) which generally remain stable during hydrothermal alteration of granitic rocks (e.g., Alderton et al., 1980; Baldwin and Pearce, 1982), so that one possible interpretation of their moderate variability is that they have not been disturbed significantly relative to their magmatic values.

High-field-strength cations in the least altered equigranular host rocks and porphyritic dikes of the Catheart Mountain pluton are similar in abundance and probably indicate that both the host rocks and the dikes originated from consanguineous granitic magmas (Fig. 10).

Assuming that the relatively low contents of Nb, Ta, Zr, Hf, Th, Yb, and Y and that the ratios of these elements in the Catheart Mountain pluton are meaningful, it is important to note that they resemble those of granitic rocks from calc-alkaline and calcic suites exemplified by the Sierra Nevada batholith (Dodge et al., 1982) and Peninsular Ranges batholith (Gottfried and Dinnin, 1965; Gottfried et al., 1961). More importantly, however, contents of the highly-charged cations in the Catheart Mountain pluton overlap those of the Devonian granodiorites from northern Maine (Ayuso, 1986b) (Fig. 10). In addition, as mentioned previously, REE contents and their chondrite-normalized pat-

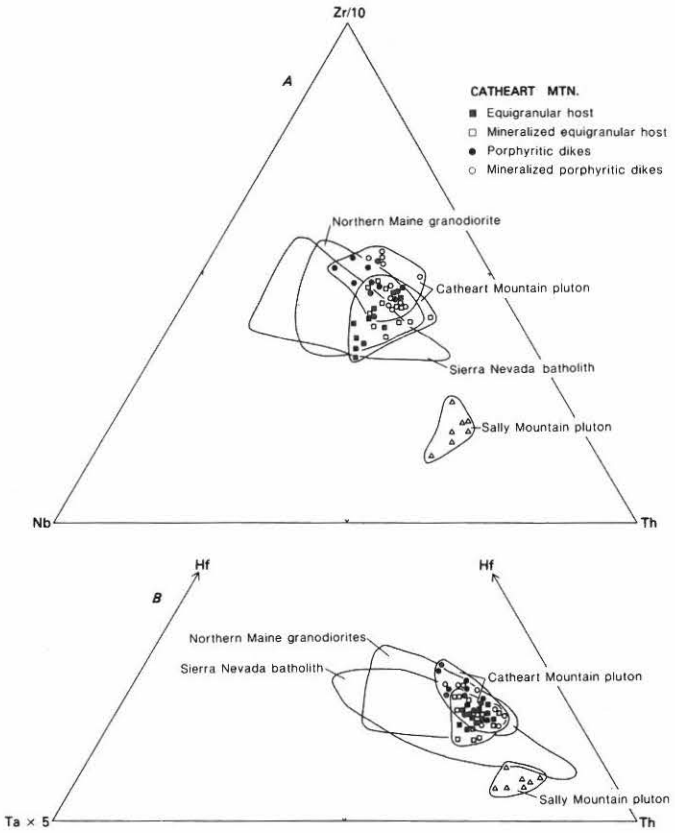

Figure 10. Ternary Nb-Zr-Th and Ta-Hf-Th diagrams of the equigranular host rocks and porphyritic dikes from the Catheart Mountain pluton. Granodiorites from northern Maine (Ayuso, 1986b) and from the Sierra Nevada batholith (Dodge et al., 1982) are also shown for comparison. Note that the Catheart Mountain pluton has compositions that overlap those found in the northern Maine granodiorites and in the Sierra Nevada batholith. The Sally Mountain pluton is not compositionally equivalent to the Catheart Mountain pluton, indicating that it was probably generated from a different source.

terns, and the relatively unradiogenic Pb and low ^{18}O values of the Catheart Mountain pluton are also similar to those found in granodiorites from northern Maine.

The most likely interpretation of this overlap in trace element and isotopic compositions between the Catheart Mountain pluton and granodiorites from northern Maine is that they have a common source. This source is probably in the continental lithosphere and consists of a mixture of mantle-derived material and continental crust as represented by Grenville basement (or possibly Chain Lakes) (Ayuso et al., 1987, 1988). All of the chemical features are also compatible with formation of the Catheart Mountain pluton from sources characteristically invoked for igneous rocks formed in continental magmatic arcs; such sources consist of mixtures of mantle-derived rocks (e.g., altered basalts) and immature eugeosynclinal sedimentary rocks and volcaniclastic rocks (e.g., Taylor, 1986; Gromet and Silver, 1987).

In contrast, comparison of the Catheart Mountain and Sally Mountain plutons indicates significant differences in the content and ratios involving Nb, Ta, Zr, Hf, and Th (e.g., Fig. 10). Diagrams combining these relatively stable elements and elements whose contents changed during hydrothermal alteration (exemplified by Sr and possibly by Yb) demonstrate that the Sally Mountain pluton lies along a different alteration trend than the Catheart Mountain pluton (Fig. 11). Thus, in the Catheart Mountain pluton the alteration trend in the equigranular host rocks and porphyritic dikes is toward decreasing Sr along generally similar Ta/Hf ratios. There is, however, no direct way of relating the chemical variation in the Sally Mountain pluton to the compositions of the equigranular host rocks and porphyritic dikes of the Catheart Mountain pluton, or to the alteration trends of these rocks. Also, the Sally Mountain pluton is significantly more radiogenic in Pb than the Catheart Mountain pluton, suggesting that it was not generated from the same source (Ayuso et al., 1987, 1988).

Relatively few unaltered samples of the Attean quartz monzonite have been analyzed to date, but preliminary Pb and O isotopic results indicate that the Catheart Mountain pluton and the Attean quartz monzonite are similar in composition.

The trace element composition of the Attean quartz monzonite has not been characterized adequately, so that it is difficult to preclude an origin of the Catheart Mountain pluton as a more evolved phase of the Attean quartz monzonite. The Pb isotopic similarity tentatively indicates, however, that Catheart Mountain and the Attean pluton were generated from a similar source.

A Model for the Evolution of the Catheart Mountain Pluton

A consistent model accounting for the evolution of the Catheart Mountain pluton involves the generation of water-undersaturated granitic magma (Burnham and Ohmoto, 1980) from a heterogeneous mixture of sialic basement and mantle-derived rocks in the continental lithosphere. The granitic melt must have been water-undersaturated to be capable of intruding to shallow levels in the Attean quartz monzonite. Both the equigranular host and the porphyritic dikes were derived from this melt, but the equigranular rocks preceded the intrusion of the mineralizing porphyritic dikes.

During the waning stages of consolidation of the shallowly emplaced Catheart Mountain pluton, an evolved and volatile-rich vapor phase was generated (Schmidt, 1978) that carried base-metal complexes (Helgeson, 1964; Roedder, 1971), KCl, and NaCl near the top of the magma chamber (Hemley and Jones, 1964). These chloride-rich acidic fluids migrated explosively through fractures that formed when fluid pressure exceeded lithostatic pressure (Burnham and Davis, 1971; Whitney, 1975; Burnham, 1979), producing mineral reactions characteristic of porphyry copper systems which deposited chalcopyrite and molybdenite especially near the interface between the phyllic and potassic alteration zones.

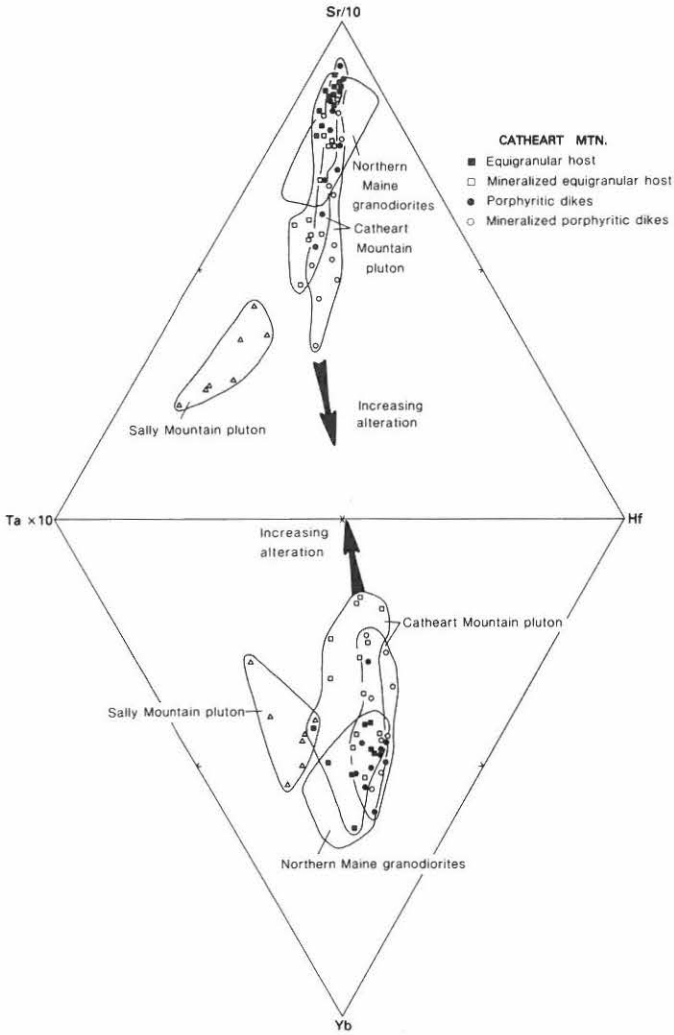

Figure 11. Ternary diagram showing a combination of incompatible and mobile elements Ta-Sr-Hf and Ta-Yb-Hf and the alteration trends in the Catheart Mountain and the Sally Mountain plutons. The field of the northern Maine granodiorites is also shown for comparison. Note that in the Ta-Sr-Hf portion of the diagram, both the equigranular host rock and the porphyritic dikes of the Catheart Mountain pluton trend away from the Sr apex as a result of increasing alteration. The equigranular host rock and the porphyritic dikes also trend away from the Yb apex in the Ta-Yb-Hf portion of the diagram. The Sally Mountain pluton does not lie within the general alteration trends found at the Catheart Mountain pluton.

At the height of hydrothermal activity the fluid was hot, oxidizing, and saline, and mineral assemblages of the potassic alteration zone were formed. Migration and reaction of this chloride-rich acidic fluid with the wall rock resulted in the influx of K, Rb, H, S, and the base metals, as well as the oxidation of Fe^{2+} to Fe^{3+}, loss of Ca and Na, increase in the K/Na ratio, and remobilization of many of the trace elements (e.g., Sr). Reaction with igneous plagioclase released Ca and Na (and also Sr). It also produced the precipitation of K-feldspar and enrichment of K in the hydrothermally-altered rocks by base exchange reactions (Hemley and Jones, 1964) which produced an increase in the KCl/HCl of the aqueous phase (Burnham, 1979; Burnham and Ohmoto, 1980). The formation of sericite also explains the overall enrichment of K and H in the system. The loss of Mg in the equigranular rocks of the Catheart Mountain pluton is as expected from the effects of phyllic alteration and as a function of the degree of mineralization (e.g. Meyer and Hemley, 1967).

The near constancy in the content of total iron indicates that the iron liberated from the magmatic mafic silicates was used for the most part in the formation of pyrite, chalcopyrite, and hydrothermal biotite during hydrothermal alteration. No contribution of iron from outside of the system is necessary. These compositional changes are consistent with the effects of wall-rock reactions including leaching of Ca and Na, and the introduction of K during potassic and phyllic alteration. Decrease of Sr and Ca in the equigranular host rocks and porphyritic dikes suggests that hydrothermal reactions produced albite from more calcic igneous plagioclase, but that the Sr content of hydrothermal albite is lower than that of the magmatic plagioclase. The net effect was a reduction of Sr content (e.g., Dickin and Jones, 1983; Humphris and Thompson, 1978; Andre and Deutsch, 1986) and higher Rb/Sr ratios in the sulfide-rich rocks.

Ti remained relatively unchanged in the Catheart Mountain pluton because sphene and possibly rutile were formed following the decomposition of biotite. Silica might have remained relatively immobile because destruction of primary magmatic minerals was probably followed immediately by precipitation of new silica-bearing phases.

The fluids were primarily magmatic in the early stages of alteration and analogous to those found in many other porphyry copper systems (e.g., Rose, 1970; Taylor, 1974). These results are compatible with suggestions that the source of the base metals, S, and K was also magmatic, and that the aqueous chloride fluids acquired Cu from magmatic sources as advocated by Holland (1965) for porphyry systems in general and is shown in detailed studies by Chivas (1981) and Hendry et al. (1985). With the collapse of the hydrothermal cell, the aqueous chloride solutions were cooler, containing perhaps predominantly meteoric water (e.g., Sheppard et al., 1969). The fluid also contained a component of high ^{18}O (Ayuso et al., 1988) and produced minerals of the sericitic alteration zone through hydrolysis reactions.

SUMMARY

(1) The Catheart Mountain pluton is the best example of a porphyry copper system in the eastern United States. It consists of equigranular granodiorite and porphyritic dikes. Both units contain pyrite, chalcopyrite, and molybdenite.

(2) The range in silica content is narrow in the Catheart Mountain pluton. There are no progressive, smooth, and consistent chemical gradients between the major rock units. The majority of the rocks are hydrated, contain high CO_2, and high S. The most intensely altered parts of the pluton are potassic (up

to 6.9 wt % K_2O) and contain copper mineralization (up to about 3900 ppm Cu). Lower Ca, Na, and Sr are characteristic of rocks containing high abundances of the ore minerals. Sulfide-rich rocks also contain the highest Fe^{3+}/Fe^{2+} and K/Na ratios.

(3) Variation of the high-valence cations (Zr, Hf, Ta, and Th) suggests that these elements were not strongly affected by the hydrothermal activity. The compositional range of these elements is especially informative because it indicates that the host rocks and dikes in the Catheart Mountain pluton are consanguineous. The Catheart Mountain pluton resembles the Devonian granodiorites from northern Maine, as well as plutonic rocks formed in magmatic continental arcs. The Sally Mountain pluton is probably not a comagmatic phase of the Catheart Mountain pluton.

(4) The Catheart Mountain pluton was generated in the continental lithosphere from a source consisting of a mixture of sialic basement (possibly Grenville craton) and mantle-derived rocks. The equigranular granodiorites represent a water-undersaturated melt which intruded high in the upper crust. Volatile and chloride-rich fluids in the porphyritic dikes transported the base metals and produced wall-rock reactions leading to the intense leaching of magmatic minerals, remobilization of the major and trace elements, oxidation of iron, and precipitation of the ore minerals. These fluids may have been magmatic at the start of the alteration event, but they included a component of high-^{18}O possibly from meteoric sources toward the waning stages.

ACKNOWLEDGMENTS

This study would have been impossible without the generous help of R. G. Schmidt. His assistance during the selection of core samples kindly made available by Scott Paper Co. for geochemical work, and especially our discussions on the nature of the mineralization and alteration in the Catheart Mountain pluton, were critical in the successful completion of this project. I have benefited from challenging discussions on the geochemistry of granitic rocks with J. G. Arth and D. Gottfried who also provided constructive criticism of the manuscript. I am also indebted to D. R. Lux and M. Yeats for their helpful comments on a version of this paper.

REFERENCES CITED

Albee, A., and Boudette, E. L., 1972, Geology of the Attean quadrangle, Somerset County, Maine: U.S. Geol. Surv., Bull. 1297, 110 p.

Alderton, D. H. N., Pearce, J. A., and Potts, P. J., 1980, Rare earth element mobility during granite alteration: evidence from southwest England: Earth Planet. Sci. Lett., v. 49, p. 149-165.

Andre, L., and Deutsch, S., 1986, Magmatic $^{87}Sr/^{86}Sr$ relicts in hydrothermally altered quartz diorites (Brabant massif, Belgium) and the role of epidote as a Sr filter: Contrib. Mineral. Petrol., v. 92, p. 104-112.

Appleyard, E. C., 1980, Mass balance computations in metasomatism: metagabbro/nepheline syenite pegmatite interaction in northern Norway: Contrib. Mineral. Petrol., v. 73, p. 131-144.

Atkinson, D., 1977, Catheart Mountain, an Ordovician porphyry copper molybdenum occurrence in northern Appalachia: Ph.D. dissert., Univ. Western Ontario, London, Ontario, 192 p.

Ayuso, R. A., 1986a, Lead isotopic evidence for distinct sources of granite and for distinct basements in the northern Appalachians, Maine: Geology, v. 14, p. 322-325.

Ayuso, R. A., 1986b, Geochemistry of mineralized and unmineralized felsic plutons in the northern Maine plutonic belt: Geol. Soc. Amer., Abs. with Prog., v. 18, p. 530.

Ayuso, R. A., 1987, Mineralized rocks of the Catheart Mountain Cu-Mo porphyry, Maine: aluminous white micas as indices of mineralization: U.S. Geol. Surv., Bull. 1803, 16 p.

Ayuso, R. A., Horan, M., and Criss, R. E., 1987, Pb and oxygen isotopic geochemistry of the northern Maine plutonic belt: Geol. Soc. Amer., Abs. with Prog., v. 19, p. 3.

Ayuso, R. A., Horan, M., and Criss, R. E., 1988, Pb and O isotopic geochemistry of granitic plutons from northern Maine: Am. Jour. Sci., Wones Volume, v. 288-A, p. 421-460.

Baldwin, A. J., and Pearce, J. A., 1982, Discrimination of productive and non-productive porphyritic intrusions in the Chilean Andes: Econ. Geol., v. 77, p. 664-674.

Barker, F., 1981, Introduction to special issue on granites and rhyolites: a commentary for the nonspecialist: Jour. Geophys. Res., v. 86, p. 10131-10135.

Beane, R. E., and Titley, S. R., 1981, Porphyry copper deposits, Part II - Hydrothermal alteration and mineralization: Econ. Geol., 75th Anniversary vol., p. 214-269.

Boone, G. M., Boudette, E. L., and Moench, R. H., 1970, Bedrock geology of the Rangeley Lakes-Dead River basin region, western Maine, *in* Boone, G. M. (ed.), New England Intercollegiate Geological Conference guidebook for field trips in the Rangeley Lakes-Dead River basin, western Maine, p. 1-24.

Burnham, C. W., 1979, Magmas and hydrothermal fluids, in Barnes, H. L. (ed.), Geochemistry of hydrothermal ore deposits, 2nd edition: John Wiley and Sons Inc., New York, p. 71-136.

Burnham, C. W., and Davis, N. F., 1971, The role of H_2O in silicate melts: I. P-V-T relations in the system $NaAlSi_3O_8$-H_2O to 10 kilobars and 1000oC: Am. Jour. Sci., v. 270, p. 54-79.

Burnham, C. W., and Ohmoto, H., 1980, Late-stage processes of felsic magmatism: Mining Geol., Special Issue, No. 8, p. 1-11.

Chaffee, M. A., 1976, The zonal distribution of selected elements above the Kalamazoo porphyry copper deposit, San Manuel district, Pinal County, Arizona: Jour. Geochem. Expl., v. 5, p. 145-165.

Cheatham, M. N., Olszewski, W. J., and Gaudette, H. E., 1985, The Chain Lakes massif, west central Maine: northern Appalachian basement or suspect terrane?: Geol. Soc. Amer., Abs. with Prog., v. 17, p. 543.

Chivas, A. R., 1981, Geochemical evidence for magmatic fluids in porphyry copper mineralization, Part I - Mafic silicates from the Kolula igneous complex: Contrib. Mineral. Petrol., v. 78, p. 389-403.

Cox, D. P., Gonzalez, I. P., and Nash, J. T., 1975, Geology, geochemistry, and fluid inclusion petrography of the Sapo Alegre porphyry copper prospect and its metavolcanic wallrocks, west-central Puerto Rico: U.S. Geol. Surv., Jour. Res., v. 3, p. 313-327.

Creasey, S. C., 1965, Geology of the San Manuel area, Pinal County, Arizona: U.S. Geol. Surv., Prof. Paper 471, 64 p.

DePaolo, D. J., 1981, Trace element and isotopic effects of combined wall-rock assimilation and fractional crystallization: Earth Planet. Sci. Lett., v. 53, p. 189-202.

Dickin, A. P., and Jones, N. W., 1983, Relative elemental mobility during hydrothermal alteration of a basic sill, Isle of Skye, N.W. Scotland: Contrib. Mineral. Petrol., v. 82, p. 147-153.

Dodge, F. C. W., Millard, H. T., Jr., and Elshemer, H. N., 1982, Compositional variations and abundances of selected elements in granitoid rocks and constituent minerals, central Sierra Nevada batholith, California: U.S. Geol. Surv., Prof. Paper 1248, 24 p.

Ericksen, G. E., and Salas, R. O., in press, Geology and resources of salars in the Central Andes: U.S. Geol. Surv., Open-File Report.

Floyd, P. A., and Winchester, J. A., 1975, Magma type and tectonic setting discrimination using immobile elements: Earth Planet. Sci. Lett., v. 53, p. 255-265.

Flynn, R. T., and Burnham, C. W., 1978, An experimental determination of rare earth partition coefficients between chloride-containing vapor phase and silicate melts: Geochim. Cosmochim. Acta, v. 42, p. 679-684.

Ford, J. H., 1978, A chemical study of alteration at the Panguna Porphyry copper deposit, Bougainville, Papua New Guinea: Econ. Geol., v. 73, p. 703-720.

Gottfried, D., and Dinnin, J., 1965, Distribution of tantalum in some igneous rocks and coexisting minerals of the southern California batholith: U.S. Geol. Surv., Prof. Paper 525-B, p. B96-B1OO.

Gottfried, D., Jenkins, L., and Grimaldi, F., 1961, Distribution of niobium in three contrasting comagmatic series of igneous rocks: U.S. Geol. Surv., Prof. Paper 424-B, p. B256-B258.

Gresens, R. L., 1967, Composition-volume relationships of metasomatism: Chem. Geol., v. 72, p. 527-548.

Gromet, L. P., and Silver, I. T., 1987, REE variations across the Peninsular Ranges batholith: implications for batholithic petrogenesis and crustal growth in magmatic arcs: Jour. Petrol., v. 28, p. 75-125.

Gustafson, L. B., and Hunt, J. P., 1975, The porphyry copper deposits at El Salvador, Chile: Econ. Geol., v. 70, p. 857-912.

Harris, N. B. W., Pearce, J. A., and Tindle, A. G., 1986, Geochemical characteristics of collision zone magmatism, *in* Coward, N. P., and Ries, A. C. (eds.), Collision tectonics: Geol. Soc. Pub. No. 19, p. 67-81.

Helgeson, H. C., 1964, Complexing and hydrothermal ore deposition: The Macmillan Co., New York, 128 p.

Hemley, J. J., and Jones, W. R., 1964, Chemical aspects of hydrothermal alteration with emphasis on hydrogen metasomatism: Econ. Geol., v. 59, p. 538-569.

Hendry, D. A. F., Chivas, A. R., Long, J. V. P., and Reed, S. J. B., 1985, Chemical differences between minerals from mineralizing and barren intrusions from some North American porphyry copper deposits: Contrib. Mineral. Petrol., v. 89, p. 317-329.

Holland, H. D., 1965, Some applications of thermochemical data to problems of ore deposits, II. Mineral assemblages and the composition of ore forming fluids: Econ. Geol., v. 60, p. 1101-1166.

Hollister, V. F., 1978, Geology of the porphyry copper deposits of the western hemisphere: Soc. Mining Eng., Am. Inst. Mining, Metall., and Petrol. Eng., New York, 219 p.

Hollister, V. F., Potter, R. R., and Barker, A. L., 1974, Porphyry-type deposits of the Appalachian orogen: Econ. Geol., v. 69, p. 618-630.

Hudson, T., and Arth, J. G., Jr., 1983, Tin granites of Seward peninsula, Alaska: Geol. Soc. Amer., Bull., v. 94, p. 768-790.

Humphris, S. E., and Thompson, G., 1978, Trace element mobility during hydrothermal alteration of oceanic basalts: Chem. Geol., v. 23, p. 125-137.

Jambor, J. L., 1974, Trace element variations in porphyry copper deposits, Babine Lake area, B.C.: Canada Geol. Surv., Paper 74-9, 30 p.

Jamieson, R. A., and Strong, D. F., 1981, A metasomatic mylonite zone within the ophiolite aureole, St. Anthony Complex, Newfoundland: Am. Jour. Sci., v. 281, p. 264-281.

Lowell, J. D., and Guilbert, J. M., 1970, Lateral and vertical alteration-mineralization zoning in porphyry ore deposits: Econ. Geol., v. 63, p. 645-654.

Lyons, J. B., Aleinikoff, J. N., and Zartman, R. E., 1986, Uranium-thorium-lead ages of the Highlandcroft plutonic suite, northern New England: Am. Jour. Sci., v. 286, p. 489-509.

Meyer, C., and Hemley, J. J., 1967, Wall rock alteration, *in* Barnes, H. L. (ed.), Geochemistry of hydrothermal ore deposits: Holt, Rinehart, and Winston, New York, p. 166-235.

Naylor, R. S., Boone, G. M., Ashenden, D. D., and Robinson, P., 1973, Pre-Ordovician rocks in the Bronson Hill and Boundary Mountain anticlines, New England, U.S.A. (abs.): Am. Geophys. Union Trans., v. 54, p. 459.

Nockolds, S. R., 1954, Average chemical compositions of some igneous rocks: Geol. Soc. Amer., Bull., v. 65, p. 1007-1032.

Olade, M. A., and Fletcher, W. K., 1975, Primary dispersion of rubidium and strontium around porphyry copper deposits, Highland Valley, British Columbia: Econ. Geol., v. 70, p. 15-21.

Pearce, J. A., and Cann, J. R., 1973, Tectonic setting of basic volcanic rocks investigated using trace element analyses: Earth Planet. Sci. Lett., v. 19, p. 290-300.

Petrov, L. L., 1973, Behavior of beryllium in crystallization of granitoid magmas: Geochem. Internat., v. 10, p. 627-640.

Roedder, E., 1971, Fluid inclusion studies on the porphyry-type ore deposits at Bingham, Utah; Butte, Montana; and Climax, Colorado: Econ. Geol., v. 66, p. 98-120.

Rose, A. W., 1970, Zonal relations of wallrock alteration and sulfide distribution at porphyry copper deposits: Econ. Geol., v. 65, p. 920-936.

Schmidt, R. G., 1974, Preliminary study of rock alteration in the Catheart Mountain molybdenum-copper deposit, Maine: U.S. Geol. Surv., Jour. Res., v. 2, p. 189-194.

Schmidt, R. G., 1978, The potential for porphyry copper-molybdenum deposits in the eastern United States: U.S. Geol. Surv., Prof. Paper 907-E, 31 p.

Schwartz, M. O., 1982, Geochemistry of the porphyry copper deposit at La Granja, Peru: Geol. Jb., v. D-57, p. 3-35.

Sheppard, S. M. F., Nielsen, R. L., and Taylor, H. P., Jr., 1969, Oxygen and hydrogen isotope ratios of clay minerals from porphyry copper deposits: Econ. Geol., v. 64, p. 755-777.

St-Julien, P., Slivitsky, A., and Feininger, T., 1983, A deep structural profile across the Appalachians of southern Quebec, *in* Hatcher, R. D., Williams, H., and Zietz, I. (eds.), Contributions to the tectonics and geophysics of mountain chains: Geol. Soc. Amer., Mem. 158, p. 103-111.

Stewart, D. B., Luetgert, J. H., Unger, J. D., and Phillips, J. D., 1985, Characterization of the crust of Maine by seismic reflection and refraction (abs.): Geol. Soc. Amer., Abs. with Prog., v. 17, p. 727.

Taylor, H. P., Jr., 1974, The application of oxygen and hydrogen isotope studies to problems of hydrothermal alteration and ore deposition: Econ. Geol., v. 69, p. 843-883.

Taylor, H. P., Jr., 1980, The effects of assimilation of country rocks by magmas on $^{18}O/^{18}O$ and $^{87}Sr/^{86}Sr$ systematics in igneous rocks: Earth Planet. Sci. Lett., v. 47, p. 243-254.

Taylor, H. P., Jr., 1986, Igneous rocks: II. Isotopic case studies of circumpacific magmatism, *in* Valley, J. W., Taylor, H. P., Jr., and O'Neil, J. R. (eds.), Reviews in Mineralogy, Stable isotopes in high temperature geological processes, v. 16: Mineral. Soc. Am., p. 273-317.

Taylor, R. P., and Fryer, B. J., 1980, Multiple-stage hydrothermal alteration in porphyry copper systems in northern Turkey: the temporal interplay of potassic, propylitic, and phyllic fluids: Can. Jour. Earth Sci., v. 17, p. 901-926.

Taylor, R. P., and Fryer, B. J., 1982, Rare earth element geochemistry as an aid to interpreting hydrothermal ore deposits, *in* Evans, A. M. (ed.), Metallization associated with acid magmatism: John Wiley and Sons, New York, p. 357-365.

Theodore, T. G., and Nash, J. T., 1973, Geochemical and fluid zonation at Copper Canyon, Lander County, Nevada: Econ. Geol. 68, p. 565-570.

Titley, S. R., 1975, Geological characteristics and environment of some porphyry copper occurrences in the southwestern Pacific: Econ. Geol., v. 70, p. 499-514.

Titley, S. R., 1982, The style and progress of mineralization and alteration in porphyry copper systems, *in* Titley, S. R. (ed.), Advances in geology of the porphyry copper deposits, southwestern North America, p. 93-116.

Titley, S. R., and Beane, R. E., 1981, Porphyry copper deposits, Part I. Geologic settings, petrology, and tectogenesis: Econ. Geol., 75th Anniversary Volume, p. 214-235.

Turekian, K., and Wedepohl, K., 1961, Distribution of the elements in some major units of the Earth's crust: Geol. Soc. Amer., Bull., v. 72, p. 175-192.

Whitney, J. A., 1975, Vapor generation in a quartz monzonite magma: a synthetic model with application to porphyry copper deposits: Econ. Geol., v. 72, p. 346-358.

Zen, E-an, 1983, Exotic terranes in the New England Appalachians-limits, candidates, and ages: a speculative essay: Geol. Soc. Amer., Mem. 158, p. 55-81.

Maine Geological Survey
Studies in Maine Geology: Volume 4
1989

Multiple Thermal Metamorphism of the Digdeguash Formation in the Contact Aureole of the Pocomoonshine Gabbro-diorite, Southeastern Maine

Allan Ludman
Department of Geology
Queens College of the City University of New York
Flushing, New York 11367

Sandra L. Bromble
Lamont-Doherty Geological Observatory
Palisades, New York 10964

James M. DeMartinis
Roux Associates
Huntington, New York 11743

ABSTRACT

Intrusion of the Pocomoonshine gabbro-diorite into turbidites of the Digdeguash Formation in southeastern Maine produced a broad contact aureole in which andalusite-biotite, sillimanite, and sillimanite-potassic feldspar mineral zones are recognized. Anatectic temperatures were reached near the pluton/host rock contact, where a distinctive migmatite marks the highest intensity of metamorphism. Pluton and aureole mineralogy confirm an epizonal environment for intrusion (P=2.5 to 3.0 kbars). Textural studies reveal that the aureole is a composite feature that resulted from two episodes of prograde mineral growth separated by a retrograde event. Assemblage and phase chemistry data indicate that the second thermal pulse was the most intense, with maximum temperatures of approximately 700°C. A two-stage magmatic injection history involving early emplacement of gabbro followed by intrusion of a larger mass of diorite is postulated to explain this thermal history.

INTRODUCTION

The coastal lithotectonic block of Maine has been intruded by a suite of several post-deformational, epizonal plutons that extends for over 320 kilometers from the mid-coastal region to the St. George batholith of southern New Brunswick (Osberg et al., 1985; Potter et al., 1979). The suite was first recognized in east-coastal Maine by Chapman (1962), who named it the Bays of Maine Igneous Complex and described it as a bimodal assemblage of gabbro and granite. Recent work in eastern Maine reveals that there is a large volume of diorite and quartz diorite as well (Ludman and Hill, 1986).

The most prominent of the mafic bodies in southeastern Maine is the Pocomoonshine gabbro-diorite, a differentiated complex exposed in the Big Lake and Wesley quadrangles (Fig. 1). Previous workers have mapped its boundaries (Larrabee, 1964), studied the magmatic processes by which it evolved (Westerman, 1972), related it to the Acadian thermal events responsible for the entire plutonic suite (Thompson, 1984), or used it to help establish the timing of regional accretion (Ludman, 1981). All who have studied it have noted its prominent contact aureole, particularly along its western margin where

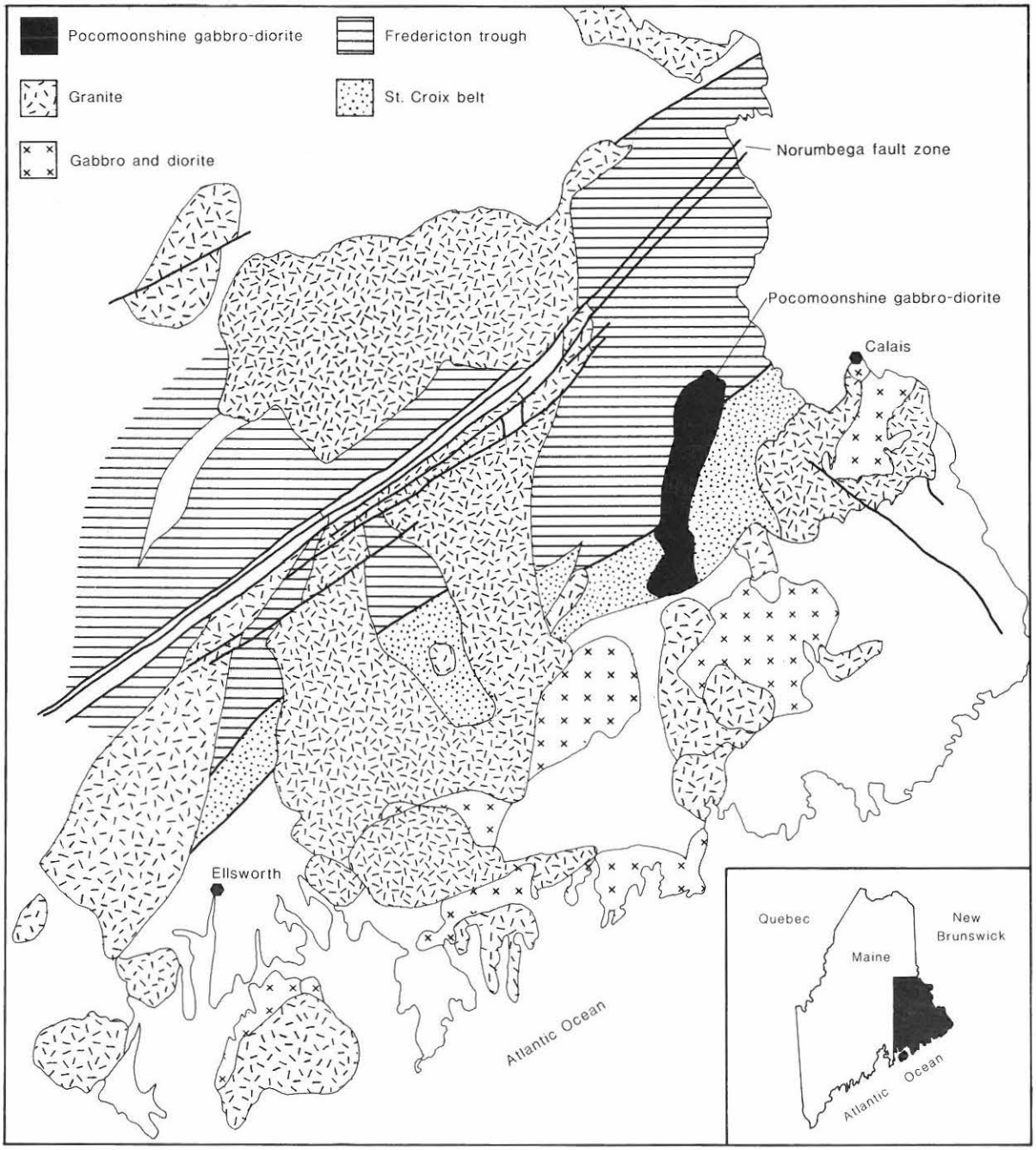

Figure 1. Geological setting of the Pocomoonshine gabbro-diorite. Inset shows location of detailed map. Modified after Osberg et al. (1985).

thermal metamorphic effects extend several kilometers from the contact, but no one has examined the metamorphism in detail. Our field, petrographic, and chemical studies show that rocks of the aureole have had an unexpectedly complex thermal history involving at least two episodes of prograde mineral growth. The purpose of this paper is to describe and document this history, and to relate it to local and regional events.

Geologic Setting

The Pocomoonshine gabbro-diorite has intruded the contact between two major components of the coastal lithotectonic block, the St. Croix belt and the Fredericton trough (Fig. 1). To the southeast, the St. Croix belt consists mostly of Cambrian through lowest Ordovician pelitic and psammitic strata. To the

northwest, the Fredericton trough is a thick sequence of calcareous and non-calcareous turbidites probably of Late Ordovician through Early Devonian age. Rocks of both belts were folded during the Acadian orogeny prior to intrusion of the pluton, and the map pattern is dominated by these large upright folds (F_1) with northeast-trending hinge surfaces. F_2 recumbent folds associated with northwest-directed thrusting, and small-scale F_3 folds related to north-trending normal faulting deform the early folds and cleavage, but do not significantly alter the map pattern. The entire region, including the Pocomoonshine pluton, was affected by northeast-, north-, and northwest-trending late or post-Acadian faults (Ludman, 1986; Ludman and Hill, 1986). Small granitic plugs cut the western and central parts of the Pocomoonshine pluton, and pegmatite and aplite veins occur sparsely within it.

Regional metamorphic grade is low in both the Fredericton trough and St. Croix tracts, generally not surpassing conditions of the chlorite zone. As a result, well-developed contact aureoles surround the numerous plutons in the region. The Pocomoonshine body has an asymmetric aureole, with contact effects extending up to 8.5 km from the contact on the west, north, and northeast, but only 0.8 km to the east. This is due partly to the shape of the pluton, a gently west-dipping tabular mass (Westerman, 1972), and partly to faults that cut it and its host rock on the east (Ludman, 1986).

Southeastern Maine is a heavily glaciated region of gently rolling hills that rise only a few hundred feet above ubiquitous lakes and swamps. The Pocomoonshine gabbro-diorite occupies an elongate lowland in the Big Lake quadrangle, but is bordered by a resistant hornfels rim that underlies Huntley, Hawkins, and Seavey Ridges on the west, and Cedar Grove Ridge on the east. Bedrock exposures comprise less than 1% of the region, but are much more abundant on these ridges. An extensive network of new lumber roads provides unprecedented access and many new outcrops throughout the western part of the Big Lake quadrangle, particularly along Huntley and Seavey Ridges. The western aureole of the pluton was thus chosen for this study because of its extent, exposure, and accessibility.

Rocks of the Pocomoonshine gabbro-diorite exposed in the study area are medium to coarse grained hornblende diorites and quartz diorites. Their host rocks along the western contact are the Flume Ridge and Digdeguash Formations of the Fredericton trough (Ludman, 1986). The Flume Ridge Formation consists of calcareous sandstones and siltstones interbedded with minor amounts of non-calcareous shale. These are converted to dense hornfelses near the pluton, and occur as alternating bands of calc-silicate (with actinolite, diopside, or wollastonite) and biotite-rich quartzo-feldspathic granofels. The Digdeguash Formation contains interbedded granule and pebble conglomerates, lithic and quartzo-feldspathic wackes, and gray shale, and is almost entirely non-calcareous. Spectacular chiastolitic andalusite porphyroblasts up to 20 cm long typify pelites of the Digdeguash Formation in much of the aureole. Sillimanite occurs near the pluton, and rare cordierite, garnet, and staurolite have been identified in middle grade exposures. Textural and phase relationships among andalusite, sillimanite, and white micas record a complicated metamorphic history for these pelites, and the remainder of this paper is devoted to unraveling that history.

Previous Works

The Pocomoonshine gabbro-diorite was not shown at all on the geologic map of Maine compiled by Keith (1933). It was first mapped in the Big Lake quadrangle and named by Larrabee (1964), and Westerman (1978) showed that it probably extends into the adjacent Wesley quadrangle on the south. Larrabee et al. (1965) described the variety of mafic and intermediate rock types that comprise the pluton, but Westerman (1972) was the first to study the body systematically and show that it is compositionally zoned. He proposed a differentiation model to explain the petrologic relationships in the pluton and used metamorphic and gravity data to postulate its tabular shape.

Larrabee (1964) outlined the contact aureole surrounding the Pocomoonshine pluton with a stippled pattern on his geologic map, but made no attempt to subdivide it. Westerman (1972) recognized four mineral zones in pelitic Digdeguash Formation hornfelses and three in the calcareous rocks of the Flume Ridge Formation, although he used a stratigraphic nomenclature that has since been abandoned. Ludman (1978, 1986) remapped the Big Lake quadrangle, revised the stratigraphies of the Fredericton trough and St. Croix belt, modified Westerman's zones and isograds, and showed that contact metamorphic anatexis of the Digdeguash Formation had occurred along Huntley and Seavey Ridges. Bromble (1983) used feldspar and garnet-biotite geothermometry to estimate temperatures in the high-grade zones and to study the cooling history of the Pocomoonshine pluton, and DeMartinis' (1986) detailed petrographic studies confirmed the aureole's polymetamorphic history. This paper updates our studies of the thermal history of the Digdeguash Formation on the west flank of the pluton.

METAMORPHIC ZONATION OF THE DIGDEGUASH FORMATION

The Digdeguash Formation is a thick pile of wackes, conglomerates, and shales intercalated in generally well graded beds. It is tightly folded, but in areas unaffected by plutonic activity it is regionally metamorphosed only to conditions of the chlorite zone (lower greenschist facies). This regional metamorphism, designated as M_1, accompanied Acadian upright folding of the Fredericton trough. Mineral growth during M_1 was minor; no M_1 porphyroblasts have been recognized, and the pelites of the Digdeguash Formation are uniformly fine grained. A faint phyllitic sheen in the low-grade pelites results from alignment (S_1 foliation) of small muscovite and chlorite flakes parallel to the hinge surfaces of the Acadian F_1 folds. Primary sedimentary features such as cross- and graded bedding and load structures

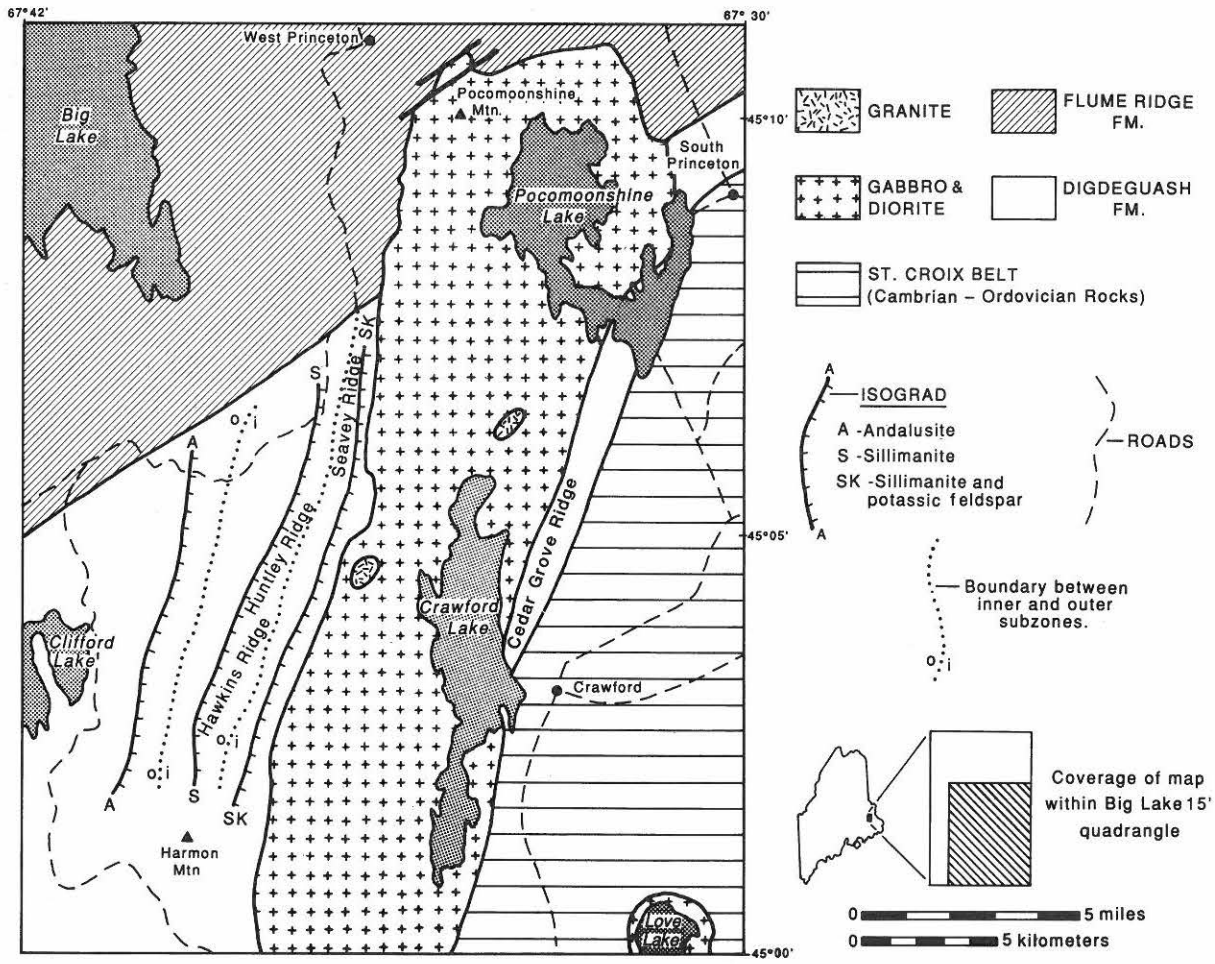

Figure 2. Simplified geologic map of part of the Big Lake quadrangle showing metamorphic zonation in pelites of the Digdeguash Formaion on the western margin of the Pocomoonshine gabbro-diorite. Modified after Ludman (1986).

are well preserved, as are original textures in the coarser rocks. Distinctions between clasts and matrix are obvious in thin section, and polymineralic or multigranular rock fragments are easily identified.

Thermal effects superimposed on this low-grade terrane by emplacement of the Pocomoonshine body are recognized by progressive changes in the color, mineralogy, and texture of the pelites as the contact is approached, and by progressive obliteration of primary textures in the psammites. The first contact effect, originally described by Westerman (1972), and visible as far as 8.5 km from the pluton, is a coarsening of the normally fine grained chlorite and muscovite flakes and growth of unfoliated chlorite. Closer to the pluton, andalusite-biotite, sillimanite, and sillimanite-potassic feldspar zones have been delineated, but variations in texture and phase relationships permit subdivision of the outer two zones. The result is the five-fold division of the aureole shown in Figure 2.

Isograds defined by the first appearance of sillimanite and of the assemblage sillimanite + potassic feldspar are easily mappable, but poor outcrop control prevents tracing individual biotite and andalusite isograds in the outer part of the aureole. Westerman (1972) stated that andalusite appears farther from the pluton than does biotite, but available exposures are not sufficient to conclusively demonstrate which formed at the lower temperature. A single boundary thus separates chlorite grade exposures from an andalusite-biotite zone. Characteristics of the three major zones will be described briefly below.

Andalusite-Biotite Zone

The andalusite-biotite zone is the broadest zone in the aureole surrounding the Pocomoonshine gabbro-diorite, extending a maximum of 3.25 km from the first appearance of biotite and andalusite to the sillimanite isograd. Primary sedimentary features are well preserved throughout the zone. Recrystallization commonly heightens compositional differences in graded beds and facilitates facing determinations. More delicate features such as cross-bedding and flame structures are visible in

the outer part of the zone, but disappear as the sillimanite isograd is approached. Microtextures are altered somewhat, but identification of clasts and distinctions between clast and matrix are still possible in conglomerates and coarse wackes.

Mineralogy. Biotite and andalusite first appear in the pelites approximately 6.4 km from the pluton and produce a darker color (purplish gray) than is typical of the pale greenish gray chlorite grade exposures. Most of the biotite in wackes and pelites occurs as small brown to red-brown flakes that, along with thermally coarsened muscovite, mimetically enhance the S_1 foliation. A few larger poikiloblastic biotite flakes have been observed in the inner part of the andalusite-biotite zone. The grain size of the micas increases as the sillimanite isograd is approached, and the phyllitic sheen eventually becomes a pronounced schistosity parallel to S_1.

Andalusite is the most prominent mineral in hornfelses of the Digdeguash Formation. It occurs sparsely as slender gray porphyroblasts in pelites in the outer part of the andalusite-biotite zone, but increases in size and abundance closer to the pluton where it also appears in the wackes. Andalusite is generally chiastolitic, ranges from 2.5 to 20 cm in length, and comprises as much as 50% of the pelitic hornfels along Huntley and Seavey Ridges.

Garnet and staurolite have been identified in andalusite-biotite zone exposures, but are very rare. Small euhedral reddish garnet crystals occur most commonly in thin bands rich in pyrite, but are also present in a few "normal" pelite horizons. The garnets are clouded with inclusions in their centers and are clear at their rims, a texture interpreted as indicating initially rapid growth followed by growth at a slower rate. The sulfide-garnet bands are separated from the typical pelite by selvages of abnormally coarse-grained muscovite and biotite flakes. Staurolite has only been observed in a few thin sections and has never been identified in the field. It occurs as small, pale yellow-brown, subhedral prisms, and in some instances as inclusions in large chiastolite crystals. A few cordierite porphyroblasts have been identified in the outer part of the andalusite-biotite zone, and round aggegrates of chlorite and muscovite in the same area are probably retrograde pseudomorphs after cordierite.

Variations within the Andalusite-Biotite Zone. Several textural and mineralogical variations have been noted in the andalusite-biotite zone. Some are attributable to distance from the pluton, but others are more problematic and show that the aureole is not as simple as had originally been thought. The steady increase in grain size of matrix micas and andalusite porphyroblasts from the outer part of the zone to the sillimanite isograd is a textural variation that is expected in a "normal" aureole. It is difficult to map the distribution of cordierite, garnet, and staurolite with the current outcrop and sampling density. Their occurrence is undoubtedly also temperature related, but bulk pelite composition is clearly a major factor as well. If the chlorite-muscovite aggregates described above are indeed pseudomorphous after cordierite, cordierite would seem to be restricted to the outer part of the andalusite-biotite zone. Garnet appears in the inner part of the zone and is stable through the rest of the aureole.

Complicating these simple patterns is the systematic distribution of severely retrograded andalusite crystals in the inner part of the zone, and fresh, nearly unaltered andalusite in the outer part. This distinction, recognizable in the field as well as with the microscope, has led us to divide the andalusite-biotite zone into inner (strongly retrograded) and outer (weakly retrograded) subzones (Fig. 2). Andalusite of the outer subzone is typically fresh to slightly altered and is surrounded at most by a thin sheath of sericite grains (Fig. 3a). Chiastolitic inclusion trains are easily visible in hand sample and thin section. In contrast, andalusite porphyroblasts of the inner subzone are strongly altered (Figs. 3b, c), sericitization commonly proceeding most rapidly along fractures and lines of inclusions. Many crystals have been completely replaced (Fig. 3d), but some of the pseudomorphs preserve traces of the original chiastolitic inclusion pattern.

Further complexity is indicated by the growth of coarse muscovite flakes from the sericite of these pseudomorphs in the high-temperature part of the inner subzone (Fig. 4). This suggests a second episode of prograde mineral growth and implies at least two pulses of heat associated with the aureole.

Sillimanite Zone

Entry to the sillimanite zone is marked by the appearance of fibrolite in pelitic horizons as far as 3.2 km from the Pocomoonshine pluton. Most of the minerals characteristic of the andalusite-biotite zone persist into the sillimanite zone as stable phases or, in some instances, as armored relicts. Porphyroblasts composed of relict andalusite armored by sericite and/or coarse muscovite are prominent throughout the zone. Garnet is abundant in pyrite-rich bands and in a few normal pelite layers, but staurolite and cordierite are very rare. Veins of white granite, quartz, quartz + muscovite, and quartz + muscovite + pink andalusite are widespread in the zone and become more abundant near the sillimanite-potassic feldspar isograd. These veins cut and strongly distort layering, but bedding is recognizable in most exposures. Cross-bedding and load features are also preserved in the outer part of the sillimanite zone, but are destroyed in the inner part.

Original clast outlines are still visible in the wackes, but the fine-grained matrix typical of lower grades has completely recrystallized. Biotite and muscovite generally occur as coarse flakes in both wacke and pelite, and most pelitic rocks display a strong schistosity mimetic after S_1 foliation. Some layers are deformed by tight F_2 folds, and a second, north-trending foliation (S_2) defined by coarse muscovite and biotite is locally well developed parallel to the F_2 hinge surfaces.

Variations within the Sillimanite Zone. The sillimanite zone is divided into inner and outer subzones of nearly equal width based on the mode of occurrence of sillimanite. In the

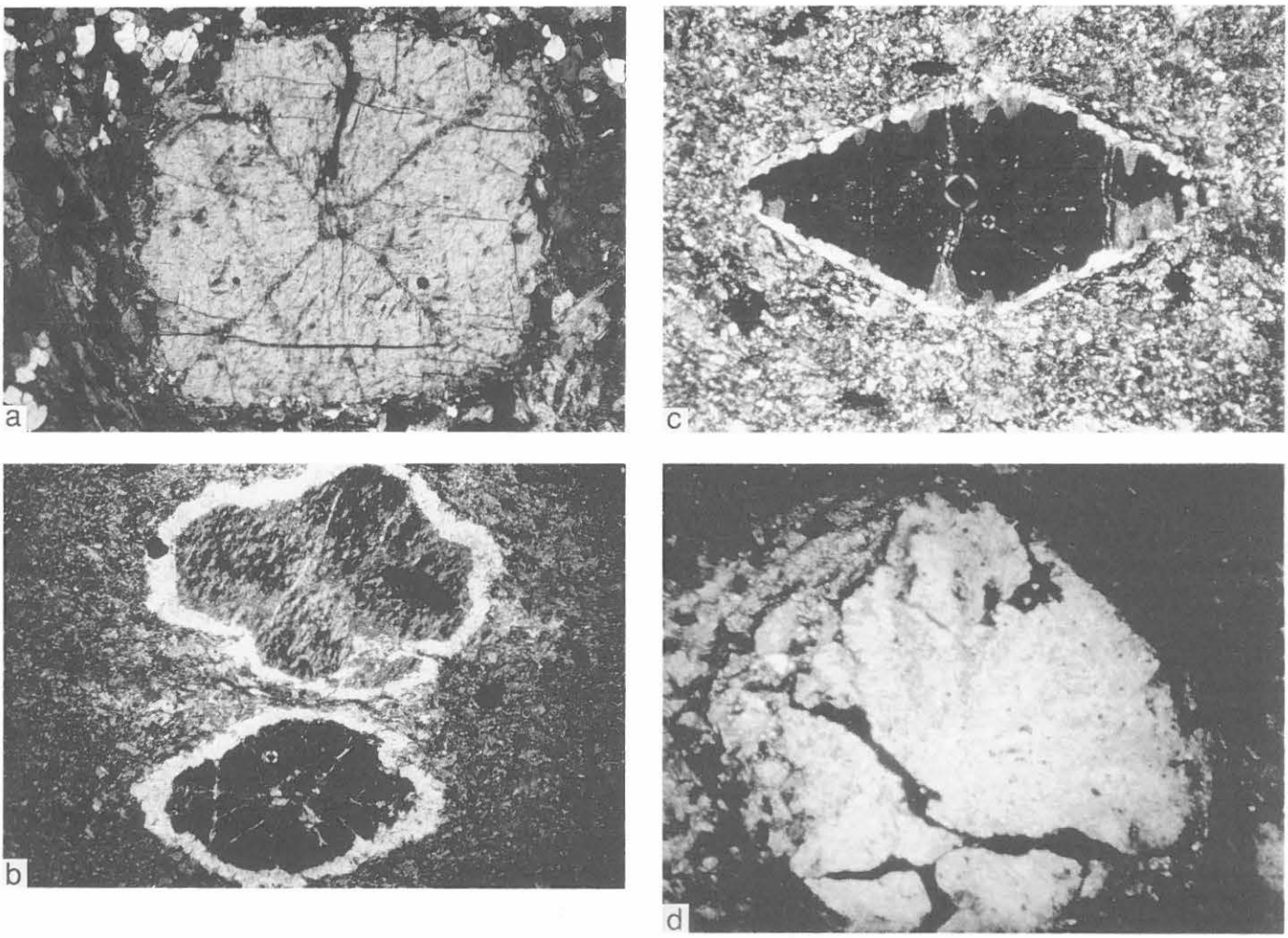

Figure 3. Photomicrographs showing types of andalusite porphyroblasts from the andalusite-biotite zone. (a) Fresh chiastolitic porphyroblast from outer andalusite-biotite subzone. O-polarizers. Porphyroblast width = 2.7 mm. (b,c) Retrograded andalusite porphyroblasts (partly replaced by sericite) from inner andalusite-biotite subzone. X-polarizers. Width of field = 3.5 mm. (d) Complete replacement of andalusite by sericite from inner andalusite-biotite subzone. X-polarizers. Width of field = 2.1 mm.

outer subzone it is totally fibrolitic and is restricted to pelitic layers immediately adjacent to large veins. In the inner subzone fibrolite is found throughout the pelitic layers and in some metawacke horizons, and coarser prismatic sillimanite is also present.

The outer sillimanite subzone is very similar to the adjacent part of the andalusite-biotite zone. Relict gray andalusite occurs in the cores of partial pseudomorphs, armored by sericite and chlorite and commonly surrounded by coarse muscovite growing from the sericite. A second, younger andalusite occurs with muscovite in the quartz veins. It is pink, unaltered, smaller than the gray porphyroblasts, and non-chiastolitic. Fibrolitic sillimanite is found only in coarse muscovite-biotite "schists" adjacent to these veins. It is not found in contact with the older generation of andalusite or with the micas of the pseudomorphs, but locally is in contact with or is included within the pink andalusite. Only a single staurolite porphyroblast, corroded and partially replaced by biotite and muscovite, has been observed in this subzone.

Fibrolitic sillimanite in the inner sillimanite subzone is not restricted to layers in contact with quartz veins, but is ubiquitous in pelites where it is intimately intergrown with biotite. Bundles of fine grained prismatic sillimanite are also present. Relict gray andalusites are surrounded by pseudomorphs of coarse muscovite and biotite, and fibrolite is commonly present in the outer parts of these pseudomorphs (Fig. 5). In a few instances it is also in contact with the relict andalusite in the pseudomorph cores. Euhedral garnets occur in sillimanite-rich pelite layers as well as in bands with abundant pyrite, but neither staurolite nor cordierite have been identified. Accessory tourmaline and zircon grains are coarser and thus more prominent than in the outer parts of the aureole.

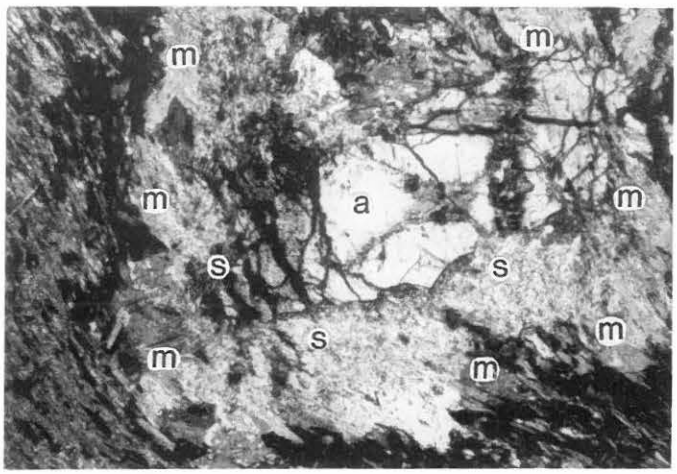

Figure 4. Photomicrograph showing second episode of prograde mineral growth in inner andalusite-biotite subzone. Pseudomorph consists of first stage gray andalusite (a) replaced by sericite (s). Coarse grained muscovite (m) of the second contact metamorphic event has grown from the sericite on the rim of the pseudomorph. X-polarizers. Width of field = 3.5 mm.

Figure 6. Pavement exposure from the sillimanite-potassic feldspar zone showing anatectic leucosome engulfing rafts of pelitic and psammitic restite. Pocketknife for scale.

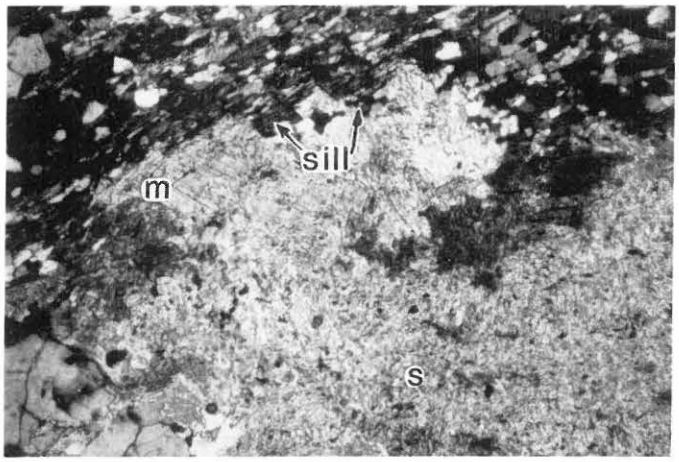

Figure 5. Photomicrograph showing relationships among sillimanite, muscovite, and sericite in the sillimanite zone. Sericite pseudomorphous (s) after first stage gray andalusite has been overgrown by coarse muscovite (m) and fibrolitic sillimanite (sill). X-polarizers. Width of field = 3.5 mm.

Sillimanite-Potassic Feldspar Zone

The highest grade portion of the contact aureole is characterized not only by the coexistence of sillimanite and potassic feldspar in the pelites, but also by a migmatitic appearance caused by segregation of quartzo-feldspathic and pelitic components during contact metamorphic anatexis. Discontinuous buff-weathering rafts of relict metawacke in addition to lenses and layers of gray melanosome are engulfed or injected by white leucosome masses within about 1 km of the contact with the pluton (Fig. 6). In the contact area along Seavey and Huntley Ridges, pods and veins of coarse grained leucosome also intrude some Pocomoonshine diorites. Sedimentary features have been completely obliterated and bedding is replaced by a well-defined gneissic banding. Quartz veins and small pegmatite lenses are abundant, further accentuating the chaotic, swirling nature of the layers. In some exposures the migmatite is deformed by F_2 folds, and thin tabular leucosome masses have been emplaced along the hinge surfaces of these folds. Anatexis of the Digdeguash Formation thus appears to have accompanied F_2 folding.

The typical leucosome is a medium to coarse grained assemblage of quartz, potassic feldspar, and plagioclase with subordinate biotite and sillimanite ± muscovite ± garnet. The melanosome contains abundant biotite, sillimanite, quartz and lesser amounts of ilmenite, muscovite, zircon, and plagioclase. Phase relationships in this zone are complex and indicate several stages of mineral growth.

Andalusite occurs as it did in the sillimanite zone, as relict gray cores of pseudomorphs surrounded by coarse muscovite and biotite, and as younger pink prisms in quartz veins. Fibrolite mats and prismatic sillimanite comprise much of the melanosome and are intergrown with biotite and quartz. There appear to be two generations of prismatic sillimanite in the melanosome. Early sillimanite prisms are bent, broken, and cut by needles and mats of younger fibrolitic sillimanite. A second generation of prisms is undeformed and appears to be coeval with the fibrolite. Fibrolite in the leucosome lies between quartz and feldspar grains and rarely forms the large aggregates typical of the melanosome. Biotite is very abundant in the melanosome and occurs in three different habits: (1) red-brown flakes intergrown with fibrolite and fine prismatic sillimanite; (2) brown to olive-brown flakes in garnet-sulfide layers and in some

leucosome pods; and (3) green, clearly late-stage flakes in folia with muscovite and incorporating inclusions of sillimanite. The first of these habits is by far the most common, the third the rarest.

Potassic feldspar is present throughout the leucosomes and in some melanosomes as coarse, anhedral grains of orthoclase and microcline crypto-, micro-, and macro-perthites. Several generations of exsolution lamellae are apparent in most grains, and the exsolved plagioclase is polysynthetically twinned in some instances, untwinned in others. Most plagioclase feldspar is present as either untwinned blebs in myrmekitic intergrowths that replace orthoclase, or as discrete anhedral to subhedral grains that exhibit zoning. Plagioclase also occurs as inclusions in garnet and in the inclusion assemblage quartz + biotite + ilmenite + plagioclase.

Muscovite is much less abundant than at lower grades. It occurs as a part of the andalusite pseudomorphs, as coarse sieved porphyroblasts in some melanosomes, as flakes in leucosome pods, and with green biotite as described above. Some very late sericite is also present, produced by alteration of feldspar and sillimanite. Ilmenite is generally concentrated in cleavage traces of brown biotite, but also occurs as discrete grains in the granoblastic leucosome.

SEQUENCE OF CONTACT METAMORPHIC EVENTS

The mineral assemblages, habits, and textural relationships outlined above indicate at least two episodes of prograde metamorphism in the contact aureole of the Pocomoonshine gabbro-diorite. Evidence for two pulses of prograde mineral growth includes: (a) partial pseudomorphs in which gray andalusite cores are replaced by sericite that is itself overgrown by coarse muscovite and sillimanite; (b) two generations of andalusite (gray chiastolitic porphyroblasts and later pink non-chiastolitic prisms); and (c) two episodes of prismatic sillimanite growth in the innermost part of the aureole. Retrograde reactions are widespread throughout the aureole and also appear to have occurred at two different times: one between the prograde events and the other following the second thermal pulse. The first retrograde episode is clearly marked by the extensive sericitization of gray andalusite and the second by sericitization of sillimanite and feldspar in the sillimanite-potassic feldspar zone. Alteration of cordierite in the outer part of the aureole is probably associated with the earlier of these events.

The sequence of metamorphic events interpreted for the western contact of the Pocomoonshine gabbro-diorite with the Digdeguash Formation is thus:

M_1: Regional chlorite grade metamorphism accompanying Acadian upright folding; development of S_1 cleavage and foliation.

M_2: First thermal metamorphism. Development of M_2 biotite, cordierite, staurolite, garnet, gray chiastolitic andalusite, and early prismatic sillimanite. Mimetic enhancement of S_1 to produce a well defined schistosity.

First retrograde event: Sericitization of gray andalusite close to the pluton; muscovite + chlorite replacement of cordierite in the outer part of the aureole.

M_3: Growth of coarse muscovite from retrograde sericite; growth of fibrolite and second generation of prismatic sillimanite; partial melting of the Digdeguash Formation and segregation of leucosome and melanosome bodies to form anatectic migmatite adjacent to diorites of the Pocomoonshine pluton; generation of quartz veins with pink andalusite. The segregation of some leucosome masses in the hinge surfaces of folds in which S_1 schistosity is deformed indicates coincidence of M_3 and F_2.

Second retrograde event: Formation of muscovite-green biotite folia; sericitization of late sillimanite and feldspars.

M_4: Small granite bodies cut the Pocomoonshine pluton as shown in Figure 2, and another has been mapped on Love Ridge just west of the study area (Ludman, 1986). Biotite and andalusite occur in a narrow aureole around the Love Ridge body, and widespread andalusite-biotite assemblages on the west flank of Harmon Mountain (see Fig. 2) are probably due to another granite that is not exposed at the present erosion level. The three mappable bodies are all composed of pale gray biotite granite, and all are thought to be younger than the Pocomoonshine pluton, so that their contact metamorphism is designated as M_4. Relationships among M_2, M_3, and M_4 are masked by thick glacial cover on Hawkins Ridge and Harmon Mountain and cannot be determined without more outcrops.

The geographic distribution of features associated with the prograde and retrograde events supplies valuable information about the thermal history of the aureole. The source of heat for both prograde pulses appears to have been the Pocomoonshine pluton, and the metamorphic zonation shown in Figure 2 is the result of superposition of M_3 on an older M_2 aureole (see Fig. 7). It is difficult to precisely define the M_2 sillimanite isograd because of the scarcity of early prismatic sillimanite, but the distribution of fibrolite and retrograded gray andalusite indicates that the presently mapped sillimanite isograd is probably an M_3 feature as is the sillimanite-potassic feldspar isograd.

The M_2 aureole probably had a narrower andalusite zone than the present composite aureole. Additional exposures and more detailed sampling are required to delineate M_2 cordierite-andalusite and staurolite-andalusite subzones, and future work is planned to attempt this. M_2 sillimanite was apparently confined to locations closer to the present pluton/Digdeguash contact than was M_3 sillimanite. This fact, along with attainment of anatexis only during M_3, shows that the second thermal pulse produced higher temperatures than the first.

CONDITIONS OF METAMORPHISM

In order to fully understand the thermal history of the Digdeguash Formation adjacent to the Pocomoonshine pluton,

absolute temperature/pressure conditions for each metamorphic event must be determined. Constraints on these conditions come from estimates of the liquidus temperature of the pluton, equilibrium mineral assemblages in the aureole, and cation exchange geothermometry.

Westerman (1972) suggested P_{H2O} of 2 to 3 kb during emplacement of the pluton based on the presence of primary magmatic hornblende ($P_{H2O} > 1$ kb) and on textures showing that plagioclase crystallized before hornblende ($P_{H2O} < 2.7$ kb). For this pressure range, he inferred liquidus temperatures of 1150 $\pm 50^{\circ}$C. This serves as a maximum possible temperature for the aureole.

Assemblage Data

Figure 8 is a petrogenetic grid for mineral assemblages of the Digdeguash pelites that greatly narrows the possible range of metamorphic conditions. The absence of kyanite, transition from the stability field of andalusite to that of sillimanite during M_2, and the occurrence of the reaction muscovite + quartz → sillimanite + potassic feldspar + water during M_3 constrain

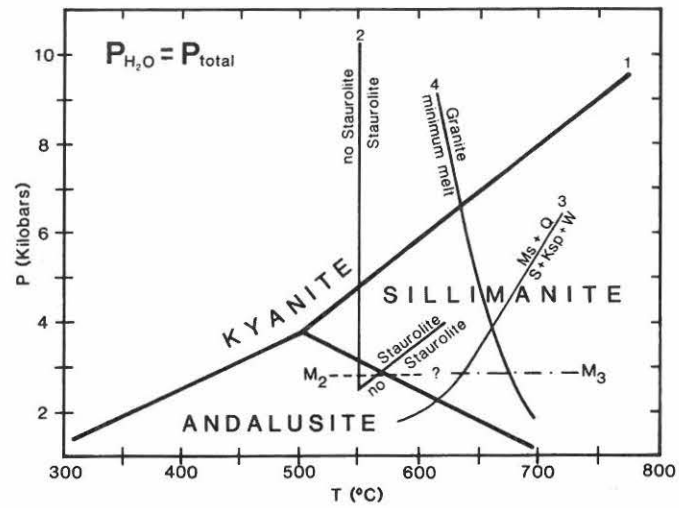

Figure 8. Petrogenetic grid for pelitic assemblages in the Digdeguash Formation showing interpreted metamorphic conditions. Curve (1) after Holdaway, 1971; (2) after Hoschek, 1969, and Richardson, 1968; (3) after Evans, 1965; (4) after Luth et al., 1964.

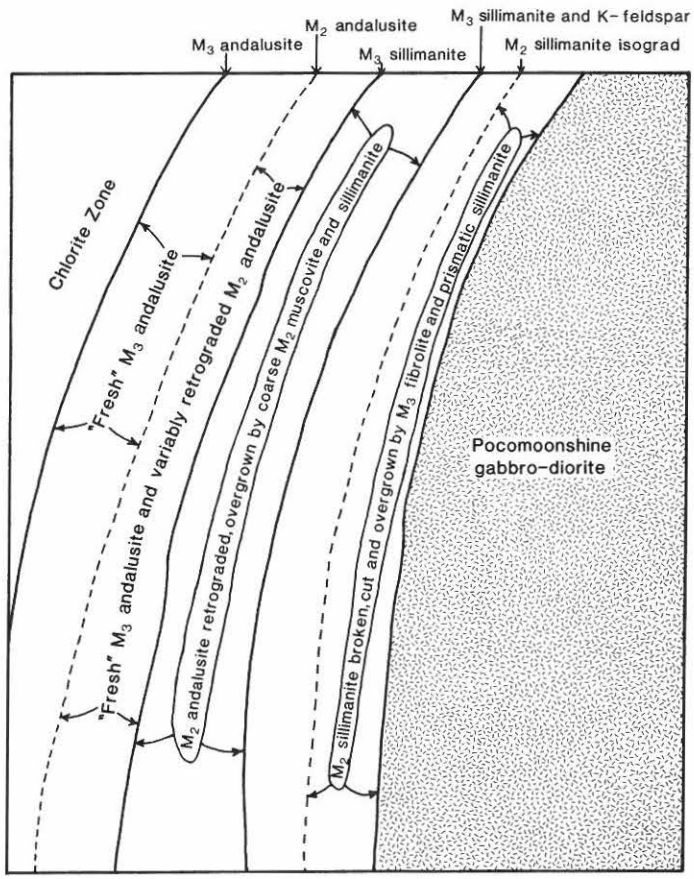

Figure 7. Schematic map showing evolution of the composite contact aureole. Dashed lines indicate interpreted extent of sillimanite and andalusite zones after initial M_2 metamorphism. Solid lines show present zonation developed during M_3.

pressure between 3.7 and 2.25 kb. The apparently stable coexistence of staurolite and andalusite further limits pressure to between 2.5 and 3.0 kb, as shown by the intersections of curves 1 and 2 in Figure 8. The effects of solid solution on curve 2 are unknown because we do not know the precise composition of the staurolite from the aureole, but this value for pressure is in close agreement with Westerman's estimate.

The restriction of the assemblage sillimanite + potassic feldspar to the anatectic migmatites implies that there should be only a small temperature difference (at about 2.75 kb) between the second sillimanite reaction and the onset of melting. This field relationship is in accord with the small difference in temperature indicated between curves 3 and 4 in Figure 8. Because all curves in Figure 8 are drawn for conditions of $P_{H2O} = P_{total}$, this suggests that P_{H2O} was approximately equal to P_{total} during M_2 and M_3. If P_{H2O} had been less than P_{total}, curve 3 would shift to the left and curve 4 to the right, increasing the temperature difference between them.

Cation-Exchange Thermometry

Preliminary microprobe studies of selected phases from the sillimanite-potassic feldspar zone were carried out in an attempt to determine the temperatures during M_3 anatexis using the biotite-garnet geothermometer. Garnet, biotite, and ilmenite from one leucosome sample and from one sulfide-garnet melanosome layer were analyzed on the JEOL electron microprobe at the American Museum of Natural History under the supervision of Drs. Jerry Delaney and Martin Prinz. Although our study can only be considered as preliminary, its results point toward a reasonable peak temperature for M_3 and

TABLE 1. AVERAGE COMPOSITIONS (IN FORMULA UNITS) OF BIOTITES FROM SILLIMANITE-POTASSIC FELDSPAR PELITIC ASSEMBLAGES IN THE DIGDEGUASH FORMATION*.

	LEUCOSOME			PYRITIFEROUS MELANOSOME		
	Green	Red-Brown	Inclusion	Green	Brown	Red-Brown
No.	1	3	1	7	6	13
Si	5.271	5.288	5.128	5.300	5.322	5.248
Al^{IV}	2.729	2.712	2.872	2.700	2.678	2.750
Ti	0.039	0.294	0.179	0.025	0.089	0.313
Al^{VI}	1.216	0.962	0.912	1.182	1.118	0.902
Fe	2.654	2.953	3.025	2.790	2.852	3.065
Mg	1.774	1.347	1.834	1.778	1.540	1.290
Ca	0.006	0.008	0.016	0.007	0.006	0.008
Na	0.033	0.056	0.042	0.067	0.073	0.055
K	1.925	1.914	1.926	1.866	1.894	1.923
$\frac{Fe}{Fe+Mg}$	0.599	0.687	0.622	0.610	0.649	0.703

* Based on 22 oxygens

at the same time confirm the thermal complexities revealed by the textural relationships.

Biotite. Analyses of each of the three different types of biotite recognized in petrographic studies are reported in Table 1. Coarse red-brown grains generally have the highest Fe/Fe+Mg ratios and titanium contents, followed in order by the olive-brown and green varieties. Olive-brown biotites always contain large numbers of ilmenite grains in their cleavage traces. The average composition of the five analyzed ilmenite grains was $Fe_{.983}Mn_{.059}Ti_{.96603}$ using the calculation method of Buddington and Lindsley (1964). Only very small traces of magnesium were detected. These biotite-ilmenite assemblages suggest a retrograde reaction for biotite during which excess iron and titanium entered a newly formed oxide phase, e.g. red-brown biotite → olive-brown biotite + ilmenite.

Garnet. Garnet grains are zoned, but much more work is needed to unravel their complexities. The reconnaissance nature of our work allowed only two-point analyses of most grains (rim and core), and most showed the calcium and manganese enrichment of rims indicative of retrograde metamorphism. More detailed traverses were possible for one garnet from the leucosome and melanosome samples (Fig. 9). These reveal the complexity of metamorphism in the aureole by their compositional asymmetry (Fig. 9a) and the irregular pattern of change of Fe, Mg, and Mn outward from core to rim (Fig. 9b). Once again, more data are needed, but prograde and retrograde trends are suggested.

Estimated Temperatures. Temperatures for the garnet-biotite pairs shown in Table 2 were estimated using the calibration diagram of Spear and Chamberlain (1986; Fig. 10). Most of these pairs consist of olive-brown biotite and the rims of adjacent garnets, and yield temperatures of 530-550°C for what is intepreted as retrograde equilibration. Results are the same for leucosome and melanosome samples. Results from a biotite inclusion and the contiguous part of the surrounding garnet yield a similar temperature (525°C), probably also reflecting reequilibration during retrograde metamorphism. These temperatures presumably represent conditions attained during the *second* retrograde event, and do not record the peak of M_3 metamorphism. The pervasive nature of this retrograde metamorphism is indicated by the reequilibration of the system involving the included biotite and its host garnet.

We plan to continue microprobe studies in order to pinpoint peak M_3 temperatures. Red-brown (i.e. prograde) biotites adjacent to garnet grains were not observed in our preliminary study, and these should yield the highest temperatures. Some idea of these temperatures may be suggested by pairing average red-brown biotite compositions with core compositions of the zoned, retrograded garnets from the same slide (Fig. 10). Results from both leucosome and melanosome are about 670°C. These are in surprisingly good agreement with estimates based on the petrogenetic grid shown in Figure 8, where minimum melt temperatures of about 680°C are suggested.

TABLE 2. Fe/Fe+Mg RATIOS FOR ADJACENT GARNET/BIOTITE PAIRS.

	LEUCOSOME				
Pair #	1	2	3	4	5
Garnet core	.916	.916	---	---	---
Garnet rim	---	---	.910	.918	.909
Adjacent biotite	.696	---	.696	.696	.696
Included biotite	---	.623	---	---	---
	MELANOSOME				
Pair #	1	2	3	4	
Garnet rim	.911	.927	.918	.917	
Adjacent biotite	.642	.691	.648	.648	

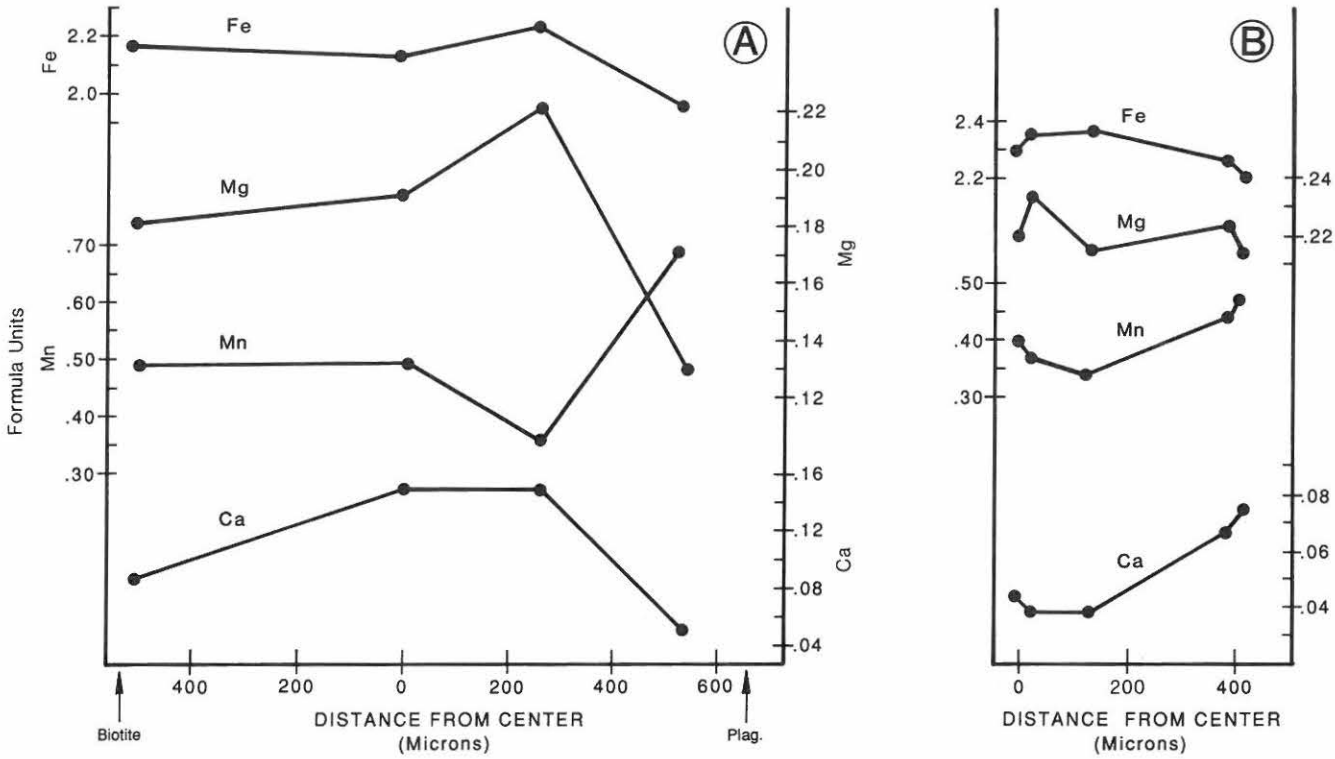

Figure 9. Compositional zoning of garnets from sillimanite-potassic feldspar zone-leucosome (a) and melanosome (b).

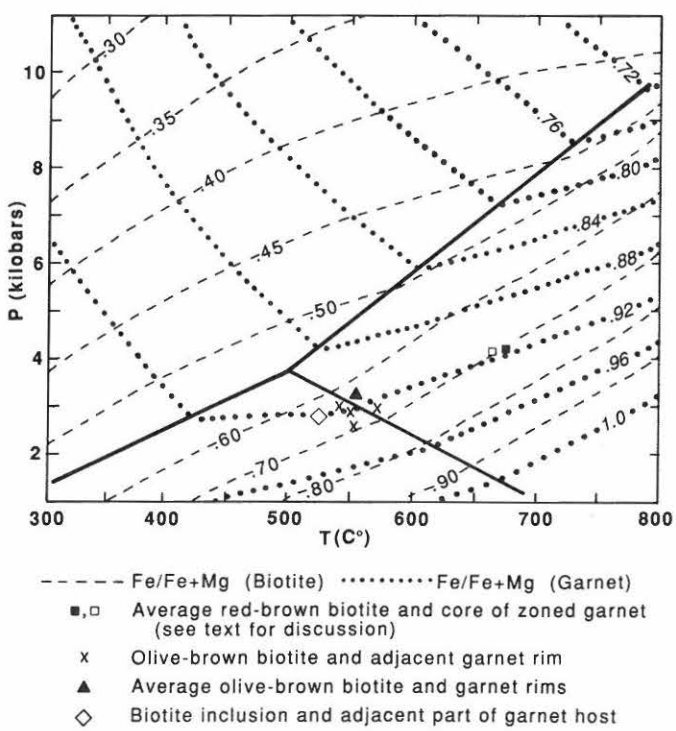

Figure 10. Calibration diagram for biotite-garnet geothermometer (after Spear and Chamberlain, 1986). Solid symbols = melanosome; open symbols = leucosome.

DISCUSSION

Figure 11 shows the interpreted thermal evolution of the hornfelsed pelites from the Digdeguash Formation based on petrographic and thermometric details given above. Although the estimated contact temperatures of >700°C are appropriate for the diorites along Hawkins, Huntley, and Seavey Ridges, the observed history is not consistent with the cooling of a simple gabbro-diorite body. The igneous sheets commonly used in theoretical studies of the cooling of plutons and their host rocks are comparable to the shape of the Pocomoonshine pluton, and this permits rapid comparison of the observed and theoretical histories. None of the theoretical cooling curves shown in Figure 11 fit the interpreted sequence of prograde M2 -- retrograde event 1 -- M_3.

Models such as those of Jaeger (1957, 1959) that invoke cooling totally by conduction yield smooth temperature-time curves (Fig. 11, dashed curve), quite unlike that interpreted for the study area. A model involving convective heat flow in water-saturated host rocks (Norton and Knight, 1977) produces perturbations of this simple curve that more closely resemble the observed relationships (Fig. 11, dotted curve). It also takes into account what must have been a high water content in the rapidly deposited turbidites of the Digdeguash Formation. Each successive peak in this model, however, must be at a lower temperature than the initial maximum, in conflict with the fact that M_3

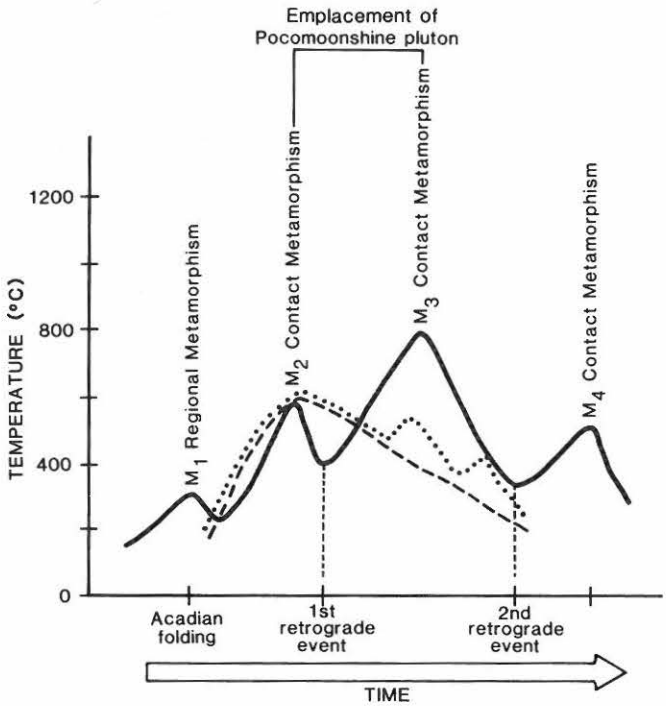

Figure 11. Comparison of interpreted thermal evolution of the Digdeguash Formation (solid line is the contact aureole of the Pocomoonshine gabbro-diorite) with theoretical cooling curves. Dashed line = conductive cooling model (after Jaeger, 1957); dotted line = conductive cooling modified by convective heat transfer by fluids in the host rock (after Norton and Knight, 1977).

produced higher temperatures than M_2 in the aureole surrounding the Pocomoonshine gabbro-diorite. Thus, M_3 cannot simply be attributed to convective heat transfer. A heat source *other than that which caused M_2* is required.

Field relationships and the estimated M_3 contact temperatures make it unlikely that this source could have been a granitic body such as those responsible for the later M_4 event. The most likely explanation is that the Pocomoonshine gabbro-diorite was emplaced in two episodes of magmatic injection, the first causing M_2, the second M_3. Enough time must have separated the two magmatic pulses to permit the cooling indicated by the early retrograde event that separates M_2 and M_3. Based on a simple conductive model (Jaeger, 1957), the epizonal environment, and a postulated thickness of 1600-4800 m for the pluton (Westerman, 1972), this time gap may have been less than 250,000 years. The concentration of mafic rocks in the northern part of the pluton and of diorites in the south near the contacts where M_3 anatexis took place implies that a sheet of mafic magma was injected first and was followed by a less regularly shaped dioritic mass. The Love Lake quartz diorite in the southeastern corner of the Big Lake quadrangle (Fig. 2) may be an extension of this second magma.

Although Westerman (1972) did not discuss a multiple injection history for the Pocomoonshine pluton, his data do not preclude this model, and he has suggested that the mafic rocks in the northern part of the body may have been emplaced earlier than the intermediate rocks of the study area (Westerman, pers. commun., 1987). The two-stage mechanism postulated here would seem to require higher temperatures for the initial gabbro phase (M_2) than for the later dioritic stage (M_3), unless the gabbro had been a partially solidified crystal-rich mush rather than a simple liquid. It is unlikely that the former possibility was involved because none of the gabbros contain the crushed and broken crystals expected if they had been largely crystallized at the time of emplacement. We believe that the relative proportions of the gabbro and diorite phases of the pluton explain this apparent incongruity. The early gabbros comprise only about 25% of the pluton; they may well have been hotter than the subsequent diorites, but the total heat contribution from the latter to the country rock was much greater.

This history for the Pocomoonshine pluton based on its contact aureole is in accord with that which has emerged for the regional plutonism (Ludman and Hill, 1986; Hill and Abbott, this volume). Early Acadian folding and thrusting were followed closely by emplacement of mafic, intermediate, and then granitic magmas. Gabbros intruding the St. Croix belt in the Calais quadrangle were apparently still somewhat liquid when the younger granites were emplaced, indicating the short time period involved in the plutonism. The time span in the case of the Pocomoonshine gabbro-diorite may have been longer, since none of the contacts between granite and the Pocomoonshine pluton exhibit the "mafic pillows" that typify the magma commingling zones in the Calais area (Ludman and Hill, 1986). In addition, the two episodes of retrograde metamorphism described above imply at least some time for cooling from peak metamorphic temperatures between (1) gabbro and diorite phases of the Pocomoonshine pluton, and (2) diorite and later granites.

ACKNOWLEDGMENTS

This study was supported by the Maine Geological Survey, by National Science Foundation Grant EAR78-03329, and by PSC-BHE grants from the City University of New York to A. Ludman. Susan Coughlin, Fran Dragan, Charles LoBue, and Neal Madnick aided in sampling, and Drs. Jerry Delaney and Martin Prinz of the American Museum of Natural History helped with the microprobe analyses. We are grateful to Patrick Brock, Hannes Brueckner, and Peter Mattson for their helpful comments on earlier versions of the work reported here.

REFERENCES CITED

Bromble, S. L., 1983, Thermal metamorphic history of the Digdeguash Formation in the inner portion of the Pocomoonshine gabbro-diorite contact aureole, Big Lake quadrangle, southeastern Maine: M.S. thesis, Queens College, Flushing, N.Y., 118 p.

Buddington, A. F., and Lindsley, D. H., 1964, Iron-titanium oxide minerals and synthetic equivalents: Jour. Petrol., v. 5, p. 310-357.

Chapman, C. A., 1962, Bays-of-Maine Igneous Complex: Geol. Soc. Amer., Bull., v. 73, p. 883-888.

DeMartinis, J. M., 1986, Multiple thermal metamorphism of the Digdeguash Formation in the contact aureole of the Pocomoonshine gabbro, eastern Maine: M.A. thesis, Queens College, Flushing, N.Y., 78 p.

Evans, B. W., 1965, Application of a reaction-rate method to the breakdown equilibria of muscovite and muscovite plus quartz: Am. Jour. Sci., v. 263, p. 647-667.

Holdaway, M. J., 1971, Stability of andalusite and the aluminum silicate phase diagram: Am. Jour. Sci., v. 271, p. 97-131.

Hoschek, G., 1969, The stability of staurolite and chloritoid and their significance in metamorphism of pelitic rocks: Contrib. Mineral. Petrol., v. 22, p. 208-232.

Jaeger, J. C., 1957, The temperature in the neighborhood of a cooling intrusive sheet: Am. Jour. Sci., v. 255, p. 306-318.

Jaeger, J. C., 1959, Temperatures outside a cooling intrusive sheet: Am. Jour. Sci., v. 257, p. 44-54.

Keith, A., 1933, Preliminary geologic map of Maine: U.S. Geol. Surv./Maine Geol. Surv.

Larrabee, D. M., 1964, Bedrock geologic map of the Big Lake quadrangle, Washington County, Maine: U.S. Geol. Surv., Geol. Quad. GQ-358.

Larrabee, D. M., Spencer, C. W., and Swift, D. J. P., 1965, Bedrock geology of the Grand Lake area, Aroostook, Hancock, Penobscot, and Washington Counties, Maine: U.S. Geol. Surv., Bull. 1201-E, 38 p.

Ludman, A., 1978, Stratigraphy, structure, and progressive metamorphism of Lower Paleozoic rocks in the Calais area, southeastern Maine, *in* Ludman, A. (ed.), New England Intercollegiate Geological Conference guidebook for field trips in southeastern Maine and southwestern New Brunswick: Queens College Geol. Bull. 6, p. 78-101.

Ludman, A., 1981, Significance of transcurrent faulting in eastern Maine and location of the suture between Avalonia and North America: Am. Jour. Sci., v. 281, p. 463-483.

Ludman, A., 1986, Bedrock geology of the Big Lake quadrangle, eastern Maine: Maine Geol. Surv., Open-File Rept. 86-1, 42 p.

Ludman, A., and Hill, M. D., 1986, Bedrock geology of the Calais quadrangle, Maine: Maine Geol. Surv., Open-File Rept. 86-72, 54 p.

Luth, W. C., Jahns, R. H., and Tuttle, O. F., 1964, The granite system at P=4-10 kb: Jour. Geophys. Res., v. 69, p. 759-773.

Norton, D., and Knight, J., 1977, Transport phenomena in hydrothermal systems: cooling plutons: Am. Jour. Sci., v. 277, p. 937-981.

Osberg, P. H., Hussey, A. M., II, and Boone, G. M., 1985, Bedrock geologic map of Maine: Maine Geol. Surv., 1:500,000.

Potter, R. R., Hamilton, J. B., and Davies, J. L., 1979, Geological map of New Brunswick, 2nd edition: New Brunswick Dept. Natural Resources, Mineral Resources Div., Fredericton, New Brunswick.

Richardson, S. W., 1968, Staurolite stability in a part of the system Fe-Al-Si-O-H: Jour. Petrol., v. 9, p. 467-488.

Spear, F. S., and Chamberlain, C. P., 1986, Metamorphic and tectonic evolution of the Fall Mountain nappe complex and adjacent Merrimack synclinorium, *in* Robinson, P., and Elbert, D. C. (eds.), Regional metamorphism and metamorphic phase relations in northwestern and central New England: Internat. Mineral. Assoc. Guidebook, p. 121-144.

Thompson, J. F. H., 1984, Acadian synorogenic mafic intrusions in the Maine Appalachians: Am. Jour. Sci., v. 284, p. 462-483.

Westerman, D. S., 1972, Petrology of the Pocomoonshine gabbro-diorite, Big Lake quadrangle, Maine: Ph.D. dissert., Lehigh University, Bethlehem, Pa., 175 p.

Westerman, D. S., 1978, Bedrock geology of the Wesley quadrangle, *in* Ludman, A. (ed.), New England Intercollegiate Geological Conference guidebook for field trips in southeastern Maine and southwestern New Brunswick: Queens College Geol. Bull. 6, p. 120-132.